IMPROVING CHRONOLOGIES IN ISLAND ENVIRONMENTS: A GLOBAL PERSPECTIVE

by

MATTHEW F. NAPOLITANO

A DISSERTATION

Presented to the Department of Anthropology
and the Division of Graduate Studies of the University of Oregon
in partial fulfillment of the requirements
for the degree of
Doctor of Philosophy

June 2021

DISSERTATION APPROVAL PAGE

Student: Matthew F. Napolitano

Title: Improving Chronologies in Island Environments: A Global Perspective

This dissertation has been accepted and approved in partial fulfillment of the requirements for the Doctor of Philosophy degree in the Department of Anthropology by:

Scott M. Fitzpatrick	Chairperson
Jon Erlandson	Core Member
Alison Carter	Core Member
Geoffrey Clark	Core Member
Ryan Jones	Institutional Representative

and

Andy Karduna	Interim Vice Provost for Graduate Studies

Original approval signatures are on file with the University of Oregon Division of Graduate Studies

.

Degree awarded June 2021

DISSERTATION ABSTRACT

Matthew F. Napolitano

Doctor of Philosophy

Department of Anthropology

June 2021

Title: Improving Chronologies in Island Environments: A Global Perspective

Chronology building is a fundamental part of archaeology. Questions related to the timing and duration of events are inextricably connected to larger questions about human activity in the past. Given its wide applicability and temporal range that covers the last ca. 50 kya, radiocarbon dating is the most frequently used chronometric technique in archaeology. Preserved carbon-based organic materials such as charcoal, shell, and bone are often key sources of information for determining the onset and duration of cultural events that occurred in the past. Limitations of radiocarbon dating have long been identified, yet with advances, including accelerator mass spectrometry (AMS) and applications of Bayesian modeling (see below), archaeologists and other scientists have continued to improve the accuracy and precision of chronologies. For archaeologists working in island regions, these techniques have allowed archaeologists to engage with a number of complex issues including island colonization events (i.e., initial human settlement), paleoenvironmental reconstruction, and long-distance exchange and interaction between groups of people living on different islands.

To examine chronological issues as they specifically relate to islands, I present four case studies as part of this dissertation in which various techniques are applied to archaeological datasets to improve the accuracy and precision of understanding human activity in the past. By applying a suite of methods, including chronometric hygiene, Bayesian modeling, glass chemical composition analysis, and marine reservoir corrections to case studies from four island regions around the world, I improve upon some of the limitations imposed by radiocarbon dating to create a more nuances understanding the past. These approaches allow me to address both large-scale questions such as the timing of human settlement across the circum-Caribbean, site-specific questions such as when stone money quarrying activity took place in a rockshelter site in Palau, western Micronesia, and how settlement patterns in southern Yap, western Micronesia was influenced by sea-level change around 2000 years.

This dissertation includes unpublished and previously published co-authored material.

CURRICULUM VITAE

NAME OF AUTHOR: Matthew F. Napolitano

GRADUATE AND UNDERGRADUATE SCHOOLS ATTENDED:

University of Oregon, Eugene, OR
University of West Florida, Pensacola, FL
State University of New York at Stony Brook, Stony Brook, NY

DEGREES AWARDED:

Doctor of Philosophy, Anthropology, 2021, University of Oregon
Master of Arts, Anthropology, 2012, University of West Florida
Bachelor of Arts, Anthropology, 2006, State University of New York at Stony Brook

AREAS OF SPECIAL INTEREST:

Island and coastal archaeology, long-term human-environment interactions, initial settlement of previously uninhabited islands, traditional ecological knowledge, long-distance migration and interaction, chronology building, ceramic analyses

PROFESSIONAL EXPERIENCE:

Principal Investigator, Archaeological Inventory of Koror Rock Island Southern Lagoon, Phase I, Bureau of Cultural and Historical Preservation, Ministry of Community and Cultural Affairs (National Park Service grant no: P17AF00153), 2020

Principal Investigator, Archaeology Inventory of Yapese Stone Money Sites in the Republic of Palau, Bureau of Cultural and Historical Preservation, Ministry of Community and Cultural Affairs (National Park Service grant no: P19AF00236), 2020

Graduate Teaching Employee, Department of Anthropology, University of Oregon, 2014-2021

Laboratory Manager and Field Director, North American Archaeology Lab, American Museum of Natural History, New York, 2012-2014

Assistant Laboratory Supervisor, North American Archaeology Lab, American Museum of Natural History, New York, 2010-2012

GRANTS, AWARDS, AND HONORS:

Centurion Award, The Graduate School, University of Oregon, 2021

Lokey Science Dissertation Fellowship, University of Oregon, 2020-2021

Lewis and Clark Fund for Fieldwork and Exploration, 2019

Sigma Xi Grant-in-Aid of Research, 2019

Small Professional Grant, Center for Asian and Pacific Studies, 2019

Wenner-Gren Dissertation Fieldwork grant, "First colonization of the land of stone money: Archaeological investigations on the remote island of Yap, western Micronesia," 2019

National Geographic Standard Grant (Team Member with advisor Fitzpatrick; HJ2-184R-18), "First colonization of the land of stone money: Archaeological investigations on the remote island of Yap, western Micronesia," 2018

Sigma Xi Grant-in-Aid of Research, "First Colonization of the Land of Stone Money: Archaeological Investigations of the Remote Island of Yap, Western Micronesia," 2018

Special "Opps" Travel and Research Award for travel to attend the Indo-Pacific Prehistory Association meetings in Hue, Vietnam, 2018

First Place, Anthropology, Sigma Xi Student Research Showcase, 2018

Edna English Trust for Archaeological Research summer research award, Edna English Trust for Archaeological Research and the Museum of Natural and Cultural History, 2017

First place, Poster presentation, Graduate Student Research Forum, University of Oregon, "Colonization of the land of stone money: New investigations on the early settlement of Yap, western Caroline Islands," 2017

People's Choice Award winner, Graduate Student Research Forum, University of Oregon, "Colonization of the land of stone money: New investigations on the early settlement of Yap, western Caroline Islands," 2017

Small Professional Grant, Center for Asian and Pacific Studies, 2016

Global Oregon Graduate Research Award, Global Studies Institute, 2016

Small Professional Grant, Center for Asian and Pacific Studies, 2016

Best Poster Presentation for the category "Breaking New Ground in the Sciences: Approaches to reproducibility and data management, shifting paradigms, and innovative research practices", Graduate Research Forum, University of Oregon, "Time is of the Essence: Establishing Chronological Baselines for Archaeological Research in the Florida Keys," 2016

People's Choice Award, Graduate Student Research Forum, University of Oregon, Poster presentation, "Before the clock runs out: Archaeology in the face of erosion on St. Catherines Island, Georgia (USA)," 2015

Small Professional Grant, Center for Asian and Pacific Studies, 2015

American Museum of Natural History grant for fieldwork on Bull Island Hammock, Georgia, 2009

Scholarly and Creative Activity Award, University of West Florida for work on stable isotope analysis of archaeological shell from Bull Island Hammock, Georgia, 2009

Tibor T. Polgar Fellowship, Hudson River Foundation, New York to analyze multibeam bathymetry data from the Hudson River to identify targets of anthropogenic origin, 2003

PUBLICATIONS:

Matthew C. Sanger and Matthew F. Napolitano. Ceramic Analyses. In press. In: *The Late Archaic on St. Catherines Island, Georgia* by Matthew C. Sanger. Anthropological Papers of the American Museum of Natural History, New York.

Matthew C. Sanger, Anna Semon, Ginessa Mahar, Matthew F. Napolitano, and David Hurst Thomas. In press. Shell Arc Excavations. In: *The Late Archaic on St. Catherines Island, Georgia* by Matthew C. Sanger. Anthropological Papers of the American Museum of Natural History, New York.

Matthew C. Sanger, Anna Semon, Ginessa Mahar, Matthew F. Napolitano, and David Hurst Thomas. In press. Plaza Excavations. In: *The Late Archaic on St. Catherines Island, Georgia* by Matthew C. Sanger. Anthropological Papers of the American Museum of Natural History, New York.

Matthew F. Napolitano, Jessica H. Stone, and Robert J. DiNapoli (editors). 2021. *The Archaeology of Island Colonization: Global Approaches to Initial Human Settlement*. Society and Ecology in Island and Coastal Archaeology Series. Gainesville: University Press of Florida.

Matthew F. Napolitano, Robert J. DiNapoli, and Jessica H. Stone. 2021. Introduction: The archaeology of island colonization. In: *The Archaeology of*

Island Colonization: Global Approaches to Initial Human Settlement, Matthew F. Napolitano, Jessica H. Stone, and Robert J. DiNapoli (editors). Society and Ecology in Island and Coastal Archaeology Series. Gainesville: University Press of Florida.

Scott M. Fitzpatrick, Matthew F. Napolitano, and Jessica H. Stone. 2021. What is the most parsimonious explanation for where pre-Columbian Caribbean peoples originated? In: *The Archaeology of Island Colonization: Global Approaches to Initial Human Settlement*, Matthew F. Napolitano, Jessica H. Stone, and Robert J. DiNapoli (editors). Society and Ecology in Island and Coastal Archaeology Series. Gainesville: University Press of Florida.

Robert J. DiNapoli, Scott M. Fitzpatrick, Matthew F. Napolitano, Torben C. Rick, Jessica H. Stone, and Nicholas P. Jew. 2021. Marine reservoir corrections for the Caribbean show high intra- and inter-island variability. *Quaternary Geochronology* 61(101126). doi.org/10.1016/j.quageo.2020.101126.

Matthew F. Napolitano, Robert J. DiNapoli, Jessica H. Stone, Maureece J. Levin, Nicholas P. Jew, Brian G. Lane, John T. O'Connor, and Scott M. Fitzpatrick. 2019. Reevaluating the Pre-Columbian colonization of the Caribbean using chronometric hygiene and Bayesian modeling. *Science Advances* 5(12):eaar7806.

Matthew C. Sanger, Brian D. Padgett, Clark Spenser Larsen, Mark Hill, Gregory D. Lattanzi, Carol Colaninno, Brendan J. Culleton, Douglas J. Kennett, Matthew F. Napolitano, Sébastien Lacombe, Robert J. Speakman, and David Hurst Thomas. 2019. Great Lakes copper and shared mortuary practices on the Atlantic Coast: Implications for long-distance exchange during the Late Archaic. *American Antiquity* 84(4):591-609.

Matthew F. Napolitano, Scott M. Fitzpatrick, Geoffrey R. Clark, and Jessica H. Stone New archaeological research sheds light on Yap's early prehistoric settlement. 2019. *The Journal of Island and Coastal Archaeology* 14(1):101-107.

Matthew C. Sanger, Mark Hill, Gregory Lattanzi, Brian Padgett, Clark Spenser Larsen, Brendan Culleton, Douglas Kennett, Laure Dussubieux, Matthew F. Napolitano, Sébastian Lacombe, and David Hurst Thomas. Early metal use and crematory practices in the American Southeast. 2018. *Proceedings of the National Academy of Sciences* 115(33):E7672-E7679.

Matthew F. Napolitano. Book review: Unearthing the Polynesian Past: Explorations and Adventures of an Island Archaeologist. 2018. *The Journal of Island and Coastal Archaeology* 13(1):153-155.

Jessica H. Stone, Scott M. Fitzpatrick, and Matthew F. Napolitano. 2017. Disproving claims for small-bodied humans in the Palauan archipelago. *Antiquity* 91(360):1546-1560.

Scott M. Fitzpatrick, Victor D. Thompson, Aaron Poteate, Matthew F. Napolitano, and Jon M. Erlandson. 2016. Marginalization of the Margins: The Importance of Smaller Islands in Prehistory. *The Journal of Island and Coastal Archaeology* 11(2):155-170.

Matthew F. Napolitano. 2013. The Role of Small Islands in Foraging Economies of St. Catherines Island. In: *Life among the Tides: Recent Archaeology on the Georgia Bight*, Victor Thompson and David Hurst Thomas (editors and contributors). Anthropological Papers of the American Museum of Natural History 98: 191–210.

Matthew F. Napolitano. 2012. *The Role of Back-barrier Islands in the Native American Economies of St. Catherines Island, Georgia*. Laboratory of Archaeology Series Reports 85, University of Georgia, Athens.

Matthew F. Napolitano, Robert J. DiNapoli, Scott M. Fitzpatrick, Traci Ardren, Victor D. Thompson, Alexander Cherkinsky, and Michelle Lefebvre. New Marine Reservoir Corrections for the Florida Keys and Chronology Building at the Clupper Site, Upper Matecumbe Key. In second review with *Radiocarbon*.

Matthew F. Napolitano, Elliot H. Blair, Laure Dussubieux, and Scott M. Fitzpatrick. Chemical analysis of glass beads in Palau, western Micronesia reveals 19th century inter-island exchange systems in transition. In first review with *Journal of Archaeological Science: Reports*.

Fitzpatrick, Scott M., Maaike S. De Waal, Matthew F. Napolitano, and Philippa Jorissen. Results of preliminary archaeological investigation at Walkers Reserve, St. Andrew, Barbados. In first review with *Barbados Museum and Historical Society*.

Hackenberger, Steve, Scott M. Fitzpatrick, Jessica H. Stone, and Matthew F. Napolitano. Rescue recovery of the earliest known burials from Barbuda, West Indies (ca. 3500-3200 BP). In first review with *The Journal of Island and Coastal Archaeology*.

ACKNOWLEDGEMENTS

I would like to thank a number of people for their support of my research and in my career. I would like to first thank my committee chairperson, Scott M. Fitzpatrick, for his mentorship that has been foundational in my professional development. His support was instrumental to my success as a graduate student and it started with a promise that I would love working in Micronesia. Thank you to my committee members Jon Erlandson, Alison Carter, Geoffrey Clark, and Ryan Jones who provided valuable feedback on my dissertation chapters. Thank you to Madonna Moss, Gyoung-Ah Leee, Aletta Biersack, and Tory Byington, each of whom made significant contributions to my professional development. I am indebted to Leah Frazier and Lisa Clawson for the behind the scenes help in managing grants.

I would also like to thank David Hurst Thomas and Lorann S.A. Pendelton for their unwavering support of me since I was an intern at the American Museum of Natural History. Thank you to my North American Archaeology family Matthew Sanger, Elliot Blair, Rachel Cajigas, Diana Rosenthal, Christina Friberg, Elizabeth Cottrell, Anna Semon, and Ginessa Mahar. No matter where I live and how many islands I work on, St. Catherines Island will always be “the island.”

Thank you to my mother Cathy Napolitano and my brother David Napolitano for their encouragement and support for nearly 15 years of me being a college student. Thank you to the crew: Jasmine Alvarez, Mea Stout, Jessica Carlos, Lisseth Corral. They are support network through all the ups and downs. I already miss the dinners at the house.

My research would not have been possible without support from my collaborators on Yap and Palau. Thank you to Francis Reg, Acting Director of the Yap State Historic

Preservation Office, Chief James Limar (Gilman municipality), Sebastian and Lisa Tamagken, Philip Kentun, and my extended family on Yap: Flo, Yasuyo, Orlando, Kathy, Ginny, Francy, and Debi. Thank you to my Palauan colleagues, especially Sunny Ngirmang, Director of the Palau Historic Preservation Office, Calvin Emesiochel, Deputy of the Historic Preservation Office, Sylvia Kloulubak, Linda Tellames, and the staff of the Palau Bureau of Historic Preservation. Fieldwork in Yap would not have been possible without the help of Kaylien Rungun, Dabei Davis, Paul Gerard, Shelby Medina, Lauren Pratt, Yan Cai, Haden Kingray, Shade Streeter, Hayley May, Michael Young, and Madeleine Getz.

I would like to thank the following for their roles as co-authors and collaborators on this research that has been published or will be published: Scott M. Fitzpatrick, Robert J. DiNapoli, Jessica H. Stone, Geoffrey Clark, John Swogger, Esther Mietes, Amy Gusick, Traci Ardren, Victor D. Thompson, Alexander Cherkinsky, Michelle LeFevbre, Elliot Blair, Laure Dussubieux, Maureece Levin, Brian Lane, John O’Connor, and Nicholas Jew.

Funding for this project was provided by the National Geographic Society (Grant #HJ2-184R-18), the Wenner-Gren Foundation for Anthropological Fieldwork (Grant #9710), the Lewis and Clark Fund for Exploration and Field Research, Sigma Xi, the Edna English Trust for Archaeological Research, University of Oregon Center for Asian and Pacific Studies, and the University of Oregon Global Studies Institute. The work presented in Chapter V was supported, in part, by a National Science Foundation grant to Scott M. Fitzpatrick (SBR-0001531).

TABLE OF CONTENTS

Chapter Page

Chapter Page

Chapter Page

LIST OF FIGURES

LIST OF TABLES

Table Page

CHAPTER I

INTRODUCTION: CHRONOLOGY BUILDING IN ISLAND ENVIRONMENTS

Introduction

Chronology building is a fundamental part of archaeology. Questions related to the timing and duration of events are inextricably connected to larger questions about human activity in the past. Prior to the development of radiocarbon (^{14}C) dating by Willard Libby in the late 1940s, archaeologists primarily relied on relative techniques such as stratigraphic superposition and seriation to discern temporal divisions, however coarse (Libby 1955; see Ihm 2005; Wood 2015). Given its wide applicability and temporal range that covers the last ca. 50 kya, radiocarbon dating is the most frequently used chronometric technique in archaeology. Preserved carbon-based organic materials such as charcoal, shell, and bone are often key sources of information for determining the onset and duration of cultural events that occurred in the past. Limitations of radiocarbon dating have long been identified, yet with advances, including accelerator mass spectrometry (AMS) and applications of Bayesian modeling (see below), archaeologists and other scientists have continued to improve the accuracy and precision of chronologies. This often includes using radiocarbon dating in conjunction with other chronometric sequencing techniques or temporally specific information like stratigraphy. For archaeologists working in island regions, these techniques have allowed archaeologists to engage with a number of complex issues such as the development of seafaring capabilities (Anderson et al. 2010a and papers therein), island colonization (i.e., initial human settlement) (e.g., Church et al. 2013; 2021; Rieth and Hunt 2008; chapter 2), changes in human demography and long-term human-environmental interactions (e.g., Douglass et al. 2019; Prebble and Wilmshurst 2009; Rick et al. 2013), population dispersals (e.g., Bedford and Spriggs 2019; Kirch 1997, 2017; Montenegro et al. 2016; Stone 2020), extinction or extirpation events (e.g., Anderson et al. 2010b; Clark et al. 2013; Louys et al. 2021; Rijsdijk et al. 2011; Rawlence et al. 2016), the development of social complexity (e.g., Dye 2016; Weisler et al. 2006), and monumentality (e.g., DiNapoli et al. 2020; Martinsson-Wallin et al. 2013; McCoy et al. 2016; Sharp et al. 2010), to name a few.

Over the last few decades, island colonization chronologies have been more highly scrutinized and debated given ongoing disagreements over data reliability, taphonomy, analytical approaches, and uncertainties in radiometric techniques, particularly as they relate to marine environments (Napolitano et al. 2021). Most scholars agree that the most parsimonious archaeological identification of colonization sites is restricted to the earliest observable events that are clearly anthropogenic (Lipo et al. 2021: 68). Problems in locating these sites can be difficult, however, given the ephemeral nature of evidence for founding populations. Early sites on islands, many times found on low-lying beaches in close proximity to productive marine resources, are often at risk of erosion and inundation from rising sea levels (Erlandson 2008, 2012). However, not all colonization events are difficult to identify. A notable, but rare example is the colonization of Iceland (*Landnám*), which appears to have been rapid and large-scale, suggesting a high degree of planning, ideological motivation, and a relatively large founding population (Schmid et al. 2018, 2019, 2021). As a result, archaeologists must often look outside the discipline to consider theory-based models and other lines of evidence such as paleoenvironmental, paleoclimate, and paleoshoreline data to reconstruct the conditions under which such colonization ventures took place (e.g., Callaghan 2010; Goodwin et al. 2014; Kayanne et al. 2011; Montenegro et al. 2016).

One key example from the Pacific is the direct dating of foraminifera sand grains under the guise of trying to constrain when humans could have colonized geologically young atolls (Weisler et al. 2012). At issue is determining when atolls were large enough to support life (i.e., having suitable freshwater lenses) and when reef flats were mature and large enough to support human populations. Given that atolls develop from accumulated sediment deposits comprised of biogenetic material (e.g., coral, shell, foraminifera) that were transported not long after death of the animal, dating these materials should be closely related to the time of island development (Weisler et al. 2012). Similar to dating algal bioclasts (see Carson and Peterson 2012), radiocarbon dates from foraminifera must be calibrated and corrected for local marine carbon offsets. Although the dates do not result from anthropogenic activities, they serve as a potential marker for when atolls could have been occupied. In this case, dates from Utrōk Atoll and Maloeap Atoll in the Marshall Islands were used to reconstruct past sea level rise and island development (Weisler et al. 2012). Other recent applications of dating biogenetic material include a case from southeastern ‘Upolu (Sāmoa) to better understand why only one early Lapita settlement site has been found (ca. 2800 BP), which stands out as a curious anomaly compared to other island groups in the region (Cochrane and Rieth 2016; Kane et al. 2017).

To examine chronological issues as they specifically relate to islands, I present four case studies as part of this dissertation in which various techniques are applied to archaeological datasets to improve the accuracy and precision of understanding human activity in the past. By applying a suite of methods, including chronometric hygiene, Bayesian modeling, glass chemical composition analysis, and marine reservoir corrections, I improve upon some of the limitations imposed by radiocarbon dating. These approaches allow me to address both large-scale questions such as the timing of human settlement across the circum-Caribbean and site-specific questions such as when stone money quarrying activity took place in a rockshelter site in Palau, western Micronesia. This chapter first discusses chronometric sequencing techniques commonly using on islands, their potential limitations, and ways that archaeologists can overcome them.

Chronology building using radiocarbon dating

Methodological advances in radiocarbon dating, including the development of high-precision techniques and improved pretreatment protocols, have resulted in higher-precision dates from samples not previously considered suitable. AMS was developed in the 1970s, but it was not until the mid-to-late 1990s when archaeologists began to use the technique more widely. As accessibility increased with more commercial radiocarbon laboratories offering the service and prices decreasing, it ushered in a new era of radiocarbon dating (Spriggs 1991). For example, AMS dating is more precise than “conventional” radiocarbon dating because carbon isotopes are directly measured, allowing for more accurate ion counting and requiring a significantly smaller sample size and often results in more precise dates (i.e., typically smaller standard error ranges of less than 50 years) (Tuniz et al. 1998). A reduction in sample size allows for direct dating of artifacts to be “minimally destructive,” eliminates the need for dating aggregate or bulk samples comprised of multiple specimens, and creates new opportunities for researchers to date new types of materials (e.g., small seeds, foraminifera), many of which are short-lived.

In addition, advances in pretreatment protocols have resulted in a wider array of suitable material for dating (Wood 2015). Conventional dates on human bone are no longer considered acceptable because collagen—the preferred datable material—was not sufficiently purified through pretreatment procedures that isolated specific amino acids. Over the years, radiocarbon and isotopic laboratories have developed new, refined pretreatments to remove contaminants from bone and teeth, which are now widely used (e.g., Brock et al. 2010; Bronk Ramsey et al. 2004; Petchey et al. 2011). This was an important development as insufficient pretreatment methods can result in inaccurate or misleading dates. For example, insufficient pretreatment processing of rat (*Rattus exulans*) bone suggested that human colonization of New Zealand occurred as early as 2000 years ago. As a result, those radiocarbon dates are no longer considered valid and the most recent settlement chronologies for New Zealand now place human arrival much later in time, ca. 750 years ago (Anderson 1996, 2000; Argiriadis et al. 2018; Wilmshurst et al. 2008). Dates produced by the Gakushuin Laboratory in Japan, primarily in the 1980s, are also considered unreliable due to significant errors when compared to dates from other labs (e.g., Blakeslee 1994; Spriggs 1989, 1990). Pretreatment protocols for wood older than 20 kya have also improved in recent decades. Acid-base-wet-oxidation

(ABOX) is an improvement on the acid-base-acid (ABA) pretreatment technique by removing additional contaminants from old charcoal samples (Bird et al. 1999, 2014). This is particularly relevant for studying Pleistocene-age sites and has been routinely used in Australia since its development.

Radiocarbon dating can sometimes be problematic and lead to misinterpretations, especially when the timing of the targeted event approaches the upper or lower limits of radiocarbon dating. Establishing when anatomically modern humans (AMH) arrived in Sahul (present day Australia and New Guinea) has been debated for decades and has far-reaching implications for our understanding of the timing of human dispersals across Eurasia, the development of watercraft technologies, and the role humans may have played in megafaunal extinction events, among others (e.g., Anderson 2018; Barlett et al. 2016; Boivin et al. 2016; Field et al. 2008, 2013; Louys et al. 2021). It is generally accepted that AMH reached Sahul by at least 50 kya (Bulbeck 2007; Allen and O'Connell 2008; Hamm et al. 2016; Tobler et al. 2017), but recent research from the site of Madjedbede in northern Australia suggests that people may have arrived as early as 65 kya (Clarkson et al. 2017; Florin et al. 2020). These latter dates come from a sequence of radiocarbon and optically stimulated luminescence (OSL) dates. Skeptics argue that there is too much uncertainty in the chronological sequence and also point to a paucity of sites between South China and Sahul dating this early (O'Connell et al. 2018).

For decades, archaeologists have understood the potential problems introduced by radiocarbon dating long-lived species or specimens with significant inbuilt age. In the Pacific, there are limited data on the lifespans of mature trees and the potential for the "old wood effect" (Schiffer 1986) or inbuilt age (IA). Some species, like the tamanu tree

(*Calophyllum inophyllum*) are expected to have an IA of at least 250 years (Allen and Wallace 2007). The most effective way to avoid issues with IA is to identify wood or charcoal specimens prior to dating and submit only specimens such as seeds that are short-lived (e.g., Allen 2014; Allen and Huebert 2014; for examples of misleading dates, see Allen and Wallace 2007; Spriggs and Anderson 1993). Nunn and Petchey (2013) echo these results after reevaluating a suite of radiocarbon dates from Viti Levu Island, Fiji, demonstrating an offset of 149 years in unidentified charcoal. Similarly, in a meta-analysis of more than 900 dates from Hawaii Island, Rieth et al. (2011) stressed that radiocarbon dates on charcoal should be identified to taxon and be from short-lived species, defined as 50 years of younger though Allen and Huebert (2014: 261) suggest that "short-lived" should be defined as 10 years or less. Examples of short-lived terrestrial samples include candlenut (*Aleurites moluccana*), coconut (*Cocos nucifera*), and bottlegourd (*Lagenaria siceraria*) (Allen and Huebert 2014: table 2). Relying on short- and medium-lived species for dating has resulted in the occupational sequence on Aitutaki, Cook Islands to be 300 years younger than previously proposed, now dating to ca. 725-520 cal yrs BP (Allen and Huebert 2014; Allen and Wallace 2007; see also Allen 1998; Allen and Morrison 2013; Allen et al. 2017). Beyond the Pacific, archaeologists working in other island regions like the Mediterranean (e.g., Micó 2006) and the North Atlantic (e.g., Schmid et al. 2018) have also demonstrated the importance of selecting short-lived samples from plants or animals for dating.

Radiocarbon dates from shell can also pose potential problems for archaeologists. Similar to the "old wood" problem in which a date could be taken from a wood fragment that is older than when the cultural event occurred (Schiffer 1986), "old shell" from fossils, subfossils, or reused material may also provide misleading results (Rick et al. 2005). Juveniles or short-lived species such as *Atacodea striata*, which only live between 1-3 years, work well for dating and can also be used to reconstruct paleoenvironmental conditions (e.g., Jew and Fitzpatrick 2015). However, when studying temporal trends in environmental conditions, longer-lived species might be preferable (see Dodrill et al. 2018).

Potential problems can also occur when dating bone samples from organisms that have a marine or unknown diet. For example, dating bone from humans who consumed a mixed marine and terrestrial diet must be calibrated differently (Cook et al. 2015). Without knowing the ratio of terrestrial-to-marine dietary contributions, calibrations may introduce an unknown degree of error. One way to address this is to conduct dietary reconstruction using stable isotopes, when possible (Arneborg et al. 1999; Bonsall et al. 2004; Cook et al. 2001, 2002; Lanting and van der Plicht 1998; Schulting and Richards 2002). Alternatively, the $\delta^{13}C$ endpoints of plants and animals can be extrapolated. This approach has been used at the well-known Lapita cemetery site of Teouma on Efate Island, Vanuatu and elsewhere (Petchey et al. 2014, 2015; see also Petchey et al. 2011).

Chronometric hygiene

Unfortunately, building refined chronologies in many regions can be hampered by a lack of critical evaluation of previously published radiocarbon dates. In addition, many “legacy dates” that were run on composite or bulk samples, those that were not corrected for $\delta^{13}C$ fractionation, or others lacking proper pretreatment have likely not produced reliable radiocarbon ages (Hamilton and Krus 2018; Sanchez et al. 2018). In many regions such as the Caribbean, these dates are still routinely incorporated into archaeological chronologies. To address this issue, chronometric hygiene is used to improve the reliability of radiocarbon datasets by evaluating individual dates based on predetermined criteria. Dates deemed unreliable are culled from the database and careful application of stricter criteria then improves confidence that the reported date range is reflective of when human activity occurred. The first formal attempt at chronometric hygiene compared radiocarbon dates from ancient Egypt to dates from Nubia, Palestine, and Mesopotamia (Hassan and Robinson 1987). In the Pacific, Matthew Spriggs (1989) first used the technique to reevaluate the connection between historical linguistics and the spread of agriculture (see also Fitzpatrick 2006; Hunt and Lipo 2006; Petchey et al. 2015; Schmid et al. 2019; Spriggs and Anderson 1993).

The efficacy of chronometric hygiene hinges upon the criteria used to evaluate radiocarbon dates, but there are no standardized criteria. Essentially, most applications of this require: 1) dates from short-lived plants and/or plant or faunal material that lack a significant inbuilt age (e.g., terrestrial bird shell, juvenile shellfish); 2) when possible, charcoal identified to the lowest taxon; 3) dates from bone identified to taxon, thoroughly purified, and dated using AMS; and 4) samples with sufficient provenience information (i.e., not from surface contexts, evidence of archaeological context), and the laboratory name and number (e.g., Wilmshurst et al. 2011; chapters 2 and 4). Unacceptable dates usually lack some component of the above contextual information and include marine shell not identified to taxon or bulk sediment, shell samples containing more than one individual, and charcoal taken from more than one fragment when association cannot be established. One unresolved issue is whether marine shell is a suitable sample material because of problems with inbuilt age and local marine reservoir corrections which are not always well-established (see Hutchinson 2020; Wilmshurst et al. 2011 and reply by Mulrooney et al. 2011).

Despite advantages inherent with using chronometric hygiene, the technique is not without its detractors. Some critiques focus on overly strict criteria that result in valid dates being culled (e.g., Kirch and Ellison 1994). The validity of dates depends on multiple factors including the confidence that the dated sample is unambiguously linked to human activity and full reporting of relevant information so that other scholars can evaluate the data. Failure to adequately report the processing laboratory, provenience, or sample material creates a black box the prevents others from utilizing those data. As detailed in Chapter 2, after applying chronometric hygiene protocols to more than 2400 radiocarbon dates from 55 Caribbean islands, nearly half (46%) were eliminated. Remarkably, 74% of those dates were rejected because of insufficient reporting of provenience, laboratory numbers, sample material, or radiocarbon age. Many of these would have otherwise been considered valid. If more information becomes available, these dates could eventually be incorporated into the database.

Perhaps the most contentious application of chronometric hygiene was by Janet Wilmshurst et al. (2011). In their study, they reassessed more than 1,400 radiocarbon dates from East Polynesia and assigned them into one of three classes. Dates that were assigned a Class 2 or Class 3 rating were expunged. Calculating the summed probability of only the acceptable (i.e., Class 1) dates resulted in significantly shorter and younger settlement histories for many Polynesian islands, including Hawaii, New Zealand, and Rapa Nui (Wilmshurst et al. 2011; see also Hunt and Lipo 2008). As a result of the chronometric hygiene protocol they imposed, their results were sharply criticized by others who argued that their overly strict criteria resulted in otherwise acceptable dates being discarded (Mulrooney et al. 2011). In a rejoinder, Mulrooney et al. (2011) took issue with dates from marine shell being assigned Class 2 or Class 3 and subsequently discarded when there are suitable regional marine reservoir corrections that could have been applied (e.g., Petchey et al. 2009). Further, they argue that calculating summed probabilities with dates as young as 300 years B.P. and not from basal deposits (i.e., after colonization and early settlement) skewed the summed probabilities, resulting in misleadingly young dates.

In a separate study, Hunt and Lipo (2008) argued that relying on an early colonization date for Rapa Nui requires incorporating isolated and spurious dates that do not meet the minimum chronometric hygiene criteria. When these dates are expunged, the colonization estimate for Rapa Nui is ca. AD 1200 rather than AD 400-800 (Hunt and Lipo 2008). While a recent multi-proxy study by Sear et al. (2020) suggests an earlier settlement of the Cook Islands ca. AD 900, this revision to East Polynesia's colonization chronology does highlight the strength of using the chronometric hygiene approach for building accurate chronologies. Taken together, these studies suggest that colonizing ventures into East Polynesia may have been more episodic than previously thought and that more multiproxy research is needed on places like Rapa Nui to look for earlier evidence of human occupation prior to the earliest unambiguous archaeological evidence.

Bayesian modeling

Bayesian statistics are increasingly being used by archaeologists for modeling various temporal phenomena, ranging from individual site chronologies to large-scale regional processes (Bayliss 2009, 2015). They are particularly useful for radiocarbon datasets because they allow the analyst to incorporate prior information such as stratigraphy or other known chronological information into the estimation of probability distributions for groups of radiocarbon dates (Bronk Ramsey 2009a, 2015; see for example Dye 2015; Dye and Buck 2015; Petchey and Nunn 2013; Petchey et al. 2015). The recent proliferation of archaeological studies that use Bayesian statistical models could arguably be called the next revolution in radiocarbon dating (Bayliss 2009, 2015; Hamilton and Krus 2018). The strength of Bayesian modeling is that it provides estimated date ranges for undated archaeological contexts, such as the onset, temporal duration, or end of a phenomenon of interest. Three key parameters of any Bayesian model are the *prior*, the *likelihood*, and the *posterior*. In archaeological applications, the *prior* is information or observations that are inferred before any data are collected or processed (e.g., stratigraphy); the *likelihood* is information obtained from the calibrated radiocarbon date range; and the *posterior* is an estimated calendar date range expressed probabilistically as the highest posterior density region based on the relationship between the prior and likelihood (Bronk Ramsey 2009a). An evaluation of how well the model fits the radiocarbon data is expressed quantitatively as an agreement index, with agreement indices over 60 being the commonly accepted threshold (Bronk Ramsey 2009a).

Recent applications of Bayesian modeling have led to increasingly precise colonization models in various regions, including the Pacific (e.g., Athens et al. 2014;

Burley et al. 2015; DiNapoli et al. 2020; Fitzpatrick and Jew 2018; Lipo et al. 2021; Dye 2012, 2015; Green et al. 2008; Petchey et al. 2015; Rieth and Athens 2019), North Atlantic (Batt et al. 2015; Schmid et al. 2018), and Caribbean (Hanna 2019; Chapter 2).

An example of a study that may have had a different outcome if it had included Bayesian modeling is the aforementioned Wilmshurst et al. (2011) paper on East Polynesian settlement. One of their chronometric hygiene protocols was to discard any date with a large standard error, which was defined as >10% of the radiocarbon age (Wilmshurst et al. 2011: 1819). Such standard errors could apply to many dates obtained with "conventional" radiometric dating techniques prior to the development of AMS. Although these dates are now considered imprecise, the probability ranges for many dates may well be accurate and have been routinely incorporated into studies with successful results (Hamilton and Krus 2018; see Krus et al. 2015; chapter 2), although Glassow (2015) notes that dates with large standard errors can also be spurious. The best way to approach this issue it to redate the original sample, although in many cases this may not be possible (Hamilton and Krus 2018). This is especially important for dates run on human and animal bone as pretreatment methods have dramatically improved the quality of the dates.

Marine reservoir correction

In coastal sites around the world where people often harvested vast quantities of marine resources, shell remains are often the best means for dating archaeological components, especially if there is a paucity of charcoal. Mollusks are also typically more abundant, better preserved, less susceptible to vertical shifting, and easily recoverable compared to other types of samples such as carbonized wood and bone (Hutchinson 2020; D. Thomas 2008:346; K. Thomas 2015). As such, the dating of marine shells has proven to be a critical tool for examining a host of issues, including population movements, settlement history, changing adaptations over time, and many others.

The interaction of deep ocean water depleted in ^{14}C, atmospheric carbon, and dissolved inorganic carbon in surface waters are now known to produce a modeled global reservoir age (R) of ca. 500 years in subtropical oceans (formerly globally calculated at ca. 400 years) according to recently updated calibration curves (Heaton et al. 2020; Reimer et al. 2013; Stuiver et al. 1986). Calibrating marine dates also requires an additional offset to account for local marine reservoir effects (ΔR) that corrects for localized factors such as regional upwelling, seasonal variations in sea surface temperature (SST), changes in ocean circulation, shifting stratification of ocean surface waters, proximity to freshwater outputs, geological substrates containing limestone, and environmental preferences of animals. Not only do local offsets have the potential to influence radiocarbon dates on marine and estuarine shell, but fauna whose diet comprises marine food to some degree will also be influenced (e.g., Carlson and Keegan 2004; Harris and Weisler 2017; Laffoon et al. 2016;). In addition, certain species of shell are susceptible to additional environmental conditions like the hardwater effect which can influence the ^{14}C age of shell (Cherkinsky et al. 2014; McKinnon 1999; Petchey and Clark 2011, 2021; Petchey et al. 2017, 2018). ΔR also often fluctuated over time, which adds another variable to consider when using a ΔR to calibrate archaeological shell (e.g., Druffel et al. 2008; Toth et al. 2017; Kennett et al. 1997).

ΔR can be calculated using multiple approaches, including the use of paired terrestrial-marine samples found in secure, contemporaneous archaeological contexts with proper taxonomic identification; paired $^{234}U/^{230}Th$ and ^{14}C samples on coral; tephra isochrones; or dating known-age, pre-bomb, live-collected shells found in museum collections (e.g., Alves et al. 2018; Ascough et al. 2005; Hadden and Cherkinsky 2015; Hadden and Schwadron 2019; Toth et al. 2017; Yoneda et al. 2000, 2007). The absence of ΔR in some regions is related to the difficulty in locating suitable pre-bomb samples for dating. Atomic bomb testing in the early 1950s artificially increased atmospheric and oceanic ^{14}C levels by nearly 100% (Berger et al. 1966) and it is therefore necessary that samples be live-collected before ca. 1955. Museum collections containing pre-bomb specimens continue to be the most relied upon source and have aided in establishing the ΔR for various regions (e.g., Yoneda et al. 2007; but see Yoneda et al. 2000 for a discussion on the reliability of museum collections).

While archaeologists have long recognized the potential for local offsets to significantly influence the age of marine samples, ΔR corrections are lacking for many islands and coastal regions. As a result, archaeologists sometimes use the closest available ΔR, even if it was developed for a location hundreds of miles away (Hutchinson 2020). This is problematic because ΔR can vary widely within a region and sometimes from one side of an island to another, depending on local hydrology and oceanographic conditions, as is clearly demonstrated by DiNapoli et al. (2021) for the Caribbean. In addition, diet and habitat preference of the dated specimen can influence the ^{14}C age and ΔR. Recently, Hutchinson (2020) pointed out many of the inherent issues with radiocarbon dating archaeological shell without a suitable ΔR, using the Pacific coast of

North America as an example, questioning whether radiocarbon dates should be "reluctantly cast aside" unless fine-grained spatial and temporal ΔRs can be determined. Although the potential problems with dating shell might seem expensive or complicated, there are ways to appropriately address these issues.

In the Pacific, this has been done by analyzing the $^{13}\delta C$ and $^{18}\delta O$ in samples to understand how local conditions may have influenced ^{14}C. For example, depleted $^{13}\delta C$ values may indicate a mollusk's preference for estuarine habitat or terrestrial freshwater runoff, while enriched values may indicate a preference for more productive marine habitats and CO_2 atmospheric absorption in reefs (Keith et al. 1964; Petchey et al. 2013). Depletion of $\delta^{18}O$ also indicates an increase in temperature and less saline water caused by evaporation of ^{16}O (e.g., Emiliani et al. 1966; Epstein and Mayeda 1953; Epstein et al. 1953; Swart et al. 1983). By analyzing ^{14}C, ^{13}C, and ^{18}O together, archaeologists can develop more accurate and species specific ΔR that can account for changes over time and identify potential species that may not be suitable for radiocarbon dating (Kennett et al. 1997; Petchey and Clark 2011, 2021; Petchey et al. 2012, 2013, 2017, 2018).

Beyond radiocarbon dating

Uranium-thorium

Applications of high-precision uranium-thorium dating in archaeology have created a new avenue for developing chronological baselines for site use. This technique measures the decay chain for ^{238}U-^{234}U-^{230}Th and, when calibrated, often has a standard error of less than 10 years, making it more precise than most AMS dates. Ideal samples for dating are coral artifacts and manuports that were live-collected and found in secure archaeological contexts. Common coral artifacts from Oceanic archaeology sites include files or abraders typically made from *Acropora* sp. and ritual offerings of live-collected branch coral (*Pocillopora* sp.). In Hawai‘i, coral abraders were also made from *Porities* sp. that were manufactured from beach rubble and contains an inbuilt age and therefore is not well-suited for dating (Weisler et al. 2006).

A strength of uranium-thorium dating is that, given its high-resolution, it can be used in place of AMS dating when the calibration curves are unreliable. This is particularly useful in Hawai‘i where Polynesian chiefdoms underwent rapid and dramatic culture change, population increase, and environmental change from ca. 500-300 years ago, a period when radiocarbon dating is notoriously unreliable due to the Seuss Effect and stochastic calibration curves (Weisler et al. 2012; see Stuvier and Pearson 1993). Implementation of uranium-thorium has also helped generate a more nuanced understanding of temple construction episodes and has been used to support the argument that Hawai‘i was an emergent archaic state level society (e.g., Kirch 1984, 2017, Kirch and Sharp 2005; Sharp et al. 2010; Weisler et al. 2012).

Elsewhere, uranium-thorium dates on *Acropora* sp. abraders from fresh (i.e., unworn) coral recovered from the site of Nukuleka in the Kingdom of Tonga position this site as the “founding Polynesian site” for West Polynesia (Burley et al. 2012). Uranium-thorium dates support the radiocarbon dates and suggest an early human arrival at Nukuleka, now dated to 2830-2846 cal years BP In Micronesia, uranium-thorium dates have helped to identify the early construction period of Nan Madol, a large megalithic site on Pohnpei (McCoy et al. 2015, 2016). Dates obtained from *Symphyllia* sp. coral used as building material at Leluh, a separate megalithic structure on Kosrae, suggests a slightly younger date of construction (Richards et al. 2015). Taken together, it is understood that the onset of megalithic construction in Micronesia began ~700-600 years ago. Uranium-thorium dating has also been used by archaeologists in the Pacific to develop sea-levels curves as an independent line of evidence for evaluating early human occupation (Allen et al. 2017).

Obsidian hydration

Other techniques like obsidian hydration provide a way to get dates on inorganic material like stone. Obsidian hydration dating is based on the premise that the hydration process—the absorption of moisture into a fresh surface or rim of obsidian—is proportional to the square root of time (Ambrose 1994; Friedman and Smith 1960). Temperature and chemical composition of obsidian have the biggest influence on hydration rates as obsidian will hydrate faster in higher temperatures and certain types of obsidian absorb water faster than others. This technique is suitable for archaeological sites lacking abundant organic material, like the Pamwak rockshelter on Manus Island, Papua New Guinea (Ambrose 1994: 138) or can be used as a way of corroborating radiocarbon data. However, the efficacy of obsidian hydration dating has been limited by a host of issues, including relative humidity, soil chemistry, and establishing the hydration rate constants needed for calibrating dates. Differences in laboratory standards and protocols, including criteria as rudimentary as the power of magnification, an operator’s bias can produce different ages on the same piece of obsidian and has led to frustration among archaeologists in various regions using this technique (e.g., Anovitz et al. 1996; Ridings 1996; Stevenson et al. 1996, 2001).

Over the last two decades, there have been various attempts at improving the precision and accuracy of obsidian hydration dating using new protocols (Liritzis and Laskarsi 2011). Obsidian diffusion dating by secondary ion mass spectrometry (ODDSIMS) purportedly improves upon the shortcomings of "first-wave" obsidian hydration with a more sensitive approach to tracking hydration. Overall, this approach to chronometric sequencing is considered problematic because there are still issues with reproducibility and control of external variables.

In contrast, tephrochronology uses tephra layers, the accumulation of unconsolidated rock debris from a volcanic eruption (i.e., volcanic ash) as chronostratigraphic markers that can be used as a relative dating technique or to refine the accuracy of associated radiocarbon dates (Lowe et al. 2000). More recent volcanic eruptions have been accurately dated using historical accounts or associated dates of known-age derived from tree-rings and radiocarbon dates. Tephra deposits are isochronous because ash deposits generally accumulate for just days or weeks (Lowe et al. 2000; Shane 2000) and therefore can be dated through associated radiocarbon dates or, depending on the age of the eruption, could increase the precision of associated radiocarbon dates or understanding stratigraphic deposits. Other times, OSL dates can be used (Torrence et al. 2004). More recently, researchers advocate incorporating Bayesian statistical modeling on radiocarbon sequences to refine tephrochronographic interpretations (Buck et al. 2003; Petrie and Torrence 2008).

In terms of application, tephrochronology has been used to date one of the largest eruptions in Oceania, that of Witori in West New Britain, Papua New Guinea ca. 3300 years ago. The W-K2 eruption—named for being the second of five major eruptions from

Witori between ca. 5600-1200 BP—devastated the surrounding landscape and created much of the coastal plains that were subsequently utilized by humans (Machida et al. 1996; see Callaghan 2010; Torrence 2008 for a discussion of the impacts of volcanic eruptions on social landscapes). The W-K2 tephra coincide with the appearance of Lapita pottery (Torrence and Swadling 2008).

Another example is the colonization of New Zealand which has been an intensely debated issue for decades. New Zealand was settled as part of the final burst of migration and exploration across East Polynesia, but three different settlement models have been proposed: "early," "intermediate," and "late" (e.g., Lowe et al. 2000: table 1). Early settlement of New Zealand ca. 1950-1450 years ago was suggested on the basis of paleoenvironmental data (Elliot et al. 1995; Kirch 1986; Kirch and Ellison 1994; Sutton 1994; Sutton et al. 2008) and now-discredited radiocarbon dates on rat bones (see Anderson 2000). An "intermediate" settlement has been proposed by Davidson (1984) and suggests a settlement by ca. 1200-1000 BP. The "short" settlement has been proposed by Anderson (1991) and others (e.g., Horrocks and Ogden 1998; Newnham et al. 1998; Wilmshurst 1997; Wilmshurst et al. 1997, 2011) and places human arrival ca. 800-600 BP (Lowe et al. 2000). That much of New Zealand's North Island is covered with tephra provides ideal conditions to better understand stratigraphic sequences and depositional history with regard to human occupation after eruption events (Shane 2000). Lowe et al. (2000) found that a shorter chronology history is supported and that ash layers could help improve precision of the existing radiocarbon record and early human activity on New Zealand. More recent multiproxy studies also support a later settlement (Argiriadis et al. 2018).

Chronometric sequencing using proxy evidence

The use of paleoecological records of human arrival and environmental impact can also be an independent method of identifying colonization and early human settlement (e.g., Athens et al. 2014; Braje et al. 2017; Jacomb et al. 2014; Lawson et al. 2008), but is sometimes used in lieu of direct archaeological data. The first major attempt in the Pacific to identify colonization using paleoenvironmental data was on the island of Mangaia in the Cook Islands (Ellison 1994; Kirch and Ellison 1994; Kirch et al. 1992). Increases in heavy (i.e., macroscopic) charcoal, decreases in forest pollen (indicative of a reduction in tree cover), and increases in *Dicranopteris* fern spores (indicative of increased savanna area) "strongly signal human presence" on the island despite direct archaeological evidence (Kirch and Ellison 1994; Kirch et al. 1992, 1995: 47). Analysis of charcoal sediment from Australia, Indonesia, the Philippines, and Papua New Guinea show increased evidence for burning ca. 53-40 kya and are interpreted as anthropogenic signatures of human arrival in the region (Pope and Terrell 2008), although dates in Australia may extend human presence in Sahul even earlier (Clarkson et al. 2017).

There are multiple approaches to assessing human activity through paleoenvironmental data. The identification of substantial amounts of micro-charcoal entering wetland sediments has been interpreted as evidence of forest clearing through anthropogenic burning. Natural fires from lightning strikes and volcanism can also result in the introduction of low levels of micro-charcoal, particularly after the mid-Holocene when El Niño Southern Oscillation (ENSO) events intensified, but rapid and sustained increase in charcoal production evidences human arrival on many islands (McWethy et al. 2010, 2014; Connor et al. 2012). This landscape change is consistent with what is expected when early colonizing populations establish an agricultural base. Ideally, cores would contain evidence of human-introduced taxa such as giant swamp taro (*Cyrtosperma chamissonis*) or breadfruit (*Artocarpus altilis*), but these are usually lacking.

In some instances, the presence of human-introduced taxa must still be critically evaluated. In Palau, radiocarbon dates of giant swamp taro pollen from paleoenvironmental cores from northeast Babeldaob date to ca. 4300 cal BP (Athens and Ward 2001). However, a lack of archaeological evidence directly associated with the pollen means these data should be treated cautiously for the time being. The date of ca. 4300 BP is also out of range with the timing of the colonization for the rest of western Micronesia (e.g., Clark 2005; Fitzpatrick 2003, Liston 2005; Petchey et al. 2016; Stone 2020; Stone et al. 2017), Remote Oceania (e.g., Rieth and Athens 2019), and the emergence of the Neolithic in Island Southeast Asia.

In the absence of direct evidence for anthropogenically-introduced taxa in sediment cores, it is important to consider equifinality. Fires caused by lightning strikes may also contribute to increased charcoal levels in paleoenvironmental records. Butler (2008) provides several scenarios from New Zealand that could account for widespread burning prior to human arrival (see also Prebble and Wilmshurst 2009). This issue is not unique to the Pacific. In the Caribbean, some scholars have proposed that archaeology is ill-equipped to identify colonization and early settlements on islands (Siegel et al. 2015, 2019), yet these types of arguments are not persuasive without direct proof of human activity or human-introduced pollen (see Caffrey and Horn 2015; Fitzpatrick et al. 2021; Giovas 2018), particularly in a region rife with vulcanism.

Project Overview

This dissertation presents four case studies, each from a different island region, including the Caribbean (Florida Keys, Antilles chain) and Pacific (Palau and Yap) where various methodological approaches have been applied to improve chronologies. Chapter Two uses chronometric hygiene and Bayesian modeling to reevaluate initial human colonization of the Caribbean where human settlement represents the only example in the Americas of peoples colonizing islands that were not visible from surrounding mainland areas or other islands. Unfortunately, many interpretive models have relied on radiocarbon dates that do not meet standard criteria for reporting because they lack critical information or sufficient provenience, often leading to spurious interpretations. After a detailed literature review, 2,484 radiocarbon dates were evaluated and assigned to classes based on chronometric hygiene criteria. Using only the most reliable dates, Bayesian modeled colonization estimates were used to examine patterns of initial settlement. Colonization estimates for 26 islands suggest that: 1) the region was settled in two major population dispersals that likely originated from South America; 2) colonists reached islands in the northern Antilles before the southern islands; and 3) the results support the southward route hypothesis and refute the “stepping-stone model.” This paper was previously published with Robert J. DiNapoli, Jessica H. Stone, Maureece J. Levin, Brian G. Lane, John T. O’Connor, Nicholas P. Jew, and Scott M. Fitzpatrick in *Science Advances* (Napolitano et al. 2019b).

Chapter 3 presents a case study from the Florida Keys where new regional and subregional ΔRs were calculated to improve the reliability of radiocarbon dates from archaeological shell. Results show high variability between islands and shell species, demonstrating the need for an error-weighted pooled mean ΔR as an additional offset from the modeled global average. Broad regional and intra-island variability also demonstrates that using a single value ΔR correction from one nearby location is not recommended. Two ΔRs were used to calibrate the first archaeological radiocarbon dates reported from intact stratigraphic contexts in the Florida Keys. Samples from shell midden deposits at the Clupper site in Upper Matecumbe Key demonstrate the importance of using island- and species-specific ΔR, when possible, to build more accurate site chronologies. This paper was coauthored with Robert J. DiNapoli, Scott M. Fitzpatrick, Traci Ardren, Victor D. Thompson, Alexander Cherkinsky, and Michelle LeFebvre and is presently in its second review with *Radiocarbon*.

Chapter 4 presents a case study from Yap, a group of four small islands in western Micronesia, the initial human settlement of which, is one of the least understood colonization events in Remote Oceania. In contrast to Polynesia where multiple lines of evidence (linguistics, genetics, material culture) provide a coherent narrative of initial occupation, there are major chronological discrepancies for Yap. Potential dates for initial human colonization span more than a millennium and are based on archaeological and paleoenvironmental chronologies. Archaeological data suggest early settlement occurred around 2000 years ago, but paleoenvironmental data hint that settlement may have occurred as early as around 3300 years ago. To help address this issue, we present a suite of 31 new radiocarbon dates from Yap, including the oldest archaeological dates yet reported, and compiled a database of 61 previously published radiocarbon dates (total = 92). Using chronometric hygiene protocols to cull potentially unreliable dates, we then created the first Bayesian modeled colonization estimate for Yap, which produced a modeled estimate of *2450-2165 cal years BP (95.4% HPD)*. The dates presented in this study also provide the first baseline data for understanding sea-level drawdown after around 2500 years ago. This paper is coauthored with Scott M. Fitzpatrick, Geoffrey Clark, Amy E. Gusick, Esther Mietes, Jessica H. Stone, and Robert J. DiNapoli and is being prepared for submission to *Quaternary International*.

Chapter 5 presents a study that uses chemical compositional analysis of glass beads to gain a better understanding of activity at stone money quarry site in Palau, western Micronesia. For centuries, money beads (*udoud*) have played a critical role in cultural and economic exchanges in Palau since they first appeared ca. AD 600-950 from East Java and mainland Southeast Asia. Later, as part of their stone money quarrying activities, visiting Yapese islanders negotiated access to quarry sites and purchased provisions using glass beads, offers of corvée labor, and other exchange valuables. Morphological and chemical composition analyses of 38 glass beads recovered from the Chelechol ra Orrak site reveal that most of the beads were manufactured in Europe, with many originating in Bohemia (present-day Czech Republic) ca. 1830-1850. Many of these beads would have been regarded as *cheldoech*, a category of *udoud* that largely went out of circulation in the 1920s. Although this category of *udoud* could be easily counterfeited and beads from Yap lacked the requisite life histories associated with traditional *udoud*, Palauans accepted them as authentic. However, our research suggests that *cheldoech* may have depreciated in value well before the 1920s and Palauans valued and exchanged this category of *udoud* in new ways, including interment with burials. This paper was co-authored by Elliot H. Blair, Laure Dussubieux, and Scott M. Fitzpatrick and is currently under review with the *Journal of Archaeological Science:*

Reports.

Chapter 6 provides a summary of the case studies presented in this dissertation and outlines a best practices approach to sample selection and reporting radiocarbon dates. I highlight several studies from island regions around the world where overlapping, interdisciplinary datasets allow for a more detailed understanding of the past. Finally, I offer a brief discussion of how these approaches can be used to benefit stakeholder and descendant communities, especially those whose cultural heritage sites are at-risk for erosion, inundation, and destruction due to sea-level rise, commercial development, and climate change. In many regions, archaeologists and stakeholder/descendant communities are racing a rise tide (sensu Erlandson 2008) and archaeologists may not be able to return to these sites in the future. Adhering to the best practices approaches outlined in this dissertation will ensure that archaeological research on islands will result in a more precise and holistic retelling of the past.

CHAPTER II

REEVALUATING HUMAN COLONIZATION OF THE CARIBBEAN USING CHRONOMETRIC HYGIENE AND BAYESIAN MODELING

From: Matthew F. Napolitano, Robert J. DiNapoli, Jessica H. Stone, Maureece J. Levin, Nicholas P. Jew, Brian G. Lane, John T. O'Connor, and Scott M. Fitzpatrick. 2019. Reevaluating human colonization of the Caribbean using chronometric hygiene and Bayesian modeling. *Science Advances* 5(12):eaar7806.

Introduction

Radiocarbon (^{14}C) dating is the most frequently used chronometric technique in archaeology given its wide applicability and temporal range that covers the last ca. 50 kya. Preserved carbon-based organic materials such as charcoal, shell, and bone are often key sources of information for determining the onset and duration of cultural events that occurred in the past. Unfortunately, building refined chronologies in many regions has been hampered by a lack of critical evaluation and application of radiocarbon dating. The Caribbean is no exception in this regard.

Initial human colonization of the insular Caribbean, which comprises more than 2.75 million km^2 of open water, represents one of the most significant, but least understood population dispersals in human history. In archaeology, the term colonization as it applies to initial human settlement of a landscape has not always been readily defined. For the purposes of this paper, we follow other case studies that define colonization as the earliest reliable (i.e., unambiguous) evidence for human arrival to previously uninhabited landmasses (e.g., Anderson 1995; Lipo et al. 2021). What sets the Caribbean apart from the rest of the Americas is that these colonization events are the only instances where ancient Amerindian groups would have crossed hundreds or even thousands of kilometers of open sea using watercraft—likely single-hulled canoes—to reach new islands after losing sight of land, either from surrounding mainland areas or between the islands themselves (Fitzpatrick 2013). However, the onset, tempo, and origin of these movements are still debated (Fitzpatrick 2015; Keegan and Hofman 2017) and persistent problems with how radiocarbon dates are used and reported have plagued Caribbean archaeology. Many published dates lack the necessary information essential to adequately examine potential sources of error (e.g., contamination, poor cultural associations, taphonomic issues, publication of uncorrected marine dates), all of which can greatly influence archaeological interpretation (Fitzpatrick 2006; Keegan 1989, 1994).

This lack of rigor in reporting radiocarbon dates brings into question the temporal efficacy of the region's cultural-historical framework for various phases of settlement and subsequent cultural behaviors. One major outcome has been an ongoing debate regarding how, when, and from where the Caribbean islands were first colonized during both the Archaic (ca. 7000-2500 BP) and Ceramic Ages (beginning ca. 2500 BP) during which groups are thought to have ventured north from somewhere along the South American mainland. This is highlighted in two competing models: 1) the "stepping-stone" model, which suggests a general south-to-north settlement from South America through the Lesser Antilles into the Greater Antilles (Rouse 1986); and 2) the "southward route hypothesis", which proposes that the northern Antilles were settled directly from South

America followed by progressively southward movement(s) into the Lesser Antilles (Figure 2.1) (Fitzpatrick et al. 2010).

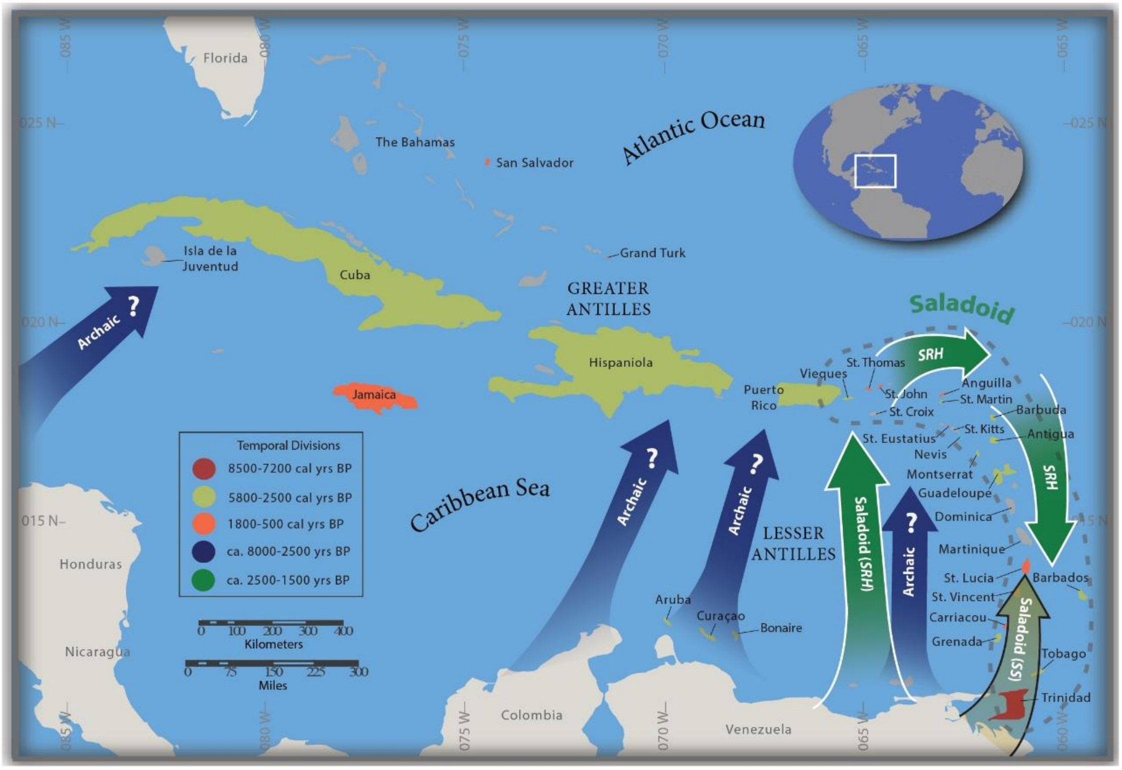

Figure 2.1. Bayesian modeled colonization estimates for 26 Caribbean islands suggest three distinct population dispersals. Colonists reached islands in the northern Antilles bypassing islands in the southern Lesser Antilles, refuting a "stepping stone" pattern. SS denotes the "stepping stone" model and SRH denotes the "southward route hypothesis."

Like other world regions where humans appear to have moved rapidly through landscapes or seascapes, such as the Pacific colonization of Remote Oceania that took place in stages from different points of origin—or in North America where the coastal migration versus the ice-free corridor debate has raged for decades—support for one model or another largely depends on the number, quality, and suitability of radiocarbon dates used in analysis. For the Caribbean, this has relevance not only for establishing the routes of dispersal, but has important implications for understanding other natural and social variables that would have influenced the movement of peoples in watercraft that possibly encouraged (or discouraged) travel, including prevailing oceanographic conditions (e.g., currents, winds), climatic anomalies (e.g., El Niño), technological capabilities, or natural events (e.g., vulcanism) (Fitzpatrick 2013, 2015).

A common approach to improving the efficacy of large radiocarbon inventories in the event of unreliable or inadequately reported dates is to apply a chronometric hygiene protocol (e.g., Fitzpatrick 2006; Hassan and Robinson 1987; Spriggs 1989; Wilmshurst et al. 2011; see Methods and Materials section below). In this selection process, dates are assigned to different reliability classes that effectively cull spurious radiocarbon dates. To resolve many of the issues related to our understanding of the timing and trajectories of Caribbean colonization, we have compiled the largest publicly available database of radiocarbon dates for the region (n = 2,484), applied a chronometric hygiene protocol, and found that only 54% of dates meet current reporting standards. Radiocarbon dates from 55 islands were obtained through an extensive literature review, including available English, Spanish, and French publications, and were bolstered by contacting more than 100 researchers and radiocarbon laboratories to obtain unpublished or under-reported dates and their associated data. These efforts have more than tripled the number of radiocarbon dates used in the last assessment (Fitzpatrick 2006). Bayesian analysis of the resulting acceptable 1,348 dates for 26 Caribbean islands provide the first model-based age estimates for initial human arrival in the Caribbean and help resolve long-standing debates about initial settlement of the region.

Following results of the first chronometric hygiene study done for the Caribbean more than a decade ago (Fitzpatrick 2006), we expect that many islands will have younger colonization estimates after the hygiene protocol is applied, a result also seen in other similar studies (Wilmshurst 2011). As such, we examine competing colonization models using only the most reliable dates from this enhanced database.

Background

For decades, archaeologists have assumed that the Caribbean was settled in multiple stages and directions. The first, termed "Lithic" (Keegan 2000; Rouse 1986; Wilson et al. 1998), was said to originate in Mesoamerica with dispersal into Cuba and through parts of the Greater Antilles ca. 6000-5000 cal yrs BP. The evidence for this is based almost solely on the perceived similarity in stone tools, ephemeral archaeological assemblages, and a limited number of radiocarbon dates (Fitzpatrick 2015; Keegan 2000). The second was a northward movement from South America around the same time or slightly earlier known as the "Archaic". While both the Lithic and Archaic Ages are now generally referred to as the Archaic regardless of supposed origin, it is evident that not all islands in the Antilles were settled during this time for reasons that are still unclear (Fitzpatrick 2015). It was not until thousands of years later, ca. 2500 BP, that an apparently new migratory group known as Saladoid—named after the Saladero site in Venezuela where distinctive pottery was first identified—moved into Puerto Rico and much of Lesser Antilles. However, Saladoid dates are not all contemporaneous and some islands remained uninhabited until much later.

Apart from Trinidad, which today is only 10 km from Venezuela and was connected to the mainland by a land bridge during the Late Pleistocene/Early Holocene (Tankersly et al. 2018), it was recognized that the oldest radiocarbon dates in the region—both for initial colonization (Lithic/Archaic) and later Saladoid populations—

were found in the northern Caribbean (e.g., Cuba, Puerto Rico, St. Martin, Anguilla). Yet there had been no substantive attempt to compile or critically examine larger datasets to investigate this model in more detail until Fitzpatrick's study in 2006.

The long-held stepping-stone model in which groups originating in South America moved northward through the Lesser Antilles and Puerto Rico, and then eventually west into the rest of the Greater Antilles, does not discount a possible earlier migration eastward from Mesoamerica into Cuba (e.g., Rouse 1986). In this model, groups were able to move quickly through the Lesser Antilles because of the close proximity and inter-visibility of islands once peoples reached Grenada. Chronological support for this model would require that the oldest radiocarbon dates be found in the southern Lesser Antilles with those in Puerto Rico occurring later in time (presuming a slight lag as movement progressed northward) or at the very least, contemporaneous if movement was rapid (Fitzpatrick et al. 2010). This has been the prevailing model for decades, in part because of the ubiquity of Saladoid pottery found throughout Puerto Rico and the Lesser Antilles and the assumption that their presence was coeval. Despite some scholars noting a discrepancy in which dates in the northern Antilles were older than those in the south, the SS model had not been explicitly tested, despite evidence that pottery styles were not always reliable chronological markers (Fitzpatrick 2010; Keegan 1994).

The prevailing stepping-stone model was challenged more than two decades ago when computer simulations of seafaring suggested that migrants voyaging from South America would have had the highest probability of initial landfall in the northern Caribbean due to the consistently strong easterly trade winds blowing through the southern Lesser Antilles and ocean currents that flow in the same direction, making eastward progress difficult, if not impossible (Callaghan 2001). Fitzpatrick (2006) was the first to examine this problem using quantitative archaeological data. After reviewing more than 600 radiocarbon dates from 36 Caribbean islands, he came to a similar conclusion, showing that the earliest acceptable dates for Saladoid—as well as earlier Archaic settlement—were found in the northern islands, with first settlement of the southern Lesser Antilles, Bahamas, and Jamaica occurring centuries later after a 'long pause' of around 1,000 years (Fitzpatrick 2006).

As a result of these studies, a second model, termed the southward route hypothesis, suggests that there was instead a direct movement from South America to the northern Caribbean (Puerto Rico and the northern Lesser Antilles) that initially bypassed the southern Lesser Antilles (see Fitzpatrick 2006, 2013; Fitzpatrick et al. 2010; Keegan 2000). This model largely rejects a Mesoamerican origin based on spurious data and assumes that the oldest radiocarbon dates are found in the northern Lesser Antilles and Puerto Rico based on previous chronometric hygiene analysis (Fitzpatrick 2006). Giovas and Fitzpatrick (2014) further explored this scenario using an ideal free distribution framework. Their results indicated that settlement location was likely influenced by the attractiveness of resources, available land, and seafaring limitations. Together, these factors suggested that dispersals were fluctuating and opportunistic, leading to settlement of the largest and most productive islands first, followed by a gradual southward movement ca. 2000 cal yrs BP. Only around 500 years later ca. 1400 cal yrs BP were Jamaica and the Bahamas occupied for the first time (Fig. 1).

More recently, analyses of paleoenvironmental data from lake cores showing an increase in charcoal particle concentrations and changes in vegetation regimes through time have also recently been used as proxy evidence in support of an even earlier settlement of many islands, in some cases thousands of years before the archaeological evidence (Siegel 2018; Siegel et al. 2015, 2019). However, we do not view the results of these paleoenvironmental surveys as convincing evidence of human colonization as the data used in these analyses are often not clearly from cultural contexts, nor do they contain unequivocal anthropogenic signatures such as pollen or other micro- or macrobotanical remains from introduced cultigens (see also Caffrey and Horn 2015; Giovas 2018; Prebble and Wilmshurst 2009). Nonetheless, the argument has revitalized the notion of a northward stepping-stone population movement, one that is much earlier than archaeological records indicate.

Fitzpatrick's previous chronometric hygiene study more than 10 years ago revealed that 87.6% of the radiocarbon dates available at that time were acceptable (Fitzpatrick 2006). In addition, only 21 (58.3%) of the 36 islands examined had any archaeological sites with at least three radiocarbon dates; astonishingly, 127 (73.8%) of the 172 sites in the dataset had three or fewer dates. While this earlier study was relatively thorough, there were still an unknown number of dates unavailable due to issues of accessibility (e.g., contract-based gray literature) or non-reporting. Fortunately, there has been a considerable increase in published radiocarbon dates over the last decade that has substantially expanded the amount of chronological data available. The greater number of radiocarbon dates for the Caribbean now has the potential to significantly improve our understanding of the mode and tempo of prehistoric colonization and a host of other issues, such as measuring human impacts on island ecosystems and reconstructing paleoecological and paleoclimatological conditions through time. However, many of the same problems with radiocarbon dating that were prevalent 13 years ago persist today, including the use of unidentified wood from potentially long-lived taxa, unknown marine reservoir corrections, and/or the inclusion of dates from contexts that are not clearly anthropogenic. Because all of these issues require chronometric hygiene before colonization models can be sufficiently reevaluated, the data presented here comprise the largest compendium of radiocarbon dates yet assembled for the Caribbean, which are used to create the first model-based colonization estimates for 26 islands.

Results

A total of 2,484 radiocarbon dates were compiled from 585 sites on 55 islands (Appendix A). Dates were assigned to one of four classes using chronometric hygiene protocols (see Materials and Methods for criteria). Only 10 dates (0.40%) met criteria for Class 1 (most acceptable dates) and 1,338 (53.9%) dates met the criteria for Class 2, for a total of 1,348 (54.3%) dates that were considered acceptable for Bayesian analysis (see Methods and Materials for a description of class criteria). Seventeen islands (31.0%) with radiocarbon dates did not have any Class 1 or 2 dates (Table 2.1). Despite a tremendous increase in research and publication over the last decade, 433 (74.0%) archaeological sites still have three or fewer radiocarbon dates and 237 (40.5%) sites only have a single date representing an entire site. This is a minimal change compared to the earlier study a decade ago where 164 (39.4%) sites had a single reported radiocarbon date (Fitzpatrick

2006). Surprisingly, only 881 published radiocarbon dates (35.5%) contained $^{13}C/^{12}C$ values ($\delta^{13}C$‰), many of which were only made available after contacting the author or radiocarbon laboratory. These values are important for understanding whether dates were corrected with estimated values, the $\delta^{13}C$‰ in the sample itself, and whether the fractionation was calculated using accelerated mass spectrometry (AMS) or isotope ratio mass spectrometry (IRMS).

Consequently, many islands settled prior to European contact were excluded from our Bayesian modeling, which only utilized Class 1 and 2 dates. For example, while it is clear that Saba has a rich prehistoric record (Hoogland and Hofman 1993), it was not modeled due to the lack of acceptable radiocarbon dates (two Class 2 dates out of 41 total dates) based on our chronometric hygiene criteria. Similarly, our chronometric hygiene protocol and Bayesian analyses show that the modeled colonization estimate for Nevis is *1425-1000 cal yrs BP (95% HPD)*, despite the presence of the Hichmans site, which was identified as an earlier Archaic settlement containing an assemblage similar to other Archaic sites on nearby islands (Davis 2000; Wilson 2006). Our results suggest a more recent settlement chronology for many islands similar to other chronometric hygiene studies (e.g., Wilmshurst et al. 2011) and highlight significant problems with the quality of radiocarbon dates in the region and/or misinterpretation of supposed earlier dates, as many of those previously reported fail to meet criteria for accurate, reliable reporting.

Class 1 dates include those from the Coralie site on Grand Turk (Carlson 1999); a cenote from Manantial de la Aleta on Hispaniola (Conrad et al. 2001); Cave 18 on Mona Island (Samson and Cooper, personal communication); and two sites on Puerto Rico: AR-39 (Carlson and Steadman 2009) and Cag-3 (Turvey et al. 2007) (Table 2.2).

Table 2.1. Results of chronometric hygiene by island.

	Abaco	Andros	Anegada	Anguilla	Antigua	Aruba	Baliceaux
Class 1	—	—	—	—	—	—	—
Class 2	1	—	—	41	18	25	2
Class 3	5	2	1	10	51	19	1
Class 4	—	—	—	—	10	6	—
Total	6	2	1	51	79	50	3

	Barbados	Barubda	Bonaire	Carriacou	Cayman Brac	Crooked Island	Cuba
Class 1	—	—	—	—	—	—	—
Class 2	9	19	16	45	—	4	169
Class 3	13	24	8	1	2	7	31
Class 4	8	6	1	1	8	1	6
Total	30	49	25	47	10	12	206

	Curaçao	Dominica	Eleuthera	Grand Turk	Great Camanoe	Grenada	Guadeloupe
Class 1	—	—	—	3	—	—	—
Class 2	26	5	1	14	—	27	23
Class 3	54	2	4	8	—	8	24
Class 4	6	1	11	1	1	22	16
Total	86	8	16	26	1	57	63

	Guana Island	Hispaniola	Inagua	Isle de la Gonâve	Jamaica	Jost Van Dyke	Long Island
Class 1	—	1	—	—	—	—	—
Class 2	—	43	—	—	10	2	—
Class 3	—	99	5	2	36	—	—
Class 4	1	83	—	—	32	—	7
Total	1	226	5	2	78	2	7

	Los Roques	Marie-Galante	Martinique	Middle Caicos	Mona Island	Montserrat	Mustique
Class 1	—	—	—	—	2	—	—
Class 2	1	—	5	—	2	15	3
Class 3	—	—	5	7	4	5	6
Class 4	3	2	14	1	—	11	—
Total	4	2	24	8	8	31	9

	Nevis	Pine Cay	Providenciales	Puerto Rico	Saba	San Salvador	St. Croix
Class 1	—	—	—	4	—	—	—
Class 2	10	—	—	447	2	14	5
Class 3	12	1	8	35	37	7	1
Class 4	—	—	—	48	2	18	5
Total	22	1	8	534	41	39	11

	St. Eustatius	St. John	St. Kitts	St. Lucia	St. Martin	St. Thomas	St. Vincent
Class 1	—	—	—	—	—	—	—
Class 2	12	14	2	18	81	61	6
Class 3	6	8	—	6	42	16	3
Class 4	1	2	1	9	5	47	—
Total	19	24	3	33	128	124	9

	Tobago	Trinidad	Union Island	Vieques	Water Island	West Caicos
Class 1	—	—	—	—	—	—
Class 2	15	49	—	68	7	—
Class 3	10	15	1	53	—	1
Class 4	2	31	—	—	—	—
Total	27	95	1	121	7	1

One of the three Class 1 radiocarbon dates from the Coralie site is the oldest acceptable date from Grand Turk, but three Class 1 dates are not enough to produce a robust colonization estimate. The remaining Class 1 dates from Hispaniola, Puerto Rico, and Mona Island likely do not date to first colonization of those islands. Taken together, these 10 dates cannot be used to evaluate different colonization models. Therefore, we have chosen to instead generate colonization models using Class 1 dates and the larger, more robust Class 2 data set.

Out of 55 islands, 26 met the criteria for Bayesian modeling. Nearly all Class 2 dates from wood samples were from unidentified taxa or could potentially be long-lived species that can present inbuilt age problems. Therefore, modeled colonization estimates were produced using the *Charcoal_Outlier* analysis in OxCal, which treats radiocarbon dates on unidentified wood as having 100% probability of having as much as 100 years of inbuilt age (Bronk Ramsey 2009b; Dee and Bronk Ramsey 2014; see Materials and Methods). All islands selected for Bayesian modeling possessed nine or more acceptable dates and produced a model agreement (A_{model}) ≥77.9%, and an overall agreement ($A_{overall}$) ≥72.0% (Table 2.3; see Materials and Methods).

Table 2.2. Class 1 dates from the Caribbean.

Island	Site	Sample material	Sample Type	Provenience	Lab number	Conventional Radiocarbon Age (BP)	Error	δ^{13}C (‰)	Reference
Grand Turk	Coralie Site	charcoal: palm	charcoal/charred material	124N 100E FS #35 47-62cmbd, Hearth Feature 5	Beta-80910	1160	60	—	Carlson 1999
Grand Turk	Coralie Site	charcoal: Wild Lime	charcoal/charred material	110N 110E, FS #81, 92-93.5 cmbd, Ash lens Area 10	Beta-80911	1280	60	—	Carlson 1999
Grand Turk	Coralie Site	wood, cf. Bullwood	wood	Mangroves Paddle, peat Layer	Beta-96700	940	60	—	Carlson 1999
Hispaniola	Manantial de la Aleta	gourd	plant material	cenote	Beta-107023	940	30	—	Conrad et al. 2001:14
Mona Island	Cave 18	*Amyris elemifera*	charcoal/charred material	Cave 18	OxA-31209	454	23	-28.2	Samson and Cooper personal communication
Mona Island	Cave 18	*Bursera simaruba*	charcoal/charred material	Cave 18	OxA-31536	682	26	-26.9	Samson and Cooper personal communication
Puerto Rico	AR-39	*Nesotrochis debooyi*	faunal material	Feature 3 (Norther area); EU 17, Level 3	Beta-221018	1340	40	-21.1	Carlson and Steadman 2009
Puerto Rico	Cag-3	*Heteropsomys insulans* (mandible)	faunal material	grave infill	OxA-15142	1219	26	-19.6	Turvey et al. 2007:195
Puerto Rico	Cag-3	*Nesophontes edithae* (mandible)	faunal material	grave infill	OxA-15141	990	24	-19.3	Turvey et al. 2007:195
Puerto Rico	Cueva María de la Cruz	Sapotaceae seed	plant material	Unit 102: 95-113 cm BD	Beta-347456	1910	30	-22.7	Oliver and Rivera Collazo 2015

Table 2.3. Modeled colonization estimates using the 100-yr outlier model. Puerto Rico was modeled with the 100 oldest dates (see Materials and Methods).

Island	Total number of dates	Number of modeled dates	Results			
			68.2 (cal BP)	95.4 (cal BP)	A_{model}	$A_{overall}$
Anguilla	51	41	*1420-1260*	*1510-1180*	77.9	77.1
Antigua	79	18	*3100-2830*	*3385-2750*	103.2	102.9
Aruba	50	25	*3670-3450*	*3895-3295*	100.8	98.1
Barbados	30	9	*4985-4485*	*5885-4440*	100.2	100.1
Barbuda	49	19	*3455-3265*	*3715-3225*	99.6	99.6
Bonaire	25	16	*3715-3470*	*4060-3410*	98.1	98.0
Carriacou	47	45	*1500-1415*	*1550-1385*	81.3	62.8
Cuba	206	169	*5055-4790*	*5360-4675*	85.6	80.4
Curaçao	86	26	*5350-4970*	*5685-4845*	97.8	94.5
Grand Turk	25	17	*1300-1105*	*1435-1025*	82.6	82.4
Grenada	57	27	*2675-2495*	*2835-2430*	95.5	95.7
Guadeloupe	63	24	*3460-3135*	*3770-2635*	104.0	86.8
Hispaniola	226	44	*4385-4040*	*4545-3930*	97.4	96.0
Jamaica	78	10	*980-575*	*1015-475*	108	107.8
Montserrat	31	15	*3045-2780*	*3355-2590*	100.0	100.1
Nevis	22	10	*1220-1050*	*1425-1000*	101.0	101.5
Puerto Rico	518	100	*4580-4390*	*4655-4305*	116.1	105.4
San Salvador	37	14	*1115-935*	*1230-795*	88.9	89.4
St. Eustatius	19	11	*1760-1570*	*1835-1340*	100.5	100.3
St. John	24	14	*1555-1305*	*1670-1095*	100.4	98.5
St. Lucia	33	18	*790-705*	*885-685*	109.6	72.0
St. Martin	105	81	*5155-4995*	*5275-4940*	96.0	93.6
St. Thomas	116	61	*2880-2620*	*2970-2485*	119.7	96.4
Tobago	27	15	*2990-2770*	*3355-2750*	110.5	108.1
Trinidad	95	49	*8160-7900*	*8420-7285*	103.8	100.4
Vieques	121	68	*4065-3855*	*4200-3745*	91.9	93.1

The oldest modeled dates for Cuba (LE-4283) and Vieques (I-16153) had poor agreement indices, but the model agreement (A_{model}) and overall agreement ($A_{overall}$) remained high (Table 2.3, Appendix A). Poor agreement indices were likely caused by a gap between the oldest modeled dates and the rest of the *Phase*, caused by both the chronometric hygiene protocol and a relative dearth of radiocarbon dates dating to early settlement when compared to later periods.

Bayesian modeling of Class 1 and 2 radiocarbon dates from each island dramatically truncates the earliest estimated date of human settlement for six modeled islands. The biggest differences are for Anguilla, Cuba, Hispaniola, and Puerto Rico, which are as much as ca. 2,100-2,300 years younger than previously reported. Although still dating to the Archaic Age (ca. >2500 cal yrs BP), the new colonization estimate places human settlement of Puerto Rico and Hispaniola after other islands such as Cuba, Curaçao, St. Martin, and possibly Barbados.

Discussion

The results of our chronometric hygiene and Bayesian modeling both support and offer new perspectives on the pattern of Pre-Columbian colonization of the Caribbean islands. Trinidad produced the oldest colonization model estimate of *8420-7285 cal yrs BP (95% HPD)*. This is not surprising given that lower sea-levels in the late Pleistocene and early Holocene either connected or placed Trinidad close enough to the South American mainland to allow for settlement that would not have necessarily required sophisticated (or any) watercraft (Tankersly et al. 2018). Consequently, early sites on Trinidad should be considered differently when compared to other islands in the Antilles where long-distance seafaring and more advanced wayfinding skills were likely required to colonize (Fitzpatrick 2015; Keegan 2000). After Trinidad, our results suggest two distinct clusters of colonization estimates modeled from ca. 5800 to 2500 cal yrs BP and 1800-500 cal yrs BP (Figures. 2.1 and 2.2).

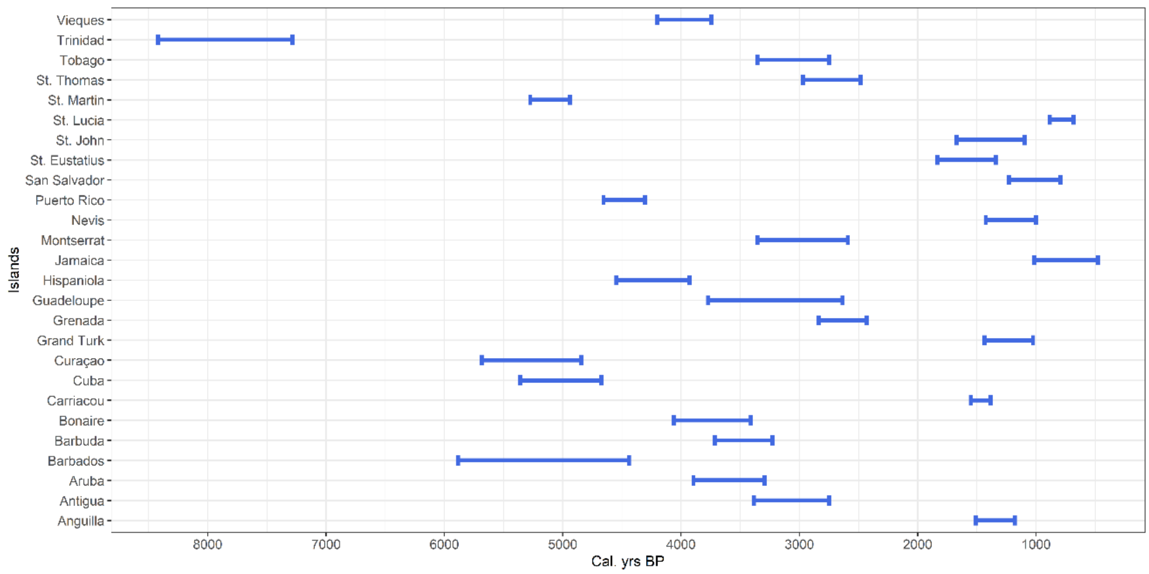

Figure 2.2. Modeled colonization age estimates (95.4% HPD) after chronometric hygiene and Bayesian modeling.

The two clusters fit well with generally accepted cultural divisions in the Caribbean. The first cluster, ca. 5800-2500 cal yrs BP suggests two distinct population dispersals into the Caribbean that span the Archaic and the inception of the Ceramic Age. The earliest settled islands in the first cluster of our model, ca. 5800-2500 cal yrs BP are Cuba, Hispaniola, and Puerto Rico in the Greater Antilles; Gaudeloupe, St. Martin, Vieques, St. Thomas, Barbuda, Antigua, and Montserrat in the northern Lesser Antilles; Barbados and Grenada in the southern Lesser Antilles; and Aruba, Bonaire, and Curaçao, located relatively close (27 km, 88 km, and 65 km, respectively) to mainland South America, along with Tobago, which is 35 km northeast of Trinidad (Fig. 1). Prior to our chronometric hygiene, the oldest reported radiocarbon dates in the Greater Antilles suggested that Archaic populations reached the area as early as ca. 7400 to 6900 cal yrs BP (Fitzpatrick 2006, 2015). Taken together, these results for earliest settlement are consistent with the southward route hypothesis and suggest that some of the largest and most resource-rich islands in the northern Caribbean were settled first (Giovas and

Fitzpatrick 2014). Additionally, our analysis places Curaçao in the earliest cluster, which may be explained by its close proximity to mainland South America. Barbados represents an exception and has long been thought to be an interesting case of anomalous early settlement of the southern Lesser Antilles; our results continue to support this notion (Callaghan 2010; Fitzpatrick 2015).

These results suggest that after the initial settlement of larger islands in the Greater Antilles and some of the smaller islands close to the mainland during the Archaic period, subsequent Ceramic Age settlement focused again on additional smaller islands close to the mainland and several in the northern Lesser Antilles, including those close to islands previously settled during the Archaic. This is not entirely unexpected, for subsequent population dispersals such as Saladoid are likely to have followed similar trajectories, particularly if there had been a long tradition of ancestral groups traveling between the mainland and the Antilles over the course of centuries or even millennia.

The second cluster of colonization estimates fall between ca. 1800 to 500 cal yrs BP, and corresponds to another burst of activity in which several islands in both the northern (St. John, St. Eustatius, Nevis, Anguilla) and southern (St. Lucia, Carriacou) Lesser Antilles were colonized. Settlement of the Bahamian Archipelago also takes place within this time period on Grand Turk and San Salvador. It is possible that the chronologies reflect multiple groups moving in various directions (northern and southern) simultaneously, an expected outcome as trade and exchange relationships quickly accelerated after Saladoid occupation (Keegan and Hofman 2017).

Interestingly, our results place Anguilla within this later cluster, which likely reflects the results of chronometric hygiene and the removal of the oldest dates for the island given that many of these are reported without provenience and had to be excluded from analysis. The previously accepted earliest radiocarbon dates from Anguilla were on *Lobatus* sp. shell tools from surface contexts. However, given the lack of stratigraphic control, those dates were discarded from our analysis. This does not rule out an earlier settlement of the island, but currently well-anchored radiocarbon evidence is lacking.

The research presented here has important implications for examining previous explanatory models of human dispersal into the Caribbean. First, using only the most secure radiocarbon dates, our results do not support an initial northward stepping-stone pattern, once the dominant scenario and resurrected by proponents of recently collected paleoenvironmental data (Siegel et al. 2015). Instead, our results suggest that islands in the Greater Antilles, northern Lesser Antilles, and those located very close to the South American mainland have the earliest reliable radiocarbon dates and modeled chronologies. These data are consistent with the general predictions of island biogeography in which the closest and largest islands are colonized first (Keegan and Diamond 1987; MacArthur and Wilson 1967), as well as the southern route hypothesis whereby the largest and/or most northerly islands in the Antilles were initially colonized with subsequent settlement proceeding southward through the Lesser Antilles. These results are also supported by previous chronometric hygiene analyses (Fitzpatrick 2006), seafaring simulations (Callaghan 2010), fine-grained ceramic analysis (Hanna 2019), and predictions of the ideal free distribution model (Fitzpatrick and Giovas 2014).

Despite consistency with previously proposed models, there are some islands that were settled anomalously later than would be expected, or not at all. For example, Jamaica has no known Archaic or Saladoid settlements, with the earliest sites containing

Ostionoid ceramics (post-ca.1400 BP). Interestingly, the Cayman Islands have no evidence for settlement prior to European arrival, despite several attempts by researchers to locate archaeological sites (Fitzpatrick 2015; Stokes and Keegan 1996). The disparity in these dates could be attributed to environmental factors, such as rough sea conditions that complicated successful navigation to these islands (Callaghan 2008), survey and excavation bias, the obscuring of evidence due to natural and/or cultural processes (e.g., sea level changes, volcanism, commercial development), or other unknown reasons. This demonstrates that the investigation of when and how island regions were colonized must be treated on an island-by-island basis and not generalized across whole regions or archipelagos, as many other variables (e.g., cultural, oceanographic, geologic) likely influenced population dispersals.

Our analysis, while utilizing the most robust chronological dataset yet compiled for the Caribbean, is still limited by incomplete or unpublished information as well as biased survey coverage for various sites and islands. Suggested colonization estimates are presented using only the most secure chronological data available, but doing so led to the exclusion of more than 1,000 radiocarbon dates. The very nature of chronometric hygiene means that in addition to removing erroneous assays, it is likely some dates that were discarded from further analysis are in fact representative of cultural activities during that time, but do not fulfill the imposed criteria (Schmid et al. 2018, 2019). A recent discussion by Dye (2015) suggests that these problems of chronometric hygiene and single-phase Bayesian models can potentially be resolved using two-phase models. Dye (2015) took this approach for examining Pacific Island colonization and modeled the first phase using radiocarbon dates from pre-colonization paleoenvironmental data that directly preceded the first evidence for human colonization. This first phase of the model helps to establish a cut-off point for the second colonization phase of the model, which serves as a step in conjunction with chronometric hygiene in deciding what chronometric data are most reliable. While robust and reliable pre-colonization paleoenvironmental data is currently lacking for most Caribbean islands (cf. Siegel et al. 2015), the use of two-phase Bayesian models in future studies will likely improve the accuracy and precision of our colonization estimates. Another argument is that temporally diagnostic objects such as pottery could be used in the absence of radiocarbon dates to potentially fill in gaps created by chronometric hygiene. However, without the inclusion of additional absolute chronometric techniques (e.g., thermoluminescence, uranium-thorium), pottery and other diagnostic artifacts such as typologically distinct lithics only serve as good chronological markers when they are first anchored by reliable absolute dates. For example, Cedrosan Saladoid pottery, thought only to occur in pre-2000 yr BP sites, has been recovered on some islands like Carriacou where the earliest acceptable dates are much later in time ca. *1550-1375 cal yrs BP (95% HPD)* (with only 4.3% of dates from the island rejected). Indeed, one implication of our revised colonization chronologies is that other long-accepted temporal events in Caribbean culture-history such as subdivisions within pottery typologies during the Ceramic Age (e.g., Troumassoid, Ostionoid) are also likely in need of critical reexamination.

Limitations resulting from the chronometric hygiene protocol could also be circumvented in the future with more detailed reporting and calibration of radiocarbon data, including taxonomic identification of samples, laboratory number, and radiocarbon age. More complete reporting would increase the reliability and thus, the number of acceptable radiocarbon dates (i.e., Class 1 and 2) for many sites and islands across the region, an issue that is still pervasive even in more recent syntheses of data for the Archaic (e.g., Hofman and Antczak 2019). To return to the example of the Hichmans site on Nevis, all nine dates were designated as Class 3 because they were from unidentified marine shell or reported without sufficient provenience (Wilson 2006). If this information was published or made available by the author or the radiocarbon laboratory, then this could possibly aid in refining the colonization estimate for Nevis.

The present database will be further advanced as new information is made available or if part of the original dated samples were saved and redated. A "best practice" approach to managing legacy dates is to rerun the radiocarbon sample if any part of the original sample remains to improve precision. For other samples, if part of the original specimen remains, it may be possible to identify the taxon to avoid issues such as the "old wood" problem. Regardless, the results show spatiotemporal patterns consistent with previous chronometric hygiene studies, seafaring simulations, and theoretical models of population ecology. Our supporting evidence of previously proposed hypotheses is also potentially falsifiable with additional archaeological evidence. For example, recently published radiocarbon dates from Grenada suggest a previously unidentified Archaic component (Hanna 2019). It is quite possible that expanded research programs on other islands could also push back dates of colonization and strengthen existing chronologies.

Conclusions

Interpretations of archaeological sites, assemblages, and other remnants of human behavior hinge on developing temporal frameworks largely built on radiocarbon dates.

This study, which involved compiling the largest dataset of radiocarbon dates from more than 50 islands in the Caribbean, subjecting them to a rigorous chronometric hygiene protocol, and constructing Bayesian models to derive probabilistic colonization estimates, demonstrates that only around half of the currently available radiocarbon dates are acceptable for chronology building. The paltry number of Class 1 dates (n = 10) is especially concerning as these are considered by scholars elsewhere to be the only form of acceptable samples to use in archaeological research (e.g., Wilmshurst et al. 2011). This means that only 0.4% of the available 2,484 radiocarbon dates from the Caribbean would be acceptable if the same standards used in other regions were applied here. That many of the radiocarbon dates in our database were discarded because of a lack of reporting of critical information underscores the importance of transparency when presenting results and conclusions. Given that the average cost of a single radiocarbon date can be hundreds of dollars, it is not unreasonable to assume that this database represents an investment of around $1 million worth of radiocarbon dates that have been largely funded by government agencies, not including the associated costs of obtaining sample material. Many radiocarbon dates are paid for with taxpayer money, and with recent increased scrutiny of publicly funded research in many parts of the world, archaeologists must take responsibility to ensure that their samples are robust, reported in full, and widely available.

Overall, results from chronometric hygiene and Bayesian analysis of acceptable radiocarbon dates suggest direct movement from South America to the northern Caribbean (Cuba, Hispaniola, and Puerto Rico and the northern Lesser Antilles) that initially bypassed the southern Lesser Antilles, with the exception of Barbados and possibly Grenada, which have evidence—albeit limited—for Archaic colonization. The later colonization estimate for islands in the southern Lesser Antilles supports the southern route hypothesis and the predictions of ideal free distribution and does not support the oft-cited and recently reinvigorated stepping-stone model.

Like many of the current models used by Caribbean scholars to explain past human lifeways that hinge on secure and reliable radiocarbon dates, these will require further quantitative testing and closer scrutiny of samples used for developing both local and regional chronologies. The analyses presented in this study can also be used to develop testable hypotheses for predicting when those islands not included in our analysis were colonized. Overall, this study demonstrates the need for increased rigor in the reporting of radiocarbon dates to adequately assess their efficacy and maintain chronological control to ensure that interpretive models are satisfactorily anchored in time and accurately reflect, to the best of our ability, the multitude of cultural behaviors that happened in the past.

Materials and Methods

Chronometric hygiene protocol

A chronometric hygiene protocol was applied to critically assess the reliability of radiocarbon dates in relation to target events. Careful application of stricter criteria improves confidence that the dated radiocarbon event reliably relates to human activity (Fitzpatrick 2006; Hassan and Robinson 1987; Spriggs 1989; Wilmshurst et al. 2011). Dates were placed into four separate classes, the two most acceptable of which were modeled using Bayesian analysis (Bronk Ramsey 2009a). Class 1 dates, which fit the most stringent criteria, are from short-lived terrestrial material (i.e., plant remains or juvenile fauna) identified to taxon, terrestrial animal bone identified to taxon and sampled using AMS, and must include both sufficient provenience information (i.e., not from surface contexts, evidence of secure archaeological context) and the processing laboratory name and number. Class 2 dates include charcoal or charred material not identified to taxon, marine shell identified to taxon, and culturally modified shell (e.g., adzes). These dates must also include sufficient provenience information and the processing laboratory number. Class 3 dates are without some component of the above contextual information and also include marine shell dates not identified to taxon, bulk sediment, or shell samples containing multiple individuals, radiometric dates on human bone apatite, or have a radiocarbon age of 300 years BP or younger. Radiocarbon dates less than 300 years BP were excluded from analysis because the 95% posterior probability would exceed beyond the range of modern age. Unidentified marine shell was given a Class 3 value because some may belong to long-lived species or have other unresolved issues, such as the inbuilt age associated with mobile and/or carnivorous gastropods that ingest older carbon from limestone substrates. Class 4 dates were rejected because they lacked critical information, were not from a secure cultural context, or were originally published as modern dates and rejected by the original author(s). Radiocarbon dates from paleoenvironmental studies were rejected as Class 4 unless a date was collected on anthropogenically introduced plant taxa or were from a secure archaeological context because their association with anthropogenic activity cannot otherwise be demonstrated, and thus may date contexts prior to human arrival.

Terrestrial and marine radiocarbon dates were calibrated using Intcal13 and Marine13, respectively (Bronk Ramsey 2009a, Reimer et al. 2013). Radiocarbon dates on human bone were calibrated using a 50%:50% Intcal13/Marine13 curve with a ± 12% error to account for the mixed marine and terrestrial diet common in the region. This 50%/50% ratio has been applied in other dietary studies (e.g., Hofman et al. 2015), although few published studies address how dietary ratio may influence radiocarbon date calibration. Cook et al. (2015) recommend using an error of 10% when groups are not consuming C4 plants; however, we selected a more conservative error of 12% to account for the presence of C4 plants in prehistoric Caribbean diets. Furthermore, marine-based subsistence strategies varied between individuals, across islands or archipelagos, and through time (Carlson and Keegan 2014; Laffoon et al. 2016). At this stage, it is not possible to develop a template for calibrating human bone other than to say that diets were likely mixed to some degree (Keegan and DeNiro 1988; Krigbaum et al. 2013). Future isotopic research on island-specific and temporally-specific dietary ratios can be used to refine marine and terrestrial ratios for human bones. Additionally, given both the paucity of inter-island and intra-island local marine carbon offsets for the Caribbean (Fitzpatrick 2006, Diaz et al. 2016) no local marine reservoir correction (ΔR) was applied to marine dates, though there should be a concerted effort to obtain these in the future (see DiNapoli et al. 2021). However, we have applied the standard reservoir correction to marine dates.

Bayesian statistical modeling

Bayesian statistical models are increasingly used by archaeologists for modeling a range of temporal phenomena, from individual site chronologies to large-scale regional processes and are particularly useful for radiocarbon datasets because they allow the analyst to incorporate prior information, such as stratigraphy or other known chronological information, into the estimation of probability distributions for groups of radiocarbon dates. A strength of Bayesian models for archaeological studies is their ability to provide estimated date ranges for undated archaeological contexts, such as the onset, temporal duration, or end of a phenomenon of interest. Three key parameters of any Bayesian model are the *prior*, the *likelihood*, and the *posterior*. In archaeological applications, the *prior* is any chronological information or observations that are inferred before any radiocarbon data are collected or processed (e.g., stratigraphy), the *likelihood* is information obtained from the calibrated radiocarbon date range, and the *posterior* is an estimated calendar date range expressed probabilistically as the highest posterior density (HPD) region based on the relationship between the prior and likelihood (Bronk Ramsey 2009a). An evaluation of how well the model fits the radiocarbon data is expressed quantitatively as an agreement index, with agreement indices over 60% being the commonly accepted threshold for a good fit (Bronk Ramsey 2009a).

Following recent Bayesian approaches to island colonization modeling in the Pacific (e.g., Athens et al. 2014; Burley 2015; Rieth and Athens 2019; Dye 2015), here we model the colonization of the Caribbean islands using single-phase Bayesian models in OxCal 4.3.2 (Bronk Ramsey 2009a). This method involves combining radiocarbon dates from multiple strata and sites into a single group with the goal of providing a simple structural framework to estimate the onset of colonization using the collective dates for the island. Using this approach, all uncalibrated conventional radiocarbon age (CRA) dates were grouped into a single unordered *phase* by island (S4) using the *Sequence*, *Boundary*, and *Phase* functions in OxCal. The model then calibrates these dates based on prior information (other early dates in the *Phase*), and the modeled range of the *Boundary* start provides the colonization estimate. Here, we provide both 68% and 95% HPD probabilities for these colonization estimates, and all date ranges were rounded outward to the nearest 5 using Oxcal's round function (Hamilton and Krus 2018).

Nearly all Class 2 dates are from potentially long-lived species or unidentified wood samples and present inbuilt age problems. To address this issue, we treated each of these radiocarbon dates as having a 100% probability of including some amount of inbuilt age using an Exponential Outlier (Charcoal) model using the *Charcoal_Outlier* model (Bronk Ramsey 2009b; Dee and Bronk Ramsey 2014). The prior assumption in this type of model is that the correct age of the modeled events is younger than the unmodeled calibrated dates by some unknown amount of time. Thus, the *Charcoal_Outlier* model is expected to produce somewhat younger age estimates (Dee and Bronk Ramsey 2014). We selected a 100-year outlier model because although Caribbean peoples were likely using dry scrub forest taxa, many of which were slow-growth species, use of these trees for fuelwood likely involved coppicing which would have sustained forests while providing younger limbs for anthropogenic use. Commonly recovered tree species include lignum-vitae (*Guaiacum* sp.), buttonwood (*Conocarpus erectus*), caper tree (*Capparis* sp.), strong bark (*Bourreria* sp.), wild lime (*Zanthoxylum* *fagara*), and mangrove (Newsom and Wing 2004). Given this ethnobotanical information, we elected to use a 100-year outlier model.

Sensitivity analyses

A large proportion of our dataset is composed of radiocarbon dates on unidentified wood and wood charcoal that likely have unknown inbuilt ages. Thus, the modeled date estimates derived from these samples may also be too old. To address this, we modeled each island with unidentified wood samples in three ways: 1) as a simple single-phase models with no additional parameters; 2) treating each radiocarbon date as having 100% probability of having between 1 and 100 years of inbuilt age using a Charcoal_Outlier model; and 3) treating each radiocarbon date as having 100% probability of having between 1 and 1000 years inbuilt age using a Charcoal_Outlier model (Dee and Bronk Ramsey 2014) (S4; see supplementary text). Assuming a 100% probability of samples having inbuilt age is intentionally conservative as not all samples may have significant inbuilt age.

In another set of sensitivity analyses, Cuba was modeled with and without legacy dates—radiocarbon dates with large standard errors (e.g., >100 years)—because, although imprecise, these samples likely still provide an accurate measurement of the target event when derived from secure archaeological contexts. Bayesian modeling accounts for imprecision of legacy dates and can still produce acceptable models (Hamilton and Krus 2018). To test the efficacy of incorporating legacy dates, we modeled Cuba with and without legacy dates.

The third set of sensitivity analyses was to test how the model for Puerto Rico improves when modeled with fewer radiocarbon dates. Modeling all 445 radiocarbon dates does not produce an acceptable model, but the model agreement increases when fewer dates are modeled (S5, S6; supplementary text). Additionally, the oldest radiocarbon date in the *Phase* does not have an acceptable agreement index until it is only modeled with 100 radiocarbon dates.

Lastly, we tested how islands with many younger dates potentially skew the models and produce younger colonization estimates. To test this, we modeled Trinidad and Puerto Rico using the *Tau Boundary* function in OxCal, which exponentially weights radiocarbon dates at one end of the grouping.

CHAPTER III

NEW MARINE RESERVOIR CORRECTIONS FOR THE FLORIDA KEYS AND CHRONOLOGY BUILDING AT THE CLUPPER SITE, UPPER MATECUMBE KEY

From: Matthew F. Napolitano, Robert J. DiNapoli, Scott M. Fitzpatrick, Traci Ardren, Victor D. Thompson, Alexander Cherkinsky, and Michelle LeFebvre. New Marine Reservoir Corrections for the Florida Keys and Chronology Building at the Clupper Site, Upper Matecumbe Key. In second review with *Radiocarbon*.

Introduction

In coastal sites around the world, where people often harvested vast quantities of marine species, shells are a common and readily available material for dating archaeological deposits, particularly if archaeobotanical remains (e.g., carbonized wood, nuts, seeds) are lacking. Marine shells are typically more abundant, better preserved, less susceptible to vertical shifting, and easily recoverable compared to other types of samples such as carbonized wood (Thomas 2008:346). As such, the dating of marine shells has proven to be a critical tool for examining a host of issues, including population movements, settlement histories, long-term changes in human-environment interactions, paleoenvironmental conditions, and many others (e.g., Culleton et al. 2006; DiNapoli et al. 2021; Dye 1994; Erlandson and Moss 1999; Kennett et al. 1997; Marquardt et al.

2020; Petchey 2009; Petchey and Clark 2011, 2021; Petchey et al. 2017, 2018; Thompson and Krus 2018).

Radiocarbon dates from marine organisms, however, can pose potential problems for archaeologists. The interaction of deep ocean water depleted in ^{14}C, atmospheric carbon, and dissolved inorganic carbon in surface waters are now known to produce a modeled global reservoir age (R) of ca. 500 years in subtropical oceans (formerly globally calculated at ca. 400 years) according to recently updated calibration curves (Heaton et al. 2020; Reimer et al. 2013; Stuiver et al. 1986). Calibrating marine dates also requires an additional offset to account for local marine reservoir effects (ΔR) that corrects for localized factors such as regional upwelling, seasonal variations in sea surface temperature (SST), changes in ocean circulation, shifting stratification of ocean surface waters, proximity to freshwater outputs, geological substrates containing limestone, and environmental preferences of animals. In addition, certain species of shell are susceptible to additional environmental conditions like the hardwater effect which can influence the ^{14}C age of shell (Cherkinsky et al. 2014; McKinnon 1999; Petchey and Clark 2011, 2021; Petchey et al. 2017, 2018). These offsets can vary dramatically within the same region—sometimes by hundreds of years on the same island—and can shift dramatically over time (e.g., DiNapoli et al. 2021; Druffel et al. 2008; Hutchinson 2020; Kuzmin et al. 2007; Petchey and Clark 2021; Petchey and Schmid 2020; Toth et al. 2017). Calculating a ΔR requires either paired terrestrial-shell samples found in secure, contemporaneous archaeological contexts with proper taxonomic identification, paired $^{234}U/^{230}Th$ and ^{14}C samples on coral; tephra isochrones; or known-age, pre-bomb, live-collected shells found in museum collections (e.g., Alves et al. 2018; Ascough et al.

2005; Hadden and Cherkinsky 2015; Hadden and Schwadron 2019; Yoneda et al. 2000, 2007).

While archaeologists have long recognized the potential for local offsets to significantly influence the age of marine samples, there is a distinct lack of ΔR corrections for many islands and coastal regions. This is gradually improving, but many areas have no or few corrections, which limits more accurate chronology building in archaeology and geosciences (DiNapoli et al. 2021; Rick et al. 2012; Petchey and Schmid 2020; Thomas 2008; Thomas et al. 2013). A common approach for calculating ΔR is to obtain radiocarbon determinations on known-age, pre-atomic testing marine shells. Because atomic bomb testing in the late 1950s and 1960s artificially increased atmospheric ^{14}C levels by nearly 100%, it is necessary that samples be live-collected prior to these events (Berger et al. 1966; Hua and Berbetti 2004).

The absence of ΔR in some regions is related to the difficulty in locating suitable live-collected pre-bomb samples for dating that were often collected by naturalists in the eighteenth and nineteenth centuries. As such, museum collections containing pre-bomb specimens continue to be the most relied upon source and have aided significantly in establishing the ΔR for various regions (e.g., DiNapoli et al. 2021; O'Connor et al. 2010; Yoneda et al. 2007; but see Petchey 2009; Ulm 2006; and Yoneda et al. 2000 for discussions on the reliability of museum collections).

One region that currently suffers from a lack of high-resolution locality-specific ΔRs is the circum-Caribbean Basin and the Gulf Coast of the United States. There are 241 ΔR values from areas adjacent to the Florida Keys region, including northwest Cuba, the western tropical Atlantic, the western Gulf of Mexico, and southwestern peninsular

Florida, calculated from pre-bomb shell or paired ^{14}C-$^{234}U/^{230}Th$ dates on coral (Broecker and Olson 1961; Diaz et al. 2017; DiNapoli et al. 2021; Druffel 1982, 1997; Druffel and Linick 1978; Hadden and Cherkinsky 2015, 2017; Hadden and Schwadron 2019; Lighty et al. 1982; Toth et al. 2017; http://calib.qub.ac.uk/marine/). These studies have provided an important baseline to investigate the ΔR on marine shell from nearshore and open ocean environments. However, ΔR values recently updated for the Marine20 calibration curve result in a more negative marine reservoir age and greater uncertainty than the Marine13 curve until ca. 11,600 years ago (Heaton et al. 2020). Further, ΔR may vary spatially and temporally by species, the influence of oceanographic currents, geological (limestone) substrates, and freshwater outputs. In a region as oceanographically complex as the Florida Keys Reef Tract, we must assess whether there are significant differences between islands and island regions. With the development of a new archaeological project initiated by three of the authors (TA, VDT, and SMF) at the Clupper site (8MO17) on Upper Matecumbe Key, one of the primary goals has been to establish a baseline chronology of midden deposits in these islands as there are currently no published radiocarbon dates from stratigraphically intact archaeological deposits anywhere in the Florida Keys. Given the region's complex of currents, limestone substrate, and susceptibility to terrestrial runoff, the dating of marine shell requires understanding variations in ΔR, especially in the general absence of carbonized wood and other terrestrial samples (Ardren et al. 2019).

In this paper, we radiocarbon date 10 historically-collected marine shells from the Florida Keys and combine them with previously published ΔRs to produce error weighted pool mean ΔRs for three islands, nearshore and open ocean environments, and six environmental regions. In addition to ^{14}C, we compare $\delta^{13}C$ and $\delta^{18}O$ isotope values to regional baseline data to infer habitat preference, overall marine productivity, water temperature, and salinity (see Culleton et al. 2006; Petchey 2009; Petchey and Clark 2011; Petchey et al. 2008a, 2008b, 2013, 2017, 2018). We then apply these ΔRs to radiocarbon dates on marine shell from the Clupper Site on Upper Matecumbe Key. Using stratigraphically associated shell and terrestrial dates, we are able to evaluate the accuracy of our ΔRs. We first provide an environmental and historical overview for the area, and discuss new research focused on investigating the region's early inhabitants. We then describe the samples used to determine the ΔR corrections and contextualize the results based on geographical distribution. Overall, our study illustrates the importance of examining variation in ΔR across an expansive chain of islands in an oceanographically complex region.

Environmental and archaeological background

Environmental background

The Florida Keys, and the associated Florida Keys Reef Tract, are an archipelago consisting of more than 1700 low-lying limestone islands on a shallow and narrow section of the continental shelf off the southern tip of Florida. The region can be divided into six subregions based on ecology, geology, and hydrology: Biscayne National Park, the Upper Keys, the Middle Keys, Lower Keys, Marquesas, and Dry Tortugas National Park (Toth et al. 2017) (Figure 3.1). The latter two are considered open-ocean environments, whereas the remaining four subregions are nearshore and influenced by peninsular Florida hydrology (Toth et al. 2017). The Upper Keys refer to the area from

Key Largo to Lower Matecumbe Key, and Middle Keys refer to Long Key to Boot Key and are both situated between the western tropical Atlantic and Florida Bay. To the east is a narrow shelf that drops sharply into the Atlantic Ocean. The Lower Keys stretch from Big Pine Key to Key West and open to the Gulf of Mexico.

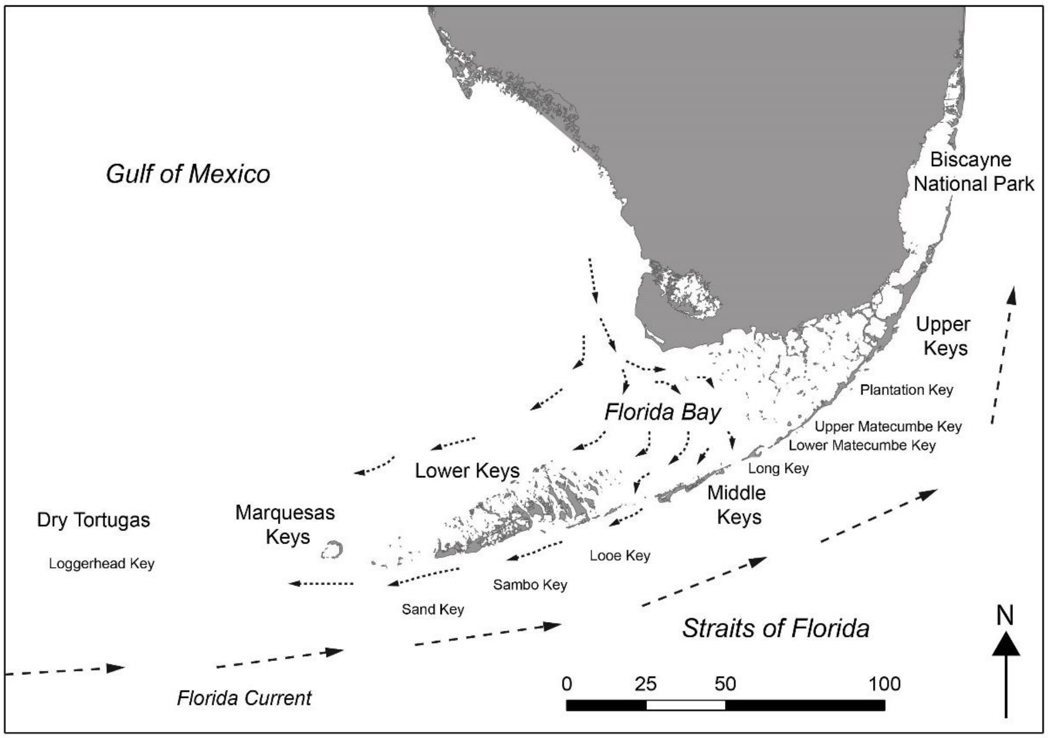

Figure 3.1. The Florida Keys with regional boundaries, sample sites, and flow regimes.

The islands from Key Largo to Big Pine Key stretch in a closely-clustered north-south orientation and are made up of coral reef rock known as Key Largo Limestone (Hoffmeister and Multer 1968). The islands from Newfound Harbor Keys to Key West lie in an east-west direction and are made up of oolitic Miami Limestone (Hoffmeister and Multer 1968). The Keys in general are sandy deposits overlying Key Largo Limestone and subject to a mix of tidal energy from the Gulf of Mexico and the Florida Straits (Shinn et al. 1977). Limestone in a restricted environment like an enclosed lagoon has the potential to produce a hardwater effect as the water travels through openings in the limestone and may influence the radiocarbon age of some shells, although the presence of limestone is not the only predictor of the hardwater effect (McKinnon 1999; Petchey et al. 2008a, 2008b, 2018).

The region has also been subjected to intensive commercial development and tourism. Prior to these activities, the Florida Keys were essentially an estuarine environment with access to open water and unconsolidated shorelines (Ardren et al. 2016, 2019). In addition to commercial development, the islands have experienced rising sea levels over the past 6,000 years, perhaps as much as 30 cm since AD 1850 (Maul and Martin 1993).

Oceanography and hydrology

The Florida Keys region is defined by complex oceanography and hydrology. Florida Bay is a ca. 1550 km^2 triangular, shallow estuary bounded by peninsular Florida and the Upper Keys and contains a number of “mud keys” that comprise muddy carbonate sediments and lack Pleistocene substrate (Enos and Perkins 1979:61). The area was flooded ca. 8,000 years ago by rising sea-levels and receives freshwater input from Shark River Slough and Taylor Slough (Lidz and Shinn 1991; Nuttle et al. 2000). Given its limited circulation and shallowness, temperature, salinity, and nutrients vary widely (see Toth et al. 2017). The Straits of Florida (the passage between the Keys and Cuba), flow to the east and north and the Florida Bay is located to the west. The Florida Current, considered part of the Gulf Stream system, begins at the Straits of Florida, receives water from the Caribbean Sea via the Yucatan Current and Loop Current, and exhibits considerable seasonal and interannual fluctuation in mean water transport (Lee et al. 1996; Schott et al. 1988; https://oceancurrents.rsmas.miami.edu/caribbean/florida.html). The area off the Lower Keys is subject to large, slow moving cyclonic gyres that contribute to water-column mixing and upwelling (Toth et al. 2017). The Upper Keys receive brief, but high-frequency periods of upwelling due to the Florida Current flowing so close to the reef system (Toth et al. 2017). Tidal passages between the Middle Keys are wider than in the Upper Keys, so there is more mixing of the Gulf of Mexico and the Florida Currents in the Middle Keys reef system than in the Upper Keys (Enos and Perkins 1979; Lee and Williams 1999; Toth et al. 2017).

Chronologies and traditions

Culturally, much of our understanding of native groups who lived in the Florida Keys derive from Spanish accounts written during the sixteenth century. Inhabitants here were described as a distinct group who traded and shared cultural traditions with the Calusa of southwestern Florida and the Tequesta of Miami and were at different times and degrees variously allied to, and paid tribute to, these groups (Hann 1991; Thompson et al. 2018). Defined as persistent foragers, their diet primarily consisted of marine foods, including fish and shellfish and they were well adapted to traveling by canoe to fish in nearby deep waters (Ardren et al. 2018a). Sixteenth century documents reinforce the archaeological record and state that the main food of the Keys inhabitants was fish, turtles, and shellfish, some terrestrial mammals, as well as marine mammals such as whales and seals, the latter reserved for higher status individuals (Worth 2014:199-200).

Population estimates for some of the named groups of the Keys, such as Guarugunbe, number as much as a 1000 (Worth 2014). Given this population density and the limited availability of settlement locations with access to key resources, it appears that many sites in the region were occupied over several archaeologically defined periods. However, the ceramic series and assemblages themselves are based, in part, on radiocarbon dates derived from shell (Griffin 1988:232), which potentially makes the dates for these series problematic and underscores the importance of calculating reliable regional reservoir corrections to establish accurate and precise chronologies. This ceramic chronology only provides a rough guide to the chronology and settlement history of these sites, highlighting the need for better developed chronologies based on radiocarbon dating that is not reliant on static culture histories.

As a result of the issues pointed out above, archaeologists do not have a detailed understanding of the occupational history of these sites and how they fit into the larger social geography of the South Florida landscape. Given the diet of the Keys inhabitants there are few animal remains that could be radiocarbon dated, save for deer, which would not require some form of marine reservoir correction.

To illustrate how the variability in ΔR impacts the interpretation of archaeological radiocarbon dates, we calibrated the first radiocarbon dates from secure archaeological contexts in the Florida Keys. The Clupper site (8MO17) covers a large (ca. 85 × 52 m) area with extensive midden deposits that was first excavated in the 1940s and again more recently in 2014 and 2015 as part of the Matecumbe Chiefdom Project. Ceramics recovered from the site suggest that deposits date to multiple cultural periods, including Glades IIa (AD 700-900), IIb (AD 900-1000), IIc (AD 1000-1200), IIIa (AD 1200-1400), and IIIb (AD 1400-1510), although the ceramic chronology in the Keys is not as well refined as it is in southern peninsular Florida (Ardren et al. 2018a). The Glades ceramic series was developed from stratigraphic excavations in the Everglades, Calusa area, and Keys early in the twentieth century and first tied to carbon dates from the Everglades in the 1980's (Goggin 1944; Griffin 2002).

Methods

Modern samples

In this study, we calculated a suite of marine reservoir corrections from live-collected, known-age, pre-bomb bivalves. Ten samples were provided by the Department of Invertebrate Zoology at the Smithsonian National Museum of Natural History (SNMNH), Washington D.C. We sampled *Argopecten gibbus Euvola* cf. *papyraceum* (formerly *Amusium papyraceum)*, *Caribachlamys sentis* (formerly *Chlamys ornata sentis*), *Caribachlamys munda* (formerly *Chlamys munda*), and *Brachtechlamys antillarum* (formerly *Decatopallium* (*Scalaris*) *antillarum*), all of which are species from the Pectinidae family (scallops) (Waller 1991, 1993). Preference was given to suspension feeding bivalves that mostly consume plankton. Understanding the animal's feeding strategy is important because variation in feeding strategies can result in differences in ^{14}C dates as a result of differential carbon intake (Petchey et al. 2013).

A. gibbus is a facultatively mobile, epibiotic suspension feeder that lives in benthic zones and seagrass beds on soft substrate with a lifespan of up to ca. 24 months (Blake and Shumway 2006; Turgeon et al. 2009). *C. sentis* and *C. ornata* are epibiotic, stationary suspension feeders that live in benthic zones on hard substrate (Turgeon et al.

2009; Waller 1993). *B. antillarum* is a benthic, epibiotic animal that lives on hard substrate in seagrass beds (Turgeon et al. 2009). With the exception of *C. ornata*, which is found only in shallow depths, sampled species live in both shallow (<35 m) and deep (>35 m) waters (Bieler and Mikkelsen 2004), although the mollusks in this study were collected from shallow depths. According to museum records, all samples were live-collected between 1885-1954.

Ten samples were pretreated and processed at the University of Oregon Island and Coastal Archaeology Laboratory (ICAL) and submitted to DirectAMS for accelerator mass spectrometry (AMS) dating (see http://www.directams.com/publications-methods-and-other-references). Samples were prepared in a 10% HCl "leach" to remove 10-25% of surface material potentially subject to recrystallization and contamination, then 3 mg of shell was drilled from each specimen using a Sherline micromill 5410 and a carbide drill bit. Shells were sampled across multiple growth bands to avoid dating intra-growth band radiocarbon variability (Culleton et al. 2006). The shell samples derive from seven islands: Lower Matecumbe Key (n=1), Looe Key (n=1), Key West (n=1), Sambo Key (n=1) (Lower Keys); Loggerhead Key (n=1), Plantation Key (n=2) and Sand Key (n=1) (Upper Keys). Another six AMS dates were run on shells from Plantation Key, Lower Matecumbe Key, Long Key, Sambo Key, and Loggerhead Key at the Center for Isotopic Analysis at the University of Georgia (UGAMS). The powdered shell samples from the University of Oregon ICAL were pumped out overnight and treated with 100% phosphoric acid to recover CO_2 for analysis. The resulting carbon dioxide was cryogenically purified from the other reaction products and catalytically converted to graphite using the method of Cherkinsky et al. (2010).

$\delta^{13}C$ and $\delta^{18}O$ values for all samples were calculated using IRMS at UGAMS to compare against regional baseline values of 1.6‰ (Tagliabue and Bopp 2008) and 1.4‰ (LeGrande and Schmidt 2006), respectively. Depletion of $\delta^{13}C$ and $\delta^{18}O$ is often an indication of freshwater or terrestrial input while enriched values indicate increased marine productivity and CO_2 atmospheric absorption in reefs (Keith et al. 1964; Petchey et al. 2013). Depletion of $\delta^{18}O$ also indicates an increase in temperature and less saline water caused by evaporation of ^{16}O (e.g., Emiliani et al. 1966; Epstein and Mayeda 1953; Epstein et al. 1953; Swart et al. 1983).

A database of existing ΔRs was built using the 14CHRONO Marine Reservoir Database. One additional study by Toth et al. (2017) not in 14CHRONO because it used paired ^{14}C/uranium-thorium samples collected from natural coral was added to the database and updated for Marine20 ΔR values using the CALIB *deltar* application and presented with a 68% confidence range (Reimer and Reimer 2017; Stuiver et al. 2020; http://calib.org/JS/JSdeltar20/).

For known age shells, ΔR was calculated using the following (after Stuiver et al. 1986):

$$\Delta R = P - Q$$

where P is the measured ^{14}C age of a known-age marine sample and Q is the expected marine model age based on the Marine20 calibration curve (Heaton et al. 2020). For known-age samples, the uncertainty for an individual ΔR, σ_i, is the uncertainty of P (Reimer and Reimer 2017). For islands with more than one date (Plantation Key, Lower

Matecumbe Key, and Loggerhead Key), we calculated the weighted average. Using the ΔR values and previously published data, we then calculated error-weighted pooled means for the six regions (Biscayne National Park, Upper Keys, Middle Keys, Lower Keys, Marquesas, and Dry Tortugas National Park) as well as a second comparison of nearshore versus open-ocean (sensu Toth et al. 2017). Because we were unable to obtain live-collected pre-bomb shells from Upper Matecumbe Key to compare to archaeological radiocarbon determinations, we calculated a weighted mean ΔR for Plantation Key and Lower Matecumbe Key, which are the islands that bound Upper Matecumbe Key directly to the north and south. We calculated the error-weighted pooled mean, ΔR_μ, (following Stuiver et al. 1986), by:

$$\Delta R_\mu = \frac{\sum_i \frac{\Delta R_i}{\sigma_i^2}}{\sum_i \frac{1}{\sigma_i^2}}$$

and the weighted uncertainty,

$$\sigma_\mu = \sqrt{\frac{1}{\sum_i \frac{1}{\sigma_i^2}}}$$

Following recent applications (e.g., Couthard et al. 2010; DiNapoli et al. 2021; Mangerud et al. 2006; Petchey et al. 2008), we statistically evaluate the internal variability in ΔR_μ

using a χ^2 test with critical value α=0.05. If the normalized χ^2 value is greater than 1, i.e., $\frac{\chi^2}{n-1} > 1$, then additional uncertainty is added to σ_μ to give the total uncertainty, S_{total}, or:

$$S_{total} = \sqrt{\sigma_\mu{}^2 + \sqrt{\sigma_{\Delta R}^2 - (\sigma_\mu * \sqrt{n})^2}}$$

Where *n* is the number of samples, $\sigma_\mu * \sqrt{n}$ is the measurement variance, and $\sigma_{\Delta R}^2$ is the total population ΔR variance. Data files and R code necessary to reproduce these analyses are available in the supplementary material files 1-3.

Archaeological shell

AMS dates on seven archaeological shells and three deer bones from the Clupper site were processed at the DirectAMS Laboratory, UGAMS, and Beta Analytic (https://www.radiocarbon.com/pretreatment-carbon-dating.htm). Six samples were from *Codakia orbicularis*, a facultatively mobile suspension feeder that burrows in shallow seagrass beds (Reynolds et al. 2007; Turgeon et al. 2009). The other sample is from *Cittarium pica*, a gastropod that can live above and below mean water level on calcareous and non-calcareous surfaces (Robertson 2003). Its diet consists of algae scraped off rocks, algae from the splash zone, sand, and detritus such as calcareous debris (Robertson 2003). One study of stomach contents demonstrated that calcareous material ranged between 13-49% in individuals (Randall 1964:428), which suggests that the radiocarbon age of this species may be heavily influenced by the intake of old carbonates.

To test the utility of our calculated ΔRs, we calibrated three sets of stratigraphically associated samples of *C. orbicularis* and white-tailed deer (*Odocoileus virginianus*) in a single-phase Bayesian model in OxCal v 4.4.4 (Bronk Ramsey 2009a). Samples were selected from Test Pit 4, a 50×50 cm test unit; suitable carbonized wood/botanical samples were lacking. Site stratigraphy and cross-mending of deer bone between levels suggests that deposition at the site occurred relatively rapidly, which provides the *prior* information for grouping these determinations into a single-phase model. AMS dates were calibrated using the Marine20 curve (Heaton et al. 2020). (i.e., ΔR = 0 ^{14}C yrs), the ΔR for the weighted average for Plantation Key/Lower Matecumbe, the weighted average for the Upper Keys, and the weighted average for the entire Florida Keys region. Dates on deer bone were calibrated using the IntCal20 curve (Reimer et al. 2020) as Key deer diet is primarily forbs and woody plants like red mangrove (*Rhizophora mangle*), black mangrove (*Avicennia germinans*), and thatch palm berries with no marine contribution (Klimstra and Dooley 1990).

Results

Modern shell radiocarbon

Radiocarbon ages and ΔRs for the 10 historically collected shell dates are presented in Table 3.1. The shell samples from Long Key and Sambo Key date to ca. 10,000 and ca. 15,000 years old, respectively. Both DirectAMS and UGAMS returned similar radiocarbon ages, which suggests that the shells were not live-collected in 1905 or 1915, respectively, as the Smithsonian records indicate. These two results were discarded from further analysis. The ΔRs for the remaining samples ranged from −257 ± 21 to −34

± 22 ^{14}C yrs (Table 3.1). Both high and low values come from different species that were collected in the same year off Plantation Key (Upper Keys). The difference in value could be attributed to interspecies susceptibility to the hardwater effect or upwelling and is discussed below.

The $\delta^{13}C$ values from DirectAMS are from AMS. ΔRs for all groupings are presented in Table 3.2 (see also Appendix B). In all cases the χ^2 tests indicate greater than statistically expected dispersion in the underlying ΔR values. Thus, the pooled mean ΔRs with external variance added (S_{total}) are the most conservative estimates. The ΔR for Plantation Key is ($\frac{\chi^2}{n-1} = 23.6$) −144 ± 99 ^{14}C yrs. The ΔR for Lower Matecumbe Key is ($\frac{\chi^2}{n-1} = 3.6$) −153 ± 36 ^{14}C yrs. The ΔR for the entire Florida Keys region is ($\frac{\chi^2}{n-1} = 4.9$) −169 ± 55 ^{14}C yrs. The ΔR for Loggerhead Key is ($\frac{\chi^2}{n-1} = 1.9$) −131 ± 23 ^{14}C yrs. Following individual islands, nearshore versus offshore ΔR values were compared. For these calculations, we included previously published ΔR values, which were all recalculated using the Marine20 calibration curve (Heaton et al. 2020). The ΔR for nearshore environment is ($\frac{\chi^2}{n-1} = 4.5$) −166 ± 48 ^{14}C yrs and the ΔR for open-ocean environment is ($\frac{\chi^2}{n-1} = 7.09$) −190 ± 78 ^{14}C yrs (Figure 3.2). The next group compares ΔR values by subregion. ΔRs were calculated for six ecological zones: Biscayne National Park is ($\frac{\chi^2}{n-1} = 2.4$); Upper Keys is ($\frac{\chi^2}{n-1} = 3.4$) −167 ± 39 ^{14}C yrs; Middle Keys is ($\frac{\chi^2}{n-1} = 35.5$) −96 ± 156 ^{14}C yrs; Lower Keys ($\frac{\chi^2}{n-1} = 4.7$) −179 ± 50 ^{14}C yrs; Marquesas is ($\frac{\chi^2}{n-1} = 6.3$) −192 ± 63 ^{14}C yrs; and Dry Tortugas ($\frac{\chi^2}{n-1} = 7.6$) −190 ± 82 ^{14}C yrs (Figure

3.3). Finally, the ΔR for Plantation Key/Lower Matecumbe Key is ($\frac{\chi^2}{n-1} = 14.9$) −147 ± 78 ^{14}C yrs (Figure 3.3).

Modern shell stable isotopes

δ^{13}C values for the historically collected shell range from a low of 0.13‰ to a high of 2.00‰ and δ^{18}O values range from a low −0.02‰ to a high value of 1.87‰. *A. gibbus*, *C. sentis*, and *B. antillarum* have depleted δ^{13}C values compared to the regional average of 1.6‰, with *A. gibbus* from Loggerhead Key showing the greatest depletion compared to the modern regional average. Most δ^{13}C values were below the expected regional average, with the lowest values from the open-ocean environment. As enriched δ^{13}C values indicate more productive marine environments, this suggests that the hardwater effect or upwelling is influencing these values. *B. antillarum* and *C. munda* both had slightly enriched δ^{13}C values. δ^{18}O values for open-ocean samples (from Loggerhead Key) were slightly above average, indicating mollusk preference for cooler, less saline water. The lower isotope values from nearshore environments suggest freshwater input as well as warmer water. *A. gibbus* exhibited a wide range with δ^{13}C of −0.13‰ to 1.17‰ and −0.02‰ to 1.6‰ for δ^{18}O. Given that these shells were sampled from four islands, it suggests that local influences in hardwater and hydrology may influence these values.

Archaeological radiocarbon

The ΔR from Plantation Key/Lower Matecumbe Key produced the best fit for the stratigraphically associated samples (Figure 3.4; Appendix B). Results of sensitivity analyses are presented in Appendix B. When calibrated with IntCal20 (Reimer et al.

2020), the dates from deer bone appear to date ca. 300-400 years older than the associated shell. When the ΔRs for the Upper Keys and the entire Florida Keys region were used, the models produced agreement indices above 60, but there was little temporal overlap in the 95.4% highest posterior density (HPD) ranges between the shell and the terrestrial dates (Appendix B). This suggests that the weighted average ΔRs for the Upper Keys and the entire Florida Keys region are inappropriate for Upper Matecumbe Key given that these terrestrial and marine dates derive from the same depositional context. When the weighted average ΔR for Plantation Key/Lower Matecumbe Key is used, the modeled 95.4% HPD ranges show statistical overlap between the shell and terrestrial dates, indicating this ΔR is more appropriate for the site. This ΔR was then applied to the four remaining dates from other excavation units at the site (Figure 3.5; Appendix B).

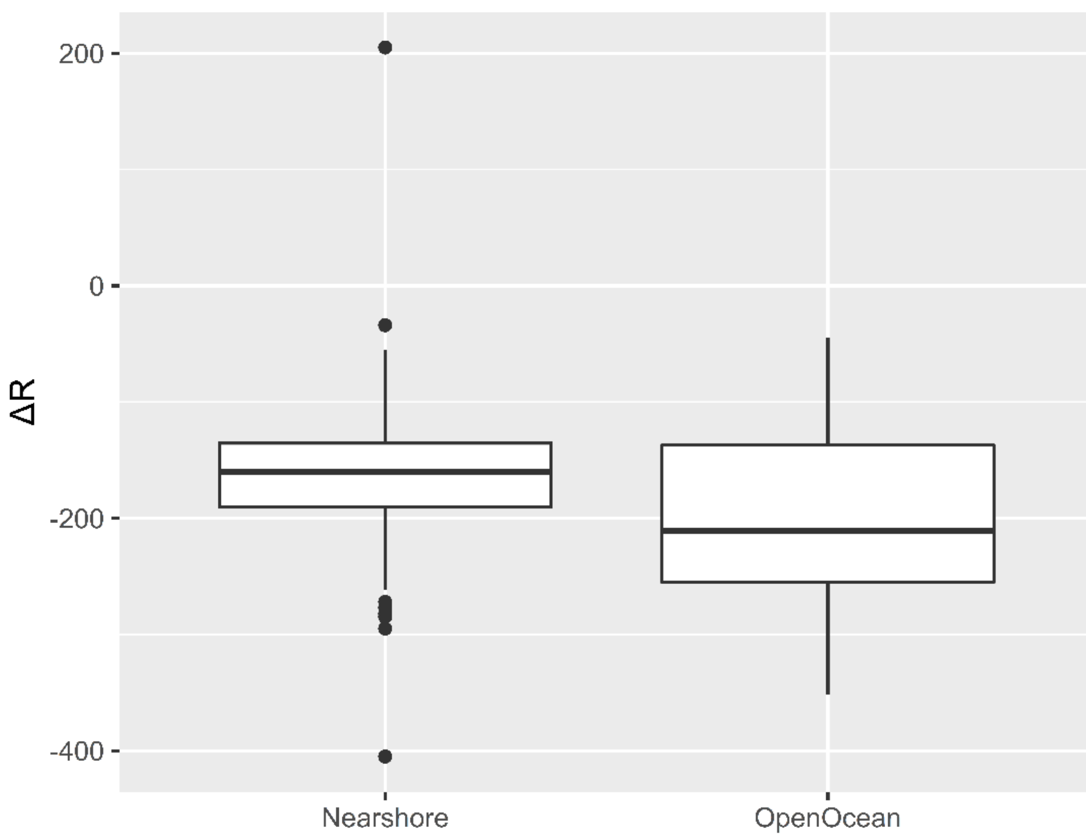

Figure 3.2. Nearshore and open ocean ΔR with external variance.

Table 3.1. AMS dates and ΔR for known-age shell from the Florida Keys. $\delta^{13}C$ and $\delta^{18}O$ values were determined at UGAMS using IRMS.

Lab Number	Location	Subregion	USNM Identification	Catalog Number (USNM)	Year Collected	Radiocarbon Age	Stable Isotope Lab Number	$\delta^{13}C$ (‰)	$\delta^{18}O$ (‰)	Reservoir Age	ΔR
UGAMS-40210	Florida Keys, Loggerhead Key	O	*Argopecten gibbus* (Linné, 1758)	609347	1954	466±18	40210	0.13	1.45	603±56	-137±18
D-AMS-015389	Florida Keys, Loggerhead Key	O	*Argopecten gibbus* (Linné, 1758)	609347	1954	512±21	—	—	—	603±56	-91±21
D-AMS-015392	Florida Keys, Loggerhead Key	O	*Argopecten gibbus* (Linné, 1758)	609346	1954	465±21	—	-0.31	1.60	603±56	-138±21
D-AMS-015393	Florida Keys, Loggerhead Key	O	*Euvola cf. papyraceum* (formerly *Amusium papyraceum*)	421734	1932	444±22	—	1.48	1.87	604±61	-160±22
D-AMS-015390	Florida Keys, Looe Key Reef	LK	*Caribachlamys sentis* (formerly *Chlamys ornata sentis*)	457120	1910	490±21	—	1.14	-.89	607±64	-117±21
D-AMS-015391	Florida Keys, Key West, Sand Key	LK	*Caribachlamys sentis (formerly Chlamys ornata sentis)*	457117	1910	415±20	—	1.45	-1.05	607±64	-192±20
UGAMS-40208	Florida Keys, Sambo Key Reef	LK	*Argopecten gibbus* (Linné, 1758)	457879	1915	15082±31	40208	1.10	2.50	—	—
D-AMS-015394	Florida Keys, Sambo Key Reef	LK	*Argopecten gibbus* (Linné, 1758)	457879	1915	15144±53	—	—	—	—	—
UGAMS-40209	Florida Keys, Long Key Reef	MK	*Argopecten gibbus* (Linné, 1758)	458050	1905	10368±25	—	-0.52	1.17	—	—
D-AMS-015395	Florida Keys, Long Key Reef	MK	*Argopecten gibbus* (Linné, 1758)	458050	1905	10581±39	—	—	—	—	—
UGAMS-40207	Florida Keys, Plantation Key, Conch Reef	UK	*Argopecten gibbus* (Linné, 1758)	450324	1910	415±18	40207	1.17	-0.02	607±64	-192±18
D-AMS-015396	Florida Keys, Plantation Key, Conch Reef	UK	*Argopecten gibbus* (Linné, 1758)	450324	1910	350±21	—	—	—	607±64	-257±21
UGAMS-40211	Florida Keys, Plantation Key, Conch Reef	UK	*Caribachlamys munda* (formerly *Chlamys munda*)	748870	1910	519±18	40211	1.73	0.12	607±64	-88±18
D-AMS-015398	Florida Keys, Plantation Key, Conch Reef	UK	*Caribachlamys munda* (formerly *Chlamys munda)*	748870	1910	573±22	—	—	—	607±64	-34±22

Table 3.3, continued.

Lab Number	Location	Subregion	USNM Identification	Catalog Number (USNM)	Year Collected	Radiocarbon Age	Stable Isotope Lab Number	$\delta^{13}C$ (‰)	$\delta^{18}O$ (‰)	Reservoir Age	ΔR
UGAMS-40206	Florida Keys, Lower Matecumbe Key	UK	*Brachtechlamys antillarum* (formerly *Decatopallium (Scalaris) antillarum*)	2140	1885	451±19	40206	2.00	1.35	627±64	-176±19
D-AMS-015397	Florida Keys, Lower Matecumbe Key	UK	*Brachtechlamys antillarum (formerly Decatopallium (Scalaris) antillarum)*	2140	1885	506±22	—	—	—	627±64	-121±22

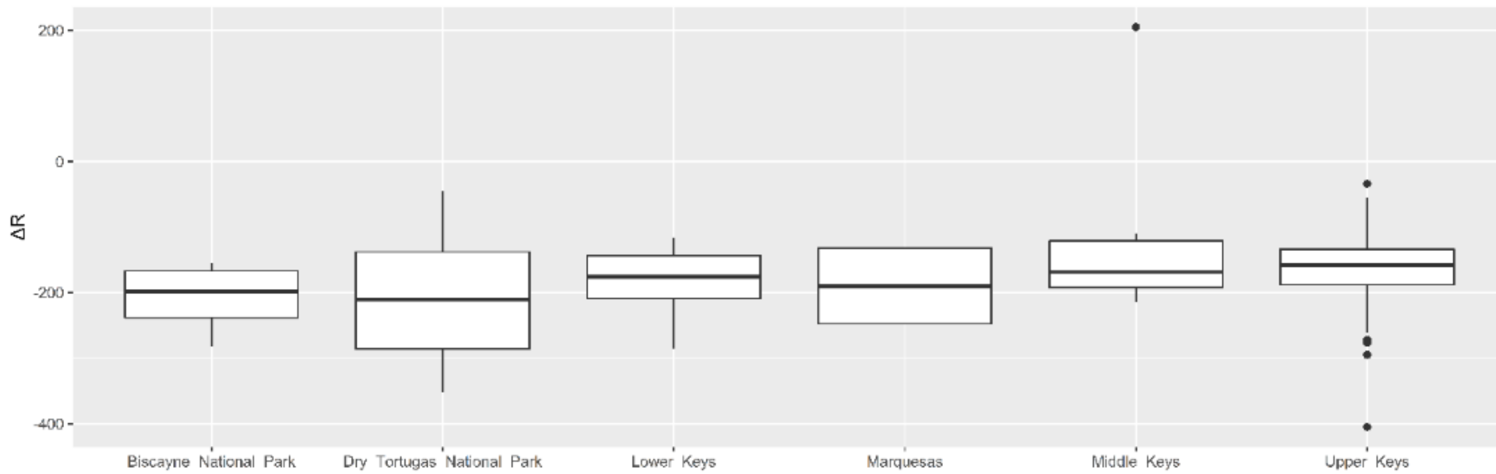

Figure 3.3. ΔR with external variance by ecological zone.

Table 3.2. Error-weighted pooled means ΔRs.

Number of pooled dates	ΔR pooled (ΔR_{μ}) + error (σ_{μ}) ^{14}C yrs	χ2 test	χ2/(n-1)	ΔR with external variance (S_{total}) ^{14}C yrs	Notes
4	-144±10	$\chi^2_{3:0.05} = 70.7<7.8$	23.6	-144±99	
2	-153±14	$\chi^2_{1:0.05} = 3.6<3.8$	3.6	-153±36	
4	-131±10	$\chi^2_{3:0.05} = 5.6<7.8$	1.9	-131±23	
2	-147±8	$\chi^2_{5:0.05} = 74.5<11.1$	14.9	-147±79	
175	-166±2	$\chi^2_{174:0.05} = 786.2<205.8$	4.5	-166±48	
25	-190±6	$\chi^2_{24:0.05} = 170.2<36.4$	7.09	-190±78	
6	-210±13	$\chi^2_{5:0.05} = 12.0<11.1$	2.4	-210±41	
155	-167±2	$\chi^2_{154:0.05} = 517.5<184.0$	3.4	-167±39	
6	-96±12	$\chi^2_{5:0.05} = 177.5<11.1$	35.5	-96±156	
8	-179±9	$\chi^2_{7:0.05} = 32.8<14.1$	4.7	-179±50	
4	-192±13	$\chi^2_{3:0.05} = 18.8<7.8$	6.3	-192±63	
16	-190±6	$\chi^2_{20:0.05} = 151.4<31.4$	7.6	-190±82	
200	-169±2	$\chi^2_{20:0.05} = 971.7<232.9$	4.9	-169±55	
11	33±16	$\chi^2_{13:0.05} = 99.2<22.4$	7.6	33±158	
17	5±6	$\chi^2_{17:0.05} = 1107.4<27.6$	65.1	5±185	
22	-106 ± 8	$\chi^2_{21:0.05} = 111.3<32.7$	5.29	-106 ± 80	from DiNapoli et al. 2021
7	-230 ± 15	$\chi^2_{6:0.05} = 44.1<12.6$	7.35	-230 ± 131	from DiNapoli et al. 2021

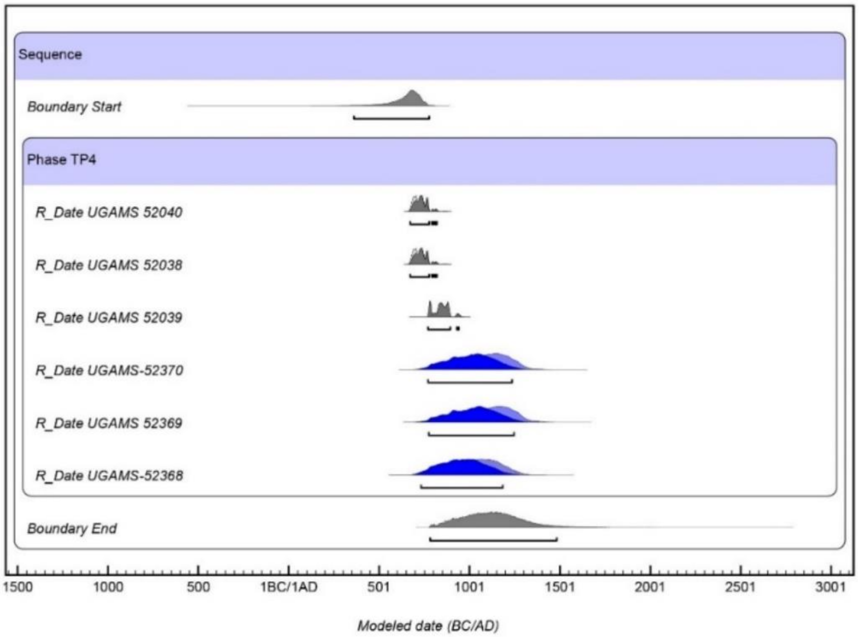

Figure 3.4. Bayesian modeled plots of stratigraphically associated samples from Test Pit 4.

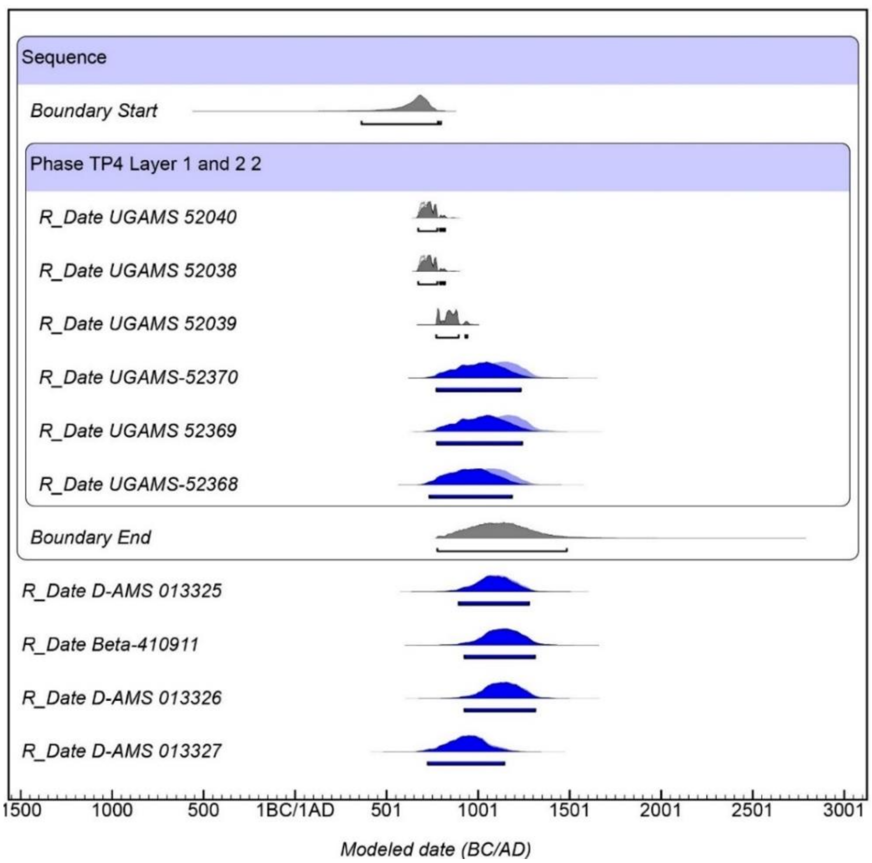

Figure 3.5. Calibrated dates from the Clupper site. Gray plots are on deer bone calibrated with IntCal20 curve (Reimer et al. 2020) and blue plots are shell dates calibrated with Marine20 curve (Heaton et al. 2020) and a ΔR of −147 ± 79 ^{14}C yrs.

Table 3.3. Calibration of radiocarbon determinations from the Clupper site, Upper Matecumbe Key. Dates were calibrated using OxCal v4.4 (Bronk Ramsey 2009a) and calibrated using the Marine20 curve (Heaton et al. 2020). Bayesian modeled dates are presented in italics (Bronk Ramsey 2009a). Lab codes: DirectAMS (D-AMS), University of Georgia Center for Isotopic Studies (UGAMS), Beta Analytic (Beta).

Lab Number	Sample Type	Provenience	Radiocarbon Age	$\delta(^{13}C)$‰	$\delta(^{15}N)$‰	$\delta(^{18}O)$‰	No ΔR (2σ cal)	Calibrated Age Range with ΔR −147±78 ^{14}C yrs (2σ cal)
D-AMS 013325	*Codakia orbicularis*	Test Unit 3, level 3, 20-30 cmbs	1323±21	2.33	—	-0.95	860-590 BP (AD 1090-1360)	1060-670 BP (AD 890-1280)
UGAMS-52038	*Odocoileus virginianus* long bone shaft bioapatite	Test Unit 4, Level 1, Layer 1	1270±20	-6.85	—	—	1280-1150 BP (AD 670-800)	*1280-1130 BP (AD 670-820)*
UGAMS-52368	*Codakia orbicularis*	Test Unit 4, Level 1, Layer 1	1340±20	3.12	—	0.75	880-610 BP (AD 1070-1340)	*1220-765 BP (AD 730-1185)*
UGAMS-52039	Mammalia long bone shaft collagen	Test Unit 4, level 2	1180±20	-8.63	6.57	—	1180-1000 BP (AD 770-950)	*1180-1005 (770-945)*
UGAMS-52369	*Codakia orbicularis*	Test Unit 4, level 2	1260±20	2.54	—	0.47	770-530 BP (AD 1180-1420)	*1175-700 (AD 775-1250)*
UGAMS-52040	*Odocoileus virginianus* long bone shaft collagen	Test Unit 4, level 3	1270±20	-5.49	10.73	—	1280-1150 BP (AD 670-800)	*1280-1130 BP (AD 670-820)*
UGAMS-52370	*Codakia orbicularis*	Test Unit 4, level 3	1280±20	1.74	—	0.68	790-540 BP (AD 1160-1410)	*1180-710 BP (AD 770-1240)*
Beta-410911	*Codakia orbicularis*	Test Unit 4, level 6, 50-60 cmbs	1280±30	1.6	—	—	800-540 BP (AD 1150-1410)	1040-640 BP (AD 910-1310)
D-AMS 013326	*Cittarium pica*	Test Unit 4, level 6, 50-60 cmbs	1278±27	2.27	—	-0.10	790-540 BP (AD 1160-1410)	1030-630 BP (AD 920-1320)
D-AMS 013327	*Codakia orbicularis*	Test Unit 3, level 7, 60-70 cmbs	1463±22	2.08	—	-0.92	970-700 BP (AD 980-1250)	1230-800 BP (AD 720-1150)

Archaeological stable isotopes

$\delta^{13}C$ and $\delta^{15}N$ values for the deer collagen samples were enriched compared to values reported in studies of modern and archaeological deer from Florida (Cormie and Schwarcz 1994; Hutchinson and Norr 2006; Schoeninger and DeNiro 1984). One sample (UGAMS 52038), measured from bioapatite, produced a value that is close to a terrestrial diet of C3 plants (−6.85‰), but the other two samples measured on collagen (UGAMS 52039 and 52040) have $\delta^{13}C$ values of −8.63‰ and −5.49‰ and $\delta^{15}N$ 6.57‰ and 10.73‰, respectively. As Key deer have an herbivorous diet, it would be expected that the $\delta^{13}C$ and $\delta^{15}N$ values would fall in the typical range for deer eating primarily C3 plants (Klimstra and Dooley 1990). For example, deer sampled from the Tatham Mound site from the central Gulf Coast of Florida returned a $\delta^{13}C$ value of −23.6‰ (adjusted for pre-industrial enrichment of atmospheric ^{12}C) and a $\delta^{15}N$ value of 4.3 (Hutchinson and Norr 2006: Table 4). These values are similar to those reported for other species of deer in Florida (Cormie and Schwarcz 1994; Schoeninger and DeNiro 1984). The isotopic values from the Clupper site would suggest an herbivorous diet almost exclusively made up of C4 plants, which is unusual for southern Florida (Table 3.3). The $\delta^{13}C$ values for *C. orbicularis* are also enriched compared to the modern samples from the region. The enriched values likely reflect the complex combination of limestone geology within the Florida Bay estuary and its hydrology, which can increase $\delta^{13}C$ and $\delta^{15}N$ across the food-web (Corbett et al. 1999; Nuttle et al. 2000). The potential impacts of the Seuss effect, anthropogenic activity, and habitat preference on these archaeological and modern mollusks is discussed in more detail below (e.g., Druffel and Benavides 1986; Swart et al. 1996).

Discussion and conclusion

Modern samples

Marine reservoir corrections for the Florida Keys demonstrate negative offsets to the modeled global average marine calibration curve (Heaton et al. 2020) ranging from −34 ± 22 ^{14}C yrs to −257 ± 21 ^{14}C yrs. Wide inter- and intra-island variability indicates that, for now, it would be prudent to use the regionally-specific error-weighted pooled mean ΔRs. Geographic variability is not surprising as this is seen throughout the circum-Caribbean (e.g., DiNapoli et al. 2021); however, given the fact that the highest and lowest ΔR value of the 10 samples used in this study came from the same island—collected from Conch Reef just off Plantation Key in 1910 from a depth of 64 m—suggests that there are additional factors to consider such as interspecies susceptibility to the hardwater effect or upwelling (Table 3.1). The least negative ΔR was calculated from *C. munda* and had a slightly enriched $\delta^{13}C$ value and depleted in $\delta^{18}O$. This is likely the result of the upwelling caused by the Florida Current as it passes by the Upper Keys and produces cooler SST. However, the most negative value was from *A. gibbus* and had a slightly depleted $\delta^{13}C$ value of 1.17‰ and a depleted $\delta^{18}O$ value of −0.02‰. *A. gibbus* had uniformly depleted $\delta^{13}C$ values relative to the regional average, suggesting that this species may be susceptible to the hardwater effect which may produce older than expected ^{14}C years and a greater ΔR value. Although ontogenesis can produce a lower-than-expected $\delta^{13}C$ value as it incorporates more metabolic carbon (C_{meta}) that results in decreased $\delta^{13}C$ values, *A. gibbus* is a short-lived species that only has a life expectancy of ca. 24 months (Blake and Shumway 2006; Lartaud et al. 2010); therefore, it is more likely that this is a result of the hardwater effect.

B. antillarum has the most enriched $\delta^{13}C$ value (2.00‰). This sample was collected in 1885, prior to the 1905-1912 construction of the Florida East Coast Railway. Construction of the railway, which stretches from Miami to Key West, restricted the exchange of water between the Gulf of Mexico and Florida Bay and led to increased eutrophication (Swart et al. 1996). Following construction of the railway, $\delta^{13}C$ values in the region uniformly depleted as a result of anthropogenic activity (Swart et al. 1996). It is therefore noteworthy that our highest $\delta^{13}C$ value was from the one sample collected prior to the construction of the railway. There may also be additional contributing external factors to depleted isotopic values that reflect local conditions. The samples from the Lower Keys also have depleted $\delta^{13}C$ and $\delta^{18}O$ values which could reflect conditions in the Florida Straits where slow-moving gyres contribute to mixing in the water column and upwelling.

Open-ocean ΔR is slightly more negative than nearshore and this finding supports the results from a previous study that found no significant difference between the two zones for the last 300 years and suggests a minimal influence of groundwater in the nearshore collection zones and along shelf-edge coral reefs (Toth et al. 2017). The most negative offset is from Biscayne National Park, suggesting that both terrestrial runoff and currents play significant roles in local variation. The least negative offset from the six subregions comes from the Middle Keys and is likely the result from a single outlier date from the Middle Holocene (sample MK-AR-7-0, CAMS-167744) reported by Toth et al. (2017:135). It is unclear why this sample produced a strong positive ΔR (205 ± 26 ^{14}C yrs, updated for Marine20 curve [Heaton et al. 2020]) as the sample met the threshold for analysis (see Toth et al. 2017).

Lastly, we compared the result for the Florida Keys to ΔRs from northwest Cuba, the Bahamas, Apalachicola Bay, and Southwest Florida (DiNapoli et al. 2021; Hadden and Cherkinsky 2015, 2017; Hadden and Schwadron 2019; see Table 2). The regional variation between these areas highlights the problem with using the "nearest" available ΔR. While some are relatively close, particularly the Florida Keys and northwest Cuba, complex currents and hydrology lead to divergent marine reservoir offsets. Overall, we consider ΔR values to be valid considering what is known about invertebrate feeding strategies and external influences.

Archaeological samples

The isotopic values taken from deer collagen appear to be unique in the region as deer from the Florida Keys and peninsular Florida would be expected to have an herbivorous diet heavy in C3 plants (e.g., Cormie and Schwarcz 1994; Klimstra and Dooley 1990; Land et al. 1980). Their $\delta^{13}C$ values are consistent with a diet of primarily C4 plants or for deer living in an arid regions like Arizona or Texas (Land et al. 1980). A diet heavily made up of C4 plants would be in sharp contrast to modern studies of Key deer populations, which found that C4 plants (i.e., grasses) made up just ~11% of their diet with red mangrove (*R. mangle*) leaves and black mangrove (*A. germinans*) fruits being the most important foods (Klimstra and Dooley 1990). Although the ratio of woody plants leaves and stems, fruits, forbs, palms, and grasses/pine needles/mushrooms changes throughout the year, the latter group made up less than 5% of Key deer diet in all seasons (Klimstra and Dooley 1990:Figure 3). Enriched $\delta^{13}C$ values occur among mangroves found in scrub forests where trees are shorter and would be well within Key deer feeding range (Lin and Sternberg 1992). However, values are only enriched by 1-4‰ and these values are still within the range of other species of mangroves (Lin and Sternberg 1992) and does not produce $\delta^{13}C$ values like the ones in our sampled deer after adjusting for trophic shifts. By discounting the possibility of $\delta^{13}C$-enriched mangrove species, this raises multiple possible scenarios. The first scenario is that the deer sampled in this study were primarily eating grasses as there were no other C4 plants like maize. Pre-industrial tropical grasses typically produce $\delta^{13}C$ values around −11.5‰; when consumed as food, there is an estimated 5‰ shift in the signature in bone collagen of large herbivores and humans, producing an expected result of ~−6.5‰, which is similar to the values from the Clupper site (Dewar and Pfeiffer 2010; van der Merwe and Vogel 1978). The stable isotope data presented in this study would suggest that the pre-industrial diets of deer were significantly different or that there were other contributing factors such as drought, population stress, or starvation at this time (Cormie and Schwarcz 1994).

A second scenario is that the $\delta^{13}C$ values became enriched because of post deposition taphonomy resulting from a chemical reaction with the surrounding soil. Land et al. (1980) report that Pleistocene- and Holocene-aged deer bone from Texas were very enriched compared to modern samples and their values were closer to equilibrium with groundwater bicarbonate. The exact ages of the Pleistocene and Holocene deer bones are not reported so it is unclear how long this process takes, but it is possible that the deer bone was subjected to this process and enriched values reflect—or partially reflect—this reaction.

A third scenario is that the complex combination of limestone lithology, hydrology, seasonal hypersalinity, and freshwater influences into the Florida Bay contributed to enriched values in shallow nearshore habitats. The presence of organic matter like macroaglae in areas with low turbidity like lakes can result in enriched $\delta^{13}C$ and $\delta^{15}N$ values (Guiry 2019). The Florida Bay estuary is notable for its low turbidity and low rates of water exchange because of the location of small keys which act as a buffer to the Gulf of Mexico and Atlantic Ocean. In addition, the interaction of groundwater input and surface water discharge along the Florida Bay side of the Florida Keys provides nutrients to the eastern Florida Bay and results in ^{15}N-enriched macroalgae, seagrasses, and seepages (Corbett et al. 1999). Enrichment in nitrogen at the lowest trophic levels would have an impact across the entire food-web as there is an estimated 3.5‰ enrichment of $\delta^{15}N$ across higher tropic levels (Schoeninger and DeNiro 1984).

It is possible that a combination of these conditions resulted in enriched $\delta^{13}C$ and $\delta^{15}N$ values in the archaeological deer bone, and this will be studied in the future. The isotopic values from *C. orbicularis* were enriched in $\delta^{13}C$ and depleted in $\delta^{18}O$ to the modeled present-day averages. The enriched $\delta^{13}C$ values compared to the modern collected samples likely reflect the Seuss effect, pre-Florida East Coast Railway construction, filter feeding carbon-enriched particulate organic matter (POM) (Lamb and Swart 2008) and their preference for warmer, less saline water like seagrass beds. The one sample from *C. pica*, a gastropod, did not yield significantly older results and its $\delta^{13}C$ and $\delta^{18}O$ values are comparable to *C. orbicularis* isotopic values. It is possible that this sample was from a juvenile, indicating that ontogenesis had not yet caused depletion in $\delta^{13}C$ or that the isotopic values reflect a diet low in calcareous materials.

The calibrated dates from the Clupper site now span the Glades IIa, IIb, IIc, and IIIa periods (Griffin 2002). The more accurate calibrations place the Clupper site occupation completely within the Glades II Period, a time of cultural growth and prosperity and into the Glades III period, a period during which was there was a shift to increased regionalism (Griffin 2002:158). This is supported by pottery recovered from the site which predominately date to Glades II (AD 700-1200). Diagnostic pottery types recovered from Test Pits 3 and 5 include Key Largo Incised (Glades II1-IIb), Miami Incised (Glades II1-IIb), and Matecumbe Incised (Glades IIb); however, Test Pit 4 only yielded undecorated pottery that was not temporally diagnostic (Ardren et al. 2018b). Thus far, the calibrated shell dates appear to be more consistent with the established chronology rather than the deer bone dates. It is worth noting that the shell dates were consistent across three different radiocarbon laboratories. Understanding the temporal range allows us to put the site in a broader regional and global context, as the time frame lines up with the latter part of the Medieval Warm Period (ca. AD 850 to 1200) and its effects on southern Florida (Walker 2013). Thus, we can now begin to ask questions about site occupation and shifting culture traditions that require more fine-grained temporalities without the homogenizing effects of culture history-based ceramic sequences (see Feinman and Neitzel 2020). Further, we can also begin to ask how well suited the broader, southern Florida Glades ceramic sequence is for the Florida Keys.

Finally, it is possible that ΔRs calculated on post-industrial era shell may not be appropriate for archaeological shell given millennial-scale shifts in ΔR documented in previous studies (e.g., Druffel et al. 2008; Toth et al. 2017). However, large shifts in ΔR over time appear to be greater during the Middle Holocene rather than in the Late

Holocene (Toth et al. 2017: Figure 2). ΔRs from ca. 1200-1000 BP appear to be similar to more recent values. Although the ΔR reported in these previous studies are calculated with Marine13 (Reimer et al. 2013), we would expect the modeled temporal trends to uniformly shift when recalibrated with Marine20 (Heaton et al. 2020).

These possibilities still do not explain why the deer bone returned dates that were unexpectedly older than the shell in each of the three pairs. It is possible that there was more post-depositional mixing of the deposit, a 1.75 cm thick midden of domestic refuse, than was noted by excavators and that the deer bone represents part of an older deposit (Ardren et al. 2018b). If this were true, then it is possible that hunting by early inhabitants in the region depleted Key deer populations and the deer bone will reflect earlier human hunting activity. For now, we discount this possibility and assume that the disparity in ^{14}C ages relates to local conditions that influence the age of the bone since the dates on shell are consistent across the site and across three radiocarbon dating laboratories.

Given the ubiquity of marine and estuarine shell found in island and coastal contexts worldwide, they provide important sample types for radiocarbon dating. However, when samples are selected and calibrated uncritically, shell can be a problematic material to radiocarbon date for many reasons. In a recent publication, Hutchinson (2020) takes a critical view of calibrating radiocarbon dates on shell using time- or regionally-averaged ΔR. He argues that local variation in ΔR caused by shoreline orientation, backshore topography, and geology may be overlooked by relying on large-scale latitudinal patterns (Hutchinson 2020:680). This is further complicated by the feeding habits of mollusks, especially estuarine species, that consume suspended detritus, POM, and other materials that can contribute to inaccurate ^{14}C ages. His study focuses on the Pacific Coast of North America, but his observations and reservations apply to many, if not all, island and coastal regions, although the spatiotemporal conditions vary widely from region to region.

We take a less pessimistic view of radiocarbon dating shell. Hutchinson (2020) stops short of highlighting how archaeologists have dealt with these problems in other island and coastal regions, as we have done in this paper. We argue that radiocarbon dates on archaeological shells can be as valid as dates on carbonized wood or charcoal when the appropriate samples were selected and attention is given to the external factors that can influence an organisms' ^{14}C age, δ^{13}C, and δ^{18}O. These programs have proven very successful in other regions of the world where dedicated programs have identified site-specific and species-specific ΔRs (e.g., Petchey and Clark 2011, 2021; Petchey et al. 2012, 2013, 2017, 2018). Just as archaeologists have developed ways to deal with the potential problems of inbuilt age when calibrating unidentified charcoal wood remains (Dee and Bronk Ramsey 2014), there are ways to develop accurate ΔRs. In some situations, it may be required to look beyond the trio of ^{14}C age, δ^{13}C, and δ^{18}O isotopes and examine the external factors that influence these values. For example, as this and many other studies have illustrated, however, mollusk habitat, diet, and susceptibility to external factors like upwelling, the hardwater effect, and anthropogenic activity must be considered when calculating a local ΔR as has been demonstrated in the Pacific (see Petchey and Clark 2011; Petchey and Schmid 2020; Petchey et al. 2013, 2017, 2018). The results of this study indicate that the weighted average ΔR for Plantation/Lower Matecumbe Key is better for calibrating archaeological dates on marine shell from the Clupper site on Upper Matecumbe Key and the regional error weighted average ΔR for the Upper Keys and Florida Keys are not appropriate. This study provides important new baseline data for establishing a ΔR for different parts of the Florida Keys. By performing sensitivity analyses to compare the calibrations of stratigraphically-associated shell and deer bone samples, we were able to identify an appropriate subregional ΔR. Given the variation in ΔRs by island and subregion, we recommend using a local weighted mean with external variance to provide the most accurate calibrations rather than a regional one.

CHAPTER IV

CHRONOLOGICAL MODELING OF EARLY SETTLEMENT ON YAP, WESTERN MICRONESIA

From: Matthew F. Napolitano, Scott M. Fitzpatrick, Geoffrey Clark, Amy Gusick, Esther Mietes, Jessica H. Stone, and Robert J. DiNapoli. Chronological modeling of early settlement on Yap, Western Micronesia. To be submitted to Quaternary International.

Introduction

Human settlement of the Pacific, comprising the most remote landmasses on the planet, represents what were arguably some of the greatest maritime accomplishments in history. These long-distance, open-water crossings—many of which spanned thousands of kilometers and required the development of specialized sailing technologies and wayfinding skills—have been the subject of anthropological and archaeological inquiry for nearly a century (e.g., Anderson 2008; Bell et al. 2015; Best 1923; Finney 1996; Gladwin 2009; Hīroa 1938; Irwin 1989; 1992, 2008; Kirch 1997, 2017; Montenegro et al. 2016; Smith 1910). Yet, despite a long tradition of research, many significant questions still exist about when and how early settlement took place. This is particularly true of Micronesia in the northwest tropical Pacific, which is home to thousands of smaller islands stretching across an expanse of ocean the size of the United States (Figure 4.1). Given their small size and remoteness, both of which pose severe logistical issues for conducting fieldwork, Micronesia is relatively understudied compared to other parts of the Pacific such as Polynesia and different island regions like the Mediterranean and Caribbean (Fitzpatrick et al. 2016). Building a refined chronology for initial human settlement on Yap is one of the most important questions to address in order to establish cultural connections, identify potential homelands, and contextualize early settlement within a broader regional context (see Napolitano et al. 2021).

Over the last few decades there has been a steady increase in research on the two largest archipelagos in western Micronesia, Palau and the Mariana Islands, which has resulted in a clearer picture of episodic entries into the region ca. 3200-3000 years ago, likely from somewhere in Island Southeast Asia (ISEA) (e.g., Clark 2005; Fitzpatrick 2003; Fitzpatrick and Jew 2018; Montenegro et al. 2016; Petchey and Clark 2021; Petchey et al. 2017, 2018; Rieth and Athens 2019; Stone 2020; Stone et al. 2017). Unfortunately, the early settlement chronology for Yap—a group of four small, interconnected islands situated between Palau and the Mariana Islands—remains one of the biggest enigmas in the Pacific. Potential dates for colonization span more than a millennium, with dates from paleoenvironmental cores suggesting human arrival as early as ca. 3300 years ago (Dodson and Intoh 1999), but with archaeological radiocarbon dates only dating to around 2000 years BP (Intoh and Leach 1985; Napolitano et al. 2019a; Takayama 1982). In addition, multiple lines of evidence suggest a broad range of possible homelands from ISEA to New Guinea and/or the Bismarck Archipelago (e.g., Lum and Cann 2000; Ross 1996; Zerega et al. 2004). If people first arrived to Yap from the south (i.e., New Guinea and/or the Bismarck Archipelago) as much as 3300 years ago, then they would have likely been affiliated with the Lapita culture. This would have profound implications for our understanding of how Remote Oceania was settled as there is no documented evidence for Lapita in Micronesia. Resolving this question partly rests on building an adequate chronology for Yap's early settlement.

Figure 4.1. Yap Islands and its location in the Pacific.

Given the uncertainty surrounding Yap's early settlement, and the potential to establish the first cultural links from western Micronesia to groups in New Guinea or the Bismarck Archipelago, we conducted the first systematic survey to locate and excavate early settlement sites and critically re-examine all previously published radiocarbon dates for Yap (n = 61) and present a suite of 31 unpublished radiocarbon dates from southern Yap for a total of 92 dates. We then subjected these dates to chronometric hygiene in which unreliable or inadequately reported dates were culled from the database (Spriggs 1989). This technique improves the strength of radiocarbon databases and has been successfully used in many other parts of the world, especially in regions where databases reflect sample selection and reporting standards that are no longer considered acceptable (e.g., bulk samples and published sample provenience) (Fitzpatrick 2006; Liston 2005; Napolitano et al. 2019b; Petchey et al. 2015; Rieth et al. 2008; Schmid et al. 2019; Spriggs 1989; Spriggs and Anderson 1993; Taché and Hart 2013; Wilmshurst et al. 2011).

Below, we discuss our efforts to find archaeological deposits that predate 2000 years ago and to develop baseline data on sea-level change over the last 2500 years. After providing environmental and archaeological background for Yap, w present 31 new radiocarbon dates and use carbon and oxygen isotopes to discuss paleoenvironmental conditions and how that might influence radiocarbon ages. As there are no spatially or temporally suitable local marine reservoir corrections (ΔR) for Yap, we then develop a Bayesian-modeled ΔR using stratigraphically associated radiocarbon dates on shell and carbonized wood. Finally, we create the first Bayesian modeled estimate for initial human settlement of Yap.

Background

Environment

Yap is located in western Micronesia, equidistant approximately 900 km east of the southern Philippines and north of New Guinea. Micronesia stretches 5000 km^2 eastward from the Western Carolines (Palau, Yap, the Marianas) across the Central and

Eastern Carolines to the Marshall Islands and Kiribati (see Figure 4.1). Yap comprises four main islands (Yap or *Marbaq*, *Maap'*, *Gagil-Tamil*, and *Rumung*) connected through narrow waterways. The main islands have a total land area of ca. 7900 ha surrounded by a fringing reef system within the west-flowing North Equatorial Current (NEC) with a mean transport of 42-82 Sv (1 Sv = 10^6 m^3 s^{-1}) (Wang et al. 2016; Yu et al. 2000). Yap is situated about 9° north of the equator, not far from the boundary between the NEC and the North Equatorial Counter Current (NECC) and has a tropical environment, receiving an average of 310 mm rainfall per year. The wet season is from July-October with a drought and tradewinds season from December-April. The average temperature is 29°C (Blumenstock 1960).

The Yap Islands are geologically unique in the region as there are no major uplifted limestone sections, with just a few small limestone outcrops not far from the present day shoreline. Southern Yap is geologically defined by alluvium, tidal mangrove forests, and Tomil volcanics comprising agglomerate, breccia, tuff, and lava overlain by upland soil (Johnson et al. 1960; Shade et al. 1992; Smith 1983). The central part of Yap, Rumung, and Maap contains upland soils underlain by green schist, which is often used with coral blocks as building material for platforms that supported structures (e.g., *dayif*, *chamog*), dancing areas (*malal*), sitting areas (*wunubey*, *sumuruw*), and walking paths (Furness 1910; Nunn et al. 2017).

Evidence for early settlement

Direct and indirect lines of evidence have resulted in an unclear picture of Yap's early settlement. Radiocarbon dates on peat samples from paleoenvironmental cores taken from wetlands located ca. 1-2 km from the southern coast show evidence for widespread burning and a decline in forest cover that was eventually replaced by savanna grasses ca. 3300 BP (Dodson and Intoh 1999). This type of activity is often associated with colonizing groups on islands as they modify the landscape in anticipation of establishing villages and agricultural fields. However, there is no evidence of plant taxa, particularly cultigens such as taro or breadfruit, having been introduced that would signify human arrival at that time. Therefore, this line of proxy evidence should be used cautiously when discussing initial human settlement (e.g., Napolitano et al. 2021:5-6; Prebble and Wilmshurst 2009).

Linguistic data provide a second circumstantial line of evidence. Yapese is an Austronesian outlier language identified as an "Oceanic isolate" and is highly unusual given Yap's position in western Micronesia (Finney 1998; Ross 1996). Analysis suggests that Yapese is likely to have developed after diverging from a closely-related language spoken in northern New Guinea or the Bismarck Archipelago approximately 3000 years ago (Finney 1998; Lynch et al. 2013; Ross 1996). This connection to one of these regions is tentatively supported with genetic data from breadfruit, as Yapese breadfruit (*Artocarpus altilis*, Moraceae) is a hybrid species that originated in Near Oceania (Zerega et al. 2004).

In contrast to these other lines of evidence, preliminary genetic data from modern Yapese people suggest an early arrival from ISEA with extensive gene flow from central and eastern Micronesia, although further study is needed (Lum and Cann 2000). Based on this circumstantial evidence, humans may have settled Yap ca. 3300-3000 years ago, contemporary with the initial movement of the Lapita culture out of the Bismarck

Archipelago to West Polynesia and the initial colonization of western Micronesia from ISEA (e.g., Bedford and Spriggs 2019; Clark 2005; Fitzpatrick 2003; Kirch 1997; Petchey and Clark 2021; Petchey et al. 2016, 2017, 2018; Rieth and Athens 2019; Rieth et al. 2017; Sheppard 2019; Stone 2020; Stone et al. 2017).

Archaeological investigation suggests that the oldest cultural deposits on Yap date to around 2000 B.P. and are found at Rungluw (spelled Rungruw in Intoh and Leah [1985]) and Pemrang, both shell midden sites located on beach flats in southern Yap (Napolitano et al. 2019a). Excavation at each site yielded large amounts of shell and calcareous sand tempered (CST) pottery, the oldest known type on Yap (Descantes 2005:75; Intoh and Leach 1985; Napolitano et al. 2019a; Takayama 1982). Following patterns seen on other islands in the Pacific, we expect that early sites would have been located on former beach flats adjacent to productive reef habitats (Bedford et al. 2006; Clark et al. 2006; Dickinson 2014; Kirch 2017). However, the lack of data on paleoshoreline reconstruction, local sea-level change, and tectonic activity (i.e., uplift, subsidence) makes it difficult to model where these early sites might be found.

Resolving the discrepancy between the linguistic, paleoenvironmental, and archaeological data is best addressed through further archaeological research. In 2016 three of the authors (MFN, SMF, and GC) began an interdisciplinary research program to identify archaeological evidence for human settlement prior to 2000 years ago with the following goals: 1) identify intact stratigraphic deposits to develop a refined chronology for early settlement; 2) assess the existing inventory of radiocarbon dates and cull unreliable dates; 3) develop the first model-based estimate for when early settlement may have taken place on Yap; and 4) collect baseline data on past sea-level change and paleoenvironmental conditions. For the initial stages of this project, we conducted a systematic auger survey in various deposits across southern Yap that would have high potential for discovering former beach flats and intact stratigraphic deposits.

Fieldwork and site descriptions

Archaeological research on Yap began in the 1950s when Gifford and Gifford (1959) excavated five sites to try and establish the island's chronology and look for possible external connections to other places. In their excavations they identified two pottery types, laminated and unlaminated, the latter of which was seen as "identical" to Marianas plain by Alexander Spoehr (Gifford and Gifford 1959). However, these connections have since been disproven through typological and petrographic research (Descantes et al. 2004; Dickinson 1982, 2000; Fitzpatrick et al. 2003; Intoh and Leach 1985). The island's ceramic sequence now comprises three types with five temper groups: 1) CST; 2) iron oxide/grog tempered ware; 3) quartz-feldspar ware; 4) Yapese plain; and 5) laminated (Descantes et al. 2004; Dickinson 2000). Iron oxide/grog tempered and quartz-feldspar are considered variants of Yapese plain. Both types are generally thought to have been produced from ca. 2000-600 years ago, after which laminated pottery replaces both types (Descantes 2005). Yapese plain became the dominant type ca. 800 years ago. Other than early survey projects by the Giffords (1959), Takayama (1982), and Intoh (1989; Intoh and Leach 1985), the majority of fieldwork and anthropological inquiry has focused on understanding settlement patterns (Adams 1997; Aoyagi 1982; Cordy 1986; Craib and Price 1978; Hunter-Anderson 1983, 1984), the *sawei* exchange/tribute system (Berg 1992; Descantes 2005; Hunter-Anderson and Zan

1996), stone money quarrying activity on Palau (Fitzpatrick 2001, 2002a, 2002b, 2003, 2008; Fitzpatrick and McKeon 2020; Hazell and Fitzpatrick 2006; chapter 5), and traditional ecological knowledge or intangible cultural heritage (e.g., Cushing Falanruw and Ruegorong 2007; Hunter-Anderson 1981, 1991; Jeffery 2013; Nunn et al. 2017; Perkins and Krause 2018).

The site of Pemrang has received the most attention from archaeologists, having been previously excavated by Gifford and Gifford (1959), Takayama (1982), and again in 2016-2017 (Napolitano et al. 2019a). The site is recognized by an extensive surface scatter of shell and pottery. An oral history of the site indicates that shellfish was brought here and offered as tribute to the priest that lived and was later buried at the site (Gifford and Gifford 1959:157). Later oral histories collected by Takayama (1982:85) explain that the shell was brought to Pemrang in exchange for coconuts by people who lived in Malway village in Map, Gargey village in Tomil, and Ul village in Gagil.

In our first field season at Pemrang, exploratory excavation of a single 1×1 m unit revealed the oldest cultural radiocarbon date from Yap (Napolitano et al. 2019a). This date, taken from a *Tridacna maxima* shell adze fragment, offered preliminary evidence that pre-2000 year old deposits could be identified. However, more research was required to corroborate this date and rule out the possibility of subfossil shell tool use (Rick et al. 2005). Excavation continued at Pemrang the following year, and over the next three field seasons, we conducted a systematic auger survey in the villages of Guror, Anoth, and Magachagil in which multiple discrete cultural deposits were identified, many with abundant CST pottery. In addition, we found a buried beach deposit ca. 2.5 m below the surface (Napolitano et al. forthcoming) (Figure 4.2). Although this beach deposit was not cultural in nature, radiocarbon dates from this context provide an important baseline to consider paleoshoreline location and begin modeling sea-level changes through time. Additional samples for dating were collected from two augers approximately 100 m apart both of which contained large amounts of burnt organics and CST pottery. The first auger (AH2019-39) is located in an area known as Balech'lee and the second (AH2019-29) is located in an area named Dulul (see Figure 4.2). At Balech'lee, CST pottery was recovered from 0.5–3.0 m below surface (bs) with an absence of laminated and Yapese plain sherds. This is notable because other sites in southern Yap usually contain abundant laminated sherds at shallower depths (Intoh and Leach 1985; Napolitano et al. 2019a). To explore this area further, a 1×1 m unit (Test Unit 1) was excavated at Balech'lee (Napolitano et al. forthcoming).

Improving the reliability of radiocarbon date calibrations

On many islands around the world, mollusks are a major source of subsistence and are often radiocarbon dated because of their ubiquity (Hutchinson 2020; Thomas 2015). Calibrating radiocarbon dates on marine shell, however, requires an additional offset to the modeled global reservoir age in subtropical oceans to reflect local conditions (Heaton et al. 2020; Reimer et al. 2013; Stuiver et al. 1986). Local marine reservoir effects (ΔR) can be influenced by factors such as regional upwelling, seasonal variations in sea surface temperature, changes in ocean circulation, shifting stratification of ocean surface waters, proximity to freshwater outputs, geological substrates containing limestone, and environmental preferences of animals selected for dating. These offsets can vary dramatically within the same region—sometimes by hundreds of years on the same island or between lagoonal and open ocean environment—and can shift over time (e.g., see DiNapoli et al. 2021; Hutchinson 2020; Kennett et al. 1997; Petchey and Clark 2010, 2011, 2021; Petchey and Schmid 2020; chapter 3). As a result, they are useful for improving the accuracy of radiocarbon date calibrations and reconstructing paleoenvironmental and paleoclimatic conditions (e.g., DiNapoli et al. 2021; Petchey 2009; Petchey and Clark 2010, 2011, 2021; Petchey and Schmid 2020; Petchey et al. 2012, 2013, 2017, 2018; Yoneda et al. 2000, 2007; chapter 3).

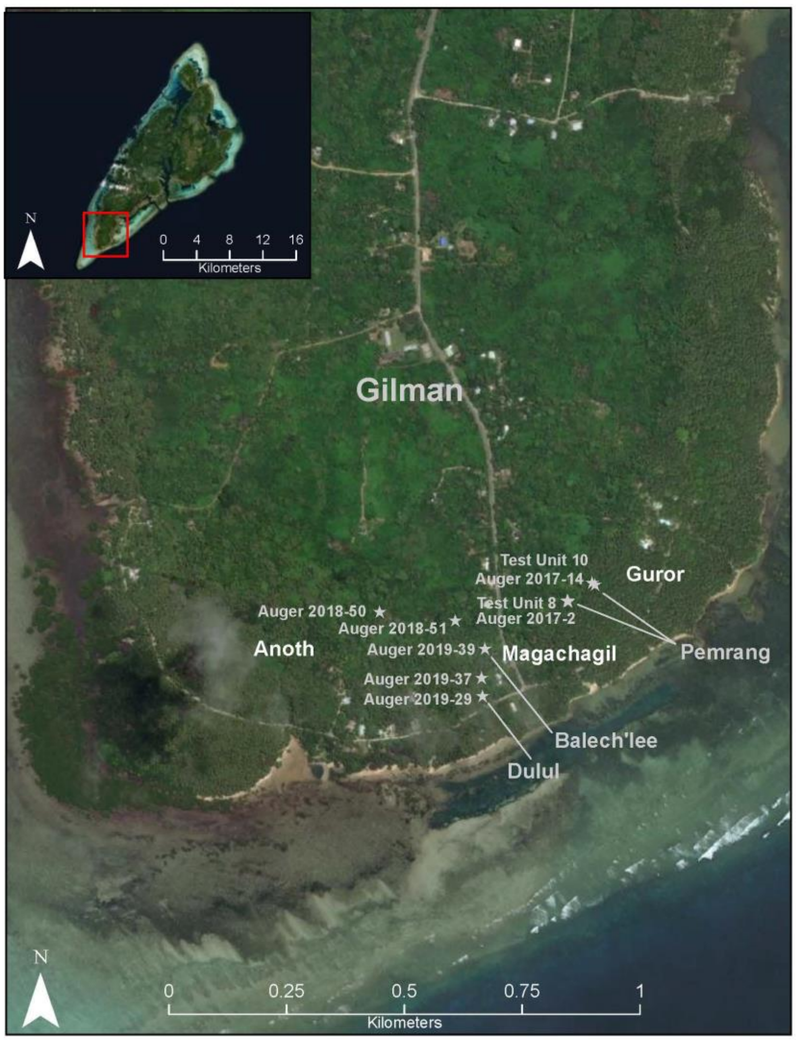

Figure 4.2. Gilman municipality with dated sites mentioned in the text.

Positive ΔRs are expected in areas with upwellings and in lagoons bounded by limestone and negative ΔRs are associated with freshwater input as a result of terrestrial influences or atmospheric absorption of CO_2 (Culleton et al. 2006; Petchey and Clark 2011; Petchey et al. 2016; Stuiver and Braziunas 1993; Southon et al. 2002). ΔR values can be calculated with paired shell-carbon samples from short-lived species identified to taxon, live-collected pre-bomb (before the mid-1950s) shell, tephra isochrones, paired ^{14}C uranium-thorium samples from banded corals, or otoliths from fish that swim in surface waters (Alves et al. 2018; Ascough et al. 2015; Kalish 1993; Petchey and Clark 2011; Yoneda et al. 2000, 2007). Museum collections are often the most ideal place to search for pre-bomb samples. However, there are currently no ΔR values available for Yap (calib.org/marine) and access to museum samples of known-age shell from Yap has not been possible during the pandemic.

While the ΔR for Yap is currently unknown, we expect there to be some offset that reflects local conditions. New radiocarbon dates on archaeological shell presented here, collected from southern Yap, were likely harvested from the adjacent coral reef system that is characterized as having high water exchange rates, moderate wave energy, low water turbidity, and less temperature variability (Houk et al. 2012). Multiple studies have demonstrated that ΔRs vary by a selected specimen's habitat and diet preference, which can influence its ^{14}C age. This is particularly true for Palau and the Mariana Islands (Petchey and Clark 2010, 2021; Petchey et al. 2017, 2018). For example, analysis of ^{14}C in combination with $\delta^{13}C$ and $\delta^{18}O$, indicates that the filter-feeding bivalve *Anadara antiquata* is susceptible to the effects of hardwater—the process where bicarbonate ions seep through karstic or calcareous substrate and can cause variability that differs from other marine species of the same age (McKinnon 1999). As such, this requires a species-specific ΔR (Petchey et al. 2013, 2017). At the site of Bapot-1 in Saipan, *A. antiquata* shells were shown to have a ΔR of 218 ± 57 ^{14}C yrs from the modeled global average (Petchey et al. 2017). Although this value was calculated with the Marine13 curve (Reimer et al. 2013) and will be different when recalculated for Marine20 (Heaton et al. 2020), it underscores the importance of understanding how various species may require their own offset. Unlike Saipan, however, Yap is geologically unique in the region and lacks limestone substrate, though the presence of limestone is not the only predictor of the hardwater effect and should still be examined for Yap (Petchey et al. 2017, 2018). Other species, like herbivorous, omnivorous, or carnivorous gastropods that feed along limestone substrates can also produce problematic ^{14}C dates (Beesley et al. 1998; Dye 1994). Beach sand in southern Yap contains calcareous materials and several small limestone outcrops within 100 m from the present-day southern shoreline would easily be within foraging range for people living in southern Yap. Therefore, it is possible that local hardwater effect will influence the ^{14}C age of marine shells and their isotopic values. To address the lack of a ΔR, we used stratigraphically-associated charcoal and shell dates from Test Unit 8 at Pemrang to build a Bayesian-modeled ΔR. This approach allows us to develop a ΔR that likely reflects a time-averaged ΔR across species. Stable isotope analysis of radiocarbon dated shells in this study are also used to infer paleoenvironmental and paleoclimate conditions at the time of death.

Methods

Laboratory pretreatment

Radiocarbon samples were processed at DirectAMS and The Australian National University (ANU). Samples D-AMS 019902-019909 were pretreated and sampled at the University of Oregon Island and Coastal Archaeology Laboratory (ICAL) and submitted to DirectAMS for dating. These marine shell samples were etched in a 10% HCl solution to remove 10-25% of surface material potentially subject to recrystallization and contamination and 3 mg of shell was drilled from each specimen using a Sherline micromill 5410 using a carbide drill bit. Shells were sampled across multiple growth bands to avoid dating intra-growth band radiocarbon variability (see Culleton et al. 2006). Samples D-AMS-26457, 26458, 31805-31811, and 38871-38880 were pretreated at DirectAMS (see http://www.directams.com/publications-methods-and-other-references). Terrestrial samples were prepared and analyzed at ANU (https://earthsciences.anu.edu.au/research/facilities/anu-radiocarbon-laboratory/laboratory-methods). Four samples of 11 (36%) were identified as short-lived samples. Samples YP-2, YP-3, YP-8 were identified as nut endocarp and S-ANU-57912 was identified as coconut endocarp.

$\delta^{13}C$ and $\delta^{18}O$ values for all samples reported in this study were measured at the Center for Isotopic Study at the University of Georgia (UGAMS) using isotope ratio mass spectrometer (IRMS) combined with gas bench expressed as $\delta^{13}C$ with respect to PDB with an error of less than 0.1‰. Values were compared against regional baseline values of 1.3‰ for $\delta^{13}C$ (Tagliabue and Bopp 2008) and 0.2‰ for $\delta^{18}O$ (LeGrande and Schmidt 2006), respectively. $\delta^{13}C$ values can be used to infer if shells were collected from estuarine or marine environments (Petchey et al. 2018). Depletion of $\delta^{13}C$ and $\delta^{18}O$ is often an indication of freshwater input while an increase in value indicates increased productivity and CO_2 atmospheric absorption in reefs (Keith et al. 1964; Petchey et al. 2013). $\delta^{13}C$ can reveal changes in water source and marine productivity (Petchey et al. 2016). Enriched $\delta^{18}O$ values indicate increased salinity and temperature (e.g., Emiliani et al. 1966; Epstein and Mayeda 1953; Epstein et al. 1953; Swart et al. 1983).

Sample selection, habitat, and diet preferences

It is important to understand the habitat and diet preferences of shell samples selected for dating because they can influence the animal's radiocarbon age. In this study, we report data from five species of bivalves (*A. antiquata*, *Quidnipagus palatam*, and *Gafrarium pectinatum*, *Mactra* sp., and *Tridacna maxima*) and three species of gastropods (*Gibberulus gibberulus, Cypraea* sp., *Cerithium* sp.). *A. antiquata* is an epifaunal bivalve that lives on rocks or in rocky crevices in estuaries (Broom 1985). *Q. palatam* is a filter-feeding, infaunal bivalve found in shallow silty offshore sands, typically burrowing between 20-30 cm deep (Kay 1979; Thomas 2001). They are harvested by hand fanning after spotting the siphonal openings (Thomas 2001). *G. pectinatum* are found in high intertidal regions such as seagrass beds and mangrove forests (Baron and Clavier 1992; Petchey and Clark 2011; Petchey et al. 2018; Tebano and Paulay 2000). *Mactra* sp. is a facultatively mobile suspension feeder that lives in sandy bottoms (Sepkoski 2002). *Tridacna maxima* is a stationary bivalve found in shallow marine environments with a complex diet involving both suspension feeding and endosymbiotic zooxanthellae photosynthesis, but are primarily suspension feeders as juveniles (Klumpp et al. 1992; Petchey and Clark 2011; Petchey et al. 2017; van Wynsberge et al. 2017). *G. gibberulus* is an herbivorous gastropod that prefers more productive marine environments like sandy, subtidal coral reef flats (Carpenter and Niem 1998; Petchey et al. 2016). *Cypraea* sp. live in coral reefs or along sandy bottoms and exhibit a range of feeding behavior with juveniles consuming algae and adults consuming coral or invertebrates. *Cerithium* sp. are deposit feeding gastropods found that prefer mangrove habitats (Reid et al. 2008).

These shells were selected because of their abundance in the archaeological record as they were clearly a preferred source of food. However, the ^{14}C ages of these species may vary from other species of the same age as *A. antiquata* and *G. pectinatum* are susceptible to the effects of hardwater and *Q. palatam* may directly ingest carbonate or indirectly through algae (Petchey and Clark 2011; Petchey et al. 2013, 2017, 2018:183). The hardwater effect on *Gafrarium* sp. should result in a more positive ΔR compared to the regional average (Petchey and Clark 2011). By comparing the $\delta^{13}C$ and $\delta^{18}O$ to modern values, we should be able to identify whether the ^{14}C age is influenced by hardwater. Gastropods are likely to return significantly older dates compared to their true age because of their dietary preferences which can include grazing on rock or seagrasses.

Modeling ΔR

We calculated a hypothetical Bayesian-modeled ΔR using one set of stratigraphically associated *A. antiquata* shell and a carbonized coconut endocarp (YP-8) dates from Layer 5 in Test Unit 8 at Pemrang. The endocarp fragment serves as the prior for the shell in an unordered phase. programmed the model to run 1,000,000 iterations in

OxCal v4.4.4 to ensure that the MCMC converged on the posterior distribution (Bronk Ramsey 2009a).

Chronometric hygiene

More than 60 years have passed since the first radiocarbon dates were produced and given a host of issues that are sample- and context-dependent, it is necessary to critically evaluate each date for potential problems. These include potential inbuilt age from long-lived taxa (Allen and Huebert 2014), the old-wood or old-shell problem (Rick et al. 2005; Schiffer 1986), and excluding dates where it is not possible to know whether dates were corrected or calibrated. To address these concerns, we first implemented a chronometric hygiene protocol. This technique—used to cull unreliable or inadequately reported radiocarbon dates—is an increasingly common approach for refining radiocarbon chronologies, particularly in island and coastal regions.

In the Pacific, the use of chronometric hygiene techniques has improved the chronological resolution of colonization events, site-specific activities, and temporal shifts in material culture (e.g., Fitzpatrick and Jew 2018; Petchey and Kirch 2019; Petchey et al. 2015; Rieth and Hunt 2008; Rieth et al. 2008; Schmid et al. 2019 Spriggs 1989; Spriggs and Anderson 1993; Wilmshurst et al. 2011). To develop the first model-based chronology for Yap, dates were first assigned to one of four classes following criteria outlined by Napolitano et al. (2019b; chapter 2), in which Class 1 dates are those that fulfill the most stringent requirements. Class 1 dates are those identified as belonging to short-lived terrestrial organisms, including plant and juvenile faunal remains that have adequately associated provenience (i.e., evidence of secure archaeological context that directly dates the associated event) and radiocarbon laboratory information (i.e., laboratory name and sample number). Unidentified charcoal or charred material and identified and/or culturally modified marine shell with sufficient provenience and laboratory information were assigned to Class 2. Dates missing contextual information, unidentified marine shell, were assigned to Class 3, while any dates that lack information necessary for class value assignment, along with those that were rejected by the original author(s), were assigned to Class 4. Radiocarbon dates reported as modern, from non-anthropogenic (i.e., paleoenvironmental), secondary contexts, or taken from bulk samples were assigned to Class 4 because they do not provide a direct date for a target event. Only dates belonging to Class 1 or 2 were selected for Bayesian modeling. When site or property names are not known, the village name was used.

Many of the existing radiocarbon samples for Yap were collected before $\delta^{13}C$ values were reported along with ^{14}C values despite their importance in understanding how dates are calibrated (Bayliss et al. 2015). In some cases, this information can be obtained through contacting the author or radiocarbon laboratory, although some laboratories have since closed or consider these data proprietary and so it is not always possible to obtain the values. As such, we have retained dates that did not have a $\delta^{13}C$ value or sample-specific $\delta^{13}C$. It is unknown if previously published $\delta^{13}C$ values presented in Table 4.1 are taken using IRMS or measured from AMS. Using offline IRMS to calculate $\delta^{13}C$ is considered more reliable for accurately correcting percent modern carbon (pMC) of ^{14}C data when compared to AMS and therefore should not be used for paleoenvironmental or dietary reconstruction (Prasad et al. 2019).

Table 4.1. Radiocarbon dates from Yap with class designation for chronometric hygiene.

Site/Village	Municipality	Class	Sample Material	Sample Type	Provenience	Lab Number	Radiocarbon Age	Error	$\delta^{13}C$ (‰)	$\delta^{18}O$ (‰)	Reference
Anoth	Gilman	4	*Quidnipagus palatam* Iredale	marine shell	Auger hole 2018-50-1, 195 cmbs	D-AMS 031805	3300	30	2.15	-1.59	this publication
Anoth	Gilman	4	*Gibberulus gibberulus*	marine shell	Auger hole 2018-50-2, 225 cmbs	D-AMS 031806	3623	30	3.74	-1.33	this publication
Anoth	Gilman	4	*Cypraea* sp.	marine shell	Auger hole 2018-50-3, 275 cmbs	D-AMS 031807	3175	33	2.04	0.75	this publication
Anoth	Gilman	4	*Mactra* sp.	marine shell	Auger hole 2018-51-1, 2450-250 cmbs	D-AMS 031808	3436	32	0.89	-0.43	this publication
Anoth	Gilman	4	*Gafrarium pectinatum*	marine shell	Auger hole 2018-51-2, 270-280 cmbs	D-AMS 031809	4226	33	2.41	-0.60	this publication
Anoth	Gilman	4	*Mactra luzonica*	marine shell	Auger hole 2018-51-3, 305-310 cmbs	D-AMS 031810	3225	34	0.84	-0.89	this publication
Anoth	Gilman	4	*Cerithium* sp.	marine shell	Auger hole 2018-51-4, 315-335 cmbs	D-AMS 031811	4699	33	0.98	-1.57	this publication
Balech'lee, Magachagil	Gilman	2	*Anadara antiquata*	marine shell	Auger hole 2019-39-1, 65-70 cmbs	D-AMS 038877	2055	22	-2.95	-3.31	this publication
Balech'lee, Magachagil	Gilman	2	*Anadara antiquata*	marine shell	Auger hole 2019-39-2, 95-105 cmbs	D-AMS 038878	1995	25	-2.60	-0.69	this publication
Balech'lee, Magachagil	Gilman	2	*Anadara antiquata*	marine shell	Auger hole 2019-39-3, 175-195 cmbs	D-AMS 038879	2123	23	-1.97	-2.73	this publication
Balech'lee, Magachagil	Gilman	2	*Anadara antiquata*	marine shell	Auger hole 2019-39-4, 300-305 cmbs	D-AMS 038880	2059	24	-0.28	-1.16	this publication
Boldanig, Malaj	Kanifay	3	charcoal	charcoal/charred material	36-42 inches	Crane M-631	320	200	—	—	Gifford and Gifford 1959: table 22
Boldanig, Malaj	Kanifay	3	*Lambis lambis*	marine shell	TP-1, Layer 4, -113 cm	N-4048	1460	490	—	—	Takayama 1980

Table 4.1, continued.

Site/Village	Municipality	Class	Sample Material	Sample Type	Provenience	Lab Number	Radiocarbon Age	Error	δ13C (‰)	δ18O (‰)	Reference
Boldanig-Wolom, Malaj	Kanifay	2	charcoal	charcoal/charred material	60-66 inches	Crane M-791	1110	200	—	—	Gifford and Gifford 1959: table 22
Dulul, Magachagil	Gilman	2	*Anadara antiquata*	marine shell	Auger hole 2019-29-1, 75-90 cmbs	D-AMS 038871	1716	22	-0.52	-0.1	this publication
Dulul, Magachagil	Gilman	2	*Quidnipagus palatam* Iredale	marine shell	Auger hole 2019-29-2, 155-170 cmbs	D-AMS 038872	592	22	1.51	-2.5	this publication
Dulul, Magachagil	Gilman	2	*Anadara antiquata*	marine shell	Auger hole 2019-29-3, 185-195 cmbs	D-AMS 038873	1519	22	-1.02	-2.8	this publication
Dulul, Magachagil	Gilman	2	*Quidnipagus palatam* Iredale	marine shell	Auger hole 2019-29-4, 250-255 cmbs	D-AMS 038874	1541	22	1.87	-2.5	this publication
Farchee, Gachpar	Gagil	2	charcoal	charcoal/charred material	Square 1, layer 1	NZ 6651	469	66	-26.2	—	Intoh and Leach 1985:Appendix C
Foqol swamp	Rull	4	peat	organic material	125-135 cm	Beta-74944	240	50	—	—	Dodson and Intoh 1999
Foqol swamp	Rull	4	peat	organic material	225-235 cm	Beta-74935	3340	80	—	—	Dodson and Intoh 1999
Foqol swamp	Rull	4	peat	organic material	330-340 cm	Beta-74936	5230	70	—	—	Dodson and Intoh 1999
Gachpar (C36-06-I/5)	Gagil	3	unidentified charcoal	charcoal/charred material	C36-06 I/5, 98-118 cmbs	AA-21204	362	45	-26.4	—	Descantes 1998
Gachpar (C36-22.1-II/2)	Gagil	3	unidentified charcoal	charcoal/charred material	C36-22.1 II/2, 85-95 cmbs	AA-21214	257	38	-25.1	—	Descantes 1998
Gachpar (C36-27-III/2)	Gagil	2	unidentified charcoal	charcoal/charred material	C36-27 III/2, 194-204 cmbs	AA-21211	1456	40	-26.7	—	Descantes 1998
Gachpar (C36-33-I/13)	Gagil	2	unidentified charcoal	charcoal/charred material	C36-22, I/9, 132-142 cmbs	AA-21209	504	38	-25.1	—	Descantes 1998
Gachpar (C36-33-I/19)	Gagil	2	unidentified charcoal	charcoal/charred material	C36-33 I/19, 196-210	AA-21208	1037	39	-28.7	—	Descantes 1998

Table 4.1, continued.

Site/Village	Municipality	Class	Sample Material	Sample Type	Provenience	Lab Number	Radiocarbon Age	Error	δ13C (‰)	δ18O (‰)	Reference
Gachpar (C36-33-I/5)	Gagil	2	unidentified charcoal	charcoal/charred material	C36-33 1/5, 52-62 cmbs	AA-21210	317	38	-27.5	—	Descantes 1998
Gachpar (C36-75.6-I/9)	Gagil	4	unidentified charcoal	charcoal/charred material	C36-75, hole 6, layer III, 110-140 cmbs	AA-21200	542	46	-25.7	—	Descantes 1998
Gachpar (C36-77-I/10)	Gagil	4	unidentified charcoal	charcoal/charred material	C36077 1/10, Feature A, 107-117,	AA-21216	335	62	-26.7	—	Descantes 1998
Gachpar (C36-77-I/9)	Gagil	4	unidentified charcoal	charcoal/charred material	C36-77 I/9, 97-107 cmbs	AA-21205	258	44	-27.9	—	Descantes 1998
Gachpar (C36-83.1-I/14)	Gagil	3	unidentified charcoal	charcoal/charred material	C36-83.1 1/14, Feature A, 140-150 cmbs	AA-21198	658	46	-27	—	Descantes 1998
Gachpar (C36-83.1-I/7)	Gagil	4	unidentified charcoal	charcoal/charred material	C36-83.1 1/7, 70-80 cmbs	AA-21207	842	54	-26.1	—	Descantes 1998
Gachpar (C36-83.2-II)	Gagil	4	unidentified charcoal	charcoal/charred material	C36-83.2 II/1, 16-43 cmbs	AA-21206	550	45	-27.3	—	Descantes 1998
Garingmog, Gachpar	Gagil	4	unidentified charcoal	charcoal/charred material	Square 1, layer 1	NZ 6676	<250	—	-26.9	—	Intoh and Leach 1985:Appendix C
Numurui, Gachpar (C36-16-II)	Gagil	3	unidentified charcoal	charcoal/charred material	C36-06 I/5, 98-118 cmbs	AA-21203	1825	66	-26.6	—	Descantes 1998
Mab oi, Nel	Kanifay	4	unidentified charcoal	charcoal/charred material	Square 1A, layer 2	NZ 6681	<250	—	-25.4	—	Intoh and Leach 1985:Appendix C
Mab oi, Nel	Kanifay	4	unidentified charcoal	charcoal/charred material	Square 1B, layer 4	NZ 6670	<250	—	-28.2	—	Intoh and Leach 1985:Appendix C
Magachagil	Gilman	2	Quidnipagus palatam Iredale	marine shell	Auger hole 2019-37-1, 45-60 cmbs	D-AMS 038875	441	21	0.82	-1.5	this publication
Magachagil	Gilman	2	marine shell	marine shell	Auger hole 2019-37-2, 190-210 cmbs	D-AMS 038876	430	19	2.15	-1.1	this publication

Table 4.1, continued.

Site/Village	Municipality	Class	Sample Material	Sample Type	Provenience	Lab Number	Radiocarbon Age	Error	δ13C (‰)	δ18O (‰)	Reference
Pemrang, Guror	Gilman	4	charcoal	charcoal/charred material	24-30 inches	Crane M-633	100	200, -100	—	—	Gifford and Gifford 1959: table 22
Pemrang, Guror	Gilman	4	charcoal	charcoal/charred material	18-24 inches	Crane M-632	250	400, -250	—	—	Gifford and Gifford 1959: table 22
Pemrang, Guror	Gilman	2	*Quidnipagus palatam* Iredale	marine shell	TU8, Spit 6, Layer 2	D-AMS 019904	621	30	1.94	-1.2	Napolitano et al. 2019
Pemrang, Guror	Gilman	3	carbonized endocarp	charcoal/charred material	TU8, Spit 6, 50-60 cmbs	YP-3	704	29	—	—	this publication
Pemrang, Guror	Gilman	2	*Quidnipagus palatam* Iredale	marine shell	TU8, Spit 2, Layer 1	D-AMS 019902	797	40	2.61	-1.3	Napolitano et al. 2019
Pemrang, Guror	Gilman	1	carbonized endocarp	charcoal/charred material	TU8, Spit 5, 40-50 cmbs	YP-2	1107	35	—	—	this publication
Pemrang, Guror	Gilman	2	*Quidnipagus palatam* Iredale	marine shell	TU8, Spit 5, Layer 1	D-AMS 019903	1175	35	-0.31	-1.6	Napolitano et al. 2019
Pemrang, Guror	Gilman	2	*Gafrarium pectinatum*	marine shell	TU8, Spit 10, Layer 2	D-AMS 019905	1520	43	0.95	-1.9	Napolitano et al. 2019
Pemrang, Guror	Gilman	3	*Tridacna* sp.	marine shell	TP-1, Layer 2, -160 cm	N-4047	1670	60	—	—	Takayama 1980
Pemrang, Guror	Gilman	3	*Tridacna* sp.	marine shell	TP-1, Layer 2, -120 cm	N-4046	1680	85	—	—	Takayama 1980
Pemrang, Guror	Gilman	3	*Tridacna* sp.	marine shell	TP-7, Layer 3, -168 cm	N-4038	1730	75	—	—	Takayama 1980
Pemrang, Guror	Gilman	3	*Tridacna* sp.	marine shell	TP-0, Layer 4, -182 cm	N-4051	1760	60	—	—	Takayama 1980
Pemrang, Guror	Gilman	4	bulk charcoal	charcoal/charred material	48-72 inches	Crane M-634	1780	250	—	—	Gifford and Gifford 1959: table 22
Pemrang, Guror	Gilman	3	*Tridacna* sp.	marine shell	TP-3, Layer 5, -170 cm	N-4049	1790	75	—	—	Takayama 1980
Pemrang, Guror	Gilman	3	*Tridacna* sp.	marine shell	TP-6, Layer 3, -174 cm	N-4050	1830	75	—	—	Takayama 1980
Pemrang, Guror	Gilman	3	*Tridacna* sp.	marine shell	TP-6, Layer 4, -210 cm	N-4037	1830	60	—	—	Takayama 1980

Table 4.1, continued.

Site/Village	Municipality	Class	Sample Material	Sample Type	Provenience	Lab Number	Radiocarbon Age	Error	δ13C (‰)	δ18O (‰)	Reference
Pemrang, Guror	Gilman	3	*Tridacna* sp.	marine shell	TP-3, Layer 7, -225 cm	N-4035	1950	75	—	—	Takayama 1980
Pemrang, Guror	Gilman	2	*Anadara antiquata*	marine shell	TU8, Spit 14, Layer 4	D-AMS 019907	1969	57	-0.41	0.13	Napolitano et al. 2019
Pemrang, Guror	Gilman	2	*Anadara antiquata*	marine shell	TU8, Spit 12, Layer 3	D-AMS 019906	2078	37	—	—	Napolitano et al. 2019
Pemrang, Guror	Gilman	3	*Tridacna* sp.	marine shell	TP-0, Layer 5, -260 cm	N-4036	2090	60	—	—	Takayama 1980
Pemrang, Guror	Gilman	2	*Anadara antiquata*	marine shell	TU8, Spit 16, Layer 4	D-AMS 019908	2161	57	0.01	-0.2	Napolitano et al. 2019
Pemrang, Guror	Gilman	3	*Trochus* sp.	marine shell	TP-3, Layer 9, ca. 3 meters	N-4034	2310	80	—	—	Takayama 1980
Pemrang, Guror	Gilman	2	*Anadara antiquata*	marine shell	TU8, Spit 27, Layer 5	YP-1	2500	30	—	—	this publication
Pemrang, Guror	Gilman	2	*Tridacna maxima* adze	marine shell	TU8, Spit 26, Layer 5	D-AMS 019909	2592	58	—	—	Napolitano et al. 2019
Pemrang, Guror	Gilman	2	unidentified charcoal	charcoal/charred material	TU8, Spit 10, 90-100 cmbs	YP-4	1467	29	—	—	this publication
Pemrang, Guror	Gilman	2	unidentified charcoal	charcoal/charred material	TU8, Spit 14, 130-140 cmbs	YP-6	1901	30	—	—	this publication
Pemrang, Guror	Gilman	2	unidentified charcoal	charcoal/charred material	TU8, Spit 16, 150-160 cmbs	YP-7	1844	29	—	—	this publication
Pemrang, Guror	Gilman	1	carbonized endocarp (*Cocos nucifera*)	charcoal/charred material	TU8, Spit 20, 190-200 cmbs	YP-8	1939	29	—	—	this publication
Pemrang, Guror	Gilman	2	unidentified charcoal	charcoal/charred material	TU8, Spit 25, 240-250 cmbs	YP-9	2298	30	—	—	this publication
Pemrang, Guror	Gilman	2	unidentified charcoal	charcoal/charred material	TU8, Spit 24, 230-240 cmbs	YP-10	2122	35	—	—	this publication
Pemrang, Guror	Gilman	2	charcoal	charcoal/charred material	TU 10, Spits 21-23	S-ANU-57910	1923	22	-25	—	this publication
Pemrang, Guror	Gilman	2	charcoal	charcoal/charred material	TU 10, Spit 20	S-ANU-57911	1946	22	-25	—	this publication
Pemrang, Guror	Gilman	2	*Anadara antiquata*	marine shell	Auger hole 2017-14-1	D-AMS 026457	2114	26	—	—	this publication
Pemrang, Guror	Gilman	2	nut endocarp	charcoal/charred material	Auger hole 2017-2-1, 3.2-3.3, Layer 5	S-ANU-57912	2239	22	-25	—	this publication

Table 4.1, continued.

Site/Village	Municipality	Class	Sample Material	Sample Type	Provenience	Lab Number	Radiocarbon Age	Error	δ13C (‰)	δ18O (‰)	Reference
Pemrang, Guror	Gilman	2	*Anadara antiquata*	marine shell	TU10, Spits 21-23	D-AMS 026548	2344	28	—	—	this publication
Pemrang, Guror	Gilman	4	*Tridacna* sp.	marine shell	TP-1, Layer 1, -45 cm	N-4045	modern	—	—	—	Takayama 1980
Penin, Kanif	Dalipebinau	4	charcoal	charcoal/charred material	24-30 inches	Crane M-629	200	200	—	—	Gifford and Gifford 1959: table 22
Rugog's grave, Merur	Tamil	4	charcoal	charcoal/charred material	20 inches	Crane M-626	200	200	—	—	Gifford and Gifford 1959: table 22
Rungluw, Anoth	Gilman	2	charcoal	charcoal/charred material	Square 1, layer 2	NZ 6625	507	133	-25	—	Intoh and Leach 1985:Appendix C
Rungluw, Anoth	Gilman	2	charcoal	charcoal/charred material	Square 1, layer 3	NZ 6668	1905	65	-25.7	—	Intoh and Leach 1985:Appendix C
Rungluw, Anoth	Gilman	4	charcoal	charcoal/charred material	Square 2, layer 2	NZ 6667	<250	—	-24.8	—	Intoh and Leach 1985:Appendix C
Rungluw, Anoth	Gilman	4	charcoal	charcoal/charred material	Square 2, layer 4	NZ 6645	<250	—	-26.5	—	Intoh and Leach 1985:Appendix C
Thoqol swamp	Tamil	4	peat	organic material	120-130 cm	Beta-74939	140	70	—	—	Dodson and Intoh 1999
Thoqol swamp	Tamil	4	peat	organic material	210-220 cm	Beta-74940	260	60	—	—	Dodson and Intoh 1999
Thoqol swamp	Tamil	4	peat	organic material	325-335 cm	Beta-74941	2320	60	—	—	Dodson and Intoh 1999
Toru anibin, Gitam	Rull	4	charcoal	charcoal/charred material	Square 1, layer 1	NZ 6630	<250	—	-24.8	—	Intoh and Leach 1985:Appendix C
Toru anibin, Gitam	Rull	4	charcoal	charcoal/charred material	Square 1, layer 3	NZ 6650	<250	—	-26.5	—	Intoh and Leach 1985:Appendix C
Toru anibin, Gitam	Rull	3	charcoal	charcoal/charred material	Square 1, layer 4	NZ 6644	285	40	-26.2	—	Intoh and Leach 1985:Appendix C
Toru anibin, Gitam	Rull	4	charcoal	charcoal/charred material	Square 1, layer 5	NZ 6678	<250	—	-26.3	—	Intoh and Leach 1985:Appendix C

Table 4.1, continued.

Site/Village	Municipality	Class	Sample Material	Sample Type	Provenience	Lab Number	Radiocarbon Age	Error	δ13C (‰)	δ18O (‰)	Reference
Toru anibin, Gitam	Rull	4	charcoal	charcoal/charred material	Square 2, layer 2	NZ 6669	<250	—	-26.2	—	Intoh and Leach 1985:Appendix C
Toru anibin, Gitam	Rull	4	charcoal	charcoal/charred material	Square 2, layer 3	NZ 6661	<250	—	-26.4	—	Intoh and Leach 1985:Appendix C
Toru anibin, Gitam	Rull	2	charcoal	charcoal/charred material	Square 2, layer 6	NZ 6680	364	54	-26.1	—	Intoh and Leach 1985:Appendix C

Bayesian modeling

After dates were assigned a class value using chronometric hygiene criteria, those belonging to Classes 1 and 2 were selected for Bayesian modeling. Following other recent studies that use Bayesian approaches to model early settlement on islands, we use Class 1 and 2 dates from the available inventory to model Yap's early occupation (e.g., Burley et al. 2015; Dye 2015; Fitzpatrick and Jew 2018; Rieth and Athens 2019; see also chapter 2).

Applications of Bayesian modeling in archaeology vary, although it is most often used for calibrating radiocarbon dates. Archaeologists now routinely employ Bayesian modeling of radiocarbon datasets because they produce more statistically robust calibrations. Bayesian models incorporate three parameters: *prior*, *likelihood*, and *posterior*. The *prior* is any information or observations that are inferred before any data are collected or processed (e.g., stratigraphy), the *likelihood* is information obtained from the calibrated radiocarbon date range. The posterior is the estimated calendar date range presented probabilistically as the highest posterior density (HPD) region based on the relationship between the prior and likelihood that have been built into the model (Bronk Ramsey 2009a). As a result, Bayesian modeling is particularly useful for creating predictive models for undated archaeological contests, like the beginning, duration, or end of a specified event.

Class 1 and 2 dates were calibrated in Oxcal v4.4.4 with all uncalibrated conventional radiocarbon ages grouped as a single *phase* regardless of stratigraphy using the Marine20 and IntCal20 calibration curves (Heaton et al. 2020; Reimer et al. 2020). To explore the potential influence of a ΔR, marine shell dates were calibrated with a ΔR of 0 years, our modeled ΔR of −1 ± 128 ^{14}C years (see below), and a ΔR of 218 ± 57 ^{14}C years, the latter of which was calculated for *A. antiquata* at Bapot-1, Saipan (Petchey et al. 2017). Although this ΔR was calculated using the Marine13 calibration curve (Reimer et al. 2013), this positive ΔR value allows us to compare the fit of the models to our modeled negative ΔR.

Given that many dates are on unidentified charcoal and that there are multiple long-lived trees on Yap (i.e., >75 years) and the potential for driftwood to be collected and burned as fuel, radiocarbon dates on preserved wood may include an unknown inbuilt age (Allen and Huebert 2014; Falanruw 2015). To address this, we calibrated dates on unidentified carbon using a 100-year Exponential Outlier model that was added using the Charcoal Outlier model function in OxCal (Dee and Bronk Ramsey 2014). The outlier model assumes that the correct age of the modeled event is younger than the radiocarbon date and produces a younger result (Dee and Bronk Ramsey 2014). There are no dates from human or animal bone in the present database so mixed dietary ratios are not needed for any of the calibrations presented here.

To add more prior information to constrain the model, we added radiocarbon dates from Fais, one of Yap's outer islands, as *termini ante quem* (TAQ). Two dated carbon fragments (1794 ± 152 ^{14}C years [NUTA2167] and 1775 ± 73 ^{14}C years [NZ885]), found in association with calcareous sand tempered pottery and metamorphic stone both sourced to Yap, demonstrate that people were already living there and producing locally-made pottery that was exchanged with the outer islands (Intoh 2017; Intoh and Shigehara 2004).

All Bayesian-modeled dates were rounded outward to the nearest 5 years using OxCal's round function and presented in italics (Bronk Ramsey 2009a; Hamilton and Krus 2018). The 95.4% HPD probabilities for these colonization estimates and model agreement index (A_{model}) and overall agreement index ($A_{overall}$) are provided. Indices over 60 are considered an acceptable fit for the model parameters and the dates (Bronk Ramsey 2009a). There were no Class 1 or 2 dates with large standard errors (≥100 years), although these dates would still be eligible for modeling. Dates with large standard errors were not excluded from modeling because, although imprecise, they are accurate and can improve the robusticity of Bayesian models (Hamilton and Krus 2018).

Results

Modeling ΔR

Using stratigraphically associated shell and charcoal dates grouped by layers, our model produced a ΔR of −1 ± 128 ^{14}C yrs with a A_{model} agreement of 99.5 and an $A_{overall}$ agreement of 99.7 (Figure 4.3; Appendix C: Tables 1 and 2, Supplemental text). When the ΔR for *A. antiquata* from Saipan was applied to the model, the MCMC failed to converge and produced a A_{model} agreement of 33.4 and $A_{overall}$ agreement of 26.2, both well below the acceptable threshold of 60 (Appendix C: Supplemental text). These results suggest that the modeled ΔR produced by our model is more appropriate than a strong positive ΔR.

Radiocarbon ages

We present 31 new radiocarbon dates from Gilman municipality (Table 4.1). AMS dates from Pemrang reported in this paper indicate that Pemrang is a multicomponent site used for more than 2000 years. A date on a *Tridacna maxima* shell adze (D-AMS 19909, 2592 ± 58 ^{14}C yrs) produced the oldest cultural radiocarbon date for Yap, which was recovered from 2.7 m below the surface and just above the water table (Napolitano et al. 2019a). Although the use of subfossil shells as tools can be a problem for radiocarbon dating (Rick et al. 2005), associated dates on charcoal support the age of the adze (Table 4.1). Additional samples from Pemrang support the radiocarbon age of the adze, but older deposits were not located.

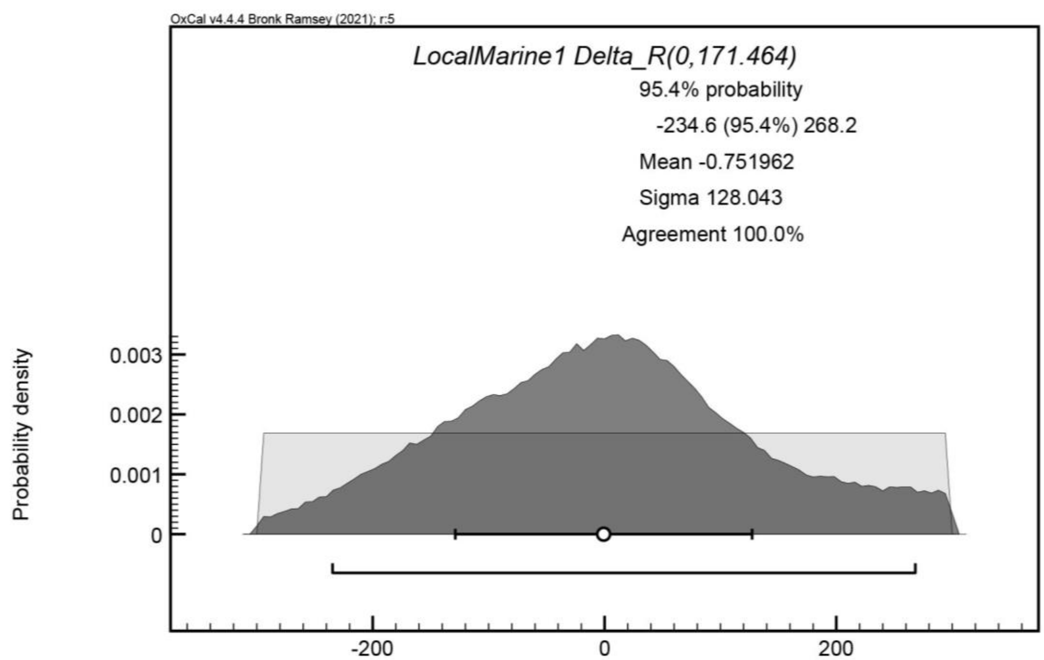

Figure 4.3. Modeled ΔR results.

Two sets of dates from Balech'lee (AH2019-39) and Dulul (AH2019-27) were selected because features were identified in each of these locations during the auger survey. The feature layers in each area, situated ca. 100 m apart, were similar and contained burned organics, shell, CST pottery, and clay, which is not naturally found in this area. The samples from Balech'lee, all from *A. antiquata,* produced dates that were ca. 2000 years old. The statistical overlap in the radiocarbon ages were unexpected given that the dates span ca. 2.5 m in depth and suggests a rapid deposit in this area. The dates from Dulul were younger, but indicate some stratigraphic reversal, which may be a product of the auger survey or site taphonomy.

When calibrated with the modeled ΔR, noncultural dates from AH2018-50 calibrate to 3790-2740 cal BP and the dates from AH2018-51 calibrate to 5220-2740 cal BP (Table 4.2). These augers were located to the north, near the transition from alluvium (i.e., sandy beach) to upland soils underlain by Tomil volcanics (Shade et al. 1992). We dated these samples with the assumption that the death of these mollusks correlates to when this area was an intertidal zone and were not subfossil shells. These dates function as a proxy to understanding former sea-level positions. Although the calibrations will likely shift when a more precise ΔR is established for each species and the Late Holocene, the calibrated dates establish a general baseline to understand that sea-level change.

Stable isotope analysis

Isotopic values varied widely with $\delta^{13}C$ values that ranged from a depleted value of −2.95‰ to an enriched value of 3.74‰ (average = 0.65‰ ± 1.72‰, n = 23) (Table 1). $\delta^{18}O$ were uniformly depleted and ranged from a strong negative value of −3.31‰ to slightly depleted value of −0.06‰ (average = −1.37‰ ± 0.92‰). *A. antiquata* had uniformly depleted $\delta^{13}C$ values and $\delta^{18}O$ values (average = −1.21‰ ± 1.14‰ and −1.34‰ ± 1.38‰, respectively, n = 8). At Balech'lee, where only *A. antiquata* were sampled, all were depleted in $\delta^{13}C$ and $\delta^{18}O$, suggesting that they were collected from an area subjected to warmer, less saline estuarine waters. *A. antiquata* from Pemrang had more enriched $\delta^{13}C$ values than at Balech'lee, but were still depleted compared to the local average. Values for *A. antiquata* were the most depleted in $\delta^{13}C$ out of all the samples in the study, which was expected given their habitat preference for seagrass beds and shallow lagoons and their predicted susceptibility to hardwater (Tebano and Paulay 2000). Both the high and low $\delta^{18}O$ values were also from *A. antiquata*.

Table 4.2. Calibrated noncultural radiocarbon dates from AH2018-50 and AH2018-51.

Name	Unmodelled (BP)		
	from	to	%
Curve Marine20			
Delta_R LocalMarine	-258	256	95.449974
R_Date D-AMS 031805	3340	2660	95.449974
R_Date D-AMS 031806	3720	2980	95.449974
R_Date D-AMS 031807	3190	2450	95.449974
R_Date D-AMS 031808	3450	2770	95.449974
R_Date D-AMS 031809	4510	3740	95.449974
R_Date D-AMS 031810	3240	2510	95.449974
R_Date D-AMS 031811	5140	4360	95.449974

Overall, $\delta^{13}C$ values for *Q. palatam* were the closest to isotopic equilibrium with the present-day average, exhibiting a slightly enriched average (1.51‰ ± 0.97‰, n = 7), but with depleted $\delta^{18}O$ values compared to the overall average (−1.75‰ ± 0.53‰). Compared to the other taxa in this study, the isotopic values of *Q. palatam* are unique in that they indicate a preference for a more marine environment, but warmer, less saline water. These values are notably different from $\delta^{13}C$ values obtained by Petchey et al. (2018) at Bapot-1 in Saipan. They attributed depleted $\delta^{13}C$ values to deposit-feeding behavior, but it does not appear to have the same influence on mollusks from Yap.

G. pectinatum exhibited averaged enriched $\delta^{13}C$ values (1.68‰ ± 1.03‰) and depleted $\delta^{18}O$ values (−1.27‰ ± 0.95‰), but these were based on a small sample size (n=2). When considered individually, one shell from Pemrang (UGAMS-52320) appears to be "estuarine" (i.e., depleted) and the other shell, collected from a nonanthropogenic context in Anoth village (AH2018-51) (UGAMS-52304), has a "marine" $\delta^{13}C$ value (i.e., enriched). Rather than this species occupying diverse habitats, the different isotopic values likely reflect differential dissolved inorganic carbon (DIC) uptake within their preferred habitat (Petchey et al. 2018:189). Petchey et al. (2018) note a difference of ca. 250 ^{14}C years between *G. pectinatum* with similar isotopic signatures; therefore, it is possible that the ^{14}C ages do not reflect the true age of the shell.

Overall, gastropods exhibited a range of $\delta^{13}C$ values with enriched values for *G. gibberulus* and *Cypraea* sp., indicating a preference for productive marine environments and warmer, less saline waters. *Mactra* sp. and *Cerithium* sp. exhibited slightly depleted $\delta^{13}C$ values, indicating a preference for a slightly estuarine habitat with less saline water.

Chronometric hygiene and Bayesian modeling

A literature review identified 61 previously published radiocarbon dates, bringing our total to 92 (Table 4.1). Although we increased the number of radiocarbon dates from Yap by 50%, the total number of dates is still relatively small considering the fact that archaeologists have worked on Yap since the 1950s. Nearly half the dates (n = 43, 43.4%) were sampled from mollusks. Most of the dates (n = 36, 38.7%) are from Pemrang, located in the village of Guror in Gilman municipality (Figure 4.2). Only two dates were assigned to Class 1, a fragment of carbonized coconut (*Cocos nucifera*) endocarp and one carbonized nut endocarp (see Table 4.1). Coconut is a well-documented ethnobotanically useful plant as all parts were utilized for water, food, oil, building material, textiles, and medicine (see Summerhayes 2018). Although YP-3 was identified as nut endocarp, its ^{14}C age is anomalously young given that it was recovered from Level 2 at Pemrang. Accordingly, we have assigned this date as Class 3. Fifty-two (56%) dates were rejected from analysis as Class 3 or 4. The previously reported dates from Pemrang were rejected because it is unclear if the dates were corrected or were sampled from multiple fragments of charcoal (Gifford and Gifford 1959; Takayama 1982). The oldest date from the site (M-634, 1780 ± 250 ^{14}C yrs) was produced from four pieces of charcoal each taken from a different level (Gifford and Gifford 1959:195). Many of the Gachpar dates, taken from charcoal from below *dayif* (hexagonal stone house platform constructions), were from secondary deposits and therefore do not directly date the target event, although they are still valid for understanding site development processes (Descantes 2005). Paleoenvironmental and other noncultural dates from this paper were also omitted from Bayesian modeling, although they are important for developing baseline data to estimate paleoshoreline location.

Table 4.3. Results of single-phase Bayesian model of Class 1 and 2 dates.

Name	Unmodelled (BP)			Modelled (BP)			Indices Amodel 116.8 Aoverall 67.2				
	from	to	%	from	to	%	Acomb	A	L	P	C
Outlier_Model Charcoal				-135	5	95.449974					99.8
Exp(1,-10,0)	-3.19	-0.05	95.449974								100
U(0,2)	1.99E-17	2	95.449974	2.69E-17	2	95.449974		100			97.5
Sequence											
Boundary Yap Start				2450	2165	95.449974					99.5
Phase											
Curve Marine20											
Delta_R LocalMarine	-258	256	95.449974	-179	247	95.449974		107.4			99.6
R_Date D-AMS 019909	2480	1710	95.449974	2320	1735	95.449974		108.6			99.7
R_Date YP-1	2330	1635	95.449974	2255	1635	95.449974		105.5			99.7
R_Date D-AMS 026548	2145	1445	95.449974	2055	1445	95.449974		105.7			99.6
Curve IntCal20											
R_Date YP-9	2360	2160	95.449974	2350	2090	95.449974		66.1			99.5
R_Date S-ANU-57912	2335	2150	95.449973	2325	2150	95.449974		101.5			99.9
Curve Marine20											
Delta_R LocalMarine	-258	256	95.449974	-270	222.5	95.449974		102.3			99.5
R_Date D-AMS 019908	1935	1260	95.449974	1940	1275	95.449974		100.8			99.6
R_Date D-AMS 038879	1870	1245	95.449974	1875	1260	95.449974		100.7			99.5
Curve IntCal20											
R_Date YP-10	2300	1990	95.449974	2295	1900	95.449973		102			99.8
Curve Marine20											
Delta_R LocalMarine	-258	256	95.449974	-312.5	214.5	95.449974		99.6			98.8
R_Date D-AMS 026457	1865	1235	95.449974	1910	1265	95.449974		97.9			99.3
R_Date D-AMS 019906	1815	1180	95.449974	1875	1230	95.449974		98.1			99.5
R_Date D-AMS 038880	1795	1170	95.449974	1850	1215	95.449974		98.4			99.3
R_Date D-AMS 038877	1790	1165	95.449974	1830	1195	95.449974		98.5			99.4
R_Date D-AMS 038878	1715	1090	95.449974	1765	1145	95.449974		100.7			99.4
R_Date D-AMS 019907	1710	1045	95.449974	1750	1090	95.449974		101.3			99.4
Curve IntCal20											
R_Date S-ANU-57911	1945	1795	95.449974	1940	1710	95.449974		99.5			99.7
R_Date YP-8	1940	1745	95.449974	1940	1745	95.449974		99.8			99.9
R_Date S-ANU-57910	1925	1745	95.449974	1925	1685	95.449974		99.5			99.7
R_Date NZ 6668	1995	1635	95.449974	1985	1610	95.449974		100			99.8
R_Date YP-6	1890	1725	95.449974	1915	1645	95.449974		99.5			99.9
R_Date YP-7	1830	1640	95.449974	1830	1595	95.449974		99.6			99.7
Delta_R LocalMarine	-258	256	95.449974	-274	279.5	95.449974		99.7			93.1
R_Date D-AMS 038871	1920	1345	95.449973	1935	1300	95.449974		100.1			92.3
R_Date D-AMS 038874	1715	1175	95.449974	1725	1175	95.449974		99.1			93.1

Table 4.3, continued.

Name	Unmodelled (BP)			Modelled (BP)			Indices Amodel 116.8 Aoverall 67.2				
	from	to	%	from	to	%	Acomb	A	L	P	C
R_Date D-AMS 019905	1715	1175	95.449974	1735	1185	95.449974		100.1			93.9
R_Date D-AMS 038873	1705	1175	95.449974	1715	1180	95.449973		98.9			92.7
Curve IntCal20											
R_Date YP-4	1390	1300	95.449974	1400	1210	95.449974		99.6			99.8
R_Date AA-21211	1400	1295	95.449974	1405	1195	95.449974		99.7			99.8
Curve Marine20											
Delta_R LocalMarine	-258	256	95.449974	-271	260.5	95.449974		97.4			99.5
R_Date D-AMS 019903	870	320	95.449974	870	320	95.449974		100.1			99.6
Curve IntCal20											
R_Date YP-2	1175	925	95.449974	1175	925	95.449974		99.8			99.9
R_Date AA-21208	1060	800	95.449974	1055	780	95.449974		99.8			99.8
Curve Marine20											
Delta_R LocalMarine	-258	256	95.449974	-239.5	196	95.449974		106.2			99.7
R_Date D-AMS 019902	480	...	95.449974	515	45	95.449974		102.6			99.8
Curve IntCal20											
R_Date YP-3	685	560	95.449973	685	560	95.449973		98.3			100
Curve Marine20											
Delta_R LocalMarine	-258	256	95.449974	-303	38.5	95.449974		89.4			99.7
R_Date D-AMS 019904	125	...	95.449974	420	10	95.449974		81			99.9
R_Date D-AMS 038872	70	...	95.449974	385	-5	95.449974		81			99.8
Curve IntCal20											
R_Date NZ 6625	725	155	95.449974	710	240	95.449974		100.8			99.8
R_Date AA-21209	625	495	95.449974	625	380	95.449973		99.6			99.8
R_Date NZ 6651	635	315	95.449974	630	290	95.449974		100			99.8
Curve Marine20											
Delta_R LocalMarine	-258	256	95.449974	-401.5	-98	95.449974		33			99.8
R_Date D-AMS 038875	245	...	95.449974	340	-5	95.449974		59.2			99.8
R_Date D-AMS 038876	245	...	95.449974	330	-5	95.449974		60.2			99.8
Curve IntCal20											
R_Date NZ 6680	505	305	95.449974	510	245	95.449974		100			99.9
R_Date AA-21210	475	300	95.449974	480	235	95.449974		100.1			99.9
Boundary Yap End				260	-120	95.449974					99.4
Before Fais pottery	...	-77.75	95.449974								
R_Date NUTA2167	2095	1365	95.449973	2095	1365	95.449974		100			99.7

The single-phase Bayesian model produced a modeled colonization estimate of *2450-2165 cal years BP (95.4% HPD)* (Table 4.3; Appendix C: Supplemental Material Table 3, Supplemental text, Supplemental Material Figure 1). The modeled estimate potentially extends the earliest unequivocal dates for human settlement of Yap by centuries, but is still much younger than both Palau and the Mariana Islands, as well as the paleoenvironmental evidence from Yap.

Discussion

Radiocarbon dates

The small radiocarbon inventory reflects the lack of systematic fieldwork on Yap. Radiocarbon dates from excavations at Pemrang extend the oldest date of human settlement by ca. 200 years (Napolitano et al. 2019a). However, additional samples did not produce substantially older dates. Expanded excavation at Pemrang yielded samples taken from below the water table were younger than expected, dating to ca. 1800-2000 BP (2 σ), and suggests that the part of the island where Pemrang is located was not a stable landform until ca. 2200 years ago and was likely subjected to shifting prograding sediments, storm surges, and king tides.

Excavation adjacent to the auger hole at Balech'lee produced turtle and shark/ray bone, a preserved portion of a CST pot and, approximately 50 cm below that, a partially burned clay floor with nine circular voids of various diameters. In addition, a small, thin, red-painted rim sherd was recovered from 60-70 cmbs. A radiocarbon date from the same depth (D-AMS 38877, 2055 ± 22 ^{14}C yrs) returned a modeled calibrated date of *1840-1210 cal yrs BP (95.4% HPD)*. Red-painted pottery is extremely rare on Yap with only four small sherds having been identified by previous archaeologists at Pemrang (Gifford and Gifford 1959; Napolitano et al. in prep). Unlike Pemrang, which has clearly stratified shell midden deposits with CST pottery only recovered from the lower *A. antiquata* midden, CST pottery was recovered at Balech'lee throughout the entire excavation, as was the absence of Yapese plain and laminated wares. This is notable because Yapese plain and CST pottery are considered contemporaneous types; however, at sites in southern Yap CST pottery is rarely recovered with Yapese plain in large numbers (Napolitano et al. 2019a). The partially burned clay floor is ca. 5-10 cm thick. There was also the presence of significant quantities of turtle bone, which was unexpected given that this is typically a high-status food reserved for chiefly consumption and distribution or consumed by outer islanders (Takayama 1982:90-91; Ushijima 1982). If the clay floor at Balech'lee is related to a structure for high-ranking males, it is possible that this was part of a men's house (*faluw*), which is typically found along coastal margins to protect the villages from outside threats (Craib and Price 1978; Cordy 1986; Intoh and Leach 1985; Nunn et al. 2017). These structures function in part as a meeting place to receive visitors and for men to sleep. In some coastal villages, *faluw* are built on top of small artificially constructed stone and coral islands (Furness 1910; Nunn et al. 2017). The similarities in features identified in Balech'lee and Dulul suggest that both areas may have been related to a meeting house structure or other type of activity area.

Stable isotopes

Based on the depleted $\delta^{13}C$ values, we suggest that *A. antiquata* are likely influenced by hardwater. *A. antiquata* are very sensitive to environmental change and will die before major changes can be recorded in their isotope values (Davenport and Wong 1986; Petchey et al. 2018; Spennemann 1987:83), which suggests that variation in their $\delta^{13}C$ reflects diet or hardwater rather than changes in habitat. Paleoclimate studies indicate that $\delta^{18}O$ of surface waters in the Western Tropical Pacific were more depleted than modern values (LeGrande and Schmidt 2009: Figure 6), but the $\delta^{18}O$ in *A. antiquata* are still depleted from these levels. At present, it is currently unclear how this may be influencing the ^{14}C age of these shells, but it is likely that *A. antiquata* will require a species specific ΔR and is a topic for future study.

More work is needed to investigate the reliability of radiocarbon dating gastropods in Yap. Petchey et al.'s (2012) study of ^{14}C marine reservoir variability in Caution Bay, Papua New Guinea found that one species of the Cerithioidea family, *Cerithium largillierti* (now referred to as *Cerithideopsis largillierti*), exhibited a wide range of $\delta^{13}C$ values, indicating both estuarine and marine resources with a large amount of variability in ΔR values for this species. Accordingly, this species was determined to be unreliable for radiocarbon dating (Petchey et al. 2012). However, unlike southern Yap, Caution Bay contains underlying limestone geology and is notable for hydrological and geological diversity that contributes to inter- and intra-species variability in ΔR values (Petchey et al. 2012, 2013) so it is possible that there will not be as much ΔR variability in Yapese samples. However, until this can be studied in more detail, the radiocarbon dates on gastropods from Yap must be interpreted cautiously. Depleted isotopic values for *G. gibberulus* are expected given their habitat preference. The $\delta^{18}O$ value was below the modeled values for the Late Holocene, but not as extreme as Late Holocene samples from Palau's Rock Islands, which reflects the importance of understanding local conditions (Dodrill et al. 2018; LeGrande and Schmidt 2009: Figure 6).

It is notable that the nonanthropogenic samples from AH2018-50 produced enriched $\delta^{13}C$ values well above the local average. Identified between two layers of gley, the stratigraphy of this deposit suggests that this area was a boggy intertidal zone. $\delta^{13}C$

values support the idea that this area was an intertidal/reef area where increased productivity and CO_2 atmospheric absorption produced enriched values. The samples from AH2018-51, located southeast from AH2018-50, were slightly depleted in $\delta^{13}C$ except for one *G. pectinatum* sample that was enriched and likely reflects the diet of this species. These samples were uniformly depleted in $\delta^{18}O$, suggesting a preference for slightly warmer, less saline waters than present day and may suggest that this area was subjected to terrestrial influences or sources of freshwater. Green schist and shell from the auger both appeared to be water-rolled and suggests that there may have been a freshwater output in this area from further inland as schist is not naturally occurring in Tomil volcanic formation.

Evidence for sea-level change and implications for early human settlement

Data from paleoreefs in the Mariana Islands suggest that in western Micronesia there was a sea-level highstand ca. 3200 years ago, after which there was a drawdown beginning ca. 2500 years ago, although this has not been empirically demonstrated for Yap (Dickinson 2003; Dickinson and Athens 2007). Higher sea-levels on Yap are inferred by a paleonotch above modern sea level on a small limestone formation off the coast of southern Yap. Further evidence for a sea-level highstand is suggested by Yapese oral histories which state that long ago, people living in the interior of Yap built up the southern part of the island to reclaim it from the sea, which was then occupied (Francis Reg, personal communication). The noncultural and cultural radiocarbon dates presented in this study lend support to these lines of evidence. The calibrated radiocarbon dates from AH2018-50 and AH2018-51 indicate that these areas were intertidal zones ca.

5000-2700 years ago, around 300-400 m inland from the current shoreline. A regional sea-level drawdown beginning ca. 2500 years ago would have exposed sandy beach flats adjacent to productive coral reef habitats and been desirable places to live. The oldest radiocarbon dates from Balech'lee, Pemrang, and Rungluw all indicate that people were living in the area by ca. 2200-2000 years ago. If future excavation at Balech'lee confirms that this structure is a *faluw*, and excavation at Dulul reveals similar structural evidence, then it is possible that this demonstrates a southern seaward progression of community structures following sea-level drawdown sometime after 2500 years ago. The practice of positioning or relocating *faluw* and *chabog* in response to sea-level change persists today on Yap and has been interpreted as a culturally grounded response to "confront" threats to Yapese identity and way of life (Furness 1910; Lingenfelter 1975; Nunn et al. 2017:966).

The shell midden excavation of Test Unit 8 at Pemrang also provides some insight on shifting habitat over time. In the older midden, between 120-160 cmbs, *A. antiquata* shells comprised the majority of the shell matrix, suggesting that an estuarine mangrove habitat was located near the site (Napolitano et al. 2019a). The younger shell midden was comprised mostly of small gastropods like *G. gibberulus* with small amounts of bivalves like *Q. palatam*, both of which prefer different habitats like sandy seagrass beds. Future detailed isotopic analysis of these taxa should help provide more details on paleoclimatic and paleoenivonmental conditions in the area.

There are currently three excavated sites in southern Yap which date to ca. 2000 years ago. With the new dates from Pemrang, Balech'lee, and previously published dates from Rungluw, we have a reasonably clear picture that settlement was extensive, yet is unlikely to pre-date ca. 2200-2000 years ago.

Thus far, there is little new evidence to suggest that Yap was settled contemporaneously with Palau and the Mariana Islands. The question remains, however, is if this interpretation is biased by the lack of systematic fieldwork or if Yap was, in fact, settled nearly a millennium after Palau and the Mariana Islands. If sea-level in southern Yap were higher until ca. 2500 years ago, then early settlement would have been located further inland or possibly in another part of the island. Our auger survey in the Tomil volcanic section of southern Yap, topographically higher than the alluvium section, did not produce any cultural material. In addition, Yapese oral traditions refer to the oldest settlements as being in the northern part of the islands. The possibility also remains that Yap was settled significantly later in time than the other major archipelagos in western Micronesia. If a later settlement date continues to be supported by archaeological evidence, it will be necessary to consider what factors may explain a relatively late colonization date considering that people were moving throughout western Micronesia by 3200 years ago.

Conclusions

We have compiled a total of 92 radiocarbon dates from Yap, including 31 new dates that increased the number available by 51%. After chronometric hygiene and Bayesian-modeling, we now have a colonization estimate for Yap of *2450-2165 cal years BP (95.4% HPD)*. When contextualized with regional evidence for a sea-level drawdown ca. 2500 years ago (e.g., Dickinson 2003; Dickinson and Athens 2007), evidence suggests that Yap was not settled until ca. 2500-2100 years ago, but that earlier sites could still be located elsewhere on the island (possibly the northern half), as suggested by Yapese oral traditions.

To produce a more accurate modeled chronology, we calculated a hypothetical ΔR of -1 ± 128 ^{14}C yrs. Isotopic analysis indicates that, like elsewhere in western Micronesia, *A. antiquata* is likely influenced by hardwater and will require its own ΔR despite the lack of limestone substrate in Yap. A more intensive excavation and dating program will be needed to investigate this further, however, so that more temporally specific and species-specific ΔRs can be established. However, by comparing our modeled ΔR with a strong positive ΔR developed for Saipan, it appears as though a negative offset to the modeled global average is appropriate for sites in southern Yap where the majority of dates presented here derive from. When results from the sites of Pemrang (Napolitano et al. 2019a) and Balech'lee are combined with that of Rungluw (Intoh and Leach 1985), we now have more robust evidence that settlement in southern Yap was more extensive than previously thought. Newly recovered data from our systematic auger survey also help establish an important baseline for understanding sea-level change over the last 3000 years though additional work is needed to better understand nuances involved with landscape development and site formation processes as they relate to human occupation.

In a recent publication, Hutchinson (2020) cautions against dating marine and estuarine shell because of the potential to produce ^{14}C ages that do not reflect the true date of the organism's death. However, as Thomas (2015) noted, archaeologists in Australia and the Pacific have demonstrated how it is possible to deal with the uncertainties of radiocarbon dating shell (e.g., Petchey 2009; Petchey and Clark 2010, 2011, 2021; Petchey et al. 2012, 2013, 2017, 2018; Ulm 2006). Doing so requires carefully selecting samples from adequate contexts and understanding how a mollusks diet and habitat preference may influence the ^{14}C age and potential inter- and intra-species variation in ΔR by looking at ^{14}C age, $\delta^{13}C$, and $\delta^{18}O$ values. Our study presents a first attempt at identifying how local conditions may influence the calibration of radiocarbon dates and understanding paleoclimatic and paleoenvironmental conditions on Yap.

At this stage, the data do not support an initial settlement from a group affiliated with the Lapita culture. However, the data cannot be used to rule out a point of entry from Near Oceania because pottery and other artifacts recovered from survey and excavation all appear to be produced on Yap. This study suggests that southern Yap was not the location of Yap's earliest settlement and is a crucial step in developing and refining models that couple archaeological data, rigorous radiocarbon dating regimes, and paleoshoreline reconstruction that can be used to model where early colonization sites might be located.

CHAPTER V

CHEMICAL ANALYSIS OF GLASS BEADS IN PALAU, WESTERN MICRONESIA REVEALS 19TH CENTURY INTER-ISLAND EXCHANGE SYSTEMS IN TRANSITION

From: Matthew F. Napolitano, Elliot H. Blair, Laure Dussubieux, Scott M. Fitzpatrick. Chemical analysis of glass beads in Palau, western Micronesia reveals 19th century inter-island exchange systems in transition. In first review with *Journal of Archaeological Science: Reports*

Introduction

Beads have long played an important role in exchange systems across the Indo-Pacific (Adhyatman and Arifin, 1993; Carter et al., 2016a; Francis, 2002). In Palau, western Micronesia, oral traditions and ethnographic accounts describe how glass beads (*udoud*) functioned as traditional forms of currency and were an integral part of traditional exchange systems (Ballendorf, 1991; Krämer, 1926; Kubary, 1873, 1895; Semper, 1873). Understanding the classification and value of *udoud* is complicated as the context in which they are exchanged, individual bead life-histories (pedigrees), and the general availability of beads all could influence their value. In addition, ethnographic and historic accounts describe pervasive secrecy around *udoud* as the types and quantities owned by clans are closely guarded. Finally, the well-documented production and exchange of counterfeit *udoud* adds an additional layer of complexity in the understanding of these valuables and the circumstances in which they are exchanged.

Despite their long-term importance in Palauan society, the provenance of *udoud* remains fairly murky (Ballendorf, 1993; Dupont, 2018a; Force, 1959; Francis, 2002; Osborne, 1966). There appears to have been two general waves of beads introduced to Palau. The first wave of *udoud* may have been introduced ca. AD 600-950 and possibly as early as AD 200, originating from East Java or mainland Southeast Asia (Francis, 1997, 2002; Osborne, 1966). Palauans may have acquired beads through sporadic trade with Chinese junk ships that may have traveled in the region (Krämer, 1926). The supply of beads into Palau appears to have been relatively fixed until later, when Yapese islanders arrived in Palau to carve their large stone money disks, and brought glass beads and other valuables from Yap and exchanged them to gain access to quarry sites and to purchase supplies (Fitzpatrick, 2003a, 2008). This more recent introduction constitutes a second wave of bead introductions into Palau.

It is presently unclear when stone money quarrying activity began in Palau—and thus when the second wave of beads introduced to Palau began—as is how the Yapese came into possession of glass beads. Yet Yapese oral traditions appear to describe the same East Java or mainland Southeast Asian beads already in circulation in Palau in addition to beads that may have been obtained from Europeans (de Beauclair, 1963). As quarrying activity increased after the permanent presence of Europeans in Palau in the mid- to late-19th century, so did the presence of other high-valued items such a metal tools (Fitzpatrick, 2008; Fitzpatrick et al., 2006). During this time, the Yapese may have acquired beads during through direct trade with Europeans or as a result of David

O'Keefe's enterprise transporting stone money disks between Palau and Yap in exchange for *bêche-de-mer* (sea cucumber) and copra (dried coconut meat), which he sold in China (Fitzpatrick, 2008; Morgan, 1996).

To examine these provenance issues, we conducted compositional analysis of glass beads from Palau that were recovered with food refuse and evidence for stone money quarrying activities at the multicomponent site of Chelechol ra Orrak. The site is notable as a Yapese stone money quarry and for containing one of the earliest cemeteries in Remote Oceania (ca. 3000–2700 cal BP) (Fitzpatrick, 2003b; Fitzpatrick and Jew, 2018; Nelson and Fitzpatrick, 2005; Stone, 2020). Chelechol ra Orrak is also the only stone money quarry site where glass beads have been recovered, so they provide a unique opportunity to anchor the site's chronology using the beads as *termini post quem* (TPQ). This is important because establishing the chronology at quarry sites can be difficult given mixing and/or subtle changes of some stratigraphic contexts within the site. This challenge is coupled with radiocarbon dates that are associated with activities which date to within the past few hundred years and, when calibrated, do not provide a reliable estimate of when these took place.

Laser ablation-inductively coupled plasma-mass spectrometry (LA-ICP-MS) and morphological analyses on 38 beads indicate that they were all manufactured in Europe or Asia during the early- or mid-19th century. These results allow us to gain better insight into when quarrying activity at Orrak occurred and provides an opportunity to speculate on Palauan interaction networks at the time of European arrival in the region. This is particularly relevant given that Palau remained relatively (or completely) isolated from European contact until 1783, centuries after other islands in Micronesia (Callaghan and

Fitzpatrick, 2007). As such, we suggest that the glass beads found at Chelechol ra Orrak were introduced to Palau via Yap and would have been considered *cheldoech*, a type of *udoud* used to purchase supplies like lumber and food while carving stone money. However, closer analysis of oral traditions, historic, and ethnographic accounts suggests that as stone money quarrying activity continued throughout the 19th century, the ways in which Palauans used and exchanged *cheldoech* was in flux, in part because of the ease and proliferation in counterfeiting them. Despite the possible depreciation of this category of *udoud*, Palauans still valued and exchanged these beads in new ways, including interment as jewelry in burials.

Background

Environmental and archaeological background

The Palauan archipelago comprises hundreds of islands with varying lithologies, including volcanic, coralline uplifted limestone, platform-reef, and atolls aligned in a southwest–northeast orientation. The two largest islands of Babeldaob and Koror are primarily volcanic rock and surrounded by smaller uplifted coralline limestone islands colloquially known as the ‘Rock Islands’. Surrounding the central islands is a barrier reef that protects a productive lagoon habitat. Palau is divided into 16 states that correspond to village district boundaries prior to European arrival.

Chelechol ra Orrak (“beach of Orrak”) is located on the western side of Orrak Island 1 km southeast of Babeldaob (Figure 5.1). Like many other cave and rock shelters in Palau, the site was used for interring or placing the dead during the earliest stages of Palau’s settlement ca. 3000 BP (Nelson and Fitzpatrick, 2005; Stone, 2020; Stone et al., 2017). Orrak is unique, however, in that it is the only known site in Palau to have a cemetery overlain with later occupational refuse (Fitzpatrick, 2003b; Fitzpatrick and Jew, 2018; Nelson and Fitzpatrick, 2005). The third component to the site clearly demonstrates its use by Yapese Islanders who journeyed ca. 400 km south to Palau to use various locations as quarries for producing stone money (Fitzpatrick, 2003a, 2008).

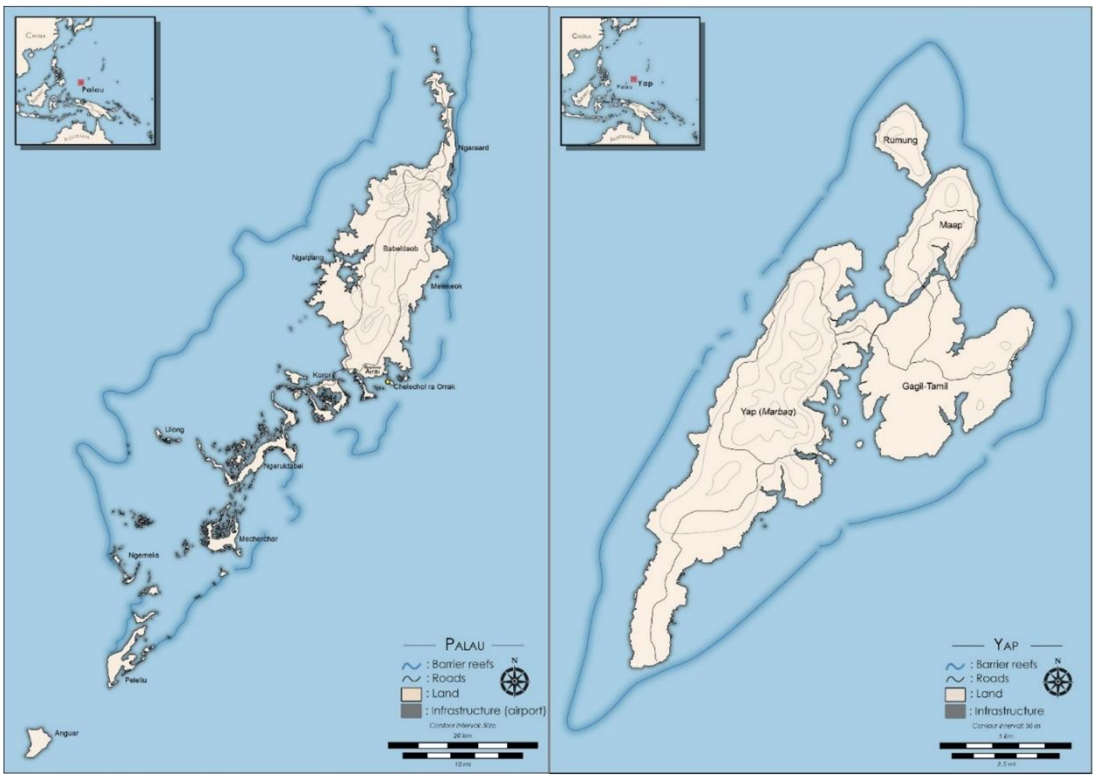

Figure 5.1. Map of Palau (A) and Yap (B).

The process of stone money production on Palau and transport to Yap was a lengthy and dangerous endeavor. According to oral traditions and ethnohistoric accounts, groups from Yap gained access to limestone quarries by providing corvée labor and offering highly valued glass beads, exotic foods, and other items such as sennit cord bundles (strong cordage made from coconut husks) to the clans or villages that controlled various islands (Fitzpatrick, 2001). For Yapese islanders, the process of traveling to

Palau, quarrying stone money, and then transporting these disks to Yap was one part of a larger system of regional interisland interaction networks that also included the *sawei* exchange with small outer island atolls in western and central Micronesia. This intricate exchange system involved the outer islands paying tribute to Yap every few years in exchange for materials not available on coral atolls, like pottery, stone, and lumber as well as providing provisions after major storms when necessary (Descantes, 2005; Fitzpatrick, 2008: fig. 6; Fitzpatrick and McKeon, 2020; Hunter-Anderson and Zan, 1996).

It is unclear exactly when Yapese stone money quarrying activity began in Palau. This is in part due to the aforementioned mixing of some stratigraphic deposits found in stone money quarry sites and rock shelters generally (Fitzpatrick, 2001). Radiocarbon determinations from deposits associated with stone money production at the only three quarry sites excavated thus far (Omis, Metuker ra Bisech, and Chelechol ra Orrak) calibrate as modern or fall on a flat part of the radiocarbon calibration curve (Fitzpatrick, 2003a; Fitzpatrick and Jew, 2018). However, oral traditions and ethnohistoric data indicate that quarrying activity was well underway before extended contact with Europeans beginning in AD 1783 (Fitzpatrick, 2003a, 2008).

Evidence for stone money quarrying at Chelechol ra Orrak includes two unfinished stone money disks, a smaller complete disk found in beach deposits outside the rockshelter, lithic debris, and a variety of stone architecture, including a dock, wall alignments, and mounds that were used during the production and transport of stone money disks (Fitzpatrick, 2003a). Unlike some Yapese quarrying sites, no metal tools were recovered here that would indicate a post-18th century use with the possible exception of one surface-collected iron tool (Fitzpatrick et al., 2006). The recovery of 38 glass beads lends additional support to Palauan and Yapese oral histories that quarrying activity was ongoing and continued until the mid- to late-19th century (Fitzpatrick, 2008).

Possible origins of beads to Palau and Yap

Douglas Osborne (1966), the first archaeologist to work extensively in Palau, surmised that beads were probably introduced sometime between ca. AD 200-950 from Indonesia or mainland Southeast Asia and was a partial catalyst for the development of Palau's social hierarchy. Bead scholar Peter Francis (1997, 2002) suggests roughly the same dates of ca. AD 600-950 years ago based on the continued circulation of numerous beads that were manufactured in East Java ca. AD 600-950, though both proposed chronologies are largely conjectural. The first written account of Palauan bead money was in AD 1783 by Captain Henry Wilson when his ship the *Antelope* wrecked on Ulong Island, leading to the first sustained contact with Europeans (Clark, 2007; Keate, 1789).

Numerous Palauan oral traditions describe the origin and use of bead money (Ballendorf, 1993; Hijikata, 1993; Kubary, 1873, 1895). According to one local legend, a fish gave birth to a girl who built an island (Ngorot Island). The girl gave birth to a bird (*Okak*) that was full of *udoud* and the bird was sent to Anguar and Ngaraard (two Palauan districts that are now states) as a reward for raising the fish and the girl (Thijssen-Etpison, 1997). A different legend recounts two Portuguese ships running aground at Ulong and near Kayangel, two islands in the Palauan archipelago. To procure supplies from Palauans, one of the ship's crew cut up the decorations and drilled holes in them to trade as money (Ritzenthaler, 1954). Another story states that *udoud* first entered the Palau economy from Yap where they were already being used as money (Parmentier, 2002:62-63).

According to Yapese oral tradition, glass beads first appeared on Yap after a man named Giluai visited the sky-world to look for a shell bracelet that was buried with his brother. During his visit he was allowed to pick magical fruits that he wore as a necklace. The largest of the fruits was crescentic shaped, corresponding to the most valuable class of Palauan *udoud*. After passing it down for several generations, it came into possession by a man named Rengenbai who used it to negotiate access to a stone money quarry on Palau (de Beauclair, 1963). Another story details a canoe party being blown off course by a typhoon and reaching Taiwan where they acquired baskets of beads. A third story describes how the chief of a high-ranking village in Yap received a large quantity of beads as tribute from a foreigner in a canoe with a square sail (de Beauclair, 1963:3-4). The beads were later distributed by the chief to people sailing on canoes for unfamiliar islands. Smaller beads remained on Yap with various accounts of them being inherited, interred with the dead, cached and buried inside large shells for protection, or accidentally found buried in gardens (de Beauclair, 1963). A consistent element in each of these oral traditions is that beads passed through the possession of chiefs were worn as necklaces or bracelets. They were also highly valuable as currency and could be traded with stone money, shell beads, banana fiber mats, or other items (de Beauclair, 1963).

When considering oral traditions from both islands and the chronologies proposed by Osborne (2002) and Francis (1997, 2002), it seems possible that there was an earlier introduction by traders from Island Southeast Asia, New Guinea, and/or mainland Southeast Asia and a later, second wave of beads introduced via Yap that may have included both older heirloom beads and beads manufactured more recently in Europe. The description of a square sail may suggest interaction with Europeans or Chinese junk boats as Micronesian watercraft typically had triangular sails.

Beads in Palauan society

In Palau today, the US dollar is used in economic transactions, but *udoud* and other forms of traditional currency like turtle shell bowls (*toluk*) are still exchanged to mark significant events such as the birth of a first child (*omengat*), funerals, weddings, and divorces (Dupont, 2018a). Beads are not, and were not, a form of currency in the strict sense that there is a fixed value per bead, but during shortages, beads would be cut up to make more money available for exchange (Krämer, 1926). The relative value of *udoud* within the same category vary as well. Historically, one bead type known as *kluk* was given a standard value of 10 coconut leaf baskets (*suálo*) holding 10-20 pounds of taro; yet one particular *kluk* could be more valuable than others depending on its life history (Ritzenthaler, 1954). In addition, the supply of beads to Palau was, at times, fixed. Coupled with beads being broken, lost, or devalued in other ways, their value generally increased as the supply decreased (Hijikata, 1993:220; Parmentier, 2002). *Udoud* can also increase in value if they are possessed by a particularly respected member of the community or have a particularly important life history; the highest valued beads were individually named (Barnett, 1949:43; Parmentier, 2002:64; Ritzenthaler, 1954:9-10). According to oral tradition, one such *udoud*, *bachel el berrak* (a yellow prismatic bead) named *Nglulmrard* was given by Ngaraard to Melekeok to settle a war between the two districts and was also later exchanged during marriages (Osborne, 1966:488).

Alternatively, the value of *udoud* can also decrease if, for example, they pass through a low-ranking household or are used to pay a fine for a penalty like adultery. The life histories of more valuable *udoud* were memorialized in formal chants (*chesol*), whereas the life history of less valuable *udoud* were tracked with informal legends (Nero, 1996).

Multiple classification schemes have been used to describe *udoud* with between three and nine broad categories usually being identified. First described in detail by Kubary (1873, 1895), Semper (1873, 1982 [1873]), and Krämer (1926), the most comprehensive discussion of *udoud* was by Ritzenthaler (1954) who identified nine families based on four criteria: material, color, shape, and social use (Figure 5.2). Many other attempts at categorization also exist (see also Barnett, 1949; Dupont, 2018a, 2018b; Krämer, 1926; Opitz, 2004; Osborne, 1966; Parmentier, 2002; Thijssen-Etpison, 1997). None of these attempts at classification schemes are completely satisfactory, with most exhibiting internal inconsistencies and conflations between *udoud* categories and individually named specimens. Some of this confusion in the literature can be traced to: 1) incorrect assumptions about *udoud* material; 2) the difficulty of ethnographers being able to view *udoud* as informants were reluctant to reveal the type and quantity of beads in their clan's possession; 3) changing terminology as some varieties disappeared from circulation; and 4) conflicting and incomplete information provided by ethnographic informants (see Parmentier, 2002).

Despite the considerable variance in classification schemes, Palauan *udoud* can be broadly, and etically, divided into three distinct categories. The first, and most important, category is *bachel* (e.g., Figure 5.2a-1, 5.2a-2, 5.2b-2). Beads in this category are considered the most valuable and are easily recognized because of their crescent shapes and are often worn as a single bead on a necklace (*iek*). When women wear these, it is typically an indication of high social rank and would be removed when entering the village or house of a higher-ranking clan (Krämer, 1926). While some of these are obviously manufactured from glass (e.g., *bachel merimer* [Figure 5.2b 18]), others (e.g, *bachel berrak* [Figure 5.2a-2, 5.2b-1], *bachel mengungau* [Figure 5.2a-1 and 5.2b-2]) have been the source of considerable debate, with many sources describing them as being made of fired clay or ceramic (e.g., Parmentier, 1985, 2002; Ritzenthaler, 1954). Archaeometric analyses of the material, however, indicates that despite its visual appearance, these *udoud* varieties are in fact made from glass and were cut from bracelets or bangles (Barnett, 1949; Force, 1959; Lövgren, 2011; Osborne, 1958, 1966). Similar intact bracelets have been recovered from burials in the Philippines, Indonesia, and Thailand and likely derive from China or mainland Southeast Asia (Force, 1959; Francis, 2002; Osborne, 1966; Thijssen-Etpison, 1997).

The second category includes polychrome bead types known as *chelbucheb* (e.g., Figure 5.2a-4, 5.2b-30-32) and *kluk* (e.g., Figure 5.2a-4), as well as thin rings cut from these types (i.e., *delobech*). The beads in this group were almost certainly manufactured in East Java, ca. AD 600-900 (Adhyatman and Arifin, 1993; Francis, 1991, 1997, 2002). The final category includes numerous varieties of beads lacking decoration. Opaque varieties, found in a number of shapes, are subsumed under the *kldait* group, while transparent and translucent beads are in the *cheldoech* group. Most of these varieties likely derive from the same sources as the first two categories, with Francis (2002) suggesting that many are varieties of Indo-Pacific beads (see Carter, 2016).

Of all *udoud* types, *cheldoech* is the least well-documented. The value of this bead type varies from low to high based on the size and quality of the bead with lower valued beads primarily used for buying supplies like food and coconut syrup (*ilaot*) and higher-valued *cheldoech* being equivalent to one *kluk* (Ritzenthaler, 1954). Krämer (1926) aso reports that *cheldoech* were worn by children and young girls. As a lower-valued type, they were not used for significant exchanges or worn like *bachel* to indicate rank, although today they are sometimes worn as bead spacers or at the end of *iek* (Watanabe and Inacio, n.d.). As they were only used for simple economic transactions, most *cheldoech* would likely not have individual names or recorded life histories. Largely disappearing from circulation in the early 1920s (Ritzenthaler, 1954), only Kubary (1873, 1895) and Semper (1873) described this type prior to its devaluation. The disappearance of *cheldoech* is widely attributed to its ease in counterfeiting (Hijikata, 1993; Ritzenthaler, 1954).

Indeed, many sources describe extensive efforts to counterfeit *udoud* (Barnett, 1949; Dupont, 2018a; Hijikata, 1993; Keate, 1789; Krämer, 1926; Kubary, 1873; Osborne, 1966; Ritzenthaler, 1954). It is unclear exactly when counterfeiting *udoud* began, though it was documented by Wilson within months of his arrival (Keate, 1789). Historically, such counterfeiting most often took three forms: 1) drilling or piercing fragments of broken bottles or plate glass for counterfeit *cheldoech* (post-European arrival) (e.g., Keate, 1789); 2) attempting to pass recently introduced foreign beads as genuine *udoud* (Hijikata, 1993); and 3) exaggerating the value or fabricating the life history of *udoud*.

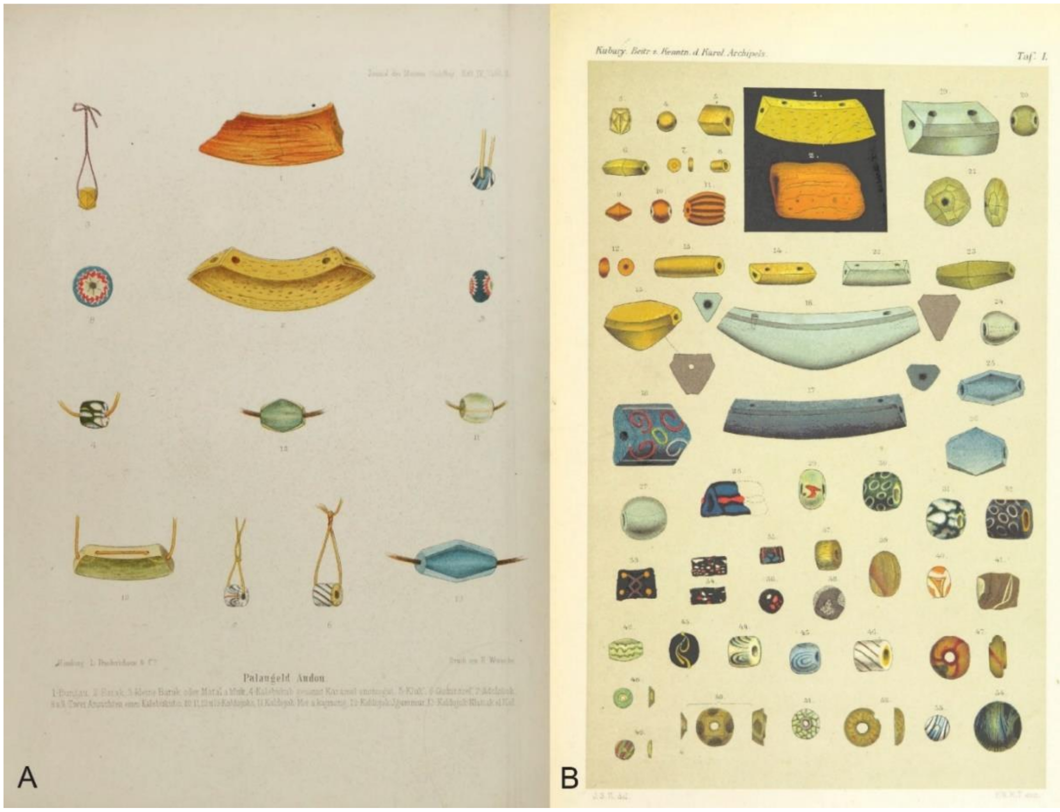

Figure 5.2. Palauan *udoud* illustrated by Kubary (1873) (A) and (1895) (B).

Hijikata (1993:217) suggests that counterfeits of the first type have been called *ngerusar* as they were extensively produced at Ngerusar village in Airai State, and Kubary (1873) reports a counterfeit of this type being manufactured from his discarded pickle jar. In an example of the second type, Krämer (1926) writes that during the German administration, when counterfeiting was at its peak, “white men, too, have attempted to create substitutes” but these were easily identified by Palauans as fraudulent they were—and still are—adept at detecting forgeries (see also Kubary, 1873). These counterfeits, when recognized, are called *udoud er a ngebard*, (“foreign *udoud*” or “*udoud* of the west”) or *ungil udoud* (good money) (Hijikata, 1993:217; Krämer, 1926); however, Krämer’s (1926) account is unclear as to what these beads looked like or how they compared to those that were already in circulation. Even today, counterfeiting *udoud* continues with East Javanese beads being looted from sites in Indonesia and then imported to Palau (Francis, 2002; Remengesau, 1997; Thijssen-Etpison, 1997; Yuping, 2012).

In an example of the third type of counterfeit, Krämer (1926) and others write about the difficulty in simply viewing *udoud* for fear that they would be lost or stolen (Parmentier, 2002:53; Thijssen-Etpison, 1997). In one such instance, after being trusted enough to look at *udoud*, Krämer (1926) later discovered that he was deceived and knowingly shown counterfeits. Attempts at counterfeiting high-valued *bachel berrak* and *bachel mengungau* by baking them from the clay found on the large island of Babeldaob, but manufacture of *cheldoech* was the most common (Krämer, 1926; Osborne 1966:488; Ritzenthaler, 1954:22).

When lacking a known life history or transaction history, Palauans inspected the beads to look for obvious signs of deception (Dupont 2018a). For example, if a bead is drilled, one way to inspect them is to look for uniform perforations made with modern equipment instead of irregular, conical, or biconical perforations; however, this would primarily apply to drilled *udoud* like *bachel* and not to beads that were of wound or drawn manufacture. Despite the heavy penalties for making transactions with counterfeit *udoud*—counterfeiting was at times heavily punished with fines and sometimes death (Ritzenthaler, 1954:22)—acceptance of may have been required, at times, because taking too long to inspect a bead may be interpreted as a sign of mistrust and cause embarrassment to both parties (*ng kora kemanget a osenged er ngii*, which translates to "the observation is taking too long because it is fake") (Kloulubak, personal communication). In this light, one could use their social status or their clan's rank as leverage to use counterfeit udoud in transactions, although this could be risky given the potential punishments.

There are, however, notable exceptions in the ways *udoud* are appraised and exchanged. Despite lacking known life histories and transaction histories, beads from Yap were trusted as *ng chuodel* (they are ancient and therefore authentic) (Kloulubak, personal communication). Kubary (1873) explains that they may have been readily accepted as authentic because people on Yap would have no way to produce counterfeit *udoud* (Thijssen Etpison and Dupont, 2017:24). There also appear to be other social contexts where counterfeit money was required for certain offerings and ritual ceremonies. In his description of burial customs, Krämer (1926:353) writes "that when the casket is delivered, a mock fight takes place on the beach in [Ngchesar], because the bearers strive to prevent the block of wood from being pulled up, and they even go so far as to cut through the ropes until they appeased with counterfeit money." Although he does not describe them, it is possible that he is referring to *cheldoech* since this category was devalued at the time Krämer was in Palau. These accounts ultimately paint a complex, and sometimes contradictory, picture of authentic and counterfeit *udoud* being exchanged, or even required in various contexts, and knowledge of clan "treasuries" was closely held information.

Glass beads in Palauan archaeology

Though ethnographic accounts indicate that *udoud* were not interred with the deceased (Ritzenthaler, 1954), many glass beads have been recovered archaeologically from *odesongel* (stone- or coral-lined clan burial platforms) or other burial contexts dating to the Stonework Era (AD 1250-1800) (Liston, 2007a, 2007b, 2010, 2011a, 2011b, 2011c; Lövgren, 2011; Masse and Snyder, 1982; Titchenal, 1999, 2001; Titchenal, et al., 1998). When recovered from burial contexts, they appear to be interred as bracelets or anklets because they are recovered near the wrist or feet (Liston, 2010a, Liston, 2010b; Lövgren, 2011), which is unexpected given that early ethnographic accounts are clear in that glass beads were not worn in this fashion (Krämer, 1926). Some of the beads reported from mortuary contexts on Palau are impossible to identify from published descriptions and photographs, but a few types are readily identifiable as beads manufactured in Europe during the 19th century. Others, however, have also been explicitly identified as examples of traditional *udoud* (Liston, 2010; Masse and Snyder, 1982; Titchenal, 1999, 2001; Titchenal et al., 1998), though in some cases, these appear to have been misidentifications.

Excavation of an *odesongel* in the village of Ngermid (Koror State, B:OR-1:1) revealed 22 burials, one of which was an adult of indeterminate sex interred with a bracelet and one or two anklets totaling 199 beads and 53 fragments (Liston, 2010). The bracelet included 78 emerald-green beads and the anklet comprised 118 emerald-green beads; blue and black beads were also recovered (Liston, 2010). Many of the beads recovered with this burial appear to be typologically similar to the *udoud* recovered at Orrak.

At a second *odesongel* at Ngerdubech (Ngatpang State, B:NT-3:9), five of 19 excavated burials contained a total of 457 glass beads. The beads were green and blue transparent glass and were all recovered near the wrist area. Photographs of the beads (Powers, 2011) show many wound varieties, as well as some pressed and drawn varieties, like those we report below. Compositional analysis indicated that many of the wound beads may have been manufactured in China (Lövgren, 2011).

At a third site in Ngerielb Village (Koror State, B:OR-1:8), 1700 beads were found with 12 individuals interred across three *odesongel* as part of a contract archaeology project for the now-defunct Hung Kuo resort. There was considerable diversity in beads at this site, with 27 different types present, including a double string of beads consisting of seven different types found around the neck of a child. Most of these (n = 1073) appear to be of Venetian origin, though numerous specimens from Bohemia and China were also reported (Lövgren, 2011; Titchenal, 1999, 2001). Three beads recovered at the site were manufactured from drilled glass and appear to be examples of the class of counterfeit *udoud* that was manufactured from bottles (Lövgren, 2011; Titchenal, 2001). Although many of the beads recovered from these sites were originally identified as *udoud* from East Java (Titchenal, 2001), compositional analysis indicated that this bead type was manufactured in Bohemia (Lövgren, 2011). Examinations of the bead photographs, descriptions, and comparisons with the Orrak assemblage make clear that most of the beads recovered from these burial contexts can be classified as *cheldoech*.

Glass beads recovered from these burial contexts suggest that, contrary to ethnographic accounts, they were worn as jewelry in large quantities, but this may have been limited to funerary contexts. Given the relatively small number of excavated burials, and the even smaller number that contain beads, it is not yet possible to test this hypothesis. The presence of Bohemian and Venetian glass beads indicate that the burials date to the end of the Stonework Era (ca. AD 1800) or immediately after. While it is possible that there were additional social contexts not described by ethnographers where *udoud* were used, including some mortuary contexts, the presence of so many glass beads—most of which can be identified as *cheldoech* (including counterfeit ones made from drilled transparent glass)—interred as jewelry suggests that the beads may have been regarded differently than traditional *udoud* since they were given away with an individual and not retained in the clan "treasury."

Despite these nuances in how *udoud* were perceived and exchanged in Palau through time, the recovery of dozens of glass beads from Orrak represents a rarely encountered archaeological context that allow us to better understand the role of *udoud* in Palauan exchange systems and provides a tangible example of inter-island exchange that supports oral traditions. Compositional analysis of glass beads provides a unique opportunity to refine the chronology as certain recipes can provide temporal markers through the presence of specific ingredients or manufacturing techniques. Below, we describe the first compositional analysis of glass beads found in this context and discuss how the results can help us establish their provenance and ways in which they might have been exchanged or valued.

Methods

Typological analysis

The 38 glass beads recovered from Orrak were analyzed using standard glass bead typological conventions (Beck, 1928; Francis, 2002; Karklins, 1982, 2012; Kidd and Kidd, 1970). Method of manufacture (e.g., drawn, wound), construction (e.g., simple, compound, complex), decoration, finishing technique (e.g., heat rounded, faceted), shape, color, diaphaneity, and size (length and diameter) were all recorded. When possible, Kidd and Kidd (1970) type-variety numbers were also assigned to individual specimens. These were then compared to documented types of *udoud* and correlations made when possible (Krämer, 1926; Kubary, 1873, 1895; Ritzenthaler, 1954; Thijssen-Etpison, 1997).

LA-ICP-MS

In addition to morphologically typing the assemblage, compositional analysis was conducted at the Elemental Analysis Facility at the Field Museum of Natural History (Chicago, USA) to identify the type of glass used to manufacture the beads (e.g., lead, potash, soda-lime) as well as identify major colorants, opacifiers, and temporally diagnostic elemental attributes. The analyses were carried out with a Thermo ICAP Q inductively coupled plasma-mass spectrometer (ICP-MS) connected to a New Wave UP213 laser for direct introduction of solid samples.

The parameters of the ICP-MS are optimized to ensure a stable signal with a maximum intensity over the full range of masses of the elements and to minimize oxides and double ionized species formation (XO^+/X^+ and $X^{++}/X^+ < 1$ to 2 %). For that purpose, the argon flows, the radio-frequency power, the torch position, the lenses, the mirror, and the detector voltages are adjusted using an auto-optimization procedure.

For better sensitivity, helium is used as a gas carrier in the laser. The choice of the laser ablation parameters not only have an effect on the sensitivity of the method and the reproducibility of the measurements, but also on the damage to the sample. The single point analysis mode with a laser beam diameter of 100 μm, operating at 80% of the laser energy (0.1 mJ) and at a pulse frequency of 20 Hz was used to determine elements with concentrations in the range of parts per million (ppm) and below while leaving a trace on the surface of the sample invisible to the naked eye. A pre-ablation time of 20 seconds is set to eliminate the transient part of the signal and to be sure that possible surface contamination or corrosion does not affect the results of the analysis. For each sample, the average of four measurements corrected from the blank is considered for the calculation of concentrations.

To improve reproducibility of measurements, the use of an internal standard is required to correct possible instrumental drifts or changes in the ablation efficiency. The element chosen as the internal standard has to be present in a relatively high and known concentration so its measurement is as accurate as possible. The isotope Si29 was used for internal standardization. Concentrations for major elements, including silica, are calculated assuming that the sum of their concentrations in weight percent in glass is equal to 100% (Gratuze, 1999).

Fully quantitative analyses are possible by using external standards. To prevent matrix effects, the composition of standards has to be as close as possible to that of the samples. Two different series of standards are used to measure major, minor, and trace elements. The first series of external standards are standard reference materials (SRM) manufactured by the National Institute of Standards and Technology (SRM 610 and SRM 612). Both of these standards are soda-lime-silica glass doped with trace elements in the range of 500 ppm (SRM 610) and 50 ppm (SRM 612). Certified values are available for a very limited number of elements. Concentrations from Pearce et al. (1997) were used for the other elements. The second series of standards were manufactured by Corning. Glass B and D are glasses that match compositions of ancient glass (Brill, 1999:544).

Results

Table 5.1 reports the complete typological analysis of the Orrak glass bead assemblage, including assignment to compositional group (Figure 5.3). Complete elemental results are reported in Appendix D, Table 1. The glass bead assemblage excavated at Orrak can be divided into two main compositional groups, with five additional beads having unique compositions (Figure 5.4).

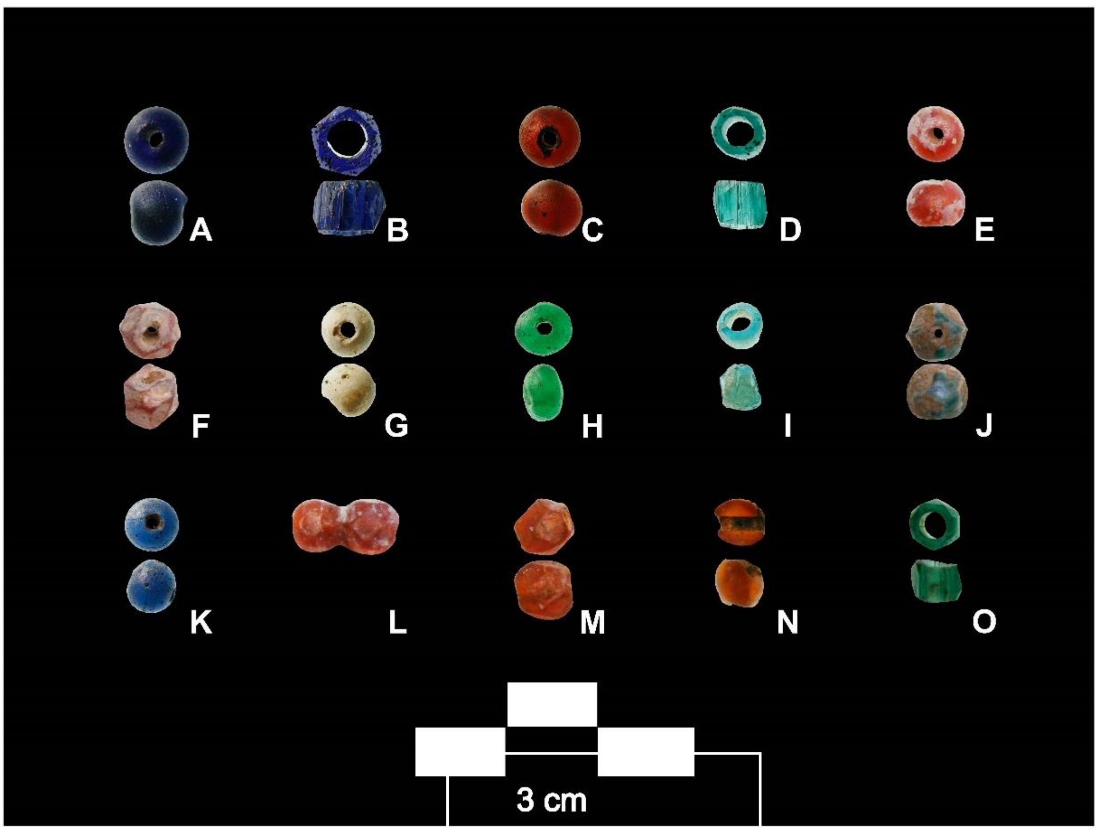

Figure 5.3. Beads recovered from Chelechol ra Orrak. Catalog numbers: A: 7; B: 4; C: 5; D: 6; E: 19; F: 26STNSP; G: 8; H: 10; I: 17; J: 85STNSP2; K: 19; L: 46NSTP-A; M: 64NSTP; N: 27MIXSP-B; O: 27MIXSP-C.

Table 5.1. Typological analysis of glass beads recovered from Chelechol ra Orrak.

Catalog Number	Unit	Glass Type	Colorant	Opacifier	Kidd and Kidd (1970) Type	Place of Manufacture	Manufacture	Construction	Finishing	Shape	Color	Munsell	Diaphaneity	Length (mm)	Diameter (mm)	Notes
4	E2/S1	K-Ca	Co	—	If5	Bohemia	Drawn	Simple	Ground facets	Hexagonal tube	Cobalt Blue	7.5PB 2/10	transparent / translucent	5.5	7.3	Uranium present
5	E2/S1	Pb-K	Au	—	—	Bohemia	Wound and Pressed (mold)	Simple	—	Oblate	Orange	1.25 YR 5/12	transparent	6.2	7.0	
6	E2/S1	K-Ca	Cu	—	If4	Bohemia	Drawn	Simple	Ground facets	Hexagonal tube	Green-blue	5.0G 6/6	transparent	4.7	5.6	
7	E2/S1	Pb-K	Co	—	WIb	Bohemia? China?	Wound	Simple	—	Oblate	Black/Dark blue	7.5PB 2/5	Opaque to translucent	5.8	7.4	
8	E2/S1	K-Ca-Al	—	—	—	Bohemia?	UID	Simple	--	Oblate	White/clear	N8	Opaque to translucent	5.2	6.1	Heavily patinated, likely of wound manufacture
9	E2/S1	K-Ca	Cu	—	Ic	Bohemia	Drawn	Simple	—	Hexagonal tube	Green-blue	10.0G 5/10	transparent	4.6	4.8	
10	E2/S1	Pb-K	Cu	—	WIb	Bohemia? China?	Wound	Simple	—	Oblate	Green	2.5G 5/10	transparent	4.0	6.5	Possible longitudinal mold seam
11	E2/S1	K-Ca	Cu	—	Ic	Bohemia	Drawn	Simple	—	Hexagonal tube	Green-blue	5.0G 6/6	transparent / translucent	5.0	5.6	
17	E2/S1	K-Ca-Mg	Cu	—	WI	China?	Wound	Simple	—	Barrel	Blue-green	7.5BG 8/4	translucent	4.3	5.1	High Zn and Ba; Coil bead?
19	E2/S1	Pb-K	Co; Cu	As	WIb	Bohemia? China?	Wound	Simple	—	Oblate	Blue	5.0PB 4/8	opaque	5.1	6.2	
37	E3/S1	Na-Ca	Cu (ext)	Sb	IVa6	Venice	Drawn	Compound	Heat rounded	Torus	Red-on-green	7.5R 3/8 over 7.5GY 7/10	Opaque over translucent	2.0	3.4	
111STNSP	E3/S4	Pb-K	Cu	As	WIb	Bohemia? China?	Wound	Simple	—	Oblate	Aqua Blue	2.5B 6/4	Opaque	5.8	6.4	
19STNSP	E2/S5	Pb-K	Au	—	—	Bohemia	Wound and Pressed (mold)	Simple	—	Oblate	Rose Wine	10.0RP 4/6	translucent	5.2	6.3	
26STNSP	E2/S5	Pb-K	Au	—	—	Bohemia	Wound and Pressed (mold)	Simple	14 molded facets, reheated	Faceted oblate	Coral	10.0R 5/8	transparent / translucent	5.4	6.1	

Table 5.1, continued.

Catalog Number	Unit	Glass Type	Colorant	Opacifier	Kidd and Kidd (1970) Type	Place of Manufacture	Manufacture	Construction	Finishing	Shape	Color	Munsell	Diaphaneity	Length (mm)	Diameter (mm)	Notes
27MIXSP-A	E2/S4	Pb-K	Au	—	—	Bohemia	Wound and Pressed (mold)	Simple	14 molded facets, reheated	Faceted oblate	Coral	10.0 R 5/8	transparent / translucent	5.2	5.4	refit w/ 51STNsp 1
27MIXSP-B	E2/S4	Pb-Ca-P	—	—	—	UID	Wound?	Compound	—	Torus	Red/ purple over brown	—	Opaque	2.5	3.7	glass?
27MIXSP-C	E2/S4	K-Ca	Cu	—	If3	Bohemia	Drawn	Simple	Ground facets	Hexagonal tube	Mint Green	5.0G 6/6	transparent	4.1	5.2	
40STNSP	E2/S4	Pb-K	Au	—	—	Bohemia	Wound and Pressed (mold)	Simple	14 molded facets, reheated	Faceted oblate	Coral	10.0 R 5/8	transparent / translucent	5.7	6.3	
46STNSP-A	E2/S4	Pb-K	Au	—	—	Bohemia	Wound and Pressed (mold)	Simple	14 molded facets, reheated	Conjoined faceted oblates	Coral	10.0 R 5/8	transparent / translucent	12.3	6.5	Conjoined, double bead
46STNSP-B	E2/S4	Pb-K	Au	—	—	Bohemia	Wound and Pressed (mold)	Simple	14 molded facets, reheated	Faceted oblate	Coral	10.0 R 5/8	transparent / translucent	6.0	6.9	
46STNSP-C	E2/S4	Pb-K	Au	—	—	Bohemia	Wound and Pressed (mold)	Simple	14 molded facets, reheated	Faceted oblate	Coral	10.0 R 5/8	transparent / translucent	6.3	6.5	
46STNSP-D	E2/S4	Pb-K	Au	—	—	Bohemia	Wound and Pressed (mold)	Simple	14 molded facets, reheated	Faceted oblate	Coral	10.0 R 5/8	transparent / translucent	5.8	6.4	
46STNSP-E	E2/S4	Pb-K	Au	—	—	Bohemia	Wound and Pressed (mold)	Simple	14 molded facets, reheated	Faceted oblate	Coral	10.0 R 5/8	transparent / translucent	6.1	7.1	
50STNSP-A	E2/S4	Pb-K	Au	—	—	Bohemia	Wound and Pressed (mold)	Simple	14 molded facets, reheated	Faceted oblate	Coral	10.0 R 5/8	transparent / translucent	5.1	6.3	
50STNSP-B	E2/S4	Pb-K	Au	—	—	Bohemia	Wound and Pressed (mold)	Simple	14 molded facets, reheated	Faceted oblate	Coral	10.0 R 5/8	transparent / translucent	5.5	6.1	

Table 5.1, continued.

Catalog Number	Unit	Glass Type	Colorant	Opacifier	Kidd and Kidd (1970) Type	Place of Manufacture	Manufacture	Construction	Finishing	Shape	Color	Munsell	Diaphaneity	Length (mm)	Diameter (mm)	Notes
51STNSP1	E2/S4	Pb-K	Au	—	—	Bohemia	Wound and Pressed (mold)	Simple	14 molded facets, reheated	Faceted oblate	Coral	10.0R 5/8	transparent / translucent	5.7	5.4	refit w/ 27MIXsp-A
64STNSP	E2/S4	Pb-K	Au	—	—	Bohemia	Wound and Pressed (mold)	Simple	14 molded facets, reheated	Faceted oblate	Coral	10.0R 5/8	transparent / translucent	6.0	6.6	
69STNsp	E3/S4	Pb-K	Au	—	—	Bohemia	Wound and Pressed (mold)	Simple	14 molded facets, reheated	Faceted oblate	Red Feather	2.5R 3/4	UID	5.8	6.8	
6STNSP-A	E2/S5	Pb-K	Co	As	—	Bohemia	Wound and Pressed (mold)	Simple	14 molded facets, reheated	Faceted oblate	Cerulean Blue	7.5B 5/10	Opaque	6.5	6.5	
6STNSP-B	E2/S5	Pb-K	Au	—	—	Bohemia	Wound and Pressed (mold)	Simple	—	Oblate	Rose Wine	10.0RP 4/6	translucent	5.6	7.3	
6STNSP-C	E2/S5	Pb-K	Au	—	—	Bohemia	Wound and Pressed (mold)	Simple	14 molded facets, reheated	Faceted oblate	Rose Wine	10.0RP 4/6	translucent	5.0	6.4	
6STNSP-D	E2/S5	Pb-K	Au	—	—	Bohemia	Wound and Pressed (mold)	Simple	14 molded facets, reheated	Faceted oblate	Rose Wine	10.0RP 4/6	translucent	5.4	6.3	
6STNSP-E	E2/S5	Pb-K	Au	—	—	Bohemia	Wound and Pressed (mold)	Simple	14 molded facets, reheated	Faceted oblate	Rose Wine	10.0RP 4/6	translucent	5.9	6.2	
6STNSP-F	E2/S5	Pb-K	Au	--	—	Bohemia	Wound and Pressed	Simple	Pressed facets	Square	Barn Red	5.0R 3/10	translucent	5.9	8.3	Pressed facets, not molded
6STNSP-G	E2/S5	Pb-Na-K	--	As	WIb	China?	Wound	Simple	—	Oblate	Oyster White	N8	Opaque	6.4	8.1	

Table 5.1, continued.

Catalog Number	Unit	Glass Type	Colorant	Opacifier	Kidd and Kidd (1970) Type	Place of Manufacture	Manufacture	Construction	Finishing	Shape	Color	Munsell	Diaphaneity	Length (mm)	Diameter (mm)	Notes
72STNSP-A	E3/S5	Pb-K	Au	—	--	Bohemia	Wound and Pressed (mold)	Simple	14 molded facets, reheated	Faceted oblate	Red Feather	2.5R 3/4	UID	6.5	7.2	
72STNSP-B	E3/S5	Pb-K	Au	—	—	Bohemia	Wound and Pressed (mold)	Simple	14 molded facets, reheated	Faceted oblate	Red Feather	2.5R 3/4	UID	5.4	6.2	
72STNSP-C	E3/S5	Pb-K	Au	—	—	Bohemia	Wound and Pressed (mold)	Simple	14 molded facets, reheated	Faceted oblate	Red Feather	2.5R 3/4	UID	6.0	6.1	
85STNSP2	E3/S5	Pb-K	Cu	—	—	Bohemia	Wound and Pressed (mold)	Simple	14 molded facets, reheated	Faceted oblate	Emerald green	10.0G 5/10	transparent	6.0	6.1	High tin content

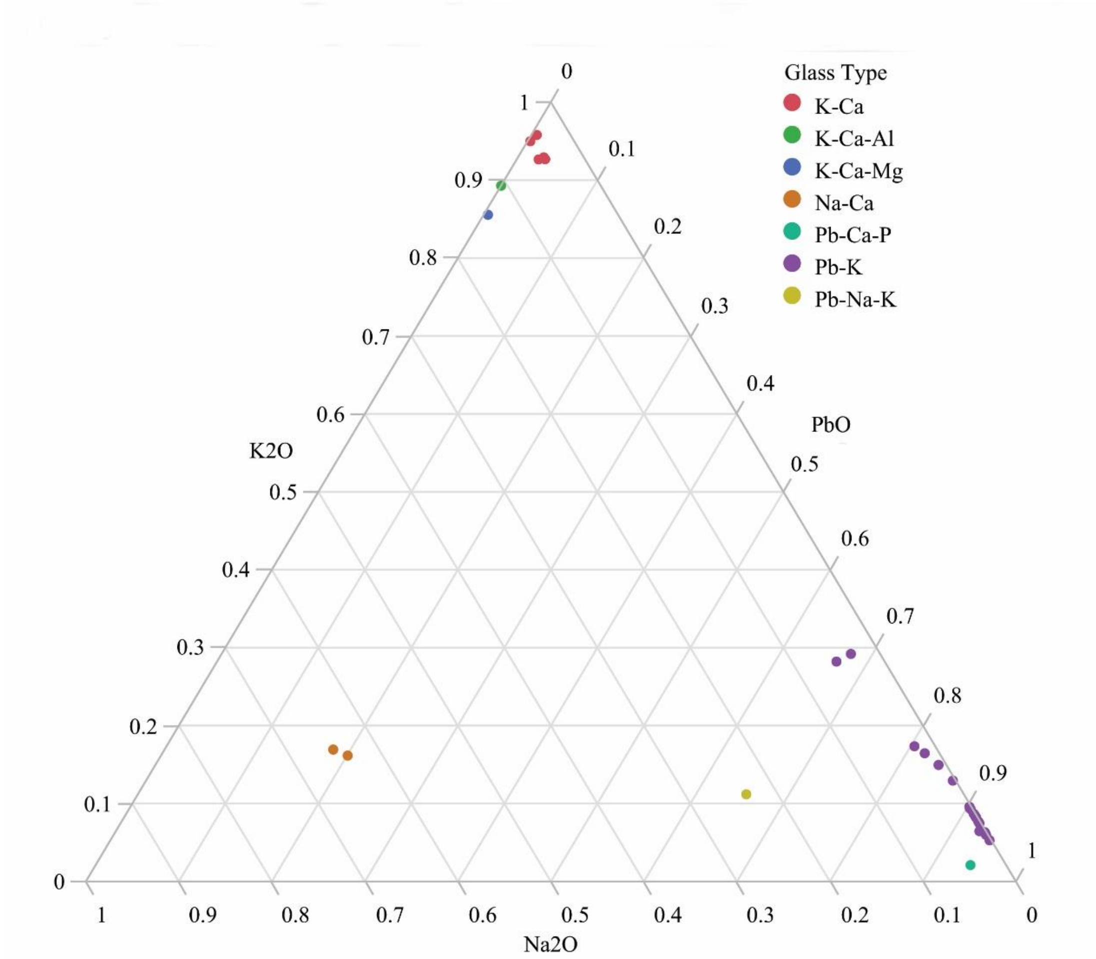

Figure 5.4. Ternary plot of Na_2O, K_2O, and PbO content of the Orrak bead assemblage, illustrating distinct compositional groups.

The largest group (n = 28) has a lead-potash composition (Pb-K), with PbO content ranging from 26.4%-57.9% and K2O ranging from 3.1%-13.3%. Twenty of the beads in this group are faceted oblates that were wound and pressed in a mold. All of these have vertical (or longitudinal) mold seams, cylindrical perforations, and were wound around a mandrel before being pressed in a mold. Each bead has 14 facets, and the edges of the facets and the mold-seam on all specimens are rounded, indicating slight reheating after pressing. One specimen (46STNSP-A) consists of two conjoined beads with the perforations and mold seams in perfect alignment (Figure 5.3L). This, and the fact that many of the single-specimens have cracked or fractured apertures, indicates that the beads were wound and pressed in a sequential mold and then separated (broken apart) when the glass was cold. This group includes orange, red, green, and blue specimens. The orange and red specimens were all colored with gold (19.5-36 ppm) (Figure 5.3F and 5.3M), while the single green specimen (85STNsp2) (Figure 5.3J) was colored with copper and the single blue specimen (6STNSP-A) was primarily colored with cobalt (Figure 5.5).

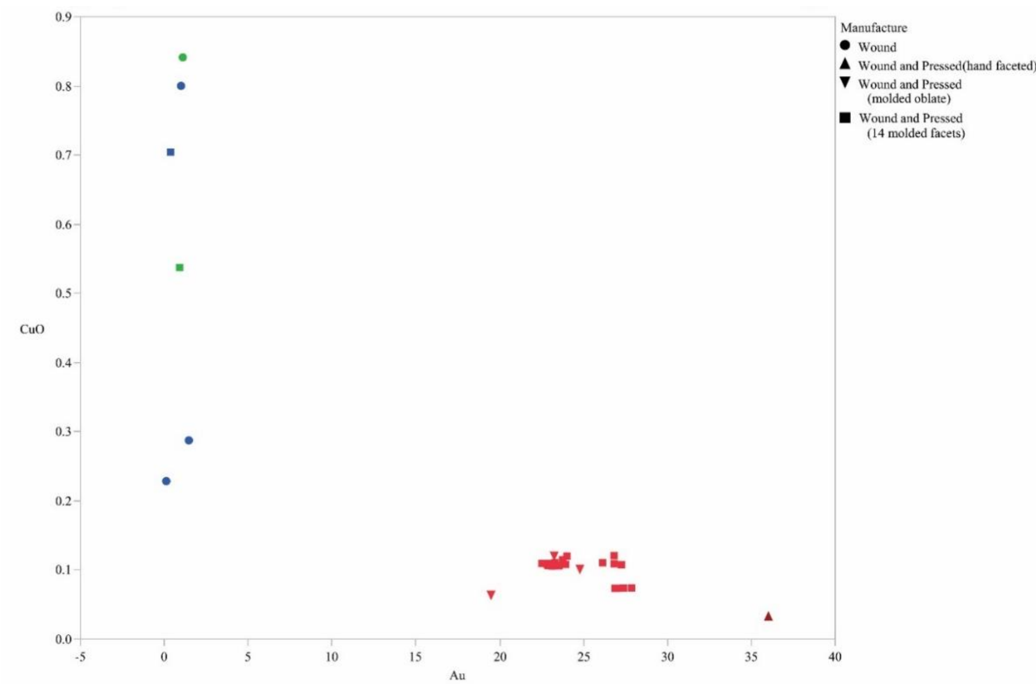

Figure 5.5. CuO (%) and Au (ppm) biplot of Pb-K beads in the Orrak assemblage. Shape indicates method of manufacture, while color (red, green, blue) reflects glass color.

While these beads are of an unusual variety (see discussion below), the morphology and technology of these beads (faceted-spheroidal, mold-pressed) is typical of Bohemian manufacture (Francis, 1988, 2009a; Kaspers, 2014; Neuwirth, 1994, 2011; Ross, 2003; Ross and Pflanz, 1989). The Pb-K formula is a good example of Bohemian “composition,” a leaded glass of brilliant color designed to imitate gemstones and be easily molded (Francis, 1979, 1988; Kaspers, 2014). The use of gold as a colorant is also typical of Bohemian “composition” (Francis, 2009a).

Four additional beads in the Pb-K group were also colored with gold and manufactured by winding and pressing. Three of these lack facets and were pressed into a simple oblate form. The fourth bead (6STNSP-F) was wound and roughly faceted and pressed into a square shape by hand (not molded). The composition and manufacturing method of these four beads is also typical of Bohemia. Four other beads, also composed of Pb-K glass, were wound, but lack evidence of pressing. Based on glass formula, these too are likely Bohemian, though wound, lead-potash beads were also manufactured in China (Brill et al. 1991; Carter, 2016; Carter, et al., 2016b).

The second major compositional group in the Orrak assemblage includes five beads made from potash glass (K-Ca) with K2O content ranging from 12.8%-16.6% and CaO content from 6.6%-11.1%. All five are of drawn manufacture and have a hexagonal cross-section. These varieties are a well-known Bohemian type (Kidd and Kidd Ic and If) and the high potassium and calcium content is typical of central European “forest glasses” (Cílová and Woitsch, 2011; Francis, 1988; Kenyon et al., 1995). Three of these specimens have facets ground into the corners.

The final five beads in the assemblage have unique compositions within the Orrak assemblage. Bead No. 37 is a compound, red-on-green, bead (Kidd and Kidd IVa6) of drawn manufacture. This type, sometimes called a “green-heart,” is a well-known variety and is the only bead in the assemblage made from soda-lime glass (N-Ca), typical of Venetian manufacture (Francis, 1988, 2009b). Bead No. 8 (Figure 5.3G) is so heavily patinated that its method of manufacture was impossible to discern. It is possibly of Bohemian manufacture, but has an extremely high potassium (19.75%) and alumina (4.91%) content (K-Ca-Al), unlike other beads of definitive Bohemian origin. Another specimen (Cat. No. 17, Figure 5.3I) is a wound bead, also of possible Bohemian origin. It was manufactured from a potash glass (K-Ca-Mg), but the magnesia content (4.32%) is significantly higher than other Bohemian beads. In form, the bead is reminiscent of Chinese “coil” beads, though those varieties are typically manufactured from leaded glass (Francis, 2002). Bead 6STNSP-G is a wound bead manufactured from a mixed alkali leaded glass (Pb-Na-K), reminiscent of some Chinese beads reported by Burgess and Dussubieux (2007). The last bead in the assemblage (27MIXSP-B) is heavily weathered but appears to be a wound bead of compound construction (red/purple over brown/tan). This specimen (Pb-Ca-P composition) contains high lead (49.6%), high calcium (19.5%), very low silica (10.0%), and has a very high phosphate (12.6%) and chlorine (2.3%) content. This is a very unusual composition for glass, and it seems most likely that this bead was either not made of glass or a section of heavily weathered glass was sampled during analysis, which can produce unexpected results.

Discussion

Chronology and origins

The bead assemblage recovered archaeologically at Orrak is notable for the ubiquity of European, primarily Bohemian, types. Several of these (i.e., the drawn Bohemian varieties manufactured from K-Ca glass) are well known in the bead literature and are the only type that can be considered a clear temporal marker (Figure 5.3B, 5.3D, 5.3O). Beads of this type—often erroneously called "Russian" beads in North America—were not manufactured until ca. 1820 (Blair, 2018; Francis, 1994; Ross, 1997). One of the Orrak specimens (Cat No. 4, Figure 5.3B) is also noteworthy for containing a notable quantity of uranium (44 ppm) compared to the rest of the beads in the assemblage. Uranium oxide was used as a colorant in some yellow and green Bohemian glasses beginning in 1830, though it did not become commonly used until the 1840s (Brill, 1964:54; Langhamer, 2003:71). The bead is blue in color and contains less uranium than would be present if this element had been used as a colorant. One explanation for the distinct presence of this element is that pieces of uranium glass cullet were used in the production of this bead, strongly suggesting that the bead could not have been manufactured prior to AD 1830. Alternatively, the uranium could be associated with the source of the cobalt ore used to color the glass, a known elemental association of the Schneeburg mine area of Germany, used from the 15th to the 18th century (Gratuze et al., 1996).

The wound and pressed, faceted beads present in the Orrak assemblage are not well documented and are rare examples of early, faceted, Bohemian beads made of "composition"—a lead glass, often colored with gold, intended to imitate faceted garnets (Hunt, 1976; Kaspers, 2014; Figures 3F, 3L, and 3M). These beads all have vertical mold seams, cylindrical perforations, and were wound before the facets were pressed into the glass. Harris (1989:5) describes the manufacture of these beads as: "[a] multi-bead, tong-mounted mold that could be clamped around a mandrel wound with glass produced a row of crude faceted beads that had to be broken apart when the glass was cold. This appears to be an early experiment" (see also Neuwirth, 2011). Ross (2003:43, citing Schreyer, 1790:93) dates this manufacturing technique to the beginning of the 18th century. The beads are distinct from the later, visually similar, mold-pressed beads that post-date the early- to mid-19th century (Ross, 2003). Similar beads have rarely been documented or recovered outside of Palau, with the closest example of this type being recovered from a pre-1630 Native American burial in a Franciscan church on St. Catherines Island, Georgia (USA) (Francis, 2009a). Though the specimens of this type recovered at Orrak could possibly have been manufactured during the 18th century (Harris, 1989; Neuwirth, 1994, 2011; Ross, 2003; Schreyer, 1790), or earlier (Francis, 2009a), the strong association in Palau between this type and the drawn Bohemian beads suggests contemporaneity, although it is possible that the beads could have been heirlooms (Power, 2011; Titchenal, 1999, 2001). The Venetian red-on-green bead variety was manufactured from the 16th-19th centuries. A similar bead type with a white center was first manufactured ca. 1830 (Billeck, 2008). The red-on-green variety beads were still manufactured after ca. 1830, but, at least at sites in western North America, they are often absent from bead assemblages after the introduction of the red-on-white variety (Billeck, 2008; Blair, 2018). The presence of the red-on-green bead at Orrak, in association with the drawn Bohemian varieties, suggests that the assemblage dates no earlier than ca. 1830 and probably no later than ca. 1850.

Manufacturing periods for bead types can provide an important TPQ that can be used to better understand when stone money quarrying activity may have taken place. The bead assemblage suggests that quarrying activity may have continued until at least ca. 1830-1850. Although it is possible that the beads may be part of a short-term Palauan use of the site after quarrying terminated, stratigraphic and artifactual evidence (e.g., limestone quarrying debitage) suggests that they are associated mostly or exclusively with quarrying activity (Fitzpatrick, 2003a, 2003c, 2008). In addition, it is well documented that quarrying activity continued into the mid- to late-19th century so the evidence from Orrak fits into the larger picture of what was happening in the Rock Islands at that time (Fitzpatrick, 2016).

It is important to note that while Europeans were Micronesia as early as the 16th century, including the arrival of the Spanish in Yap (see Hezel, 1972, 1979, 1983), there is a noticeable absence of 15th-17th centuries beads in the archaeological record and ethnographic accounts. A notable exception may be Kubary's (1873) illustration of a Venetian five-layer chevron bead (Figure 5.2a-8 and 5.2a-9), considered to be genuine *udoud*, that most likely dates to the late 16th or early 17th century (Allen, 2010). However, it can be difficult to determine the number of glass layers in chevron beads and if this analysis or illustration was inaccurate and this is a four-layer chevron bead, then its manufacture would date to the 18th-19th centuries, placing it generally within the same time as when other European beads were introduced to Palau. Interestingly, Kubary does not illustrate this bead in any later publications (Allen, 2010) and it is possible that this bead was later discovered as a counterfeit or *udoud er a ngebard* given the difficulty in outsiders gaining access to authentic *udoud*. Beyond this example, there appears to a significant gap from when beads were introduced from East Java or Southeast Asia.

Cheldoech *in transition during the 19th century*

The vast majority of glass beads in the Orrak assemblage can be correlated with the *cheldoech* category. Although the wound, pressed, and faceted Bohemian beads

(Figure 5.3F, 5.3M, 5.3L) bear a striking resemblance in shape to *klorange*, a category of *kldait udoud* (Figure 5.2a-3, 5.2b-3), the fact that these beads are made of transparent glass automatically places in the *cheldoech* category. The coral-colored Bohemian beads could possibly be considered *cheldoech mengungau* (small bright red-orange), while the beads made from opaque glass may fit into other categories. For example, the oyster white oblate bead (Figure 5.3G) and dark blue oblate bead (Figure 5.3A) can both be identified with *kldait bleob*, a category of undecorated *udoud* that was typically used for more significant exchanges than *cheldoech*, including payment to chiefs during a burial or worn around the neck of a pregnant woman to ensure a healthy baby (Watanabe and Inacio, n.d.). The transparent and translucent beads would have likely been used in economic transactions and for purchasing supplies like *ilaot* and food and not for more important exchanges like negotiating access to stone money quarries, exchanged as dowry, or to end a war between clans (see de Beauclair, 1963; Krämer, 1926; Kubary, 1873, 1895; Osborne, 1966; Watanabe and Inacio, n.d.).

When considering the Orrak bead assemblage in a wider context, there is evidence that it is important to consider large-scale shifts that were taking place in Palauan society during the 19th century. The proliferation of stone money quarrying by Yapese islanders led to a second wave of bead introduction to the Palauan economy and these beads were introduced as the manufacture of counterfeit *udoud* was increasing. At approximately the same time, beads were interred with burials for the first time. These processes were taking place against a backdrop of increasing European presence, the introduction of guns, iron, and a precipitous population decline from European-introduced diseases. Palau was under Spanish administration, including Christian missionization, by 1885 and became part of the German administration in 1899. The introduction of the Deutsche mark during the German administration, when Krämer was conducting his fieldwork, likely had an impact on the relative value of *cheldoech* as the economy transitioned to using foreign currency. This coincided with efforts by the Germans to suppress traditional interisland voyaging that eventually led to the cessation of stone money quarrying.

As such, we argue that glass beads from Orrak were introduced from Yap at a time when *cheldoech* was already being devalued as a form of currency—perhaps in conjunction with prohibitions placed on voyaging—but still retained non-monetary value to Palauans, resulting in them being used in novel ways. Many of the beads from *odesongel* are typologically identical to those recovered at Orrak. The blue-green glass beads and orange/amber beads at the Hung Kuo site originally identified by archaeologists as *kldait chesbad* are, in fact, Bohemian, suggesting an introduction contemporaneous to the Orrak assemblage during the second wave of bead introductions to Palau. Yet those Bohemian beads were interred with clear counterfeits made from drilled bottle glass and, therefore, the question remains, would the European-made glass beads interred in *odesongel* also be considered counterfeit or devalued? Or could the devaluation of *cheldoech* happened earlier than recorded by ethnographers?

According to some, small trade beads were not considered money and worn as earrings primarily by children, which supports Krämer’s (1926) account that *cheldoech* were sometimes worn as earrings by young girls (Thijssen Etpison and Dupont, 2017). Earrings, however, were typically made from pearl shell or turtle shell and it is possible that *cheldoech* were only worn as earrings only after they were devalued. If this is true, then it is possible that small trade beads, like ones manufactured in Europe, could be recognized as *udoud er a ngebard* (udoud of the west). In contrast, oral traditions indicate that beads were accepted as authentic *udoud* if they were introduced by Yapese islanders (Kloulubak, personal communication). Despite written accounts that outline what types of beads may have been considered counterfeit, we must cautiously interpret accounts when the ethnographer has a sometimes-unfavorable view of Palauans (see Kubary, 1873). It is very possible that given the complexity and sensitivity of the topic, important details about *udoud* classification and exchange were not shared, especially given the secrecy surrounding them. We are also careful not to discount Palauan oral tradition, which is clear that beads coming from Yap would have been considered authentic *udoud* (Kloulubak, personal communication). When considering these objects from a Palauan perspective, there is no contradiction. When introduced by Yapese islanders, these objects would not have been categorically thought of as European and inauthentic because of their manufacturing origin (see Silliman, 2009).

Given the changes in how beads were being used or exchanged by ca. 1830-1850, it appears likely that the process of *cheldoech* being devalued was already begun well before they officially went out of circulation in the 1920s. However, the contemporaneous interment of beads in *odesongel* suggests that *cheldoech* had come to take on new roles in funerary contexts, reflecting a larger social shift in how lower-valued *udoud*, like these, were used and exchanged. It is possible that although the beads at Orrak were likely considered authentic, they may have had little value in economic exchanges because they had already depreciated.

Despite the economic value of the beads being unknown, the recovery of glass beads from Orrak allows us to consider the nature of Yapese-Palauan interaction networks. With the exception of Captain Wilson's wreck on Ulong Island in 1783, Palau was relatively isolated from European interaction until Palau fell under the colonial rule of Spain in 1885 (Callaghan and Fitzpatrick, 2007). Stone money quarrying activity and transport between Yap and Palau was one part of Yap's extensive inter-island exchange networks across Micronesia. In addition to moving people and goods between archipelagos, they provided a new source of glass beads to local Palau economy. At the same time, the Yapese were engaged in the *sawei* tribute system involving atoll dwellers to the east. Although some highly valued items such as sennit cord were exchanged to both Palau and Yap's outer islands, glass beads were exclusively traded with Palauans—and not a part of *sawei* exchanges—likely because there was little demand for them on remote atolls where other types of exchange valuables were used or preferred. In addition to highlighting the navigational feats required to travel throughout western and central Micronesia, our research helps shed light on multiple, contemporaneous, and highly-organized exchange networks using many different types of objects or resources as part of exchange behaviors.

Conclusions

Like other types of "currency" or exchange valuables in traditional island societies, Palauan money beads were highly valued and used in a variety of different social transactions for obtaining goods or services. People from Yap negotiated access to stone money quarries by offering highly-valued glass beads, corvée labor, and marriage partners while using less valuable glass beads to purchase supplies. Despite participating in multiple overlapping long-distance exchange networks, the Yapese used glass beads exclusively in Palau where they had already been in circulation for centuries. The recovery of more than three dozen glass beads from the Yapese stone money quarry at Chelechol ra Orrak is unique in that glass beads in this quantity have never been previously recovered archaeologically from non-mortuary contexts or in a stone money quarry site. Morphological and compositional analyses indicate that the assemblage overwhelmingly consists of Bohemian varieties produced ca. 1830-1850 and, accordingly, were recent introductions to the region that provides an independent line of evidence to understand when quarrying activity took place at Orrak. The majority of the beads in the Orrak assemblage can be correlated with the *cheldoech* type of Palauan bead money.

The entire category of *cheldoech* was devalued by the 1920s because counterfeiting was so widespread. Our research suggests that the devaluation of this bead type began as early at the mid-19th century, decades earlier than ethnohistoric accounts indicate. Despite being a devalued type, multiple sources indicate that there was both a market and demand for devalued and counterfeit *udoud*, though it is difficult to know when counterfeiting began since it took many different forms. There appears to be a shift in the way Palauans used and exchanged *cheldoech*; however, these beads were still valued and exchanged in different ways.

Beyond using these beads to help better understand the nature of Palauan-Yapese interactions, they provide an important artifact class with which to help answer a number of important questions relating to pre-European exchange behaviors and post-contact interactions. Using the beads as a TPQ, they suggest that quarrying activity at the site may have continued until the 1830-1850s, which can then be used to help anchor the chronology of stone money quarrying activity at Chelechol ra Orrak.

Important questions remain that can be tested with future research. It is unknown if bead chronologies developed in Western North America are appropriate parallels or if there was a time-lag and glass beads were distributed in the Pacific at a later date (Francis, 1994). In terms of using the beads as chronological markers, it should be possible to build more refined Bayesian models using the beads as priors and model the Yapese stone money quarrying component at Orrak (see Fitzpatrick and Jew, 2018). Given that this is the only example of glass beads being recovered from a stone money quarry site, the Orrak assemblage can be used to compare with other quarries identified in Palau through archaeological survey or oral tradition. Future excavation at these types of sites may reveal if glass beads occur more frequently at stone money quarries or if the Orrak assemblage is distinct and represents a unique place to understand the nature of Palauan-Yapese interactions at a key period of time for both societies as they engaged in exchange with each other and newly arrived Europeans and Euro-Americans.

CHAPTER VI

CONCLUSION

Introduction

Chronology building is one of the most fundamental aspects of archaeological inquiry with radiocarbon dating being the most important technique in which ages can be assigned to archaeological sites and materials (Bronk Ramsey 2008; Wood 2015). The ability to develop accurate, precise, and robust temporal assignments hinges on selecting ideal samples from undisputed cultural contexts. However, there are limitations to radiocarbon dating, particularly at the upper and lower ends of the calibration curve. Other times, sites may lack suitable material for dating. In coastal sites around the world, where people often harvested vast quantities of marine species, shells are a common and readily available material for dating archaeological deposits, particularly if archaeobotanical remains (e.g., carbonized wood, nuts, seeds) are lacking. Marine shells are typically more abundant, better preserved, less susceptible to vertical shifting, and easily recoverable compared to other types of samples such as carbonized wood (Thomas 2008: 346). As such, the dating of marine shells has proven to be a critical tool for examining a host of issues, including population movements, settlement histories, long-term changes in human-environment interactions, paleoenvironmental conditions, and many others. The chapters in this dissertation have outlined multiple approaches for best practices to improve chronology building in island environments. Using four case studies from around the world, I have shown that it is possible to produce robust chronologies in these and other locations using chronometric hygiene, Bayesian modeling, marine reservoir corrections, and chemical compositional analysis of diagnostically distinct glass beads.

Summary of research

In the Caribbean, pervasive problems in the way radiocarbon dates are calibrated and reported have resulted in imprecise or incorrect interpretations of the past. After more than half a century of archaeological research in the Caribbean, two competing models of human colonization have emerged: the stepping-stone model and the southward route hypothesis. Like other world regions where humans appear to have moved rapidly through landscapes or seascapes, such as the Pacific colonization of Remote Oceania that took place in stages from different points of origin—or in North America where the coastal migration versus the ice-free corridor debate has raged for decades—support for one model or another largely depends on the number, quality, and suitability of radiocarbon dates used in analysis. In Chapter 2, I analyzed more than 2400 radiocarbon dates from 585 sites on 55 islands and subjected them to chronometric hygiene protocols and assigned them a class value of 1-4 with Class 3 and 4 dates deemed unreliable for chronology building. Just over half the total number of dates (54%) were Class 1 or 2 and considered acceptable for Bayesian modeling with only 10 dates (0.4%) being assigned as Class 1. In other regions of the world like the Pacific, chronometric hygiene studies use only Class 1 dates for chronology building (e.g., Wilmshurst et al. 2011). This means that only 0.4% of the available 2484 radiocarbon determinations from the Caribbean would be acceptable if the same standards used in other regions were applied here. Most of the Class 3 and 4 dates (74%, n = 843) were rejected because laboratory number, complete provenience, sample material type, or radiocarbon age were lacking. This work underscores the importance of complete reporting, especially of sample material and provenience.

Bayesian modeled colonization estimates suggest direct movement from South America to the northern Caribbean (Cuba, Hispaniola, and Puerto Rico and the northern Lesser Antilles) that initially bypassed the southern Lesser Antilles, with the exception of Barbados. Later colonization estimates for islands in the southern Lesser Antilles support the southern route hypothesis (Callaghan 2001; Fitzpatrick 2006; Fitzpatrick et al. 2010) and the predictions of ideal free distribution (Giovas and Fitzpatrick 2014) and does not support the oft-cited and recently reinvigorated stepping-stone model (Rouse 1986; Siegel 2018; Siegel et al. 2015, 2019).

Overall, this study demonstrates the need for increased rigor in the reporting of radiocarbon determinations to adequately assess their efficacy and maintain chronological control to ensure that interpretive models are satisfactorily anchored in time and accurately reflect, to the best of our ability, the multitude of cultural behaviors that happened in the past. One of the useful outcomes of this database is that it can be easily updated when more radiocarbon dates are made available and can be used to develop local and regional chronologies that focus topics beyond initial human settlement. With the recent publication of 33 new ΔRs for the circum-Caribbean (DiNapoli et al. 2021) and updated calibration curves (Heaton et al. 2020; Reimer et al. 2020), it will be possible to develop increasingly accurate models for many islands.

In Chapter 3, I developed multiple error-weighted pooled mean ΔRs for the Florida Keys region using known-age live-collected scallop shells and demonstrated that there were negative regional offsets to the modeled global average marine calibration curve (Heaton et al. 2020). Individual ΔRs ranges from −257 ± 21 to −34 ± 22 ^{14}C yrs with both the high and low values coming from different species collected at the same location. As such, until more site specific ΔRs can be calculated, it is recommended that error-weighted pooled means are used instead. Isotopic data also suggest that *Argopecten gibbus* may be susceptible to the hardwater effect and produce an "older" ^{14}C age. A comparison of error weighted pooled mean ΔRs show that Biscayne National Park had the most negative offset, which suggests that terrestrial runoffs and currents play a role in variation given its close proximity to peninsular Florida.

Next, I calibrated radiocarbon dates on stratigraphically associated shell and deer bone from the Clupper site, Upper Matecumbe Key, to compare how well the subregional ΔRs fit archaeological samples. It was not possible to develop a ΔR for Upper Matecumbe Key or the Clupper site using museum collections or paired charcoal and shell samples. To remedy this, we used an error weighted pooled mean ΔR for Plantation Key and Lower Matecumbe Key, the islands that border Upper Matecumbe Key. Using a single-phase Bayesian model, the ΔR (−147 ± 78 ^{14}C yrs) produced a good fit with the archaeological samples.

This study demonstrates the importance of developing local ΔRs to use when calibrating archaeological dates on shell. Although it is recommended that site-specific ΔRs be calculated, it may not be possible due to a variety of issues. One way to address this limitation is to use error weighted pooled mean ΔRs. Doing so requires careful sample selection, however, and an understanding of a mollusk's preferred habitat and diet as these factors influence the ^{14}C age and stable isotopic values. This study provides important new baseline data for establishing a ΔR for different parts of the Florida Keys and South Florida generally.

In chapter 4, I compiled a database of 92 radiocarbon dates from Yap, including 31 new dates from my own field research that increased the total number available by 51%. After chronometric hygiene, 54% of the dates were excluded from modeling. Similar to the Caribbean, only 4% (n = 4) were assigned as Class 1. This stems from many samples having been dated on unidentified charcoal. Unlike the Caribbean, where improved reporting could result in many of the Class 3 and 4 dates being reassigned to Class 2, many of the Class 3 and 4 dates from Yap were excluded because they were taken from composite samples or secondary deposits.

To produce a more accurate modeled chronology, we calculated a hypothetical ΔR of −1 ± 128 ^{14}C yrs. Isotopic analysis indicates that, like elsewhere in western Micronesia, *A. antiquata* is likely influenced by hardwater and will require its own ΔR despite the lack of limestone substrate in Yap (see Petchey and Clark 2011, 2021; Petchey et al. 2017, 2018). A more intensive excavation and dating program will be needed to investigate this further though, so that more temporally specific and species-specific ΔRs can be established.

Bayesian modeling of Class 1 and 2 dates with the modeled ΔR produced a colonization estimate for Yap of *2450-2165 cal years BP (95.4% HPD)*. When contextualized with regional evidence for a sea-level drawdown ca. 2500 years ago (e.g., Dickinson 2003; Dickinson and Athens 2007), the data suggest that Yap was not settled until ca. 2500-2100 years ago, but that earlier sites could still be located elsewhere on the island (possibly the northern half), as suggested by Yapese oral traditions.

When results from the sites of Pemrang (Napolitano et al. 2019a) and Balech'lee are combined with that of Rungluw (Intoh and Leach 1985), we now have more robust evidence that settlement in southern Yap was more extensive than previously thought. Newly recovered data from my systematic auger survey also helps to establish an important baseline for understanding sea-level change over the last 3000 years though additional work is needed to better understand nuances involved with landscape development and site formation processes as they relate to human occupation.

In chapter 5, I demonstrate how it is possible to refine site chronology when radiocarbon dates calibrate as modern or fall on a flat part of the radiocarbon calibration curve. At the multicomponent site of Chelechol ra Orrak, 38 glass beads were recovered from a Yapese stone money quarry site in Palau, western Micronesia (Blaiyok 1993; Fitzpatrick 2001, 2003b; Fitzpatrick and Jew 2018). Glass beads (*udoud*) have been exchanged as currency in Palau for centuries. People from Yap negotiated access to stone money quarries by offering highly-valued *udoud*, corvée labor, and marriage partners while using less valuable *udoud* to purchase supplies. Morphological and compositional analyses indicate that the assemblage overwhelmingly consists of Bohemian varieties produced ca. 1830-1850 and, accordingly, were recent introductions to the region that provides an independent line of evidence to understand when quarrying activity took place at Orrak. The production period of the Bohemian beads help anchor when quarrying activity at this site took place because the beads function as a *termini post quem* for site activity. In addition, the majority of the beads in the Orrak assemblage can be correlated with the *cheldoech* type of Palauan bead money. This type of udoud was devalued for economic transactions due to its ease in counterfeiting, but archaeological analysis suggests that this bead type still retained non-economic value to Palauans.

All of these case studies highlight how archaeologists can address some of the limitations imposed by radiocarbon dating, incomplete reporting of radiocarbon dates, and how various methods can be used to understand human activity in past when radiocarbon dating is unreliable. As these chapters demonstrate, chronology building should use only the most reliable and thoroughly reported dates. Bayesian statistical modeling can also incorporate prior information like stratigraphy to produce models that can estimate date ranges for undated archaeological contexts, such as the onset, temporal duration, or end of target events like initial human colonization of an island. When mollusks are selected for radiocarbon dating, samples must be selected carefully with an understanding of habitat preference and diet as these can influence the ^{14}C age. By comparing the isotopes ^{14}C, $^{13}\delta C$, and $^{18}\delta O$, it is possible to understand if certain species are susceptible to external influences like the hardwater effect, which can produce ^{14}C ages that do not reflect the actual age of the sample. Finally, when radiocarbon dating is not reliable, or a site lacks suitable samples for dating, it is possible to use other techniques that can help anchor chronology. These approaches ultimately allow archaeologists to develop increasingly precise and accurate chronologies that can be used to better understand human activities in the past.

Best practices to chronology building on islands

The case studies used in this dissertation demonstrate ways in which archaeologists can use various techniques to overcome some of the limitations with radiocarbon dating. I also outline best practices approaches to chronology building in island environments. Below, I discuss each of these separately in an effort to provide a useful guideline when selecting and analyzing radiocarbon samples.

Increasing the number of dates

Despite a dramatic increase in archaeological research in the Caribbean over the last two decades, the number of available radiocarbon dates is quite small considering it covers an expanse of more than 2.75 million km^2. The meta-analysis of radiocarbon dates in Chapter 2 highlights this problem as only 433 out of 585 (74.0%) archaeological sites still have three or fewer radiocarbon dates with 237 (40.5%) of those sites only have a single date representing an entire site. This is a minimal change compared with the results of Fitzpatrick's (2006) study where 164 (39.4%) sites had a single reported radiocarbon date. Having a small number of dates for a single site limits the ways in which radiocarbon dates can be critically evaluated and interpreted, but it is more likely that spurious dates will not be identified (Spriggs and Anderson 1993). This issue extends to many Quaternary studies and likely reflects, in part, the financial burden of rigorous dating regimes (Blaauw et al. 2018).

In addition, building Bayesian models with too few dates associated with a targeted event should also be avoided. Using hypothetical datasets to analyze the colonization of Fiji and Hawai‘i, Rieth and Hamilton (2021) outline several best practices approaches including at least five dates in a model, incorporating pre-colonization dates if available, and building multiphase models with ideal stratigraphic associations. Having too few dates results in a model that is overly imprecise. Models are also improved when calibrations fall on a steep part of the calibration curve; however, this may not be possible at times in various geographic regions.

In a separate study, using this function with radiocarbon dates group into multiple *phases* also produced more precise colonization estimate for Rapa Nui than in single-*phase* models (DiNapoli et al. 2021). The case study in Chapter 2 grouped all radiocarbon dates in a single-*phase* model regardless of stratigraphy because each island was considered a "site." Moving forward, it might be possible to produce more precise colonization estimates by building multi-*phase* models.

Sample selection

Selecting appropriate samples from secure archaeological contexts is key. Problems with "old wood" have long been identified and inbuilt age (IA) represents a significant problem in areas where species of trees can be long-lived or where it is possible that old driftwood was used for fuel (e.g., Allen and Huebert 2014; Dye 2000; Lepofsky et al. 2003; Schiffer 1986). The best way to address this is by identifying wood charcoal to taxon (preferably species) to avoid dating long-lived species (Allen and Huebert 2014). Preference should be given to short-lived taxa like seeds and nuts, but also twigs recovered from secure anthropogenic contexts to avoid environmental contamination like rootlets that may introduce additional sources of carbon (Brock et al. 2010).

When taxonomic identification is not possible, there are statistical methods that can be used to account for the potential for IA, such as the *Charcoal Outlier* function in OxCal (Dee and Bronk Ramsey 2014). This approach works well for using previously reported radiocarbon dates on identified wood charcoal or charred material. Incorporating the *Charcoal Outlier* function requires an understanding of the lifespans of long-lived tree species. The prior in this model is that the correct age of the modeled events is younger than the unmodeled calibration dates by some unknown amount of time. Thus, the *Charcoal Outlier* model is expected to produce younger age estimates than single-phase modeling without this prior assumption (Dee and Bronk Ramsey 2014). In Chapter 2, each date on unidentified charcoal or charred material was presumed to have some degree IA of up to 100 years.

Similar issues apply to marine samples. The "old shell" problem can be an issue when dating long-lived species, subfossil shells are used as tools, or if shell artifacts are passed on as heirlooms (Rick et al. 2005). Despite the potential for problems with dating marine samples with a marine component (see Hutchinson 2020; Rick et al. 2005), they can provide reliable radiocarbon dates if researchers are careful to select samples with preference given to species where the potential for inbuilt age is minimal. This includes selecting juvenile fauna to avoid potential inbuilt age, when possible.

In addition, marine shell samples should be dated in conjunction with developing marine reservoir corrections (ΔR) for specific sites, habitat, or species. More studies in the Caribbean are doing this, which has been routinely practiced in the Pacific (e.g., Chinique de Armas et al. 2020; Diaz et al. 2017; Petchey and Clark 2010, 2011, 2021; Petchey et al. 2017, 2018). When it is not feasible, because of a lack of suitable terrestrial samples or access to suitable museum collections, using error weighted pooled means from all available samples from the appropriate subregions is an option (e.g., Couthard et al. 2010; DiNapoli et al. 2021; chapter 3).

Faunal remains can also provide dating material, typically in the form of bone or teeth, and are often ideal for directly dating specific events of interest. Human skeletal remains can also be used with the appropriate ethical considerations and support from descendant or stakeholder communities. For example, in the Caribbean, human burials are often interred in existing midden or posthole features, particularly during the Late Ceramic Age (Hoogland and Hofman 2013). In doing so, the original feature's stratigraphy as well as possible dateable material in an associated context, is not only disturbed, but also mixed. In these cases, if the burial is the event of interest, directly dating the skeletal remains is the only reliable approach. However, skeletal tissue is notorious within radiocarbon dating for the numerous challenges it can present, particularly for issues of preservation, diagenesis, and calibration.

A major challenge in calibrating human bone dates in the Caribbean, as well as many other island and coastal regions, is the contribution of marine foods to overall diet. Archaeological and bioarchaeological evidence have demonstrated the utility of marine protein to human diet in many island and coastal regions, and the Caribbean is no exception (e.g., Keegan and DeNiro 1988; Sullivan et al. 2020; see also Chisholm et al. 1982). The result is that many individuals have an overall diet that reflects a combination of marine and terrestrial foods, thus requiring application of a mixed marine and terrestrial calibration curve. Cook et al. (2015) propose a best practices approach for mixed diets that involves the application of a 50% mixed marine and terrestrial curve along with a 10% error range to account for variability in cases where marine foods and C3 plants are consumed. In the Caribbean, however, archaeological and botanical evidence have suggested some consumption of maize, a C4 plant, in the form of macro- and microbotanical remains in archaeological and paleoenvironmental contexts and starch grains trapped in samples of human dental calculus (Mickleburgh and Pagan-Jiminez 2012). In Chapter 2, dates on human bone were calibrated with a 50/50% mixed curve with a 12% error range to account for additional uncertainty with C4 plants.

This problem becomes increasingly complex when individual variation and changes across the life course are considered. As bone turnover is slow, the $\delta^{13}C$ may reflect variation from mobility or changes with age. Additionally, stress and disease can impact nitrogen values. When marine curves are applied, a local marine reservoir correction must also be considered (e.g., DiNapoli et al. 2021). In the cases where people or food resources are moving or being traded, the marine carbon will vary.

Finally, it is also critical that archaeologists date single entities to avoid introducing multiple sources of radiocarbon and additional offsets (Ashmore 1999). Using bulk, or mixed, samples was common practice for both charcoal and marine dates when larger sample sizes were required prior to the development of AMS. Combining multiple specimens, even closely associated ones can introduce multiple radiocarbon ages, producing an unreliable and inaccurate sample age.

Legacy samples

In regions where archaeologists have been working for decades, it is likely that datasets contain conventional radiocarbon dates that have large standard errors. Some define large standard errors are more than 100 years (Hamilton and Krus 2018) or 10% of the radiocarbon age (Wilmsurst et al. 2011). Some chronometric hygiene studies exclude these "legacy dates" because they are considered imprecise (e.g., Wilmshurst et al. 2011). However, when used in a Bayesian model, these legacy dates do not need to be rejected because they can provide useful information in a Bayesian model provided the sample meets other criteria for reporting (Hamilton and Krus 2018; Krus et al. 2015). The best practices approach to dates with large standard errors is to redate the original sample if any is left (Hamilton and Krus 2018). In many cases this is not possible, but it is important for archaeologists currently submitting samples to retain part of the original sample or request any residual sample to be returned from the radiocarbon laboratory for archiving.

Chronometric hygiene

Chronometric hygiene is an effective way to cull unreliable or underreported dates from databases. However, overly strict hygiene protocols can result in too few dates being used for modeling (Schmid et al. 2018). The ideal way to address this is to improve the reliability of dates with complete reporting. This can be achieved by contacting archaeologists and radiocarbon laboratories to obtain missing information as was done for the larger Caribbean-wide study. Note that this may not be possible, however, if an archaeologist is deceased or a radiocarbon laboratory considers data proprietary and is unwilling to share.

Integrating multiple datasets

Given that each chronometric sequencing technique has inherent limitations, several best practices approaches have been developed to overcome these potential obstacles. One of the most effective ways to do this is to build large, interdisciplinary datasets that can produce higher precision results. For example, *Homo erectus* remains recovered on the island of Flores date to ca. 700-840 kya, would have required two open-water crossings to reach (Brumm et al. 2010, 2016; van den Bergh et al. 2016; O'Sullivan et al. 2001). The conditions under which they arrived on the island are still debated, as are the cognitive and behavioral capabilities and by extension, their ability to construct watercraft.

The final appearance of *H. erectus* on Java has also been debated, with dates from the Ngandon site, suggesting that they survived on Java until around 53-27 kya (Swisher et al. 1996). These dates, taken from electron spin resonance and U-series dates of fossil bovine teeth are anomalously young and suggest that they overlapped with *Homo sapiens* (Swisher et al. 1996). These interpretations have been challenged on the grounds that the dated material was not directly associated with *H. erectus* fossils and that taphonomic processes, such as reworking of fluvial deposits and uranium leaching, produced spurious dates (Rizal et al. 2020). Using a combination of methods to date fossil contexts and constrain site formation processes, these fossils were modeled to 117-108 kya (Rizal et al. 2020).

In another example, sea level and bathymetric reconstruction have been used to evaluate the potential for Pleistocene seafaring in the Mediterranean as a number of Greek Islands that were never connected to the mainland, including Crete, Gavdos, Naxos, and some of the southern Ionian Islands, contain some evidence of hominin activity ca. 70-13 kya, suggesting that humans may have had some degree of seafaring capabilities during the Middle Pleistocene (Cherry and Leppard 2015; Ferentinos et al. 2012; Leppard and Runnels 2017; Leppard et al. 2021; Papoulia 2017; Runnels 2014, 2021). In a similar vein, close reexamination of multiple lines of long-accepted evidence for the Balearic Islands in the western Mediterranean, including the timing of endemic faunal extinction, radiometric data, distinguishing natural from anthropogenic fire, and a lack of pre-Neolithic diagnostic artifacts, suggests a surprisingly late colonization when considering the pre-Neolithic colonization of many other nearby islands (Cherry and Leppard 2018b; Leppard et al. 2021).

Iceland is a rare, notable example of how separate lines of evidence can be used to understand initial human colonization. Schmid et al. (2018, 2019, 2021) revised the colonization of Iceland using a combination of dated tephra layers, radiocarbon dates, and temporally diagnostic artifacts. Using this combination with the application of chronometric hygiene and Bayesian modeling to radiocarbon dates, they reevaluate the notion that all dates from the Viking Age relate to the colonization of Iceland (*Landnám*). Their analyses demonstrate that less than 1% of archaeological sites are from the pre-*Landnám* period (pre-AD 877) and that 15% of sites are from the initial colonization period (AD 877-939), which has broad implications for understanding the settlement density of Icelandic colonization sites (Schmid et al. 2021). These examples demonstrate that as archaeologists continue to incorporate ancillary datasets from other fields of study, we can expect increasingly refined pictures of colonization to emerge.

Beyond chronologies: Implications for understanding the past

Having outlined multiple approaches to address some of the limitations of radiocarbon dating, it is possible to explore what the implications are for a more nuanced understanding of the past. Understanding when humans first reached previously uninhabited islands is linked to many larger anthropological themes, such as the development of seafaring technologies and wayfinding skills (Anderson et al. 2010a; Bednarik 2003; Erlandson 2010; Fitzpatrick and Callaghan 2008; Montenegro et al. 2016), understanding linguistic diasporas, particularly the spread of Austronesian languages out of Taiwan to the Pacific and Indian Ocean (e.g., Adelaar and Himmelmann 2013 and papers therein; Blust 2013; Donohue et a. 2010; Spriggs 2011), understanding extinction or extirpation events (Anderson et al. 2010b; Clark et al. 2013; Louys et al. 2021; Rijsdijk et al. 2011; Rawlence et al. 2016; Seersholm et al. 2018), and long-term anthropogenic impacts on our own planet such as the onset of the Anthropocene (e.g., Boivin et al. 2016; Braje et al. 2017; Erlandson 2013; Erlandson and Rick 2010; Rick et al. 2013). Finally, as we move forward as a discipline, many archaeologists working on islands find themselves "racing a rising tide" (sensu Erlandson 2008) and trying to mitigate the impacts of climate change and sea-level rise. In many instances, aspects of cultural heritage are at risk of being permanently lost due to erosion, inundation, or coastal commercial development. Recent projections of sea-level rise and its impacts on small and low-lying islands represents an ever-increasing threat to the preservation of cultural heritage in Small Island Developing States with some studies predicting that more than half of the Pacific's low-lying atolls will be uninhabitable by the end of the century (e.g., Barnett and Campbell 2010; Dickinson 1999; Erlandson 2012; Kelman

2010; Storlazzi et al. 2018). Unfortunately, even if global efforts to mitigate sea level rise are effective, island nations still face increasing vulnerability to natural disasters and threats to local economies, food production strategies, and cultural heritage sites (e.g., Kelman and West 2009; Terry and Chiu 2012; Storlazzi et al. 2018). One critical part to protecting and preserving cultural heritage is understanding the long-term temporal trajectories of human history in these regions especially when they are at risk of being permanently lost. Doing so requires an accurate understanding of how chronometric sequencing techniques work, their limitations, and how other lines of evidence can be used to build synthetic interpretations of the past that benefit descendant and stakeholder communities.

APPENDIX A

SUPPLEMENTARY MATERIAL FOR CHAPTER II

Supplementary text
Sensitivity analyses for inbuilt age on unidentified wood

Nearly all Class 2 radiocarbon determinations from wood samples were not identified to taxon or identified as long-lived species, potentially presenting inbuilt age problems. To address this, our analysis presents modeled colonization estimates with a 100-year Exponential Outlier model using the *Charcoal_Outlier* model (Bronk Ramsey 2009a; Dee and Bronk Ramsey 2014). The prior assumption in this model is that the correct age of the modeled events is younger than the unmodeled calibration dates by some unknown amount of time. Thus, the *Charcoal_Outlier* model is expected to produce younger age estimates than single-phase modeling without this prior assumption (Dee and Bronk Ramsey 2014). To demonstrate the effect of including 100% probability of some amount of inbuilt age on colonization estimates, we modeled Class 2 wood dates in three ways: 1) as simple single-phase models with no additional parameters, which assumes that each radiocarbon determination is close in age to the actual activity being dated; 2) as having 100% probability of having between 1 and 100 years of inbuilt age; and 3) as having 100% probability of including between 1 and 1,000 years of in-built age using the *Charcoal_Outlier* model (Bronk Ramsey 2009a; Dee and Bronk Ramsey 2014; Napolitano et al. 2019b; Appendix A). 1,000-year Outlier models for Cuba and Puerto Rico were run with the 100 oldest determinations because the models would not converge when modeled with all dates. The 1,000-year outlier models for Trinidad and Guadeloupe would not converge with so many younger radiocarbon determinations. Trinidad's three youngest determinations were removed from the model (I-10766, ISGS-A2629, ISGS-A2630).

Results of sensitivity analyses

As expected, the outlier models produced somewhat younger and more precise colonization estimates than the single-phase modeling (Schmid et al. 2018, 2019); however, some of the 1,000-year models produced spurious results (Napolitano et al. 2019b). As such, we selected the 100-year outlier models for colonization estimates (Napolitano et al. 2019b; Appendix A). Overall, the single-phase and 1,000-year outlier models do not improve upon the 100-year outlier models (Napolitano et al. 2019b; Appendix A). The 1,000 year outlier models from Barbados, Bonaire, Carriacou, Curaçao, Grand Turk, Hispaniola, Nevis, Puerto Rico, San Salvador, St. Martin, St. Thomas, Tobago, Trinidad, and Vieques are reasonable, but we reject the 1,000-year outlier models from Anguilla, Antigua, Aruba, Cuba, Guadeloupe, Jamaica, Montserrat, St. Eustatius, St. John, and St. Lucia because they produced results that conflict with prior archaeological knowledge of these islands. For the 1,000-year outlier model, Jamaica produced a colonization estimate that was out of range at 68% and 95% HPD, and Montserrat produced an estimate that was out of range at 95% HPD; thus, both models were rejected. As prior archaeological research clearly shows pre-contact occupation of these islands, these results are unrealistic and the models were therefore not considered in our final results. The models for Anguilla, St. Eustatius, and St. John were rejected because they produced colonization estimates that span almost the entire *Phase* of acceptable radiocarbon determinations and are therefore uninformative.

In the case of Anguilla, there are 51 radiocarbon determinations in our database, 41 of which are considered acceptable after chronometric hygiene. Prior to chronometric hygiene, the oldest radiocarbon determinations for Anguilla were on shell tools and vessels recovered from surface contexts (see Appendix A). This truncates the previous colonization estimate of ca. 3620 cal yrs BP (Fitzpatrick 2013) to *1510-1185 cal yrs BP (95% HPD)* with the 100 year outlier model. Out of the 41 acceptable determinations, 30 are on unidentified wood charcoal and the remaining 11 are marine shell identified to species. The single-phase model produced a colonization estimate of *1535-1315 cal yrs BP (95% HPD)* and the 1000 year outlier model produced colonization estimate of *1320-745 cal yrs BP (95% HPD)*. This latter estimate encompasses 34 of the 41 oldest dates in the *Phase* and is not a robust colonization estimate. Material culture from Anguilla demonstrates that the island was occupied by Late Ceramic Age. *Zemis/cemís* such as ground three-pointed objects thought to embody Amerindian spirituality, snuffing tubes for inhaling the South American-introduced hallucinogenic substance *cohoba* (*Anadenenthera peregrina*), vomit spatulas, and pottery all suggest that island was colonized and integrated into a large Taíno culture that extended across the Greater Antilles and northern Lesser Antilles (e.g., Crock and Petersen 2004; Fitzpatrick 2015, Hofman et al. 2008), Crock (2000, 2004) suggests that it was possible that residents of Anguilla were part of a "lesser Chiefdom" or part of a multi-island chiefdom by ca. 800 years ago. Ceramic evidence also indicates that there were populations on Anguilla by the Late Ceramic Age (2000, 2004). Based on these lines of evidence, it seems the 1,000-year outlier model for Anguilla adds too much potential inbuilt age to the radiocarbon determinations because the modeled colonization estimate is incongruent with archaeological evidence. The 1,000-year outlier model for Antigua was rejected because it was more than ca. 1500 years younger than the simple single-phase models and produced a large colonization range of almost 1200 years. The result was that the estimate spanned almost the entire known prehistoric occupation of Antigua (after chronometric hygiene) and therefore is not a considered a robust colonization model. Similarly, the 1000-year model for Aruba was rejected because at 95% HPD the colonization estimate is modeled at *3575-1540 cal yrs BP*. We do not consider a ca. 2,000 year range to be a robust model. The 1000-year outlier model for Cuba was rejected because it produced a colonization estimate that was ca. 1000 years younger than that produced by single-phase modeling. Given the presence of pottery-bearing sites on Cuba that extend into the Archaic period, we reject the *Charcoal_Outlier* model for being too conservative and contradicting our prior archaeological knowledge of the island's archaeology (see Fitzpatrick 2015; Keegan and Hofman 2017).

Legacy dates

Cuba has 40 legacy dates—determinations with standard errors (SE) of 100 years or more, typically conventional radiocarbon dates sampled prior to the development of AMS—including the three oldest acceptable determinations from the island. In a single phase model with legacy dates, Cuba's modeled colonization estimate is *5950-5335 cal yrs BP* (95% HPD). Without legacy dates, the modeled colonization date is *4800-4535 cal yrs BP* (95% HPD). While in some cases using legacy dates with large SE has a negligible impact on model precision and accuracy (Hamilton and Krus 2018), our results show that in the case of Cuba, these determinations with large SE produce modeled ages that are substantially older than when using more precise data. In both models, however, the colonization estimate is still younger than previously reported. Our modeling still supports a colonization during the Archaic period and Cuba remains one of the earliest islands colonized in the Greater Antilles (e.g., Fitzpatrick 2015; chapter 2: Table 1).

Puerto Rico

Modeling all 451 determinations resulted in a low model agreement (40.0%) (Appendix A, Table 1). The low model agreement is caused by an over-representation of dates in the middle and late part of the *Phase*, thus biasing the early end of the *Phase* because the determinations are not uniformly distributed. To assess how the model for Puerto Rico improves with fewer younger determinations, models were run in increments of 25 until only the 100 oldest determinations were modeled. Modeled colonization estimates do not change significantly when younger determinations were removed from the model, but the model agreement (A_{model}) increases from 40.0% with 451 dates to 117.7% with 100 dates and becomes acceptable with 425 and 375 and fewer dates; the overall agreement ($A_{overall}$) increases from 76.0% with 445 dates to 104.6% with 100 dates. The overall agreement increases significantly with 325 dates.

Tau Boundary

One potential limitation to this study is that we have included all radiocarbon determinations and grouped them in a single *Phase*. For islands that have a large number of radiocarbon determinations, many of them likely do not closely relate to colonization and can potentially produce younger colonization estimates. The *Tau_Boundary* function in OxCal can be used to exponentially weight activity within a *Phase* toward the one end by placing the *Tau Boundary* as the beginning or end event (Bronk Ramsey 2009a). Because we are more interested in the older radiocarbon determinations, we modeled Trinidad and Puerto Rico with the *Tau_Boundary* as the end event (Bronk Ramsey 2009a). The *Tau Boundary* for Trinidad with a 100-year Outlier Model produced a colonization estimate of *8365-7835 cal yrs BP (95% HPD)*, which is a slightly more precise range than that produced by the single-phase modeling or the *Charcoal_Outlier* analyses (Appendix A). A single phase model with the *Tau_Boundary* for Puerto with all 451 radiocarbon determinations produced a model with an unacceptable model index of 35.4%. When modeled with 325 dates, the Tau Boundary produced a modeled estimate of *4500-4425 cal yrs BP (95% HPD)* with a model agreement of 84.2%. With a range of just 75 years, the *Tau_Boundary* appears to have improved the precision of the modeled colonization estimate without shifting the estimated colonization date. One possible avenue for future research is to add a *Tau Boundary* to other islands with radiocarbon determinations that span millennia to improve precision of the modeled colonization estimates.

Table 1. Radiocarbon dates from 55 Caribbean islands with their assigned class value. Class 1 and 2 radiocarbon dates qualified for Bayesian modeling. Original taxonomic names are reported, see Appexndix A, Table 2 for the current classification. Commas in some lab numbers been omitted (e.g., "I-1,2345" has been standardized to "I-12345"). See Appendix A, Table 3 for list of laboratory abbreviations and names. See Appendix A, Table 4 for complete bibliographic information. $\delta^{13}C$ values published here should not be used for dietary reconstruction.

Island	Country/ Territory	Region	Class	Site	Sample Material	Sample Type	Provenience	Lab Number	CRA	Error	$\delta^{13}C$ (‰)	Reference
Abaco	Bahamas	Bahamian Archipelago	3	Gilpin Point	*Crocodylus rhombifer* post orbital bone	faunal material	—	Beta-338510	1020	30	-19.4	Steadman et al. 2014
Abaco	Bahamas	Bahamian Archipelago	3	Gilpin Point	*Chelonoidis alburyorum* left first costal	faunal material	—	Beta-338511	1010	30	-21.6	Steadman et al. 2014
Abaco	Bahamas	Bahamian Archipelago	3	Gilpin Point	*Chelonia mydas* left first costal	faunal material	—	Beta-338512	1340	30	-9.6	Steadman et al. 2014
Abaco	Bahamas	Bahamian Archipelago	3	Gilpin Point	*Conocarpus erectus*	wood	—	Beta-338518	900	30	-28.4	Steadman et al. 2014
Abaco	Bahamas	Bahamian Archipelago	3	Gilpin Point	*Sabal Palmetto*	wood	—	Beta-345519	990	30	-28.0	Steadman et al. 2014
Abaco	Bahamas	Bahamian Archipelago	2	Sawmill Sink	human bone collagen, tibia	human bone/teeth	peat	Beta-228852	870	30	-14.7	Steadman et al. 2007
Andros	Bahamas	Bahamian Archipelago	3	Sanctuary Cave	human bone collagen, radius	human bone/teeth	—	Beta-268510	520	40	-14.8	Hastings et al. 2014
Andros	Bahamas	Bahamian Archipelago	3	Stargate Cave	human bone collagen, radius	human bone/teeth	—	Beta-268511	620	40	-16.0	Hastings et al. 2014
Anegada	British Virgin Islands	Lesser Antilles	3	midden	*Strombus gigas*	marine shell	—	—	1245	80	—	Gross 1976:234; Davis and Oldfield 2003:2

Anguilla	Anguilla	Lesser Antilles	2	Barnes Bay (AL14-BB)	charcoal	charcoal/ charred material	N401 E417-418, L. 19B	Beta-106441	840	80	—	Crock 2001:132
Anguilla	Anguilla	Lesser Antilles	2	Barnes Bay (AL14-BB)	charcoal	charcoal/ charred material	N401 E423, L. 22B	Beta-106442	1120	70	—	Crock 2001:132
Anguilla	Anguilla	Lesser Antilles	2	Barnes Bay (AL14-BB)	*Strombus gigas*	marine shell	N402 E423 L. 22B	Beta-106444	1180	60	—	Crock 2001:132
Anguilla	Anguilla	Lesser Antilles	2	Barnes Bay (AL14-BB)	*Strombus gigas*	marine shell	N402 E423, L. 19B	Beta-106443	1180	60	—	Crock 2001:132
Anguilla	Anguilla	Lesser Antilles	2	Forest North (AL20-FN)	*Strombus* sp.	marine shell	N235 E252, 10-20 cm	Beta-141202	740	60	—	Crock 2001:195
Anguilla	Anguilla	Lesser Antilles	3	Forest North (AL20-FN)	*Strombus* sp.	marine shell	surface	Beta-63159	1970	60	—	Crock 2001:194; Crock and Petersen 2001
Anguilla	Anguilla	Lesser Antilles	2	Fountain Cave (AL01-FC)	charcoal	charcoal/ charred material	TP 1, 100 cmbs	Beta-15824	1530	140	—	Watters 1991; Crock and Petersen 2001; Douglas 1991
Anguilla	Anguilla	Lesser Antilles	2	Fountain Cave (AL01-FC)	*Cittarium pica*	marine shell	TP 1, 50-55 cmbs	Beta-15485	1220	70	—	Watters 1991; Crock and Petersen 2001; Douglas 1991

Anguilla	Anguilla	Lesser Antilles	2	Fountain Cave (AL01-FC)	*Cittarium pica*	marine shell	TP 1, 72-75 cmbs	Beta-15486	1130	80	—	Watters 1991; Crock and Petersen 2001; Douglas 1991
Anguilla	Anguilla	Lesser Antilles	2	Rendezvous Bay (AL02-RZ)	charcoal	charcoal/ charred material	AAHS pit B3, 45.7 cmbs	Beta-21858	1410	60	—	Crock and Petersen 2001
Anguilla	Anguilla	Lesser Antilles	2	Rendezvous Bay (AL02-RZ)	charcoal	charcoal/ charred material	AAHS pit D4, 25.4 cmbs	Beta-21861	1080	90	—	Douglas 1991 cited in Crock and Petersen 2001
Anguilla	Anguilla	Lesser Antilles	2	Rendezvous Bay (AL02-RZ)	charcoal	charcoal/ charred material	Strat. VI, 90-100 cmbs	Beta-18739	1000	110	—	Watters and Petersen 1991; Crock and Petersen 2001
Anguilla	Anguilla	Lesser Antilles	2	Rendezvous Bay (AL02-RZ)	charcoal	charcoal/ charred material	Stratum II, 30-40 cmbs	Beta-18738	1120	70	—	Watters and Petersen 1991; Crock and Petersen 2001
Anguilla	Anguilla	Lesser Antilles	2	Rendezvous Bay (AL02-RZ)	charcoal	charcoal/ charred material	Stratum II, 40-50 cmbs	Beta-19955	1150	60	—	Watters and Petersen 1991; Crock and Petersen 2001

Anguilla	Anguilla	Lesser Antilles	2	Rendezvous Bay (AL02-RZ)	charcoal	charcoal/ charred material	Stratum IV, 60-70 cmbs	PITT-0545	1135	40	—	Watters and Petersen 1991; Crock and Petersen 2001
Anguilla	Anguilla	Lesser Antilles	2	Rendezvous Bay (AL02-RZ)	charcoal	charcoal/ charred material	Stratum VI, 80-90 cmbs	Beta-19956	1290	60	—	Watters and Petersen 1991; Crock and Petersen 2001
Anguilla	Anguilla	Lesser Antilles	2	Rendezvous Bay (AL02-RZ)	charcoal	charcoal/ charred material	Stratum VI, 90-100 cmbs	Beta-19957	1550	70	—	Watters and Petersen 1991; Crock and Petersen 2001
Anguilla	Anguilla	Lesser Antilles	2	Rendezvous Bay (AL02-RZ)	charcoal	charcoal/ charred material	Stratum VII, 120-130 cmbs	Beta-18740	1430	70	—	Watters and Petersen 1991; Crock and Petersen 2001
Anguilla	Anguilla	Lesser Antilles	2	Rendezvous Bay (AL02-RZ)	*Strombus gigas*	marine shell	N194 E991, 110 cmbs	Beta-257182	890	40	+0.7	John Crock personal communication
Anguilla	Anguilla	Lesser Antilles	2	Rendezvous Bay (AL02-RZ)	*Strombus gigas*	marine shell	N194 E991, 150 cmbs	Beta-257181	910	40	+1	John Crock personal communication

Anguilla	Anguilla	Lesser Antilles	2	Rendezvous Bay (AL02-RZ)	*Strombus gigas*	marine shell	N194 E991, 40 cmbs	Beta-257185	780	40	+1	John Crock personal communication
Anguilla	Anguilla	Lesser Antilles	2	Rendezvous Bay (AL02-RZ)	*Strombus gigas*	marine shell	N194 E991, 50 cmbs	Beta-257184	860	40	+4.4	John Crock personal communication
Anguilla	Anguilla	Lesser Antilles	2	Rendezvous Bay (AL02-RZ)	*Strombus gigas*	marine shell	N194 E991, 95 cmbs	Beta-257183	680	40	+3.4	John Crock personal communication
Anguilla	Anguilla	Lesser Antilles	3	Rendezvous Bay (AL02-RZ)	charred material	charcoal/ charred material	N181 E750, N182 E750, 130 cmbs, level 51A	Beta-277834	840	50	-23.7	John Crock personal communication
Anguilla	Anguilla	Lesser Antilles	3	Rendezvous Bay (AL02-RZ)	charred material	charcoal/ charred material	N181 E750, N182 E750, 130 cmbs, level 56B	Beta-277836	1140	50	-24.9	John Crock personal communication
Anguilla	Anguilla	Lesser Antilles	3	Rendezvous Bay (AL02-RZ)	charred material	charcoal/ charred material	N181 E750, N183 E750, 130 cmbs, level 54A	Beta-277835	1020	50	-24.5	John Crock personal communication
Anguilla	Anguilla	Lesser Antilles	2	Rendezvous Bay (AL02-RZ)	charcoal	charcoal/ charred material	Feature 3, 130-140 cmbs	PITT-0546	1180	45	—	Watters and Petersen 1991; Crock and Petersen 2001

Anguilla	Anguilla	Lesser Antilles	2	Rendezvous Bay (AL02-RZ)	charcoal	charcoal/ charred material	Feature 4, 120-130 cmbs	PITT-0547	1085	55	—	Watters 1991; Crock and Petersen 2001
Anguilla	Anguilla	Lesser Antilles	2	Sandy Ground (AL03-SG)	charcoal	charcoal/ charred material	N479 E267, 40-50	Beta-110397	1310	80	—	Petersen and Crock 2001:132
Anguilla	Anguilla	Lesser Antilles	2	Sandy Ground (AL03-SG)	charcoal	charcoal/ charred material	N482 E280, 30-40	Beta-110393	1140	60	—	Petersen and Crock 2001:132
Anguilla	Anguilla	Lesser Antilles	2	Sandy Ground (AL03-SG)	charcoal	charcoal/ charred material	N482 E280, 50-60	Beta-110394	1230	70	—	Petersen and Crock 2001:132
Anguilla	Anguilla	Lesser Antilles	2	Sandy Ground (AL03-SG)	charcoal	charcoal/ charred material	N482 E280, 70-80	Beta-110395	1170	80	—	Petersen and Crock 2001:132
Anguilla	Anguilla	Lesser Antilles	2	Sandy Ground (AL03-SG)	charcoal	charcoal/ charred material	N482 E280, 90-100	Beta-110396	1290	60	—	Petersen and Crock 2001:132
Anguilla	Anguilla	Lesser Antilles	2	Sandy Ground (AL03-SG)	charcoal	charcoal/ charred material	N482 E285, 40-50	Beta-110398	780	80	—	Petersen and Crock 2001:132
Anguilla	Anguilla	Lesser Antilles	2	Sandy Hill Bay (AL08-SH)	charcoal	charcoal/ charred material	area disturbed for cistern 35.6 cmbs	Beta-21863	940	80	—	Douglas 1991 cited in Crock and Petersen 2001
Anguilla	Anguilla	Lesser Antilles	2	Sandy Hill Bay (AL08-SH)	charcoal	charcoal/ charred material	area disturbed for cistern 50.8 cmbs	Beta-21862	880	90	—	Douglas 1991 cited in Crock and Petersen 2001
Anguilla	Anguilla	Lesser Antilles	2	Sandy Hill Bay (AL08-SH)	charcoal	charcoal/ charred material	N490 E285, 10-35	Beta-120152	950	70	—	Crock 2001:101; Petersen and Crock 2001:132

Anguilla	Anguilla	Lesser Antilles	2	Sandy Hill Bay (AL08-SH)	charcoal	charcoal/ charred material	N490 E286, 30-55	Beta-120153	740	60	—	Crock 2001:101; Petersen and Crock 2001:132
Anguilla	Anguilla	Lesser Antilles	2	Sandy Hill Bay (AL08-SH)	charcoal	charcoal/ charred material	N490 E286, 50-75	Beta-120154	850	60	—	Crock 2001:102; Petersen and Crock 2001:132
Anguilla	Anguilla	Lesser Antilles	2	Sandy Hill Bay (AL08-SH)	charcoal	charcoal/ charred material	N575 E205, 20-35	Beta-106440	510	80	—	Crock 2001:102; Petersen and Crock 2001:132
Anguilla	Anguilla	Lesser Antilles	2	Shoal Bay East (AL19-SE)	charcoal	charcoal/ charred material	N375 E475, 60-65	Beta-106439	1270	60	—	Crock 2001:169; Petersen and Crock 2001:132
Anguilla	Anguilla	Lesser Antilles	2	Shoal Bay East (AL19-SE)	charcoal	charcoal/ charred material	N558 E467, 140-150	Beta-120157	880	80	—	Crock 2001:168; Petersen and Crock 2001:132
Anguilla	Anguilla	Lesser Antilles	2	Shoal Bay East (AL19-SE)	charcoal	charcoal/ charred material	N558 E467, 60-70	Beta-120155	440	70	—	Crock 2001:165; Petersen and Crock 2001:132
Anguilla	Anguilla	Lesser Antilles	2	Shoal Bay East (AL19-SE)	charcoal	charcoal/ charred material	N558 E467, 90-100	Beta-120156	710	80	—	Crock 2001:168; Petersen and Crock 2001:132
Anguilla	Anguilla	Lesser Antilles	2	Whitehead's Bluff (AL33-WB)	*Cittarium pica*	marine shell	N120 E85, 10-20 cmbs	Beta-60776	400	60	—	Crock et al. 1995

Anguilla	Anguilla	Lesser Antilles	3	Forest North (AL20-FN)	charcoal	charcoal/ charred material	N236 E252, level 8B	Beta-141201	1140	40	—	Crock 2001:195
Anguilla	Anguilla	Lesser Antilles	3	Whitehead's Bluff (AL33-WB)	charcoal	charcoal/ charred material	surface	Beta-21864	160	70	—	Crock et al. 1995
Anguilla	Anguilla	Lesser Antilles	3	Whitehead's Bluff (AL33-WB)	*Strombus* sp. axe	marine shell	surface	Beta-21865	3240	80	—	Douglas 1991
Anguilla	Anguilla	Lesser Antilles	3	Whitehead's Bluff (AL33-WB)	*Strombus* sp. vessel	marine shell	surface	Beta-60775	3410	60	—	Crock et al. 1995
Anguilla	Anguilla	Lesser Antilles	3	Whitehead's Bluff (AL33-WB)	*Strombus* sp. celt preform	marine shell	surface	Beta-63158	3380	90	—	Crock et al. 1995
Anguilla	Anguilla	Lesser Antilles	3	Whitehead's Bluff (AL33-WB)	*Strombus* sp.	marine shell	surface	PITT-1263	3605	45	—	Crock et al. 1995
Antigua	Antigua and Barbuda	Lesser Antilles	4	Big Deep Bay	charcoal	charcoal/ charred material	—	—	—	—	—	Olsen 1961
Antigua	Antigua and Barbuda	Lesser Antilles	2	Blackman's	human bone collagen, ulna	human bone/teeth	GE4-HUM-2011	SUERC-34163	950	30	-15.7	Bain, personal communication
Antigua	Antigua and Barbuda	Lesser Antilles	3	Brigits	shell	marine shell	—	UM-4005	4810	45	—	de Mille 2011; Nodine 1990
Antigua	Antigua and Barbuda	Lesser Antilles	3	Cloverleaf W	shell	marine shell	—	Beta-23547	2680	80	—	Siegel et al. 2015

Antigua	Antigua and Barbuda	Lesser Antilles	3	Coconut Hall (PE-15)	shell	marine shell	Excavation 1, Stratum F-3, level 30-40 cm	Beta-93701	1350	60	—	Healy et al. 2003
Antigua	Antigua and Barbuda	Lesser Antilles	3	Coconut Hall (PE-15)	shell	marine shell	Excavation 1, Stratum F-6, level 0-10 cm	Beta-81999	1370	60	—	Healy et al. 2003
Antigua	Antigua and Barbuda	Lesser Antilles	4	Crosby Lagoon	organic sediment	sediment	CL09-1, 132-133 cm	AA-86581	680	35	-24.4	Jones et al. 2018a
Antigua	Antigua and Barbuda	Lesser Antilles	3	Deep Bay	shell	marine shell	—	UM-4003	3450	100	—	de Mille 2011; Nodine 1990
Antigua	Antigua and Barbuda	Lesser Antilles	3	Five Islands	shell	marine shell	—	UM-4001	2390	50	—	de Mille 2011; Nodine 1990
Antigua	Antigua and Barbuda	Lesser Antilles	3	Freeman's Bay	—	unknown	—	I-7839	935	80	—	Davis 1988
Antigua	Antigua and Barbuda	Lesser Antilles	3	Freeman's Bay	—	unknown	—	I-7840	1065	80	—	Davis 1988
Antigua	Antigua and Barbuda	Lesser Antilles	3	Freeman's Bay	—	unknown	—	I-7856	480	80	—	Davis 1988
Antigua	Antigua and Barbuda	Lesser Antilles	3	Hand Point	shell	marine shell	—	UM-4002	3390	120	—	Nodine 1990; de Mille 2011
Antigua	Antigua and Barbuda	Lesser Antilles	3	Indian Creek	—	unknown	2 (C1-2)	I-7844	1000	90	—	Rouse and Morse 1999:46
Antigua	Antigua and Barbuda	Lesser Antilles	3	Indian Creek	—	unknown	2 (C3-2)	I-7982	1070	80	—	Rouse and Morse 1999:46
Antigua	Antigua and Barbuda	Lesser Antilles	3	Indian Creek	—	unknown	2 (C3-3)	I-7983	1110	80	—	Rouse and Morse 1999:46

Antigua	Antigua and Barbuda	Lesser Antilles	3	Indian Creek	—	unknown	2 (C3-5)	I-7984	1124	80	—	Rouse and Morse 1999:46
Antigua	Antigua and Barbuda	Lesser Antilles	3	Indian Creek	—	unknown	2 (C4-2)	I-7843	645	80	—	Davis 1988; Rouse and Morse 1999:46
Antigua	Antigua and Barbuda	Lesser Antilles	3	Indian Creek	—	unknown	2 (C4-3)	I-7831	785	80	—	Rouse and Morse 1999:46
Antigua	Antigua and Barbuda	Lesser Antilles	3	Indian Creek	—	unknown	3 (E4-2)	I-7832	855	80	—	Rouse and Morse 1999:46
Antigua	Antigua and Barbuda	Lesser Antilles	3	Indian Creek	—	unknown	4 (G1-2)	I-7845	1020	80	—	Rouse and Morse 1999:46
Antigua	Antigua and Barbuda	Lesser Antilles	3	Indian Creek	—	unknown	4 (G2-4)	I-7846	1140	80	—	Rouse and Morse 1999:46
Antigua	Antigua and Barbuda	Lesser Antilles	3	Indian Creek	—	unknown	4 (G3-5)	I-7834	1265	80	—	Rouse and Morse 1999:46
Antigua	Antigua and Barbuda	Lesser Antilles	3	Indian Creek	—	unknown	4 (G4-3)	I-7833	1895	80	—	Rouse and Morse 1999:46
Antigua	Antigua and Barbuda	Lesser Antilles	3	Indian Creek	—	unknown	5 (I1-2)	I-7835	845	80	—	Rouse and Morse 1999:46
Antigua	Antigua and Barbuda	Lesser Antilles	3	Indian Creek	—	unknown	5 (I1-3)	I-7847	900	90	—	Rouse and Morse 1999:46
Antigua	Antigua and Barbuda	Lesser Antilles	3	Indian Creek	—	unknown	5 (I1-4)	I-7354	1100	85	—	Rouse and Morse 1999:46
Antigua	Antigua and Barbuda	Lesser Antilles	3	Indian Creek	—	unknown	5(I2-4)	I-7357	1080	85	—	Rouse and Morse 1999:46

Antigua	Antigua and Barbuda	Lesser Antilles	3	Indian Creek	—	unknown	6 (P3-2)	I-7836	1070	80	—	Rouse and Morse 1999:46
Antigua	Antigua and Barbuda	Lesser Antilles	2	Indian Creek	charcoal	charcoal/ charred material	1 (A1-3)	I-7830	2785	80	—	Rouse and Morse 1999:46; Morse and Rouse 1995:316
Antigua	Antigua and Barbuda	Lesser Antilles	2	Indian Creek	charcoal	charcoal/ charred material	1 (A2-3)	I-7842	2785	80	—	Rouse and Morse 1999:46; Morse and Rouse1995:316
Antigua	Antigua and Barbuda	Lesser Antilles	2	Indian Creek	charcoal	charcoal/ charred material	1 (A3-2)	I-7979	1790	85	—	Haviser 1997:62; Rouse and Morse 1999:46; Morse and Rouse 1995:316
Antigua	Antigua and Barbuda	Lesser Antilles	2	Indian Creek	charcoal	charcoal/ charred material	1 (A4-2)	I-7980	1915	80	—	Rouse 1989:397; Haviser 1997:62; Rouse and Morse 1999:46; Morse and Rouse 1995:316

Antigua	Antigua and Barbuda	Lesser Antilles	2	Indian Creek	charcoal	charcoal/ charred material	1 (A4-3)	I-7981	1855	80	—	Rouse 1989:397; Haviser 1997:62; Rouse and Morse 1999:46; Morse and Rouse 1995:316
Antigua	Antigua and Barbuda	Lesser Antilles	2	Indian Creek	charcoal	charcoal/ charred material	5 (I1-5)	I-7353	1230	85	—	Rouse and Morse 1999:46, Morse and Rouse 1995:316
Antigua	Antigua and Barbuda	Lesser Antilles	2	Indian Creek	charcoal	charcoal/ charred material	5 (I1-6)	I-7352	1440	85	—	Haviser 1997:62; Rouse and Morse 1999:46; Morse and Rouse 1995:316
Antigua	Antigua and Barbuda	Lesser Antilles	2	Indian Creek	charcoal	charcoal/ charred material	5 (I2-6)	I-7355	1505	85	—	Haviser 1997:62; Rouse and Morse 1999:46; Morse and Rouse 1995:316
Antigua	Antigua and Barbuda	Lesser Antilles	2	Indian Creek	charcoal	charcoal/ charred material	5 (I2-6)	I-7356	1505	85	—	Haviser 1997:62; Rouse and Morse 1999:46, Morse and Rouse 1995:46

Antigua	Antigua and Barbuda	Lesser Antilles	2	Indian Creek	charcoal	charcoal/ charred material	6 (P2-3)	I-7854	1670	80	—	Haviser 1997:62; Rouse and Morse 1999:46; Morse and Rouse 1995:316
Antigua	Antigua and Barbuda	Lesser Antilles	2	Indian Creek	charcoal	charcoal/ charred material	6 (P2-6)	I-7838	1750	80	—	Haviser 1997:62; Rouse and Morse 1999:46; Morse and Rouse 1995:316
Antigua	Antigua and Barbuda	Lesser Antilles	2	Indian Creek	charcoal	charcoal/ charred material	6 (P3-4)	I-7837	1715	80	—	Haviser 1997:62; Rouse and Morse 1999:46; Morse and Rouse 1995:316
Antigua	Antigua and Barbuda	Lesser Antilles	2	Indian Creek	charcoal	charcoal/ charred material	6 (P3-5)	I-7855	1765	80	—	Haviser 1997:62; Rouse and Morse 1999:46; Morse and Rouse 1995:316
Antigua	Antigua and Barbuda	Lesser Antilles	3	Jolly Beach	charcoal	charcoal/ charred material	—	—	3775	90	—	Davis 1982; Davis 2000:24
Antigua	Antigua and Barbuda	Lesser Antilles	3	Jolly Beach	shell	marine shell	—	Beta-31930	3630	80	—	Nodine 1990; de Mille 2011

Antigua	Antigua and Barbuda	Lesser Antilles	4	Jolly Beach	organic sediment	sediment	JB07-1, 115 cm	AA-82473	1470	35	-25.5	Jones et al. 2018a
Antigua	Antigua and Barbuda	Lesser Antilles	4	Jolly Beach	organic sediment	sediment	JB07-1, 235 cm	AA-82474	3290	60	-28.0	Siegel et al. 2015
Antigua	Antigua and Barbuda	Lesser Antilles	4	Little Deep Bay	charred wood	charcoal/ charred material	base of post	—	—	—	—	Olsen 1961
Antigua	Antigua and Barbuda	Lesser Antilles	3	Mill Reef	—	unknown	—	O-2217	850	105	—	Davis 1988
Antigua	Antigua and Barbuda	Lesser Antilles	3	Mill Reef	—	unknown	—	O-2219	950	105	—	Davis 1988
Antigua	Antigua and Barbuda	Lesser Antilles	3	Mill Reef	—	unknown	—	O-2220	1550	105	—	Davis 1988
Antigua	Antigua and Barbuda	Lesser Antilles	3	Mill Reef	—	unknown	—	O-2258	1450	105	—	Davis 1988
Antigua	Antigua and Barbuda	Lesser Antilles	3	Mill Reef	—	unknown	—	O-2259	1450	105	—	Davis 1988
Antigua	Antigua and Barbuda	Lesser Antilles	3	Mill Reef	—	unknown	—	O-2278	1175	105	—	Davis 1988
Antigua	Antigua and Barbuda	Lesser Antilles	3	Mill Reef	—	unknown	—	O-2279	1105	105	—	Davis 1988
Antigua	Antigua and Barbuda	Lesser Antilles	3	Mill Reef	—	unknown	—	O-JG2-1	1100	105	—	Davis 1988
Antigua	Antigua and Barbuda	Lesser Antilles	3	Mill Reef	—	unknown	—	O-JG2-2	1075	105	—	Davis 1988
Antigua	Antigua and Barbuda	Lesser Antilles	3	Mill Reef	—	unknown	—	O-JG2-3	1225	105	—	Davis 1988
Antigua	Antigua and Barbuda	Lesser Antilles	3	Mill Reef	—	unknown	—	Y-692	2243	70	—	Davis 1988
Antigua	Antigua and Barbuda	Lesser Antilles	3	Muddy Bay (PH-14)	—	unknown	Unit 1 (28 cm)	Beta-74426	720	60	—	Healy and Murphy 1995:287-299; Murphy 1999

Antigua	Antigua and Barbuda	Lesser Antilles	3	Muddy Bay (PH-14)	—	unknown	Unit 1 (49 cm)	Beta-74427	735	70	—	Healy and Murphy 1995:287-299; Murphy 1999
Antigua	Antigua and Barbuda	Lesser Antilles	3	Muddy Bay (PH-14)	—	unknown	Unit 2 (28 cm)	Beta-74428	930	60	—	Healy and Murphy 1995:287-299; Murphy 1999
Antigua	Antigua and Barbuda	Lesser Antilles	3	Muddy Bay (PH-14)	—	unknown	Unit 2 (42 cm)	Beta-74429	710	60	—	Healy and Murphy 1995:287-299; Murphy 1999
Antigua	Antigua and Barbuda	Lesser Antilles	3	North Crabb's Bay	shell	marine shell	—	Beta-164056	3430	50	—	de Mille 2011
Antigua	Antigua and Barbuda	Lesser Antilles	3	North Crabb's Bay	shell	marine shell	—	Beta-164057	3800	70	—	de Mille 2011
Antigua	Antigua and Barbuda	Lesser Antilles	3	North Crabb's Bay	shell	marine shell	—	Beta-164058	3540	70	—	de Mille 2011
Antigua	Antigua and Barbuda	Lesser Antilles	4	Nonsuch Bay	carbonized wood	charcoal/ charred material	NS07-2, 349 cm	AA-82746	190	40	-25.2	Jones et al. 2018a
Antigua	Antigua and Barbuda	Lesser Antilles	4	Nonsuch Bay	organic sediment	sediment	NS07-2, 398 cm	AA-82475	250	35	-26.3	Jones et al. 2018a
Antigua	Antigua and Barbuda	Lesser Antilles	4	Nonsuch Bay	organic sediment	sediment	NS07-2, 445 cm	AA-77643	580	35	-26.5	Jones et al. 2018a
Antigua	Antigua and Barbuda	Lesser Antilles	4	Nonsuch Bay	preserved wood	wood	NS07-2, 221 cm	AA-77644	110	30	-28.2	Jones et al. 2018a
Antigua	Antigua and Barbuda	Lesser Antilles	3	Parham Road	shell	marine shell	—	UM-4004	3140	100	—	Nodine 1990; de Mille 2011
Antigua	Antigua and Barbuda	Lesser Antilles	2	Royall's	charcoal	charcoal/ charred material	Unit 4, Level 8 (70-80 cmbs)	Beta-124126	1600	50	—	Healy et al. 2001:232

Antigua	Antigua and Barbuda	Lesser Antilles	2	Royall's	charcoal	charcoal/ charred material	Unit 4, Level 9, 80-90 cmbs	Beta-124127	1610	80	—	Healy et al. 2001:232
Antigua	Antigua and Barbuda	Lesser Antilles	3	Twenty Hill	shell	marine shell	—	Beta-31931	4660	90	—	Nodine 1990; de Mille 2011
Antigua	Antigua and Barbuda	Lesser Antilles	3	Twenty Hill	shell	marine shell	—	UM-4000	2940	90	—	Nodine 1990; de Mille 2011
Antigua	Antigua and Barbuda	Lesser Antilles	3	Winthorpe's East (GE-1)	—	unknown	—	Beta-127865	710	50	—	Murphy 1999:207
Antigua	Antigua and Barbuda	Lesser Antilles	2	Winthorpe's West (GE-6)	charred material	charcoal/ charred material	Unit 4, Level 3, 54 cm	Beta-101499	720	50	—	de Mille, Murphy, and Healy 1999:105-121
Antigua	Antigua and Barbuda	Lesser Antilles	2	Winthorpe's West (GE-6)	charred material	charcoal/ charred material	Unit 4, Level 7, 140 cm	Beta-101500	1430	50	—	de Mille, Murphy, and Healy 1999:105-121
Antigua	Antigua and Barbuda	Lesser Antilles	3	Winthorpe's West (GE-6)	—	unknown	—	Beta-127864	760	50	—	Murphy 1999:207
Antigua	Antigua and Barbuda	Lesser Antilles	4	—	—	unknown	"fifth layer down" 50 cmbs	—	580	85	—	Olsen 1974
Aruba	Aruba	northern South America	3	Arashi midden	shell	marine shell	—	Beta-450522	2580	30	+4.0	Kelly and Hofman 2019
Aruba	Aruba	northern South America	4	Boca Urirama	—	unknown	—	GrN-32759	1385	35	—	Kelly and Hofman 2019
Aruba	Aruba	northern South America	3	Bringamosa 5	shell	marine shell	—	Beta-450528	3480	30	-3.2	Kelly and Hofman 2019

Aruba	Aruba	northern South America	2	Canashitu	human bone collagen	human bone/teeth	skeleton number C-1	Ua-1501	2210	95	-11.91	Versteeg et al. 1990
Aruba	Aruba	northern South America	3	Ceru Canashito	*Anadara* sp.	marine shell	—	—	1345	120	—	Gould 1971
Aruba	Aruba	northern South America	3	Ceru Canashito	*Cittarium* sp.	marine shell	midden	—	815	105	—	Gould 1971
Aruba	Aruba	northern South America	3	Ceru Canashito	*Chama* sp.	marine shell	midden	—	1685	115	—	Gould 1971
Aruba	Aruba	northern South America	2	Ceru Noka/Santa Cruz	human bone	human bone/teeth	131	GrN-17460	910	170	-7.99	Versteeg et al. 1990
Aruba	Aruba	northern South America	2	Ceru Noka/Santa Cruz	charcoal	charcoal/ charred material	1	GrN-7341	3300	35	—	Versteeg et al. 1990
Aruba	Aruba	northern South America	2	Ceru Noka/Santa Cruz	charcoal	charcoal/ charred material	8	GrN-7342	990	30	—	Versteeg et al. 1990
Aruba	Aruba	northern South America	2	Ceru Noka/Santa Cruz	human bone collagen	human bone/teeth	135	GrN-17459	870	80	-9.19	Versteeg et al. 1990
Aruba	Aruba	northern South America	4	Daimari 1	—	unknown	—	GrN-32760	1430	35	—	Kelly and Hofman 2019
Aruba	Aruba	northern South America	3	Guadirikiri 2	shell	marine shell	—	Beta-450527	1760	30	+3.0	Kelly and Hofman 2019
Aruba	Aruba	northern South America	3	Malmok	shell	marine shell	F. 114	GrN-16833	2175	85	—	Versteeg 1991
Aruba	Aruba	northern South America	3	Malmok	shell	marine shell	Malmok pit 1, center of midden, 0-10 cm	GrN-16838	2370	140	+1.15	Versteeg 1991

Aruba	Aruba	northern South America	3	Malmok	shell	marine shell	Malmok pit 1	GrN-17779	2160	40	+2.52	Van Klinken 1991
Aruba	Aruba	northern South America	3	Malmok	shell	marine shell	Malmok pit 1	GrN-17780	1080	50	+2.38	Van Klinken 1991
Aruba	Aruba	northern South America	3	Malmok	shell	marine shell	pit 1	GrN-16832	2345	140	-2.12	Versteeg 1991
Aruba	Aruba	northern South America	3	Malmok	shell	marine shell	skeleton 35	GrN-16837	2210	90	+1.53	Versteeg et al. 1990
Aruba	Aruba	northern South America	3	Malmok	shell	marine shell	skeleton 41	GrN-16836	2430	150	+2.06	Versteeg et al. 1990
Aruba	Aruba	northern South America	3	Malmok	human tooth	human bone/teeth	Malmok F111	Ua-1513	3560	220	-9.35	Van Klinken 1991
Aruba	Aruba	northern South America	3	Malmok	marine shell	marine shell	Malmok 137	GrN-16835	530	90	-3.23	Van Klinken 1991
Aruba	Aruba	northern South America	2	Malmok	collagen	human bone/teeth	skeleton 11B	Ua-1342	1520	100	-12.46	Versteeg et al. 1990
Aruba	Aruba	northern South America	2	Malmok	collagen	human bone/teeth	skeleton 21B	Ua-1340	1520	110	-12.47	Versteeg et al. 1990
Aruba	Aruba	northern South America	2	Malmok	human bone collagen	human bone/teeth	skeleton 41	Ua-1514	1420	150	-9.69	Versteeg et al. 1990
Aruba	Aruba	northern South America	2	Malmok	collagen	human bone/teeth	skeleton 59B	Ua-1341	1740	110	-10.47	Versteeg et al. 1990
Aruba	Aruba	northern South America	3	Malmok	shell	marine shell	skeleton 19	GrN-16834	2070	80	—	Versteeg et al. 1990
Aruba	Aruba	northern South America	2	Sabaneta	charcoal	charcoal/ charred material	94	GrN-7338	940	25	—	Versteeg et al. 1990

Aruba	Aruba	northern South America	2	Sabaneta	charcoal	charcoal/ charred material	154	GrN-7339	1040	45	—	Versteeg et al. 1990
Aruba	Aruba	northern South America	2	Sabaneta	charcoal	charcoal/ charred material	278	GrN-7340	1000	30	—	Versteeg et al. 1990
Aruba	Aruba	northern South America	4	Seru Colorado 3	—	unknown		Beta-450529	1930	30	-10.0	Kelly and Hofman 2019
Aruba	Aruba	northern South America	3	Spaans Lagoen 3	—	marine shell		Beta-450523	3440	30	-0.5	Kelly and Hofman 2019
Aruba	Aruba	northern South America	3	Spaans Lagoen 4	—	marine shell		Beta-450524	1630	30	+0.1	Kelly and Hofman 2019
Aruba	Aruba	northern South America	3	Spaans Lagoen 5	—	marine shell		Beta-450525	2000	30	+2.1	Kelly and Hofman 2019
Aruba	Aruba	northern South America	4	Spaans Lagoen 6	—	unknown		Beta-446966	1440	30	-8.7	Kelly and Hofman 2019
Aruba	Aruba	northern South America	4	Spaans Lagoen 6	—	unknown		Beta-450526	3450	30	+0.9	Kelly and Hofman 2019
Aruba	Aruba	northern South America	2	Tanki Flip	charcoal	charcoal/ charred material	F.I., S part site	I-4025	765	110	—	Heidecker and Siegel 1969
Aruba	Aruba	northern South America	2	Tanki Flip	charcoal	charcoal/ charred material	F.II, S part site	I-4026	740	105	—	Heidecker and Siegel 1969
Aruba	Aruba	northern South America	2	Tanki Flip	charcoal	charcoal/ charred material	F1265, stone hearth, str-5	GrA-2778	830	50	—	Versteeg 1997
Aruba	Aruba	northern South America	2	Tanki Flip	charcoal	charcoal/ charred material	F1702A, burial child, overlap F1762	GrN-21664	860	40	—	Versteeg 1997
Aruba	Aruba	northern South America	2	Tanki Flip	charcoal	charcoal/ charred material	F1762, Stone hearth, str-10	GrN-21665	1030	40	—	Versteeg 1997

Aruba	Aruba	northern South America	2	Tanki Flip	charcoal	charcoal/ charred material	F1874, stone hearth, str-10	GrN-21666	1030	30	—	Versteeg 1997
Aruba	Aruba	northern South America	2	Tanki Flip	charcoal	charcoal/ charred material	F222, ash hearth, str-3	GrN-2788	1080	50	—	Versteeg 1997
Aruba	Aruba	northern South America	2	Tanki Flip	charcoal	charcoal/ charred material	F408, posthole, pit, str-4	GrA-2790	340	50	—	Versteeg 1997
Aruba	Aruba	northern South America	2	Tanki Flip	charcoal	charcoal/ charred material	F426, posthole, str-4	GrA-2784	750	50	—	Versteeg 1997
Aruba	Aruba	northern South America	2	Tanki Flip	charcoal	charcoal/ charred material	F484, stone hearth, str-6	GrA-2789	990	50	—	Versteeg 1997
Aruba	Aruba	northern South America	2	Tanki Flip	charcoal	charcoal/ charred material	F608, posthole, str-11	GrA-2785	860	50	—	Versteeg 1997
Aruba	Aruba	northern South America	2	Tanki Flip	charcoal	charcoal/ charred material	F9, pottery kiln, outside settlement	GrN-21656	910	30	—	Versteeg 1997
Aruba	Aruba	northern South America	2	Tanki Flip	charcoal	charcoal/ charred material	TFH-197, burial, S part site	GrN-16915	825	30	—	Versteeg 1997
Aruba	Aruba	northern South America	4	Tanki Flip	charcoal	charcoal/ charred material	F49i, posthole	GrN-21657	23470	750	—	Versteeg 1997
Baliceaux	St. Vincent and the Grenadines	Lesser Antilles	2	Banana Bay	*Strombus gigas*	marine shell	10 ft. in from midden face	RL-27	720	100	—	Bullen and Bullen 1972:36-40
Baliceaux	St. Vincent and the Grenadines	Lesser Antilles	2	Banana Bay	*Cittarium pica*	marine shell	S. profile, 30 cmbs	Beta-286848	970	50	+2.8	Fitzpatrick and Giovas 2011
Baliceaux	St. Vincent and the Grenadines	Lesser Antilles	3	Banana Bay	*Strombus gigas*	marine shell	—	RL-71	530	110	—	Bullen and Bullen 1972:36-40

Barbados	Barbados	Lesser Antilles	2	Chancery Lane	charcoal	charcoal/ charred material	48 inches below surface	I-2486	1570	95	—	Bullen and Bullen 1968
Barbados	Barbados	Lesser Antilles	3	Chancery Lane	shell gouge	marine shell	—	I-16307	1770	80	—	Drewett 1991:14; O'Day and Keegan 2001:280
Barbados	Barbados	Lesser Antilles	3	Goddard	charcoal	charcoal/ charred material	Beach deposit below and west of the Goddard House*	Beta-19969	2253	55	—	Hackenberger 1988; Drewett 1989:99; Drewett 1991:14
Barbados	Barbados	Lesser Antilles	3	Goddard	human bone	human bone/teeth	—	D-AMS 009909	980	28	-7.3	Hansen 2015
Barbados	Barbados	Lesser Antilles	2	Goddard	charcoal	charcoal/ charred material	Hearth feature from the east portion of the Goddard House feature*	Beta-20723	1950	150	—	Hackenberger 1988; Drewett 1989:99; Drewett 1991:14
Barbados	Barbados	Lesser Antilles	4	Graeme Hall	shell	marine shell	core, 225	BGS-2395	1409	40	—	Ramcharan 2005
Barbados	Barbados	Lesser Antilles	4	Graeme Hall	preserved peat	peat	core, 104-114	BGS-2397	690	75	—	Ramcharan 2005
Barbados	Barbados	Lesser Antilles	4	Graeme Hall	preserved peat	peat	core, 110 cm	AA-268169	970	40	-25.3	Dunning et al. 2018b
Barbados	Barbados	Lesser Antilles	4	Graeme Hall	preserved peat	peat	core, 170-172 cm	AA-82682	1120	60	-24.9	Dunning et al. 2018b
Barbados	Barbados	Lesser Antilles	4	Graeme Hall	preserved peat	peat	core, 85 cm	AA-92658	270	35	-25.6	Dunning et al. 2018b

Barbados	Barbados	Lesser Antilles	3	Greenland	*Strombus* sp. gouge	marine shell	—	BM-128	850	150	—	Bullen and Bullen 1968:142, 1972:153; Drewett 1989:99; Drewett 1991:14; O'Day and Keegan 2001:280
Barbados	Barbados	Lesser Antilles	3	Greenland	shell gouge	marine shell	Surface collection	BM-128	850	150	—	Bullen and Bullen 1968
Barbados	Barbados	Lesser Antilles	2	Heywoods	triton shell	marine shell	Context 6, Trench 25	1-16189	1120	80	—	Drewett 1991:14; Drewett 1993:116
Barbados	Barbados	Lesser Antilles	2	Heywoods	*Eustrombus gigas* (adze)	marine shell	Context 7, Trench 39	Beta-297521	4230	50	+0.1	Fitzpatrick 2011
Barbados	Barbados	Lesser Antilles	2	Heywoods	conch lip adze	marine shell	TP 39	I-16840	3980	100	—	Drewett 1993:116; Drewett 2000:24
Barbados	Barbados	Lesser Antilles	3	Heywoods	shell	marine shell	—	I-16188	910	80	—	Drewett 1991:14
Barbados	Barbados	Lesser Antilles	3	Heywoods	—	unknown	House 1, context 125	Beta-1134099	1040	60	—	Drewett 2000:165
Barbados	Barbados	Lesser Antilles	3	Heywoods	—	unknown	House 2, context 480	Beta-1134100	1120	50	—	Drewett 2000:165
Barbados	Barbados	Lesser Antilles	3	Heywoods	—	unknown	House 3, context 510	Beta 134101	1230	60	—	Drewett 2000:165
Barbados	Barbados	Lesser Antilles	4	Heywoods	charcoal	charcoal/ charred material	Pit 44	Beta-112110	—	—	—	Drewett 2000:33
Barbados	Barbados	Lesser Antilles	4	Heywoods	wood	wood	Context 55	Beta-113021	—	—	—	Drewett 2000:33

Barbados	Barbados	Lesser Antilles	2	Heywoods	*Eustrombus gigas* (juvenile)	marine shell	Context 7, Trench 39	D-AMS 001792	4366	32	+8.8	this publication
Barbados	Barbados	Lesser Antilles	2	Heywoods	*Eustrombus gigas* (juvenile)	marine shell	Context 7, Unit 35	D-AMS 001793	4278	29	+3.5	this publication
Barbados	Barbados	Lesser Antilles	2	Heywoods	*Eustrombus gigas* (juvenile)	marine shell	Context 8, Trench 30	Beta-297522	4360	40	+0.4	Fitzpatrick 2011
Barbados	Barbados	Lesser Antilles	2	Heywoods	*Eustrombus gigas* (juvenile)	marine shell	Context 8, Unit 35	D-AMS 001794	4091	27	+ 9.2	this publication
Barbados	Barbados	Lesser Antilles	4	Heywoods	wood	wood	Potstack 39	Beta-117589	—	—	—	Drewett 2000:32
Barbados	Barbados	Lesser Antilles	3	Hillcrest	shell axe	marine shell	—	I-16187	780	80	—	Drewett 1991:14; O'Day and Keegan 2001:280
Barbados	Barbados	Lesser Antilles	3	Silver Sands	human bone	human bone/teeth	—	I-16215	650	100	—	Drewett 1991:14
Barbados	Barbados	Lesser Antilles	3	Silver Sands	human bone	human bone/teeth	—	I-16268	1000	150	—	Drewett 1991:14
Barbados	Barbados	Lesser Antilles	3	Silver Sands	shell	marine shell	—	I-16218	990	80	—	Drewett 1991:14
Barbuda	Antigua and Barbuda	Lesser Antilles	2	Burton's Field	*Stombus gigas*	marine shell	Basal Cultural Deposit	UCI-107937	2565	20	—	Rousseau 2012; Vésteinsson 2011
Barbuda	Antigua and Barbuda	Lesser Antilles	2	Burton's Field	*Stombus gigas*	marine shell	Highest Undisturbed Layer	UCI-107938	3430	15	—	Rousseau 2012; Vésteinsson 2011
Barbuda	Antigua and Barbuda	Lesser Antilles	3	Cattle Field	*Pinctada imbricata*	marine shell	associated with shell ridge	UCI-107939	3315	15	—	Rousseau 2012; Vésteinsson 2011
Barbuda	Antigua and Barbuda	Lesser Antilles	4	Grassy Island	preserved peat	peat	GI09-1, 169-170 cm	AA-86580	2820	40	-20.4	Jones et al. 2018b

Barbuda	Antigua and Barbuda	Lesser Antilles	2	Gravenor Bay Transect	*Strombus gigas*	marine shell	BA- GB2	PITT-1234	1365	45	—	Watters 1999; Vésteinsson 2011
Barbuda	Antigua and Barbuda	Lesser Antilles	2	Gravenor Bay Transect	*Strombus gigas*	marine shell	BA-GB1	PITT-1233	1135	50	—	Watters 1999; Vésteinsson 2011
Barbuda	Antigua and Barbuda	Lesser Antilles	2	Gravenor Bay Transect	*Strombus gigas*	marine shell	BA-GB3	Beta-103890	1210	60	—	Watters 1999; Vésteinsson 2011
Barbuda	Antigua and Barbuda	Lesser Antilles	2	Gravenor Bay Transect	*Strombus gigas*	marine shell	BA-GB4	Beta-103891	2030	60	—	Watters 1999; Vésteinsson 2011
Barbuda	Antigua and Barbuda	Lesser Antilles	2	Gravenor Bay Transect	*Strombus gigas*	marine shell	BA-GB5	Beta-103892	1360	60	—	Watters 1999; Vésteinsson 2011
Barbuda	Antigua and Barbuda	Lesser Antilles	2	Gravenor Bay Transect	*Strombus gigas*	marine shell	BA-GB6	Beta-103893	1350	60	—	Watters 1997:196
Barbuda	Antigua and Barbuda	Lesser Antilles	3	Indian Town Trail (BA1)	charcoal	charcoal/ charred material	—	Beta-18492	910	220	—	Watters et al. 1992
Barbuda	Antigua and Barbuda	Lesser Antilles	3	Indian Town Trail (BA1)	*Cittarium pica*	marine shell	—	PITT-0594	445	30	—	Watters et al. 1992
Barbuda	Antigua and Barbuda	Lesser Antilles	3	Indian Town Trail (BA1)	*Strombus gigas*	marine shell	—	PITT-0595	1065	45	—	Watters et al. 1992
Barbuda	Antigua and Barbuda	Lesser Antilles	2	Indian Town Trail (BA1)	charcoal	charcoal/ charred material	BA01-C [2005]	SUERC 18556	820	35	-24.5	Kendall et al. 2011
Barbuda	Antigua and Barbuda	Lesser Antilles	4	Low Pond	organic sediment	sediment	LP09-2, 148-149 cm	AA-86579	2430	45	-24.3	Jones et al. 2018b

Barbuda	Antigua and Barbuda	Lesser Antilles	3	North Sand Ground Plantation	*Strombus gigas*	marine shell	—	PITT-0718	2100	35	—	Watters 1999; Vésteinsson 2011
Barbuda	Antigua and Barbuda	Lesser Antilles	3	North Sand Ground Plantation	*Strombus gigas*	marine shell	—	SI-6695	3340	70	—	Watters and Donahue 1990; Watters et al. 1992; Vésteinsson 2011
Barbuda	Antigua and Barbuda	Lesser Antilles	3	North Sand Ground Plantation	*Strombus gigas*	marine shell	Surface collection	PITT-0590	3560	45	—	Watters et al. 1992; Vésteinsson 2011
Barbuda	Antigua and Barbuda	Lesser Antilles	2	River (JA1)	*Strombus gigas*	marine shell	Area A; Context 005 ("Cultural Layer" c. 50-70 cm)	SUERC 33605 (GU-23531)	2790	35	+3.0	Friðriksson et al. 2011; Kendall et al. 2011; Rousseau 2011
Barbuda	Antigua and Barbuda	Lesser Antilles	2	River (JA1)	*Strombus gigas*	marine shell	Area B; Context 103 (Lower Shell Midden, 27-35 cm)	SUERC-33604 (GU-23530)	3280	35	+4.0	Friðriksson et al. 2011; Kendall et al. 2011; Rousseau 2011
Barbuda	Antigua and Barbuda	Lesser Antilles	3	River (BA4)	*Strombus gigas* celt	marine shell	Surface collection	PITT-0717	3650	35	—	Watters et al. 1992; Vésteinsson 2011
Barbuda	Antigua and Barbuda	Lesser Antilles	3	River (BA4)	*Strombus gigas* celt	marine shell	Surface collection	PITT-0731	3830	25	—	Watters et al. 1992; Vésteinsson 2011

Barbuda	Antigua and Barbuda	Lesser Antilles	3	River (JA1)	*Strombus gigas*	marine shell	Surface collection	PITT-0589	1075	60	—	Watters et al. 1992; Vésteinsson 2011
Barbuda	Antigua and Barbuda	Lesser Antilles	3	Sand Ground Plantation	*Strombus gigas*	marine shell	Surface collection	PITT-0592	2900	50	—	Watters et al. 1992; Vésteinsson 2011
Barbuda	Antigua and Barbuda	Lesser Antilles	3	Sand Ground Plantation	*Strombus gigas*	marine shell	Surface collection	PITT-0719	1755	75	—	Watters et al. 1992; Vésteinsson 2011
Barbuda	Antigua and Barbuda	Lesser Antilles	3	Sand Ground Plantation	*Strombus gigas*	marine shell	Surface collection	SI-6879	5480	100	—	Watters et al. 1992; Vésteinsson 2011
Barbuda	Antigua and Barbuda	Lesser Antilles	3	Sandman	shell	marine shell	—	PITT-0721	3350	50	—	Vésteinsson 2011
Barbuda	Antigua and Barbuda	Lesser Antilles	3	Sandman	shell	marine shell	Surface collection	PITT-0593	2650	50	—	Watters et al. 1992; Vésteinsson 2011
Barbuda	Antigua and Barbuda	Lesser Antilles	3	Sandman	*Strombus gigas*	marine shell	Surface collection	SI-6880	3150	55	—	Watters et al. 1992; Vésteinsson 2011
Barbuda	Antigua and Barbuda	Lesser Antilles	3	Seaview	charcoal	charcoal/ charred material	Context 189, sample 107	SUERC 34972	1975	35	-25.0	Kendall et al. 2011
Barbuda	Antigua and Barbuda	Lesser Antilles	3	Seaview	charcoal	charcoal/ charred material	Context 256, sample 119	SUERC 34970	1900	35	-22.9	Kendall et al. 2011
Barbuda	Antigua and Barbuda	Lesser Antilles	3	Seaview	human bone	human bone/teeth	BAA016-Hum-99	SUERC 34162	1540	30	-17.2	Kendall et al. 2011
Barbuda	Antigua and Barbuda	Lesser Antilles	3	Seaview	—	unknown	from posthole	—	—	—	—	Faucher et al. 2011
Barbuda	Antigua and Barbuda	Lesser Antilles	2	Seaview Erosion	charcoal	charcoal/ charred material	BA016-A1 [804]	SUERC 18557	1755	35	-26.5	Kendall et al. 2011

Barbuda	Antigua and Barbuda	Lesser Antilles	2	Seaview Erosion	charcoal	charcoal/ charred material	BA016-A2 861-863	SUERC 18558	1785	35	-25.3	Kendall et al. 2011
Barbuda	Antigua and Barbuda	Lesser Antilles	3	Seaview Erosion	charcoal	charcoal/ charred material	BA016-A2 [857]	SUERC 18559	1690	35	-25.2	Kendall et al. 2011
Barbuda	Antigua and Barbuda	Lesser Antilles	2	Seaview Erosion	charcoal	charcoal/ charred material	Sample 154, sample 71	SUERC 34971	1565	35	-27.3	Kendall et al. 2011
Barbuda	Antigua and Barbuda	Lesser Antilles	2	Seaview Inland	charcoal	charcoal/ charred material	BA016 TRB-5 posthole	SUERC 18560	2005	35	-25.7	Kendall et al. 2011
Barbuda	Antigua and Barbuda	Lesser Antilles	2	Seaview Inland	charcoal	charcoal/ charred material	TRB-5 [1002] h=78 cm	SUERC 18561	1920	35	-25.8	Kendall et al. 2011
Barbuda	Antigua and Barbuda	Lesser Antilles	2	Seaview Inland	charcoal	charcoal/ charred material	Ba016-TRB-5 [1003] h=232 cm	SUERC 18562	2025	35	-25.0	Kendall et al. 2011
Barbuda	Antigua and Barbuda	Lesser Antilles	4	Seaview	*Ruppia maritima* achenes	plant material	27-30 cm	SUERC 37169	242	30	-15.0 (est.)	Bain et al. 2017
Barbuda	Antigua and Barbuda	Lesser Antilles	4	Seaview	*Ruppia maritima* achenes	plant material	47-49 cm	SUERC 37170	347	30	-15.0 (est.)	Bain et al. 2017
Barbuda	Antigua and Barbuda	Lesser Antilles	4	Seaview	woody fragment	wood	63-64 cm	OS-81963	1959	30	-25.17	Bain et al. 2017
Barbuda	Antigua and Barbuda	Lesser Antilles	4	Seaview	woody fragment	wood	64-65 cm	OS-81964	2121	40	-26.05	Bain et al. 2017
Barbuda	Antigua and Barbuda	Lesser Antilles	3	Singer Cave Road	*Strombus gigas*	marine shell	—	SI-6696	4085	85	—	Watters and Donahue 1990; Watters et al. 1992; Vésteinsson 2011
Barbuda	Antigua and Barbuda	Lesser Antilles	3	Singer Cave Road	*Strombus gigas*	marine shell	surface collection	PITT-0591	2830	80	—	Watters et al. 1992; Vésteinsson 2011

Barbuda	Antigua and Barbuda	Lesser Antilles	3	Singer Cave Road	*Strombus gigas*	marine shell	surface collection	PITT-0720	1930	65	—	Watters et al. 1992; Vésteinsson 2011
Barbuda	Antigua and Barbuda	Lesser Antilles	2	Sufferers	*Strombus gigas*	marine shell	BA3-RC1	PITT-1231	1050	30	—	Watters 1999; Vésteinsson 2011
Barbuda	Antigua and Barbuda	Lesser Antilles	2	Sufferers	*Strombus gigas*	marine shell	BA3-RC2	Beta-103894	1400	60	—	Watters 1999; Vésteinsson 2011
Bonaire	Bonaire	northern South America	2	Amboina (B-001)	charcoal	charcoal/ charred material	10-15 cm b.s.	PITT-0265	710	65	—	Haviser 1991
Bonaire	Bonaire	northern South America	3	Amboina (B-001)	human bone	human bone/teeth	—	GrN-9318	760	25	-10.08	Tacoma 1980
Bonaire	Bonaire	northern South America	2	Amboina (B-001)	charcoal	charcoal/ charred material	10-20 cm b.s.	PITT-0264	560	40	—	Haviser 1991
Bonaire	Bonaire	northern South America	2	Gotomeer #1 (B-073)	*Melongena* sp.	marine shell	Testpit 1, level 1 (0-10 cm)	GrN-32750	3095	20	—	Haviser 2010
Bonaire	Bonaire	northern South America	2	Gotomeer #1 (B-073)	*Melongena* sp.	marine shell	Testpit 1, level 1 (0-10 cm)	GrN-32751	3245	25	—	Haviser 2010
Bonaire	Bonaire	northern South America	2	Gotomeer #1 (B-073)	*Melongena* sp.	marine shell	Testpit 2, level 1 (0-10 cm)	GrN-32748	2412	15	—	Haviser 2010
Bonaire	Bonaire	northern South America	2	Gotomeer #1 (B-073)	*Melongena* sp.	marine shell	Testpit 2, level 1 (0-10 cm)	GrN-32749	2785	20	—	Haviser 2010
Bonaire	Bonaire	northern South America	3	Gotomeer #1 (B-073)	shell	marine shell	0-5 cm b.s.	PITT-0260	2160	55	—	Haviser 2001:118
Bonaire	Bonaire	northern South America	3	Gotomeer #1 (B-073)	shell	marine shell	10-15 cm b.s.	PITT-0261	2105	75	—	Haviser 2001:118

Bonaire	Bonaire	northern South America	3	Lagun (B-021)	shell	marine shell	10-15 cm b.s.	PITT-0258	3320	55	—	Haviser 2001:118
Bonaire	Bonaire	northern South America	3	Lagun (B-021)	shell	marine shell	15-20 cm b.s.	PITT-0259	3275	80	—	Haviser 2001:118
Bonaire	Bonaire	northern South America	3	Noord Lac (B-018)	shell	marine shell	15-20 cm b.s.	PITT-0263	1025	45	—	Haviser 1991
Bonaire	Bonaire	northern South America	2	Slagbaai	*Lobatus* sp.	marine shell	Testpit 9, level 1 (0-10 cm)	GrN-32753	2575	20	—	Haviser 2010
Bonaire	Bonaire	northern South America	2	Slagbaai	*Lobatus* sp.	marine shell	Testpit 9, level 1 (0-10 cm)	GrN-32752	2705	30	—	Haviser 2010
Bonaire	Bonaire	northern South America	2	Slagbaai Salinja #5	*Lobatus* sp.	marine shell	Trench 1, level 1 (0-10 cm)	GrN-32758	3410	20	—	Haviser 2010
Bonaire	Bonaire	northern South America	2	Slagbaai Salinja #5	*Melongena* sp.	marine shell	Testpit 1, level 1 (0-10 cm)	GrN-32754	2665	20	—	Haviser 2010
Bonaire	Bonaire	northern South America	2	Slagbaai Salinja #5	*Melongena* sp.	marine shell	Testpit 2, level 1 (0-10 cm)	GrN-32755	2735	25	—	Haviser 2010
Bonaire	Bonaire	northern South America	2	Slagbaai Salinja #5	*Melongena* sp.	marine shell	Testpit 2, level 1 (0-10 cm)	GrN-32756	3610	25	—	Haviser 2010
Bonaire	Bonaire	northern South America	2	Slagbaai Salinja #6	*Lobatus* sp.	marine shell	Testpit 2, level 1 (0-10 cm)	GrN-32757	2680	25	—	Haviser 2010
Bonaire	Bonaire	northern South America	3	Sorobon (B-008)	shell	marine shell	15-20 cm b.s.	PITT-0262	615	65	—	Haviser 1991
Bonaire	Bonaire	northern South America	2	Wanapa (B-016)	charcoal	charcoal/ charred material	10-15 cm b.s.	PITT-0266	505	35	—	Haviser 1991
Bonaire	Bonaire	northern South America	2	Wanapa (B-016)	charcoal	charcoal/ charred material	15-20 cm b.s.	PITT-0267	1480	25	—	Haviser 1991

Bonaire	Bonaire	northern South America	2	Wanapa (B-016)	charcoal	charcoal/ charred material	15-20 cm b.s.	PITT-0268	885	45	—	Haviser 2001
Bonaire	Bonaire	northern South America	3	Wanapa (B-016)	shell	marine shell	10-15 cm b.s.	PITT-0270	2975	45	—	Haviser 1991
Bonaire	Bonaire	northern South America	4	Wanapa (B-016)	charcoal	charcoal/ charred material	20-25 cm b.s.	PITT-0269	moder n	—	—	Haviser 1991
Carriacou	Grenada	Lesser Antilles	2	Grand Bay	charcoal	charcoal/ charred material	F016	AA-62282	1227	36	-25.97	Fitzpatrick and Giovas 2011
Carriacou	Grenada	Lesser Antilles	2	Grand Bay	charcoal	charcoal/ charred material	Unit 447, layer 6, Depth 110 cmbs	AA-62279	1243	36	-25.13	Fitzpatrick and Giovas 2011
Carriacou	Grenada	Lesser Antilles	2	Grand Bay	charcoal	charcoal/ charred material	Unit 447, Layer 6, Depth 93 cmbs	AA-62281	1339	36	-23.96	Fitzpatrick and Giovas 2011
Carriacou	Grenada	Lesser Antilles	2	Grand Bay	*Tayassu/Pecari* mandible	faunal material	trench 415, square 23, stratum L002, planum 5	UCIAMS-94044	990	20	-22.2	Giovas et al. 2012
Carriacou	Grenada	Lesser Antilles	2	Grand Bay	*Cavia* maxilla	faunal material	trench 446, square 9, stratum L002, planum 4	UCIAMS-94045	1020	20	-13.5	Giovas et al. 2012
Carriacou	Grenada	Lesser Antilles	2	Grand Bay	human bone (adult, rib fragment)	human bone/teeth	563; F1064	Beta-257793	870	40	-12.4	this publication

Carriacou	Grenada	Lesser Antilles	2	Grand Bay	human bone	human bone/teeth	C177; Grand Bay, Carriacou. F177	UCIAMS-111934	690	15	-10.2744801	Giovas 2013; Casto 2015
Carriacou	Grenada	Lesser Antilles	2	Grand Bay	human bone	human bone/teeth	C180; Grand Bay, Carriacou. F180	UCIAMS-111935	1565	15	-13.5740816	Giovas 2013; Casto 2015
Carriacou	Grenada	Lesser Antilles	2	Grand Bay	human bone (child, rt. fibula)	human bone/teeth	F006	AA-62283	1062	44	-14.21	Fitzpatrick and Giovas 2011
Carriacou	Grenada	Lesser Antilles	2	Grand Bay	human bone	human bone/teeth	GB1230	UCIAMS-120951	1015	15	-15.7	this publication
Carriacou	Grenada	Lesser Antilles	2	Grand Bay	*Eustrombus gigas* (juvenile)	marine shell	N.profile, Depth 108 cmbs	Beta-206685	1870	70	+2.1	Fitzpatrick and Giovas 2011
Carriacou	Grenada	Lesser Antilles	2	Grand Bay	*Cittarium pica*	marine shell	Unit 415, Layer 5	Beta-233647	1310	40	+1.8	Fitzpatrick and Giovas 2011
Carriacou	Grenada	Lesser Antilles	2	Grand Bay	*Cittarium pica*	marine shell	Unit 447, Layer 15, Depth 145 cmbs	AA-62278	1917	37	+2.53	Fitzpatrick and Giovas 2011
Carriacou	Grenada	Lesser Antilles	2	Grand Bay	*Venus* sp.	marine shell	Unit 447, layer 6, Depth 127 cmbs	AA-62280a	1789	38	+3.39	Fitzpatrick and Giovas 2011
Carriacou	Grenada	Lesser Antilles	2	Grand Bay	*Venus* sp.	marine shell	Unit 447, layer 6, Depth 127 cmbs	AA-62280b	1822	41	+3.36	Fitzpatrick and Giovas 2011
Carriacou	Grenada	Lesser Antilles	2	Grand Bay	charcoal	charcoal/ charred material	415; Sq. 20, Layer VI; planum 10	D-AMS 016648	1315	20	-23.9	this publication

Carriacou	Grenada	Lesser Antilles	2	Grand Bay	charcoal	charcoal/ charred material	415; Sq. 20, Layer VI; planum 10	D-AMS 16649	1321	20	-14.2	this publication
Carriacou	Grenada	Lesser Antilles	2	Grand Bay	charcoal	charcoal/ charred material	415; Sq. 20, Layer VI; planum 8	D-AMS 016647	1328	20	-20.2	this publication
Carriacou	Grenada	Lesser Antilles	3	Harvey Vale	human bone (rt. ulna)	human bone/teeth	—	AA-62284	1027	46	-12.55	Fitzpatrick and Giovas 2011
Carriacou	Grenada	Lesser Antilles	2	Point Bay	human bone	human bone/teeth	C001; Point Bay, Carriacou. F001	UCIAMS-111933	715	15	-12.6062241	Giovas 2013; Casto 2015
Carriacou	Grenada	Lesser Antilles	2	Sabazan	charcoal	charcoal/ charred material	Layer 11, 53-108 cmbs	AA-67529	988	42	-25.6	Fitzpatrick and Giovas 2011
Carriacou	Grenada	Lesser Antilles	2	Sabazan	charcoal	charcoal/ charred material	Layer 11, 53-108 cmbs	AA-67530	1039	35	-25.6	Fitzpatrick and Giovas 2011
Carriacou	Grenada	Lesser Antilles	2	Sabazan	charcoal	charcoal/ charred material	Layer 13, 108-115 cmbs	AA-67531	1133	38	-24.6	Fitzpatrick and Giovas 2011
Carriacou	Grenada	Lesser Antilles	2	Sabazan	charcoal	charcoal/ charred material	Layer 13, 108-115 cmbs	AA-67532	1073	38	-25.0	Fitzpatrick and Giovas 2011
Carriacou	Grenada	Lesser Antilles	2	Sabazan	charcoal	charcoal/ charred material	Layer 14, 115-154 cmbs	AA-67533	1172	36	-25.0	Fitzpatrick and Giovas 2011
Carriacou	Grenada	Lesser Antilles	2	Sabazan	charcoal	charcoal/ charred material	Layer 14, 115-154 cmbs	AA-67534	1333	57	-24.6	Fitzpatrick and Giovas 2011

Carriacou	Grenada	Lesser Antilles	2	Sabazan	charcoal	charcoal/ charred material	Layer 15, 149-164 cmbs	AA-67535	1588	36	-24.8	Fitzpatrick and Giovas 2011
Carriacou	Grenada	Lesser Antilles	2	Sabazan	charcoal	charcoal/ charred material	Layer 15, 149-164 cmbs	AA-67536	1584	36	-25.8	Fitzpatrick and Giovas 2011
Carriacou	Grenada	Lesser Antilles	2	Sabazan	charcoal	charcoal/ charred material	Layer 6, 215 cmbs	OS-41358	1030	30	-23.94	Fitzpatrick et al. 2004
Carriacou	Grenada	Lesser Antilles	2	Sabazan	charcoal	charcoal/ charred material	midden, ~60-80 cmbs	RL-29	940	100	—	Bullen and Bullen 1972:17, 161
Carriacou	Grenada	Lesser Antilles	2	Sabazan	charcoal	charcoal/ charred material	Tr 1: sq 1, layer 2, 3-13 cmbs	AA-81054	657	44	-23.8	Fitzpatrick and Giovas 2011
Carriacou	Grenada	Lesser Antilles	2	Sabazan	charred seed	charcoal/ charred material	Tr 1: sq 1, layer 4, 30-34 cmbs	OS-71407	960	15	-23.55	Fitzpatrick and Giovas 2011
Carriacou	Grenada	Lesser Antilles	2	Sabazan	charcoal	charcoal/ charred material	Tr 1: sq 1, layer 5, 43-53 cmbs	OS-71408	970	15	-25.99	Fitzpatrick and Giovas 2011
Carriacou	Grenada	Lesser Antilles	2	Sabazan	charred seed	charcoal/ charred material	Tr 1: sq 1, layer 6, 57-67 cmbs	AA-81056	994	45	-25.5	Fitzpatrick and Giovas 2011
Carriacou	Grenada	Lesser Antilles	2	Sabazan	charcoal	charcoal/ charred material	Tr 1: sq 1, layer 6, 73.5 cmbs	OS-71409	925	15	-24.73	Fitzpatrick and Giovas 2011
Carriacou	Grenada	Lesser Antilles	2	Sabazan	charred seed	charcoal/ charred material	Tr 2: sq 1, layer 3, 19-29 cmbs	OS-71462	975	20	-24.5	Fitzpatrick and Giovas 2011

Carriacou	Grenada	Lesser Antilles	2	Sabazan	charcoal	charcoal/ charred material	Tr 2: sq 1, layer 3A, 40-50 cmbs	AA-81055	1158	45	-24.1	Fitzpatrick and Giovas 2011
Carriacou	Grenada	Lesser Antilles	2	Sabazan	charcoal	charcoal/ charred material	Tr 2: sq 1, layer 3A, 75.5 cmbs	OS-71463	1140	15	-23.62	Fitzpatrick and Giovas 2011
Carriacou	Grenada	Lesser Antilles	2	Sabazan	charred seed	charcoal/ charred material	Tr 2: sq 1, layer 8, 89-91 cmbs	OS-71464	1100	20	-24.03	Fitzpatrick and Giovas 2011
Carriacou	Grenada	Lesser Antilles	2	Sabazan	charcoal	charcoal/ charred material	Tr 2: sq 1, layer 9, 115 cmbs	OS-71465	1080	15	-24.04	Fitzpatrick and Giovas 2011
Carriacou	Grenada	Lesser Antilles	2	Sabazan	charcoal	charcoal/ charred material	Tr 3: sq 1, layer 2, 8-19 cmbs	OS-71466	680	15	-24.77	Fitzpatrick and Giovas 2011
Carriacou	Grenada	Lesser Antilles	2	Sabazan	charcoal	charcoal/ charred material	Tr 3: sq 1, layer 3A, 84 cmbs	OS-71467	1220	20	-25.67	Fitzpatrick and Giovas 2011
Carriacou	Grenada	Lesser Antilles	2	Sabazan	*Didelphis* vertebra	faunal material	coastal profile, statum XIV, 115-154 cmbs	UCIAMS-94046	1265	20	-19.0	Giovas et al. 2012
Carriacou	Grenada	Lesser Antilles	2	Sabazan	*Cittarium pica*	marine shell	Layer 5, 160 cmbs	GX-30423	1400	60	+2.4	Fitzpatrick et al. 2004
Carriacou	Grenada	Lesser Antilles	2	Sabazan	*Strombus gigas*	marine shell	Layer 6, 210 cmbs	GX-30424	1570	60	+0.2	Fitzpatrick et al. 2004
Carriacou	Grenada	Lesser Antilles	2	Sabazan	*Cittarium pica*	marine shell	Layer 7, 230 cmbs	GX-30425	1460	60	+2.5	Fitzpatrick et al. 2004
Carriacou	Grenada	Lesser Antilles	4	Sabazan	charcoal	charcoal/ charred material	Tr 2: sq 1, layer 2, 2-11 cmbs	OS-71410	moder n	—	-26.05	Fitzpatrick and Giovas 2011

Cayman Brac	Cayman Islands	Greater Antilles	4	Bedding Plane II	Rodentia; Capromyidae	faunal material	back of cave	ORAU-	897	23	-19.23	Harvey et al. 2016
Cayman Brac	Cayman Islands	Greater Antilles	4	Bedding Plane II	Rodentia; Capromyidae	faunal material	entrance of cave	ORAU-	930	25	-19.54	Harvey et al. 2016
Cayman Brac	Cayman Islands	Greater Antilles	4	Green Cave	Rodentia; Capromyidae	faunal material	Cave Chamber 2	ORAU-	928	26	-18.35	Harvey et al. 2016
Cayman Brac	Cayman Islands	Greater Antilles	4	Green Cave	Rodentia; Capromyidae	faunal material	Cave Chamber 2	ORAU-	609	26	-18.32	Harvey et al. 2016
Cayman Brac	Cayman Islands	Greater Antilles	4	Green Cave	Rodentia; Capromyidae	faunal material	Cave Chamber 3	ORAU-	1588	26	-17.59	Harvey et al. 2016
Cayman Brac	Cayman Islands	Greater Antilles	4	Green Cave	Rodentia; Capromyidae	faunal material	Chamber 5, surface	ORAU-	1166	34	-18.09	Harvey et al. 2016
Cayman Brac	Cayman Islands	Greater Antilles	4	Green Cave	Rodentia; Capromyidae	faunal material	Chamber 5, surface	ORAU-	1134	34	-17.69	Harvey et al. 2016
Cayman Brac	Cayman Islands	Greater Antilles	4	Pebble Cave	Rodentia; Capromyidae	faunal material	Cave Chamber 4	ORAU-	393	25	-19.03	Harvey et al. 2016
Cayman Brac	Cayman Islands	Greater Antilles	3	Great Cave, Pollards Bay	*Cittarium pica*	marine shell	—	I-17143	1230	80	—	Scudder and Quitmyer 1998
Cayman Brac	Cayman Islands	Greater Antilles	3	Great Cave, Pollards Bay	*Cittarium pica*	marine shell	—	I-17144	1480	80	—	Scudder and Quitmyer 1998
Crooked Island	Bahamas	Bahamian Archipelago	3	1702 Cave	*Chelonoidis* sp.	faunal material	CR-26, surface	Beta-445995	2510	30	-19.7	Steadman et al. 2017
Crooked Island	Bahamas	Bahamian Archipelago	4	Acklins	*Cordia* sp.	wood	—	OxA-18449	395	25	-28.9	Ostapkowicz 2015
Crooked Island	Bahamas	Bahamian Archipelago	3	Crossbed Cave	*Geocaproms ingrahami*	faunal material	CR-25; surface	Beta-411055	250	30	-20.1	Steadman et al. 2017
Crooked Island	Bahamas	Bahamian Archipelago	3	Crossbed Cave	*Crocodylus rhombifer*	faunal material	CR-26; surface	Beta-411056	460	30	-17.3	Steadman et al. 2017
Crooked Island	Bahamas	Bahamian Archipelago	2	McKay's Bluff	*Geocaproms ingrahami*	faunal material	CR-5; Unit 1, Level 2	Beta-411057	280	30	-20.7	Steadman et al. 2017

Crooked Island	Bahamas	Bahamian Archipelago	2	McKay's Bluff	*Geocaproms ingrahami*	faunal material	CR-5; Unit 1, Level 4	Beta-411058	300	30	-19.1	Steadman et al. 2017
Crooked Island	Bahamas	Bahamian Archipelago	2	McKay's Bluff	*Chelonoidis* sp.	faunal material	CR-5; Unit 2, Level 2	Beta-451745	870	30	-21.1	Steadman et al. 2017
Crooked Island	Bahamas	Bahamian Archipelago	3	McKay	wood charcoal	charcoal/ charred material	—	UGa-1584	690	75	—	Winter 1978b; Winter 1978:238-239
Crooked Island	Bahamas	Bahamian Archipelago	3	McKay	bulk fauna (fish)	faunal material	—	UGa-1583	210	80	—	Winter 1978b; Winter 1978:238-239
Crooked Island	Bahamas	Bahamian Archipelago	3	McKay	*Strombus gigas*	marine shell	—	UGa-1262	710	65	—	Winter 1978b; Winter 1978:238-239
Crooked Island	Bahamas	Bahamian Archipelago	3	McKay's Bluff	*Geocaproms ingrahami*	faunal material	CR-5; surface	Beta-411059	310	30	-20.7	Steadman et al. 2017
Crooked Island	Bahamas	Bahamian Archipelago	2	Pittstown Landing	*Crocodylus rhombifer*	faunal material	CR-14; Test Pit 2, Layer 4	Beta-445997	860	30	-16.9	Steadman et al. 2017
Cuba	Cuba	Greater Antilles	2	Abra del Cacoyuguin 1	charcoal	charcoal/ charred material	Excavation 1, enlargement 1, level 0.10-0.20 m	Beta-133947	1210	60	—	Ulloa Hung and Valcárcel Rojas 2002:232
Cuba	Cuba	Greater Antilles	2	Abra del Cacoyuguin 1	charcoal	charcoal/ charred material	Excavation 1, enlargement 1, level 0.30-0.40 m	Beta-133948	1640	130	—	Ulloa Hung and Valcárcel Rojas 2002:232

Cuba	Cuba	Greater Antilles	2	Abra Rio Cacoyuguin II	charcoal	charcoal/ charred material	Excavation 2, grid square 1, level 0.40-0.50 m	Beta-133950	2780	40	—	Ulloa Hung and Valcárcel Rojas 2002:232
Cuba	Cuba	Greater Antilles	2	Abra Rio Cacoyuguin II	charcoal	charcoal/ charred material	Excavation 2, grid square 1, level 0.50-0.60 m	Beta-133951	3720	70	—	Ulloa Hung and Valcárcel Rojas 2002:232
Cuba	Cuba	Greater Antilles	2	Abra Rio Cacoyuguin IV	charcoal	charcoal/ charred material	Cut 1, level 0.30-0.40 m	Beta-140079	4180	80	—	Ulloa Hung and Valcárcel Rojas 2002:232
Cuba	Cuba	Greater Antilles	3	Aguas Gordas	charcoal	charcoal/ charred material	Midden 2, pit 1, level 0.50-0.75 m. Assoc. Assoc. with ceramics, some shell and stone artifacts	GD-620	165	60	—	Pino 1995:6; Valcárcel Rojas 2002:140
Cuba	Cuba	Greater Antilles	2	Aguas Gordas	charcoal	charcoal/ charred material	Midden 1, sample depth 1.75 m	Mo-399	1000	105	—	Vinogradov 1968:462; Pazdur et al. 1982:174; Pino 1995:6; Valcárcel Rojas 2002:140
Cuba	Cuba	Greater Antilles	2	Aguas Gordas	charcoal	charcoal/ charred material	Midden 2, pit 1, level 1.25-1.50 m. Assoc. with ceramics, shell and stone artifacts	GD-621	705	65	—	Pino 1995:6; Valcárcel Rojas 2002:140

Cuba	Cuba	Greater Antilles	2	Aguas Gordas	charcoal	charcoal/ charred material	Midden 2, pit 1, level 1.00-1.25 m	GD-1055	575	60	—	Pazdur et al. 1982:174; Pino 1995:6
Cuba	Cuba	Greater Antilles	2	Aguas Gordas	charcoal	charcoal/ charred material	Mound 2, pit 1, level 0.75-1.00 m	GD-1054	485	50	—	Pino 1995:6; Valcárcel Rojas 2002:140
Cuba	Cuba	Greater Antilles	2	Arroyo del Palo, Mayari	charcoal	charcoal/ charred material	Cave no. 1, sample depth .25m	Y-1556	970	80	—	Pino 1995:3
Cuba	Cuba	Greater Antilles	2	Arroyo del Palo, Mayari	charcoal	charcoal/ charred material	Trench 2B, level 0.75-1.00 m (sample depth .75 m)	Y-1555	760	60	—	Pino 1995:3
Cuba	Cuba	Greater Antilles	3	Belleza	charcoal	charcoal/ charred material	Trench 1, level 0.40 m	—	1120	60	—	Ulloa Hung and Valcárcel Rojas 2002:233
Cuba	Cuba	Greater Antilles	3	Birama	charcoal	charcoal/ charred material	—	—	820	40	—	Angelbello 2002:69
Cuba	Cuba	Greater Antilles	2	El Boniato (El Palmar)	charcoal	charcoal/ charred material	Unit 2, grid square 9, level spit depth 0.40-0.50 m, natural layer 2	Beta-148958	670	70	—	Valcárcel Rojas 2002:142
Cuba	Cuba	Greater Antilles	3	Los Buchillones	wood	wood	Sample Number = 33	OxA-15147	157	24	-27.2	Cooper and Thomas 2012
Cuba	Cuba	Greater Antilles	3	Los Buchillones	wood	wood	Post 1, Structure F1-1	TO-8067	240	60	—	Pendergast et al. 2002:72
Cuba	Cuba	Greater Antilles	3	Los Buchillones	wood	wood	Post 3, Structure F1-1	TO-8069	230	70	—	Pendergast et al. 2002:72

Cuba	Cuba	Greater Antilles	3	Los Buchillones	wood	wood	Post 4, Structure F1-1	TO-8070	280	60	—	Pendergast et al. 2002:72
Cuba	Cuba	Greater Antilles	3	Los Buchillones	wood	wood	Post 5, Structure F1-1	TO-8071	250	60	—	Pendergast et al. 2002:72
Cuba	Cuba	Greater Antilles	3	Los Buchillones	wood	wood	Post 7, Structure D2-1,	TO-7619	300	50	—	Pendergast et al. 2002:69
Cuba	Cuba	Greater Antilles	2	Los Buchillones	*Strombus gigas*	marine shell	Sample Number = 37	OxA-15145	879	26	+2.2	Cooper and Thomas 2012
Cuba	Cuba	Greater Antilles	2	Los Buchillones	*Phacoides pectinatus*	marine shell	Sample Number = 38	OxA-15146	1557	25	+2.5	Cooper and Thomas 2012
Cuba	Cuba	Greater Antilles	2	Los Buchillones	*Fasciolaria tulipa*	marine shell	Sample Number = 39	OxA-15151	950	24	+2.6	Cooper and Thomas 2012
Cuba	Cuba	Greater Antilles	2	Los Buchillones	*Oliva recticularis*	marine shell	Sample Number = 40	OxA-15152	939	24	+1.3	Cooper and Thomas 2012
Cuba	Cuba	Greater Antilles	2	Los Buchillones	*Fasciolaria tulipa*	marine shell	Sample Number = 41	OxA-15153	714	25	+1.2	Cooper and Thomas 2012
Cuba	Cuba	Greater Antilles	2	Los Buchillones	*Codakia orbicularis*	marine shell	Sample Number = 42	OxA-15154	820	24	+2.4	Cooper and Thomas 2012
Cuba	Cuba	Greater Antilles	2	Los Buchillones	*Oliva recticularis*	marine shell	Sample Number = 43	OxA-15149	874	25	+1.6	Cooper and Thomas 2012

Cuba	Cuba	Greater Antilles	2	Los Buchillones	*Strombus gigas*	marine shell	Sample Number = 44	OxA-15148	891	23	+3.4	Cooper and Thomas 2012
Cuba	Cuba	Greater Antilles	2	Los Buchillones	wood	wood	King Post 1, Structure D2-1,	TO-7627	460	50	—	Pendergast et al. 2002:69
Cuba	Cuba	Greater Antilles	2	Los Buchillones	wood	wood	King Post 2, Structure D2-1,	TO-7628	560	50	—	Pendergast et al. 2002:69; Kepecs et al. 2010
Cuba	Cuba	Greater Antilles	2	Los Buchillones	wood	wood	Post 1, Structure D2-1,	TO-7617	330	50	—	Pendergast et al. 2002:69
Cuba	Cuba	Greater Antilles	2	Los Buchillones	wood	wood	Post 12, Structure D2-1,	TO-7621	1404	60	—	Pendergast et al. 2002:69; Kepecs et al. 2010
Cuba	Cuba	Greater Antilles	2	Los Buchillones	wood	wood	Post 13, Structure D2-1,	TO-7622	320	40	—	Pendergast et al. 2002:69; Kepecs et al. 2010
Cuba	Cuba	Greater Antilles	2	Los Buchillones	wood	wood	Post 2, Structure D2-1,	TO-7618	510	50	—	Pendergast et al. 2002:69
Cuba	Cuba	Greater Antilles	2	Los Buchillones	wood	wood	Post 2, Structure F1-1	TO-8068	480	60	—	Pendergast et al. 2002:72
Cuba	Cuba	Greater Antilles	2	Los Buchillones	wood	wood	Post 6, Structure F1-1	TO-8072	430	60	—	Pendergast et al. 2002:72
Cuba	Cuba	Greater Antilles	2	Los Buchillones	wood	wood	Post 7 sub, Structure D2-1,	TO-7620	430	50	—	Pendergast et al. 2002:69

Cuba	Cuba	Greater Antilles	2	Los Buchillones	wood	wood	Rafter 2, Structure D2-1,	TO-7623	390	50	—	Pendergast et al. 2002:69
Cuba	Cuba	Greater Antilles	2	Los Buchillones	wood	wood	Rafter 3, Structure D2-1,	TO-7624	1320	60	—	Pendergast et al. 2002:69; Kepecs et al. 2010
Cuba	Cuba	Greater Antilles	2	Los Buchillones	wood	wood	Rafter 4, Structure D2-1,	TO-7625	340	50	—	Pendergast et al. 2002:69
Cuba	Cuba	Greater Antilles	2	Los Buchillones	wood	wood	Rafter 5, Structure D2-1,	TO-7626	540	50	—	Pendergast et al. 2002:69
Cuba	Cuba	Greater Antilles	2	Los Buchillones	wood	wood	Sample Number = 32	OxA-15144	651	24	-25.7	Cooper and Thomas 2012
Cuba	Cuba	Greater Antilles	2	Los Buchillones	wood	wood	Sample Number = 34	OxA-15150	531	23	-27.3	Cooper and Thomas 2012
Cuba	Cuba	Greater Antilles	2	Los Buchillones	wood	wood	Sample Number = 36	OxA-15123	710	27	-24.9	Cooper and Thomas 2012
Cuba	Cuba	Greater Antilles	3	Cabagan	bone	human bone/teeth	—	—	1080	20	—	Rankin 1994:139
Cuba	Cuba	Greater Antilles	2	Caimanes III	charcoal	charcoal/ charred material	Test pit 4, sample depth .38 m	UM-1953	1745	175	—	Navarrete 1990:41; Pino 1995:3
Cuba	Cuba	Greater Antilles	2	Canimar 1	charcoal	charcoal/ charred material	Sample depth 0.7 m to 0.8m. Ca 3m asl. Unsecure stratigraphy	GD-203	1010	110	—	Pazdur et al. 1982:175
Cuba	Cuba	Greater Antilles	4	Canímar Abajo	charcoal	charcoal/ charred material	20 cm below surface	UNAM-0714a	800	50	-25.8	Roksandic et al. 2015

Cuba	Cuba	Greater Antilles	4	Canímar Abajo	charcoal	charcoal/ charred material	60-70 cm below surface	UNAM-0715	6460	15	-26.9	Roksandic et al. 2015
Cuba	Cuba	Greater Antilles	2	Canímar Abajo	charcoal	charcoal/ charred material	1.6-1.7 m below surface	UBAR-170	4200	79	—	Roksandic et al. 2015
Cuba	Cuba	Greater Antilles	2	Canímar Abajo	charcoal	charcoal/ charred material	1.8-1.9 meters	A-14316	2845	90	-26.3	Roksandic et al. 2015
Cuba	Cuba	Greater Antilles	2	Canímar Abajo	charcoal	charcoal/ charred material	40 cm below surface	UNAM-0717	2520	60	-27.3	Roksandic et al. 2015
Cuba	Cuba	Greater Antilles	2	Canímar Abajo	charcoal	charcoal/ charred material	45 cm below surface	UNAM-0716	3460	60	-26.2	Roksandic et al. 2015
Cuba	Cuba	Greater Antilles	2	Canímar Abajo	charcoal	charcoal/ charred material	90-100 cm below surface	A-14315	2515	75	-28.2	Roksandic et al. 2015
Cuba	Cuba	Greater Antilles	2	Canímar Abajo	charcoal	charcoal/ charred material	Layer 4	AA-101053	3057	39	-25.6	Roksandic et al. 2015
Cuba	Cuba	Greater Antilles	3	Canímar Abajo	shell	marine shell	1.8-1.9 m below surface	UBAR-171	4700	70	—	Roksandic et al. 2015
Cuba	Cuba	Greater Antilles	2	Canímar Abajo	human bone collagen	human bone/teeth	Layer 2	AA-101055	1661	52	-19.1	Roksandic et al. 2015
Cuba	Cuba	Greater Antilles	2	Canímar Abajo	human bone collagen	human bone/teeth	Layer 2	AA-101056	1289	46	-19.7	Roksandic et al. 2015
Cuba	Cuba	Greater Antilles	2	Canímar Abajo	human bone collagen	human bone/teeth	Layer 2	AA-89060	1420	59	-18.1	Roksandic et al. 2015
Cuba	Cuba	Greater Antilles	2	Canímar Abajo	human bone collagen	human bone/teeth	Layer 2	AA-89062	1536	51	-16.1	Roksandic et al. 2015
Cuba	Cuba	Greater Antilles	2	Canímar Abajo	human bone collagen	human bone/teeth	Layer 2	AA-89064	1617	46	-14.0	Roksandic et al. 2015
Cuba	Cuba	Greater Antilles	2	Canímar Abajo	human bone collagen	human bone/teeth	Layer 4	AA-101052	2946	57	-15.0	Roksandic et al. 2015
Cuba	Cuba	Greater Antilles	2	Canímar Abajo	human bone collagen	human bone/teeth	Layer 4	AA-101054	2999	61	-15.3	Roksandic et al. 2015
Cuba	Cuba	Greater Antilles	2	Canímar Abajo	human bone collagen	human bone/teeth	Layer 4	AA-101057	2996	53	-15.6	Roksandic et al. 2015

Cuba	Cuba	Greater Antilles	2	Canímar Abajo	human bone collagen	human bone/teeth	Layer 4	AA-101059	2791	51	-20.0	Roksandic et al. 2015
Cuba	Cuba	Greater Antilles	2	Canímar Abajo	human bone collagen	human bone/teeth	Layer 4	AA-89061	2960	33	-14.1	Roksandic et al. 2015
Cuba	Cuba	Greater Antilles	2	Canímar Abajo	human bone collagen	human bone/teeth	Layer 4	AA-89063	2922	34	-16.3	Roksandic et al. 2015
Cuba	Cuba	Greater Antilles	2	Los Caracoles	oyster shell	marine shell	Trench A, section 3, level 15-30 cm	Beta-422938	2350	30	-2.3	Colten and Worthington 2019
Cuba	Cuba	Greater Antilles	2	Catunda	charcoal	charcoal/ charred material	Trench 1, level 0.30 m	Beta-93866	1850	50	—	Ulloa Hung and Valcárcel Rojas 2002:233
Cuba	Cuba	Greater Antilles	2	Catunda	charcoal	charcoal/ charred material	Trench 2, level 0.40 m	Beta-93862	1890	60	—	Ulloa Hung and Valcárcel Rojas 2002:233
Cuba	Cuba	Greater Antilles	2	Catunda	charcoal	charcoal/ charred material	Trench 5, level 0.20-0.30 m	Beta-140078	1280	60	—	Ulloa Hung and Valcárcel Rojas 2002:233
Cuba	Cuba	Greater Antilles	2	Cayo Caiman Mata del Coco	*Strombus gigas*	marine shell	Sample Number = 22 (Midden 1)	OxA-15267	4408	37	+2.4	Cooper and Thomas 2012
Cuba	Cuba	Greater Antilles	2	Cayo Contrabando	*Strombus gigas*	marine shell	Sample Number = 30 (Surface Deposit 2)	OxA-15182	857	24	+3.5	Cooper and Thomas 2012
Cuba	Cuba	Greater Antilles	2	Cayo Felipe Este	*Strombus gigas*	marine shell	Sample Number = 21 (Surface Deposit 1)	OxA-15266	1978	33	+3.9	Cooper and Thomas 2012

Cuba	Cuba	Greater Antilles	2	Cayo Flores	*Strombus gigas*	marine shell	Sample Number = 23 (Surface Deposit 1)	OxA-15180	3861	28	+2.9	Cooper and Thomas 2012
Cuba	Cuba	Greater Antilles	2	Cayo Guillermo (Punta Morro)	*Strombus gigas*	marine shell	Sample Number = 19 (Midden 1)	OxA-15184	1686	26	+3.1	Cooper and Thomas 2012
Cuba	Cuba	Greater Antilles	2	Cayo Hijo de Guillermo Este	*Oliva recticularis*	marine shell	Sample Number = 1 (Cave 1)	OxA-15259	827	36	-1.6	Cooper and Thomas 2012
Cuba	Cuba	Greater Antilles	2	Cayo Hijo de Guillermo Este	*Strombus* sp.	marine shell	Sample Number = 13 (Cave 3)	OxA-15263	3271	29	+3.7	Cooper and Thomas 2012
Cuba	Cuba	Greater Antilles	2	Cayo Hijo de Guillermo Este	*Xancus angulatus*	marine shell	Sample Number = 15 (Cave 3)	OxA-15264	3273	33	+3.8	Cooper and Thomas 2012
Cuba	Cuba	Greater Antilles	2	Cayo Hijo de Guillermo Este	*Strombus gigas*	marine shell	Sample Number = 2 (Cave 1)	OxA-15260	1617	29	+3.8	Cooper and Thomas 2012
Cuba	Cuba	Greater Antilles	2	Cayo Hijo de Guillermo Este	*Strombus gigas*	marine shell	Sample Number = 20 (Rock Shelter 1)	OxA-15265	763	25	+4.3	Cooper and Thomas 2012
Cuba	Cuba	Greater Antilles	2	Cayo Hijo de Guillermo Este	*Oliva recticularis*	marine shell	Sample Number = 24 (Cave 1)	OxA-15178	709	26	+2.5	Cooper and Thomas 2012
Cuba	Cuba	Greater Antilles	2	Cayo Hijo de Guillermo Este	*Strombus gigas*	marine shell	Sample Number = 26 (Cave 1)	OxA-15179	1112	26	+3.3	Cooper and Thomas 2012

Cuba	Cuba	Greater Antilles	2	Cayo Hijo de Guillermo Este	*Oliva recticularis*	marine shell	Sample Number = 6 (Cave 1)	OxA-15261	782	26	+2.1	Cooper and Thomas 2012
Cuba	Cuba	Greater Antilles	2	Cayo Hijo de Guillermo Este	*Strombus gigas*	marine shell	Sample Number = 7 (Cave 1)	OxA-15262	2005	27	+3.1	Cooper and Thomas 2012
Cuba	Cuba	Greater Antilles	2	Cayo Hijo de Guillermo Oeste	*Strombus gigas*	marine shell	Sample Number = 31 (Surface Deposit 1)	OxA-15183	1873	26	+3.0	Cooper and Thomas 2012
Cuba	Cuba	Greater Antilles	2	Cayo Langosta	*Strombus gigas*	marine shell	Sample Number = 29 (Surface Deposit 1)	OxA-15181	1561	24	+3.1	Cooper and Thomas 2012
Cuba	Cuba	Greater Antilles	3	Los Chivos	terrestrial shell	terrestrial shell	Trench 1, level 0.45 m (preceramic)	Beta-140076	2710	80	—	Ulloa Hung and Valcárcel Rojas 2002:233
Cuba	Cuba	Greater Antilles	3	Los Chivos	terrestrial shell	terrestrial shell	Trench 1, South enlargement, level 0.10-0.20 m	Beta-140074	1150	60	—	Ulloa Hung and Valcárcel Rojas 2002:233
Cuba	Cuba	Greater Antilles	2	Chorro de Maita	charcoal	charcoal/ charred material	Unit 5, grid square 2, natural layer 1, spit depth 0.30-0.50 m	Beta-148957	730	60	—	Valcárcel Rojas 2002:142
Cuba	Cuba	Greater Antilles	2	Chorro de Maita	human bone	human bone/teeth	Skeleton no. 25, depth 0.88 m	Beta-148956	870	70	-0.19	Valcárcel Rojas 2002:142; Valcárcel Rojas and Arce 2003:511

Cuba	Cuba	Greater Antilles	2	Chorro de Maita	human bone	human bone/teeth	Skeleton no. 39, depth 0.79 m	Beta-148955	360	80	-0.19	Valcárcel Rojas 2002:142; Valcárcel Rojas and Arce 2003:511
Cuba	Cuba	Greater Antilles	3	El Convento	charcoal	charcoal/ charred material	—	—	400	20	—	Rankin 1994:138
Cuba	Cuba	Greater Antilles	2	El Convento	charcoal	charcoal/ charred material	Pit 2, level 0.25-0.50 m. sample depth 0.45 m. Assoc. with ceramic, shell, and stone artifacts	GD-1053	665	50	—	Pazdur et al. 1982:174; Pino 1995:7
Cuba	Cuba	Greater Antilles	3	Corinthia III	marine shell	marine shell	Excavation 3, grid square 3, level 0.10-0.20 m	Beta-133953	2220	70	—	Ulloa Hung and Valcárcel Rojas 2002:132
Cuba	Cuba	Greater Antilles	3	Corinthia III	marine shell	marine shell	Excavation 4, grid square 2, level 1	Beta-133952	2300	60	—	Ulloa Hung and Valcárcel Rojas 2002:132
Cuba	Cuba	Greater Antilles	3	Corinthia III	marine shell	marine shell	Unit III, level 0.00-0.10 m	Beta-140080	1700	70	—	Ulloa Hung and Valcárcel Rojas 2002:132
Cuba	Cuba	Greater Antilles	4	Cueva de los Bandoleros	—	unknown	—	—	4045	75	—	Godo 2001
Cuba	Cuba	Greater Antilles	2	Cueva Calero	collagen	human bone/teeth	Area 2, Trench 1, Secc. D, 30-40 cm	Beta-72801	1670	70	25.0	Ulloa Hung 2008

Cuba	Cuba	Greater Antilles	2	Cueva Calero	collagen	human bone/teeth	Area 2, Trench 1, Secc. E, 20-30 cm	Beta-72802	1590	60	25.0	Ulloa Hung 2008
Cuba	Cuba	Greater Antilles	2	Cueva #1 Punta del Este	charcoal	charcoal/ charred material	In front of cave, Block I, Sec. A, level .5-.75 m sample depth .57 m. Assoc. with shell and stone artifacts	GD-618	910	85	—	Pino 1995:3
Cuba	Cuba	Greater Antilles	2	Cueva #4 Punta del Este	charcoal	charcoal/ charred material	Test Pit 1 x .5m sample depth .38 m	LC-H-1106	1100	130	—	Pino 1995:3; Navarrete 1990:41
Cuba	Cuba	Greater Antilles	2	Cueva de la Lechuza	charcoal	charcoal/ charred material	Test Pit 1, block 1, level 0.25 m	LE-4269	1470	110	—	Pino 1995:5
Cuba	Cuba	Greater Antilles	2	Cueva de la Lechuza	charcoal	charcoal/ charred material	Test Pit 1, block 1, level 0.35 m	LE-4267	2220	160	—	Pino 1995:5
Cuba	Cuba	Greater Antilles	2	Cueva de la Lechuza	charcoal	charcoal/ charred material	Test Pit 1, block 1, level 0.45 m	LE-4274	2030	160	—	Pino 1995:5
Cuba	Cuba	Greater Antilles	2	Cueva de la Lechuza	charcoal	charcoal/ charred material	Test Pit 1, block 1, level 0.55 m	LE-4276	2250	150	—	Pino 1995:5
Cuba	Cuba	Greater Antilles	2	Cueva de la Lechuza	charcoal	charcoal/ charred material	Test Pit 1, block 1, level 0.65 m	LE-4272	2750	160	—	Pino 1995:5
Cuba	Cuba	Greater Antilles	2	Cueva de la Lechuza	charcoal	charcoal/ charred material	Test Pit 1, block 1, level 0.75 m	LE-4271	2380	80	—	Pino 1995:5
Cuba	Cuba	Greater Antilles	2	Cueva de la Lechuza	charcoal	charcoal/ charred material	Test Pit 1, block 1, level 0.85 m	LE-4279	2390	170	—	Pino 1995:5
Cuba	Cuba	Greater Antilles	2	Cueva de la Lechuza	charcoal	charcoal/ charred material	Test Pit 1, block 1, level 0.95 m	LE-4273	2420	100	—	Pino 1995:5

Cuba	Cuba	Greater Antilles	2	Cueva de la Lechuza	charcoal	charcoal/ charred material	Test Pit 1, block 1, level 1.05 m	LE-4270	3110	180	—	Pino 1995:5
Cuba	Cuba	Greater Antilles	2	Cueva de la Lechuza	charcoal	charcoal/ charred material	Test Pit 1, block 1, level 1.25 m	LE-4282	2930	300	—	Pino 1995:5
Cuba	Cuba	Greater Antilles	2	Cueva de la Lechuza	charcoal	charcoal/ charred material	Test Pit 1, block 1, level 1.55 m	LE-4288	3030	180	—	Pino 1995:6
Cuba	Cuba	Greater Antilles	2	Cueva de la Lechuza	charcoal	charcoal/ charred material	Test Pit 1, block 1, level 1.65 m	LE-4287	3030	180	—	Pino 1995:6
Cuba	Cuba	Greater Antilles	2	Cueva de la Lechuza	charcoal	charcoal/ charred material	Test Pit 1, block 1, level 1.95 m	LE-4283	5270	120	—	Pino 1995:6
Cuba	Cuba	Greater Antilles	2	Cueva de la Lechuza	charcoal	charcoal/ charred material	Test Pit 1, block 1, level 2.05 m	LE-4290	2610	120	—	Pino 1995:6
Cuba	Cuba	Greater Antilles	2	Cueva de la Lechuza	charcoal	charcoal/ charred material	Test Pit 1, block 1, level 2.15 m	LE-4281	2610	120	—	Pino 1995:6
Cuba	Cuba	Greater Antilles	2	Cueva de la Lechuza	charcoal	charcoal/ charred material	Test Pit 1, block 1, level 2.35 m	LE-4275	2580	90	—	Pino 1995:6
Cuba	Cuba	Greater Antilles	2	Cueva de la Pintura	charcoal	charcoal/ charred material	Excavation unit 1, block 1-I, sec. A, level 0.50-0.75 m. assoc. with shell and stone artifacts	GD-1039	2160	55	—	Pazdur et al. 1982:173; Pino 1995:6
Cuba	Cuba	Greater Antilles	2	Cueva de la Pintura	charcoal	charcoal/ charred material	Excavation unit 1, block 1-I, sec. D, level 1.00-1.25 m. assoc. with shell and stone artifacts	GD-601	2805	60	—	Pazdur et al. 1982:173; Pino 1995:6
Cuba	Cuba	Greater Antilles	2	Cueva de la Pintura	charcoal	charcoal/ charred material	Excavation unit 1, block 1-I, sec. D, level 1.5 to 1.8 m. assoc. with shell and stone artifacts	GD-591	2930	80	—	Pazdur et al. 1982:173

Cuba	Cuba	Greater Antilles	2	Cueva de la Pintura	charcoal	charcoal/ charred material	Excavation unit 2, block 5, sec. D, level 1.00-1.25 m. assoc. with shell and stone artifacts	GD-614	2720	65	—	Pazdur et al. 1982:173; Pino 1995:6
Cuba	Cuba	Greater Antilles	2	Cueva de la Pintura	charcoal	charcoal/ charred material	Excavation unit 2, block 5, sec. D, level 1.25 to 1.5m. assoc. with shell and stone artifacts	GD-1046	2840	60	—	Pazdur et al. 1982:173
Cuba	Cuba	Greater Antilles	2	Cueva de la Pintura	charcoal	charcoal/ charred material	Excavation unit 2, block 5, sec. D, level 1.5 to 1.75m. assoc. with shell and stone artifacts	GD-613	2880	70	—	Pazdur et al. 1982:173
Cuba	Cuba	Greater Antilles	2	Cueva del Perico I	charcoal	charcoal/ charred material	Trench 1, sec. 1, level 1.00-1.20 m. assoc. with human burials, shell and stone artifacts	GD-617	1495	60	—	Pino 1995:3
Cuba	Cuba	Greater Antilles	2	Cueva del Perico I	charcoal	charcoal/ charred material	Trench 1, sec. 1, level 1.30-1.40 m	GD-1051	1990	80	—	Pazdur et al. 1982:173; Pino 1995:3; Martínez Fuentes et al. 2003:65
Cuba	Cuba	Greater Antilles	2	Cueva del Perico I	charcoal	charcoal/ charred material	Trench 2, sec. 2, level 1.50-1.75 m. assoc. with human burials, shell and stone artifacts	GD-616	1350	70	—	Pino 1995:3
Cuba	Cuba	Greater Antilles	4	Cueva de San Martin	—	unknown	—	—	3200	80	—	Godo 2001
Cuba	Cuba	Greater Antilles	4	Cueva de San Martin	—	unknown	—	—	3290	120	—	Godo 2001

Cuba	Cuba	Greater Antilles	2	Cueva Funche	charcoal	charcoal/ charred material	Block II, sec. A, level 0.25-0.50 m (sample depth .50 m). With preceramic artifacts associated with Guayabo Blanco see Rouse 1942	SI-426	2070	150	—	Stuckenrath and Mielke 1973:407; Mielke and Long 1969:172; Pino 1995:4
Cuba	Cuba	Greater Antilles	2	Cueva Funche	charcoal	charcoal/ charred material	Block II, sec. D, level 0.50-0.75 m (sample depth .55 m). With preceramic artifacts associated with Guayabo Blanco see Rouse 1942	SI-427	2510	200	—	Stuckenrath and Mielke 1973:407; Mielke and Long 1969:172; Pino 1995:4
Cuba	Cuba	Greater Antilles	2	Cueva Funche	charcoal	charcoal/ charred material	Block III, sec. A, level 1.25-1.50 m (sample depth 1.40 m). With preceramic artifacts associated with Guayabo Blanco see Rouse 1942	SI-428	3110	200	—	Stuckenrath and Mielke 1973:407; Mielke and Long 1969:172; Pino 1995:4
Cuba	Cuba	Greater Antilles	2	Cueva Funche	charcoal	charcoal/ charred material	Block III, sec. A, level 1.50-1.75 m (sample depth 1.72 m). With preceramic artifacts associated with Guayabo Blanco see Rouse 1942	SI-429	4000	150	—	Stuckenrath and Mielke 1973:407; Mielke and Long 1969:172; Pino 1995:4

Cuba	Cuba	Greater Antilles	2	Damayajabo	charcoal	charcoal/ charred material	Nivel ceramico (sin datos estratigraficos)	Y-1994	1120	160	—	Pino 1995:5; Navarrete 1990; Dacal Moure and Rivero de la Calle 1996:13
Cuba	Cuba	Greater Antilles	2	Damayajabo	charcoal	charcoal/ charred material	Trench 51, level 1.34m	Y-1764	3250	100	—	Pino 1995:5; Navarrete 1990; Dacal Moure and Rivero de la Calle 1996:13
Cuba	Cuba	Greater Antilles	3	La Escondida de Bucuey	charcoal	charcoal/ charred material	Test Pits 3 y 4, 1 x1m, level .2-.3 m	—	1060	150	—	Pino 1995:3
Cuba	Cuba	Greater Antilles	2	Esterito	charcoal	charcoal/ charred material	Midden 1, trench 1, sec. C, level 0.25-0.50 m (sample depth .45 m). Assoc. with ceramic, shell, and stone artifacts. Without European contact.	SI-349	550	150	—	Mielke and Long 1969:171; Pino 1995:7; Valcárcel Rojas 2002:140
Cuba	Cuba	Greater Antilles	2	Esterito	charcoal	charcoal/ charred material	Midden 1, trench 1, sec. D, level 1.00-1.25 m (sample depth 1.15 m). Assoc. with ceramic, shell, and stone artifacts. Without European contact.	SI-350	500	100	—	Mielke and Long 1969:171; Pino 1995:7; Valcárcel Rojas 2002:140
Cuba	Cuba	Greater Antilles	2	El Guafe I	charcoal	charcoal/ charred material	Block 1, sec. 2 y 4, natural layer 3,	FS AC 2420	450	35	—	Pino 1995:5

							prof. sample depth 0.50 m					
Cuba	Cuba	Greater Antilles	2	El Guafe I	charcoal	charcoal/ charred material	Block 2, natural layer 2, prof. sample depth 0.30 m	FS AC 2419	690	50	—	Pino 1995:5
Cuba	Cuba	Greater Antilles	2	La Guira de Barajagua	charcoal	charcoal/ charred material	Midden 1, trench 1, sec. B, level 0.75-1.00 (sample depth .90 m). Assoc. with ceramic, shell, and stone artifacts.	SI-351	590	100	—	Mielke and Long 1969:171; Pino 1995:7
Cuba	Cuba	Greater Antilles	3	La Guira (Santiago de Cuba)	terrestrial shell	terrestrial shell	Trench 1, level 0.19m	Beta-140077	1390	70	—	Ulloa Hung and Valcárcel Rojas 2002:233
Cuba	Cuba	Greater Antilles	3	Herradura 1	marine shell	marine shell	Corte 5, level 0.00-0.10 m	Beta-140075	2050	70	—	Ulloa Hung and Valcárcel Rojas 2002:232
Cuba	Cuba	Greater Antilles	2	Jorajuria	charcoal	charcoal/ charred material	Pit 1, 1x1m, level .40-.50 m	LE-1784	3870	40	—	Pino 1995:4
Cuba	Cuba	Greater Antilles	2	Jorajuria	charcoal	charcoal/ charred material	Pit 1, 1x1m, level .60-.70 m	LE-1782	3760	40	—	Pino 1995:4
Cuba	Cuba	Greater Antilles	2	Jorajuria	charcoal	charcoal/ charred material	Pit 1, 1x1m, level .80-.90 m	LE-1783	4110	50	—	Pino 1995:4
Cuba	Cuba	Greater Antilles	2	Jucaro	charcoal	charcoal/ charred material	Cut A, spit depth 0.20-0.40 m, natural layer 1	Beta-148949	690	60	—	Valcárcel Rojas 2002:143

Cuba	Cuba	Greater Antilles	2	Laguna de Limones	charcoal	charcoal/ charred material	Midden 2, trench 2, sec. D. level 0.25- .50 m (sample depth .40 m)	SI-348	640	120	—	Mielke and Long 1969:171; Pino 1995:7
Cuba	Cuba	Greater Antilles	2	Levisa 1 (Far. de Lev.)	charcoal	charcoal/ charred material	sec.I-I, 0.5-0.55m, capa v	GD-204	3460	160	—	Pazdur et al. 1982:175; Pino 1995:2
Cuba	Cuba	Greater Antilles	2	Levisa 1 (Far. de Lev.)	charcoal	charcoal/ charred material	sec.I-I, 0.55-0.60m, layer 6	MC-859	4240	100	—	Pino 1995:2
Cuba	Cuba	Greater Antilles	2	Levisa 1 (Far. de Lev.)	charcoal	charcoal/ charred material	sec.I-I, 0.55-0.60m, layer 6	MC-860	4420	100	—	Pino 1995:2
Cuba	Cuba	Greater Antilles	2	Levisa 8 (Cueva S. Rita)	charcoal	charcoal/ charred material	Unit 2, sec 25, 0.20-0.40 m, layer 3	LE-2719	2160	40	—	Pino 1995:2
Cuba	Cuba	Greater Antilles	2	Levisa 8 (Cueva S. Rita)	charcoal	charcoal/ charred material	Unit 3, sec 23 A, 0.40-0.50 m, layer 1	LE-2720	2680	40	—	Pino 1995:2
Cuba	Cuba	Greater Antilles	2	Levisa 8 (Cueva S. Rita)	charcoal	charcoal/ charred material	Unit 3, sec 35 A, 0.20-0.30 m, layer 2/3	LE-2717	2010	40	—	Pino 1995:2
Cuba	Cuba	Greater Antilles	2	Levisa 8 (Cueva S. Rita)	charcoal	charcoal/ charred material	Unit 3, sec 45, 0.20-0.22 m, layer 1	LE-2718	2610	40	—	Pino 1995:2
Cuba	Cuba	Greater Antilles	2	Loma de la Campana	charcoal	charcoal/ charred material	Midden 2. Bloque I, sec. C, nivel 0.50-0.75 m. Assoc. with ceramic, shell, and stone artifacts.	GD-1057	490	45	—	Pazdur et al. 1982:174; Pino 1995:7; Valcárcel Rojas 2002:140

Cuba	Cuba	Greater Antilles	2	Loma de la Campana	charcoal	charcoal/ charred material	Midden 2. Bloque II, sec. D, nivel 0.75-1.00 m. Assoc. with ceramic, shell, and stone artifacts.	GD-624	505	40	—	Pino 1995:7; Valcárcel Rojas 2002:140; Pazdur et al. 1982:174
Cuba	Cuba	Greater Antilles	2	Loma de la Campana	charcoal	charcoal/ charred material	Midden 2. Bloque II, sec. D, nivel 1.00 -1.50 m. Assoc. with ceramic, shell, and stone artifacts.	GD-1056	600	55	—	Pino 1995:7; Valcárcel Rojas 2002:140; Pazdur et al. 1982:174
Cuba	Cuba	Greater Antilles	2	Loma de la Forestal	charcoal	charcoal/ charred material	Midden 9, trench 1, sec. A, level 0.50-0.75 m (muestra de 0.70 m). Assoc. with ceramic, shell, and stone artifacts.	SI-352	970	100	—	Mielke and Long 1969:171; Pino 1995:7
Cuba	Cuba	Greater Antilles	2	Loma de Ochile	charcoal	charcoal/ charred material	Block 1, sec. 2, natural layer 4, sample depth 0.80 - 0.90 m	FS AC 2418	880	40	—	Pino 1995:7
Cuba	Cuba	Greater Antilles	2	Loma de Ochile	charcoal	charcoal/ charred material	Block 2, sec. 1,2 y 3, natural layer 2 sample depth 0.30-0.40 m	FS AC 2415	690	50	—	Pino 1995:7
Cuba	Cuba	Greater Antilles	2	Loma de Ochile	charcoal	charcoal/ charred material	Block 2, sec. 3, natural layer 1 sample depth 0.10-0.30 m	FS AC 2414	770	35	—	Pino 1995:7
Cuba	Cuba	Greater Antilles	2	Loma de Ochile	charcoal	charcoal/ charred material	Block I, sec. 1-2, natural layer 2 sample depth 0.30-0.60 m	FS AC 2416	660	35	—	Pino 1995:7

Cuba	Cuba	Greater Antilles	2	Loma de Ochile	charcoal	charcoal/ charred material	Block I, sec. 2, natural layer 3, sample depthl 0.60-0.80 m	FS AC 2417	620	30	—	Pino 1995:7
Cuba	Cuba	Greater Antilles	2	La Luz	charcoal	charcoal/ charred material	Test Pit 3, level 1.20 m	Beta-93863	1350	50	—	Ulloa Hung and Valcárcel Rojas 2002:233
Cuba	Cuba	Greater Antilles	2	Marien 2	charcoal	charcoal/ charred material	Excavation square LL-10, level 0.10-0.20 m	Lv-2062	780	100	—	Pino 1995:2
Cuba	Cuba	Greater Antilles	2	Marien 2	charcoal	charcoal/ charred material	Excavation square M-07, level 0.20-0.30 m	Lv-2063	2020	80	—	Pino 1995:2
Cuba	Cuba	Greater Antilles	2	Meijas	charcoal	charcoal/ charred material	Trench 1, sec. B, level 0.25-0.50 m, sample depth 0.45 m.	SI-347	1020	100	—	Mielke and Long 1969:170; Pino 1995:3
Cuba	Cuba	Greater Antilles	2	Mogote de la Cueva	charcoal	charcoal/ charred material	Trench 1, level .25-.50 m (sample depth .35m) Unsafe Stratigraphy	SI-424	1620	150	—	Stuckenrath and Mielke 1973:407; Pino 1995:3; Lalueza-Fox et al. 2003:64
Cuba	Cuba	Greater Antilles	3	Mogote de la Cueva	charcoal	charcoal/ charred material	—	—	960	50	—	Navarrete 1990:41
Cuba	Cuba	Greater Antilles	2	Mogote de la Cueva	charcoal	charcoal/ charred material	Trench 1, level 1. 1.3 m (sample depth 1.25m)	SI-425	650	200	—	Stuckenrath and Mielke 1973:407; Pino 1995:3

Cuba	Cuba	Greater Antilles	2	El Morrillo	charcoal	charcoal/ charred material	Block 9-Q, sec. B, level 0.25-0.50 m, sample depth 0.45 m. Assoc. with ceramic, shell, and stone artifacts. Close to European artifacts.	SI-353	590	90	—	Mielke and Long 1969:171; Pino 1995:7
Cuba	Cuba	Greater Antilles	2	El Morrillo	human bone	human bone/teeth	burial	ICA 17B/0756	420	40	-15.5	Orihuela León et al. 2017
Cuba	Cuba	Greater Antilles	2	Las Obas	charcoal	charcoal/ charred material	sec I-I, 0.85-0.90 m	GD-250	5140	170	—	Pazdur et al. 1982:175; Pino 1995:2
Cuba	Cuba	Greater Antilles	2	Las Obas	*Melongena melongena*	marine shell	Trench A, section 1, 15 cm - 30 cm level	Beta-214957	2020	50	-1.0	Colten et al. 2009
Cuba	Cuba	Greater Antilles	2	Las Obas	*Melongena melongena*	marine shell	Trench A, section 1, 45 cm - 60 cm level	Beta-214958	1910	50	-4.7	Colten et al. 2009
Cuba	Cuba	Greater Antilles	2	El Porvenir	charcoal	charcoal/ charred material	Unit 5, grid square B, spit depth 0.40-0.50 m, natural layer 1	Beta-148960	500	50	—	Valcárcel Rojas 2002:143
Cuba	Cuba	Greater Antilles	2	El Purial	charcoal	charcoal/ charred material	Level (approximate) 0.40 m	UBAR-169	3060	180	—	Pino 1995:4
Cuba	Cuba	Greater Antilles	2	Los Pedregales	charcoal	charcoal/ charred material	Trench 2, sec. B. level 2.00-2.25 m. Sample depth 2.00 m. Assoc. with ceramic, shell, and stone artifacts.	GD-619	1170	90	—	Pazdur et al. 1982:174; Pino 1995:2
Cuba	Cuba	Greater Antilles	3	El Paraiso	charcoal	charcoal/ charred material	Test Pit 1, 1x1 m, level 0.20-0.30 m	—	1130	150	—	Pino 1995:5

Cuba	Cuba	Greater Antilles	3	Playvita (Villa Clara)	charcoal	charcoal/ charred material	—	—	1280	20	—	Pino 1995:2
Cuba	Cuba	Greater Antilles	2	Potrero del Mango	charcoal	charcoal/ charred material	Unit 1, grid square A, spit depth 0.80-0.90 m	Beta-148961	880	80	—	Valcárcel Rojas 2002:141, 143
Cuba	Cuba	Greater Antilles	2	Potrero del Mango	charcoal	charcoal/ charred material	Unit 2, grid square A, spit depth 1.00-1.10 m	Beta-148962	620	60	—	Valcárcel Rojas 2002:143
Cuba	Cuba	Greater Antilles	2	Potrero del Mango	wood	wood	Midden 1, sec, Y-5, level 0.75-1.00 m (Rouse)	Y-206	810	80	—	Stuiver 1969:627; Pino 1995:7; Valcárcel Rojas 2002:141, 143
Cuba	Cuba	Greater Antilles	3	Potrero del Mango	shell	marine shell	Excavation 3, midden 2, section L-2, 0.0-0.25 m	Beta-408952	1420	30	—	Colten and Worthington 2017
Cuba	Cuba	Greater Antilles	3	Potrero del Mango	shell	marine shell	Excavation 3, midden 3, sectin L-2, 1.00-1.25	Beta-408953	1230	30	—	Colten and Worthington 2017
Cuba	Cuba	Greater Antilles	3	Potrero del Mango	shell	marine shell	Excavation 3, midden 2, section L-2, 0.0-0.25 m	Beta-410922	850	30	—	Colten and Worthington 2017
Cuba	Cuba	Greater Antilles	3	Potrero del Mango	shell	marine shell	Excavation 3, midden 3, sectin L-2, 1.00-1.25	Beta-410923	1130	30	—	Colten and Worthington 2017

Cuba	Cuba	Greater Antilles	3	Punta de Peque	terrestrial shell	terrestrial shell	Trench 1, level 0.50 m	Beta-93860	1400	60	—	Ulloa Hung and Valcárcel Rojas 2002:233
Cuba	Cuba	Greater Antilles	4	Rio Chico	—	unknown	—	—	3100	70	—	Godo 2001
Cuba	Cuba	Greater Antilles	3	San Benito	terrestrial shell	terrestrial shell	Trench 2, level 0.40-0.50 m	Beta-93851	2020	60	—	Ulloa Hung and Valcárcel Rojas 2002:233
Cuba	Cuba	Greater Antilles	2	U.S. Naval Station Guantanamo Bay	*Strombus* sp.	marine shell	67 cmbs	Beta-184894	2980	70	—	Sara et al. 2007
Cuba	Cuba	Greater Antilles	2	U.S. Naval Station Guantanamo Bay	*Strombus* sp.	marine shell	shell midden, no other info	Beta-184896	2680	60	—	Sara et al. 2007
Cuba	Cuba	Greater Antilles	3	U.S. Naval Station Guantanamo Bay	shell	marine shell	0-13 cmbs	Beta-184893	1060	60	—	Sara et al. 2007
Cuba	Cuba	Greater Antilles	3	U.S. Naval Station Guantanamo Bay	shell	marine shell	40-50 cmbs	Beta-184895	1700	60	—	Sara et al. 2007
Cuba	Cuba	Greater Antilles	2	Vega del Palmar	charcoal	charcoal/ charred material	Unit 1, Sample depth 105- to 120-cm level of a midden, 150 cm deep, which yielded pottery only in the top two 15-cm levels.	Y-465	960	60	—	Deevey et al.1959:26; Pino 1995:4; Navarrete 1990:41
Cuba	Cuba	Greater Antilles	2	Vega del Palmar	*Lucina pectinatus*	marine shell	Unit 1, 120-135 cm level	Beta-318171	2570	30	-3.0	Colten and Worthington 2014

Cuba	Cuba	Greater Antilles	2	Vega del Palmar	*Cittarium pica*	marine shell	Unit 1, 15-30 cm level	Beta-318170	1750	30	+2.6	Colten and Worthington 2014
Cuba	Cuba	Greater Antilles	2	Ventas de Casanova	charcoal	charcoal/ charred material	Block 1, sec. 1 y 2, natural layer 3, Sample depth 0.30-0.50 m	FS AC 2422	420	45	—	Pino 1995:6
Cuba	Cuba	Greater Antilles	2	Ventas de Casanova	charcoal	charcoal/ charred material	Block 1, sec. 1 y 2, natural layer 4, prof. Sample depth 0.50-0.60 m	FS AC 2423	315	45	—	Pino 1995:5
Cuba	Cuba	Greater Antilles	2	Ventas de Casanova	charcoal	charcoal/ charred material	Block 1, sec. 1, natural layer 4, Sample depth 0.60-0.80 m	FS AC 2424	475	35	—	Pino 1995:6
Cuba	Cuba	Greater Antilles	2	Ventas de Casanova	charcoal	charcoal/ charred material	Test Trench, sec. 4 natural layer 1 y 2, prof. Sample depth 0.0-0.23 m	FS AC 2421	375	25	—	Pino 1995:6
Cuba	Cuba	Greater Antilles	2	Victoria I	charcoal	charcoal/ charred material	Block 1, sec B, level 2.00-2.25 m	LC-H 1035	1450	70	—	Pino 1995:4; Godo Torres 1994:141
Cuba	Cuba	Greater Antilles	2	Victoria I	charcoal	charcoal/ charred material	Block 1, sec B, level 6.25-6.50 m	LC-H 1034	2070	110	—	Pino 1995:4; Godo Torres 1994:141
Cuba	Cuba	Greater Antilles	2	Victoria I	charcoal	charcoal/ charred material	Block I, Sec. B, level 2.00-2.25 m	LC-H 565	960	50	—	Pino 1995:3
Curaçao	Curaçao	northern South America	2	Gaito	charcoal	charcoal/ charred material	#8/0-25 cm	IVIC-241	340	50	—	Cruxent 1965:243
Curaçao	Curaçao	northern South America	3	Isla Simo	shell	marine shell	—	Beta-	1140	60	—	Haviser 2001:118

Curaçao	Curaçao	northern South America	3	Isla Simo	shell	marine shell	—	Beta-	1160	60	—	Haviser 2001:118
Curaçao	Curaçao	northern South America	3	Kintjan	*Cittarium pica* (?)	marine shell	midden	—	3530	140	—	Gould 1971
Curaçao	Curaçao	northern South America	3	Kintjan	*Chama* sp.	marine shell	midden	—	4150	140	—	Gould 1971
Curaçao	Curaçao	northern South America	3	Knip	*Lobatus gigas*	marine shell	surface	D-AMS 009260	1133	24	+3.8	Kraan et al. 2017
Curaçao	Curaçao	northern South America	2	Knip	charcoal	charcoal/ charred material	#26/0-25 cm	IVIC-250	1230	60	—	Cruxent 1965:243
Curaçao	Curaçao	northern South America	2	Knip	charcoal	charcoal/ charred material	#26/25-50 cm	IVIC-248	630	50	—	Cruxent 1965:243
Curaçao	Curaçao	northern South America	2	Knip	charcoal	charcoal/ charred material	#27/0-25 cm	IVIC-249	630	60	—	Cruxent 1965:243
Curaçao	Curaçao	northern South America	2	Knip	charcoal	charcoal/ charred material	#9/0-25 cm	IVIC-233	910	50	—	Cruxent 1965:243
Curaçao	Curaçao	northern South America	2	Knip	charcoal	charcoal/ charred material	#9/25-50 cm	IVIC-244	830	60	—	Cruxent 1965:243
Curaçao	Curaçao	northern South America	3	Paradise Beach	*Lima scabra*	marine shell	surface	D-AMS 009261	3965	28	+9.8	Kraan et al. 2017
Curaçao	Curaçao	northern South America	3	Punta Blanku	*Chicoreus brevifrons*	marine shell	surface	D-AMS 009258	1268	24	+1.9	Kraan et al. 2017
Curaçao	Curaçao	northern South America	3	Punta Mangusa	marine shell	marine shell	surface	D-AMS 010112	3803	23	+2.6	Kraan et al. 2017
Curaçao	Curaçao	northern South America	3	Rooi Rincon	charcoal	charcoal/ charred material	midden	—	3990 - 4490	50	—	Gould 1971

Curaçao	Curaçao	northern South America	3	Rooi Rincon	*Chama* sp.	marine shell	midden	—	4090	140	—	Gould 1971
Curaçao	Curaçao	northern South America	3	Rooi Rincon	*Cittarium* sp.	marine shell	midden	—	4705	160	—	Gould 1971
Curaçao	Curaçao	northern South America	2	Rooi Rincon	charcoal	charcoal/ charred material	#28/0-25 cm	IVIC-247	4490	60	—	Cruxent 1965:243; Haviser 1987
Curaçao	Curaçao	northern South America	2	Rooi Rincon	charcoal	charcoal/ charred material	#28/25-50 cm	IVIC-246	4160	80	—	Cruxent 1965:243; Haviser 1987
Curaçao	Curaçao	northern South America	2	Rooi Rincon	charcoal	charcoal/ charred material	#5/25-50 cm	IVIC-240	3990	50	—	Cruxent 1965:243; Haviser 1987
Curaçao	Curaçao	northern South America	2	Rooi Rincon	charcoal	charcoal/ charred material	P.H./0-20 cm	IVIC-234	4110	65	—	Cruxent 1965:243; Haviser 1987
Curaçao	Curaçao	northern South America	2	Rooi Rincon	charcoal	charcoal/ charred material	P.H./20-30 cm	IVIC-242	4070	65	—	Cruxent 1965:243; Haviser 1987
Curaçao	Curaçao	northern South America	2	San Hironimo	charcoal	charcoal/ charred material	Trench B, Unit I, level 3, 10-15 cm	GrN-9997	420	15	—	Haviser 1987
Curaçao	Curaçao	northern South America	2	San Hironimo	charcoal	charcoal/ charred material	Trench B, Unit IV, level 3, 10-15 cm	GrN-9998	325	35	—	Haviser 1987
Curaçao	Curaçao	northern South America	3	San Hironimo	shell	marine shell	Trench B, Unit I, level 3, 10-15 cm	GrN-9996	350	50	—	Haviser 1987
Curaçao	Curaçao	northern South America	2	San Juan	charcoal	charcoal/ charred material	C.B./25-50cm	IVIC-237	1440	60	—	Cruxent 1965:243

Curaçao	Curaçao	northern South America	4	San Juan	organic sediment	sediment	CC09-1, 245 cm	AA-92660	680	35	-14.3	Dunning et al. 2018a
Curaçao	Curaçao	northern South America	4	San Juan	organic sediment	sediment	CC09-1, 308-309 cm	AA-84145	1070	30	-17.5	Dunning et al. 2018a
Curaçao	Curaçao	northern South America	3	San Juan	charcoal	charcoal/ charred material	—	—	1440	60	—	Haviser 1985
Curaçao	Curaçao	northern South America	3	Santa Cruz	*Chione cancellata*	marine shell	surface	D-AMS 09259	834	21	-11.1	Kraan et al. 2017
Curaçao	Curaçao	northern South America	4	Santa Barbara	charcoal	charcoal/ charred material	unit 77/103 level 7-8 (30-40 cm bs)	PITT-1199	moder n	—	—	Haviser 1987
Curaçao	Curaçao	northern South America	2	Santa Barbara	charcoal	charcoal/ charred material	unit 118/117 level 3-4 (10-20 cm bs)	PITT-1195	590	50	—	Haviser 1987
Curaçao	Curaçao	northern South America	2	Santa Barbara	charcoal	charcoal/ charred material	unit 118/117 level 7-8 (30-40 cm bs)	PITT-1196	775	60	—	Haviser 1987
Curaçao	Curaçao	northern South America	2	Santa Barbara	charcoal	charcoal/ charred material	unit 118/117 level 9-10 (40-50 cm bs), small sample, diluted	PITT-1197	395	115	—	Haviser 1987
Curaçao	Curaçao	northern South America	2	Santa Barbara	charcoal	charcoal/ charred material	unit 120/142 level 7 (30-35 cm bs)	PITT-1198	875	35	—	Haviser 1987
Curaçao	Curaçao	northern South America	3	Savaan	charcoal	charcoal/ charred material	WP4, 0-25 cm	IVIC-236	70	60	—	Cruxent 1965:243
Curaçao	Curaçao	northern South America	3	Savaan	human bone	human bone/teeth	—	DIC-3137	1500	200	—	Ayubi et al. 1990
Curaçao	Curaçao	northern South America	3	Savaan	human bone	human bone/teeth	Skeleton S-1 (primary urn burial)	GrN-12014	1500	200	—	Tacoma 1990

Curaçao	Curaçao	northern South America	3	Savaan	human bone	human bone/teeth	Skeleton S-3 (secondary urn burial)	GrN-12979	660	20	-10.58	Tacoma 1990
Curaçao	Curaçao	northern South America	2	Savaan	human bone	human bone/teeth	S-2, 0-25 cm	DIC-3138	660	20	—	Ayubi et al. 1990
Curaçao	Curaçao	northern South America	2	Savaan	human bone collagen	human bone/teeth	Savaan 1, 0-25 cm	GrN-12914	1500	200	-10.58	Haviser 1989:16
Curaçao	Curaçao	northern South America	3	Savaan	molar	human bone/teeth	Savaan I	Ua-1498	1040	100	-11.27	Tacoma 1990
Curaçao	Curaçao	northern South America	3	Savaan	shell	marine shell	Unit 106/98, level 3, 35-45 cm	GrN-9995	740	60	—	Haviser 1987
Curaçao	Curaçao	northern South America	2	Savonet	charcoal	charcoal/ charred material	Unit A level 1, small sample, diluted	PITT-1183	1875	430	—	Haviser 2001:118
Curaçao	Curaçao	northern South America	3	Savonet	shell	marine shell	Unit A/B level 2 (20-40 cm)	PITT-1185	3355	25	—	Haviser 2001:118
Curaçao	Curaçao	northern South America	3	St. Joris #1	shell	marine shell	—	Beta-	4340	70	—	Haviser 2001:118
Curaçao	Curaçao	northern South America	3	St. Joris #1	shell	marine shell	—	Beta-	4450	70	—	Haviser 2001:118
Curaçao	Curaçao	northern South America	3	St. Michielsberg	shell	marine shell	Trench A, Unit BA west, level 7	GrN-9994	3820	70	—	Haviser 2001:118
Curaçao	Curaçao	northern South America	3	St. Michielsberg	shell	marine shell	Unit B/70-80 cm	AAINA-102	3820	65	—	Havier 1989
Curaçao	Curaçao	northern South America	3	St. Michielsberg	shell	marine shell	Unit B/70-80 cm	AAINA-103	3790	50	—	Haviser 1987

Curaçao	Curaçao	northern South America	3	St. Michielsberg	shell	marine shell	Unit B/70-80 cm	DIC-3158	3790	50	—	Haviser 2001:118
Curaçao	Curaçao	northern South America	3	St. Michielsberg	shell	marine shell	Unit B/70-80 cm	DIC-3159	3820	65	—	Haviser 2001:118
Curaçao	Curaçao	northern South America	2	Seru Boca	charcoal	charcoal/ charred material	07 S77-01 F01	GrN-32016	450	30	—	Hoogland and Hofman 2011:636
Curaçao	Curaçao	northern South America	2	Seru Boca	charcoal	charcoal/ charred material	08 S77-01 F01	GrN-32017	370	25	—	Hoogland and Hofman 2011:636
Curaçao	Curaçao	northern South America	3	Seru Boca	shell	marine shell	02 10-77-35 unit 1	GrN-32015	4570	35	—	Hoogland and Hofman 2011:636
Curaçao	Curaçao	northern South America	2	Spaanse Water	charcoal	charcoal/ charred material	378, unit 1	GrN-31926	605	15	—	Hoogland and Hofman 2011:636
Curaçao	Curaçao	northern South America	3	Spaanse Water	charcoal	charcoal/ charred material	296, Unit 8	GrN-31920	280	15	—	Hoogland and Hofman 2011:636
Curaçao	Curaçao	northern South America	3	Spaanse Water	shell	marine shell	13, unit 1	GrN-31917	4435	15	—	Hoogland and Hofman 2011:636
Curaçao	Curaçao	northern South America	3	Spaanse Water	shell	marine shell	139, unit 4	GrN-31918	3195	20	—	Hoogland and Hofman 2011:636
Curaçao	Curaçao	northern South America	3	Spaanse Water	shell	marine shell	176, unit 8	GrN-31919	1915	20	—	Hoogland and Hofman 2011:636

Curaçao	Curaçao	northern South America	3	Spaanse Water	shell	marine shell	297, unit 12	GrN-31921	2680	20	—	Hoogland and Hofman 2011:636
Curaçao	Curaçao	northern South America	3	Spaanse Water	shell	marine shell	300, unit 3	GrN-31922	2625	20	—	Hoogland and Hofman 2011:636
Curaçao	Curaçao	northern South America	3	Spaanse Water	shell	marine shell	301, unit 2	GrN-31923	2450	15	—	Hoogland and Hofman 2011:636
Curaçao	Curaçao	northern South America	3	Spaanse Water	shell	marine shell	307, unit 6	GrN-31924	2005	15	—	Hoogland and Hofman 2011:636
Curaçao	Curaçao	northern South America	3	Spaanse Water	shell	marine shell	333, unit 7	GrN-31925	2255	20	—	Hoogland and Hofman 2011:636
Curaçao	Curaçao	northern South America	3	Spaanse Water	shell	marine shell	C-215, unit 1	GrN-32018	4455	20	—	Hoogland and Hofman 2011:636
Curaçao	Curaçao	northern South America	3	Spaanse Water	shell	marine shell	C-215/6, unit 1	GrN-31915	4415	20	—	Hoogland and Hofman 2011:636
Curaçao	Curaçao	northern South America	3	Spaanse Water	shell	marine shell	C-215/9 unit 1	GrN-31916	4400	20	—	Hoogland and Hofman 2011:636
Curaçao	Curaçao	northern South America	2	Spaanse Water	*Strombus* sp.	marine shell	unit 105/112 level 3 (10-15 cm bs)	PITT-1200	1965	35	—	Haviser 2001:118

Curaçao	Curaçao	northern South America	3	Spaanse Water	bulk shell (pecten, *Strombus* sp., *Anadara* sp., C*hama* sp.)	marine shell	unit 105/112 level 5 (20-25 cm bs)	PITT-1201	3105	40	—	Haviser 2001:118
Curaçao	Curaçao	northern South America	3	Spaanse Water	bulk shell (*Cittarium pica*, *Anadara* sp.)	marine shell	unit 105/112 level 7 (30-35 cm bs)	—	2965	40	—	Haviser 2001:118
Curaçao	Curaçao	northern South America	4	Spanish Water	organic sediment	sediment	SW09-1, 95 cm	AA-92659	1790	40	-25.2	Dunning et al. 2018a
Curaçao	Curaçao	northern South America	4	Spanish Water	preserved wood	wood	SW09-1, 157-158 cm	AA-90821	3970	45	-25.0	Dunning et al. 2018a
Curaçao	Curaçao	northern South America	3	Spaanse Water	—	unknown	—	PITT-	2180	55	—	Haviser 2001:118
Curaçao	Curaçao	northern South America	4	Spanish Water	preserved wood	wood	SW09-1, 223 cm	AA-84144	4850	40	-25.4	Dunning et al. 2018a
Curaçao	Curaçao	northern South America	3	Tafelberg	*Cittarium* sp.	marine shell	midden	—	3665	140	—	Gould 1971
Curaçao	Curaçao	northern South America	3	Tafelberg	*Chama* sp.	marine shell	midden	—	3830	140	—	Gould 1971
Curaçao	Curaçao	northern South America	3	Tomasitu Cave	shell	marine shell	—	Beta-	4030	70	—	Haviser 2001:118
Curaçao	Curaçao	northern South America	3	Tomasitu Cave	shell	marine shell	—	Beta-	2970	70	—	Haviser 2001:118
Curaçao	Curaçao	northern South America	3	Tomasitu Cave	shell	marine shell	—	Beta-	3060	70	—	Haviser 2001:118
Curaçao	Curaçao	northern South America	3	Tomasitu Cave	shell	marine shell	—	Beta-	3080	70	—	Haviser 2001:118

Curaçao	Curaçao	northern South America	3	Veeris	shell	marine shell	—	Beta-	4170	65	—	Haviser 2001:118
Curaçao	Curaçao	northern South America	3	Veeris	shell	marine shell	—	Beta-	4180	70	—	Haviser 2001:118
Curaçao	Curaçao	northern South America	3	Zuurzak	shell	marine shell	level 10 b.s. (180-200 cm)	PITT-1187	3290	35	—	Haviser 2001:118
Curaçao	Curaçao	northern South America	3	Zuurzak	shell	marine shell	level 8 b.s. (140-160 cm)	PITT-1186	2045	30	—	Haviser 2001:118
Curaçao	Curaçao	northern South America	2	Zuurzak	charcoal	charcoal/ charred material	level 15 b.s. (140-150 cm)	PITT-1188	475	50	—	Haviser and Simmons-Brito 1995
Dominica	Commonwealth of Dominica	Lesser Antilles	2	CB-3	charred material	charcoal/ charred material	Test unit 1, NW quad, 91 cmbd	Beta-366738	890	30	—	Shearn 2014
Dominica	Commonwealth of Dominica	Lesser Antilles	3	CB-1	bulk sherd organics	pottery organics	Test pit 1, 0-10 cmbs	Beta-366737	840	30	—	Shearn 2014
Dominica	Commonwealth of Dominica	Lesser Antilles	3	cave, Dominica	*Guaiacum* sp., terminus date	wood	Museum collections	OxA-17917	556	25	-23.9	Ostapkowicz et al. 2012
Dominica	Commonwealth of Dominica	Lesser Antilles	2	DEL-2	charred material	charcoal/ charred material	Test unit 1, NE quad, 78 cmbd	Beta-366739	1450	30	—	Shearn 2014
Dominica	Commonwealth of Dominica	Lesser Antilles	2	DEL-2	charred material	charcoal/ charred material	Test unit 1, NE quad, 96 cmbd	Beta-366740	2380	30	—	Shearn 2014
Dominica	Commonwealth of Dominica	Lesser Antilles	2	DEL-3	charred material	charcoal/ charred material	Test pit 1, 49 cmbs	Beta-366741	1900	30	—	Shearn 2014
Dominica	Commonwealth of Dominica	Lesser Antilles	2	HS-2	organic residue on sherd	organic material	Test unit 1, NE quad, 110-120 cmbd	Beta-367733	870	30	—	Shearn 2014

Dominica	Commonwealth of Dominica	Lesser Antilles	4	Soufrière site	—	unknown	Complex C	—	1800	40	—	Berard 2007
Eleuthera	Bahamas	Bahamian Archipelago	3	Broad Creek Cay	charred material	charcoal/ charred material	—	Beta-302306	820	40	—	Peter Sinelli, Personal Communication
Eleuthera	Bahamas	Bahamian Archipelago	4	cave	*Guaiacum* sp.	wood	—	OxA-21155	804	25	—	Ostapkowicz 2015
Eleuthera	Bahamas	Bahamian Archipelago	3	Broad Creek Cay	charred material	charcoal/ charred material	—	Beta-302307	490	40	—	Peter Sinelli, Personal Communication
Eleuthera	Bahamas	Bahamian Archipelago	4	Garden Cave (EL-229)	*Geocapromys ingrahami* ulna	faunal material	Room 1:0-10 cmbs	Beta-338513	1390	30	-19.9	Steadman et al. 2017
Eleuthera	Bahamas	Bahamian Archipelago	4	Garden Cave (EL-229)	*Geocapromys ingrahami* humerus	faunal material	Room 1:10-20 cmbs	Beta-330403	4180	30	-19.3	Steadman et al. 2017
Eleuthera	Bahamas	Bahamian Archipelago	4	Garden Cave (EL-229)	*Geocapromys ingrahami* femur	faunal material	Room 1:20-30 cmbs	Beta-330404	3880	30	-18.9	Steadman et al. 2017
Eleuthera	Bahamas	Bahamian Archipelago	4	Garden Cave (EL-229)	*Geocapromys ingrahami* femur	faunal material	Room 1:surface	Beta-330401	2180	30	-19.1	Steadman et al. 2017
Eleuthera	Bahamas	Bahamian Archipelago	4	Garden Cave (EL-229)	*Geocapromys ingrahami* femur	faunal material	Room 2:surface	Beta-330400	210	30	-20.1	Steadman et al. 2017
Eleuthera	Bahamas	Bahamian Archipelago	3	Greenstone	charred material	charcoal/ charred material	—	Beta-334794	1010	30	—	Peter Sinelli, Personal Communication

Eleuthera	Bahamas	Bahamian Archipelago	3	Greenstone	charred material	charcoal/ charred material	—	Beta-356054	730	30	—	Peter Sinelli, Personal Communication
Eleuthera	Bahamas	Bahamian Archipelago	4	Preacher's Cave	human bone collagen	human bone/teeth	Burial 1	Beta-260751	—	—	-21.8	Schaffer et al. 2012
Eleuthera	Bahamas	Bahamian Archipelago	4	Preacher's Cave	human bone collagen	human bone/teeth	Burial 2	Beta-260752	—	—	-17.1	Schaffer et al. 2012
Eleuthera	Bahamas	Bahamian Archipelago	4	Preacher's Cave	human bone collagen	human bone/teeth	Burial 3	Beta-260753	—	—	-19.7	Schaffer et al. 2012
Eleuthera	Bahamas	Bahamian Archipelago	4	Preacher's Cave	*Tellina* sp.	marine shell	Burial 3	Beta-242393	—	—	-0.7	Schaffer et al. 2012
Eleuthera	Bahamas	Bahamian Archipelago	4	Preacher's Cave	triton shell	marine shell	Burial 3	Beta-242394	—	—	+3.5	Schaffer et al. 2012
Eleuthera	Bahamas	Bahamian Archipelago	2	Preacher's Cave	enamel	human bone/teeth	cave burial, sample PC537	ORAU-X-2623-21	1082	29	-8.3	Schroeder et al. 2018
Grand Turk	Turks and Caicos	Bahamian Archipelago	2	Coralie Site	charcoal	charcoal/ charred material	100 N 110 E FS #178 70-80cmbd, Hearth Feature 25	Beta-98698	1230	60	—	Carlson 1999
Grand Turk	Turks and Caicos	Bahamian Archipelago	2	Coralie Site	charcoal	charcoal/ charred material	110N 102 E FS #41 70cmbd, Post Layer Zone 2	Beta-98697	1010	50	—	Carlson 1999
Grand Turk	Turks and Caicos	Bahamian Archipelago	2	Coralie Site	charcoal	charcoal/ charred material	148N 104E FS #353 70-80cmbd, Zone 2 Level 2	Beta-114924	1120	50	—	Carlson 1999
Grand Turk	Turks and Caicos	Bahamian Archipelago	2	Coralie Site	charcoal	charcoal/ charred material	96N 100E FS #198 55-74cmbd, Hearth Feature 28	Beta-98699	900	50	—	Carlson 1999
Grand Turk	Turks and Caicos	Bahamian Archipelago	1	Coralie Site	charcoal: Wild Lime	charcoal/ charred material	110N 110E, FS #81, 92-93.5 cmbd, Ash lens Area 10	Beta-80911	1280	60	—	Carlson 1999

Grand Turk	Turks and Caicos	Bahamian Archipelago	1	Coralie Site	charcoal: palm	charcoal/ charred material	124N 100E FS #35 47-62cmbd, Hearth Feature 5	Beta-80910	1160	60	—	Carlson 1999
Grand Turk	Turks and Caicos	Bahamian Archipelago	2	Coralie Site	*Stombus gigas*	marine shell	100N 108E FS #168, 78-90cmbd, midden Feature 23	Beta-93912	1170	60	—	Carlson 1999
Grand Turk	Turks and Caicos	Bahamian Archipelago	2	Coralie Site	*Stombus gigas*	marine shell	99N 99E FS #216 Post Layer Zone 2	Beta-93913	930	60	—	Carlson 1999
Grand Turk	Turks and Caicos	Bahamian Archipelago	1	Coralie Site	wood, cf. Bullwood	wood	Mangroves Paddle, peat Layer	Beta-96700	940	60	—	Carlson 1999
Grand Turk	Turks and Caicos	Bahamian Archipelago	2	Coralie Site	charcoal	charcoal/ charred material	ca. 120N 110E FS #353 70-80cmbd, Zone 2	Beta-66151	1120	120	—	Carlson 1999
Grand Turk	Turks and Caicos	Bahamian Archipelago	3	Gibbs Cay	*Strombus gigas* pick	marine shell	Unit A, Level 2, 25cm	Beta-242676	260	50	—	Sinelli 2010
Grand Turk	Turks and Caicos	Bahamian Archipelago	2	Gibbs Cay	charcoal	charcoal/ charred material	Unit A, Level 4	Beta-253527	780	40	—	Sinelli 2010
Grand Turk	Turks and Caicos	Bahamian Archipelago	3	GT-2	charcoal	charcoal/ charred material	—	Beta-42983	830	80	—	Carlson 1999
Grand Turk	Turks and Caicos	Bahamian Archipelago	3	GT-2	charcoal	charcoal/ charred material	—	Beta-42985	820	50	—	Carlson 1999
Grand Turk	Turks and Caicos	Bahamian Archipelago	3	GT-2	charcoal	charcoal/ charred material	—	Beta-61150	910	60	—	Sinelli 2010
Grand Turk	Turks and Caicos	Bahamian Archipelago	3	GT-2	charcoal	charcoal/ charred material	—	Beta-66150	910	60	—	Carlson 1999
Grand Turk	Turks and Caicos	Bahamian Archipelago	3	GT-2	*Stombus gigas*	marine shell	—	Beta-42984	1170	60	—	Carlson 1999

Grand Turk	Turks and Caicos	Bahamian Archipelago	3	GT-2	*Stombus gigas*	marine shell	—	Beta-42986	1080	50	—	Carlson 1999
Grand Turk	Turks and Caicos	Bahamian Archipelago	3	GT-3	charcoal	charcoal/ charred material	—	Beta-61151	1130	120	—	Sinelli 2010
Grand Turk	Turks and Caicos	Bahamian Archipelago	2	Middleton Cay	*Strombus gigas*, punched	marine shell	Unit D, Level 3, 30cm (on sterile soil)	Beta-242673	790	50	—	Sinelli 2010
Grand Turk	Turks and Caicos	Bahamian Archipelago	2	Middleton Cay	*Strombus gigas*, punched	marine shell	Unit H, Level 3	Beta-242674	460	40	—	Sinelli 2010
Grand Turk	Turks and Caicos	Bahamian Archipelago	2	Pelican Cay	small conch	marine shell	Unit B, Level 3, on bedrock	Beta-242675	850	50	—	Sinelli 2010
Grand Turk	Turks and Caicos	Bahamian Archipelago	2	Spud Cay	charcoal	charcoal/ charred material	Unit A, Level 4	Beta 242670	690	40	—	Sinelli 2010
Grand Turk	Turks and Caicos	Bahamian Archipelago	2	Spud Cay	charcoal	charcoal/ charred material	Unit E, Level 5	Beta-242671	610	40	—	Sinelli 2010
Grand Turk	Turks and Caicos	Bahamian Archipelago	2	Spud Cay	charcoal	charcoal/ charred material	Unit E, Level 6	Beta-242672	910	40	—	Sinelli 2010
Grand Turk	Turks and Caicos	Bahamian Archipelago	4	—	*Guaiacum* sp.	wood	museum collections	OxA-19116	860	24	-24.2	Ostapkowicz 2015
Great Camanoe	British Virgin Islands	Lesser Antilles	4	Cam Bay	carved shell (tadpole)	unknown	unknown	—	—	—	—	Davis 2011
Inagua	Bahamas	Bahamian Archipelago	3	GI-12	*Strombus gigas*	marine shell	—	Beta-61910	800	50	—	Keegan 1993
Inagua	Bahamas	Bahamian Archipelago	3	GI-3	*Strombus gigas*	marine shell	—	Beta-61909	480	60	—	Keegan 1993
Grenada	Grenada	Lesser Antilles	2	Beausejour (GREN-G-34)	charcoal	charcoal/ charred material	Burial 1, 95 cmbs	PSUAMS-1287	1500	25	—	Hanna 2019

Grenada	Grenada	Lesser Antilles	2	Beausejour (GREN-G-34)	charcoal	charcoal/ charred material	STP1-SS4, 80 cmbs	PSUAMS-1317	1685	20	—	Hanna 2019
Grenada	Grenada	Lesser Antilles	4	Black Point (GREN-G-20)	charcoal	charcoal/ charred material	G20-STP8-SS1, 30-40 cmbs	PSUAMS-1315	moder n	—	—	Hanna 2019
Grenada	Grenada	Lesser Antilles	4	Black Point (GREN-G-20)	*Lobatus* sp.	marine shell	G20-SF-S1, SF on beach, waypt. 130 (STP-1)	PSUAMS-3019	3525	20	—	Hanna 2019
Grenada	Grenada	Lesser Antilles	3	Cato Beach (GREN-G-28)	*Lobatus* sp.	marine shell	G20-SF-S2 [G-28], SF at beach rock, waypt. 137	PSUAMS-3021	1560	15	—	Hanna 2019
Grenada	Grenada	Lesser Antilles	2	Duquense (GREN-M-3)	charcoal	charcoal/ charred material	5N/5W, upper profile (20-40 cmbs)	Beta-85938	850	40	—	Cody 1998
Grenada	Grenada	Lesser Antilles	2	Duquense (GREN-M-3)	charcoal	charcoal/ charred material	5N/5W, lower profile (40-60 cmbs)	Beta-98365	1080	50	—	Cody 1998
Grenada	Grenada	Lesser Antilles	2	La Filette (GREN-A-11)	charcoal	charcoal/ charred material	STP1-SS4, ~2mbs (top of concentration)	PSUAMS-1565	1215	20	—	Hanna 2019
Grenada	Grenada	Lesser Antilles	4	Grand Anse (GREN-G-7)	*Lobatus* sp.	marine shell	Locus B, Unknown unit, 38 cmbs	—	1520	80	—	Banks 1988
Grenada	Grenada	Lesser Antilles	4	Grand Anse (GREN-G-7)	*Lobatus* sp.	marine shell	Locus B, Unknown unit, 71 cmbs	—	1300	80	—	Banks 1988
Grenada	Grenada	Lesser Antilles	4	Grand Bacolet (GREN-D-7)	charcoal	charcoal/ charred material	D7-STP12-SS3, 80-90 cmbs	PSUAMS-1323	moder n	—	—	Hanna 2019
Grenada	Grenada	Lesser Antilles	4	Grand Bacolet (GREN-D-7)	charcoal	charcoal/ charred material	D7-STP12-SS2, 50-60 cmbs	PSUAMS-3943	moder n	—	—	Hanna 2019

Grenada	Grenada	Lesser Antilles	2	Grand Bay (GREN-G-22)	*Lobatus* sp.	marine shell	G22-SF4-S1, top of shell midden, waypt 149	PSUAMS-3022	2145	20	—	Hanna 2019
Grenada	Grenada	Lesser Antilles	2	Grand Bay (GREN-G-22)	*Lobatus* sp.	marine shell	G22-SF5-S2, 20 cm below top of shell midden, waypt 149	PSUAMS-3017	2820	20	—	Hanna 2019
Grenada	Grenada	Lesser Antilles	2	High Cliff Point (GREN-P-7)	charcoal	charcoal/ charred material	STP12-SS3, 22-30 cmbs	PSUAMS-3945	380	25	—	Hanna 2019
Grenada	Grenada	Lesser Antilles	4	Lake Antoine	lake sediment	sediment	Antoine 12_VII-08-6, 611-613 cm	AA-91728	4860	45	-29.2	Siegel et al. 2015
Grenada	Grenada	Lesser Antilles	4	Lake Antoine	preserved peat	organic material	Antoine 12_VII-08-1, 146 cm	Beta-377885	1290	30	-23.2	Siegel et al. 2015
Grenada	Grenada	Lesser Antilles	4	Lake Antoine	lake sediment	sediment	Antoine 12-VII-08-3, 311-313 cm	AA-91729	2030	40	-34.2	Siegel et al. 2015
Grenada	Grenada	Lesser Antilles	4	Lake Antoine	lake sediment	sediment	Antoine 12-VII-08-7, 700 cm	Beta-377883	7340	40	-28.4	Siegel et al. 2015
Grenada	Grenada	Lesser Antilles	4	Marlmont (GREN-D-24)	charcoal	charcoal/ charred material	Waypt. 137-SS1, 43 cmbs	PSUAMS-3944	240	20	—	Hanna 2019
Grenada	Grenada	Lesser Antilles	4	Meadow Beach	peat	peat	MB08-1, 215-217 cm	AA-84798	2880	40	-27.0	Siegel et al. 2015
Grenada	Grenada	Lesser Antilles	4	Meadow Beach	peat	peat	MB08-1, 330-332 cm	AA-84799	4220	40	-30.4	Siegel et al. 2015
Grenada	Grenada	Lesser Antilles	4	Meadow Beach	lake sediment	sediment	Antoine 12-VII-08-7, 736-738 cm	AA-91730	8050	50	-28.6	Siegel et al. 2015

Grenada	Grenada	Lesser Antilles	4	Meadow Beach	preserved wood	wood	MB08-1, 492 cm	AA-82678	4860	45	-29.2	Siegel et al. 2015
Grenada	Grenada	Lesser Antilles	4	Montreuil (GREN-P-2)	charcoal	charcoal/ charred material	PS-STP1-SS4, 40-50 cmbs	PSUAMS-1318	moder n			
Grenada	Grenada	Lesser Antilles	4	Montreuil (GREN-P-2)	charcoal	charcoal/ charred material	PS-STP1-SS6, 70-76 cmbs	PSUAMS-1319	moder n			
Grenada	Grenada	Lesser Antilles	2	Montreuil (GREN-P-2)	charcoal	charcoal/ charred material	Unit A-5d,SS8, 56 cmbs	PSUAMS-3946	1215	20		
Grenada	Grenada	Lesser Antilles	3	Pearls (GREN-A-1)	*Astraea* sp.	marine shell	Unit B, 75-80 cmbd, (55-60 cmbd, 15-20 cmbo)	UGa-	1914	51	—	Cody 1991
Grenada	Grenada	Lesser Antilles	3	Pearls (GREN-A-1)	*Astraea* sp.	unknown	Unit B, 74 cmbd (54 cmbs, 14 cmbo)	UGa-	1725	54	—	Cody 1991
Grenada	Grenada	Lesser Antilles	3	Pearls (GREN-A-1)	*Astraea* sp.	unknown	Unit B, 110-120 cmbd (90-100 cmbs, 50-60 cmbo)	UGa-	1711	74	—	Haviser 1997:60
Grenada	Grenada	Lesser Antilles	2	Pearls (GREN-A-1)	charcoal	charcoal/ charred material	W 195, 103-113 cmbs	PSUAMS-1322	835	25	—	Hanna 2019
Grenada	Grenada	Lesser Antilles	3	Pearls (GREN-A-1)	charcoal	charcoal/ charred material	—	GX-14202	1600	340	—	Hanna 2019
Grenada	Grenada	Lesser Antilles	3	La Sagesse (GREN-D-1)	charcoal	charcoal/ charred material	Unit 28S-4E (bag 41), 60-70 cmbs [D1-28S-7-FW1]	PSUAMS-1316	155	20	—	Hanna 2019
Grenada	Grenada	Lesser Antilles	2	Salt Pond 2 (GREN-G-21)	charcoal	charcoal/ charred material	STP7-SS3, 14-25 cmbs	PSUAMS-1320	1180	25	—	Hanna 2019
Grenada	Grenada	Lesser Antilles	2	Salt Pond 2 (GREN-G-21)	cf. *Anadara* sp.	marine shell	STP7-SS5, 34-45 cmbs	PSUAMS-3020	1510	20	—	Hanna 2019

Grenada	Grenada	Lesser Antilles	4	Salt Pond 3 (GREN-G-21)	charcoal	charcoal/ charred material	G21-STP6-SS4, 45-60 cmbs	PSUAMS-1566	moder n	—	—	Hanna 2019
Grenada	Grenada	Lesser Antilles	4	Salt Pond 3 (GREN-G-21)	charcoal	charcoal/ charred material	G21-STP6-SS9, 110-119 cmbs	PSUAMS-1321	moder n	—	—	Hanna 2019
Grenada	Grenada	Lesser Antilles	2	Sauteurs Bay-1 (GREN-P-5)	charcoal	charcoal/ charred material	Locus 1, 111N/117.5W, posthole, 80-90 cmbs	Beta-86832	790	60	—	Cody 1998
Grenada	Grenada	Lesser Antilles	2	Sauteurs Bay-1 (GREN-P-5)	charcoal	charcoal/ charred material	Locus 1, 127.5N/137.5W, burial layer	Beta-98368	980	60	—	Cody 1998
Grenada	Grenada	Lesser Antilles	2	Sauteurs Bay-1 (GREN-P-5)	charcoal	charcoal/ charred material	Locus 1, 120N/127.5W, burial layer	Beta-86831	1050	90	—	Cody 1998
Grenada	Grenada	Lesser Antilles	2	Sauteurs Bay-2 (GREN-P-5)	charcoal	charcoal/ charred material	Locus 2, 18.5S/7.5W	Beta-98366	340	50	—	Cody 1998
Grenada	Grenada	Lesser Antilles	2	Sauteurs Bay-2 (GREN-P-5)	charcoal	charcoal/ charred material	Locus 2, 45N-114.5W, base of hearth	Beta-98367	510	60	—	Cody 1998
Grenada	Grenada	Lesser Antilles	2	Sauteurs Bay-3 (GREN-P-5)	charcoal	charcoal/ charred material	Locus 3, SC-D (locus SW)	Beta-85941	1270	50	—	Cody 1998
Grenada	Grenada	Lesser Antilles	3	Savanne Suazey-1 (GREN-P-3)	*Strombus* sp.	marine shell	southern locus (#1), "burial area" 0-38 cmbs	RL-76 FSM-BF-14	957	115	—	Bullen and Bullen 1972:153; Rouse et al. 1978:462
Grenada	Grenada	Lesser Antilles	2	Savanne Suazey-1 (GREN-P-3)	charcoal	charcoal/ charred material	southern locus (#1), "burial area" 15-31 cmbs	Beta-86827	900	60	—	Cody 1998
Grenada	Grenada	Lesser Antilles	2	Savanne Suazey-1 (GREN-P-3)	charcoal	charcoal/ charred material	southen (#1), 8.5N/21W, 10-20 cmbs	Beta-86833	810	50	—	Cody 1998
Grenada	Grenada	Lesser Antilles	2	Savanne Suazey-1 (GREN-P-3)	charcoal	charcoal/ charred material	southern locus (#1), 5N/17W, posthole, 15-31 ccmbs	Beta-85935	1110	40	—	Cody 1998

Grenada	Grenada	Lesser Antilles	4	Savanne Suazey-3 (GREN-P-3)	charcoal	charcoal/ charred material	Historic "northeast" locus (#3), probably west of hotel	Beta-85934	120	40	—	Cody 1998
Grenada	Grenada	Lesser Antilles	4	St. John's River (GREN-G-8)	*Hymenaea courbaril*	charcoal/ charred material	G8-P4-6-SRF, Unit 4, 30-45 cmbs	UCIAMS-15873	moder n	—	—	Hanna 2019
Grenada	Grenada	Lesser Antilles	4	St. John's River (GREN-G-8)	*Lobatus* sp.	marine shell	G8-P4-6-SRF, Unit 4, 30-45 cmbs	PSUAMS-1435	3560	60	—	Hanna 2019
Grenada	Grenada	Lesser Antilles	3	St. John's River (GREN-G-8)	*Canis familiaris*	faunal material	G8-P5, Level III, Unit 5, 26-40 cmbs	PSUAMS-1484	230	20	—	Hanna 2019
Grenada	Grenada	Lesser Antilles	2	St. John's River (GREN-G-8)	cf. *Anadara* sp.	marine shell	G8-P3-Final STP(2), Unit 3, 64-82 cmbs	UCIAMS-179806	1380	20	—	Hanna 2019
Grenada	Grenada	Lesser Antilles	2	La Tante (GREN-D-4)	charcoal	charcoal/ charred material	118.5S/36W, 85-110 cmbs (pieces of same sample)	Beta-86829	550	60	—	Cody 1998
Grenada	Grenada	Lesser Antilles	2	La Tante (GREN-D-4)	charcoal	charcoal/ charred material	118.5S/36W, 85-110 cmbs (pieces of same sample)	Beta-86828	650	40	—	Cody 1998
Grenada	Grenada	Lesser Antilles	2	La Tante (GREN-D-4)	charcoal	charcoal/ charred material	118.5S/36W, 85-110 cmbs	Beta-85939	770	60	—	Cody 1998
Grenada	Grenada	Lesser Antilles	2	La Tante (GREN-D-4)	charcoal	charcoal/ charred material	118.5S/36W, 85-110 cmbs	Beta-86830	770	50	—	Cody 1998
Grenada	Grenada	Lesser Antilles	4	True Blue (GREN-G-23)	—	unknown	—	—	800	—	—	Hanna 2019
Guadeloupe	Guadeloupe	Lesser Antilles	3	l'Anse-a-l'Eau	charcoal	charcoal/ charred material	—	Esso	1160	100	—	Bullen and Bullen 1972:153

Guadeloupe	Guadeloupe	Lesser Antilles	4	Baie du Nord Ouest	—	marine shell	—	Erl-8228	2606	58	—	Paulet-Locard and Stouvenot 2005
Guadeloupe	Guadeloupe	Lesser Antilles	4	Baie du Nord Ouest	—	marine shell	—	Erl-8229	3258	59	—	Paulet-Locard and Stouvenot 2005
Guadeloupe	Guadeloupe	Lesser Antilles	4	Blanchard 2	human bone	human bone/teeth	—	Erl-10155	—	—	—	Lenoble et al. 2018:124
Guadeloupe	Guadeloupe	Lesser Antilles	2	Cadet 3	charcoal	charcoal/ charred material	D E3-F1	Erl-10159	1056	36	-26.1	Stouvenot et al. 2014
Guadeloupe	Guadeloupe	Lesser Antilles	2	Cadet 3	charcoal	charcoal/ charred material	G E3-C6	Erl-10156	3052	41	-25.5	Stouvenot et al. 2014
Guadeloupe	Guadeloupe	Lesser Antilles	3	CHU Belle-Plaine	charcoal	charcoal/ charred material	—	Poz-63016	870	30	—	Van den Bel 2017
Guadeloupe	Guadeloupe	Lesser Antilles	3	CHU Belle-Plaine	charcoal	charcoal/ charred material	—	Poz-63019	875	30	—	Van den Bel 2017
Guadeloupe	Guadeloupe	Lesser Antilles	3	CHU Belle-Plaine	charcoal	charcoal/ charred material	—	Poz-63017	885	30	—	Van den Bel 2017
Guadeloupe	Guadeloupe	Lesser Antilles	3	CHU Belle-Plaine	charcoal	charcoal/ charred material	—	Poz-63022	890	30	—	Van den Bel 2017
Guadeloupe	Guadeloupe	Lesser Antilles	3	CHU Belle-Plaine	charcoal	charcoal/ charred material	—	Poz-63015	900	30	—	Van den Bel 2017
Guadeloupe	Guadeloupe	Lesser Antilles	3	CHU Belle-Plaine	charcoal	charcoal/ charred material	—	Poz-63018	915	30	—	Van den Bel 2017
Guadeloupe	Guadeloupe	Lesser Antilles	3	CHU Belle-Plaine	charcoal	charcoal/ charred material	—	Poz-63020	930	30	—	Van den Bel 2017
Guadeloupe	Guadeloupe	Lesser Antilles	3	CHU Belle-Plaine	charcoal	charcoal/ charred material	—	Poz-63014	960	40	—	Van den Bel 2017

Guadeloupe	Guadeloupe	Lesser Antilles	3	CHU Belle-Plaine	charcoal	charcoal/ charred material	—	Poz-63024	960	30	—	Van den Bel 2017
Guadeloupe	Guadeloupe	Lesser Antilles	3	CHU Belle-Plaine	charcoal	charcoal/ charred material	—	Poz-63021	1030	35	—	Van den Bel 2017
Guadeloupe	Guadeloupe	Lesser Antilles	3	Couronne	*Strombus* sp.	marine shell	—	RL-155	780	100	—	Bullen and Bullen 1972:153
Guadeloupe	Guadeloupe	Lesser Antilles	4	Fété 2	—	unknown	—	Beta-407285	3110	30	—	Stouvenot 2017
Guadeloupe	Guadeloupe	Lesser Antilles	3	Grand Anse	shell	marine shell	—	GrN-20874	1210	30	—	Hofman 1995:35
Guadeloupe	Guadeloupe	Lesser Antilles	4	Grotte Morne Rita	—	unknown	—	Ly-11571	4295	30	—	Fouéré et al. 2015
Guadeloupe	Guadeloupe	Lesser Antilles	2	Grotte Papin	charcoal	charcoal/ charred material	test pit near entrance	Ly-8466	770	30	—	Grouard et al. 2014
Guadeloupe	Guadeloupe	Lesser Antilles	2	Morel	charcoal	charcoal/ charred material	base Morel IV, interpreted as Terminal Saladoid	Y-1246	1100	80	—	Bullen and Bullen 1972:153; Rouse et al. 1978:462
Guadeloupe	Guadeloupe	Lesser Antilles	2	Morel	wood	wood	bottom of post (center)	Ly-9162	1815	30	—	Stouvenot et al. 2013:480
Guadeloupe	Guadeloupe	Lesser Antilles	2	Morel	wood	wood	bottom of post (peripherial)	Ly-9161	1580	30	—	Stouvenot et al. 2013:480

Guadeloupe	Guadeloupe	Lesser Antilles	3	Morel	charcoal	charcoal/ charred material	Morel I	Y-1137	1730	70	—	Clerc 1968; Bullen and Bullen 1972:153; Rouse et al. 1978:462; Rouse 1989:397; Haviser 1997:61
Guadeloupe	Guadeloupe	Lesser Antilles	3	Morel	charcoal	charcoal/ charred material	Morel I, interpreted as early Modified Saladoid	Y-1138	1710	100	—	Clerc 1968; Bullen and Bullen 1972:153; Rouse et al. 1978:462; Rouse 1989:397; Haviser 1997:61
Guadeloupe	Guadeloupe	Lesser Antilles	3	Morel	charcoal	charcoal/ charred material	Morel II	Y-1136	1380	100	—	Clerc 1968; Bullen and Bullen 1972:153; Rouse et al. 1978:462; Rouse 1989:397; Haviser 1997:61
Guadeloupe	Guadeloupe	Lesser Antilles	3	Morel	—	unknown	—	GrN-20163	1635	30	—	Haviser 1997:61
Guadeloupe	Guadeloupe	Lesser Antilles	3	Morel	—	unknown	—	GrN-20165	1720	35	—	Haviser 1997:61

Guadeloupe	Guadeloupe	Lesser Antilles	3	Morel	—	unknown	—	GrN-20166	1910	30	—	Haviser 1997:61
Guadeloupe	Guadeloupe	Lesser Antilles	4	Morel	—	unknown	listed as Y-1245 in Bullen; interprted as modified Saladoid	Y-1245	1400	80	—	Bullen and Bullen 1972:153; Rouse et al. 1978:462; Haviser 1997:61; Clerc 1968
Guadeloupe	Guadeloupe	Lesser Antilles	4	Morel Zéro	—	marine shell	—	Erl-9069	3481	47	—	Paulet-Locard and Stouvenot 2005
Guadeloupe	Guadeloupe	Lesser Antilles	4	Morel Zéro	—	marine shell	—	Erl-9070	3493	48	—	Paulet-Locard and Stouvenot 2005
Guadeloupe	Guadeloupe	Lesser Antilles	3	Pointe Canot	shell	marine shell	—	GrN-20876	2050	30	—	Hofman and Hoogland 2003:21
Guadeloupe	Guadeloupe	Lesser Antilles	3	Pointe des Pies	—	unknown	—	Ly-6423	2830	50	—	Richard 1994
Guadeloupe	Guadeloupe	Lesser Antilles	2	La Pointe de Grande Anse, Trois-Rivières	charcoal	charcoal/ charred material	House location 1, number 7 (post hole)	KIA-36671	1230	30	—	Van den Bel and Romon 2010
Guadeloupe	Guadeloupe	Lesser Antilles	2	La Pointe de Grande Anse, Trois-Rivières	charcoal	charcoal/ charred material	House location 1, number 32 (post hole)	KIA-36672	1340	25	—	Van den Bel and Romon 2010
Guadeloupe	Guadeloupe	Lesser Antilles	2	La Pointe de Grande Anse, Trois-Rivières	charcoal	charcoal/ charred material	House location 1, number 1 (burial)	KIA-36673	945	35	—	Van den Bel and Romon 2010

Guadeloupe	Guadeloupe	Lesser Antilles	2	La Pointe de Grande Anse, Trois-Rivières	human bone, collagen	human bone/teeth	House location 1, number 1 (burial)	KIA-36675	915	50	—	Van den Bel and Romon 2010
Guadeloupe	Guadeloupe	Lesser Antilles	2	La Pointe de Grande Anse, Trois-Rivières	human bone, collagen	human bone/teeth	House location 1, number 2 (burial)	KIA-36676	565	25	—	Van den Bel and Romon 2010
Guadeloupe	Guadeloupe	Lesser Antilles	2	La Pointe de Grande Anse, Trois-Rivières	human bone, apatite A	human bone/teeth	House location 1, number 2 (burial)	KIA-36676	348	39	—	Van den Bel and Romon 2010
Guadeloupe	Guadeloupe	Lesser Antilles	2	La Pointe de Grande Anse, Trois-Rivières	human bone, apatite B	human bone/teeth	House location 1, number 2 (burial)	KIA-36676	431	22	—	Van den Bel and Romon 2010
Guadeloupe	Guadeloupe	Lesser Antilles	2	La Pointe de Grande Anse, Trois-Rivières	charcoal	charcoal/ charred material	House location 1, number 3 (pit)	KIA-36674	945	30	—	Van den Bel and Romon 2010
Guadeloupe	Guadeloupe	Lesser Antilles	2	La Pointe de Grande Anse, Trois-Rivières	charcoal	charcoal/ charred material	House location 2, number 935 (post hole)	KIA-36677	1245	30	—	Van den Bel and Romon 2010
Guadeloupe	Guadeloupe	Lesser Antilles	2	La Pointe de Grande Anse, Trois-Rivières	charcoal	charcoal/ charred material	House location 2, number 81 (post hole)	KIA-36678	1065	30	—	Van den Bel and Romon 2010
Guadeloupe	Guadeloupe	Lesser Antilles	2	La Pointe de Grande Anse, Trois-Rivières	charcoal	charcoal/ charred material	House location 2, number 33 (burial)	KIA-36679	625	30	—	Van den Bel and Romon 2010
Guadeloupe	Guadeloupe	Lesser Antilles	2	La Pointe de Grande Anse, Trois-Rivières	human bone, apatite B	human bone/teeth	House location 2, number 33 (burial)	KIA-36681	620	25	—	Van den Bel and Romon 2010
Guadeloupe	Guadeloupe	Lesser Antilles	2	La Pointe de Grande Anse, Trois-Rivières	human bone, apatite A	human bone/teeth	House location 2, number 33 (burial)	KIA-36681	625	25	—	Van den Bel and Romon 2010

Guadeloupe	Guadeloupe	Lesser Antilles	2	La Pointe de Grande Anse, Trois-Rivières	charcoal	charcoal/ charred material	House location 2, number 351 (burial)	KIA-36680	690	30	—	Van den Bel and Romon 2010
Guadeloupe	Guadeloupe	Lesser Antilles	4	La Pointe de Grande Anse, Trois-Rivières	human bone, collagen	human bone/teeth	House location 2, number 351 (burial)	KIA-36682	650	140	—	Van den Bel and Romon 2010
Guadeloupe	Guadeloupe	Lesser Antilles	2	La Pointe de Grande Anse, Trois-Rivières	charcoal	charcoal/ charred material	Number 265, post hole	KIA-36683	330	25	—	Van den Bel and Romon 2010
Guadeloupe	Guadeloupe	Lesser Antilles	2	La Pointe de Grande Anse, Trois-Rivières	charcoal	charcoal/ charred material	Number 834, post hole	KIA-36684	1000	30	—	Van den Bel and Romon 2010
Guadeloupe	Guadeloupe	Lesser Antilles	4	La Pointe de Grande Anse, Trois-Rivières	human bone, apatite A	human bone/teeth	Number 571, burial	KIA-36685	1435	20	—	Van den Bel and Romon 2010
Guadeloupe	Guadeloupe	Lesser Antilles	4	La Pointe de Grande Anse, Trois-Rivières	human bone, apatite B	human bone/teeth	Number 571, burial	KIA-36685	1340	20	—	Van den Bel and Romon 2010
Guadeloupe	Guadeloupe	Lesser Antilles	2	La Pointe de Grande Anse, Trois-Rivières	charcoal	charcoal/ charred material	Number 9, pit	KIA-31187	1210	20	—	Van den Bel and Romon 2010
Guadeloupe	Guadeloupe	Lesser Antilles	3	Pointe Helleux	shell	marine shell	—	GrN-20880	1125	35	—	Hoogland 1995:33
Guadeloupe	Guadeloupe	Lesser Antilles	3	Pointe Helleux	shell	marine shell	—	GrN-20881	925	35	—	Hoogland 1995:33
Guadeloupe	Guadeloupe	Lesser Antilles	3	Pointes des Mangles	shell	marine shell	—	Beta-239750	2620	20	—	Richard 1994
Guadeloupe	Guadeloupe	Lesser Antilles	4	Pointe des Mangles 2	*Lobatus gigas*	marine shell	30-40 cmbs	Erl-9067	—	—	—	Lenoble et al. 2018:124

Guadeloupe	Guadeloupe	Lesser Antilles	4	Pointe des Mangles 2	*Codakia orbicularis*	marine shell	ca. 50 cmbs	Erl-8232	—	—	—	Lenoble et al. 2018:124
Guadeloupe	Guadeloupe	Lesser Antilles	4	Roseau's Seaside	—	unknown	level I	—	865	30	—	Richard 2003:20
Guadeloupe	Guadeloupe	Lesser Antilles	4	Roseau's Seaside	—	unknown	level II	—	1080	30	—	Richard 2003:20
Guadeloupe	Guadeloupe	Lesser Antilles	4	Roseau's Seaside	—	unknown	Level III	—	1370	30	—	Richard 2003:20
Guana Island	British Virgin Islands	Lesser Antilles	4	unnamed cave site	charcoal	charcoal/ charred material	—	—	—	—	—	Lazell 2005:314
Hispaniola	Dominican Republic	Greater Antilles	4	Altos de Vireya	—	unknown	—	I-6146	920	90	—	Morbán Laucer 1979
Hispaniola	Dominican Republic	Greater Antilles	4	Atajadizo	—	unknown	—	—	1410	80	—	Morbán Laucer 1979
Hispaniola	Dominican Republic	Greater Antilles	4	Atajadizo	—	unknown	—	—	1110	80	—	Morbán Laucer 1979
Hispaniola	Dominican Republic	Greater Antilles	4	Bao Bog 2	charcoal	charcoal/ charred material	Core 97 I	Beta-103598	28400	180	-24.8	Horn et al. 2000:16
Hispaniola	Dominican Republic	Greater Antilles	4	Barrera II	charcoal	charcoal/ charred material	Pit 1	I-6145	4115	95	—	Veloz Maggiolo and Ortega 1973
Hispaniola	Dominican Republic	Greater Antilles	4	Barrera-Mordán	charcoal	charcoal/ charred material	—	I-8738	1975	300	—	Morbán Laucer 1979
Hispaniola	Dominican Republic	Greater Antilles	3	Barrera-Mordán	charcoal	charcoal/ charred material	—	Tx-1975-300	1350	80	—	Morbán Laucer 1979
Hispaniola	Dominican Republic	Greater Antilles	2	Batey Negro	charcoal	charcoal/ charred material	Pit 1, . 40 m below surface	I-6781	2585	90	—	Morbán Laucer 1979
Hispaniola	Dominican Republic	Greater Antilles	4	Batey Negro	charcoal	charcoal/ charred material	—	—	2515	85	—	Morbán Laucer 1979

Hispaniola	Dominican Republic	Greater Antilles	4	Bavaro	—	unknown	—	—	1180	80	—	Morbán Laucer 1979
Hispaniola	Haiti	Greater Antilles	4	Bois Charrite	Bulk shell (*Cittarium pica* and *Stombus gigas*)	marine shell	Level 3, .2-.3 m	Instituto de Ciencias Weizman de Israel 560 B	730	190	—	Ortega and Guerrero 1981
Hispaniola	Haiti	Greater Antilles	4	Bois Charrite	Bulk shell (Cittarium pica and Stombus gigas)	marine shell	Level 3, .6-.7 m	Instituto de Ciencias Weizman de Israel 560 A	630	170	—	Ortega and Guerrero 1981
Hispaniola	Haiti	Greater Antilles	4	Le Boucanier	shell	marine shell	—	Beta-42231	1090	80	—	Moore and Tremmel 1997
Hispaniola	Haiti	Greater Antilles	4	Cabaret	*Strombus* sp.	marine shell	—	Beta-	—	—	—	Moore 1991
Hispaniola	Haiti	Greater Antilles	4	Caberet	—	unknown	—	Beta-	2280	80	—	Wilson 1995:397
Hispaniola	Dominican Republic	Greater Antilles	2	El Cabo	charcoal	charcoal/ charred material	75-26-62/layer 9	GrN-31412	1230	40	—	Samson 2010
Hispaniola	Dominican Republic	Greater Antilles	2	El Cabo	charcoal, edge of burnt post	charcoal/ charred material	84-29-F178	GrN-30534	600	25	—	Samson 2010
Hispaniola	Dominican Republic	Greater Antilles	2	El Cabo	charcoal, edge of burnt post	charcoal/ charred material	84-29-F249	GrN-30535	580	30	—	Samson 2010
Hispaniola	Dominican Republic	Greater Antilles	2	El Cabo	charcoal, edge of burnt post	charcoal/ charred material	84-29-F30; Structure 6	GrN-29035	535	25	—	Samson 2010
Hispaniola	Dominican Republic	Greater Antilles	2	El Cabo	charcoal, edge of burnt post	charcoal/ charred material	85-04-F01	GrN-29931	815	35	—	Samson 2010
Hispaniola	Dominican Republic	Greater Antilles	2	El Cabo	charcoal, edge of burnt post	charcoal/ charred material	85-50-F156	GrN-31417	915	20	—	Samson 2010
Hispaniola	Dominican Republic	Greater Antilles	2	El Cabo	charcoal, edge of burnt post	charcoal/ charred material	85-50-F193	GrN-31418	925	30	—	Samson 2010

Hispaniola	Dominican Republic	Greater Antilles	2	El Cabo	*Gercarcinus lateralis*	faunal material	85-44-00/layer 10a	GrN-29934	1110	25	—	Samson 2010
Hispaniola	Dominican Republic	Greater Antilles	2	El Cabo	*Cittarium pica*	marine shell	75-26-62/layer 12	GrN-31413	1705	20	—	Samson 2010
Hispaniola	Dominican Republic	Greater Antilles	2	El Cabo	*Cittarium pica*	marine shell	75-26-62/layer 9	GrN-31414	1435	20	—	Samson 2010
Hispaniola	Dominican Republic	Greater Antilles	2	El Cabo	*Cittarium pica*	marine shell	84-34-06/layer 3	GrN-30531	1170	25	—	Samson 2010
Hispaniola	Dominican Republic	Greater Antilles	2	El Cabo	*Cittarium pica*	marine shell	84-34-16/layer 1	GrN-30533	1040	25	—	Samson 2010
Hispaniola	Dominican Republic	Greater Antilles	2	El Cabo	*Cittarium pica*	marine shell	84-39-29/1	GrN-29932	1495	30	—	Samson 2010
Hispaniola	Dominican Republic	Greater Antilles	2	El Cabo	*Cittarium pica*	marine shell	85-31-01/layer 4	GrN-30532	1525	25	—	Samson 2010
Hispaniola	Dominican Republic	Greater Antilles	2	El Cabo	*Cittarium pica*	marine shell	85-34-81/layer 10	GrN-31416	1745	20	—	Samson 2010
Hispaniola	Dominican Republic	Greater Antilles	2	El Cabo	*Cittarium pica*	marine shell	85-34-90/layer 4	GrN-31415	1520	20	—	Samson 2010
Hispaniola	Dominican Republic	Greater Antilles	2	El Cabo	*Cittarium pica*	marine shell	85-44-00/layer 10b	GrN-29933	1750	30	—	Samson 2010
Hispaniola	Dominican Republic	Greater Antilles	3	La Cacique	charcoal	charcoal/ charred material	—	GrN-6578	740	60	—	Veloz Maggiolo et al. 1981
Hispaniola	Dominican Republic	Greater Antilles	3	La Caleta	charcoal	charcoal/ charred material	—	I-6938	2495	80	—	Morbán Laucer 1979
Hispaniola	Dominican Republic	Greater Antilles	3	La Caleta	charcoal	charcoal/ charred material	—	I-7179	965	85	—	Morbán Laucer 1979
Hispaniola	Dominican Republic	Greater Antilles	3	La Caleta	charcoal	charcoal/ charred material	—	I-7163	780	50	—	Morbán Laucer 1979
Hispaniola	Dominican Republic	Greater Antilles	3	La Caleta	charcoal	charcoal/ charred material	—	I-7183	740	130	—	Morbán Laucer 1979

Hispaniola	Dominican Republic	Greater Antilles	3	La Caleta	charcoal	charcoal/ charred material	—	I-1650	1680	100	—	Morbán Laucer 1979
Hispaniola	Dominican Republic	Greater Antilles	3	La Caleta	charcoal	charcoal/ charred material	—	IVIC-422	670	70	—	Morbán Laucer 1979
Hispaniola	Dominican Republic	Greater Antilles	3	El Caimito	terrestrial shell (*Pleurodontes* sp., *Polydontes* sp., *Caracolus* sp.)	faunal material	—	I-6924	1965	90	—	Veloz Maggiolo et al. 1973
Hispaniola	Dominican Republic	Greater Antilles	3	El Caimito	terrestrial shell (Pleurodontes sp., Polydontes sp., Caracolus sp.)	faunal material	—	I-7821	1830	85	—	Veloz Maggiolo et al. 1973
Hispaniola	Dominican Republic	Greater Antilles	3	El Caimito	terrestrial shell (Pleurodontes sp., Polydontes sp., Caracolus sp.)	faunal material	—	I-7822	1865	85	—	Veloz Maggiolo et al. 1973
Hispaniola	Dominican Republic	Greater Antilles	3	El Caimito	terrestrial shell (Pleurodontes sp., Polydontes sp., Caracolus sp.)	faunal material	—	I-7823	2130	85	—	Veloz Maggiolo et al. 1973
Hispaniola	Dominican Republic	Greater Antilles	4	La Cangrejera	*Stombus pugilis*	marine shell	0-20 cm	NOSAMS -	—	—	—	Nold 2018

Hispaniola	Dominican Republic	Greater Antilles	4	La Cangrejera	*Stombus pugilis*	marine shell	0-20 cm	NOSAMS -	—	—	—	Nold 2018
Hispaniola	Dominican Republic	Greater Antilles	4	La Cangrejera	*Stombus pugilis*	marine shell	0-20 cm	NOSAMS -	—	—	—	Nold 2018
Hispaniola	Dominican Republic	Greater Antilles	4	La Cangrejera	*Stombus pugilis*	marine shell	0-20 cm	NOSAMS -	—	—	—	Nold 2018
Hispaniola	Dominican Republic	Greater Antilles	4	La Cangrejera	*Stombus pugilis*	marine shell	40-60 cm	NOSAMS -	—	—	—	Nold 2018
Hispaniola	Dominican Republic	Greater Antilles	4	La Cangrejera	*Stombus pugilis*	marine shell	40-60 cm	NOSAMS -	—	—	—	Nold 2018
Hispaniola	Dominican Republic	Greater Antilles	4	La Cangrejera	*Stombus pugilis*	marine shell	40-60 cm	NOSAMS -	—	—	—	Nold 2018
Hispaniola	Dominican Republic	Greater Antilles	4	La Cangrejera	*Stombus pugilis*	marine shell	80-100 cm	NOSAMS -	—	—	—	Nold 2018
Hispaniola	Dominican Republic	Greater Antilles	4	La Cangrejera	*Stombus pugilis*	marine shell	80-100 cm	NOSAMS -	—	—	—	Nold 2018
Hispaniola	Dominican Republic	Greater Antilles	4	La Cangrejera	*Stombus pugilis*	marine shell	80-100 cm	NOSAMS -	—	—	—	Nold 2018
Hispaniola	Dominican Republic	Greater Antilles	3	El Carril	charcoal	charcoal/ charred material	—	CSIC-104	1030	100	—	Veloz Maggiolo et al. 1981
Hispaniola	Dominican Republic	Greater Antilles	3	Cave Isabella, Dominican Republic	*Guaiacum* sp., terminus date	wood	—	OxA-21153	606	25	-16.2	Ostapkowicz et al. 2013
Hispaniola	Haiti	Greater Antilles	4	Complejo Cordillera Central	—	unknown	—	I-6165	2790	190	—	Veloz Maggiolo and Ortega 1973
Hispaniola	Dominican Republic	Greater Antilles	3	Corrales	charcoal	charcoal/ charred material	—	I-6594	1090	90	—	Morbán Laucer 1979
Hispaniola	Dominican Republic	Greater Antilles	3	Corrales	charcoal	charcoal/ charred material	—	I-6593	1080	90	—	Morbán Laucer 1979
Hispaniola	Haiti	Greater Antilles	3	Couri II	—	marine shell	—	Beta-41783	1710	70	—	Moore and Tremmel 1997

Hispaniola	Haiti	Greater Antilles	3	Couri II	—	marine shell	—	Beta-71640	3430	70	—	Moore and Tremmel 1997
Hispaniola	Dominican Republic	Greater Antilles	3	La Cucama	charcoal	charcoal/ charred material	—	I-7889	1545	100	—	Morbán Laucer 1979
Hispaniola	Dominican Republic	Greater Antilles	2	Cueva de Berna	charcoal	charcoal/ charred material	Corte 6, .75-1.00 m	I-9539	3205	90	—	Veloz Maggiolo et al. 1977
Hispaniola	Dominican Republic	Greater Antilles	2	Cueva de Berna	charcoal	charcoal/ charred material	Corte 2, nivel 1.7-1.8	I-5940	3840	130	—	Veloz Maggiolo et al. 1977
Hispaniola	Dominican Republic	Greater Antilles	2	Cueva de Berna	conch shell	marine shell	Corte 5, nivel 2.50-2.75	I-9541	3575	90	—	Veloz Maggiolo et al. 1977
Hispaniola	Dominican Republic	Greater Antilles	4	Cueva Elizabeth	—	—	—	I-6448	1125	90	—	Morbán Laucer 1979
Hispaniola	Dominican Republic	Greater Antilles	3	Cueva del Ferrocarril	charcoal	charcoal/ charred material	—	I-8737	1315	80	—	Morbán Laucer 1979
Hispaniola	Dominican Republic	Greater Antilles	3	El Curro	—	unknown	—	—	3400	95	—	Morbán Laucer 1979
Hispaniola	Haiti	Greater Antilles	4	Des Cahots	—	unknown	—	—	—	—	—	Moore 1991
Hispaniola	Haiti	Greater Antilles	4	Des Cahots	—	unknown	—	Beta-	4340	80	—	Wilson 1995:397
Hispaniola	Dominican Republic	Greater Antilles	3	Don Julio	conch	marine shell	—	GrN-32761	763	15	—	University of Leiden
Hispaniola	Dominican Republic	Greater Antilles	3	Don Julio	charcoal	charcoal/ charred material	—	DSH-3784	754	39	—	University of Leiden
Hispaniola	Dominican Republic	Greater Antilles	3	Don Julio	charcoal	charcoal/ charred material	—	DSH-3785	1031	45	—	University of Leiden
Hispaniola	Dominican Republic	Greater Antilles	2	Edilio Cruz	*Lobatus gigas*	marine shell	Trench 5, Unit 1 N1992.65-E1955.54, Stratum 2	Beta-293244	1340	40	-0.6	Oliver personal communication 2018

Hispaniola	Dominican Republic	Greater Antilles	2	Edilio Cruz	*Lobatus gigas*	marine shell	Unit 1: N1990-E1995, base Stratum 1	Beta-293242	1120	40	+1.3	Oliver personal communication 2018
Hispaniola	Dominican Republic	Greater Antilles	2	Edilio Cruz	*Cittarium pica*	marine shell	Unit 1: N1990-E1995, base Stratum 2 (top of ash lens)	Beta-293243	1030	40	+2.9	Oliver personal communication 2018
Hispaniola	Haiti	Greater Antilles	2	En Ba Saline	charcoal	charcoal/ charred material	FS7399 (A18) Mound structure	Beta-47758	810	70	-25.0 (est.)	Deagan 2004
Hispaniola	Haiti	Greater Antilles	2	En Ba Saline	charcoal	charcoal/ charred material	FS7126 (A2, L3) Mound structure	Beta-46760	800	60	-25.0 (est.)	Deagan 2004
Hispaniola	Haiti	Greater Antilles	2	En Ba Saline	charcoal	charcoal/ charred material	FS7123 (F26, L4) Mound structure	Beta-46759	720	50	-25.0 (est.)	Deagan 2004
Hispaniola	Haiti	Greater Antilles	2	En Ba Saline	charcoal	charcoal/ charred material	FS6851 (PM6) Mound structure	Beta-18173	680	80	-25.0 (est.)	Deagan 2004
Hispaniola	Haiti	Greater Antilles	2	En Ba Saline	charcoal	charcoal/ charred material	FS7185 (F31, L2) Non-elite ridge structure	Beta-046761	320	70	-0.25	Deagan 2004
Hispaniola	Haiti	Greater Antilles	2	En Ba Saline	charcoal	charcoal/ charred material	FS3888 (A6) Post underlying burial pit	Beta-01527	640	260	-0.25	Deagan 2004
Hispaniola	Haiti	Greater Antilles	2	En Ba Saline	charcoal	charcoal/ charred material	FS6316 (F11, L5) Feast pit	Beta-18172	600	70	-25.0 (est.)	Deagan 2004
Hispaniola	Haiti	Greater Antilles	2	En Ba Saline	charcoal	charcoal/ charred material	FS3885 (F4, L11) Burial pit	Beta-10526	430	80	-0.25	Deagan 2004
Hispaniola	Haiti	Greater Antilles	2	En Ba Saline	charcoal	charcoal/ charred material	FS6882 (A6, L6) Burial pit	Beta-018469	440	60	-0.25	Deagan 2004
Hispaniola	Haiti	Greater Antilles	2	En Ba Saline	charcoal	charcoal/ charred material	FS3897 (F8, L3) Burial pit	Beta-010528	340	70	-0.25	Deagan 2004

Hispaniola	Dominican Republic	Greater Antilles	3	Estero Hondo (Las Paredes)	charcoal	charcoal/ charred material	—	—	2570	85	—	Morbán Laucer 1979
Hispaniola	Haiti	Greater Antilles	4	Gillote	—	marine shell	—	Beta-52888	3260	60	—	Moore and Tremmel 1997
Hispaniola	Dominican Republic	Greater Antilles	3	Guzmancito	conch	marine shell	—	GrN-31419	1170	20	—	University of Leiden
Hispaniola	Dominican Republic	Greater Antilles	3	Guzmancito	conch	marine shell	—	GrN-31420	1195	20	—	University of Leiden
Hispaniola	Dominican Republic	Greater Antilles	3	Guzmancito	conch	marine shell	—	GrN-31421	1190	20	—	University of Leiden
Hispaniola	Dominican Republic	Greater Antilles	3	Hatillo Palma II	charcoal	charcoal/ charred material	—	I-6016	605	90	—	Veloz Maggiolo et al. 1981
Hispaniola	Dominican Republic	Greater Antilles	3	Hatillo Palma I	charcoal	charcoal/ charred material	—	I-6015	515	90	—	Veloz Maggiolo et al. 1981
Hispaniola	Dominican Republic	Greater Antilles	4	Honduras del Oeste	—	unknown	Level 1; 30 cmbs	I-6012	2310	95	—	Morbán Laucer 1979
Hispaniola	Dominican Republic	Greater Antilles	2	Hoyo de Toro	charcoal	charcoal/ charred material	Pit 1, 30-60 cmbs	I-6756	3890	95	—	Morbán Laucer 1979
Hispaniola	Dominican Republic	Greater Antilles	4	Hoyo de Toro	charcoal	charcoal/ charred material	—	—	2540	85	—	Morbán Laucer 1979
Hispaniola	Dominican Republic	Greater Antilles	3	Humilde López	charcoal	charcoal/ charred material	—	GrN-32770	915	30	—	University of Leiden
Hispaniola	Dominican Republic	Greater Antilles	3	Humilde López	charcoal	charcoal/ charred material	—	GrN-32771	925	20	—	University of Leiden
Hispaniola	Haiti	Greater Antilles	3	Ile a Rat	charcoal	charcoal/ charred material	52 cm below datum	Beta-108547	690	70	—	Keegan 1999
Hispaniola	Haiti	Greater Antilles	3	Ile a Rat	charcoal	charcoal/ charred material	69 cm below datum	Beta-108548	1130	50	—	Keegan 1999

Hispaniola	Dominican Republic	Greater Antilles	4	Los Indios	plant material (from core)	plant material	123-124	Beta - 437562	920	30	-28.2	Hooghiemstra et al. 2018
Hispaniola	Dominican Republic	Greater Antilles	4	Los Indios	plant material	plant material	224-225	Beta - 437563	1840	30	-25.9	Hooghiemstra et al. 2018
Hispaniola	Dominican Republic	Greater Antilles	4	Los Indios	plant material	plant material	36-37 cmbs	Beta- 437560	moder n	—	-15.4	Hooghiemstra et al. 2018
Hispaniola	Dominican Republic	Greater Antilles	4	Los Indios	bulk organic sediment	sediment	105-106 cmbs	Beta - 437561	1060	30	-23.8	Hooghiemstra et al. 2018
Hispaniola	Dominican Republic	Greater Antilles	4	Los Indios	bulk organic sediment	sediment	165-166	Beta - 420881	870	30	-24.5	Hooghiemstra et al. 2018
Hispaniola	Dominican Republic	Greater Antilles	4	Los Indios	bulk organic sediment	sediment	179-180	Beta - 420882	980	30	-25.0	Hooghiemstra et al. 2018
Hispaniola	Dominican Republic	Greater Antilles	4	Los Indios	bulk organic sediment	sediment	80-81 cmbs	Beta - 420880	260	30	-25.0	Hooghiemstra et al. 2018
Hispaniola	Dominican Republic	Greater Antilles	4	La Isabela	—	—	—	Tx-	800	390	—	Morbán Laucer 1979
Hispaniola	Dominican Republic	Greater Antilles	3	La Isleta	—	unknown	—	I-7852	1230	90	—	Morbán Laucer 1979
Hispaniola	Dominican Republic	Greater Antilles	3	La Isleta	—	unknown	—	—	3180	90	—	Morbán Laucer 1979
Hispaniola	Dominican Republic	Greater Antilles	4	Laguna Biajaca	bulk sediment	sediment	127-126 cmbs	Beta - 469283	740	30	-23.0	Castilla-Beltran et al. 2018
Hispaniola	Dominican Republic	Greater Antilles	4	Laguna Biajaca	bulk sediment	sediment	185-183 cmbs	Beta - 469282	660	30	-23.7	Castilla-Beltran et al. 2018
Hispaniola	Dominican Republic	Greater Antilles	4	Laguna Biajaca	bulk sediment	sediment	224-225 cmbs	Beta - 420888	1060	30	-24.8	Castilla-Beltran et al. 2018

Hispaniola	Dominican Republic	Greater Antilles	4	Laguna Biajaca	bulk sediment	sediment	75-76 cmbs	Beta - 469284	430	30	-21.9	Castilla-Beltran et al. 2018
Hispaniola	Dominican Republic	Greater Antilles	4	Laguna Biajaca	bulk sediment	sediment	90-91 cmbs	Beta - 420887	290	30	-19.4	Castilla-Beltran et al. 2018
Hispaniola	Dominican Republic	Greater Antilles	3	Laguna Castilla	organic macrofossils	organic macrofossils	204-207 cm	Beta-204702	110	40	-24.5	Lane et al. 2008
Hispaniola	Dominican Republic	Greater Antilles	4	Laguna Castilla	bulk sediment	sediment	66-68 cm depth	Beta-196817	modern	—	-25.6	Lane et al. 2008
Hispaniola	Dominican Republic	Greater Antilles	3	Laguna Castilla	bulk sediment	sediment	536-537 cm	Beta-171499	1000	40	-24.2	Lane et al. 2008
Hispaniola	Dominican Republic	Greater Antilles	3	Laguna Castilla	bulk sediment	sediment	329-331 cm	Beta-196818	730	40	-25.9	Lane et al. 2008
Hispaniola	Dominican Republic	Greater Antilles	4	Laguna Grande de Macutico	charcoal	charcoal/ charred material	Core 97 I	Beta-106384	11040	60	-24.9	Horn et al. 2000:16
Hispaniola	Dominican Republic	Greater Antilles	3	Laguna de Salvador	wood fragment	wood	204 cm	Beta-204696	410	40	-27.5	Lane et al. 2008
Hispaniola	Dominican Republic	Greater Antilles	3	Laguna de Salvador	wood fragment	wood	75-76 cm	Beta-219035	100	40	-25.7	Lane et al. 2008
Hispaniola	Dominican Republic	Greater Antilles	3	Loma Perenal	charcoal	charcoal/ charred material	—	R-3318	806	63	—	De Grossi et al. 2008
Hispaniola	Dominican Republic	Greater Antilles	3	López	charcoal	charcoal/ charred material	—	T-6446	900	90	—	Veloz Maggiolo et al. 1981
Hispaniola	Dominican Republic	Greater Antilles	4	La Llamada	—	unknown	—	I-6018	730	95	—	Veloz Maggiolo et al. 1981
Hispaniola	Dominican Republic	Greater Antilles	3	Macao	charcoal	charcoal/ charred material	—	I-6314	1125	90	—	Morbán Laucer 1979
Hispaniola	Dominican Republic	Greater Antilles	3	Macao	charcoal	charcoal/ charred material	—	I-7163	780	50	—	Morbán Laucer 1979
Hispaniola	Dominican Republic	Greater Antilles	3	Macao	charcoal	charcoal/ charred material	—	I-6445	925	110	—	Morbán Laucer 1979

Hispaniola	Dominican Republic	Greater Antilles	3	La Madama, Cabo Samaná	charcoal	charcoal/ charred material	—	I-9780	2795	140	—	Morbán Laucer 1979
Hispaniola	Dominican Republic	Greater Antilles	3	Madrigales	charcoal	charcoal/ charred material	—	I-7388	2030	95	—	Morbán Laucer 1979
Hispaniola	Dominican Republic	Greater Antilles	2	Manantial de la Aleta	duho	wood	cenote	Beta-112400	910	40	—	Conrad et al. 2001:14
Hispaniola	Dominican Republic	Greater Antilles	1	Manantial de la Aleta	gourd	plant material	cenote	Beta-107023	940	30	—	Conrad et al. 2001:14
Hispaniola	Dominican Republic	Greater Antilles	2	Manantial de la Aleta	duho fragment	wood	cenote	Beta-96781	680	60	—	Conrad et al. 2001:14
Hispaniola	Dominican Republic	Greater Antilles	2	Manantial de la Aleta	basket	plant material	cenote	Beta-108314	620	70	—	Conrad et al. 2001:14
Hispaniola	Dominican Republic	Greater Antilles	2	Manantial de la Aleta	flaring bowl	wood	cenote	Beta-108313	990	70	—	Conrad et al. 2001:14
Hispaniola	Dominican Republic	Greater Antilles	2	Manantial de la Aleta	macana	wood	cenote	Beta-108315	540	50	—	Conrad et al. 2001:14
Hispaniola	Dominican Republic	Greater Antilles	2	Manantial de la Aleta	haft	wood	cenote	Beta-96782	870	60	—	Conrad et al. 2001:14
Hispaniola	Haiti	Greater Antilles	4	Matelas	—	unknown	—	Beta-	4370	90	—	Wilson 1995:397
Hispaniola	Dominican Republic	Greater Antilles	3	Mordan	charocal	charcoal/ charred material	—	IVIC-5	4400	170	—	Wilson 1995:397
Hispaniola	Dominican Republic	Greater Antilles	3	Mordan	charocal	charcoal/ charred material	—	Tx-54	4140	130	—	Wilson 1995:397
Hispaniola	Dominican Republic	Greater Antilles	3	Mordan	charcoal	charcoal/ charred material	—	Y-1422	4560	80	—	Wilson 1995:397
Hispaniola	Dominican Republic	Greater Antilles	4	El Morro	—	unknown	—	I-6443	970	90	—	Morbán Laucer 1979

Hispaniola	Dominican Republic	Greater Antilles	3	La Muchacha	charcoal	charcoal/ charred material	—	GrN-32767	390	35	—	University of Leiden
Hispaniola	Dominican Republic	Greater Antilles	3	La Muchacha	charcoal	charcoal/ charred material	—	GrN-32766	540	50	—	University of Leiden
Hispaniola	Dominican Republic	Greater Antilles	4	Musie Pedro, San Pedro de Macoris	charcoal	charcoal/ charred material	—	Tx-	2255	80	—	Morbán Laucer 1979
Hispaniola	Dominican Republic	Greater Antilles	3	museum collection	*Carapa* sp.	wood	outer wood: 125 mm from pith sample	OxA-21149	801	24	-24.4	Brock et al. 2012; Ostapkowicz et al. 2013
Hispaniola	Dominican Republic	Greater Antilles	3	museum collection	*Carapa* sp. (pith)	wood	pith (bird and turtle canopied cemi)	OxA-21148	805	24	-24.8	Brock et al. 2012; Ostapkowicz et al. 2013
Hispaniola	—	Greater Antilles	3	museum collection	Pinaceae, resin (platter)	wood	Museum collections	OxA-18331	383	25	-21.1	Ostapkowicz et al. 2012:4
Hispaniola	—	Greater Antilles	3	museum collection	wood, terminus, cohoba stand	wood	Museum collections	OxA-18457	923	27	-23.2	Ostapkowicz et al. 2012:4
Hispaniola	Haiti	Greater Antilles	3	museum collection	*Guaiacum* sp. Terminus (platter)	wood	Museum collections	OxA-19175	547	28	-22.6	Ostapkowicz et al. 2012:4
Hispaniola	Haiti	Greater Antilles	3	museum collection	*Guaiacum* spp. (duho); outer edge: 112.9 mm from pith sample	wood	Museum collections	OxA-19176	369	28	-26.4	Brock et al. 2012; Ostapkowicz et al. 2012
Hispaniola	Haiti	Greater Antilles	3	museum collection	*Guaiacum* spp. (duho); 4.1 mm from center of pith	wood	Museum collections	OxA-19178	491	27	-26.7	Brock et al. 2012; Ostapkowicz et al. 2012

Hispaniola	Dominican Republic	Greater Antilles	3	museum collection	*Guaiacum* spp.; reliquary? Pith inner edge~25 mm from out edge	wood	Museum collections	OxA-19398	904	28	-24.1	Brock et al. 2012; Ostapkowicz et al. 2012
Hispaniola	Dominican Republic	Greater Antilles	3	museum collection	*Guaiacum* spp.; reliquary? Pith outer edge	wood	Museum collections	OxA-19399	927	28	-25.6	Brock et al. 2012; Ostapkowicz et al. 2012
Hispaniola	Dominican Republic	Greater Antilles	3	museum collection	*Guaiacum* spp.; pith (cohoba stand)	wood	Museum collections	OxA-20675	1107	26	-25.9	Brock et al. 2012; Ostapkowicz et al. 2012
Hispaniola	Dominican Republic	Greater Antilles	3	museum collection	*Guaiacum* spp.; pith (cohoba stand)	wood	Museum collections	OxA-20676	1144	27	-25.6	Brock et al. 2012; Ostapkowicz et al. 2012
Hispaniola	Dominican Republic	Greater Antilles	3	museum collection	*Guaiacum* spp.; pith (cohoba stand), left side terminus	wood	Museum collections	OxA-21855	1093	24	-24.8	Brock et al. 2012; Ostapkowicz et al. 2012
Hispaniola	—	Greater Antilles	3	museum collection	*Guaiacum* spp.	wood	Pith (cohoba stand) Right 115.4 mm from pit, 4.1 mm from outer edge	OxA-20627	1031	27	-25.8	Ostapkowicz et al. 2012:4; Brock et al. 2012

Hispaniola	—	Greater Antilles	3	museum collection	*Guaiacum* spp.	wood	Pith (left: 89.8 mm for pith, 7.5 mm from outer edge) cohoba stand	OxA-20626	1165	28	-25.6	Ostapkowicz et al. 2012:4; Brock et al. 2012
Hispaniola	—	Greater Antilles	4	museum collection	Protium or *Bursera* sp. resin	wood	Museum collections	OxA-19170	150	25	-12.9	Ostapkowicz et al. 2012:4
Hispaniola	Dominican Republic	Greater Antilles	3	museum collection	*Guaiacum* sp., terminus date	wood	—	OxA-15483	621	26	-23.7	Ostapkowicz et al. 2013
Hispaniola	Dominican Republic	Greater Antilles	4	Musiepedro	bulk shell (*Cittarium pica*, *Tectarius muricatus*, and *Stombus gigas*)	marine shell	Unit 1, level 4 (02-2-1A-4)	I-8646	2255	80	—	Veloz Maggiolo et al. 1976
Hispaniola	Dominican Republic	Greater Antilles	4	La Nevera	charcoal	charcoal/ charred material	Excavation 4	Beta-125067	4910	50	-27.8	Horn et al. 2000:16
Hispaniola	Dominican Republic	Greater Antilles	4	La Nevera	charcoal	charcoal/ charred material	Excavation 9	Beta-125066	3220	60	-27.7	Horn et al. 2000:16
Hispaniola	Dominican Republic	Greater Antilles	3	Los Patos	conch	marine shell	—	GrN-32764	1480	20	—	University of Leiden
Hispaniola	Haiti	Greater Antilles	4	Phaeton	—	unknown	—	—	—	—	—	Moore 1991
Hispaniola	Haiti	Greater Antilles	4	Phaeton	—	unknown	—	Beta-	3260	70	—	Wilson 1995:397
Hispaniola	Dominican Republic	Greater Antilles	3	Los Pérez	conch	marine shell	—	GrN-32769	1041	15	—	University of Leiden
Hispaniola	Dominican Republic	Greater Antilles	3	Los Pérez	charcoal	charcoal/ charred material	—	GrN-32768	855	25	—	University of Leiden
Hispaniola	Dominican Republic	Greater Antilles	4	La Piedra	bulk shell (*Crassostrea rhizophorae*)	marine shell	Unit 4, level 2	I-8740	3585	85	—	Rímoli and Nadal 1983

Hispaniola	Dominican Republic	Greater Antilles	4	La Piedra	bulk shell (*Crassostrea rhizophorae*)	marine shell	Unit 6, level 3	I-8741	3625	85	—	Rímoli and Nadal 1983
Hispaniola	Dominican Republic	Greater Antilles	3	Playa de Bavaro	charcoal	charcoal/ charred material	—	I-10337	945	80	—	Morbán Laucer 1979
Hispaniola	Dominican Republic	Greater Antilles	4	El Pleicito	charcoal	charcoal/ charred material	—	I-6147	865	90	—	Morbán Laucer 1979
Hispaniola	Dominican Republic	Greater Antilles	3	Popi	charcoal	charcoal/ charred material	—	GrN-32772	972	15	—	University of Leiden
Hispaniola	Dominican Republic	Greater Antilles	4	El Porvenir	—	unknown	—	I-6615	2855	90	—	Wilson 1995:397
Hispaniola	Dominican Republic	Greater Antilles	3	El Porvenir	charcoal	charcoal/ charred material	—	I-6792	2980	95	—	Wilson 1995:397
Hispaniola	Dominican Republic	Greater Antilles	4	El Porvenir	—	unknown	—	—	3980	95	—	Veloz Maggiolo and Ortega 1973
Hispaniola	Dominican Republic	Greater Antilles	3	El Porvenir (Seralles)	charcoal	charcoal/ charred material	—	—	3135	90	—	Morbán Laucer 1979
Hispaniola	Dominican Republic	Greater Antilles	4	Puerto Alejandro	charcoal	charcoal/ charred material	—	I-10338	3400	95	—	Morbán Laucer 1979
Hispaniola	Dominican Republic	Greater Antilles	3	Puerto Juanita	conch	marine shell	—	GrN-31913	1075	15	—	University of Leiden
Hispaniola	Dominican Republic	Greater Antilles	3	Puerto Juanita	conch	marine shell	—	GrN-31912	1010	15	—	University of Leiden
Hispaniola	Dominican Republic	Greater Antilles	3	Puerto Juanita	conch	marine shell	—	GrN-31911	1025	15	—	University of Leiden
Hispaniola	Dominican Republic	Greater Antilles	3	La Punta De Bayahibe	shell	marine shell	level 0.60/0.40	Beta-199781	3380	60	—	Atiles and López Belando 2006:543
Hispaniola	Dominican Republic	Greater Antilles	3	La Punta De Bayahibe	shell	marine shell	level 0.80/0.60	Beta-199782	3530	70	—	Atiles and López Belando 2006:543

Hispaniola	Dominican Republic	Greater Antilles	4	Punta Bayahibe	—	marine shell	—	Beta-222903	3550	50	—	Atiles and López Belando 2006:543
Hispaniola	Dominican Republic	Greater Antilles	4	Punta Bayahibe	—	marine shell	—	Beta-222904	3600	80	—	Atiles and López Belando 2006:543
Hispaniola	Dominican Republic	Greater Antilles	4	Punta Bayahibe	—	marine shell	—	Beta-222905	3460	50	—	Atiles and López Belando 2006:543
Hispaniola	Dominican Republic	Greater Antilles	4	Punta Bayahibe	—	marine shell	—	Beta-222906	3150	50	—	Atiles and López Belando 2006:543
Hispaniola	Dominican Republic	Greater Antilles	4	Punta Cana	—	unknown	—	Beta-179653	1750	50	—	Ortega et al. 2003:413
Hispaniola	Dominican Republic	Greater Antilles	4	Punta Garza	—	unknown	—	I-6858	705	85	—	Morbán Laucer 1979
Hispaniola	Dominican Republic	Greater Antilles	4	Punta Garza	—	unknown	—	—	650	90	—	Morbán Laucer 1979
Hispaniola	Haiti	Greater Antilles	3	Riviere Maurice	shell	marine shell	—	Beta-52434	4170	60	—	Moore and Tremmel 1997
Hispaniola	Dominican Republic	Greater Antilles	4	Río Bao	charcoal	charcoal/ charred material	Cutbank 1	Beta-128791	1280	30	-24.9 (est.)	Horn et al. 2000:16
Hispaniola	Dominican Republic	Greater Antilles	4	Río Bao	charcoal	charcoal/ charred material	Cutbank 1	Beta-128792	3060	40	-25.6	Horn et al. 2000:16
Hispaniola	Dominican Republic	Greater Antilles	4	Río Bao	charcoal	charcoal/ charred material	Cutbank 2	Beta-128789	42480	680	-25.0	Horn et al. 2000:16
Hispaniola	Dominican Republic	Greater Antilles	3	Río Joba	—	unknown	—	—	920	100	—	Olsen et al. 2000

Hispaniola	Dominican Republic	Greater Antilles	3	Río Joba	charcoal	charcoal/ charred material	—	GrN-31914	985	15	—	University of Leiden
Hispaniola	Dominican Republic	Greater Antilles	3	Río Joba	charcoal	charcoal/ charred material	—	N-3517	1150	85	—	Veloz Maggiolo et al. 1981
Hispaniola	Dominican Republic	Greater Antilles	3	Río Joba	charcoal	charcoal/ charred material	—	N-3516	1080	65	—	Veloz Maggiolo et al. 1981
Hispaniola	Dominican Republic	Greater Antilles	3	Río Joba	charcoal	charcoal/ charred material	—	—	1080	60	—	Olsen et al. 2000
Hispaniola	Dominican Republic	Greater Antilles	3	Río Joba	charcoal	charcoal/ charred material	—	—	740	60	—	Olsen et al. 2000
Hispaniola	Dominican Republic	Greater Antilles	3	Río Verde/Cutupú	charcoal	charcoal/ charred material	—	N-3360	1210	75	—	Veloz Maggiolo et al. 1981
Hispaniola	Dominican Republic	Greater Antilles	3	Río Verde	charcoal	charcoal/ charred material	—	GrN-6577	1095	60	—	Veloz Maggiolo et al. 1981
Hispaniola	Dominican Republic	Greater Antilles	3	Río Verde	charcoal	charcoal/ charred material	—	GrN-6576	1145	30	—	Veloz Maggiolo et al. 1981
Hispaniola	Dominican Republic	Greater Antilles	3	Río Verde	charcoal	charcoal/ charred material	—	GrN-6575	965	30	—	Veloz Maggiolo et al. 1981
Hispaniola	Dominican Republic	Greater Antilles	3	La Romana	charcoal	charcoal/ charred material	—	Y-1896	940	80	—	Morbán Laucer 1979
Hispaniola	Dominican Republic	Greater Antilles	4	Sabana de los Robles 1b	charcoal (*Pinus occidentalis*?)	charcoal/ charred material	40-44 cm	Beta-93754	4160	60	-25.0	Horn et al. 2000:16
Hispaniola	Dominican Republic	Greater Antilles	4	Sabana Macutico 1	charcoal (*Pinus occidentalis*?)	charcoal/ charred material	45-50 cm	Beta-111207	9380	80	-25.0 (est.)	Horn et al. 2000:16
Hispaniola	Dominican Republic	Greater Antilles	3	Sabaneta de Juan Dolio	charcoal	charcoal/ charred material	Pit 1	I-6755	2195	90	—	Morbán Laucer 1979
Hispaniola	Haiti	Greater Antilles	3	Savane Caree II	shell	marine shell	—	Beta-42232	4160	90	—	Moore and Tremmel 1997

Hispaniola	Dominican Republic	Greater Antilles	4	El Soco	—	unknown	—	—	1020	80	—	Morbán Laucer 1979
Hispaniola	Dominican Republic	Greater Antilles	4	El Soco	—	unknown	—	—	655	80	—	Morbán Laucer 1979
Hispaniola	Dominican Republic	Greater Antilles	3	Sonador	charcoal	charcoal/ charred material	—	UG2-433	1255	115	—	Morbán Laucer 1979
Hispaniola	Dominican Republic	Greater Antilles	3	Sonador	charcoal	charcoal/ charred material	—	UG-432	580	65	—	Veloz Maggiolo et al. 1973
Hispaniola	Dominican Republic	Greater Antilles	3	Sonador	charcoal	charcoal/ charred material	—	UG-434	480	65	—	Rouse and Cruxent 1979
Hispaniola	Haiti	Greater Antilles	4	Source Matelas	shell	marine shell	—	Beta-	—	—	—	Moore 1991
Hispaniola	Dominican Republic	Greater Antilles	2	Taveras I	charcoal	charcoal/ charred material	Pit 4, 4.6 m	I-5818	2095	135	—	Morbán Laucer 1979
Hispaniola	Dominican Republic	Greater Antilles	2	Taveras II	charcoal	charcoal/ charred material	Pit 4, 3.6 m	SI-991	1805	70	—	Morbán Laucer 1979
Hispaniola	Dominican Republic	Greater Antilles	4	Valle de Bao	charcoal	charcoal/ charred material	Excavation in fan	Beta-128793	6780	40	-22.8	Horn et al. 2000:16
Hispaniola	Dominican Republic	Greater Antilles	4	Valle de Bao	charcoal	charcoal/ charred material	Excavation in fan	Beta-128794	3040	40	-25.6	Horn et al. 2000:16
Hispaniola	Dominican Republic	Greater Antilles	4	Valle Nuevo 1	charcoal (*Pinus occidentalis*?)	charcoal/ charred material	65-70 cm	Beta-93755	4110	80	-20.0	Horn et al. 2000:16
Hispaniola	Dominican Republic	Greater Antilles	3	El Vigia	charcoal	charcoal/ charred material	—	I-8742	3920	85	—	Morbán Laucer 1979
Hispaniola	Dominican Republic	Greater Antilles	3	El Vigia	charcoal	charcoal/ charred material	—	I-08763	3775	85	—	Morbán Laucer 1979
Hispaniola	Haiti	Greater Antilles	4	Vignier II	—	unknown	—	—	—	—	—	Moore 1991

Hispaniola	Haiti	Greater Antilles	4	Vignier III	shell	marine shell	—	Beta-	—	—	—	Moore 1991
Hispaniola	Haiti	Greater Antilles	4	Vignier III	—	unknown	—	Beta-	5580	80	—	Wilson 1995:397
Hispaniola	Haiti	Greater Antilles	4	Vignier III	—	unknown	—	Beta-	5270	100	—	Wilson 1995:397
Inagua	Dominican Republic	Bahamian Archipelago	3	Ike's Cut (GI-3)	charred material	charcoal/ charred material	—	Beta-334793	760	30	—	Sinelli, Personal Communicatio n
Inagua	Bahamas	Bahamian Archipelago	3	Ike's Cut (GI-3)	charred material	charcoal/ charred material	—	Beta-356052	730	30	—	Sinelli, Personal Communicatio n
Inagua	Bahamas	Bahamian Archipelago	3	Ike's Cut (GI-3)	charred material	charcoal/ charred material	—	Beta-356053	710	30	—	Sinelli, Personal Communicatio n
Isle de la Gonâve	Haiti	Greater Antilles	3	cave, Isle de La Gonave	*Guaiacum* sp. terminus (reliquary?)	wood	Museum collections	OxA-19169	617	29	-25.0	Ostapkowicz et al. 2012:4
Isle de la Gonâve	Haiti	Greater Antilles	3	cave, Isle de La Gonave	*Guaiacum* sp. terminus (drum)	wood	Museum collections	OxA-19171	1139	27	-24.6	Ostapkowicz et al. 2012:4
Jamaica	Jamaica	Greater Antilles	3	Aboukir	*Swietenia* sp.	marine shell	Museum collections	Beta-153380	690	40	-23.8	Ostakopwicz et al. 2012: 2241; Allsworth-Jones 2008: 99
Jamaica	Jamaica	Greater Antilles	3	Aboukir	—	unknown	Museum collections	OxA-21055	536	24	-13.5	Ostapkowicz et al. 2012: 2241

Jamaica	Jamaica	Greater Antilles	3	Aboukir	*Guaiacum* sp.	wood	Museum collections	Beta-153379	820	40	-25.2	Brock et al. 2012: 681; Ostapkowicz et al. 2012: 6641; Allsworth-Jones 2008: 99
Jamaica	Jamaica	Greater Antilles	3	Aboukir	*Guaiacum* sp.	wood	Museum collections	OxA-21052	600	24	-23.7	Ostakopwicz et al. 2012: 2242
Jamaica	Jamaica	Greater Antilles	3	Aboukir	Protium or *Bursera* sp.	wood	Museum collections	OxA-21053	634	28	-16.4	Ostakopwicz et al. 2012: 2241
Jamaica	Jamaica	Greater Antilles	3	Aboukir	*Guaiacum* sp.	wood	Museum collections	OxA-21054	886	26	-26.5	Brock et al. 2012: 681; Ostapkowicz et al. 2012: 2241
Jamaica	Jamaica	Greater Antilles	3	Aboukir	*Guaiacum* sp.	wood	Museum collections	OxA-23004	646	22	-24.2	Brock et al. 2012: 681: Ostakowicz et al. 2012: 2241
Jamaica	Jamaica	Greater Antilles	3	Bengal (A8)	charcoal	charcoal/ charred material	—	IVIC-190	770	100	—	Allsworth-Jones 2008: 99, 137
Jamaica	Jamaica	Greater Antilles	3	Bottom Bay (M4)	—	unknown	—	Y-1987	1300	120	—	Allsworth-Jones 2008: 101, 159

Jamaica	Jamaica	Greater Antilles	4	Bottom Bay (M4)	—	unknown	—	—	—	—	—	Fitzpatrick 2006:400
Jamaica	Jamaica	Greater Antilles	3	Bull Savannah Cave	human bone	human bone/teeth	—	OxA-12995	1101	27	-13.9	Higham et al. 2007: S9; Santos et al. 2013: 493
Jamaica	Jamaica	Greater Antilles	3	Bull Savannah Cave	human bone	human bone/teeth	—	OxA-13614	1123	25	-14.0	Higham et al. 2007: S9; Santos et al. 2013: 493
Jamaica	Jamaica	Greater Antilles	3	Bull Savannah Cave	human bone	human bone/teeth	—	OxA-13664	1069	23	-13.9	Higham et al. 2007: S9; Santos et al. 2013: 493
Jamaica	Jamaica	Greater Antilles	2	Cambridge Hill	*Guaiacum* sp.	wood	Duho (high-back): terminus	OxA-21058	615	24	-25.3	Ostakopwicz et al. 2012: 2241
Jamaica	Jamaica	Greater Antilles	3	Cedar Valley, St. Ann's Parish	*Guaiacum* sp.	wood	Museum collections	OxA-19055	152	24	-25.3	Ostakopwicz et al. 2012: 2242
Jamaica	Jamaica	Greater Antilles	3	Chancery Hall (K11)	charcoal	charcoal/ charred material	—	Beta-53703	690	50	—	Allsworth-Jones 2008: 99, 154
Jamaica	Jamaica	Greater Antilles	3	Cinnamon Hill (J10)	charcoal	charcoal/ charred material	lower stratum, 10-20 in. below surface	—	935	180	—	Allsworth-Jones 2008: 99, 151
Jamaica	Jamaica	Greater Antilles	3	Cinnamon Hill (J10)	charcoal	charcoal/ charred material	upper stratum, 0-10 in. below surface	—	625	195	—	Allsworth-Jones 2008: 99, 151
Jamaica	Jamaica	Greater Antilles	3	Cinnamon Hill (J10)	human bone	human bone/teeth	burial, 20 in. below surface	—	350	90	—	Allsworth-Jones 2008: 151

Jamaica	Jamaica	Greater Antilles	2	cave, St. Catherine's Parish	*Guaiacum* sp.	wood	Museum collections	Beta-153378	970	40	-26.0	Ostakopwicz et al. 2012: 2242
Jamaica	Jamaica	Greater Antilles	2	cave, St. Catherine's Parish	*Guaiacum* sp.	wood	Museum collections	OxA-21056	384	24	-23.8	Ostakopwicz et al. 2012: 2242
Jamaica	Jamaica	Greater Antilles	2	cave, St. Catherine's Parish	*Protium* or *Bursera* sp.	wood	Museum collections	OxA-21057	396	24	-29.4	Ostakopwicz et al. 2012: 2242
Jamaica	Jamaica	Greater Antilles	4	Coleraine (Y19)	—	unknown	trench 4.5-6S 6-7W	Beta-182412	790	70	—	Allsworth-Jones 2008:100, 179
Jamaica	Jamaica	Greater Antilles	4	Cranbrook	charcoal	charcoal/ charred material	Area 1 West, Level 7 (Layer 4)	Beta-	—	—	—	Conolley 2011
Jamaica	Jamaica	Greater Antilles	4	Cranbrook	charcoal	charcoal/ charred material	Area 2 West, Layer 6	Beta-	—	—	—	Conolley 2011
Jamaica	Jamaica	Greater Antilles	4	Fairfield	charcoal	charcoal/ charred material	Area 1 West, Level 6 (Layer 1)	Beta-	—	—	—	Conolley 2011
Jamaica	Jamaica	Greater Antilles	4	Fairfield	charcoal	charcoal/ charred material	Section 1 East, Level 11 (Layer 5)	Beta-	—	—	—	Conolley 2011
Jamaica	Jamaica	Greater Antilles	4	Fairfield	charcoal	charcoal/ charred material	Trench 5, Layer 8	Beta-	—	—	—	Conolley 2011
Jamaica	Jamaica	Greater Antilles	4	Green Castle (Y25)	—	unknown	Mid Trench, level 2	Beta-134378	70	50	—	Allsworth-Jones 2008:181
Jamaica	Jamaica	Greater Antilles	4	Green Castle (Y25)	—	unknown	Mid Trench, level 3	Beta-158967	750	60	—	Allsworth-Jones 2008:100, 181
Jamaica	Jamaica	Greater Antilles	4	Green Castle (Y25)	—	unknown	Mid Trench, level 7	Beta-158968	480	80	—	Allsworth-Jones 2008:100, 181

Jamaica	Jamaica	Greater Antilles	3	Green Castle (Y25)	human bone?	unknown	Mid Trench, burial 1	Beta-158969	660	40	—	Allsworth-Jones 2008: 100, 181
Jamaica	Jamaica	Greater Antilles	4	Green Castle (Y25)	—	unknown	Southern Trench, occupation 3, level 2	Beta-134379	330	60	—	Allsworth-Jones 2008:100, 181
Jamaica	Jamaica	Greater Antilles	4	Green Castle (Y25)	—	unknown	Southern Trench, occupation 1, level 13	Beta-158964	920	60	—	Allsworth-Jones 2008:100, 181
Jamaica	Jamaica	Greater Antilles	4	Green Castle (Y25)	—	unknown	Southern Trench, occupation 1, level 13	Beta-158965	820	60	—	Allsworth-Jones 2008:100, 181
Jamaica	Jamaica	Greater Antilles	4	Green Castle (Y25)	—	unknown	Southern Trench, occupation 2, level 7	Beta-158963	760	60	—	Allsworth-Jones 2008:100, 181
Jamaica	Jamaica	Greater Antilles	4	Green Castle (Y25)	—	unknown	Southern Trench, occupation 3, level 3	Beta-158966	430	80	—	Allsworth-Jones 2008:100, 181
Jamaica	Jamaica	Greater Antilles	4	Little River, St. Ann	—	unknown	—	—	—	—	—	Reid 1992:16
Jamaica	Jamaica	Greater Antilles	2	Maima East	charcoal	charcoal/ charred material	House 8 Strata, IVb	WK 43114	627	20	—	Burley et al. 2017
Jamaica	Jamaica	Greater Antilles	2	Maima East	charcoal	charcoal/ charred material	House 8, Stata V	WK 43115	938	20	—	Burley et al. 2017
Jamaica	Jamaica	Greater Antilles	4	Newry (Y27)	—	unknown	13-14 S 6-7 E, level 4	Beta-170433	850	60	—	Allsworth-Jones 2008:100, 184
Jamaica	Jamaica	Greater Antilles	4	Newry (Y27)	—	unknown	13-14 S 6-7 E, level 6	Beta-170434	1020	60	—	Allsworth-Jones 2008:100, 184

Jamaica	Jamaica	Greater Antilles	4	Newry (Y27)	—	unknown	9-10 S 1-2 W, level 4	Beta-170435	950	60	—	Allsworth-Jones 2008:100, 184
Jamaica	Jamaica	Greater Antilles	4	Newry (Y27)	—	unknown	9-10 S 1-2 W, level 8	Beta-170436	1040	40	—	Allsworth-Jones 2008:100, 184
Jamaica	Jamaica	Greater Antilles	3	Paradise Park (Wes-15a)	conch shell	marine shell	—	Beta-125832	1180	60	—	Keegan et al. 2003: 1609; Allsworth-Jones 2008: 101
Jamaica	Jamaica	Greater Antilles	3	Paradise Park (Wes-15b)	charcoal	charcoal/ charred material	—	Beta-125833	490	60	—	Keegan et al. 2003: 1609; Allsworth-Jones 2008: 99
Jamaica	Jamaica	Greater Antilles	4	St. Ann's Bay	wood	wood	Transect 1	A-6063	moder n	—	-27.6	Waters et al. 1993
Jamaica	Jamaica	Greater Antilles	3	St. Ann's Bay	organic debris	plant material	Transect 1	A-6399	545	45	-27.2	Waters et al. 1993
Jamaica	Jamaica	Greater Antilles	3	St. Ann's Bay	wood	wood	Transect 1	A-6048	4080	45	-26.0	Waters et al. 1993
Jamaica	Jamaica	Greater Antilles	3	St. Ann's Bay	wood	wood	Transect 1	A-6049	910	45	-26.4	Waters et al. 1993
Jamaica	Jamaica	Greater Antilles	3	St. Ann's Bay	wood	wood	Transect 1	A-6056	2410	45	-26.8	Waters et al. 1993
Jamaica	Jamaica	Greater Antilles	3	St. Ann's Bay	wood	wood	Transect 1	A-6062	105	35	-26.8	Waters et al. 1993
Jamaica	Jamaica	Greater Antilles	3	St. Ann's Bay	wood	wood	Transect 1	A-6139	150	35	-27.2	Waters et al. 1993
Jamaica	Jamaica	Greater Antilles	3	St. Ann's Bay	wood	wood	Transect 2	A-6051	740	45	-26.0	Waters et al. 1993
Jamaica	Jamaica	Greater Antilles	3	St. Ann's Bay	wood	wood	Transect 2	A-6052	905	40	-26.4	Waters et al. 1993
Jamaica	Jamaica	Greater Antilles	3	St. Ann's Bay	wood	wood	Transect 2	A-6053	1315	50	-28.7	Waters et al. 1993

Jamaica	Jamaica	Greater Antilles	3	St. Ann's Bay	wood	wood	Transect 2	A-6055	1575	45	-26.8	Waters et al. 1993
Jamaica	Jamaica	Greater Antilles	3	St. Ann's Bay	wood	wood	Transect 2	A-6060	1260	40	-29.4	Waters et al. 1993
Jamaica	Jamaica	Greater Antilles	3	St. Ann's Bay	wood	wood	Transect 3	A-6050	1970	50	-30.7	Waters et al. 1993
Jamaica	Jamaica	Greater Antilles	3	St. Ann's Bay	wood	wood	Transect 3	A-6057	1400	35	-26.8	Waters et al. 1993
Jamaica	Jamaica	Greater Antilles	3	St. Ann's Bay	wood	wood	Transect 3	A-6059	290	35	-28.7	Waters et al. 1993
Jamaica	Jamaica	Greater Antilles	2	St. Ann's Bay	charcoal	charcoal/ charred material	Transect 1, midden with burned fishbone	A-6061	525	45	-25.7	Waters et al. 1993
Jamaica	Jamaica	Greater Antilles	2	St. Ann's Bay	Charcoal	charcoal/ charred material	Transect 2, hearth	A-6058	570	45	-29.0	Waters et al. 1993
Jamaica	Jamaica	Greater Antilles	2	St. Ann's Bay	Wood	wood	Transect 1, treenail from ship	A-6140	630	40	-23.0	Waters et al. 1993
Jamaica	Jamaica	Greater Antilles	2	Wentworth (Y8)	charcoal	charcoal/ charred material	layer 3	Beta-167740	680	60	—	Allsworth-Jones 2008: 100, 178
Jamaica	Jamaica	Greater Antilles	4	White Marl (S1)	—	unknown	—	—	—	—	—	Fitzpatrick 2006:400
Jamaica	Jamaica	Greater Antilles	4	White Marl (S1)	—	unknown	—	—	—	—	—	Reid 1992:16
Jamaica	Jamaica	Greater Antilles	4	White Marl (S1)	—	unknown	midden 2, 40-50 in. below surface	Y-1118	1073	95	—	Allsworth-Jones 2008:99, 165
Jamaica	Jamaica	Greater Antilles	4	White Marl (S1)	—	unknown	midden 3, 40-50 in. below surface	Y-1119	617	95	—	Allsworth-Jones 2008:164
Jamaica	Jamaica	Greater Antilles	4	White Marl (S1)	—	unknown	midden 3, 50-60 in. below surface	Y-1117	1016	95	—	Allsworth-Jones 2008:99, 165

Jamaica	Jamaica	Greater Antilles	4	White Marl (S1)	—	unknown	Trench A, 6‘M, level II	Y-1753	650	60	—	Allsworth-Jones 2008:99, 165
Jamaica	Jamaica	Greater Antilles	4	White Marl (S1)	—	unknown	Trench A, 6‘M, level VII	Y-1754	720	60	—	Allsworth-Jones 2008:99, 165
Jamaica	Jamaica	Greater Antilles	4	White Marl (S1)	—	unknown	Trench A, 6‘N, level I	Y-1750	460	120	—	Allsworth-Jones 2008:99, 165
Jamaica	Jamaica	Greater Antilles	4	White Marl (S1)	—	unknown	Trench A, 6‘N, level V	Y-1751	760	60	—	Allsworth-Jones 2008:99, 165
Jamaica	Jamaica	Greater Antilles	4	White Marl (S1)	—	unknown	Trench B, 13F, level IV	Y-1785	650	60	—	Allsworth-Jones 2008:99, 165
Jamaica	Jamaica	Greater Antilles	4	White Marl (S1)	—	unknown	Trench B, 13F, level IX	Y-1784	780	60	—	Allsworth-Jones 2008:99, 165
Jamaica	Jamaica	Greater Antilles	3	White Marl (S1)	human bone	human bone/teeth	Trench B, 12G, Burial 3	Y-1786	800	80	—	Allsworth-Jones 2008: 99, 165
Jamaica	Jamaica	Greater Antilles	3	White Marl (S1)	human bone	human bone/teeth	Trench B, 13F, Burial 2	Y-1755	600	60	—	Allsworth-Jones 2008: 165
Jost Van Dyke	British Virgin Islands	Lesser Antilles	2	Cape Wright	charcoal	charcoal/ charred material	Test Unit G, 135 cm (2 intercepts)	Beta-144547	1350	40	-25.1	Bates 2001:222-224
Jost Van Dyke	British Virgin Islands	Lesser Antilles	2	Cape Wright	charcoal	charcoal/ charred material	Test Unit G, 35 cm	Beta-144548	1030	40	-0.26	Bates 2001:222-224
Long Island	Antigua and Barbuda	Greater Antilles	4	Jolly Beach	—	unknown	15 cmbs	I-7687	—	—	—	Nicholson 1975:265

Long Island	Antigua and Barbuda	Greater Antilles	4	Jumby Bay	—	unknown	—	GrA-18850	860	60	—	Knippenberg 2001
Long Island	Antigua and Barbuda	Greater Antilles	4	Sugar Mill	—	unknown	—	GrA-18849	600	60	—	Knippenberg 2001
Long Island	Antigua and Barbuda	Greater Antilles	4	cave, Mortimers	*Cordia* sp.	wood	cave	OxA-19173	623	27	-23.2	Ostapkowicz 2015
Long Island	Antigua and Barbuda	Greater Antilles	4	cave, Mortimers	*Cordia* sp.	wood	cave	Oxa-18912	524	22	-22.4	Ostapkowicz 2015
Long Island	Antigua and Barbuda	Greater Antilles	4	cave, Mortimers	*Guaiacum* sp.	wood	cave	OxA-18793	454	24	-24.1	Ostapkowicz 2015
Long Island	Antigua and Barbuda	Greater Antilles	4	cave, Mortimers	*Cordia* sp.	wood	cave	OxA-18448	424	24	-26.5	Ostapkowicz 2015
Los Roques	Venezuela	northern South America	2	Las Cuevas, La Isla Blanquilla	charcoal	charcoal/ charred material	exterior niche 26 cmbs	I-16293	1130	120	—	Antczak et al. 1991
Los Roques	Venezuela	northern South America	4	Domusky Norte	—	unknown	multicomponent site	I-15089	620	80	—	Antczak et al. 1991:495-496
Los Roques	Venezuela	northern South America	4	Dos Mosquises	—	unknown	multicomponent site	I-15087	470	80	—	Antczak et al. 1991:495-496
Los Roques	Venezuela	northern South America	4	Dos Mosquises	—	unknown	multicomponent site	I-15088	520	80	—	Antczak et al. 1991:495-496
Marie-Galante	Guadeloupe	Lesser Antilles	4	Vieux Fort	carbonized wood	charcoal/ charred material	—	AA-84884	4380	60	-26.7	Siegel et al. 2015
Marie-Galante	Guadeloupe	Lesser Antilles	4	Vieux Fort	organic sediment	sediment	—	AA-84883	—	—	-31.2	Siegel et al. 2015
Martinique	Martinique	Lesser Antilles	4	Baie de Fort-de-France	preserved plant matter	plant material	KC08-1, 575 cm	Beta-341060	4220	30	-25.4	Siegel et al. 2015
Martinique	Martinique	Lesser Antilles	4	Baie de Fort-de-France	organic sediment	sediment	KC08-1, 229-230 cm	AA-92562	1710	30	-27.7	Siegel et al. 2015

Martinique	Martinique	Lesser Antilles	4	Baie de Fort-de-France	organic sediment	sediment	KC08-1, 674-676 cm	AA-82676	5000	50	-27.3	Siegel et al. 2015
Martinique	Martinique	Lesser Antilles	2	Diamant	*Strombus* sp.	marine shell	level 1	ARC-999	1815	50	—	Vidal 1999:11
Martinique	Martinique	Lesser Antilles	2	Diamant	*Strombus* sp.	marine shell	level 13	ARC-1017	1780	50	—	Vidal 1999:11
Martinique	Martinique	Lesser Antilles	2	Diamant	*Strombus* sp.	marine shell	level 18	ARC-1018	1880	50	—	Vidal 1999:11
Martinique	Martinique	Lesser Antilles	2	Diamant	*Strombus* sp.	marine shell	level 2	ARC-1000	1260	50	—	Vidal 1999:11
Martinique	Martinique	Lesser Antilles	2	Diamant	*Strombus* sp.	marine shell	level 7	ARC-1016	1845	50	—	Vidal 1999:11
Martinique	Martinique	Lesser Antilles	3	Diamant (lower)	charcoal	charcoal/ charred material	—	Y-1762	1475	60	—	Bullen and Bullen 1972:153; Haviser 1997:61
Martinique	Martinique	Lesser Antilles	4	Fond Brûlé	—	unknown	—	Ly-2196	1630	210	—	Rouse 1989:397; Haviser 1997:61
Martinique	Martinique	Lesser Antilles	4	Fond Brûlé	—	unknown	—	Ly-2197	2100	210	—	Rouse 1989:397; Haviser 1997:61
Martinique	Martinique	Lesser Antilles	4	Fond Brûlé	—	unknown	—	Ny-	2215	115	—	Rouse 1989:397; Haviser 1997:61
Martinique	Martinique	Lesser Antilles	4	Fond Brûlé	—	unknown	—	Ny-	2480	140	—	Rouse 1989:397; Haviser 1997:61
Martinique	Martinique	Lesser Antilles	4	Fond Brûlé	—	unknown	—	Ny-478	1650	260	—	Rouse 1989:397; Haviser 1997:61
Martinique	Martinique	Lesser Antilles	4	Fond Brûlé	—	unknown	—	—	265	115	—	Mattioni 1979

Martinique	Martinique	Lesser Antilles	4	Fond Brûlé	—	unknown	—	—	530	140	—	Mattioni 1979
Martinique	Martinique	Lesser Antilles	3	Grand Anse du Lorrain	charcoal	charcoal/ charred material	—	Y-1337	1450	80	—	Bullen and Bullen 1972:153
Martinique	Martinique	Lesser Antilles	3	La Salle	charcoal	charcoal/ charred material	—	Y-1116	1770	80	—	Bullen and Bullen 1972:153; Rouse 1989:397; Haviser 1997:61
Martinique	Martinique	Lesser Antilles	4	Pointe Figuier	organic sediment	sediment	PF08-1, 222-223 cm	AA-82677	2600	50	-29.1	Siegel et al. 2015
Martinique	Martinique	Lesser Antilles	4	Pointe Figuier	preserved wood	wood	PF08-1, 128 cm	AA-92561	330	35	-27.8	Siegel et al. 2015
Martinique	Martinique	Lesser Antilles	4	Vivé	—	unknown	—	S-85	1655	150	—	Rouse 1989:397; Haviser 1997:61
Martinique	Martinique	Lesser Antilles	3	Vivé	charcoal	charcoal/ charred material	—	RL-156	1730	100	—	Bullen and Bullen 1972:153, 156; Rouse 1989:397; Haviser 1997:61
Martinique	Martinique	Lesser Antilles	3	Vivé	charcoal	charcoal/ charred material	—	UGa-113	1530	75	—	Bullen and Bullen 1972:95; Rouse 1989:397; Haviser 1997:61
Martinique	Martinique	Lesser Antilles	4	—	—	unknown	—	—	294	150	—	Petitjean-Roget 1970

Middle Caicos	Turks and Caicos	Bahamian Archipelago	3	Kendrick	charcoal	charcoal/ charred material	—	Beta-146873	900	50	—	Sinelli 2001
Middle Caicos	Turks and Caicos	Bahamian Archipelago	3	MC-12	charcoal	charcoal/ charred material	—	Beta-70335	950	60	—	Carlson 1999
Middle Caicos	Turks and Caicos	Bahamian Archipelago	3	MC-12	charcoal	charcoal/ charred material	—	IGS-1098	680	70	—	Carlson 1999
Middle Caicos	Turks and Caicos	Bahamian Archipelago	3	MC-12	charcoal	charcoal/ charred material	—	IGS-896	800	70	—	Carlson 1999
Middle Caicos	Turks and Caicos	Bahamian Archipelago	3	MC-32	charcoal	charcoal/ charred material	—	Beta-67886	660	50	—	Carlson 1999
Middle Caicos	Turks and Caicos	Bahamian Archipelago	3	MC-36	charcoal	charcoal/ charred material	—	Beta-70608	740	80	—	Carlson 1999
Middle Caicos	Turks and Caicos	Bahamian Archipelago	3	MC-6	charcoal	charcoal/ charred material	—	IGS-2633	450	70	—	Carlson 1999
Middle Caicos	Turks and Caicos	Bahamian Archipelago	4	MC-16 (Cave)	—	unknown	—	IGS-2670	820	70	—	Carlson 1999
Mona Island	Puerto Rico	Greater Antilles	1	Cave 18	*Amyris elemifera*	charcoal/ charred material	Cave 18	OxA-31209	454	23	-28.2	Samson and Cooper personal communication
Mona Island	Puerto Rico	Greater Antilles	1	Cave 18	*Bursera simaruba*	charcoal/ charred material	Cave 18	OxA-31536	682	26	-26.9	Samson and Cooper personal communication
Mona Island	Puerto Rico	Greater Antilles	3	Cave 6	Bursera simaruba	charcoal/ charred material	Cave art on wall	OxA-31199	—	—	—	Samon et al. 2017
Mona Island	Puerto Rico	Greater Antilles	3	Cave 8	Bursera simaruba	charcoal/ charred material	Cave art on wall	OxA-31348	—	—	—	Samon et al. 2017

Mona Island	Puerto Rico	Greater Antilles	2	Cueva de los Caracoles	charcoal	charcoal/ charred material	0-10 cmbs	I-13671	3290	90	—	Davila Davila 2003
Mona Island	Puerto Rico	Greater Antilles	2	Cueva de los Caracoles	*Strombus gigas*	marine shell	10-20 cmbs	I-13674	4330	100	—	Davila Davila 2003
Mona Island	Puerto Rico	Greater Antilles	3	Cueva de los Caracoles	charcoal	charcoal/ charred material	—	I-13672	630	80	—	Davila Davila 2003
Mona Island	Puerto Rico	Greater Antilles	3	Cueva de los Caracoles	charcoal	charcoal/ charred material	—	I-13673	610	80	—	Davila Davila 2003
Montserrat	Montserrat	Lesser Antilles	4	Radio Antilles	—	unknown	—	Beta-18490	2210	70	—	Rouse 1989:397; Haviser 1997:61
Montserrat	Montserrat	Lesser Antilles	4	Radio Antilles	—	unknown	—	Beta-18491	2390	60	—	Rouse 1989:397; Haviser 1997:61
Montserrat	Montserrat	Lesser Antilles	4	Radio Antilles	—	unknown	—	Beta-18581	2120	60	—	Rouse 1989:397; Haviser 1997:61
Montserrat	Montserrat	Lesser Antilles	2	Trants Site	charcoal	charcoal/ charred material	Feature 5 burial	Beta-83048	1860	100	—	Petersen, Bartone, and Watters 1999:50-51
Montserrat	Montserrat	Lesser Antilles	2	Trants Site	charcoal	charcoal/ charred material	Stripped Area	Beta-83043	2770	60	—	Petersen, Bartone, and Watters 1999:50-51

Montserrat	Montserrat	Lesser Antilles	2	Trants Site	charcoal	charcoal/ charred material	Stripped Area	Beta-83047	1270	130	—	Petersen, Bartone, and Watters 1999:50-51
Montserrat	Montserrat	Lesser Antilles	2	Trants Site	charcoal	charcoal/ charred material	Stripped Area	Beta-83049	1730	100	—	Petersen, Bartone, and Watters 1999:50-51
Montserrat	Montserrat	Lesser Antilles	2	Trants Site	charcoal	charcoal/ charred material	Stripped Area	Beta-83050	2140	110	—	Petersen, Bartone, and Watters 1999:50-51
Montserrat	Montserrat	Lesser Antilles	2	Trants Site	charcoal	charcoal/ charred material	Stripped Area	Beta-83051	1540	120	—	Petersen, Bartone, and Watters 1999:50-51
Montserrat	Montserrat	Lesser Antilles	2	Trants Site	charcoal	charcoal/ charred material	Trench 1	Beta-83044	1650	130	—	Petersen, Bartone, and Watters 1999:50-51
Montserrat	Montserrat	Lesser Antilles	2	Trants Site	charcoal	charcoal/ charred material	Trench 1	Beta-83045	1950	90	—	Petersen, Bartone, and Watters 1999:50-51

Montserrat	Montserrat	Lesser Antilles	2	Trants Site	charcoal	charcoal/ charred material	Trench 1	Beta-83046	2050	80	—	Petersen, Bartone, and Watters 1999:50-51
Montserrat	Montserrat	Lesser Antilles	3	Trants Site	shell	marine shell	Trench 1	Beta-83052	1180	60	—	Petersen, Bartone, and Watters 1999:50-51
Montserrat	Montserrat	Lesser Antilles	3	Trants Site	shell	marine shell	Trench 1	Beta-83053	1280	80	—	Petersen, Bartone, and Watters 1999:50-51
Montserrat	Montserrat	Lesser Antilles	4	Trants Site	—	unknown	—	Beta-18489	2140	80	—	Rouse 1989:397; Haviser 1997:61
Montserrat	Montserrat	Lesser Antilles	4	Trants Site	—	unknown	—	Beta-18582	1620	90	—	Rouse 1989:397; Haviser 1997:61
Montserrat	Montserrat	Lesser Antilles	4	Trants Site	—	unknown	—	Beta-41678	1890	70	—	Haviser 1997:61
Montserrat	Montserrat	Lesser Antilles	4	Trants Site	—	unknown	—	Beta-41679	1750	80	—	Haviser 1997:61
Montserrat	Montserrat	Lesser Antilles	4	Trants Site	—	unknown	—	Beta-41680	1960	90	—	Haviser 1997:61
Montserrat	Montserrat	Lesser Antilles	4	Trants Site	—	unknown	—	Beta-41681	1740	90	—	Haviser 1997:61
Montserrat	Montserrat	Lesser Antilles	4	Trants Site	—	unknown	—	Beta-41682	2390	90	—	Haviser 1997:61
Montserrat	Montserrat	Lesser Antilles	4	Trants Site	—	unknown	—	Beta-44828	2480	80	—	Haviser 1997:61

Montserrat	Montserrat	Lesser Antilles	3	Upper Blakes	charcoal	charcoal/ charred material	Feature 206, 10 cmbs	Beta-451179	4170	30	-25.8	John Cherry personal communication
Montserrat	Montserrat	Lesser Antilles	3	Valentine Ghaut	charcoal	charcoal/ charred material	Midden Pit 3	Beta-326555	230	30	-26.5	John Cherry personal communication
Montserrat	Montserrat	Lesser Antilles	2	Valentine Ghaut	charcoal	charcoal/ charred material	Midden Pit 1	Beta-282299	980	40	-23.4	John Cherry personal communication
Montserrat	Montserrat	Lesser Antilles	2	Valentine Ghaut	charcoal	charcoal/ charred material	Midden Pit 1	Beta-282300	1070	40	-26.9	John Cherry personal communication
Montserrat	Montserrat	Lesser Antilles	2	Valentine Ghaut	charcoal	charcoal/ charred material	Midden Pit 1	Beta-282301	980	40	-25.6	John Cherry personal communication
Montserrat	Montserrat	Lesser Antilles	2	Valentine Ghaut	charcoal	charcoal/ charred material	Midden Pit 1	Beta-282302	1120	40	-27.9	John Cherry personal communication
Montserrat	Montserrat	Lesser Antilles	2	Valentine Ghaut	"faunal material" - bone collagen	faunal material	Surface of Midden Pit 1	Beta-277241	1010	40	-9.8	John Cherry personal communication
Montserrat	Montserrat	Lesser Antilles	2	Valentine Ghaut	"faunal material" - bone collagen	faunal material	Surface of Midden Pit 1	Beta-277242	880	40	-20.1	John Cherry personal communication

Montserrat	Montserrat	Lesser Antilles	3	Valentine Ghaut	charcoal	charcoal/ charred material	Midden Pit 4	Beta-350069	130	30	-22.8	John Cherry personal communication
Mustique	St. Vincent and the Grenadines	Lesser Antilles	3	Desal Plant	*Cittarium pica*	marine shell	Unit: 2, Layer: Pl. 8, cmbs: 70-80	UGa-12515	1810	20	+1.7	this publication
Mustique	St. Vincent and the Grenadines	Lesser Antilles	3	Desal Plant	*Cittarium pica*	marine shell	Unit: 2, Layer: Pl. 8, cmbs: 75	D-AMS 006289	1784	27	+1.6	this publication
Mustique	St. Vincent and the Grenadines	Lesser Antilles	3	Desal Plant	*Cittarium pica*	marine shell	Unit: 2, Layer: Pl. 9, cmbs: 80-90	UGa-12516	2120	20	+1.8	this publication
Mustique	St. Vincent and the Grenadines	Lesser Antilles	3	Desal Plant	charcoal	charcoal/ charred material	Unit: 2, Layer: Pl. 6, cmbs: 55	D-AMS 006801	40	23	-22.5	this publication
Mustique	St. Vincent and the Grenadines	Lesser Antilles	3	Desal Plant	*Cittarium pica*	marine shell	Unit: 2, Layer: Pl. 4, cmbs: 35	D-AMS 006288	2526	32	+7.2	this publication
Mustique	St. Vincent and the Grenadines	Lesser Antilles	3	Desal Plant	*Nerita tessellata*	marine shell	Unit: 2, Layer: Pl. 8, cmbs: 75	D-AMS 006798	3272	25	-3.5	this publication
Mustique	St. Vincent and the Grenadines	Lesser Antilles	2	Lagoon Bay	*Cittarium pica*	marine shell	Unit: 3, Layer: 4, cmbs: 90	Beta-302725	1540	50	+1.7	this publication
Mustique	St. Vincent and the Grenadines	Lesser Antilles	2	Lagoon Bay	*Cittarium pica*	marine shell	Unit: 6, Layer: Pl. 8, cmbs: 80	D-AMS 009264	2186	33	-9.6	this publication
Mustique	St. Vincent and the Grenadines	Lesser Antilles	2	Lagoon Bay	*Eustrombus gigas* (juvenile)	marine shell	Unit 2, Layer 3, 70-80 cmbs	Beta-286849	1370	50	+0.5	Fitzpatrick and Giovas 2011

Nevis	Federation of St. Kitts and Nevis	Lesser Antilles	2	Coconut Walk (JA-1)	*Donax denticulatus*	marine shell	Nev-11	D-AMS 007668	1541	33	-1.1	Jew et al. 2016
Nevis	Federation of St. Kitts and Nevis	Lesser Antilles	2	Coconut Walk (JA-1)	*Donax denticulatus*	marine shell	Nev-11	D-AMS 07667	1464	24	+5.7	Jew et al. 2016
Nevis	Federation of St. Kitts and Nevis	Lesser Antilles	2	Coconut Walk (JA-1)	*Cittarium pica*	marine shell	Unit: 2273, Square: 25, Planum: 3, Feature: L001, 20-30 cmbs	Beta-324951	570	30	+0.3	Giovas et al. 2013
Nevis	Federation of St. Kitts and Nevis	Lesser Antilles	2	Coconut Walk (JA-1)	*Eustrombus gigas* (juvenile)	marine shell	Unit: 2273, Square: 6, Planum: 1, Feature: Top, 0-10 cmbs	Beta-290340	1350	40	+1.8	Giovas et al. 2013
Nevis	Federation of St. Kitts and Nevis	Lesser Antilles	2	Coconut Walk (JA-1)	*Cittarium pica*	marine shell	Unit: 2273, Square: 8, Planum: 4, Feature: L003, 30-40 cmbs	Beta-290341	1420	40	+2.6	Giovas et al. 2013
Nevis	Federation of St. Kitts and Nevis	Lesser Antilles	2	Coconut Walk (JA-1)	*Cassis tuberosa*	marine shell	Unit: 2273, Square: 9, Planum: 4, Feature: L003, 30-40 cmbs	Beta-324952	720	30	+2.7	Giovas et al. 2013
Nevis	Federation of St. Kitts and Nevis	Lesser Antilles	3	Hichmans (GE-5)	charcoal	charcoal/ charred material	—	Beta-106769	1690	50	—	Wilson 2006:196-197

Nevis	Federation of St. Kitts and Nevis	Lesser Antilles	3	Hichmans (GE-5)	charcoal	charcoal/ charred material	—	Beta-106770	1620	60	—	Wilson 2006:196-197
Nevis	Federation of St. Kitts and Nevis	Lesser Antilles	3	Hichmans (GE-5)	charcoal	charcoal/ charred material	—	Beta-106771	1720	60	—	Wilson 2006:196-197
Nevis	Federation of St. Kitts and Nevis	Lesser Antilles	3	Hichmans (GE-5)	charcoal	charcoal/ charred material	—	Beta-106772	1900	60	—	Wilson 2006:196-197
Nevis	Federation of St. Kitts and Nevis	Lesser Antilles	3	Hichmans (GE-5)	charcoal	charcoal/ charred material	—	Beta-106773	1540	50	—	Wilson 2006:196-197
Nevis	Federation of St. Kitts and Nevis	Lesser Antilles	3	Hichmans (GE-5)	charcoal	charcoal/ charred material	—	Beta-106774	1580	60	—	Wilson 2006:196-197
Nevis	Federation of St. Kitts and Nevis	Lesser Antilles	3	Hichmans (GE-5)	charcoal	charcoal/ charred material	—	Beta-46944b	1160	60	—	Wilson 2006:196-197
Nevis	Federation of St. Kitts and Nevis	Lesser Antilles	3	Hichmans (GE-5)	shell	marine shell	—	Beta-19328	2490	60	—	Wilson 1989:435
Nevis	Federation of St. Kitts and Nevis	Lesser Antilles	3	Hichmans Shell Heap (GE-6)	shell	marine shell	—	Beta-63256	3110	60	—	Wilson 2006: 196-197
Nevis	Federation of St. Kitts and Nevis	Lesser Antilles	3	Indian Castle (GE-1)	charcoal	charcoal/ charred material	—	Beta-19327	670	60	—	Wilson 1989:436
Nevis	Federation of St. Kitts and Nevis	Lesser Antilles	2	Sulphur Ghaut (JO-2)	charcoal	charcoal/ charred material	Unit 3S, 104-114 cmbs	Beta-47807	1070	70	—	Wilson 2006: 56, 196-197
Nevis	Federation of St. Kitts and Nevis	Lesser Antilles	2	Sulphur Ghaut (JO-2)	charcoal	charcoal/ charred material	Unit 9N, 20-30 cmbs	Beta-46940	1060	50	—	Wilson 2006: 56, 196-197
Nevis	Federation of St. Kitts and Nevis	Lesser Antilles	2	Sulphur Ghaut (JO-2)	charcoal	charcoal/ charred material	Unit 9N, 50-60 cmbs	Beta-46944a	940	60	—	Wilson 2006: 56, 196-197
Nevis	Federation of St. Kitts and Nevis	Lesser Antilles	2	Sulphur Ghaut (JO-2)	charcoal	charcoal/ charred material	Unit 9N, 85-95 cmbs	Beta-46942	880	60	—	Wilson 2006: 56, 196-197

Nevis	Federation of St. Kitts and Nevis	Lesser Antilles	3	Sulphur Ghaut (JO-2)	shell	marine shell	Unit 10N, 20 cmbs	Beta-46941	920	60	—	Wilson 2006: 56, 196-197
Nevis	Federation of St. Kitts and Nevis	Lesser Antilles	3	Sulphur Ghaut (JO-2)	sediment	sediment	Unit 3N, 73-83 cmbs	Beta-47806	940	80	—	Wilson 2006: 56, 196-197
Pine Cay	Turks and Caicos	Bahamian Archipelago	3	PC-1	charcoal	charcoal/ charred material	—	Beta-70799	690	50	—	Carlson 1999
Providenciales	Turks and Caicos	Bahamian Archipelago	4	Blue Hills Settlement	*Carapa* sp.	wood	cave	OxA-21854	498	24	-24.2	Ostapkowicz 2015
Providenciales	Turks and Caicos	Bahamian Archipelago	4	Blue Hills Settlement	*Carapa* sp.	wood	cave	OxA-20843	475	27	-22.9	Ostapkowicz 2015
Providenciales	Turks and Caicos	Bahamian Archipelago	4	Blue Hills Settlement	*Carapa* sp.	wood	cave	OxA-21894	464	26	-25.9	Ostapkowicz 2015
Providenciales	Turks and Caicos	Bahamian Archipelago	3	P-1	charcoal	charcoal/ charred material	—	IGS-2632	660	70	—	Carlson 1999
Providenciales	Turks and Caicos	Bahamian Archipelago	3	P-4	shell	marine shell	—	Beta-70797	960	50	—	Carlson 1999
Providenciales	Turks and Caicos	Bahamian Archipelago	3	P-5	shell	marine shell	—	Beta-70798	1250	50	—	Carlson 1999
Providenciales	Turks and Caicos	Bahamian Archipelago	3	Palmetto Junction	charred material	charcoal/ charred material	—	Beta-384424	590	30	—	Sinelli, Personal Communication
Providenciales	Turks and Caicos	Bahamian Archipelago	3	Palmetto Junction	charred material	charcoal/ charred material	—	Beta-384425	660	30	—	Sinelli, Personal Communication
Providenciales	Turks and Caicos	Bahamian Archipelago	3	Palmetto Junction	charred material	charcoal/ charred material	—	Beta-384426	570	30	—	Sinelli, Personal Communication

Providenciales	Turks and Caicos	Bahamian Archipelago	3	Palmetto Junction	charred material	charcoal/ charred material	—	Beta-384427	460	30	—	Sinelli, Personal Communication
Providenciales	Turks and Caicos	Bahamian Archipelago	3	Palmetto Junction	charred material	charcoal/ charred material	—	Beta-384428	600	30	—	Sinelli, Personal Communication
Puerto Rico	Puerto Rico	Greater Antilles	1	AR-39	*Nesotrochis debooyi*	faunal material	Feature 3 (Norther area); EU 17, Level 3	Beta-221018	1340	40	-21.1	Carlson and Steadman 2009
Puerto Rico	Puerto Rico	Greater Antilles	1	Cag-3	*Nesophontes edithae* (mandible)	faunal material	grave infill	OxA-15141	990	24	-19.3	Turvey et al. 2007:195
Puerto Rico	Puerto Rico	Greater Antilles	1	Cag-3	*Heteropsomys insulans* (mandible)	faunal material	grave infill	OxA-15142	1219	26	-19.6	Turvey et al. 2007:195
Puerto Rico	Puerto Rico	Greater Antilles	2	Angostura	charcoal	charcoal/ charred material	Mound - B forest soil/first habitation surface (>99 cmbs)	GX-28807	3920	40	-27.5	Rivera-Collazo et al. 2015
Puerto Rico	Puerto Rico	Greater Antilles	2	Angostura	charcoal	charcoal/ charred material	Mound B - habitation surface (39-63 cmbs)	GX-28805	3700	30	-24.5	Rivera-Collazo et al. 2015
Puerto Rico	Puerto Rico	Greater Antilles	2	Angostura	charcoal	charcoal/ charred material	Mound B - midden, ca. 39-63 cmbs	GX-28809	3470	40	-28.5	Rivera-Collazo et al. 2015
Puerto Rico	Puerto Rico	Greater Antilles	2	Angostura	charcoal	charcoal/ charred material	Mound B - midden, ca. 7-39 cmbs	GX-28806	3570	40	-26.9	Rivera-Collazo et al. 2015
Puerto Rico	Puerto Rico	Greater Antilles	2	Angostura	charcoal	charcoal/ charred material	Mound B - midden, ca. 7-39 cmbs	GX-28808	3670	40	-28.8	Rivera-Collazo et al. 2015
Puerto Rico	Puerto Rico	Greater Antilles	2	Angostura	charcoal	charcoal/ charred material	Mound B - shell layer (63-99 cmbs)	GX-28814	3740	100	-27.0	Rivera-Collazo et al. 2015

Puerto Rico	Puerto Rico	Greater Antilles	2	Angostura	charred material	charcoal/ charred material	Mound C - midden/shell layer (12-14 cmbs)	Beta-294434	3680	40	-26.3	Rivera-Collazo et al. 2015
Puerto Rico	Puerto Rico	Greater Antilles	2	Angostura	charred material	charcoal/ charred material	Unit 3 - shell layer/anthrosol (74-80 cmbs)	Beta-294435	2120	30	-23.7	Rivera-Collazo et al. 2015
Puerto Rico	Puerto Rico	Greater Antilles	3	Angostura	shell	marine shell	Mound B - forest soil/first habitation surface (>99 cmbs)	GX-28812	4120	80	—	Rivera-Collazo et al. 2015
Puerto Rico	Puerto Rico	Greater Antilles	3	Angostura	shell	marine shell	Mound B - shell layer (63-99 cmbs)	GX-28810	3980	80	—	Rivera-Collazo et al. 2015
Puerto Rico	Puerto Rico	Greater Antilles	4	Angostura	charred material	charcoal/ charred material	Offsite core 3, Unit 8b, 440 cmbs	Beta-297766	660	30	—	Rivera-Collazo et al. 2015
Puerto Rico	Puerto Rico	Greater Antilles	4	Angostura	plant material	plant material	Offsite Core 2, 538 cmbs	Beta-294440	3740	30	-28.1	Rivera-Collazo et al. 2015
Puerto Rico	Puerto Rico	Greater Antilles	4	Angostura	plant material	plant material	Offsite core 3, 353 cmbs	Beta-294438	840	30	-28.1	Rivera-Collazo et al. 2015
Puerto Rico	Puerto Rico	Greater Antilles	4	Angostura	organic sediment	sediment	Offsite core 4, 178 cmbs	Beta-294439	1890	30	-17.2	Rivera-Collazo et al. 2015
Puerto Rico	Puerto Rico	Greater Antilles	4	Angostura	wood	wood	Offsite core 1, Unit 7a, 280 cmbs	Beta-294437	1430	30	-26.8	Rivera-Collazo et al. 2015
Puerto Rico	Puerto Rico	Greater Antilles	3	Angostura	shell	marine shell	Mound B - shell layer (63-99 cmbs)	GX-28813	4010	70	—	Rivera-Collazo et al. 2015

Puerto Rico	Puerto Rico	Greater Antilles	3	Angostura	charcoal	charcoal/ charred material	Mound B - unknown	Beta-29778	5960	250	—	Rivera-Collazo et al. 2015
Puerto Rico	Puerto Rico	Greater Antilles	3	Angostura	shell	marine shell	Mound B -shell layer, ca. 63-99 cmbs	GX-28811	3830	90	—	Rivera-Collazo et al. 2015
Puerto Rico	Puerto Rico	Greater Antilles	2	AR-38	charcoal	charcoal/ charred material	Feature 131(post); Structure 3	Beta-223568	490	60	-24.6	Carlson and Steadman 2009
Puerto Rico	Puerto Rico	Greater Antilles	2	AR-38	human bone	human bone/teeth	Burial 1; Structure 3	Beta-220581	790	40	-19.6	Carlson and Steadman 2009
Puerto Rico	Puerto Rico	Greater Antilles	2	AR-38	human bone	human bone/teeth	Burial 4; Structure 6	Beta-220582	1010	40	-19.4	Carlson and Steadman 2009
Puerto Rico	Puerto Rico	Greater Antilles	2	AR-39	charcoal	charcoal/ charred material	Feature 200; EU 18, Level 1	Beta-223566	1460	60	-25.4	Carlson and Steadman 2009
Puerto Rico	Puerto Rico	Greater Antilles	2	AR-39	charcoal	charcoal/ charred material	Feature 200; EU 18, Level 3	Beta-225064	1220	40	-25.1	Carlson and Steadman 2009
Puerto Rico	Puerto Rico	Greater Antilles	2	AR-39	charcoal	charcoal/ charred material	Feature 3 (Northern area); EU 16, Level1	Beta-223565	1370	40	-25.1	Carlson and Steadman 2009
Puerto Rico	Puerto Rico	Greater Antilles	2	AR-39	charcoal	charcoal/ charred material	Feature 3 (Southern area); EU 4, Level 1	Beta-223977	1430	70	-27.0	Carlson and Steadman 2009
Puerto Rico	Puerto Rico	Greater Antilles	2	AR-39	human bone	human bone/teeth	Feature 3 (Southern area); EU 12, Level 4	Beta-222869	1630	40	-19.0	Carlson and Steadman 2009

Puerto Rico	Puerto Rico	Greater Antilles	4	Batey Yagüez	—	unknown	Unit S41/W4, Feat 5 (postmold), 62-75 cmbs	GrN-30061	790	30	-27.67	Oliver personal communication 2018
Puerto Rico	Puerto Rico	Greater Antilles	2	Bateyes de Vivi	charcoal	charcoal/ charred material	Site U-1 Unit B1 Lev 6, 47-49cm	GrN-30058	710	40	-27.60	Oliver and Rivera Fontan 2007
Puerto Rico	Puerto Rico	Greater Antilles	2	Bateyes de Vivi	charcoal	charcoal/ charred material	Site U-1, Feat 4-2 116 cm	GrN-30057	610	50	-26.25	Oliver and Rivera Fontan 2007
Puerto Rico	Puerto Rico	Greater Antilles	2	Bateyes de Vivi	charcoal	charcoal/ charred material	Site U-1, Feat 4-2, 102-116 cm	GrN-30056	600	50	-26.42	Oliver and Rivera Fontan 2007
Puerto Rico	Puerto Rico	Greater Antilles	2	Bateyes de Vivi	charcoal	charcoal/ charred material	Site U-1, Unit 4 Feat 4-2, 74 cm	GrN-30055	510	30	-25.97	Oliver and Rivera Fontan 2007
Puerto Rico	Puerto Rico	Greater Antilles	2	Bateyes de Vivi	charcoal	charcoal/ charred material	Site U-1, Unit 4: 43-51cm Stratum II	GrN-30053	630	40	-24.53	Oliver and Rivera Fontan 2007
Puerto Rico	Puerto Rico	Greater Antilles	2	Bateyes de Vivi	charcoal	charcoal/ charred material	Site U-1, Unit 4: 53-71cm Stratum III	GrN-30054	410	40	-25.43	Oliver and Rivera Fontan 2007
Puerto Rico	Puerto Rico	Greater Antilles	4	Caño Hondo	—	unknown	Stratum I	UGa-995	3010	70	—	Figueredo 1976:250; Rouse and Alegria 1990:25
Puerto Rico	Puerto Rico	Greater Antilles	4	Caño Hondo	—	unknown	Stratum II	UGa-997	2705	70	—	Figueredo 1976:250; Rouse and Alegria 1990:25

Puerto Rico	Puerto Rico	Greater Antilles	4	Caño Hondo	—	unknown	Stratum III	UGa-996	2855	65	—	Figueredo 1976:250; Rouse and Alegria 1990:25
Puerto Rico	Puerto Rico	Greater Antilles	4	Cayo Cofresí	—	unknown	0.7	I-7424	2275	85	-24.7	Veloz Maggiolo 1975:91; Rouse and Alegria 1990:25
Puerto Rico	Puerto Rico	Greater Antilles	4	Cayo Cofresí	—	unknown	0.7	I-7425	2245	85	-24.4	Veloz Maggiolo 1975:91; Rouse and Alegria 1990:25
Puerto Rico	Puerto Rico	Greater Antilles	2	CE-34	charcoal	charcoal/ charred material	Unit 10, level 2	Beta-386615	1270	30	-24.2	Carlson et al. 2017
Puerto Rico	Puerto Rico	Greater Antilles	2	CE-34	charcoal	charcoal/ charred material	Unit 16, level 3	Beta-386073	1230	30	-23.8	Carlson et al. 2017
Puerto Rico	Puerto Rico	Greater Antilles	2	CE-34	charcoal	charcoal/ charred material	Unit 16, level 4	Beta-386074	1230	30	-25.7	Carlson et al. 2017
Puerto Rico	Puerto Rico	Greater Antilles	2	CE-34	charcoal	charcoal/ charred material	Unit 1, level 5	Beta-283565	1190	40	-25.4	Carlson et al. 2017
Puerto Rico	Puerto Rico	Greater Antilles	2	CE-34	charcoal	charcoal/ charred material	Unit 15, level 3	Beta-386072	720	30	-25.6	Carlson et al. 2017
Puerto Rico	Puerto Rico	Greater Antilles	2	CE-34	charcoal	charcoal/ charred material	Unit 7, level 3	Beta-386698	1120	30	-25.7	Carlson et al. 2017
Puerto Rico	Puerto Rico	Greater Antilles	2	CE-34	charcoal	charcoal/ charred material	Unit 14, level 3	Beta-386071	1260	30	-25.1	Carlson et al. 2017
Puerto Rico	Puerto Rico	Greater Antilles	2	CE-34	charcoal	charcoal/ charred material	Unit 7, level 4	Beta-386068	1260	30	-23.3	Carlson et al. 2017

Puerto Rico	Puerto Rico	Greater Antilles	2	Convento	charcoal	charcoal/ charred material	Church floor (1.45)	I-11297	1995	80	—	Rouse and Alegria 1990:55-56; Haviser 1997:63
Puerto Rico	Puerto Rico	Greater Antilles	2	Convento	charcoal	charcoal/ charred material	Church floor (1.50)	I-11296	2100	80	—	Rouse and Alegria 1990:55-56; Haviser 1997:63
Puerto Rico	Puerto Rico	Greater Antilles	2	Convento	charcoal	charcoal/ charred material	Interior patio	I-11266	1865	80	—	Rouse and Alegria 1990:55-56; Haviser 1997:63
Puerto Rico	Puerto Rico	Greater Antilles	3	Cueva del Abono	marine shell	marine shell	CA-1	UGM-30015	4780	30	0	Rodríguez-Ramos 2017
Puerto Rico	Puerto Rico	Greater Antilles	3	Cueva del Abono	black pigment	organic material	FP-8	UGM-30025	280	30	-31.9	Rodríguez-Ramos 2017
Puerto Rico	Puerto Rico	Greater Antilles	2	Cueva del Abono	black pigment	organic material	FP-7	UGM-30024	320	30	-29.6	Rodríguez-Ramos 2017
Puerto Rico	Puerto Rico	Greater Antilles	2	Cueva del Gemelos	black pigment	organic material	FP-10	UGM-30027	410	40	-26.8	Rodríguez-Ramos 2017
Puerto Rico	Puerto Rico	Greater Antilles	2	Cueva del Gemelos	black pigment	organic material	FP-12	UGM-30028	870	40	-30.1	Rodríguez-Ramos 2017
Puerto Rico	Puerto Rico	Greater Antilles	2	Cueva del Gemelos	black pigment	organic material	FP-9	UGM-30026	1230	65	-25.3	Rodríguez-Ramos 2017
Puerto Rico	Puerto Rico	Greater Antilles	2	Cueva de los Lagartos	black pigment	organic material	FP-14	UGM-30029	610	40	-28.5	Rodríguez-Ramos 2017

Puerto Rico	Puerto Rico	Greater Antilles	2	Cueva Lucero	black pigment	organic material	FP-24	UGM-30039	630	20	-27.7	Rodríguez-Ramos 2017
Puerto Rico	Puerto Rico	Greater Antilles	2	Cueva Lucero	black pigment	organic material	FP-27	UGM-30042	3140	40	-27.1	Rodríguez-Ramos 2017
Puerto Rico	Puerto Rico	Greater Antilles	2	Cueva Lucero	black pigment	organic material	FP-28	UGM-30043	630	50	-28.7	Rodríguez-Ramos 2017
Puerto Rico	Puerto Rico	Greater Antilles	2	Cueva Lucero	black pigment	organic material	FP-30	UGM-30045	730	35	-28.7	Rodríguez-Ramos 2017
Puerto Rico	Puerto Rico	Greater Antilles	2	Cueva Lucero	black pigment	organic material	FP-33	UGM-30048	310	35	-29.8	Rodríguez-Ramos 2017
Puerto Rico	Puerto Rico	Greater Antilles	2	Cueva Lucero	black pigment	organic material	FP-34	UGM-30049	400	35	-29.4	Rodríguez-Ramos 2017
Puerto Rico	Puerto Rico	Greater Antilles	2	Cueva Lucero	black pigment	organic material	FP-35	UGM-30050	380	30	-28.1	Rodríguez-Ramos 2017
Puerto Rico	Puerto Rico	Greater Antilles	3	Cueva Lucero	black pigment	organic material	FP-25	UGM-30040	220	30	-26.6	Rodríguez-Ramos 2017
Puerto Rico	Puerto Rico	Greater Antilles	3	Cueva Lucero	black pigment	organic material	FP-26	UGM-30041	110	30	-29.8	Rodríguez-Ramos 2017
Puerto Rico	Puerto Rico	Greater Antilles	4	Cueva Lucero	black pigment	organic material	FP-29	UGM-30044	modern	—	-32.4	Rodríguez-Ramos 2017
Puerto Rico	Puerto Rico	Greater Antilles	4	Cueva Lucero	black pigment	organic material	FP-31	UGM-30046	modern	—	-29.8	Rodríguez-Ramos 2017
Puerto Rico	Puerto Rico	Greater Antilles	4	Cueva Lucero	black pigment	organic material	FP-32	UGM-30047	modern	—	-31.6	Rodríguez-Ramos 2017
Puerto Rico	Puerto Rico	Greater Antilles	4	Cueva María de la Cruz	—	unknown	Pit A, 60-89 cm	Beta-41051	2220	70	—	Oliver and Rivera Collazo 2015

Puerto Rico	Puerto Rico	Greater Antilles	1	Cueva María de la Cruz	Sapotaceae seed	plant material	Unit 102: 95-113 cm BD	Beta-347456	1910	30	-22.7	Oliver and Rivera Collazo 2015
Puerto Rico	Puerto Rico	Greater Antilles	3	Cueva Matos	marine shell	marine shell	CM-1	UGM-30016	3200	30	-7.1	Rodríguez-Ramos 2017
Puerto Rico	Puerto Rico	Greater Antilles	2	Cueva Matos	black pigment	organic material	FP-1	UGM-30018	410	25	-31.0	Rodríguez-Ramos 2017
Puerto Rico	Puerto Rico	Greater Antilles	2	Cueva Matos	black pigment	organic material	FP-2	UGM-30019	640	45	-28.3	Rodríguez-Ramos 2017
Puerto Rico	Puerto Rico	Greater Antilles	2	Cueva Matos	black pigment	organic material	FP-3	UGM-30020	330	30	-31.8	Rodríguez-Ramos 2017
Puerto Rico	Puerto Rico	Greater Antilles	2	Cueva Matos	black pigment	organic material	FP-4	UGM-30021	580	40	-28.2	Rodríguez-Ramos 2017
Puerto Rico	Puerto Rico	Greater Antilles	2	Cueva Negra	charcoal	charcoal/ charred material	flowstone ledge (east side of chamber)	Beta-86999	380	60	-29.6	Frank 1998:101
Puerto Rico	Puerto Rico	Greater Antilles	4	Cueva del Perro	charcoal	charcoal/ charred material	0-2 cm interval	OxA-15129	3512	28	-27.3	Turvey et al. 2007:195
Puerto Rico	Puerto Rico	Greater Antilles	4	Cueva del Perro	charcoal	charcoal/ charred material	Combined, 0-4 cm	OxA-15132	2407	28	-26.8	Turvey et al. 2007:195
Puerto Rico	Puerto Rico	Greater Antilles	3	Cueva Soto	black pigment	organic material	FP-15	UGM-30030	moder n	—	-34.7	Rodríguez-Ramos 2017
Puerto Rico	Puerto Rico	Greater Antilles	2	Cueva Soto	black pigment	organic material	FP-16	UGM-30031	2910	50	-26.1	Rodríguez-Ramos 2017
Puerto Rico	Puerto Rico	Greater Antilles	2	Cueva Soto	black pigment	organic material	FP-5	UGM-30022	480	30	-34.5	Rodríguez-Ramos 2017
Puerto Rico	Puerto Rico	Greater Antilles	2	Cueva Soto	black pigment	organic material	FP-6	UGM-30023	1030	20	-31.3	Rodríguez-Ramos 2017

Puerto Rico	Puerto Rico	Greater Antilles	3	Cueva Tembladera	marine shell	marine shell	CT-1	UGM-30017	4160	30	-4.8	Rodríguez-Ramos 2017
Puerto Rico	Puerto Rico	Greater Antilles	3	Cueva Ventana	charcoal	charcoal/ charred material	Unit A, Stratum B-2	UGM-5109	100	20	-28.3	Rodríguez-Ramos 2014
Puerto Rico	Puerto Rico	Greater Antilles	3	Cueva Ventana	charcoal	charcoal/ charred material	Unit A, Stratum C-3	UGM-17563	140	20	-26.7	Rodríguez-Ramos 2014
Puerto Rico	Puerto Rico	Greater Antilles	2	Cueva Ventana	charcoal	charcoal/ charred material	Unit C, Stratum C-4	UGM-17565	3810	25	-12	Rodríguez-Ramos 2014
Puerto Rico	Puerto Rico	Greater Antilles	2	Cueva Ventana	charcoal	charcoal/ charred material	Unit C, Stratum C-6	UGM-5106	3740	30	-13.4	Rodríguez-Ramos 2014
Puerto Rico	Puerto Rico	Greater Antilles	2	Cueva Ventana	*Nerita* sp.	marine shell	Unit A, Stratum B-2	UGM-5105	3170	30	-8.1	Rodríguez-Ramos 2014
Puerto Rico	Puerto Rico	Greater Antilles	2	Cueva Ventana	*Nerita* sp.	marine shell	Unit A, Stratum B-3	UGM-17561	3640	25	-8.5	Rodríguez-Ramos 2014
Puerto Rico	Puerto Rico	Greater Antilles	2	Cueva Ventana	*Nerita* sp.	marine shell	Unit A, Stratum C-1	UGM-17562	3630	25	-7.0	Rodríguez-Ramos 2014
Puerto Rico	Puerto Rico	Greater Antilles	2	Cueva Ventana	*Nerita* sp.	marine shell	Unit B, Stratum C-1	UGM-5108	3740	30	-8.3	Rodríguez-Ramos 2014
Puerto Rico	Puerto Rico	Greater Antilles	2	Cueva Ventana	*Nerita* sp.	marine shell	Unit B, Stratum C-3	UGM-5107	3520	30	-7.3	Rodríguez-Ramos 2014
Puerto Rico	Puerto Rico	Greater Antilles	2	Cueva Ventana	*Nerita* sp.	marine shell	Unit C, Stratum C-1	UGM-17564	3120	20	-7.1	Rodríguez-Ramos 2014
Puerto Rico	Puerto Rico	Greater Antilles	2	Cueva Ventana	*Phaecoides* sp.	marine shell	Unit C, Stratum D-2	UGM-17566	4250	25	-4.1	Rodríguez-Ramos 2014
Puerto Rico	Puerto Rico	Greater Antilles	3	Cueva Ventana Int.	black pigment	organic material	FP-17	UGM-30032	300	20	-26.4	Rodríguez-Ramos 2017

Puerto Rico	Puerto Rico	Greater Antilles	2	Cueva Ventana Int.	black pigment	organic material	FP-18	UGM-30033	2390	35	-29.5	Rodríguez-Ramos 2017
Puerto Rico	Puerto Rico	Greater Antilles	2	Cueva Ventana Int.	black pigment	organic material	FP-19	UGM-30034	1050	30	-29.1	Rodríguez-Ramos 2017
Puerto Rico	Puerto Rico	Greater Antilles	2	Cueva Ventana Int.	black pigment	organic material	FP-20	UGM-30035	1440	30	-26.6	Rodríguez-Ramos 2017
Puerto Rico	Puerto Rico	Greater Antilles	2	Cueva Ventana Int.	black pigment	organic material	FP-21	UGM-30036	1050	80	-25.5	Rodríguez-Ramos 2017
Puerto Rico	Puerto Rico	Greater Antilles	2	Cueva Ventana Int.	black pigment	organic material	FP-22	UGM-30037	1280	30	-27.5	Rodríguez-Ramos 2017
Puerto Rico	Puerto Rico	Greater Antilles	3	Cueva Ventana Int.	black pigment	organic material	FP-23	UGM-30098	190	30	-28.1	Rodríguez-Ramos 2017
Puerto Rico	Puerto Rico	Greater Antilles	2	Finca de Dona Rosa (Utu-44)	wood charcoal	charcoal/ charred material	Unit N999-990, 99.03 masl	GrN-24760	600	40	-27.20	Oliver and Narganes Storde 2003
Puerto Rico	Puerto Rico	Greater Antilles	2	Finca de Dona Rosa (Utu-44)	wood charcoal	charcoal/ charred material	Unit N999-W988, 98.5 masl	GrN-24758	680	50	-26.61	Oliver and Narganes Storde 2003
Puerto Rico	Puerto Rico	Greater Antilles	2	Finca de Dona Rosa (Utu-44)	wood charcoal Sapotacea cf. *Manikara* sp.	charcoal/ charred material	Unit N999-W988, 98.63 masl	GrN-24757	760	70	-26.7	Oliver and Narganes Storde 2003
Puerto Rico	Puerto Rico	Greater Antilles	2	Finca de Dona Rosa (Utu-44)	wood charcoal	charcoal/ charred material	Unit N999-W990, 98.71 masl	GrN24762	880	40	-29.11	Oliver and Narganes Storde 2003
Puerto Rico	Puerto Rico	Greater Antilles	2	Finca de Dona Rosa (Utu-44)	wood charcoal	charcoal/ charred material	Unit N999-W990, 98.71 masl	GrN-24763	860	40	-26.55	Oliver and Narganes Storde 2003

Puerto Rico	Puerto Rico	Greater Antilles	2	Finca de Dona Rosa (Utu-44)	wood charcoal (Sterculiaceae)	charcoal/ charred material	Unit N999-W991, 98.97 masl	GrN-24761	900	60	-25.58	Oliver and Narganes Storde 2003
Puerto Rico	Puerto Rico	Greater Antilles	2	Finca de Dona Rosa (Utu-44)	Moraceae cf. *Cercopia* sp.	charcoal/ charred material	Unit N999-W991, 99.08 masl	GrN-24759	970	30	-26.03	Oliver and Narganes Storde 2003
Puerto Rico	Puerto Rico	Greater Antilles	2	Hacienda Grande	charcoal	charcoal/ charred material	Section D (0.50-0.75)	Y-1232	1580	80	—	Rouse and Alegria 1990:55-56; Haviser 1997:63
Puerto Rico	Puerto Rico	Greater Antilles	2	Hacienda Grande	charcoal	charcoal/ charred material	Section D (1.25-1.50)	Y-1233	1830	80	—	Rouse 1963; Bullen and Bullen 1972:152; Rouse and Alegria 1990:55-56; Haviser 1997:63
Puerto Rico	Puerto Rico	Greater Antilles	2	Hacienda Grande	charred seeds	charcoal/ charred material	W127, S55 (30-40)	Beta-9970	2060	70	—	Rouse and Alegria 1990:55; 57
Puerto Rico	Puerto Rico	Greater Antilles	2	Hacienda Grande	charred seeds	charcoal/ charred material	W128, S55 (40-50)	Beta-9972	1840	50	—	Rouse and Alegria 1990:55; 57 Haviser 1997:63
Puerto Rico	Puerto Rico	Greater Antilles	2	Hacienda Grande	charred seeds	charcoal/ charred material	W129, S55 (40-50)	Beta-9971	1320	70	—	Rouse and Alegria 1990:55, 57

Puerto Rico	Puerto Rico	Greater Antilles	3	Hacienda Luisa Josefa	shell	marine shell	deposit 1, Unit S-1	I-10554	515	75	—	Narganes Storde 2005:280-281
Puerto Rico	Puerto Rico	Greater Antilles	3	Hacienda Luisa Josefa	shell	marine shell	deposit 1, Unit S-1	I-10555	785	80	—	Narganes Storde 2005:280-281
Puerto Rico	Puerto Rico	Greater Antilles	3	Hacienda Luisa Josefa	shell	marine shell	deposit 1, Unit S-1	I-10556	670	80	—	Narganes Storde 2005:280-281
Puerto Rico	Puerto Rico	Greater Antilles	3	Juan Miguel Cave	charcoal	charcoal/ charred material	Unit N52/W50, Feature 4	GrA-18767	65	45	-27.82	Oliver personal communication 2018
Puerto Rico	Puerto Rico	Greater Antilles	3	Juan Miguel Cave	wood charcoal	charcoal/ charred material	Unit N52-W50: F4, 31 cmbs	GrA-187657	65	45	—	Oliver and Narganes Storde 2003
Puerto Rico	Puerto Rico	Greater Antilles	2	Juan Miguel Cave	charcoal	charcoal/ charred material	Unit N51-W50: F4, 57cmbs	GrN-16414	790	50	—	Oliver and Narganes Storde 2003
Puerto Rico	Puerto Rico	Greater Antilles	2	Juan Miguel Cave	wood charcoal	charcoal/ charred material	Unit N51-W55: F7, 29.5cmbs	GrN-24769	1140	40	-27.83	Oliver and Narganes Storde 2003
Puerto Rico	Puerto Rico	Greater Antilles	2	Juan Miguel Cave	wood charcoal	charcoal/ charred material	Unit N51-W55: S11, 12 cmbs	GrN-24768	990	40	-26.45	Oliver and Narganes Storde 2003
Puerto Rico	Puerto Rico	Greater Antilles	2	Juan Miguel Cave	wood charcoal	charcoal/ charred material	Unit N52-W52: F11, 44cmbs, base of conical feature	GrN-24770	420	30	-27.07	Oliver and Narganes Storde 2003
Puerto Rico	Puerto Rico	Greater Antilles	2	Juan Miguel Cave	wood charcoal	charcoal/ charred material	Unit N52-W54: F7, 22cmbs	GrN-24767	1180	40	-26.83	Oliver and Narganes Storde 2003

Puerto Rico	Puerto Rico	Greater Antilles	2	Juan Miguel Cave	*Montezuma* sp.	faunal material	Unit N51-W54: F6, 17cmbs	GrN-24764	1060	40	-26.90	Oliver and Narganes Storde 2003
Puerto Rico	Puerto Rico	Greater Antilles	2	Juan Miguel Cave	Rutaceae (*Amyris*?)	wood	Unit N51-W54: F6, 17cmbs	GrN-24766	890	30	-27.34	Oliver and Narganes Storde 2003
Puerto Rico	Puerto Rico	Greater Antilles	2	Juan Miguel Cave	*Psidium* sp.	wood	Unit N51-W54; S1b, 10cmbs	GrN-24765	680	40	-27.06	Oliver and Narganes Storde 2003
Puerto Rico	Puerto Rico	Greater Antilles	4	Juan Miguel Cave	—	unknown	Feature 4, 57 cmbs	GrN-26414	790	50	-24.29	Oliver personal communication 2018
Puerto Rico	Puerto Rico	Greater Antilles	2	Los Muertos Cave	charcoal	charcoal/ charred material	Test Unit 1, Lev. 4, stratum 3a - base	GrN-30059	1200	40	-27.93	Oliver personal communication 2018
Puerto Rico	Puerto Rico	Greater Antilles	3	Los Muertos Cave	charcoal	charcoal/ charred material	Test Unit 1, Lev. 3, stratum 3a - middle	GrN-30060	930	40	-27.67	Oliver personal communication 2018
Puerto Rico	Puerto Rico	Greater Antilles	2	Maisabel	carbon	charcoal/ charred material	Burial 22, Cemetery	Beta-17637	1580	120	—	Siegel 1996:325
Puerto Rico	Puerto Rico	Greater Antilles	2	Maisabel	carbon	charcoal/ charred material	House, N342W12, F101, 30-40 cmbs (ditch feature)	Beta-17632	1070	70	—	Siegel 1989:218, 1996:325
Puerto Rico	Puerto Rico	Greater Antilles	2	Maisabel	carbon	charcoal/ charred material	House, N36W10, F95, 50-60 cmbs (earthoven feature)	Beta-17638	1260	60	—	Siegel 1989:221, 1996:325
Puerto Rico	Puerto Rico	Greater Antilles	2	Maisabel	carbon	charcoal/ charred material	House, N36W10, F95, 60-70 cmbs	Beta-17639	1150	70	—	Siegel 1989:218, 1996:325
Puerto Rico	Puerto Rico	Greater Antilles	2	Maisabel	carbon	charcoal/ charred material	House, N36W10, F95, 70-80 cmbs	Beta-17640	1300	70	—	Siegel 1989:221, 1996:325

Puerto Rico	Puerto Rico	Greater Antilles	2	Maisabel	carbon	charcoal/ charred material	House, N36W10, F95, 80-90 cmbs	Beta-17641	1440	70	—	Siegel 1989:221, 1996:325
Puerto Rico	Puerto Rico	Greater Antilles	2	Maisabel	carbon	charcoal/ charred material	House, N36W12, 20-30 cmbs	Beta-15007	1040	50	—	Siegel 1989:218, 1996:325
Puerto Rico	Puerto Rico	Greater Antilles	2	Maisabel	carbon	charcoal/ charred material	House, N40W10, 30-40 (Below Burial 18)	Beta-17631	1530	90	—	Siegel 1989:221, 1996:325
Puerto Rico	Puerto Rico	Greater Antilles	2	Maisabel	carbon	charcoal/ charred material	House, N40W10, F105, 60-70 cmbs	Beta-17633	1310	60	—	Siegel 1989:221, 1996:325
Puerto Rico	Puerto Rico	Greater Antilles	2	Maisabel	carbon	charcoal/ charred material	House, N43W8, F117, 40-50 cmbs	Beta-17636	1160	70	—	Siegel 1989:218, 1996:325
Puerto Rico	Puerto Rico	Greater Antilles	2	Maisabel	carbon	charcoal/ charred material	House, N4W38, F117, 30-40 cmbs (hearth feature)	Beta-17635	1360	70	—	Siegel 1989:221, 1996:325
Puerto Rico	Puerto Rico	Greater Antilles	2	Maisabel	carbon	charcoal/ charred material	HouseN40W10, F105, 80-90 cmbs (hearth feature)	Beta-17634	1140	60	—	Siegel 1989:218, 1996:325
Puerto Rico	Puerto Rico	Greater Antilles	2	Maisabel	charred material	charcoal/ charred material	Lm-2, 107-109 cm	Beta-127523	1240	40	—	Siegel et al. 2005
Puerto Rico	Puerto Rico	Greater Antilles	2	Maisabel	carbon	charcoal/ charred material	Mounded Midden 1, N100W13 100-110 cmbs	Beta-14381	1960	90	—	Siegel 1989:221, 1996:325; Rouse and Alegria 1990:55; Haviser 1997:63
Puerto Rico	Puerto Rico	Greater Antilles	2	Maisabel	carbon	charcoal/ charred material	Mounded Midden 1, N100W13, 150-160	I-14744	2270	80	—	Siegel 1996:325

Puerto Rico	Puerto Rico	Greater Antilles	2	Maisabel	carbon	charcoal/ charred material	Mounded Midden 1, N102, W14 (50-60)	Beta-14992	1660	100	—	Siegel 1989:221, 1996:325; Rouse and Alegria 1990:55; Haviser 1997:63
Puerto Rico	Puerto Rico	Greater Antilles	2	Maisabel	carbon	charcoal/ charred material	Mounded Midden 1, N102W14, 60-70 cmbs	Beta-14994	1520	50	—	Siegel 1989:221, 1996:325; Rouse and Alegria 1990:55; Haviser 1997:63
Puerto Rico	Puerto Rico	Greater Antilles	2	Maisabel	carbon	charcoal/ charred material	Mounded Midden 1, N106W11, 0-20 cmbs	Beta-14993	1810	60	—	Siegel 1989:221, 1996:325
Puerto Rico	Puerto Rico	Greater Antilles	2	Maisabel	carbon	charcoal/ charred material	Mounded Midden 1, N90W13 40-50 cmbs	Beta-14997	1810	70	—	Siegel 1989:221, 1996:325; Rouse and Alegria 1990:55; Haviser 1997:63
Puerto Rico	Puerto Rico	Greater Antilles	2	Maisabel	carbon	charcoal/ charred material	Mounded Midden 1, N90W13, 150-160 cmbs	I-14745	3340	90	—	Siegel 1996:325
Puerto Rico	Puerto Rico	Greater Antilles	2	Maisabel	carbon	charcoal/ charred material	Mounded Midden 1, N98W13 140-150 cmbs	Beta-14380	2060	60	—	Siegel 1989:221, 1996:325; Rouse and Alegria 1990:55; Haviser 1997:63

Puerto Rico	Puerto Rico	Greater Antilles	2	Maisabel	carbon	charcoal/ charred material	Mounded Midden 2, N2W7, 20-30 cmbs	Beta-15001	340	50	—	Siegel 1996:325
Puerto Rico	Puerto Rico	Greater Antilles	2	Maisabel	carbon	charcoal/ charred material	Mounded Midden 2, N2W7, Area A, 60-70 cmbs	I-14746	1180	80	—	Siegel 1996:325
Puerto Rico	Puerto Rico	Greater Antilles	2	Maisabel	carbon	charcoal/ charred material	Mounded Midden 2, N2W7, Area A, 70-80 cmbs	Beta-15003	1370	60	—	Siegel 1996:325
Puerto Rico	Puerto Rico	Greater Antilles	2	Maisabel	carbon	charcoal/ charred material	Mounded Midden 2, N2W7, Area A, 70-80 cmbs	I-14747	1080	80	—	Siegel 1996:325
Puerto Rico	Puerto Rico	Greater Antilles	2	Maisabel	carbon	charcoal/ charred material	Mounded Midden 2, N2W7, F38, 74-79 cmbs	I-14748	1240	80	—	Siegel 1996:325
Puerto Rico	Puerto Rico	Greater Antilles	2	Maisabel	carbon	charcoal/ charred material	Mounded Midden 2, N2W9, 90-100 cmbs	Beta-15006	1130	60	—	Siegel 1996:325
Puerto Rico	Puerto Rico	Greater Antilles	2	Maisabel	carbon	charcoal/ charred material	Mounded Midden 2, N2W9, 90-100 cmbs	I-14749	1160	80	—	Siegel 1996:325
Puerto Rico	Puerto Rico	Greater Antilles	2	Maisabel	carbon	charcoal/ charred material	Mounded Midden 2, S36W18, 30-40 cmbs	AA-4115	1295	45	—	Siegel 1996:325
Puerto Rico	Puerto Rico	Greater Antilles	2	Maisabel	carbon	charcoal/ charred material	Mounded Midden 2, S38W18, Area A, 30-40 cmbs	AA-4114	1315	45	—	Siegel 1996:325
Puerto Rico	Puerto Rico	Greater Antilles	2	Maisabel	collagen	human bone/teeth	Burial 1, Cemetery, N52E100, 50-70 cmbs	AA-6805	1525	55	-18.3	Siegel 1996:324-325
Puerto Rico	Puerto Rico	Greater Antilles	2	Maisabel	collagen	human bone/teeth	Burial 10, Cemetery, N84E72, 26-43	AA-4100	1515	50	-21.5	Siegel 1996:324-325
Puerto Rico	Puerto Rico	Greater Antilles	2	Maisabel	collagen	human bone/teeth	Burial 14, Cemetery, N90E42, 100-122 cmbs	AA-6809	1600	55	-13.0	Siegel 1996:324-325

Puerto Rico	Puerto Rico	Greater Antilles	2	Maisabel	collagen	human bone/teeth	Burial 16, Cemetery, N90E42, 60-73 cmbs	AA-4103	1335	45	-17.8	Siegel 1996:324-325
Puerto Rico	Puerto Rico	Greater Antilles	3	Maisabel	carbon	charcoal/ charred material	Mounded Midden 2, N2W25, F28, 60-70 cmbs	Beta-14387	240	70	—	Siegel 1996:325
Puerto Rico	Puerto Rico	Greater Antilles	3	Maisabel	carbon	charcoal/ charred material	Mounded Midden 2, N2W27, 30-40 cmbs	Beta-14389	250	80	—	Siegel 1996:325
Puerto Rico	Puerto Rico	Greater Antilles	3	Maisabel	human bone	human bone/teeth	Burial 2, Cemetery, N52E100, 76-93 cmbs	Beta-15886	1325	100	—	Siegel 1996:324-325
Puerto Rico	Puerto Rico	Greater Antilles	2	Maisabel	collagen	human bone/teeth	Burial 17, Cemetery, N84E72, 50-70 cmbs	AA-6810	1295	60	-16.4	Siegel 1996:324-325
Puerto Rico	Puerto Rico	Greater Antilles	2	Maisabel	collagen	human bone/teeth	Burial 18, House Area, N40W10, 20-34 cmbs	AA-4104	1195	45	-21.9	Siegel 1996:325
Puerto Rico	Puerto Rico	Greater Antilles	2	Maisabel	collagen	human bone/teeth	Burial 20, Cemetery, N84E72, 41-54 cmbs	AA-4106	1045	45	-21.0	Siegel 1996:324-325
Puerto Rico	Puerto Rico	Greater Antilles	2	Maisabel	collagen	human bone/teeth	Burial 21, Cemetery, N84E72, 47-58 cmbs	AA-4107	1360	50	-20.8	Siegel 1996:324-325

Puerto Rico	Puerto Rico	Greater Antilles	2	Maisabel	collagen	human bone/teeth	Burial 22, Cemetery, N84E72, 53-62 cmbs	AA-6811	1180	85	—	Siegel 1996:324-325
Puerto Rico	Puerto Rico	Greater Antilles	2	Maisabel	collagen	human bone/teeth	Burial 23, House Area, N42E20, Ext. 1, 46-63 cmbs	AA-4108	1025	55	-24.1	Siegel 1996:325
Puerto Rico	Puerto Rico	Greater Antilles	2	Maisabel	collagen	human bone/teeth	Burial 25, House Area, N42W21, 26-36 cmbs	AA-4109	1335	45	-19.2	Siegel 1996:325
Puerto Rico	Puerto Rico	Greater Antilles	2	Maisabel	collagen	human bone/teeth	Burial 27, House Area, N35W21, 23-34	AA-4110	1405	50	-21.9	Siegel 1996:325
Puerto Rico	Puerto Rico	Greater Antilles	2	Maisabel	collagen	human bone/teeth	Burial 29, House Area, N31W23, 22-30 cmbs	AA-4111	1110	50	-21.3	Siegel 1996:325
Puerto Rico	Puerto Rico	Greater Antilles	2	Maisabel	collagen	human bone/teeth	Burial 3, Cemetery, N32E32, 40-50 cmbs	AA-4096	1140	45	-18.9	Siegel 1996:324-325
Puerto Rico	Puerto Rico	Greater Antilles	2	Maisabel	collagen	human bone/teeth	Burial 30, House Area, N4E50, 43-56 cmbs	AA-4112	1040	45	-19.0	Siegel 1996:325

Puerto Rico	Puerto Rico	Greater Antilles	2	Maisabel	collagen	human bone/teeth	Burial 31, House Area, N44E0, 50-55	AA-4113	1065	50	-19.4	Siegel 1996:325
Puerto Rico	Puerto Rico	Greater Antilles	2	Maisabel	collagen	human bone/teeth	Burial 4, Cemetery, N84E72, 28-48 cmbs	AA-6806	1145	55	-19.5	Siegel 1996:324-325
Puerto Rico	Puerto Rico	Greater Antilles	2	Maisabel	collagen	human bone/teeth	Burial 7, Cemetery, N84E72, 50-70 cmbs	AA-6807	1188	55	-18.6	Siegel 1996:324-325
Puerto Rico	Puerto Rico	Greater Antilles	2	Maisabel	collagen	human bone/teeth	Burial 8, House Area, N38W14, 24-35 cmbs	AA-4099	1045	45	-18.8	Siegel 1996:325
Puerto Rico	Puerto Rico	Greater Antilles	2	Maisabel	collagen	human bone/teeth	Cemetery	AA-4097	1330	45	-18.1	Siegel 1996:325
Puerto Rico	Puerto Rico	Greater Antilles	2	Maisabel	collagen	human bone/teeth	House Area	AA-6812	1080	55	-18.9	Siegel 1996:325
Puerto Rico	Puerto Rico	Greater Antilles	2	Maisabel	wood	wood	MAN-1, 203-205 cmbs	Beta-130450	2730	70	—	Siegel et al. 2005
Puerto Rico	Puerto Rico	Greater Antilles	2	Maisabel	wood	wood	MAN-1, 274-281 cmbs	Beta-130451	3640	70	—	Siegel et al. 2005
Puerto Rico	Puerto Rico	Greater Antilles	3	Maisabel	carbon	charcoal/ charred material	Mounded Midden 1, N100W13, 150-160 cmbs	Beta-14996	2300	80	—	Siegel 1989:221, 1996:325
Puerto Rico	Puerto Rico	Greater Antilles	3	Maisabel	carbon	charcoal/ charred material	Mounded Midden 1, N90W13, 150-160 cmbs	Beta-14998	2810	70	—	Siegel 1989:221, 1996:325
Puerto Rico	Puerto Rico	Greater Antilles	3	Maisabel	carbon	charcoal/ charred material	Mounded Midden 1, N90W13, 40-50 cmbs	Beta-14999	3370	60	—	Siegel 1989:221, 1996:325

Puerto Rico	Puerto Rico	Greater Antilles	4	Maisabel	carbon	charcoal/ charred material	Mounded Midden 1, N106W13, 100-110	Beta-15000	1190	90	—	Siegel 1989:221, 1996:325
Puerto Rico	Puerto Rico	Greater Antilles	4	Maisabel	collagen	human bone/teeth	Burial 11, Cemetery, N54E50, 49-65 cmbs	AA-6808	750	60	—	Siegel 1996:324-325
Puerto Rico	Puerto Rico	Greater Antilles	4	Maisabel	collagen	human bone/teeth	Burial 15, Cemetery, N90E42, 89-114 cmbs	AA-4102	1420	100	too small	Siegel 1996:324-325
Puerto Rico	Puerto Rico	Greater Antilles	4	Maisabel	collagen	human bone/teeth	Burial 19c, Cemetery, N54E50, 48-67 cmbs	AA-5031	995	80	—	Siegel 1996:325
Puerto Rico	Puerto Rico	Greater Antilles	4	Maisabel	collagen	human bone/teeth	Burial 19c, Cemetery, N54E50, 48-67 cmbs	AA-7030	580	50	-25.0	Siegel 1996:325
Puerto Rico	Puerto Rico	Greater Antilles	4	Maisabel	collagen	human bone/teeth	Burial 6, Cemetery, N90E42, 72-86 cmbs	AA-4098	1505	65	-19.0	Siegel 1996:324-325
Puerto Rico	Puerto Rico	Greater Antilles	4	Maisabel	collagen	human bone/teeth	Burial 9, Cemetery, N90E42	AA-5030	1145	75	—	Siegel 1996:325
Puerto Rico	Puerto Rico	Greater Antilles	4	Maisabel	collagen	human bone/teeth	Burial 9, Cemetery, N90E42	AA-7029	1280	50	-17.5	Siegel 1996:325
Puerto Rico	Puerto Rico	Greater Antilles	2	Maisabel	wood	wood	MAN-1, 385-394 cmbs	Beta-116372	3820	70	—	Siegel et al. 2005

Puerto Rico	Puerto Rico	Greater Antilles	4	Maisabel	peat	peat	LM-2, 141-146 cmbs	Beta-116369	1660	50	—	Siegel et al. 2005
Puerto Rico	Puerto Rico	Greater Antilles	4	Maisabel	peat	peat	LM-2, 160-165 cmbs	Beta-127524	2270	60	—	Siegel et al. 2005
Puerto Rico	Puerto Rico	Greater Antilles	4	Maisabel	peat	peat	LM-2, 200-205cmbs	Beta-116370	2560	50	—	Siegel et al. 2005
Puerto Rico	Puerto Rico	Greater Antilles	4	Maisabel	organic sediment	sediment	LM-2, 90-95cm	Beta-127522	710	40	—	Siegel et al. 2005
Puerto Rico	Puerto Rico	Greater Antilles	4	Maisabel	wood	wood	LM-2, 151 cmbs	Beta-127525	1450	40	—	Siegel et al. 2005
Puerto Rico	Puerto Rico	Greater Antilles	2	María de la Cruz	charcoal	charcoal/ charred material	Section A (0.125-0.25)	Y-1234	1910	100	—	Bullen and Sleight 1963:41; Rouse 1963; Rouse and Alegria 1990:25
Puerto Rico	Puerto Rico	Greater Antilles	2	María de la Cruz	charcoal	charcoal/ charred material	Section A (0.50-0.625)	Y-1235	1920	120	—	Bullen and Sleight 1963:41; 43; Rouse 1963; Rouse and Alegria 1990:25
Puerto Rico	Puerto Rico	Greater Antilles	4	Maruca	—	marine shell	—	Beta-69878	3080	90	-25.0	Pantel 1994
Puerto Rico	Puerto Rico	Greater Antilles	4	Maruca	—	marine shell	—	Beta-69879	3870	130	-25.0	Pantel 1994
Puerto Rico	Puerto Rico	Greater Antilles	4	Maruca	—	marine shell	—	Beta-70866	2960	110	-25.0	Pantel 1994
Puerto Rico	Puerto Rico	Greater Antilles	4	Maruca	—	marine shell	—	Beta-92890	2950	50	-25.3	Rodríguez Lopez 2004
Puerto Rico	Puerto Rico	Greater Antilles	4	Maruca	—	marine shell	—	Beta-92891	4160	50	-25.8	Rodríguez Lopez 2004

Puerto Rico	Puerto Rico	Greater Antilles	4	Maruca	—	unknown	—	Beta-92892	2870	60	-25.4	Rodríguez Lopez 2004
Puerto Rico	Puerto Rico	Greater Antilles	4	Maruca	—	unknown	—	Beta-92893	2650	60	-26.7	Rodríguez Lopez 2004
Puerto Rico	Puerto Rico	Greater Antilles	4	Maruca	—	marine shell	—	Beta-92894	2820	70	—	Rodríguez Lopez 2004
Puerto Rico	Puerto Rico	Greater Antilles	3	Playa Blanca	charcoal	charcoal/ charred material	—	Beta-31692	1190	90	—	Rodríguez López and Rivera 1991
Puerto Rico	Puerto Rico	Greater Antilles	3	Playa Blanca	*Strombus* sp.	marine shell	—	Beta-21694	450	70	—	Rivera and Rodríguez 1991
Puerto Rico	Puerto Rico	Greater Antilles	3	Playa Blanca	*Strombus* sp.	marine shell	—	Beta-31693	590	60	—	Rodríguez López and Rivera 1991
Puerto Rico	Puerto Rico	Greater Antilles	3	Playa Blanca	*Strombus* sp.	marine shell	—	Beta-31695	1150	70	—	Rodríguez López and Rivera 1991
Puerto Rico	Puerto Rico	Greater Antilles	2	Paso del Indio	charcoal	charcoal/ charred material	6N-18/13	Beta-81844	960	50	—	Walker 2005
Puerto Rico	Puerto Rico	Greater Antilles	2	Paso del Indio	charcoal	charcoal/ charred material	6N-18/13	Beta-81845	970	50	—	Walker 2005
Puerto Rico	Puerto Rico	Greater Antilles	2	Paso del Indio	charcoal	charcoal/ charred material	6N-18/21	Beta-178668	970	40	—	Walker 2005
Puerto Rico	Puerto Rico	Greater Antilles	2	Paso del Indio	charcoal	charcoal/ charred material	6S-17/37	Beta-178666	1450	40	—	Walker 2005
Puerto Rico	Puerto Rico	Greater Antilles	2	Paso del Indio	charcoal	charcoal/ charred material	6S-17/37	Beta-77174	940	60	—	Walker 2005
Puerto Rico	Puerto Rico	Greater Antilles	2	Paso del Indio	charcoal	charcoal/ charred material	unit 6N-13/10	Beta-178669	960	130	—	Walker 2005

Puerto Rico	Puerto Rico	Greater Antilles	2	Paso del Indio	charcoal	charcoal/ charred material	unit 6N-13/13	Beta-178660	1030	50	—	Walker 2005
Puerto Rico	Puerto Rico	Greater Antilles	2	Paso del Indio	charcoal	charcoal/ charred material	unit 6N-13/13	Beta-178670	1580	90	—	Walker 2005
Puerto Rico	Puerto Rico	Greater Antilles	2	Paso del Indio	charcoal	charcoal/ charred material	unit 6N-13/13	Beta-178674	1470	40	—	Walker 2005
Puerto Rico	Puerto Rico	Greater Antilles	2	Paso del Indio	charcoal	charcoal/ charred material	Unit 6N-13/17	Beta-178661	940	60	—	Walker 2005
Puerto Rico	Puerto Rico	Greater Antilles	2	Paso del Indio	charcoal	charcoal/ charred material	Unit 6N-13/17	Beta-178662	910	40	—	Walker 2005
Puerto Rico	Puerto Rico	Greater Antilles	2	Paso del Indio	charcoal	charcoal/ charred material	unit 6N-13/17	Beta-178663	1060	40	—	Walker 2005
Puerto Rico	Puerto Rico	Greater Antilles	2	Paso del Indio	charcoal	charcoal/ charred material	unit 6N-13/17	Beta-81848	1180	70	—	Walker 2005
Puerto Rico	Puerto Rico	Greater Antilles	2	Paso del Indio	charcoal	charcoal/ charred material	Unit 6N-13/21	Beta-178664	630	40	—	Walker 2005
Puerto Rico	Puerto Rico	Greater Antilles	2	Paso del Indio	charcoal	charcoal/ charred material	Unit 6N-13/21	Beta-81849	840	60	—	Walker 2005
Puerto Rico	Puerto Rico	Greater Antilles	2	Paso del Indio	charcoal	charcoal/ charred material	unit 6N-13/21	Beta-81850	1050	50	—	Walker 2005
Puerto Rico	Puerto Rico	Greater Antilles	2	Paso del Indio	charcoal	charcoal/ charred material	unit 6N-13/21	Beta-87601	1440	60	—	Walker 2005
Puerto Rico	Puerto Rico	Greater Antilles	2	Paso del Indio	charcoal	charcoal/ charred material	unit 6N-13/25	Beta-178665	950	60	—	Walker 2005
Puerto Rico	Puerto Rico	Greater Antilles	2	Paso del Indio	charcoal	charcoal/ charred material	unit 6N-18/10	Beta-81841	990	50	—	Walker 2005
Puerto Rico	Puerto Rico	Greater Antilles	2	Paso del Indio	charcoal	charcoal/ charred material	unit 6N-18/10	Beta-87600	910	60	—	Walker 2005
Puerto Rico	Puerto Rico	Greater Antilles	2	Paso del Indio	charcoal	charcoal/ charred material	unit 6N-18/13	Beta-81843	1060	60	—	Walker 2005

Puerto Rico	Puerto Rico	Greater Antilles	2	Paso del Indio	charcoal	charcoal/ charred material	unit 6N-18/13	Beta-81846	1080	60	—	Walker 2005
Puerto Rico	Puerto Rico	Greater Antilles	2	Paso del Indio	charcoal	charcoal/ charred material	unit 6N-18/21	Beta-178667	1230	60	—	Walker 2005
Puerto Rico	Puerto Rico	Greater Antilles	2	Paso del Indio	charcoal	charcoal/ charred material	unit 6S-17/25	Beta-77168	980	50	—	Walker 2005
Puerto Rico	Puerto Rico	Greater Antilles	2	Paso del Indio	charcoal	charcoal/ charred material	unit 6S-17/29	Beta-87603	950	60	—	Walker 2005
Puerto Rico	Puerto Rico	Greater Antilles	2	Paso del Indio	charcoal	charcoal/ charred material	Unit 6S-17/33	Beta-77175	830	80	—	Walker 2005
Puerto Rico	Puerto Rico	Greater Antilles	2	Paso del Indio	charcoal	charcoal/ charred material	Unit 6S-17/33	Beta-87604	870	80	—	Walker 2005
Puerto Rico	Puerto Rico	Greater Antilles	2	Paso del Indio	charcoal	charcoal/ charred material	Unit 7-1	Beta-178671	560	60	—	Walker 2005
Puerto Rico	Puerto Rico	Greater Antilles	2	Paso del Indio	charcoal	charcoal/ charred material	unit 7-2	Beta-178672	960	40	—	Walker 2005
Puerto Rico	Puerto Rico	Greater Antilles	2	Paso del Indio	charcoal	charcoal/ charred material	unit 7-2	Beta-178673	1270	70	—	Walker 2005
Puerto Rico	Puerto Rico	Greater Antilles	2	Paso del Indio	charcoal	charcoal/ charred material	Unit 7-2	Beta-77177	640	60	—	Walker 2005
Puerto Rico	Puerto Rico	Greater Antilles	2	Paso del Indio	charcoal	charcoal/ charred material	Unit 7-4	Beta-178675	730	40	—	Walker 2005
Puerto Rico	Puerto Rico	Greater Antilles	2	Paso del Indio	charcoal	charcoal/ charred material	unit 7-4	Beta-178676	1010	40	—	Walker 2005
Puerto Rico	Puerto Rico	Greater Antilles	2	Paso del Indio	charcoal	charcoal/ charred material	unit 7-5	Beta-77183	630	50	—	Walker 2005
Puerto Rico	Puerto Rico	Greater Antilles	2	Paso del Indio	charcoal	charcoal/ charred material	unit 81-2	Beta-77164	1350	70	—	Walker 2005
Puerto Rico	Puerto Rico	Greater Antilles	2	Paso del Indio	charcoal	charcoal/ charred material	unit 81-2	Beta-87610	1550	60	—	Walker 2005

Puerto Rico	Puerto Rico	Greater Antilles	2	Paso del Indio	charcoal	charcoal/ charred material	unit 8I-2	Beta-178677	2330	110	—	Walker 2005
Puerto Rico	Puerto Rico	Greater Antilles	2	Paso del Indio	charcoal	charcoal/ charred material	unit 8I-3	Beta-178679	930	40	—	Walker 2005
Puerto Rico	Puerto Rico	Greater Antilles	2	Paso del Indio	charcoal	charcoal/ charred material	unit 8I-3	Beta-87611	1920	80	—	Walker 2005
Puerto Rico	Puerto Rico	Greater Antilles	2	Paso del Indio	charcoal	charcoal/ charred material	unit 8I-4	Beta-178681	1520	40	—	Walker 2005
Puerto Rico	Puerto Rico	Greater Antilles	2	Paso del Indio	charcoal	charcoal/ charred material	unit 8I-4	Beta-77165	4060	60	—	Walker 2005
Puerto Rico	Puerto Rico	Greater Antilles	2	Paso del Indio	charcoal	charcoal/ charred material	unit 8I-5	Beta-178680	4110	40	—	Walker 2005
Puerto Rico	Puerto Rico	Greater Antilles	2	Paso del Indio	charcoal	charcoal/ charred material	unit 8S-2	Beta-178678	2520	40	—	Walker 2005
Puerto Rico	Puerto Rico	Greater Antilles	2	Paso del Indio	human bone	human bone/teeth	Impacted/Out of context	AA-75802	710	43	-19.44	Pestle 2010
Puerto Rico	Puerto Rico	Greater Antilles	2	Paso del Indio	human bone	human bone/teeth	Impacted/Out of context	AA-82413	900	44	-20.09	Pestle 2010
Puerto Rico	Puerto Rico	Greater Antilles	2	Paso del Indio	human bone	human bone/teeth	P6 18E 21S Ent. 1	AA-79406	1040	44	-19.34	Pestle 2010
Puerto Rico	Puerto Rico	Greater Antilles	2	Paso del Indio	human bone	human bone/teeth	P6 U12 Ent. 1	AA-79407	1041	44	-18.52	Pestle 2010
Puerto Rico	Puerto Rico	Greater Antilles	2	Paso del Indio	human bone	human bone/teeth	P6 U13E 25S Ent. 4A	AA-82414	1026	44	-18.94	Pestle 2010
Puerto Rico	Puerto Rico	Greater Antilles	2	Paso del Indio	human bone	human bone/teeth	P6/T1 Ent. 1	AA-75143	932	44	-19.30	Pestle 2010
Puerto Rico	Puerto Rico	Greater Antilles	2	Paso del Indio	human bone	human bone/teeth	P6/U 13E 25S Ent. 4B	AA-83933	991	43	-19.53	Pestle 2010
Puerto Rico	Puerto Rico	Greater Antilles	2	Paso del Indio	human bone	human bone/teeth	P6/U 17E 25S Ent. 1	AA-83932	873	42	-19.39	Pestle 2010
Puerto Rico	Puerto Rico	Greater Antilles	2	Paso del Indio	human bone	human bone/teeth	P6/U 17E 25S Ent. 2	AA-83931	927	45	-19.02	Pestle 2010

Puerto Rico	Puerto Rico	Greater Antilles	2	Paso del Indio	human bone	human bone/teeth	P6/U 17E 29S Ent. 4	AA-75124	1010	42	—	Pestle 2010
Puerto Rico	Puerto Rico	Greater Antilles	2	Paso del Indio	human bone	human bone/teeth	P6/U 17E 41S Ent. 1	AA-79356	1075	44	-19.32	Pestle 2010
Puerto Rico	Puerto Rico	Greater Antilles	2	Paso del Indio	human bone	human bone/teeth	P6/U 18E 21S Ent. 2	AA-82408	953	46	-19.00	Pestle 2010
Puerto Rico	Puerto Rico	Greater Antilles	2	Paso del Indio	human bone	human bone/teeth	P6/U13 Ent. #2	AA-72888	1164	41	-19.09	Pestle 2010
Puerto Rico	Puerto Rico	Greater Antilles	2	Paso del Indio	human bone	human bone/teeth	P6/U13 Ent. 13	AA-83934	951	42	-18.50	Pestle 2010
Puerto Rico	Puerto Rico	Greater Antilles	2	Paso del Indio	human bone	human bone/teeth	P6/U13-25 Ent. 2	AA-79400	983	44	-18.97	Pestle 2010
Puerto Rico	Puerto Rico	Greater Antilles	2	Paso del Indio	human bone	human bone/teeth	P6/U17E 29S Ent. 10	AA-78488	1085	43	-18.79	Pestle 2010
Puerto Rico	Puerto Rico	Greater Antilles	2	Paso del Indio	human bone	human bone/teeth	P6/U17E 29S Ent. 5	AA-75142	1004	44	-19.50	Pestle 2010
Puerto Rico	Puerto Rico	Greater Antilles	2	Paso del Indio	human bone	human bone/teeth	P6/U17E 29S Ent. 6	AA-75818	1127	45	-19.25	Pestle 2010
Puerto Rico	Puerto Rico	Greater Antilles	2	Paso del Indio	human bone	human bone/teeth	P6/U17E 33S Ent. 1	AA-79355	1099	44	-17.63	Pestle 2010
Puerto Rico	Puerto Rico	Greater Antilles	2	Paso del Indio	human bone	human bone/teeth	P6/U17E 33S Ent. 2	AA-75826	997	44	-18.55	Pestle 2010
Puerto Rico	Puerto Rico	Greater Antilles	2	Paso del Indio	human bone	human bone/teeth	P6/U17E 37S Ent. 1	AA-82410	1098	45	-19.52	Pestle 2010
Puerto Rico	Puerto Rico	Greater Antilles	2	Paso del Indio	human bone	human bone/teeth	P6/U18E 25S Ent. 4	AA-82404	1162	60	-17.48	Pestle 2010
Puerto Rico	Puerto Rico	Greater Antilles	2	Paso del Indio	human bone	human bone/teeth	P6/U75E 35S Ent. 1	AA-82409	1150	45	-18.81	Pestle 2010
Puerto Rico	Puerto Rico	Greater Antilles	2	Paso del Indio	human bone	human bone/teeth	P6/U7E 33S Ent. 1	AA-79404	1125	45	-18.49	Pestle 2010
Puerto Rico	Puerto Rico	Greater Antilles	2	Paso del Indio	human bone	human bone/teeth	P6/U7E 33S Ent. 2	AA-82415	1054	44	—	Pestle 2010
Puerto Rico	Puerto Rico	Greater Antilles	2	Paso del Indio	human bone	human bone/teeth	P6N/U 13E 13S Ent. 1	AA-78480	1084	46	-19.95	Pestle 2010
Puerto Rico	Puerto Rico	Greater Antilles	2	Paso del Indio	human bone	human bone/teeth	P6N/U 18E 17S Ent. 1	AA-82407	1289	46	-17.42	Pestle 2010

Puerto Rico	Puerto Rico	Greater Antilles	2	Paso del Indio	human bone	human bone/teeth	P7 Ent. D Impacto	AA-82382	1007	47	—	Pestle 2010
Puerto Rico	Puerto Rico	Greater Antilles	2	Paso del Indio	human bone	human bone/teeth	P7 Impactado	AA-75822	1062	43	-19.30	Pestle 2010
Puerto Rico	Puerto Rico	Greater Antilles	2	Paso del Indio	human bone	human bone/teeth	P7/T1 Ent. 1	AA-75801	1168	43	-17.94	Pestle 2010
Puerto Rico	Puerto Rico	Greater Antilles	2	Paso del Indio	human bone	human bone/teeth	P7/T1 Ent. 4	AA-78489	1336	43	-19.05	Pestle 2010
Puerto Rico	Puerto Rico	Greater Antilles	2	Paso del Indio	human bone	human bone/teeth	P7/U1 Ent. 1	AA-72877	699	52	-18.72	Pestle 2010
Puerto Rico	Puerto Rico	Greater Antilles	2	Paso del Indio	human bone	human bone/teeth	P7/U1 Ent. 2	AA-79352	567	43	—	Pestle 2010
Puerto Rico	Puerto Rico	Greater Antilles	2	Paso del Indio	human bone	human bone/teeth	P7/U2 Ent. 11A	AA-75123	973	41	-19.11	Pestle 2010
Puerto Rico	Puerto Rico	Greater Antilles	2	Paso del Indio	human bone	human bone/teeth	P7/U2 Ent. 12B	AA-83930	1065	45	-18.94	Pestle 2010
Puerto Rico	Puerto Rico	Greater Antilles	2	Paso del Indio	human bone	human bone/teeth	P7/U2 Ent. 13	AA-83926	829	45	-19.39	Pestle 2010
Puerto Rico	Puerto Rico	Greater Antilles	2	Paso del Indio	human bone	human bone/teeth	P7/U2 Ent. 1A	AA-72875	980	41	-18.94	Pestle 2010
Puerto Rico	Puerto Rico	Greater Antilles	2	Paso del Indio	human bone	human bone/teeth	P7/U2 Ent. 3	AA-78481	798	45	-18.61	Pestle 2010
Puerto Rico	Puerto Rico	Greater Antilles	3	Paso del Indio	charcoal	charcoal/ charred material	Unit 6S-17/25	Beta-77166	260	50	—	Walker 2005
Puerto Rico	Puerto Rico	Greater Antilles	2	Paso del Indio	human bone	human bone/teeth	P7/U2 Ent. 4	AA-79351	1121	44	-19.09	Pestle 2010
Puerto Rico	Puerto Rico	Greater Antilles	2	Paso del Indio	human bone	human bone/teeth	P7/U2 Ent. 9	AA-79346	885	44	-19.48	Pestle 2010
Puerto Rico	Puerto Rico	Greater Antilles	2	Paso del Indio	human bone	human bone/teeth	P7/U3 Ent. 11	AA-72889	893	41	-19.17	Pestle 2010
Puerto Rico	Puerto Rico	Greater Antilles	2	Paso del Indio	human bone	human bone/teeth	P7/U3 Ent. 2	AA-83928	935	44	-19.57	Pestle 2010
Puerto Rico	Puerto Rico	Greater Antilles	2	Paso del Indio	human bone	human bone/teeth	P7/U3 Ent. 4	AA-83935	1092	42	-19.47	Pestle 2010
Puerto Rico	Puerto Rico	Greater Antilles	2	Paso del Indio	human bone	human bone/teeth	P7/U3 Ent. 5A	AA-83929	1086	46	-19.34	Pestle 2010
Puerto Rico	Puerto Rico	Greater Antilles	2	Paso del Indio	human bone	human bone/teeth	P7/U3 Ent. 6	AA-83936	1002	43	0.00	Pestle 2010

Puerto Rico	Puerto Rico	Greater Antilles	2	Paso del Indio	human bone	human bone/teeth	P7/U3 Ent. 7	AA-75144	941	44	-19.49	Pestle 2010
Puerto Rico	Puerto Rico	Greater Antilles	2	Paso del Indio	human bone	human bone/teeth	P7/U3 Ent. 8	AA-83925	735	44	-19.46	Pestle 2010
Puerto Rico	Puerto Rico	Greater Antilles	2	Paso del Indio	human bone	human bone/teeth	P7/U4 Ent. 10	AA-82411	1027	44	18.57	Pestle 2010
Puerto Rico	Puerto Rico	Greater Antilles	2	Paso del Indio	human bone	human bone/teeth	P7/U4 Ent. 11	AA-83927	1073	45	-18.54	Pestle 2010
Puerto Rico	Puerto Rico	Greater Antilles	2	Paso del Indio	human bone	human bone/teeth	P7/U4 Ent. 14	AA-75140	1016	45	-19.01	Pestle 2010
Puerto Rico	Puerto Rico	Greater Antilles	2	Paso del Indio	human bone	human bone/teeth	P7/U4 Ent. 2A	AA-72876	1036	42	-17.8	Pestle 2010
Puerto Rico	Puerto Rico	Greater Antilles	2	Paso del Indio	human bone	human bone/teeth	P7/U4 Ent. 2B	AA-78487	1078	46	-18.89	Pestle 2010
Puerto Rico	Puerto Rico	Greater Antilles	2	Paso del Indio	human bone	human bone/teeth	P7/U4 Ent. 2C	AA-75126	966	42	-19.09	Pestle 2010
Puerto Rico	Puerto Rico	Greater Antilles	2	Paso del Indio	human bone	human bone/teeth	P7/U4 Ent. 3A	AA-79347	1090	45	-18.96	Pestle 2010
Puerto Rico	Puerto Rico	Greater Antilles	2	Paso del Indio	human bone	human bone/teeth	P7/U4 Ent. 4A	AA-75800	907	45	-19.41	Pestle 2010
Puerto Rico	Puerto Rico	Greater Antilles	2	Paso del Indio	human bone	human bone/teeth	P7/U4 Ent. 4D	AA-75139	1011	42	-18.89	Pestle 2010
Puerto Rico	Puerto Rico	Greater Antilles	2	Paso del Indio	human bone	human bone/teeth	P7/U4 Ent. 5C	AA-75798	1071	43	-18.88	Pestle 2010
Puerto Rico	Puerto Rico	Greater Antilles	2	Paso del Indio	human bone	human bone/teeth	P7/U4 Ent. 5D	AA-79348	1039	45	-19.17	Pestle 2010
Puerto Rico	Puerto Rico	Greater Antilles	2	Paso del Indio	human bone	human bone/teeth	P7/U4 Ent. 7B	AA-79354	1098	44	-18.51	Pestle 2010
Puerto Rico	Puerto Rico	Greater Antilles	2	Paso del Indio	human bone	human bone/teeth	P7/U5 Ent . 1	AA-82412	904	44	-19.28	Pestle 2010
Puerto Rico	Puerto Rico	Greater Antilles	2	Paso del Indio	human bone	human bone/teeth	P7/U5 Ent. #11	AA-75122	1055	41	-19.31	Pestle 2010
Puerto Rico	Puerto Rico	Greater Antilles	2	Paso del Indio	human bone	human bone/teeth	P7/U5 Ent. #12	AA-78479	1128	49	-18.98	Pestle 2010
Puerto Rico	Puerto Rico	Greater Antilles	2	Paso del Indio	human bone	human bone/teeth	P7/U5 Ent. #16A	AA-75121	952	41	-19.63	Pestle 2010
Puerto Rico	Puerto Rico	Greater Antilles	2	Paso del Indio	human bone	human bone/teeth	P7/U5 Ent. #3	AA-79345	1099	45	-20.51	Pestle 2010
Puerto Rico	Puerto Rico	Greater Antilles	2	Paso del Indio	human bone	human bone/teeth	P7/U5 Ent. #4	AA-78478	1014	43	-18.78	Pestle 2010

Puerto Rico	Puerto Rico	Greater Antilles	2	Paso del Indio	human bone	human bone/teeth	P7/U5 Ent. #7	AA-72874	1053	42	-19.20	Pestle 2010
Puerto Rico	Puerto Rico	Greater Antilles	2	Paso del Indio	human bone	human bone/teeth	P7/U5 Ent. #9	AA-79344	1070	45	-18.41	Pestle 2010
Puerto Rico	Puerto Rico	Greater Antilles	2	Paso del Indio	human bone	human bone/teeth	P7/U5 Ent. 10A	AA-82381	1070	45	-19.60	Pestle 2010
Puerto Rico	Puerto Rico	Greater Antilles	2	Paso del Indio	human bone	human bone/teeth	P7/U5 Ent. 10B	AA-79402	1141	45	-19.69	Pestle 2010
Puerto Rico	Puerto Rico	Greater Antilles	2	Paso del Indio	human bone	human bone/teeth	P7/U5 Ent. 11	AA-75799	1351	44	-18.13	Pestle 2010
Puerto Rico	Puerto Rico	Greater Antilles	2	Paso del Indio	human bone	human bone/teeth	P7/U5 Ent. 13A	AA-75141	1094	44	-18.80	Pestle 2010
Puerto Rico	Puerto Rico	Greater Antilles	2	Paso del Indio	human bone	human bone/teeth	P7/U5 Ent. 13B	AA-82406	1140	47	-19.18	Pestle 2010
Puerto Rico	Puerto Rico	Greater Antilles	2	Paso del Indio	human bone	human bone/teeth	P7/U5 Ent. 13C	AA-82405	963	46	-18.71	Pestle 2010
Puerto Rico	Puerto Rico	Greater Antilles	2	Paso del Indio	human bone	human bone/teeth	P7/U5 Ent. 19A	AA-79403	725	43	-18.89	Pestle 2010
Puerto Rico	Puerto Rico	Greater Antilles	2	Paso del Indio	human bone	human bone/teeth	P7/U5 Ent. 2	AA-75820	964	44	-19.06	Pestle 2010
Puerto Rico	Puerto Rico	Greater Antilles	2	Paso del Indio	human bone	human bone/teeth	P7/U5 Ent. 20	AA-79401	870	44	-19.14	Pestle 2010
Puerto Rico	Puerto Rico	Greater Antilles	2	Paso del Indio	human bone	human bone/teeth	P7/U5 Ent. 8	AA-79353	1026	44	-18.94	Pestle 2010
Puerto Rico	Puerto Rico	Greater Antilles	2	Paso del Indio	human bone	human bone/teeth	P7/U5 Impactado	AA-78490	1392	43	-18.97	Pestle 2010
Puerto Rico	Puerto Rico	Greater Antilles	2	Paso del Indio	human bone	human bone/teeth	P8/U2 Ent. 2	AA-72892	966	41	-18.72	Pestle 2010
Puerto Rico	Puerto Rico	Greater Antilles	2	Paso del Indio	human bone	human bone/teeth	P8I/U1 Ent. 2	AA-75823	951	42	-19.31	Pestle 2010
Puerto Rico	Puerto Rico	Greater Antilles	2	Paso del Indio	human bone	human bone/teeth	P8I/U3 Ent. 3	AA-82402	1191	48	-19.66	Pestle 2010
Puerto Rico	Puerto Rico	Greater Antilles	2	Paso del Indio	human bone	human bone/teeth	P8I/U5 Ent.(1) Impactado	AA-75824	1200	44	-18.99	Pestle 2010
Puerto Rico	Puerto Rico	Greater Antilles	2	Paso del Indio	human bone	human bone/teeth	P8N/U5 Ent. #2	AA-78482	1053	42	-18.96	Pestle 2010
Puerto Rico	Puerto Rico	Greater Antilles	2	Paso del Indio	human bone	human bone/teeth	P8N/U5 Ent. 2	AA-82401	1147	87	-19.32	Pestle 2010

Puerto Rico	Puerto Rico	Greater Antilles	2	Paso del Indio	human bone	human bone/teeth	P8N/U5 Ent. 3	AA-72893	1168	42	-19.5	Pestle 2010
Puerto Rico	Puerto Rico	Greater Antilles	4	Paso del Indio	charcoal	charcoal/ charred material	stratum 8, pilaster 6	Beta 87604	—	—	—	Clark et al. 2003
Puerto Rico	Puerto Rico	Greater Antilles	2	Paso del Indio	human bone	human bone/teeth	P8S/U3 Ent. 2	AA-75825	804	43	-19.67	Pestle 2010
Puerto Rico	Puerto Rico	Greater Antilles	2	PO-29	charred material	charcoal/ charred material	Jácana 1; Midden; Unit 142, Level 17	Beta-272032	1550	40	-25.7	Espenshade 2014
Puerto Rico	Puerto Rico	Greater Antilles	2	PO-29	charred material	charcoal/ charred material	Jácana 3; Batey surface; Unit 153, Level 6	Beta-247738	940	40	-24.8	Espenshade 2014
Puerto Rico	Puerto Rico	Greater Antilles	2	PO-29	charred material	charcoal/ charred material	Jácana 3; Batey surface; Unit 153, Level 7	Beta-247739	940	40	-25.2	Espenshade 2014
Puerto Rico	Puerto Rico	Greater Antilles	2	PO-29	charred material	charcoal/ charred material	Jácana 4; Slope Wash, Batey floor, Unit 153, level 2	Beta-247736	540	40	-25.1	Espenshade 2014
Puerto Rico	Puerto Rico	Greater Antilles	2	PO-29	charred material	charcoal/ charred material	Jácana 4; Unit 153, level 4	Beta-247737	440	60	-24.1	Espenshade 2014
Puerto Rico	Puerto Rico	Greater Antilles	2	PO-29	charred material	charcoal/ charred material	Jácana 2; FX-12; Burial feature 258	Beta-272029	1100	40	-24.3	Espenshade 2014
Puerto Rico	Puerto Rico	Greater Antilles	2	PO-29	charred material	charcoal/ charred material	Jácana 2; FX-T12; Burial feature 370	Beta-272030	1240	40	-23.9	Espenshade 2014
Puerto Rico	Puerto Rico	Greater Antilles	2	PO-29	charred material	charcoal/ charred material	Jácana 2; FX-T12; Feature 222, posthole	Beta-272028	1300	40	-26.2	Espenshade 2014
Puerto Rico	Puerto Rico	Greater Antilles	2	PO-29	charred material	charcoal/ charred material	Jácana 2; FX-T12; Feature 224, charcoal lense	Beta-272023	1310	40	-25.5	Espenshade 2014
Puerto Rico	Puerto Rico	Greater Antilles	2	PO-29	charred material	charcoal/ charred material	Jácana 2; Gully Top; Feature 204, posthole	Beta-272026	1190	40	-24.2	Espenshade 2014
Puerto Rico	Puerto Rico	Greater Antilles	2	PO-29	charred material	charcoal/ charred material	Jácana 2; Gully Top; Feature 209	Beta-272027	1220	40	-26.2	Espenshade 2014

Puerto Rico	Puerto Rico	Greater Antilles	2	PO-29	charred material	charcoal/ charred material	Jácana 2; Midden Mound; Feature 105, posthole	Beta-272025	1250	40	-25.0	Espenshade 2014
Puerto Rico	Puerto Rico	Greater Antilles	2	PO-29	charred material	charcoal/ charred material	Jácana 3; posthole in Midden Mound; Feature 112, posthole	Beta-272022	860	40	-26.5	Espenshade 2014
Puerto Rico	Puerto Rico	Greater Antilles	2	PO-29	charred material	charcoal/ charred material	Jácana 4; FX-F feature; Feature 454, posthole	Beta-272024	580	40	-25.6	Espenshade 2014
Puerto Rico	Puerto Rico	Greater Antilles	2	PO-29	charred material	charcoal/ charred material	Jácana 4; upper Midden Mound; Unit 108, Level 5	Beta-272031	710	40	-25.7	Espenshade 2014
Puerto Rico	Puerto Rico	Greater Antilles	2	PO-29	charred material	charcoal/ charred material	Jácana 4; upper Midden Mound; Unit 150, Level 8	Beta-272033	550	40	-26.5	Espenshade 2014
Puerto Rico	Puerto Rico	Greater Antilles	2	Punta Candelero	charcoal	charcoal/ charred material	Postmold E-1	I-15678	1170	80	—	Rodríguez 1991:627
Puerto Rico	Puerto Rico	Greater Antilles	3	Punta Candelero	human bone	human bone/teeth	C-6, no prov	AA-79380	948	44	—	Pestle 2013
Puerto Rico	Puerto Rico	Greater Antilles	2	Punta Candelero	charcoal	charcoal/ charred material	Postmold E-4	I-15679	1230	80	—	Rodríguez 1991:627
Puerto Rico	Puerto Rico	Greater Antilles	2	Punta Candelero	charcoal	charcoal/ charred material	Test A (60-70)	I-14978	2020	80	—	Rouse and Alegria 1990:58; Haviser 1997:63
Puerto Rico	Puerto Rico	Greater Antilles	2	Punta Candelero	charcoal	charcoal/ charred material	Unit F (60-70)	I-15407	690	80	—	Rodríguez 1989:259
Puerto Rico	Puerto Rico	Greater Antilles	2	Punta Candelero	charcoal	charcoal/ charred material	Unit F4 (40-50)	I-15410	1260	80	—	Rodríguez 1989:259
Puerto Rico	Puerto Rico	Greater Antilles	2	Punta Candelero	charcoal	charcoal/ charred material	Unit I (70-80)	I-15432	1000	110	—	Rodríguez 1989:259
Puerto Rico	Puerto Rico	Greater Antilles	2	Punta Candelero	charcoal	charcoal/ charred material	Unit J (60-70)	I-15408	1310	80	—	Rodríguez 1989:259

Puerto Rico	Puerto Rico	Greater Antilles	2	Punta Candelero	human bone	human bone/teeth	Area Cuevas Pozo A3 Ent. 29	AA-75137	1372	44	-16.28	Pestle 2013
Puerto Rico	Puerto Rico	Greater Antilles	2	Punta Candelero	human bone	human bone/teeth	Area Cuevas Pozo B-3 Ent. 9	AA-75816	1455	46	-15.34	Pestle 2013
Puerto Rico	Puerto Rico	Greater Antilles	2	Punta Candelero	human bone	human bone/teeth	Area Cuevas Pozo B-3, Ent. 10	AA-79408	1208	45	-18.08	Pestle 2013
Puerto Rico	Puerto Rico	Greater Antilles	2	Punta Candelero	human bone	human bone/teeth	Area Cuevas Pozo B-6, Ent. 9	AA-78509	1179	43	-17.87	Pestle 2013
Puerto Rico	Puerto Rico	Greater Antilles	2	Punta Candelero	human bone	human bone/teeth	Area Cuevas Pozo D-1 Ent. 1	AA-75813	1214	46	-18.79	Pestle 2013
Puerto Rico	Puerto Rico	Greater Antilles	2	Punta Candelero	human bone	human bone/teeth	Area Cuevas Pozo D-1 Ext. S.O. Ent. 45	AA-72884	1118	44	-18.75	Pestle 2013
Puerto Rico	Puerto Rico	Greater Antilles	2	Punta Candelero	human bone	human bone/teeth	Area Cuevas Pozo D-8 Ent. 47	AA-75135	1082	42	-18.43	Pestle 2013
Puerto Rico	Puerto Rico	Greater Antilles	2	Punta Candelero	human bone	human bone/teeth	Area Cuevas, Pozo A-2	AA-79381	1162	45	-18.29	Pestle 2013
Puerto Rico	Puerto Rico	Greater Antilles	2	Punta Candelero	human bone	human bone/teeth	Area Cuevas, Pozo A-2	AA-79382	1235	45	-18.36	Pestle 2013
Puerto Rico	Puerto Rico	Greater Antilles	2	Punta Candelero	human bone	human bone/teeth	Area Cuevas, Pozo A-3, Ent. 16	AA-79413	1154	44	-16.92	Pestle 2013

Puerto Rico	Puerto Rico	Greater Antilles	2	Punta Candelero	human bone	human bone/teeth	Area Cuevas, Pozo B-4	AA-79383	1389	45	-17.18	Pestle 2013
Puerto Rico	Puerto Rico	Greater Antilles	2	Punta Candelero	human bone	human bone/teeth	Area Cuevas, Pozo B-6	AA-79384	1408	46	-15.94	Pestle 2013
Puerto Rico	Puerto Rico	Greater Antilles	2	Punta Candelero	human bone	human bone/teeth	Area Cuevas. Pozo A-2 Ent. 33	AA-72881	1251	42	-17.98	Pestle 2013
Puerto Rico	Puerto Rico	Greater Antilles	2	Punta Candelero	human bone	human bone/teeth	Blq 2 Pozo B-1 Ent. 13 Area Huecoide	AA-75129	1260	42	-17.70	Pestle 2013
Puerto Rico	Puerto Rico	Greater Antilles	2	Punta Candelero	human bone	human bone/teeth	Blq 2 Pozo Q Ent. 1	AA-75810	1582	46	-16.35	Pestle 2013
Puerto Rico	Puerto Rico	Greater Antilles	2	Punta Candelero	human bone	human bone/teeth	Blq 3 Pozo A Ent. 3	AA-75130	1374	43	-16.49	Pestle 2013
Puerto Rico	Puerto Rico	Greater Antilles	2	Punta Candelero	human bone	human bone/teeth	Blq II L-2 Pozo D Ent. 1	AA-75805	1369	45	-15.95	Pestle 2013
Puerto Rico	Puerto Rico	Greater Antilles	2	Punta Candelero	human bone	human bone/teeth	Blq II Pozo F-8 Ent. 1	AA-75128	1539	43	-18.06	Pestle 2013
Puerto Rico	Puerto Rico	Greater Antilles	2	Punta Candelero	human bone	human bone/teeth	Blq. 2 Pozo F Ent. 1 Hueso 5	AA-75812	1339	45	-17.75	Pestle 2013
Puerto Rico	Puerto Rico	Greater Antilles	2	Punta Candelero	human bone	human bone/teeth	Blq. II Pozo J Nivel 6.5-34 Ent. 1	AA-75804	1401	45	-17.29	Pestle 2013
Puerto Rico	Puerto Rico	Greater Antilles	2	Punta Candelero	human bone	human bone/teeth	Blq. II Pozo W Ent. 1	AA-82377	1260	46	-16.97	Pestle 2013
Puerto Rico	Puerto Rico	Greater Antilles	2	Punta Candelero	human bone	human bone/teeth	C-21	AA-82380	1174	45	-18.67	Pestle 2013

Puerto Rico	Puerto Rico	Greater Antilles	2	Punta Candelero	human bone	human bone/teeth	F-2	AA-82378	1347	45	-16.73	Pestle 2013
Puerto Rico	Puerto Rico	Greater Antilles	2	Punta Candelero	human bone	human bone/teeth	Paredes Pozo W-X, Ent. 1	AA-79415	1566	46	-16.87	Pestle 2013
Puerto Rico	Puerto Rico	Greater Antilles	2	Punta Candelero	human bone	human bone/teeth	Pedestal F 14 Ent. 57 Area Huecoide	AA-72887	1322	42	-17.42	Pestle 2013
Puerto Rico	Puerto Rico	Greater Antilles	2	Punta Candelero	human bone	human bone/teeth	Pozo A-2 Ent. 1 Area Cuevas	AA-75134	1098	43	-17.54	Pestle 2013
Puerto Rico	Puerto Rico	Greater Antilles	2	Punta Candelero	human bone	human bone/teeth	Pozo A-2 Ent. 30	AA-75127	1160	42	-18.42	Pestle 2013
Puerto Rico	Puerto Rico	Greater Antilles	2	Punta Candelero	human bone	human bone/teeth	Pozo A3 Area Cuevas Ent. 17	AA-75136	1061	42	-18.86	Pestle 2013
Puerto Rico	Puerto Rico	Greater Antilles	2	Punta Candelero	human bone	human bone/teeth	Pozo A-3, nivel 40-50	AA-78510	1189	45	-18.00	Pestle 2013
Puerto Rico	Puerto Rico	Greater Antilles	2	Punta Candelero	human bone	human bone/teeth	Pozo A6 Ent. 2	AA-75809	1350	46	-16.31	Pestle 2013
Puerto Rico	Puerto Rico	Greater Antilles	2	Punta Candelero	human bone	human bone/teeth	Pozo B3 Area Cuevas Ent. 2	AA-75806	1186	45	-18.87	Pestle 2013
Puerto Rico	Puerto Rico	Greater Antilles	2	Punta Candelero	human bone	human bone/teeth	Pozo B-3 Area Cuevas Ent. 5	AA-75133	1173	42	-18.53	Pestle 2013
Puerto Rico	Puerto Rico	Greater Antilles	4	Punta Candelero	—	unknown	Unit L (40-50)	I-15409	1230	80	—	Rodríguez 1989:259
Puerto Rico	Puerto Rico	Greater Antilles	2	Punta Candelero	human bone	human bone/teeth	Pozo B3 Ent 10	AA-75814	1175	45	-17.87	Pestle 2013
Puerto Rico	Puerto Rico	Greater Antilles	2	Punta Candelero	human bone	human bone/teeth	Pozo B-4 Ent. 1	AA-78483	1427	44	-16.19	Pestle 2013
Puerto Rico	Puerto Rico	Greater Antilles	2	Punta Candelero	human bone	human bone/teeth	Pozo B-4, Ent. 1	AA-79414	1255	45	-17.25	Pestle 2013

Puerto Rico	Puerto Rico	Greater Antilles	2	Punta Candelero	human bone	human bone/teeth	Pozo B-5, Ent. 9	AA-79412	1257	47	-18.19	Pestle 2013
Puerto Rico	Puerto Rico	Greater Antilles	2	Punta Candelero	human bone	human bone/teeth	Pozo B-6 Area Cuevas. Ent. 6	AA-75807	1231	77	-16.65	Pestle 2013
Puerto Rico	Puerto Rico	Greater Antilles	2	Punta Candelero	human bone	human bone/teeth	Pozo B6 Ent. 7	AA-75803	1331	68	-17.14	Pestle 2013
Puerto Rico	Puerto Rico	Greater Antilles	2	Punta Candelero	human bone	human bone/teeth	Pozo C3 Ent. 1	AA-78484	1004	45	-19.05	Pestle 2013
Puerto Rico	Puerto Rico	Greater Antilles	2	Punta Candelero	human bone	human bone/teeth	Pozo C5 Ent. 1	AA-75817	1135	45	-17.86	Pestle 2013
Puerto Rico	Puerto Rico	Greater Antilles	2	Punta Candelero	human bone	human bone/teeth	Pozo D-2, Ent. 1	AA-79409	1421	48	-15.96	Pestle 2013
Puerto Rico	Puerto Rico	Greater Antilles	2	Punta Candelero	human bone	human bone/teeth	Pozo F-8, Ent. 2	AA-78512	1430	43	-16.86	Pestle 2013
Puerto Rico	Puerto Rico	Greater Antilles	2	Punta Candelero	human bone	human bone/teeth	Pozo Q-1	AA-78513	1557	44	-15.85	Pestle 2013
Puerto Rico	Puerto Rico	Greater Antilles	2	Punta Candelero	human bone	human bone/teeth	Pozo S-2, nivel 30-40	AA-79410	1387	45	-15.60	Pestle 2013
Puerto Rico	Puerto Rico	Greater Antilles	2	Punta Candelero	human bone	human bone/teeth	Pozo T, nivel 0-80	AA-79411	1271	45	-17.70	Pestle 2013
Puerto Rico	Puerto Rico	Greater Antilles	2	Punta Candelero	human bone	human bone/teeth	Pozo U Ent. 1	AA-75815	1218	46	-16.47	Pestle 2013
Puerto Rico	Puerto Rico	Greater Antilles	2	Punta Candelero	human bone	human bone/teeth	Pozo Z	AA-78511	1287	43	-17.45	Pestle 2013
Puerto Rico	Puerto Rico	Greater Antilles	2	Punta Candelero	human bone	human bone/teeth	UIUC173	AA-72886	1006	41	-18.86	Pestle 2013
Puerto Rico	Puerto Rico	Greater Antilles	2	Punta Candelero	human bone	human bone/teeth	Unidad B Pozo B-3 Ent. 7 Zona Cuevas	AA-75808	1228	47	-18.57	Pestle 2013
Puerto Rico	Puerto Rico	Greater Antilles	2	Punta Candelero	*Strombus* sp.	marine shell	C4 60-70 cm	I-15430	850	80	—	Rodríguez 1991:627

Puerto Rico	Puerto Rico	Greater Antilles	2	Punta Candelero	*Strombus gigas*	marine shell	Test C (80-90)	I-14979	2120	80	—	Rodríguez 1989:259; Rouse and Alegria 1990:58; Haviser 1997:63
Puerto Rico	Puerto Rico	Greater Antilles	2	Punta Candelero	*Strombus* sp.	marine shell	Unit C (80-90)	I-15431	1220	80	—	Rodríguez 1989:259
Puerto Rico	Puerto Rico	Greater Antilles	2	Punta Candelero	*Strombus* sp.	marine shell	Unit L2 (80-90)	I-15429	860	80	—	Rodríguez 1989:259
Puerto Rico	Puerto Rico	Greater Antilles	2	Punta Ostiones	charcoal	charcoal/ charred material	Unit A-4	I-6595	1545	90	—	Narganes Storde 2005:280-281
Puerto Rico	Puerto Rico	Greater Antilles	2	Tecla	charcoal	charcoal/ charred material	Section B-3 (0.50-0.60)	I-10921	1705	85	—	Rouse and Alegria 1990:55-56; Haviser 1997:63
Puerto Rico	Puerto Rico	Greater Antilles	2	Tecla	charcoal	charcoal/ charred material	Section M-12 (0.60-0.70)	I-10914	1780	85	—	Rouse and Alegria 1990:55-56; Haviser 1997:63
Puerto Rico	Puerto Rico	Greater Antilles	4	Tecla	—	unknown	—	I-13820	1950	80	—	Haviser 1997:63
Puerto Rico	Puerto Rico	Greater Antilles	4	Tecla	—	unknown	—	I-13856	2380	80	—	Haviser 1997:63
Puerto Rico	Puerto Rico	Greater Antilles	4	Tecla	—	unknown	—	I-13866	1900	80	—	Haviser 1997:63
Puerto Rico	Puerto Rico	Greater Antilles	4	Tecla	—	unknown	—	I-13867	2050	80	—	Haviser 1997:63
Puerto Rico	Puerto Rico	Greater Antilles	4	Tecla	—	unknown	—	I-13868	1850	80	—	Haviser 1997:63
Puerto Rico	Puerto Rico	Greater Antilles	4	Tecla	—	unknown	—	I-13921	2020	80	—	Haviser 1997:63

Puerto Rico	Puerto Rico	Greater Antilles	4	Tecla	—	unknown	—	I-13929	1920	80	—	Haviser 1997:63
Puerto Rico	Puerto Rico	Greater Antilles	2	Tecla	charcoal	charcoal/ charred material	Section P-9 (1.10-1.20)	I-10916	1720	80	—	Rouse and Alegria 1990:55-56; Haviser 1997:63
Puerto Rico	Puerto Rico	Greater Antilles	2	Tecla	charcoal	charcoal/ charred material	Unit A-3	I-9679	1220	80	—	Narganes Storde 1991
Puerto Rico	Puerto Rico	Greater Antilles	2	Tecla I	charcoal	charcoal/ charred material	T-I	I-10915	1390	85	—	Narganes Storde 1991
Puerto Rico	Puerto Rico	Greater Antilles	2	Tecla I	charcoal	charcoal/ charred material	Unit JJ-69	I-13930	1950	80	—	Narganes Storde 1991
Puerto Rico	Puerto Rico	Greater Antilles	2	Tecla I	charcoal	charcoal/ charred material	Unit N-12	I-10912	1295	85	—	Narganes Storde 1991
Puerto Rico	Puerto Rico	Greater Antilles	2	Tecla I	charcoal	charcoal/ charred material	Unit O-12	I-10913	1315	85	—	Narganes Storde 1991
Puerto Rico	Puerto Rico	Greater Antilles	2	Tecla I	charcoal	charcoal/ charred material	Unit A-2	I-9108	1480	95	—	Narganes Storde 1991
Puerto Rico	Puerto Rico	Greater Antilles	2	Tecla I	charcoal	charcoal/ charred material	Unit B-2	I-9107	1285	95	—	Narganes Storde 1991
Puerto Rico	Puerto Rico	Greater Antilles	2	Tecla I	charcoal	charcoal/ charred material	Unit II-69	I-13922	1780	85	—	Narganes Storde 1991
Puerto Rico	Puerto Rico	Greater Antilles	2	Tecla I	charcoal	charcoal/ charred material	Unit II-70	I-13923	1490	80	—	Narganes Storde 1991
Puerto Rico	Puerto Rico	Greater Antilles	2	Tecla I	charcoal	charcoal/ charred material	Unit II-72	I-13855	2020	80	—	Narganes Storde 1991

Puerto Rico	Puerto Rico	Greater Antilles	2	Tecla I	charcoal	charcoal/ charred material	Unit JJ-68	I-13924	1480	80	—	Narganes Storde 1991
Puerto Rico	Puerto Rico	Greater Antilles	2	Tecla I	charcoal	charcoal/ charred material	Unit JJ-70	I-13931	1360	80	—	Narganes Storde 1991
Puerto Rico	Puerto Rico	Greater Antilles	2	Tecla I	charcoal	charcoal/ charred material	Unit K-11	I-9678	1055	80	—	Narganes Storde 1991
Puerto Rico	Puerto Rico	Greater Antilles	2	Tecla I	charcoal	charcoal/ charred material	Unit L-12	I-9680	1775	80	—	Narganes Storde 1991
Puerto Rico	Puerto Rico	Greater Antilles	2	Tecla I	charcoal	charcoal/ charred material	Unit L-9	I-9677	1515	80	—	Narganes Storde 1991
Puerto Rico	Puerto Rico	Greater Antilles	2	Tecla I	charcoal	charcoal/ charred material	Unit MM-63	I-14360	1460	80	—	Narganes Storde 1991
Puerto Rico	Puerto Rico	Greater Antilles	2	Tecla I	charcoal	charcoal/ charred material	Unit MM-64	I-14429	1550	80	—	Narganes Storde 1991
Puerto Rico	Puerto Rico	Greater Antilles	2	Tecla I	charcoal	charcoal/ charred material	Unit MM-65	I-14428	1600	150	—	Narganes Storde 1991
Puerto Rico	Puerto Rico	Greater Antilles	2	Tecla I	charcoal	charcoal/ charred material	Unit MM-66	I-14361	1650	80	—	Narganes Storde 1991
Puerto Rico	Puerto Rico	Greater Antilles	2	Tecla I	charcoal	charcoal/ charred material	Unit NN-64	I-14362	1560	80	—	Narganes Storde 1991
Puerto Rico	Puerto Rico	Greater Antilles	2	Tecla I	charcoal	charcoal/ charred material	Unit ÑÑ-65	I-14430	1610	80	—	Narganes Storde 1991
Puerto Rico	Puerto Rico	Greater Antilles	2	Tecla I	charcoal	charcoal/ charred material	Unit ÑÑ-65	I-14431	1650	80	—	Narganes Storde 1991
Puerto Rico	Puerto Rico	Greater Antilles	2	Tecla I	charcoal	charcoal/ charred material	Unit NN-66	I-14382	1530	80	—	Narganes Storde 1991

Puerto Rico	Puerto Rico	Greater Antilles	2	Tecla I	charcoal	charcoal/ charred material	Unit OO-65	I-14383	1600	80	—	Narganes Storde 1991
Puerto Rico	Puerto Rico	Greater Antilles	2	Tecla I	charcoal	charcoal/ charred material	Unit QQ-76	I-14427	1610	80	—	Narganes Storde 1991
Puerto Rico	Puerto Rico	Greater Antilles	2	Tecla I	charcoal	charcoal/ charred material	Unit S-2	I-9873	1460	80	—	Narganes Storde 1991
Puerto Rico	Puerto Rico	Greater Antilles	2	Tecla I	charcoal	charcoal/ charred material	Unit VV-97	I-13853	1370	80	—	Narganes Storde 1991
Puerto Rico	Puerto Rico	Greater Antilles	2	Tecla I	charcoal	charcoal/ charred material	Unit VV-97	I-13854	1400	150	—	Narganes Storde 1991
Puerto Rico	Puerto Rico	Greater Antilles	2	Tecla II	charcoal	charcoal/ charred material	Unit B-2	I-10920	1410	85	—	Narganes Storde 1991
Puerto Rico	Puerto Rico	Greater Antilles	2	Tecla II	charcoal	charcoal/ charred material	Unit Y-56	I-13932	1500	80	—	Narganes Storde 1991
Puerto Rico	Puerto Rico	Greater Antilles	2	Tecla II	charcoal	charcoal/ charred material	Unit Y-60	I-13933	1350	110	—	Narganes Storde 1991
Puerto Rico	Puerto Rico	Greater Antilles	2	Tibes	charcoal	charcoal/ charred material	N184 E55, level 6, Feat. 03-2, deposit H	Beta-198877	990	40	-23.9	Curet et al. 2006
Puerto Rico	Puerto Rico	Greater Antilles	2	Tibes	charcoal	charcoal/ charred material	N215 E70, evel 4	Beta-198876	750	40	-25.0	Curet et al. 2006
Puerto Rico	Puerto Rico	Greater Antilles	2	Tibes	charcoal	charcoal/ charred material	N93.95/E98.05, level 3 deposit H	Beta-136324	950	40	-25.9	Curet et al. 2006
Puerto Rico	Puerto Rico	Greater Antilles	2	Tibes	charcoal	charcoal/ charred material	N93.95/E98.05, level 4 deposit H	Beta-136325	1040	50	-25.9	Curet et al. 2006
Puerto Rico	Puerto Rico	Greater Antilles	2	Tibes	charcoal	charcoal/ charred material	N94.05/E98.05, level 3, deposit H	Beta-136326	1080	60	-25.3	Curet et al. 2006
Puerto Rico	Puerto Rico	Greater Antilles	2	Tibes	charcoal	charcoal/ charred material	N94.05/E98.05, level 4, deposit H	Beta-136327	1010	40	-25.0	Curet et al. 2006

Puerto Rico	Puerto Rico	Greater Antilles	2	Tibes	charcoal	charcoal/ charred material	OP19E, Feature 5, level 3	Beta-136328	930	40	-25.9	Curet et al. 2006; Curet 2010
Puerto Rico	Puerto Rico	Greater Antilles	2	Tibes	charcoal	charcoal/ charred material	Unit 1, level 3, deposit A	Beta-110631	900	60	-25.0	Curet et al. 2006
Puerto Rico	Puerto Rico	Greater Antilles	2	Tibes	charcoal	charcoal/ charred material	Unit 1, level 6, deposit A	Beta-109680	1270	40	-23.8	Curet et al. 2006
Puerto Rico	Puerto Rico	Greater Antilles	2	Tibes	charcoal	charcoal/ charred material	Unit 3, level 5, deposit C	Beta-109679	890	40	-28.6	Curet et al. 2006
Puerto Rico	Puerto Rico	Greater Antilles	2	Tibes	charcoal	charcoal/ charred material	Unit 8, post mold, deposit H	Beta-103329	880	50	-27.6	Curet et al. 2006
Puerto Rico	Puerto Rico	Greater Antilles	2	Tibes	human bone	human bone/teeth	A-3	AA-79368	1253	52	-18.50	Pestle 2010
Puerto Rico	Puerto Rico	Greater Antilles	2	Tibes	human bone	human bone/teeth	Batey de la Herradura, E-3	AA-74636	1365	45	-17.04	Pestle 2010
Puerto Rico	Puerto Rico	Greater Antilles	2	Tibes	human bone	human bone/teeth	Batey de la Herradura, E-3(1)	AA-74638	1493	45	-18.18	Pestle 2010
Puerto Rico	Puerto Rico	Greater Antilles	2	Tibes	human bone	human bone/teeth	Batey de la Herradura, E-3(3)	AA-74637	1434	45	-17.28	Pestle 2010
Puerto Rico	Puerto Rico	Greater Antilles	2	Tibes	human bone	human bone/teeth	Batey Herradura, EH-1	AA-79367	1367	45	-17.19	Pestle 2010
Puerto Rico	Puerto Rico	Greater Antilles	2	Tibes	human bone	human bone/teeth	Burial 07-01	AA-82416	1302	45	-17.99	Pestle 2010
Puerto Rico	Puerto Rico	Greater Antilles	2	Tibes	human bone	human bone/teeth	CE-10	AA-79362	1422	46	-17.54	Pestle 2010
Puerto Rico	Puerto Rico	Greater Antilles	2	Tibes	human bone	human bone/teeth	CE-4	AA-79365	1358	48	-16.97	Pestle 2010
Puerto Rico	Puerto Rico	Greater Antilles	2	Tibes	human bone	human bone/teeth	CE-5	AA-72896	1428	42	-17.72	Pestle 2010

Puerto Rico	Puerto Rico	Greater Antilles	2	Tibes	human bone	human bone/teeth	CE-5	AA-79369	1359	50	-17.62	Pestle 2010
Puerto Rico	Puerto Rico	Greater Antilles	2	Tibes	human bone	human bone/teeth	CE-6	AA-79364	1411	45	-16.77	Pestle 2010
Puerto Rico	Puerto Rico	Greater Antilles	2	Tibes	human bone	human bone/teeth	CE-7	AA-79363	1397	50	-18.02	Pestle 2010
Puerto Rico	Puerto Rico	Greater Antilles	2	Tibes	human bone	human bone/teeth	CE-9	AA-82397	1469	47	-16.69	Pestle 2010
Puerto Rico	Puerto Rico	Greater Antilles	2	Tibes	human bone	human bone/teeth	E-1	AA-72869	1302	42	-16.92	Pestle 2010
Puerto Rico	Puerto Rico	Greater Antilles	2	Tibes	human bone	human bone/teeth	E-13	AA-72871	1352	43	-17.21	Pestle 2010
Puerto Rico	Puerto Rico	Greater Antilles	2	Tibes	human bone	human bone/teeth	E-20	AA-72872	1443	50	-17.87	Pestle 2010
Puerto Rico	Puerto Rico	Greater Antilles	2	Tibes	human bone	human bone/teeth	E-20	AA-74639	1319	42	-17.23	Pestle 2010
Puerto Rico	Puerto Rico	Greater Antilles	2	Tibes	human bone	human bone/teeth	E-28	AA-78496	1338	43	-17.28	Pestle 2010
Puerto Rico	Puerto Rico	Greater Antilles	2	Tibes	human bone	human bone/teeth	E-40	AA-74656	1403	44	-17.39	Pestle 2010
Puerto Rico	Puerto Rico	Greater Antilles	2	Tibes	human bone	human bone/teeth	E-43	AA-83938	1326	44	-17.19	Pestle 2010
Puerto Rico	Puerto Rico	Greater Antilles	2	Tibes	human bone	human bone/teeth	E-46	AA-82383	1321	46	-18.29	Pestle 2010
Puerto Rico	Puerto Rico	Greater Antilles	2	Tibes	human bone	human bone/teeth	E-47	AA-83940	1353	43	-17.27	Pestle 2010
Puerto Rico	Puerto Rico	Greater Antilles	2	Tibes	human bone	human bone/teeth	E-48	AA-72894	1366	44	—	Pestle 2010
Puerto Rico	Puerto Rico	Greater Antilles	2	Tibes	human bone	human bone/teeth	E-57	AA-83942	1381	43	-16.09	Pestle 2010
Puerto Rico	Puerto Rico	Greater Antilles	2	Tibes	human bone	human bone/teeth	E-59	AA-74657	1305	44	-17.98	Pestle 2010
Puerto Rico	Puerto Rico	Greater Antilles	2	Tibes	human bone	human bone/teeth	E-60	AA-72897	1351	44	-17.23	Pestle 2010
Puerto Rico	Puerto Rico	Greater Antilles	2	Tibes	human bone	human bone/teeth	E-71	AA-74662	1322	44	-18.49	Pestle 2010
Puerto Rico	Puerto Rico	Greater Antilles	2	Tibes	human bone	human bone/teeth	E-72	AA-74663	1355	54	-18.40	Pestle 2010
Puerto Rico	Puerto Rico	Greater Antilles	2	Tibes	human bone	human bone/teeth	E-74A	AA-74664	1285	43	-18.72	Pestle 2010

Puerto Rico	Puerto Rico	Greater Antilles	2	Tibes	human bone	human bone/teeth	E-74B	AA-74665	1301	43	-18.60	Pestle 2010
Puerto Rico	Puerto Rico	Greater Antilles	2	Tibes	human bone	human bone/teeth	E-80	AA-83951	1413	64	-17.74	Pestle 2010
Puerto Rico	Puerto Rico	Greater Antilles	2	Tibes	human bone	human bone/teeth	E-85	AA-82391	1355	46	-16.59	Pestle 2010
Puerto Rico	Puerto Rico	Greater Antilles	2	Tibes	human bone	human bone/teeth	E-8B	AA-74643	1347	45	-17.45	Pestle 2010
Puerto Rico	Puerto Rico	Greater Antilles	2	Tibes	human bone	human bone/teeth	ES-3	AA-72895	1392	42	-17.15	Pestle 2010
Puerto Rico	Puerto Rico	Greater Antilles	2	Tibes	human bone	human bone/teeth	ES-7	AA-78492	1434	44	-17.14	Pestle 2010
Puerto Rico	Puerto Rico	Greater Antilles	2	Tibes	human bone	human bone/teeth	ES-8	AA-79366	1364	45	-17.47	Pestle 2010
Puerto Rico	Puerto Rico	Greater Antilles	2	Tibes	human bone	human bone/teeth	IA	AA-78493	1424	44	-17.95	Pestle 2010
Puerto Rico	Puerto Rico	Greater Antilles	2	Tibes	human bone	human bone/teeth	IB	AA-79370	1344	62	-17.75	Pestle 2010
Puerto Rico	Puerto Rico	Greater Antilles	2	Tibes	human bone	human bone/teeth	IC	AA-82399	1156	46	-17.98	Pestle 2010
Puerto Rico	Puerto Rico	Greater Antilles	2	Tibes	human bone	human bone/teeth	IIA	AA-78494	1138	43	-17.85	Pestle 2010
Puerto Rico	Puerto Rico	Greater Antilles	2	Tibes	human bone	human bone/teeth	P1-12-6	AA-78491	1249	43	-16.68	Pestle 2010
Puerto Rico	Puerto Rico	Greater Antilles	2	Tibes	human bone	human bone/teeth	P1-3-2-E-3	AA-79372	1038	47	-18.30	Pestle 2010
Puerto Rico	Puerto Rico	Greater Antilles	2	Tibes	human bone	human bone/teeth	P1-A-E-3B	AA-79371	1456	45	-18.03	Pestle 2010
Puerto Rico	Puerto Rico	Greater Antilles	2	Tibes	human bone	human bone/teeth	P1-E3C	AA-78495	1505	44	-18.31	Pestle 2010
Puerto Rico	Puerto Rico	Greater Antilles	2	Tibes	human bone	human bone/teeth	Pozo 12, Batey Santa Elena	AA-79374	1369	45	-18.14	Pestle 2010
Puerto Rico	Puerto Rico	Greater Antilles	2	Tibes	human bone	human bone/teeth	Pozo L2	AA-82400	1008	46	-17.63	Pestle 2010
Puerto Rico	Puerto Rico	Greater Antilles	2	Vega de Nelo Vargas	charcoal	charcoal/ charred material	Test Unit 2, W. Extension - Stratum 2	GrN-26412	650	25	-25.83	Oliver personal communication 2018

Puerto Rico	Puerto Rico	Greater Antilles	2	Vega de Nelo Vargas	charcoal	charcoal/ charred material	Test Unit, (2x1.5m), Lev. 3-Strat 2b, 27 cmbs	GrN-26413	590	45	-26.52	Oliver personal communication 2018
Puerto Rico	Puerto Rico	Greater Antilles	2	Vega de Nelo Vargas	charcoal	charcoal/ charred material	Test Unit, (2x1.5m), Lev. 7-Strat 3, 50-60 cmbs	GrN-30051	625	25	-25.19	Oliver personal communication 2018
Puerto Rico	Puerto Rico	Greater Antilles	2	Vega de Nelo Vargas	charcoal	charcoal/ charred material	Test Unit, (2x1.5m, Lev. 11, Strat 3	GrN-30052	640	30	-26.48	Oliver personal communication 2018
Puerto Rico	Puerto Rico	Greater Antilles	2	Villa Taina	charcoal	charcoal/ charred material	shell midden, (18° 02' 27" N, 67° 11' 33" W, 27cm below surface, duplicate run of UM-399	UM-398	1300	90	—	Eldridge et al. 1976
Puerto Rico	Puerto Rico	Greater Antilles	2	Villa Taina	charcoal	charcoal/ charred material	shell midden, (18° 02' 27" N, 67° 11' 33" W, 27cm below surface, duplicate run of UM-399	UM-399	1090	100	—	Eldridge et al. 1976
Puerto Rico	Puerto Rico	Greater Antilles	3	Villa Taina	shell	marine shell	30 cm below surface	UM-400	1050	80	—	Eldridge et al. 1976
Saba	The Netherlands	Lesser Antilles	3	The Bottom	shell	marine shell	—	GrN-16030	1490	60	—	Hofman 1993:25; Haviser 1997:62
Saba	The Netherlands	Lesser Antilles	3	The Bottom	shell	marine shell	—	GrN-16031	1120	50	—	Hofman 1993:25; Haviser 1997:62
Saba	The Netherlands	Lesser Antilles	3	Fort Bay	shell adze	marine shell	—	UM-1478	3155	65	—	Roobol et al. 1980; Hofman and Hoogland 2003:12

Saba	The Netherlands	Lesser Antilles	3	Fort Bay Ridge	shell	marine shell	—	Beta-409000	3670	30	+0.6	Hofman et al. 2019
Saba	The Netherlands	Lesser Antilles	3	Fort Bay Ridge	shell	marine shell	—	Beta-409001	2880	30	+1.3	Hofman et al. 2019
Saba	The Netherlands	Lesser Antilles	3	Fort Bay Ridge	shell	marine shell	—	GrA-63874	3005	35	—	Hofman et al. 2019
Saba	The Netherlands	Lesser Antilles	3	Fort Bay Ridge	shell	marine shell	—	GrA-63875	3620	35	—	Hofman et al. 2019
Saba	The Netherlands	Lesser Antilles	3	Fort Bay Ridge	shell	marine shell	—	GrA-63876	2770	30	—	Hofman et al. 2019
Saba	The Netherlands	Lesser Antilles	3	Fort Bay Ridge	shell	marine shell	—	GrA-63878	2800	30	—	Hofman et al. 2019
Saba	The Netherlands	Lesser Antilles	4	Kelbey's Ridge	dentine	human bone/teeth	—	OxA-3618	moder n	—	-14.9	Hoogland and Hofman 1993
Saba	The Netherlands	Lesser Antilles	3	Kelbey's Ridge	charcoal	charcoal/ charred material	—	GrN-16032	595	30	—	Hoogland and Hofman 1993
Saba	The Netherlands	Lesser Antilles	3	Kelbey's Ridge	charcoal	charcoal/ charred material	—	GrN-18737	597	18	—	Hoogland and Hofman 1993
Saba	The Netherlands	Lesser Antilles	3	Kelbey's Ridge	charcoal	charcoal/ charred material	—	GrN-18738	625	25	—	Hoogland and Hofman 1993
Saba	The Netherlands	Lesser Antilles	3	Kelbey's Ridge	charcoal	charcoal/ charred material	F516	GrN-18736	172	17	—	Hoogland and Hofman 1993
Saba	The Netherlands	Lesser Antilles	3	Kelbey's Ridge	land crab	faunal material	—	GrN-16033	1280	60	—	Hoogland and Hofman 1993
Saba	The Netherlands	Lesser Antilles	3	Kelbey's Ridge	dentine	human bone/teeth	—	OxA-2951	500	65	-13.9	Hoogland and Hofman 1993

Saba	The Netherlands	Lesser Antilles	3	Kelbey's Ridge	dentine	human bone/teeth	—	OxA-3617	900	60	-15.1	Hoogland and Hofman 1993
Saba	The Netherlands	Lesser Antilles	3	Kelbey's Ridge	dentine	human bone/teeth	—	OxA-3619	690	65	-15.2	Hoogland and Hofman 1993
Saba	The Netherlands	Lesser Antilles	3	Kelbey's Ridge	dentine	human bone/teeth	—	OxA-3843	795	60	-13.2	Hoogland and Hofman 1993
Saba	The Netherlands	Lesser Antilles	3	Kelbey's Ridge	dentine	human bone/teeth	—	OxA-3844	450	60	-16.8	Hoogland and Hofman 1993
Saba	The Netherlands	Lesser Antilles	3	Kelbey's Ridge	shell	marine shell	F504	GrN-16776	1084	35	—	Hoogland and Hofman 1993
Saba	The Netherlands	Lesser Antilles	2	Kelbey's Ridge	charcoal	charcoal/ charred material	F504	GrN-16775	610	30	—	Hoogland and Hofman 1993
Saba	The Netherlands	Lesser Antilles	2	Kelbey's Ridge	charcoal	charcoal/ charred material	F504	GrN-16777	630	30	—	Hoogland and Hofman 1993
Saba	The Netherlands	Lesser Antilles	4	Old Booby Hill Cave	shell	marine shell	—	Beta-450521	3980	30	+0.8	Hofman et al. 2019
Saba	The Netherlands	Lesser Antilles	3	Plum Piece	land crab	faunal material	undisturbed midden	GrN-27562	3430	30	—	Hofman and Hoogland 2003
Saba	The Netherlands	Lesser Antilles	3	Plum Piece	land crab	faunal material	undisturbed midden	GrN-27563	3300	30	—	Hofman and Hoogland 2003

Saba	The Netherlands	Lesser Antilles	3	Plum Piece	land crab	faunal material	undisturbed midden	GrN-27564	3320	30	—	Hofman and Hoogland 2003
Saba	The Netherlands	Lesser Antilles	3	Spring Bay	charcoal	charcoal/ charred material	—	GrN-16772	1205	30	—	Hofman 1993:25
Saba	The Netherlands	Lesser Antilles	3	Spring Bay	charcoal	charcoal/ charred material	—	GrN-16774	645	30	—	Hofman 1993:25
Saba	The Netherlands	Lesser Antilles	3	Spring Bay	charcoal	charcoal/ charred material	—	GrN-18735	620	25	—	Hofman 1993:25
Saba	The Netherlands	Lesser Antilles	3	Spring Bay	human bone	human bone/teeth	—	OxA-2950	535	65	-17.6	Hofman 1993:25
Saba	The Netherlands	Lesser Antilles	3	Spring Bay	shell	marine shell	—	GrN-16026	1560	60	—	Hofman 1993:25; Haviser 1997:62
Saba	The Netherlands	Lesser Antilles	3	Spring Bay	shell	marine shell	—	GrN-16027	1240	50	—	Hofman 1993:25
Saba	The Netherlands	Lesser Antilles	3	Spring Bay	shell	marine shell	—	GrN-16028	1130	60	—	Hofman 1993:25
Saba	The Netherlands	Lesser Antilles	3	Spring Bay	shell	marine shell	—	GrN-16029	1310	60	—	Hofman 1993:25
Saba	The Netherlands	Lesser Antilles	3	Spring Bay	shell	marine shell	—	GrN-16773	1125	30	—	Hofman 1993:25
Saba	The Netherlands	Lesser Antilles	3	Spring Bay	shell	marine shell	—	GrN-19321	1320	35	—	Hofman 1993:25
Saba	The Netherlands	Lesser Antilles	3	Spring Bay	shell	marine shell	—	GrN-19322	1320	45	—	Hofman 1993:25
Saba	The Netherlands	Lesser Antilles	3	Spring Bay	shell	marine shell	—	GrN-19323	1445	30	—	Hofman 1993:25
Saba	The Netherlands	Lesser Antilles	3	Spring Bay	shell	marine shell	—	GrN-19771	1065	30	—	Hofman 1993:25
Saba	The Netherlands	Lesser Antilles	3	Spring Bay	land crab	faunal material	—	GrN-18558	1640	35	—	Hofman 1993:25; Haviser 1997:62

San Salvador	Bahamas	Bahamian Archipelago	2	Barker's Point Shell Midden	*Strombus gigas*	marine shell	beach rock	AA-51432	1028	34	+3.3	Blick et al. 2007
San Salvador	Bahamas	Bahamian Archipelago	2	Barker's Point Shell Midden	*Strombus gigas*	marine shell	recovered projectile point	UGa-00836	1054	37	—	Blick et al. 2007
San Salvador	Bahamas	Bahamian Archipelago	2	Blue Hole	*Zanthoxylum flavum* (Yellow wood tree), mortar	wood	blue hole (underwater)	Beta-16732	530	65	—	Winter 1987
San Salvador	Bahamas	Bahamian Archipelago	4	Cat Island	*Cordia* sp.	wood	—	OxA-20839	409	25	-23.1	Ostapkowicz 2015
San Salvador	Bahamas	Bahamian Archipelago	4	Cat Island	*Guaiacum* sp.	wood	—	OxA-18101	355	25	-24.4	Ostapkowicz 2015
San Salvador	Bahamas	Bahamian Archipelago	2	Major's Cave	*Guaiacum* sp. (Lignum vitae tree), bowl fragment	wood	High Density Area D	Beta-105988	450	50	—	Winter et al. 1999
San Salvador	Bahamas	Bahamian Archipelago	2	Minnis-Ward	wood charcoal	charcoal/ charred material	22-28, hearth	UM-2244	660	100	—	Winter and Stipp 1983
San Salvador	Bahamas	Bahamian Archipelago	2	Minnis-Ward	*Strombus gigas*	marine shell	22cm, hearth	UM-2245	425	75	—	Winter and Stipp 1983
San Salvador	Bahamas	Bahamian Archipelago	4	Minnis-Ward	burnt turtle shell	faunal material	22-28cm, hearth	UM-2243	750	55	—	Winter and Stipp 1983
San Salvador	Bahamas	Bahamian Archipelago	4	Palmetto Grove Site	—	unknown	unknown	Beta-66089	1483	60	—	Berman and Gnivecki 1995
San Salvador	Bahamas	Bahamian Archipelago	4	Palmetto Grove Site	—	unknown	unknown	Beta-67064	1410	80	—	Berman and Gnivecki 1995

San Salvador	Bahamas	Bahamian Archipelago	2	Pigeon Creek	wood charcoal	charcoal/ charred material	26cm	UM-2274	620	70	—	Rose 1987
San Salvador	Bahamas	Bahamian Archipelago	2	Pigeon Creek	wood charcoal	charcoal/ charred material	30-40cm	UM-2271	305	75	—	Rose 1982
San Salvador	Bahamas	Bahamian Archipelago	2	Pigeon Creek	wood charcoal	charcoal/ charred material	30-40cm	UM-2273	580	90	—	Rose 1987
San Salvador	Bahamas	Bahamian Archipelago	2	Pigeon Creek	fish bone	faunal material	40-50cm	UM-2275	1384	65	—	Rose 1982
San Salvador	Bahamas	Bahamian Archipelago	3	Pigeon Creek	wood charcoal	charcoal/ charred material	—	Beta-17839	840	60	—	Rose 1987
San Salvador	Bahamas	Bahamian Archipelago	3	Pigeon Creek	wood charcoal	charcoal/ charred material	—	UM-2733	540	60	—	Rose 1987
San Salvador	Bahamas	Bahamian Archipelago	3	Pigeon Creek	wood charcoal	charcoal/ charred material	—	UM-2736	390	60	—	Rose 1987
San Salvador	Bahamas	Bahamian Archipelago	3	Pigeon Creek	wood charcoal	charcoal/ charred material	—	UM-2738	480	70	—	Rose 1987
San Salvador	Bahamas	Bahamian Archipelago	3	Pigeon Creek	wood charcoal	charcoal/ charred material	10-20cm	UM-2272	215	60	—	Rose 1982
San Salvador	Bahamas	Bahamian Archipelago	4	Pigeon Creek	—	unknown	—	Beta-17840	790	70	—	Rose 1987
San Salvador	Bahamas	Bahamian Archipelago	2	Storr's Lake	charcoal	charcoal/ charred material	38cm	YSU #2	350	70	—	Shaklee et al. 2007
San Salvador	Bahamas	Bahamian Archipelago	2	Storr's Lake	charcoal	charcoal/ charred material	38cm	YSU #4	470	60	—	Shaklee et al. 2007
San Salvador	Bahamas	Bahamian Archipelago	2	Storr's Lake	charcoal	charcoal/ charred material	50cm	YSU #3	1130	40	—	Shaklee et al. 2007
San Salvador	Bahamas	Bahamian Archipelago	2	Storr's Lake	charcoal	charcoal/ charred material	60cm	YSU #1	840	40	—	Shaklee et al. 2007
San Salvador	Bahamas	Bahamian Archipelago	3	Storr's Lake	charcoal	charcoal/ charred material	—	YSU #5	800	60	—	Shaklee et al. 2007

San Salvador	Bahamas	Bahamian Archipelago	4	Three Dog Site	wood charcoal	charcoal/ charred material	unknown	Beta-26138, ETH-4266	—	—	—	Berman and Gnivecki 1995
San Salvador	Bahamas	Bahamian Archipelago	4	Three Dog Site	wood charcoal	charcoal/ charred material	unknown	Beta-26894	—	—	—	Berman and Gnivecki 1995
San Salvador	Bahamas	Bahamian Archipelago	4	Three Dog Site	wood charcoal	charcoal/ charred material	unknown	Beta-55102	—	—	—	Berman and Gnivecki 1995
San Salvador	Bahamas	Bahamian Archipelago	4	Three Dog Site	wood charcoal	charcoal/ charred material	unknown	Beta-55103, CAMS 3549	—	—	—	Berman and Gnivecki 1995
San Salvador	Bahamas	Bahamian Archipelago	3	Three Dog Site	wood charcoal	charcoal/ charred material	unknown	Beta-26896	685	90	—	Berman and Gnivecki 1995
San Salvador	Bahamas	Bahamian Archipelago	4	Three Dog Site	turtle bone	faunal material	—	Beta-18562	490	70	—	Berman and Gnvecki 1991
San Salvador	Bahamas	Bahamian Archipelago	4	Triangle Pond	charcoal	charcoal/ charred material	Core depth: 35 cm	—	—	—	—	Kjellmark and Blick 2016
San Salvador	Bahamas	Bahamian Archipelago	4	Triangle Pond	snail	faunal material	Core depth: 54 cm	UGAMS-12732a	2610	25	-11.64	Kjellmark and Blick 2016
San Salvador	Bahamas	Bahamian Archipelago	4	Triangle Pond	clam	marine shell	Core depth 43 cm	UGAMS-10497	2450	25	-1.24	Kjellmark and Blick 2016
San Salvador	Bahamas	Bahamian Archipelago	4	Triangle Pond	clam	marine shell	Core depth: 54 cm	UGAMS-12772b	2360	25	-0.7	Kjellmark and Blick 2016
San Salvador	Bahamas	Bahamian Archipelago	4	Triangle Pond	leaf fragment	organic material	Core depth: 11 cm	UGAMS-10495	moder n	—	-29.27	Kjellmark and Blick 2016

San Salvador	Bahamas	Bahamian Archipelago	4	Triangle Pond	bark fragment	organic material	Core depth: 28-30 cm	UGAMS-10496	180	20	-26.71	Kjellmark and Blick 2016
San Salvador	Bahamas	Bahamian Archipelago	4	Triangle Pond	peat	peat	Core depth: 50-53 cm	UGAMS-12731	2090	25	-22.02	Kjellmark and Blick 2016
St. Croix	U.S. Virgin Islands	Lesser Antilles	2	Aklis	*Strombus gigas*	marine shell	Unit 1-L 5	Beta-82357	1650	80	—	Cinquino, Hayward, and Hoffman 1999:74, Hayward and Cinquino 2002:94-96; 182
St. Croix	U.S. Virgin Islands	Lesser Antilles	2	Aklis	*Strombus gigas*	marine shell	Unit 1-L-1	Beta-82566	1630	80	—	Cinquino, Hayward, and Hoffman 1999:74, Hayward and Cinquino 2002:94-96; 182
St. Croix	U.S. Virgin Islands	Lesser Antilles	2	Aklis	*Strombus gigas*	marine shell	Unit 3-L 2/3	Beta-82360	1500	70	—	Cinquino, Hayward, and Hoffman 1999:74, Hayward and Cinquino 2002:94-96; 182

St. Croix	U.S. Virgin Islands	Lesser Antilles	2	Aklis	*Strombus gigas*	marine shell	Unit 3-L 7	Beta-82358	1530	70	—	Cinquino, Hayward, and Hoffman 1999:74, Hayward and Cinquino 2002:94-96; 182
St. Croix	U.S. Virgin Islands	Lesser Antilles	4	Aklis	human bone	human bone/teeth	Early Ostionoid ceramic vessel	—	—	—	—	Doran 1990; Hayward and Cinquino 2002:94-96; 182
St. Croix	U.S. Virgin Islands	Lesser Antilles	2	Aklis	*Strombus gigas*	marine shell	Unit 5-L 2	Beta-82359	530	70	—	Cinquino, Hayward, and Hoffman 1999:74, Hayward and Cinquino 2002:94-96; 182
St. Croix	U.S. Virgin Islands	Lesser Antilles	3	Coakley Bay	organic sediment	sediment	—	Beta-376843	2900	30	—	Siegel et al. 2015
St. Croix	U.S. Virgin Islands	Lesser Antilles	4	Coakley Bay	organic sediment	sediment	140 cm	AA-99901	2320	30	-9.4	Pearsall et al. 2018
St. Croix	U.S. Virgin Islands	Lesser Antilles	4	Coakley Bay	organic sediment	sediment	249 cm	AA-77642	3500	40	-18.8	Pearsall et al. 2018
St. Croix	U.S. Virgin Islands	Lesser Antilles	4	Coakley Bay	preserved wood	wood	67 cm	AA-82471	1350	35	-26.9	Pearsall et al. 2018
St. Croix	U.S. Virgin Islands	Lesser Antilles	4	Robin Bay	wood charcoal	charcoal/ charred material	Magens Bay - Salt River 1 level	Beta-32129	—	—	—	Payne 1995
St. Eustatius	Netherlands	Lesser Antilles	3	Corre Corre-1	marine shell	marine shell	40 cm	GrN-17073	2400	50	—	Versteeg et al. 1993

St. Eustatius	Netherlands	Lesser Antilles	3	Corre Corre-2	marine shell	marine shell	70 cm	GrN-17071	2740	40	—	Versteeg et al. 1993
St. Eustatius	Netherlands	Lesser Antilles	3	Godet 1	shell	shell	–	GrN-11518	680	70	+3.16	Van Klinken 1991
St. Eustatius	Netherlands	Lesser Antilles	3	Godet 2	human tooth	human bone/teeth	–	Ua-1481	585	80	-16.18	Van Klinken 1991
St. Eustatius	Netherlands	Lesser Antilles	3	Golden Rock	shell	marine shell	H2	GrN-11511	1600	50	—	Versteeg and Schinkel 1992:204
St. Eustatius	Netherlands	Lesser Antilles	2	Golden Rock	bone collagen	human bone/teeth	B9	Ua-1488	1735	220	-16.56	Versteeg and Schinkel 1992:204
St. Eustatius	Netherlands	Lesser Antilles	2	Golden Rock	charcoal	charcoal/ charred material	1021 (Structure 1)	GrN-11514	1350	60	—	Versteeg and Schinkel 1992:204; Haviser 1997:62
St. Eustatius	Netherlands	Lesser Antilles	2	Golden Rock	charcoal	charcoal/ charred material	1022 (S1)	GrN-11512	1755	20	—	Versteeg and Schinkel 1992:204; Haviser 1997:62
St. Eustatius	Netherlands	Lesser Antilles	2	Golden Rock	charcoal	charcoal/ charred material	1084 (S1)	GrN-11513	1635	20	—	Versteeg and Schinkel 1992:204; Haviser 1997:62
St. Eustatius	Netherlands	Lesser Antilles	2	Golden Rock	charcoal	charcoal/ charred material	149 (S4)	GrN-11515	1205	30	—	Versteeg and Schinkel 1992:204

St. Eustatius	Netherlands	Lesser Antilles	2	Golden Rock	charcoal	charcoal/ charred material	1866 (S5)	GrN-17075	1260	30	—	Versteeg and Schinkel 1992:204
St. Eustatius	Netherlands	Lesser Antilles	2	Golden Rock	charcoal	charcoal/ charred material	2030 (S5)	GrN-17074	1325	30	—	Versteeg and Schinkel 1992:204; Haviser 1997:62
St. Eustatius	Netherlands	Lesser Antilles	2	Golden Rock	charcoal	charcoal/ charred material	209 (S4)	GrN-11516	1340	20	—	Versteeg and Schinkel 1992:204; Haviser 1997:62
St. Eustatius	Netherlands	Lesser Antilles	2	Golden Rock	charcoal	charcoal/ charred material	210 (S4)	GrN-11517	1210	20	—	Versteeg and Schinkel 1992:204
St. Eustatius	Netherlands	Lesser Antilles	2	Golden Rock	charcoal	charcoal/ charred material	H1	GrN-11510	1545	35	—	Versteeg and Schinkel 1992:204; Haviser 1997:62
St. Eustatius	Netherlands	Lesser Antilles	2	Golden Rock	charcoal	charcoal/ charred material	H2	GrN-11509	1415	30	—	Versteeg and Schinkel 1992:204; Haviser 1997:62
St. Eustatius	Netherlands	Lesser Antilles	3	Smoke Alley	charcoal	charcoal/ charred material	—	GrN-17072	1720	30	—	Versteeg et al. 1993
St. Eustatius	Netherlands	Lesser Antilles	2	Smoke Alley	bone collagen	human bone/teeth	8F50	GrN-17070	1105	30	-14.10	Versteeg et al. 1993
St. Eustatius	Netherlands	Lesser Antilles	4	Smoke Alley	—	unknown	—	GrN-18448	160	70	—	Versteeg et al. 1993

St. John	U.S. Virgin Islands	Lesser Antilles	2	Calabash Boom	charcoal	charcoal/ charred material	Pit 13, 20-40 cmbs	Beta-16647	1210	80	—	Caesar et al. 1991; Lundberg et al. 1992
St. John	U.S. Virgin Islands	Lesser Antilles	2	Calabash Boom	charcoal	charcoal/ charred material	Pits 3+4, Level H, 50-90 cmbs	Beta-19863	660	60	—	Caesar et al. 1991; Lundberg et al. 1992
St. John	U.S. Virgin Islands	Lesser Antilles	2	Calabash Boom	charcoal	charcoal/ charred material	Pit 13, level H	Beta-17080	1630	100	—	Lundberg et al. 1992:table 1
St. John	U.S. Virgin Islands	Lesser Antilles	2	Calabash Boom	charcoal	charcoal/ charred material	Pit 17, 35-55 cmbs	Beta-18513	970	70	—	Lundberg et al. 1992:table 1
St. John	U.S. Virgin Islands	Lesser Antilles	2	Calabash Boom	charcoal	charcoal/ charred material	Pit 23, 40-50 cmbs	Beta-20605	1050	60	—	Caesar et al. 1991; Lundberg et al. 1992
St. John	U.S. Virgin Islands	Lesser Antilles	2	Calabash Boom	charcoal	charcoal/ charred material	Pit 27-NE, 60-80 cmbs	Beta-32239	1460	80	—	Lundberg et al. 1992:table 1
St. John	U.S. Virgin Islands	Lesser Antilles	2	Calabash Boom	charcoal	charcoal/ charred material	Pit 27-SE, 60-80 cmbs	Beta-26964	900	100	—	Lundberg et al. 1992:table 1
St. John	U.S. Virgin Islands	Lesser Antilles	2	Calabash Boom	charcoal	charcoal/ charred material	Pit 27-W, 60-80 cmbs	Beta-25891	1130	70	—	Lundberg et al. 1992:table 1
St. John	U.S. Virgin Islands	Lesser Antilles	2	Calabash Boom	charcoal	charcoal/ charred material	Unit 105, level D2	Beta-192223	1160	40	-25.1	Lundberg 2005:table 3
St. John	U.S. Virgin Islands	Lesser Antilles	2	Calabash Boom	charcoal	charcoal/ charred material	Unit 106, level C	Beta-192224	1140	40	-24.7	Lundberg 2005:table 3

St. John	U.S. Virgin Islands	Lesser Antilles	2	Calabash Boom	human bone	human bone/teeth	Burial 4	Beta-27793	1170	80	—	Lundberg et al. 1992:table 1
St. John	U.S. Virgin Islands	Lesser Antilles	2	Calabash Boom	human bone	human bone/teeth	Feature 20	Beta-191882	840	40	-14.4	Lundberg 2005:table 3
St. John	U.S. Virgin Islands	Lesser Antilles	3	Cinnamon Bay	charcoal	charcoal/ charred material	Unit 1, Level 3, 20-30 cmbs	Beta-69973	—	—	—	Wilds 2013
St. John	U.S. Virgin Islands	Lesser Antilles	3	Cinnamon Bay	charcoal	charcoal/ charred material	Unit 3, Level 1, 0-10 cmbs	Beta-184206	—	—	—	Wilds 2013
St. John	U.S. Virgin Islands	Lesser Antilles	3	Cinnamon Bay	charcoal	charcoal/ charred material	Unit 3, Level 2, 10-20 cmbs	Beta-184208	—	—	—	Wilds 2013
St. John	U.S. Virgin Islands	Lesser Antilles	3	Cinnamon Bay	charcoal	charcoal/ charred material	Unit 3, Level 3, 20-30 cmbs	Beta-184209	—	—	—	Wilds 2013
St. John	U.S. Virgin Islands	Lesser Antilles	3	Cinnamon Bay	charcoal	charcoal/ charred material	Unit 3, Level 4, 30-40 cmbs	Beta-184211	—	—	—	Wilds 2013
St. John	U.S. Virgin Islands	Lesser Antilles	3	Cinnamon Bay	charcoal	charcoal/ charred material	Unit 3, Level 6, 50-60 cmbs	Beta-184217	—	—	—	Wilds 2013
St. John	U.S. Virgin Islands	Lesser Antilles	3	Cinnamon Bay	charcoal	charcoal/ charred material	Unit 3, Level 7, 60-70 cmbs	Beta-184212	—	—	—	Wilds 2013
St. John	U.S. Virgin Islands	Lesser Antilles	3	Cinnamon Bay	charcoal	charcoal/ charred material	Unit 3, Level 8, 70-80 cmbs	Beta-184218	—	—	—	Wilds 2013
St. John	U.S. Virgin Islands	Lesser Antilles	4	Cinnamon Bay	bulk sample	bulk sample	Unit 1 and 3, Levels 9, 10, and 11, 80-110 cmbs	Beta-69974	—	—	—	Wilds 2013
St. John	U.S. Virgin Islands	Lesser Antilles	4	Lamesure Beach Access Road (12VAm2-63)	—	unknown	—	—	—	—	—	Bates 2001: 101

St. John	U.S. Virgin Islands	Lesser Antilles	2	Peter Bay Site	charcoal	charcoal/ charred material	BT1-I, Str. 1	Beta-59780	970	80	25.0 (est)	Lundberg 2001:224
St. John	U.S. Virgin Islands	Lesser Antilles	2	Peter Bay Site	charcoal	charcoal/ charred material	Unit 1, Level F2	Beta-59781	1120	100	25.0 (est)	Lundberg 2001:224
St. Kitts	Federation of St. Kitts and Nevis	Lesser Antilles	2	Sugar Factory Pier	*Anadana notebilis*	marine shell	interface of midden base with soil	UCLA-2111a	4100	60	—	Goodwin 1978:13
St. Kitts	Federation of St. Kitts and Nevis	Lesser Antilles	2	Sugar Factory Pier	*Arca zebra*	marine shell	interface of midden base with soil	UCLA-2111b	2175	60	—	Goodwin 1978:13
St. Kitts	Federation of St. Kitts and Nevis	Lesser Antilles	4	Sugar Factory 1	—	unknown	—	UCLA-	4100	60	—	Goodwin 1978:13
St. Lucia	St. Lucia	Lesser Antilles	2	Giraudy	*Strombus* sp.	marine shell	18-24 in.	RL-31	1120	100	—	Bullen and Bullen 1972:153; Rouse et al. 1978:462
St. Lucia	St. Lucia	Lesser Antilles	2	Giraudy	*Strombus* sp.	marine shell	6-12 in.	RL-30	1240	100	—	Bullen and Bullen 1972:153; Rouse et al. 1978:462
St. Lucia	St. Lucia	Lesser Antilles	4	Grande Anse	—	unknown	—	—	490	80	—	Bullen and Bullen 1970
St. Lucia	St. Lucia	Lesser Antilles	2	Grande Anse	charcoal	charcoal/ charred material	5.5 ft.	Y-1115	1460	80	—	Rouse et al. 1978:462; Rouse 1989:397; Haviser 1997:60

St. Lucia	St. Lucia	Lesser Antilles	2	Lavoutte	charcoal	charcoal/ charred material	F67-02	GrN-46604	645	35	—	Hofman et al. 2012
St. Lucia	St. Lucia	Lesser Antilles	2	Lavoutte	human bone	human bone/teeth	F22	GrN-31944	750	30	—	Hofman et al. 2012
St. Lucia	St. Lucia	Lesser Antilles	2	Lavoutte	human bone	human bone/teeth	F57-23	GrN-32314	740	30	—	Hofman et al. 2012
St. Lucia	St. Lucia	Lesser Antilles	2	Lavoutte	human bone	human bone/teeth	F58-23	GrN-32315	720	35	—	Hofman et al. 2012
St. Lucia	St. Lucia	Lesser Antilles	2	Lavoutte	human bone	human bone/teeth	F67-03	GrN-32317	725	35	—	Hofman et al. 2012
St. Lucia	St. Lucia	Lesser Antilles	2	Lavoutte	human bone	human bone/teeth	F67-11	GrN-32319	770	35	—	Hofman et al. 2012
St. Lucia	St. Lucia	Lesser Antilles	2	Lavoutte	bone	human bone/teeth	F67-31	GrN-46607	1000	40	—	Hofman et al. 2012
St. Lucia	St. Lucia	Lesser Antilles	2	Lavoutte	human bone	human bone/teeth	F68-01	GrN-32324	920	25	—	Hofman et al. 2012
St. Lucia	St. Lucia	Lesser Antilles	2	Lavoutte	human bone	human bone/teeth	F68-04	GrN-32325	790	35	—	Hofman et al. 2012
St. Lucia	St. Lucia	Lesser Antilles	2	Lavoutte	human bone	human bone/teeth	F68-06	GrN-32326	865	35	—	Hofman et al. 2012
St. Lucia	St. Lucia	Lesser Antilles	2	Lavoutte	human bone	human bone/teeth	F68-11	GrN-32327	745	30	—	Hofman et al. 2012
St. Lucia	St. Lucia	Lesser Antilles	2	Lavoutte	human bone	human bone/teeth	F68-20	GrN-32328	820	35	—	Hofman et al. 2012
St. Lucia	St. Lucia	Lesser Antilles	2	Lavoutte	human bone	human bone/teeth	F69-02	GrN-32329	620	40	—	Hofman et al. 2012
St. Lucia	St. Lucia	Lesser Antilles	2	Lavoutte	human bone	human bone/teeth	F69-05	GrN-32330	960	35	—	Hofman et al. 2012
St. Lucia	St. Lucia	Lesser Antilles	3	Lavoutte	*Strombus* sp.	marine shell	—	RL-26	710	100	—	Bullen and Bullen 1970; Hofman et al. 2012
St. Lucia	St. Lucia	Lesser Antilles	3	Lavoutte	marine shell	marine shell	05-69-55/2	GrN-32331	950	25	—	Hofman et al. 2012
St. Lucia	St. Lucia	Lesser Antilles	3	Lavoutte	marine shell	marine shell	05-69-55/7	GrN-32332	1070	25	—	Hofman et al. 2012
St. Lucia	St. Lucia	Lesser Antilles	3	Lavoutte	marine shell	marine shell	F67-06/1	GrN-32318	680	25	—	Hofman et al. 2012

St. Lucia	St. Lucia	Lesser Antilles	3	Lavoutte	marine shell	marine shell	F67-24	GrN-32322	805	30	—	Hofman et al. 2012
St. Lucia	St. Lucia	Lesser Antilles	3	Lavoutte	wood	wood	F67-21	GrN-46606	240	35	—	Hofman et al. 2012
St. Lucia	St. Lucia	Lesser Antilles	2	Troumassee	charcoal	charcoal/ charred material	Pit 6	Y-650	1220	100	—	Bullen and Bullen 1972:153, 161; Rouse et al. 1978:462
St. Lucia	St. Lucia	Lesser Antilles	4	Troumassee Site	—	unknown	—	—	1220	110	—	Rouse 1961
St. Lucia	St. Lucia	Lesser Antilles	4	Vieux Fort	carbonized wood	charcoal/ charred material	VF08-1, 414.5 cm	AA-84884	4380	60	-26.7	Siegel et al. 2015
St. Lucia	St. Lucia	Lesser Antilles	4	Vieux Fort	organic sediment	organic material	VF08-1, 60-65 cm	Beta-378827	630	30	-27.0	Siegel et al. 2015
St. Lucia	St. Lucia	Lesser Antilles	4	Vieux Fort	preserved peat	organic material	VF08-1, 60-65 cm	Beta-379163	230	30	-25.3	Siegel et al. 2015
St. Lucia	St. Lucia	Lesser Antilles	4	Vieux Fort	organic sediment	organic material	VF08-1, 60-65 cm	Beta-383083	660	30	-27.2	Siegel et al. 2015
St. Lucia	St. Lucia	Lesser Antilles	4	Vieux Fort	preserved peat	peat	VF08, 655-657 cm	AA-82675	5730	70	-27.4	Siegel et al. 2015
St. Lucia	St. Lucia	Lesser Antilles	4	Vieux Fort	preserved peat	peat	VF08-1, 205-207 cm	AA-84800	1980	35	-26.3	Siegel et al. 2015
St. Lucia	St. Lucia	Lesser Antilles	4	Vieux Fort	organic sediment	sediment	VF08-1, 255-257 cm	AA-84883	2960	30	-31.2	Siegel et al. 2015
St. Martin	St. Martin	Lesser Antilles	2	Anse des Peres	land crab	faunal material	AP 2-A-1	GrN-20160	1180	30	—	Hénocq 1995a:322, 324, 1995b:29
St. Martin	St. Martin	Lesser Antilles	2	Anse des Peres	land crab	faunal material	AP 3-A-2	GrN-20162	1170	30	—	Hénocq 1995a:322, 324, 1995b:29

St. Martin	St. Martin	Lesser Antilles	2	Anse des Peres	land crab	faunal material	AP 5-A-3	GrN-20161	1225	30	—	Hénocq 1995a:322, 324, 1995b:29
St. Martin	St. Martin	Lesser Antilles	2	Baie Longue 2	charcoal	charcoal/ charred material	BL2US2n°5	Beta-187937	3140	40	—	Bonnissent 2008; Watters et al. 1992
St. Martin	St. Martin	Lesser Antilles	2	Baie Longue 2	*Strombus gigas*	marine shell	BL2US2n°2	Beta-187936	3450	40	—	Bonnissent 2008
St. Martin	St. Martin	Lesser Antilles	3	Baie Nettle	—	unknown	—	Beta-261095	4150	40	—	Serrand 2009
St. Martin	St. Martin	Lesser Antilles	2	Baie Orientale 1	charcoal	charcoal/ charred material	S11L16n°2	Beta-146424	2020	40	—	Bonnissent et al. 2001
St. Martin	St. Martin	Lesser Antilles	2	Baie Orientale 1	charcoal	charcoal/ charred material	S23L20n°1	Beta-146425	2270	40	—	Bonnissent et al. 2001; Bonnissent 2008
St. Martin	St. Martin	Lesser Antilles	2	Baie Orientale 1	charcoal	charcoal/ charred material	S39L15n°4	Beta-145372	2420	40	—	Bonnissent et al. 2001
St. Martin	St. Martin	Lesser Antilles	2	Baie Orientale 1	*Strombus gigas*	marine shell	S4L24n°1	Beta-146427	2850	60	—	Bonnissent et al. 2001; Richard 1994
St. Martin	St. Martin	Lesser Antilles	3	Baie Oreintale	shell	marine shell	BO G2-4	GrN-20164	1170	30	—	Hénocq and Petit 1995
St. Martin	St. Martin	Lesser Antilles	3	Baie Orientale 2	parasite	faunal material	BO G2-4	GrN -20177	1280	50	—	Hénocq and Petit 1998
St. Martin	St. Martin	Lesser Antilles	4	Baie Orientale 2	—	unknown	BO S6J-10	Ly-1455 (OxA)	1180	30	—	Bonnissent 2008
St. Martin	St. Martin	Lesser Antilles	2	Baie Orientale 2	*Cittarium pica*	marine shell	BO G2-4	GrN-20164	1170	30	—	Hénocq and Petit 1998

St. Martin	St. Martin	Lesser Antilles	2	Baie aux Prunes	human bone	human bone/teeth	BP99SEP2S25	Ly-2019(OxA)	895	30	—	Bonnissent and Stouvenot 2005
St. Martin	St. Martin	Lesser Antilles	4	Baie aux Prunes	—	unknown	BP99S104AB	Ly-2020(OxA)	705	25	—	Bonnissent and Stouvenot 2005
St. Martin	St. Martin	Lesser Antilles	4	Baie aux Prunes	—	unknown	BP99S24O3D	Ly-2021(OxA)	1035	25	—	Bonnissent and Stouvenot 2005
St. Martin	St. Martin	Lesser Antilles	2	Baie aux Prunes	*Guaiacum* sp.	wood	BP99US213	Ly-11437	890	30	—	Bonnissent and Stouvenot 2005
St. Martin	St. Martin	Lesser Antilles	2	Baie-au-Prunes	wood	wood	bottom of post (center)	Ly-9163	1230	30	—	Stouvenot et al. 2013:480
St. Martin	St. Martin	Lesser Antilles	2	Baie-au-Prunes	wood	wood	bottom of post Peripherial	Ly-11435	890	30	—	Stouvenot et al. 2013:480
St. Martin	St. Martin	Lesser Antilles	3	Baie Rouge	shell	marine shell	BR M1C-9	Beta-82151	840	60	—	Hénocq 1995b; Hénocq 1998
St. Martin	St. Martin	Lesser Antilles	3	Baie Rouge	marine shell	marine shell	BRM1C-10	Beta-82152	880	50	—	Hénocq 1995b; Hénocq 1998
St. Martin	St. Martin	Lesser Antilles	3	Baie Rouge	marine shell	marine shell	BRM1C-2	Beta-82150	1300	60	—	Hénocq 1995b; Hénocq 1998
St. Martin	St. Martin	Lesser Antilles	3	Baie Rouge	marine shell	marine shell	BRM1C-9	Beta82151	840	60	—	Hénocq 1998
St. Martin	St. Martin	Lesser Antilles	3	Belle Créole	Strombe, lame	marine shell	—	Lyon-7579	3810	30	—	Yvon 2009

St. Martin	St. Martin	Lesser Antilles	2	Cul-de-Sac	*Strombus gigas*	marine shell	Cul-de-Sac 2007	KIA-32785	1900	25	—	Bonnissent 2008
St. Martin	St. Martin	Lesser Antilles	3	Cupecoy Bay	marine shell	marine shell	CB10-20 cm	PITT-0157	790	35	—	Haviser 1988
St. Martin	St. Martin	Lesser Antilles	3	Cupecoy Bay	marine shell	marine shell	CB20-30 cm	PITT-0158	1045	25	—	Haviser 1988
St. Martin	St. Martin	Lesser Antilles	3	Cupecoy Bay	marine shell	marine shell	CB30-40 cm	PITT-0159	1715	45	—	Haviser 1988
St. Martin	St. Martin	Lesser Antilles	2	Etang Rouge 1	charcoal	charcoal/ charred material	971270098FE2	Beta-190805	3490	40	—	Bonnissent 2008
St. Martin	St. Martin	Lesser Antilles	2	Etang Rouge 1	charcoal	charcoal/ charred material	ER(B)S2n30	KIA-28122	1494	26	—	Bonnissent 2008
St. Martin	St. Martin	Lesser Antilles	2	Etang Rouge 1	charcoal	charcoal/ charred material	ER1010(D)S1n28	KIA-28117	3095	23	—	Bonnissent 2008
St. Martin	St. Martin	Lesser Antilles	2	Etang Rouge 1	charcoal	charcoal/ charred material	ER1011(D)S1n26	KIA-28118	2951	52	—	Bonnissent 2008
St. Martin	St. Martin	Lesser Antilles	2	Etang Rouge 1	charcoal	charcoal/ charred material	ER1012(D)S1n27	KIA-28119	3655	25	—	Bonnissent 2008
St. Martin	St. Martin	Lesser Antilles	2	Etang Rouge 1	charcoal	charcoal/ charred material	ER1013b(E)S1n3 8	KIA-28120	3366	27	—	Bonnissent 2008
St. Martin	St. Martin	Lesser Antilles	2	Etang Rouge 1	charcoal	charcoal/ charred material	ER1020(E)S1n39	KIA-28121	3828	27	—	Bonnissent 2008
St. Martin	St. Martin	Lesser Antilles	2	Etang Rouge 1	charcoal	charcoal/ charred material	ER4010(E)S4n40	KIA-28123	3684	27	—	Bonnissent 2008
St. Martin	St. Martin	Lesser Antilles	2	Etang Rouge 1	charcoal	charcoal/ charred material	ER4010(E)S4n41	KIA-28124	3598	29	—	Bonnissent 2008
St. Martin	St. Martin	Lesser Antilles	2	Etang Rouge 1	charcoal	charcoal/ charred material	ER6002(D)S2n29	KIA-28125	3235	26	—	Bonnissent 2008
St. Martin	St. Martin	Lesser Antilles	2	Etang Rouge 1	charcoal	charcoal/ charred material	ER6003(D)S2n31	KIA-28126	3447	26	—	Bonnissent 2008
St. Martin	St. Martin	Lesser Antilles	2	Etang Rouge 1	charcoal	charcoal/ charred material	ER7001(E)S3n33	KIA-28127	3429	35	—	Bonnissent 2008

St. Martin	St. Martin	Lesser Antilles	2	Etang Rouge 1	*Strombus gigas*	marine shell	ER1007a(D)S1n23	KIA-28109	3105	30	—	Bonnissent 2008
St. Martin	St. Martin	Lesser Antilles	2	Etang Rouge 1	*Strombus gigas*	marine shell	ER1007a(D)S1n44	KIA-28110	3185	30	—	Bonnissent 2008
St. Martin	St. Martin	Lesser Antilles	2	Etang Rouge 1	*Strombus gigas*	marine shell	ER1007b(D)S1n21	KIA-28111	3380	40	—	Bonnissent 2008
St. Martin	St. Martin	Lesser Antilles	2	Etang Rouge 1	*Strombus gigas*	marine shell	ER1007b(D)S1n45	KIA-28112	3775	30	—	Bonnissent 2008
St. Martin	St. Martin	Lesser Antilles	2	Etang Rouge 1	*Strombus gigas*	marine shell	ER1009(D)S1n34	KIA-28113	3320	30	—	Bonnissent 2008
St. Martin	St. Martin	Lesser Antilles	2	Etang Rouge 1	*Strombus gigas*	marine shell	ER6004(E)S2n32	KIA-28114	3800	30	—	Bonnissent 2008
St. Martin	St. Martin	Lesser Antilles	2	Etang Rouge 1	blade conch	marine shell	ER6005(E)S2n43	KIA-28115	4275	30	—	Bonnissent 2008
St. Martin	St. Martin	Lesser Antilles	2	Etang Rouge 1	*Strombus gigas*	marine shell	ER7002(F)S3n35	KIA-28116	4505	35	—	Bonnissent 2008
St. Martin	St. Martin	Lesser Antilles	2	Etang Rouge 3	*Strombus gigas*	marine shell	ER3 H2	KIA-28815	4830	40	—	Martias 2005
St. Martin	St. Martin	Lesser Antilles	2	Etang Rouge 3	*Strombus gigas*	marine shell	ER3(H)1	KIA-28108	4770	40	—	Martias 2005; Bonnissent 2008
St. Martin	St. Martin	Lesser Antilles	3	Grand Case	shell	marine shell	BK 76	Beta-359544	1340	30	+1.0	Sellier-Segard and Samuelian 2017
St. Martin	St. Martin	Lesser Antilles	3	Grand Case	shell	marine shell	BK 76	Beta-386284	1580	30	+0.7	Sellier-Segard and Samuelian 2017
St. Martin	St. Martin	Lesser Antilles	3	Grand Case	shell	marine shell	BK 76	Beta-286285	1510	30	+1.9	Sellier-Segard and Samuelian 2017

St. Martin	St. Martin	Lesser Antilles	3	Grand Case	shell	marine shell	BK 77	Beta-417001	1390	30	+0.4	Sellier-Segard and Samuelian 2017
St. Martin	St. Martin	Lesser Antilles	3	Grand Case	shell	marine shell	BK 77	Beta-417000	1490	30	+0.4	Sellier-Segard and Samuelian 2017
St. Martin	St. Martin	Lesser Antilles	3	Grand Case	collagen	human bone/teeth	BK 77	Beta-416998	950	30	+14.5	Sellier-Segard and Samuelian 2017
St. Martin	St. Martin	Lesser Antilles	2	Hope Estate	charcoal	charcoal/ charred material	HE A3-2	PITT-0445	1490	35	—	Bonnissent 1998:341
St. Martin	St. Martin	Lesser Antilles	2	Hope Estate	charcoal	charcoal/ charred material	HE 13-A-14	Beta-82153	1590	70	—	Bonnissent 1998:341; Hénocq and Petit 1998
St. Martin	St. Martin	Lesser Antilles	2	Hope Estate	charcoal	charcoal/ charred material	HE 13-B-16	Beta-82154	1710	60	—	Bonnissent 1998:341; Hénocq and Petit 1998
St. Martin	St. Martin	Lesser Antilles	2	Hope Estate	charcoal	charcoal/ charred material	HE 13-D-16	Beta-82155	1540	50	—	Bonnissent 1998:341; Hénocq and Petit 1998
St. Martin	St. Martin	Lesser Antilles	2	Hope Estate	charcoal	charcoal/ charred material	HE 13-D-21	Beta-82156	1870	60	—	Bonnissent 1998:341; Hénocq and Petit 1998
St. Martin	St. Martin	Lesser Antilles	2	Hope Estate	charcoal	charcoal/ charred material	HE 16-US-18	LGQ-1099	1760	160	—	Bonnissent 1998

St. Martin	St. Martin	Lesser Antilles	2	Hope Estate	charcoal	charcoal/ charred material	HE 17-G-10	Beta-82157	1800	60	—	Bonnissent 1998:341; Hénocq and Petit 1998
St. Martin	St. Martin	Lesser Antilles	2	Hope Estate	charcoal	charcoal/ charred material	HE 17-H-10	Beta-82158	1800	50	—	Bonnissent 1998:341; Hénocq and Petit 1998
St. Martin	St. Martin	Lesser Antilles	2	Hope Estate	charcoal	charcoal/ charred material	HE 18-B-11	Beta-82160	1760	50	—	Bonnissent 1998:341; Hénocq and Petit 1998
St. Martin	St. Martin	Lesser Antilles	2	Hope Estate	charcoal	charcoal/ charred material	HE 18-D-9	Beta-82159	1910	50	—	Bonnissent 1998:341; Hénocq and Petit 1998
St. Martin	St. Martin	Lesser Antilles	2	Hope Estate	charcoal	charcoal/ charred material	HE 19-M-17	Beta-82165	1000	50	—	Bonnissent 1998:341
St. Martin	St. Martin	Lesser Antilles	2	Hope Estate	charcoal	charcoal/ charred material	HE 20-14-D	Beta-106228	1770	50	—	Bonnissent et al. 2002
St. Martin	St. Martin	Lesser Antilles	2	Hope Estate	charcoal	charcoal/ charred material	HE 22-4C/B	Beta-106229	1670	50	—	Bonnissent et al. 2002
St. Martin	St. Martin	Lesser Antilles	2	Hope Estate	charcoal	charcoal/ charred material	HE 23-5-B	Beta-106230	1960	60	—	Bonnissent et al. 2002
St. Martin	St. Martin	Lesser Antilles	2	Hope Estate	charcoal	charcoal/ charred material	HE 25-12-B	Beta-106231	1560	60	—	Bonnissent et al. 2002
St. Martin	St. Martin	Lesser Antilles	2	Hope Estate	charcoal	charcoal/ charred material	HE 25-12-C	Beta-106232	1650	70	—	Bonnissent et al. 2002
St. Martin	St. Martin	Lesser Antilles	2	Hope Estate	charcoal	charcoal/ charred material	HE 26-06-C	Beta-106233	1710	70	—	Bonnissent et al. 2002

St. Martin	St. Martin	Lesser Antilles	2	Hope Estate	charcoal	charcoal/ charred material	HE A3-3	PITT-0446	2250	45	—	Bonnissent 1998:341
St. Martin	St. Martin	Lesser Antilles	2	Hope Estate	charcoal	charcoal/ charred material	HE A3-7	PITT-0452	1660	55	—	Haviser 1991; Hoogland 1999
St. Martin	St. Martin	Lesser Antilles	2	Hope Estate	charcoal	charcoal/ charred material	HE A5-8	PITT-0448	2050	45	—	Bonnissent 1998:341
St. Martin	St. Martin	Lesser Antilles	2	Hope Estate	charcoal	charcoal/ charred material	HE T20-3	PITT-0449	2300	55	—	Bonnissent 1998:341
St. Martin	St. Martin	Lesser Antilles	2	Hope Estate	charcoal	charcoal/ charred material	HE T20-3	PITT-0450	2510	40	—	Bonnissent 1998:341
St. Martin	St. Martin	Lesser Antilles	2	Hope Estate	charcoal	charcoal/ charred material	HE Test 1-5	PITT-0219	2275	60	—	Bonnissent 1998:341
St. Martin	St. Martin	Lesser Antilles	2	Hope Estate	charcoal	charcoal/ charred material	HE Test 1-6	PITT-0220	2250	45	—	Bonnissent 1998:341
St. Martin	St. Martin	Lesser Antilles	2	Hope Estate	land crab	faunal material	HE 10-C-3 (posthole)	GrN-20168	1530	30	—	Bonnissent 1998; Haviser 1997:62
St. Martin	St. Martin	Lesser Antilles	2	Hope Estate	land crab	faunal material	HE 6-D-6	GrN-20170	1535	30	—	Hoogland 1999, Bonnissent 1998:341
St. Martin	St. Martin	Lesser Antilles	2	Hope Estate	crab	faunal material	HE 7-B-4	GrN-20169	1520	35	—	Bonnissent 1998:341
St. Martin	St. Martin	Lesser Antilles	3	Hope Estate	human bone	human bone/teeth	—	GrN-20169	1520	35	—	Haviser 1997:62
St. Martin	St. Martin	Lesser Antilles	3	Hope Estate	shell	marine shell	HE 16-US- 19	LGQ-1100	2070	140	—	Bonnissent 1998
St. Martin	St. Martin	Lesser Antilles	3	Hope Estate	marine shell	marine shell	HE 19-F-14	Beta-82163	1900	60	—	Hénocq and Petit 1998, Bonnissent 1998:341

St. Martin	St. Martin	Lesser Antilles	3	Hope Estate	marine shell	marine shell	HE 19-I-10	Beta-82162	1930	80	—	Hénocq and Petit 1998, Bonnissent 1998:341
St. Martin	St. Martin	Lesser Antilles	3	Hope Estate	marine shell	marine shell	HE 19-J-6	Beta-82161	2265	110	—	Hénocq and Petit 1998, Bonnissent 1998:341
St. Martin	St. Martin	Lesser Antilles	3	Hope Estate	marine shell	marine shell	HE 19-O-15	Beta-82164	3360	70	—	Bonnissent 1998:341; Hénocq and Petit 1998
St. Martin	St. Martin	Lesser Antilles	4	Hope Estate	—	unknown	HE 98 2917A	AA-30805	1610	45	-4.87	Serrand 1999
St. Martin	St. Martin	Lesser Antilles	2	Hope Estate	charcoal	charcoal/ charred material	HE 16-US-16	LGQ-1098	1610	150	—	Bonnissent 1998
St. Martin	St. Martin	Lesser Antilles	3	Hope Estate	shell	marine shell	HE A2 5-3	PITT-0451	1510	35	—	Bonnissent 1998
St. Martin	St. Martin	Lesser Antilles	3	Hope Hill	*Lobatus gigas*	marine shell	—	Lyon-9190	3140	40	—	Bonnissent et al. 2016
St. Martin	St. Martin	Lesser Antilles	3	Lot 73	*Lobatus gigas*	marine shell	—	Beta-361277	3120	30	—	Bonnissent et al. 2016
St. Martin	St. Martin	Lesser Antilles	3	Lot 73	*Lobatus gigas*	marine shell	—	Beta-361273	3150	30	—	Bonnissent et al. 2016
St. Martin	St. Martin	Lesser Antilles	3	Lot 73	*Lobatus gigas*	marine shell	—	Beta-361280	3330	30	—	Bonnissent et al. 2016
St. Martin	St. Martin	Lesser Antilles	3	Lot 73	*Lobatus gigas*	marine shell	—	Beta-361279	3390	30	—	Bonnissent et al. 2016
St. Martin	St. Martin	Lesser Antilles	3	Lot 73	*Lobatus gigas*	marine shell	—	Beta-390239	3390	30	—	Bonnissent et al. 2016
St. Martin	St. Martin	Lesser Antilles	3	Lot 73	*Lobatus gigas*	marine shell	—	Beta-361278	3520	30	—	Bonnissent et al. 2016
St. Martin	St. Martin	Lesser Antilles	3	Lot 73	*Codakia orbicularis*	marine shell	—	Beta-390240	3540	30	—	Bonnissent et al. 2016
St. Martin	St. Martin	Lesser Antilles	3	Lot 73	*Codakia orbicularis*	marine shell	—	Beta-390242	3550	30	—	Bonnissent et al. 2016

St. Martin	St. Martin	Lesser Antilles	3	Lot 73	*Codakia orbicularis*	marine shell	—	Beta-361282	3750	30	—	Bonnissent et al. 2016
St. Martin	St. Martin	Lesser Antilles	3	Lot 73	*Codakia orbicularis*	marine shell	—	Beta-390241	3580	30	—	Bonnissent et al. 2016
St. Martin	St. Martin	Lesser Antilles	3	Lot 73	*Lobatus gigas*	marine shell	—	Beta-361281	3830	30	—	Bonnissent et al. 2016
St. Martin	St. Martin	Lesser Antilles	3	Lot 73	*Codakia orbicularis*	marine shell	—	Beta-390243	3820	30	—	Bonnissent et al. 2016
St. Martin	St. Martin	Lesser Antilles	3	Lot 73	*Codakia orbicularis*	marine shell	—	Beta-390244	3850	30	—	Bonnissent et al. 2016
St. Martin	St. Martin	Lesser Antilles	2	Norman Estate 1	Strombidae blade	marine shell	NE92 Surf.	Beta-41782	3580	90	—	Hénocq 1995a, 1995b
St. Martin	St. Martin	Lesser Antilles	2	Norman Estate 2	charcoal	charcoal/ charred material	NE2D2	Beta-224792	2610	40	—	Bonnissent 2008
St. Martin	St. Martin	Lesser Antilles	2	Norman Estate 2	*Strombus gigas*	marine shell	NE2D4	Beta-224793	3240	60	—	Bonnissent 2008
St. Martin	St. Martin	Lesser Antilles	3	Norman Estate	shell	marine shell	NE 19-2	GrN-20158	3590	50	—	Hénocq 1995a, 1995b
St. Martin	St. Martin	Lesser Antilles	3	Norman Estate	shell	marine shell	NE 23-D-1	GrN-20157	3730	30	—	Hénocq 1995a, 1995b
St. Martin	St. Martin	Lesser Antilles	3	Norman Estate	shell	marine shell	NE 6-E-3	GrN-20159	3780	40	—	Hénocq 1995a, 1995b
St. Martin	St. Martin	Lesser Antilles	2	Petite Plage 1	*Strombus gigas*	marine shell	PPO4B2	KIA-28963	1585	25	—	Bonnissent 2008
St. Martin	St. Martin	Lesser Antilles	2	Petite Plage 2	*Strombus gigas*	marine shell	PPO4B	Beta-200098	1330	60	—	Bonnissent 2008
St. Martin	St. Martin	Lesser Antilles	2	Pinel Ouest	charcoal	charcoal/ charred material	PO1104n°3	Beta-187940	1560	40	—	Bonnissent 2008
St. Martin	St. Martin	Lesser Antilles	2	Pinel Ouest	*Strombus gigas*	marine shell	PO1706B2n°2	Beta-187941	1810	40	—	Bonnissent 2008
St. Martin	St. Martin	Lesser Antilles	2	Pointe du Bluff	*Strombus gigas*	marine shell	PTE-BLUFF surf	Erl-9064	3460	50	—	Bonnissent 2008
St. Martin	St. Martin	Lesser Antilles	2	Pointe du Canonnier	*Strombus gigas*	marine shell	PDC6006C2n°2	Beta-187938	1540	40	—	Bonnissent 2008

St. Martin	St. Martin	Lesser Antilles	4	Pointe du Canonnier	—	unknown	PDC6006C4n°5	Beta-187939	1290	40	—	Bonnissent 2008
St. Martin	St. Martin	Lesser Antilles	2	Salines d'Orient	*Strombus gigas*	marine shell	SAOR-1004-1	Erl-9071	3750	50	—	Bonnissent 2008
St. Martin	St. Martin	Lesser Antilles	2	Salines d'Orient	*Strombus gigas*	marine shell	SAOR-1004-2	Erl-9072	3610	50	—	Bonnissent 2008
St. Martin	St. Martin	Lesser Antilles	2	Sandy Ground 1	blade conch	marine shell	SAND-GR1	Erl-9065	3340	50	—	Bonnissent 2008
St. Martin	St. Martin	Lesser Antilles	2	Sandy Ground 2	blade conch	marine shell	SAND-GR2	Erl-9066	4200	50	—	Bonnissent 2008
St. Martin	St. Martin	Lesser Antilles	2	Trou David 1	charcoal	charcoal/ charred material	TD1n1	Erl-9074	3515	45	—	Bonnissent 2008
St. Martin	St. Martin	Lesser Antilles	2	Trou David 1	*Strombus gigas*	marine shell	TD1n4	Erl-9073	3510	50	—	Bonnissent 2008
St. Martin	St. Martin	Lesser Antilles	2	Trou David 2	human bone	human bone/teeth	TRD2-SURF	Erl-8235	2070	50	—	Bonnissent 2008
St. Martin	St. Martin	Lesser Antilles	3	Rue Maurasse	—	marine shell	—	Beta-435488	3140	30	—	Sellier-Ségard 2016
St. Thomas	U.S. Virgin Islands	Lesser Antilles	2	Arboretum	*Chione cancellata*	marine shell	Pit 10, Level E, 35-45 cmbs	L-1380B	2410	60	—	Tilden 1976: 244; Rouse et al. 1978:468
St. Thomas	U.S. Virgin Islands	Lesser Antilles	2	Arboretum	*Chione cancellata*	marine shell	Pit, 10, Level J, 85-95 cmbs	L-1380A	1900	70	—	Tilden 1976: 244; Rouse et al. 1978:468
St. Thomas	U.S. Virgin Islands	Lesser Antilles	3	Cancel Hill	*Arca zebra*	marine shell	—	I-8643	2820	85	—	Gross 1976:234; Rouse et al. 1978:468

St. Thomas	U.S. Virgin Islands	Lesser Antilles	4	Hull Bay	—	unknown	TP 5, 100-110 cmbs	RL-409	640	110	—	Rouse et al. 1978:468; Lundberg 1992:table 2
St. Thomas	U.S. Virgin Islands	Lesser Antilles	4	Hull Bay	—	unknown	TP 6B and 13, 80-90 cmbs	RL-411	730	110	—	Rouse et al. 1978:468; Lundberg 1992:table 2
St. Thomas	U.S. Virgin Islands	Lesser Antilles	3	Grambokola Hill	*Arca zebra*	marine shell	—	I-8642	2785	85	—	Gross 1976:234
St. Thomas	U.S. Virgin Islands	Lesser Antilles	2	Krum Bay	*Busycon gigas*	marine shell	third midden level	I-621	2400	175	—	Bullen and Sleight 1963:41; Rouse et al. 1978:46
St. Thomas	U.S. Virgin Islands	Lesser Antilles	2	Krum Bay	*Arca zebra*	marine shell	Unit 5, level N	Beta-7022	2860	70	+1.33	Lundberg 1989:table 3, 87
St. Thomas	U.S. Virgin Islands	Lesser Antilles	2	Krum Bay	*Arca zebra*	marine shell	Unit 6, level C	SI-5848	1805	75	—	Lundberg 1989:table 3
St. Thomas	U.S. Virgin Islands	Lesser Antilles	2	Krum Bay	*Arca zebra*	marine shell	Unit 6, level E	SI-5849	1595	75	—	Lundberg 1989:table 3
St. Thomas	U.S. Virgin Islands	Lesser Antilles	2	Krum Bay	*Arca zebra*	marine shell	Unit 6, level I	SI-5850	2130	60	—	Lundberg 1989:table 3
St. Thomas	U.S. Virgin Islands	Lesser Antilles	2	Krum Bay	*Arca zebra*	marine shell	Unit 6, level K	SI-5851	2700	65	—	Lundberg 1989:table 3
St. Thomas	U.S. Virgin Islands	Lesser Antilles	3	Krum Bay	charcoal	charcoal/ charred material	B1, L-III	RL-412	moder n	—	—	Gross 1976:234

St. Thomas	U.S. Virgin Islands	Lesser Antilles	3	Krum Bay	charcoal	charcoal/ charred material	Unit 6, level N	Beta-5778	3580	270	—	Lundberg 1989:table 3
St. Thomas	U.S. Virgin Islands	Lesser Antilles	3	Krum Bay	*Arca zebra*	marine shell	Unit 6, level O	SI-5852	2535	55	—	Lundberg 1989:table 3
St. Thomas	U.S. Virgin Islands	Lesser Antilles	4	Krum Bay	charcoal	charcoal/ charred material	Unit 6, level B	Beta-5777	120	90	—	Lundberg 1989:table 3
St. Thomas	U.S. Virgin Islands	Lesser Antilles	4	Krum Bay	*Arca zebra*	marine shell	Unit 6, level B	SI-5847	2030	80	—	Lundberg 1989:table 3
St. Thomas	U.S. Virgin Islands	Lesser Antilles	2	Krum Bay	*Busycon gigas*	marine shell	first midden level	I-620	2175	160	—	Bullen and Sleight 1963:41; Rouse et al. 1978:468
St. Thomas	U.S. Virgin Islands	Lesser Antilles	2	Krum Bay	*Arca zebra*	marine shell	Unit B1, Stratum III	I-8641	2775	85	+2.2	Gross 1976:234; Rouse et al. 1978:468
St. Thomas	U.S. Virgin Islands	Lesser Antilles	2	Krum Bay	*Arca zebra*	marine shell	Unit B1, Stratum VI	I-8640	2830	85	+2.3	Gross 1976:234; Rouse et al. 1978:468
St. Thomas	U.S. Virgin Islands	Lesser Antilles	3	Krum Bay A	shell	marine shell	Hatt's layer 2	Beta-445042	2600	30	+1.6	Toftgaard 2019
St. Thomas	U.S. Virgin Islands	Lesser Antilles	3	Krum Bay A	shell	marine shell	Hatt's layer 4	Beta-445861	2420	30	+1.1	Toftgaard 2019
St. Thomas	U.S. Virgin Islands	Lesser Antilles	3	Krum Bay A	shell	marine shell	Hatt's layer 3	Beta-445862	3080	30	+3.2	Toftgaard 2019
St. Thomas	U.S. Virgin Islands	Lesser Antilles	3	Krum Bay A	shell	marine shell	Hatt's layer 3	Beta-445863	2900	30	+2.1	Toftgaard 2019
St. Thomas	U.S. Virgin Islands	Lesser Antilles	3	Krum Bay B	shell	marine shell	Hatt's layer 2	Beta-445038	3280	30	+2.6	Toftgaard 2019
St. Thomas	U.S. Virgin Islands	Lesser Antilles	3	Krum Bay B	shell	marine shell	Hatt's layer 2	Beta-445039	3190	30	+1.6	Toftgaard 2019

St. Thomas	U.S. Virgin Islands	Lesser Antilles	3	Krum Bay B	shell	marine shell	Hatt's layer 2	Beta-445040	3120	30	+3.9	Toftgaard 2019
St. Thomas	U.S. Virgin Islands	Lesser Antilles	3	Krum Bay B	shell	marine shell	Hatt's layer 1	Beta-445041	2920	30	+2.8	Toftgaard 2019
St. Thomas	U.S. Virgin Islands	Lesser Antilles	2	Magens Bay	charcoal	charcoal/ charred material	Unit 3, level B	Beta-49751	1040	150	—	Lundberg et al. 1992:table 2; Wing et al. 2002
St. Thomas	U.S. Virgin Islands	Lesser Antilles	2	Main Street	charcoal	charcoal/ charred material	Utility trench, lowest cultural stratum	GX-12845	1770	235	—	Rouse 1989; Lundberg et al. 1992:table 2
St. Thomas	U.S. Virgin Islands	Lesser Antilles	4	Main Street	—	unknown	Lowest Stratum	Kreuger Ent.	—	—	—	Wing et al. 2002
St. Thomas	U.S. Virgin Islands	Lesser Antilles	2	Tutu	charcoal	charcoal/ charred material	A 1, 2097N/1821.50E (EU 3), E/gravel 1	Beta-111459	2710	120	—	Righter 2002:table 1.3; Lundberg personal communication
St. Thomas	U.S. Virgin Islands	Lesser Antilles	2	Tutu	charcoal	charcoal/ charred material	Area 1, 2097N/1821.50E (EU 3), BI	Beta-108889	1500	50	-25.3	Lundberg 2002:table 5.1
St. Thomas	U.S. Virgin Islands	Lesser Antilles	2	Tutu	charcoal	charcoal/ charred material	Area 1, 2097N/1821.50E (EU 3), BIII	Beta-111462	1980	50	—	Lundberg 2002:table 5.1
St. Thomas	U.S. Virgin Islands	Lesser Antilles	2	Tutu	charcoal	charcoal/ charred material	Area 1, 2097N/1822.50E (EU 10), D	Beta-108917	2090	50	-27.2	Lundberg 2002:table 5.1
St. Thomas	U.S. Virgin Islands	Lesser Antilles	2	Tutu	charcoal	charcoal/ charred material	Area 1, 2097N/1823.50E (EU 4), B	Beta-108888	1720	140	-24.6	Lundberg 2002:table 5.1

St. Thomas	U.S. Virgin Islands	Lesser Antilles	2	Tutu	charcoal	charcoal/ charred material	Area 9N, 2075N/1810E (EU 33), B2	Beta-65472	1580	50	-26.6	Righter 2002:table 1.3; Lundberg personal communication
St. Thomas	U.S. Virgin Islands	Lesser Antilles	2	Tutu	charcoal	charcoal/ charred material	Area 9S, 2036N/1842E (EU 26), C	Beta-111452	560	80	—	Lundberg 2002:table 5.4
St. Thomas	U.S. Virgin Islands	Lesser Antilles	2	Tutu	charcoal	charcoal/ charred material	Area 9S, 2037N/1842E (EU 25), C	Beta-111461	650	50	—	Lundberg 2002:table 5.4
St. Thomas	U.S. Virgin Islands	Lesser Antilles	2	Tutu	charcoal	charcoal/ charred material	Area 9S, 2037N/1842E (EU 25), I	Beta-48742	810	140	—	Righter 2002:table 1.3; Lundberg personal communication
St. Thomas	U.S. Virgin Islands	Lesser Antilles	2	Tutu	charred wood	charcoal/ charred material	F-20, Posthole burial 14 (unit and level)	Beta-65469	1310	60	—	Righter 2002, Lundberg personal communication
St. Thomas	U.S. Virgin Islands	Lesser Antilles	2	Tutu	charred wood	charcoal/ charred material	P-15, Str. 1 (unit and level)	Beta-42277	730	80	—	Righter 2002; Lundberg personal communication
St. Thomas	U.S. Virgin Islands	Lesser Antilles	2	Tutu	*Guaiacum* sp.	wood	P-407A, Str. 2 (unit and level)	Beta-43437	810	70	—	Righter 2002; Lundberg personal communication

St. Thomas	U.S. Virgin Islands	Lesser Antilles	3	Tutu	charcoal	charcoal/ charred material	Area 4, 2087N/1952E (EU 31), A	Beta-65470	40	50	—	Righter 2002:table 1.3; Lundberg personal communication
St. Thomas	U.S. Virgin Islands	Lesser Antilles	3	Tutu	charcoal	charcoal/ charred material	Area 4, 2087N/1952E (EU 31), BIII	Beta-65471	70	50	—	Righter 2002:table 1.3; Lundberg personal communication
St. Thomas	U.S. Virgin Islands	Lesser Antilles	3	Tutu	human bone	human bone/teeth	Burial 39, Str. 8	Beta-83002	80	30	-18.9	Righter 2002
St. Thomas	U.S. Virgin Islands	Lesser Antilles	4	Tutu	charred wood	charcoal/ charred material	P-101, Str. 3 (unit and level)	Beta-108904	—	—	—	Righter 2002
St. Thomas	U.S. Virgin Islands	Lesser Antilles	4	Tutu	charred wood	charcoal/ charred material	P-103 (unit and level)	Beta-111454	—	—	—	Righter 2002
St. Thomas	U.S. Virgin Islands	Lesser Antilles	4	Tutu	charred wood	charcoal/ charred material	P-1067 (unit and level)	Beta-112964	—	—	—	Righter 2002
St. Thomas	U.S. Virgin Islands	Lesser Antilles	4	Tutu	charred wood	charcoal/ charred material	P-114, Str. 7 (unit and level)	Beta-108885	—	—	—	Righter 2002
St. Thomas	U.S. Virgin Islands	Lesser Antilles	4	Tutu	charred wood	charcoal/ charred material	P-116(2)A, Str. 8 (unit and level)	Beta-108894	—	—	—	Righter 2002
St. Thomas	U.S. Virgin Islands	Lesser Antilles	4	Tutu	charred wood	charcoal/ charred material	P-146 (unit and level)	Beta-108899	—	—	—	Righter 2002
St. Thomas	U.S. Virgin Islands	Lesser Antilles	4	Tutu	charred wood	charcoal/ charred material	P-1763A, Str. 7 (unit and level)	Beta-108893	—	—	—	Righter 2002
St. Thomas	U.S. Virgin Islands	Lesser Antilles	4	Tutu	charred wood	charcoal/ charred material	P-1764A, Str. 7 (unit and level)	Beta-111456	—	—	—	Righter 2002
St. Thomas	U.S. Virgin Islands	Lesser Antilles	4	Tutu	charred wood	charcoal/ charred material	P-1822 (unit and level)	Beta-108921	—	—	—	Righter 2002

St. Thomas	U.S. Virgin Islands	Lesser Antilles	4	Tutu	charred wood	charcoal/ charred material	P-1841, Str. 8 (unit and level)	Beta-111463	—	—	—	Righter 2002
St. Thomas	U.S. Virgin Islands	Lesser Antilles	4	Tutu	charred wood	charcoal/ charred material	P-192 (unit and level)	Beta-108890	—	—	—	Righter 2002
St. Thomas	U.S. Virgin Islands	Lesser Antilles	4	Tutu	charred wood	charcoal/ charred material	P-2071A, Str. 5 (unit and level)	Beta-108911	—	—	—	Righter 2002
St. Thomas	U.S. Virgin Islands	Lesser Antilles	4	Tutu	charred wood	charcoal/ charred material	P-2073A, Str. 5 (unit and level)	Beta-108916	—	—	—	Righter 2002
St. Thomas	U.S. Virgin Islands	Lesser Antilles	4	Tutu	charred wood	charcoal/ charred material	P-283A, Str. 8 (unit and level)	Beta-108898	—	—	—	Righter 2002
St. Thomas	U.S. Virgin Islands	Lesser Antilles	4	Tutu	charred wood	charcoal/ charred material	P-3024A, Str. 5 (unit and level)	Beta-111458	—	—	—	Righter 2002
St. Thomas	U.S. Virgin Islands	Lesser Antilles	4	Tutu	charred wood	charcoal/ charred material	P-3063A, Str. 8 (unit and level)	Beta-108913	—	—	—	Righter 2002
St. Thomas	U.S. Virgin Islands	Lesser Antilles	4	Tutu	charred wood	charcoal/ charred material	P-3078 (unit and level)	Beta-108915	—	—	—	Righter 2002
St. Thomas	U.S. Virgin Islands	Lesser Antilles	4	Tutu	charred wood	charcoal/ charred material	P-526, Str. 6 (unit and level)	Beta-111460	—	—	—	Righter 2002
St. Thomas	U.S. Virgin Islands	Lesser Antilles	4	Tutu	charred wood	charcoal/ charred material	P-531, Str. 6 (unit and level)	Beta-111455	—	—	—	Righter 2002
St. Thomas	U.S. Virgin Islands	Lesser Antilles	4	Tutu	charred wood	charcoal/ charred material	P-535A, Str. 6 (unit and level)	Beta-111457	—	—	—	Righter 2002
St. Thomas	U.S. Virgin Islands	Lesser Antilles	4	Tutu	charred wood	charcoal/ charred material	P-53A, Str. 8 (unit and level)	Beta-108908	—	—	—	Righter 2002
St. Thomas	U.S. Virgin Islands	Lesser Antilles	4	Tutu	charred wood	charcoal/ charred material	P-54A, Str. 8 (unit and level)	Beta-108895	—	—	—	Righter 2002
St. Thomas	U.S. Virgin Islands	Lesser Antilles	4	Tutu	charred wood	charcoal/ charred material	P-552, Str. 5 (unit and level)	Beta-108892	—	—	—	Righter 2002
St. Thomas	U.S. Virgin Islands	Lesser Antilles	4	Tutu	charred wood	charcoal/ charred material	P-59, Str. 7 (unit and level)	Beta-108910	—	—	—	Righter 2002

St. Thomas	U.S. Virgin Islands	Lesser Antilles	4	Tutu	charred wood	charcoal/ charred material	P-601A, Str. 3 (unit and level)	Beta-112968	—	—	—	Righter 2002
St. Thomas	U.S. Virgin Islands	Lesser Antilles	4	Tutu	charred wood	charcoal/ charred material	P-61 (unit and level)	Beta-108901	—	—	—	Righter 2002
St. Thomas	U.S. Virgin Islands	Lesser Antilles	4	Tutu	charred wood	charcoal/ charred material	P-77 (unit and level)	Beta-108906	—	—	—	Righter 2002
St. Thomas	U.S. Virgin Islands	Lesser Antilles	4	Tutu	charred wood	charcoal/ charred material	P-78(2)A, Str. 7 (unit and level)	Beta-108909	—	—	—	Righter 2002
St. Thomas	U.S. Virgin Islands	Lesser Antilles	4	Tutu	charred wood	charcoal/ charred material	P-81A, Str. 8 (unit and level)	Beta-112969	—	—	—	Righter 2002
St. Thomas	U.S. Virgin Islands	Lesser Antilles	4	Tutu	charred wood	charcoal/ charred material	P-82A (unit and level)	Beta-108912	—	—	—	Righter 2002
St. Thomas	U.S. Virgin Islands	Lesser Antilles	4	Tutu	charred wood	charcoal/ charred material	P-830, Str. 4 (unit and level)	Beta-108897	—	—	—	Righter 2002
St. Thomas	U.S. Virgin Islands	Lesser Antilles	4	Tutu	charred wood	charcoal/ charred material	P-834, Str. 4 (unit and level)	Beta-108907	—	—	—	Righter 2002
St. Thomas	U.S. Virgin Islands	Lesser Antilles	4	Tutu	charred wood	charcoal/ charred material	P-884A(2), Str. 4 (unit and level)	Beta-112965	—	—	—	Righter 2002
St. Thomas	U.S. Virgin Islands	Lesser Antilles	4	Tutu	charred wood	charcoal/ charred material	P-92, Str. 8 (unit and level)	Beta-108900	—	—	—	Righter 2002
St. Thomas	U.S. Virgin Islands	Lesser Antilles	4	Tutu	*Acacia* sp.	wood	P-111A (unit and level)	Beta-108919	—	—	—	Righter 2002
St. Thomas	U.S. Virgin Islands	Lesser Antilles	4	Tutu	*Acacia* sp.	wood	P-131A (unit and level)	Beta-108891	—	—	—	Righter 2002
St. Thomas	U.S. Virgin Islands	Lesser Antilles	4	Tutu	*Acacia* sp.	wood	P-214A (unit and level)	Beta-108903	—	—	—	Righter 2002
St. Thomas	U.S. Virgin Islands	Lesser Antilles	4	Tutu	*Acacia* sp.	wood	P-294(1)A, Str. 8 (unit and level)	Beta-108905	—	—	—	Righter 2002

St. Thomas	U.S. Virgin Islands	Lesser Antilles	4	Tutu	*Acacia* sp.	wood	P-3, Tr-1 (unit and level)	Beta-111453	—	—	—	Righter 2002
St. Thomas	U.S. Virgin Islands	Lesser Antilles	4	Tutu	*Croton* sp.	wood	P-41A, Str. 7 (unit and level)	Beta-108887	—	—	—	Righter 2002
St. Thomas	U.S. Virgin Islands	Lesser Antilles	4	Tutu	*Acacia* sp.	wood	P-4A, Str. 7 (unit and level)	Beta-112967	—	—	—	Righter 2002
St. Thomas	U.S. Virgin Islands	Lesser Antilles	4	Tutu	*Acacia* sp.	wood	P-760A, Str. 8 (unit and level)	Beta-108896	—	—	—	Righter 2002
St. Thomas	U.S. Virgin Islands	Lesser Antilles	2	Tutu	charcoal	charcoal/ charred material	Area 1; 2096N/1827E, (EU 6), B	Beta-65474	1800	80	—	Lundberg 2002:table 5.1
St. Thomas	U.S. Virgin Islands	Lesser Antilles	2	Tutu	charcoal	charcoal/ charred material	Area 4; 2087N/1952E, (EU 31), B	Beta-50066	1610	70	—	Wing et al. 2002, Lundberg 2002:table 5.2
St. Thomas	U.S. Virgin Islands	Lesser Antilles	2	Tutu	charcoal	charcoal/ charred material	Area 4; 2090N/1948E, (EU 26), D	Beta-54646	1560	90	—	Lundberg 2002:table 5.2
St. Thomas	U.S. Virgin Islands	Lesser Antilles	2	Tutu	charcoal	charcoal/ charred material	Area 8; 2113N/1840E (EU 15), B	Beta-65473	1570	60	—	Wing et al. 2002; Righter 2002:table 1.3; Lundberg personal communication
St. Thomas	U.S. Virgin Islands	Lesser Antilles	2	Tutu	charcoal	charcoal/ charred material	Area 9N, 2075N/1810E, B2	CAMS-10696	1550	50	—	Wing et al. 2002
St. Thomas	U.S. Virgin Islands	Lesser Antilles	2	Tutu	charcoal	charcoal/ charred material	Area 9S; 2036N/1842E (EU 26), B base	Beta-51355	720	120	—	Lundberg 2002:table 5.4

St. Thomas	U.S. Virgin Islands	Lesser Antilles	2	Tutu	charcoal	charcoal/ charred material	Area 9S; 2036N/1842E (EU 26), B top	Beta-51354	560	120	—	Lundberg 2002:table 5.4
St. Thomas	U.S. Virgin Islands	Lesser Antilles	2	Tutu	charcoal	charcoal/ charred material	Area 9W; 2044N/1837E, (EU 1), D	Beta-62568	1430	90	—	Lundberg 2002:table 5.3
St. Thomas	U.S. Virgin Islands	Lesser Antilles	2	Tutu	charcoal	charcoal/ charred material	Area 9W; 2044N/1837E, (EU 1), F	Beta-62569	1400	120	—	Lundberg 2002:table 5.3
St. Thomas	U.S. Virgin Islands	Lesser Antilles	2	Tutu	charcoal	charcoal/ charred material	Area 9W; 2044N/1837E, (EU 1), I	Beta-62570	1380	90	—	Lundberg 2002:table 5.3
St. Thomas	U.S. Virgin Islands	Lesser Antilles	2	Tutu	human bone	human bone/teeth	Burial 1, N2059 E1835	Beta-73390	640	60	-17.2	Righter 2002
St. Thomas	U.S. Virgin Islands	Lesser Antilles	2	Tutu	human bone	human bone/teeth	Burial 10, N2097 E1858	Beta-88345	1390	40	-17.7	Righter 2002
St. Thomas	U.S. Virgin Islands	Lesser Antilles	2	Tutu	human bone	human bone/teeth	Burial 11, N2096 E1842	Beta-88346	390	40	-16.9	Righter 2002
St. Thomas	U.S. Virgin Islands	Lesser Antilles	2	Tutu	human bone	human bone/teeth	Burial 12, Str. in Area 4	Beta-83008	540	30	-19.8	Righter 2002
St. Thomas	U.S. Virgin Islands	Lesser Antilles	2	Tutu	human bone	human bone/teeth	Burial 13, Str. in Area 1	Beta-83009	1300	30	-17.6	Righter 2002
St. Thomas	U.S. Virgin Islands	Lesser Antilles	2	Tutu	human bone	human bone/teeth	Burial 13A, Str. in Area 1	Beta-83006	1280	40	-15.3	Righter 2002
St. Thomas	U.S. Virgin Islands	Lesser Antilles	2	Tutu	human bone	human bone/teeth	Burial 16, Area 6	Beta-73392	1190	60	-17.7	Righter 2002
St. Thomas	U.S. Virgin Islands	Lesser Antilles	2	Tutu	human bone	human bone/teeth	Burial 19, Str. in Area 9N	Beta-73393	600	60	-17.5	Righter 2002
St. Thomas	U.S. Virgin Islands	Lesser Antilles	2	Tutu	human bone	human bone/teeth	Burial 2, N2061 E1833	Beta-109070	450	50	-18.8	Righter 2002

St. Thomas	U.S. Virgin Islands	Lesser Antilles	2	Tutu	human bone	human bone/teeth	Burial 20, Str. in Area 4	Beta-109072	380	50	-18.3	Righter 2002
St. Thomas	U.S. Virgin Islands	Lesser Antilles	2	Tutu	human bone	human bone/teeth	Burial 21, Area 5	Beta-83011	1390	40	-17.5	Righter 2002
St. Thomas	U.S. Virgin Islands	Lesser Antilles	2	Tutu	human bone	human bone/teeth	Burial 22B, Str. 2	Beta-83005	600	30	-18.3	Righter 2002
St. Thomas	U.S. Virgin Islands	Lesser Antilles	2	Tutu	human bone	human bone/teeth	Burial 23B, Area 6	Beta-83000	1330	30	-19.3	Righter 2002
St. Thomas	U.S. Virgin Islands	Lesser Antilles	2	Tutu	human bone	human bone/teeth	Burial 26, Trench 6, Area 6	Beta-88347	560	40	-18.8	Righter 2002
St. Thomas	U.S. Virgin Islands	Lesser Antilles	2	Tutu	human bone	human bone/teeth	Burial 29, Str. 3	Beta-73394	630	60	-18.2	Righter 2002
St. Thomas	U.S. Virgin Islands	Lesser Antilles	2	Tutu	human bone	human bone/teeth	Burial 3, Area 9S	Beta-83010	1090	30	-19.4	Righter 2002
St. Thomas	U.S. Virgin Islands	Lesser Antilles	2	Tutu	human bone	human bone/teeth	Burial 30, Area 9N	Beta-88348	470	40	-17.7	Righter 2002
St. Thomas	U.S. Virgin Islands	Lesser Antilles	2	Tutu	human bone	human bone/teeth	Burial 31, Str. 8	Beta-83004	500	30	-22.4	Righter 2002
St. Thomas	U.S. Virgin Islands	Lesser Antilles	2	Tutu	human bone	human bone/teeth	Burial 33 Str. 4	Beta-88349	460	40	-17.1	Righter 2002
St. Thomas	U.S. Virgin Islands	Lesser Antilles	2	Tutu	human bone	human bone/teeth	Burial 36, Area 5	Beta-83003	1390	30	-16.6	Righter 2002
St. Thomas	U.S. Virgin Islands	Lesser Antilles	2	Tutu	human bone	human bone/teeth	Burial 38 N2081 E1842	Beta-73395	590	90	-16.1	Righter 2002
St. Thomas	U.S. Virgin Islands	Lesser Antilles	2	Tutu	human bone	human bone/teeth	Burial 4, N2015 E1855	Beta-83001	1330	30	-20.7	Righter 2002
St. Thomas	U.S. Virgin Islands	Lesser Antilles	2	Tutu	human bone	human bone/teeth	Burial 5, Str. 8	Beta-88344	300	40	-18.6	Righter 2002
St. Thomas	U.S. Virgin Islands	Lesser Antilles	2	Tutu	human bone	human bone/teeth	Burial 6, Str. 3	Beta-109071	480	50	-19.5	Righter 2002
St. Thomas	U.S. Virgin Islands	Lesser Antilles	2	Tutu	human bone	human bone/teeth	Burial 8B, N2083 E1839	Beta-83007	340	30	-16.9	Righter 2002

St. Thomas	U.S. Virgin Islands	Lesser Antilles	2	Tutu	human bone	human bone/teeth	Burial 9, Area 4, Str. 6	Beta-73391	580	60	-16.1	Righter 2002
St. Vincent	St. Vincent and the Grenadines	Lesser Antilles	2	Arnos Vale	charcoal	charcoal/ charred material	black cultural zone	RL-75	1540	110	—	Bullen and Bullen 1972:77; Haviser 1997:60
St. Vincent	St. Vincent and the Grenadines	Lesser Antilles	3	Battowia	*Guaiacum* sp.	wood	Museum collections	X-2345-50	775	50	—	Ostapkowicz et al. 2011
St. Vincent	St. Vincent and the Grenadines	Lesser Antilles	3	Brighton Beach	shell	marine shell	Unit A, level 3, find number 194	GrA-52054	1810	30	—	Boomert et al. 2017
St. Vincent	St. Vincent and the Grenadines	Lesser Antilles	3	Brighton Beach	shell	marine shell	Unit A, level 14-15, find number 170	GrA-52053	2100	30	—	Boomert et al. 2017
St. Vincent	St. Vincent and the Grenadines	Lesser Antilles	2	Brighton Beach	charcoal	charcoal/ charred material	Unit A, level 16, find number 190	GrA-52187	1855	30	—	Boomert et al. 2017
St. Vincent	St. Vincent and the Grenadines	Lesser Antilles	2	Buccament West	charcoal	charcoal/ charred material	120 cm; base	RL-73	1670	160	—	Bullen and Bullen 1972:79, 112, 153; Haviser 1997:60
St. Vincent	St. Vincent and the Grenadines	Lesser Antilles	2	Fitz-Hughs	charcoal	charcoal/ charred material	exposed bank	RL-74	930	110	—	Bullen and Bullen 1972:53
St. Vincent	St. Vincent and the Grenadines	Lesser Antilles	2	Indian Bay	*Livonia pica*	marine shell	deposit below midden	RL-72	370	110	—	Bullen and Bullen 1972:73

St. Vincent	St. Vincent and the Grenadines	Lesser Antilles	2	Kingston Post Office	*Strombus gigas*	marine shell	lower level	RL-28	1790	100	—	Bullen and Bullen 1972:79, 94, 153-154; Rouse 1989:397; Haviser 1997:60
Tobago	Trinidad and Tobago	northern South America	2	Golden Grove (TOB-13)	iguana vertebra	faunal material	IV/13 83/86-88/90	Beta-172209	1180	40	-22.6	Steadman and Jones 2006
Tobago	Trinidad and Tobago	northern South America	2	Golden Grove (TOB-13)	peccary pedal phalanx	faunal material	IV/16 98/100-102/103	Beta-172210	1110	40	-22.2	Steadman and Jones 2006
Tobago	Trinidad and Tobago	northern South America	2	Golden Grove (TOB-13)	agouti pelvis	faunal material	Layer II, Level 2	Beta-153149	900	40	-18.9	Steadman and Stokes 2002
Tobago	Trinidad and Tobago	northern South America	2	Golden Grove (TOB-13)	peccary thoracic vertebra	faunal material	Layer III/Level 10	Beta-153150	1170	40	-21.7	Steadman and Stokes 2002
Tobago	Trinidad and Tobago	northern South America	2	Golden Grove (TOB-13)	peccary humerus	faunal material	V/19 113/115-117-120	Beta-172211	1700	40	-20.4	Steadman and Jones 2006
Tobago	Trinidad and Tobago	northern South America	3	Golden Grove (TOB-13)	bulk shell	marine shell	Pit B7, L. 13, 60-65	GrN-14956	1100	35	—	Boomert 2000
Tobago	Trinidad and Tobago	northern South America	3	Golden Grove (TOB-13)	bulk shell (*Melongena melongena, Strombus gigas*)	marine shell	Pit B7, L 4, 15-20	GrN-14960	995	35	—	Boomert 2000
Tobago	Trinidad and Tobago	northern South America	3	Golden Grove (TOB-13)	bulk shell (*Crassostrea rhizophorae, Isognomon alatus, Strombus* sp.)	marine shell	Pit B7, L. 11, 50-55	GrN-14957	880	50	—	Boomert 2000

Tobago	Trinidad and Tobago	northern South America	3	Golden Grove (TOB-13)	bulk shell (*Crassostrea rhizophorae*, *Phacoides pectinatus*, *Strombus gigas*)	marine shell	Pit B7, L. 17, 80-85	GrN-14955	1040	35	—	Boomert 2000
Tobago	Trinidad and Tobago	northern South America	3	Golden Grove (TOB-13)	bulk shell (*Melongena melongena*, *Murex* sp., *Pacoides pectinatus*)	marine shell	Pit B7, L. 5, 20-25	GrN-14959	860	35	—	Boomert 2000
Tobago	Trinidad and Tobago	northern South America	3	Golden Grove (TOB-13)	bulk shell (Crassostrea rhizophorae, Isognomon alatus, Strombus sp.)	marine shell	Pit B7, L. 8, 35-40	GrN-14958	890	60	—	Boomert 2000
Tobago	Trinidad and Tobago	northern South America	4	Great Courtland Bay (TOB-23)	charcoal	charcoal/ charred material	Zone 4, Stratum A	Beta-129261	modern	—	—	Boomert 2000
Tobago	Trinidad and Tobago	northern South America	2	Great Courtland Bay (TOB-23)	charcoal	charcoal/ charred material	Zone 4, Stratum E	Beta-129264	550	40	-25.0	Boomert 2000
Tobago	Trinidad and Tobago	northern South America	2	Great Courtland Bay (TOB-23)	charcoal	charcoal/ charred material	Zone 5, Stratum A	Beta-129262	590	40	-25.0	Boomert 2000
Tobago	Trinidad and Tobago	northern South America	2	Great Courtland Bay (TOB-23)	charcoal	charcoal/ charred material	Zone 6, Statum F	Beta-129265	600	50	-25.0	Boomert 2000
Tobago	Trinidad and Tobago	northern South America	2	Lovers' Retreat (TOB-69)	charcoal	charcoal/ charred material	Area A, Pit A, L. 9, 80-90	Y-1336	1300	120	—	Rouse 1963:table C
Tobago	Trinidad and Tobago	northern South America	2	Lovers' Retreat (TOB-69)	charcoal	charcoal/ charred material	Area B, Pits GMQR, L. 2 & 3, 10-30 cm	Beta-4905	760	105	-23.1	Boomert 2000

Tobago	Trinidad and Tobago	northern South America	2	Lovers' Retreat (TOB-69)	bone collagen	human bone/teeth	Area B Phase 2A	Beta-221319	810	40	-14.8	Reid, personal communications
Tobago	Trinidad and Tobago	northern South America	2	Lovers' Retreat (TOB-69)	bone collagen	human bone/teeth	Area B Phase 2B	Beta-221320	810	40	-14.7	Reid, personal communications
Tobago	Trinidad and Tobago	northern South America	2	Lovers' Retreat (TOB-69)	bone collagen	human bone/teeth	Area B Phase 2C	Beta-221321	850	40	-15.6	Reid, personal communications
Tobago	Trinidad and Tobago	northern South America	3	Milford 1 (TOB-3)	bulk shell	marine shell	Pit 2, level 9, 40-45 cm	GrN-14963	4315	45	—	Boomert 1996: 80
Tobago	Trinidad and Tobago	northern South America	3	Milford 1 (TOB-3)	bulk shell	marine shell	Pit 2, level 8, 35-40 cm	GrN-14964	4020	70	—	Boomert 1996: 80
Tobago	Trinidad and Tobago	northern South America	4	Milford 1 (TOB-3)	bulk shell	marine shell	Pit 2, level 7, 30-35 cm	GrN-14965	4875	45	—	Boomert 1996: 80
Tobago	Trinidad and Tobago	northern South America	2	Milford 1 (TOB-3)	peccary humerus	faunal material	Layer II, Level 3	Beta-153151	2700	40	-21.3	Steadman and Stokes 2002
Tobago	Trinidad and Tobago	northern South America	2	Milford 1 (TOB-3)	peccary dentary	faunal material	Layer II, Level 5	Beta-153936	1750	40	-24.3	Steadman and Stokes 2002
Tobago	Trinidad and Tobago	northern South America	3	Sandy Point (TOB-1)	bulk shell	marine shell	Pit 3, L. 11, 50-55	GrN-14961	1940	35	—	Boomert 2000
Tobago	Trinidad and Tobago	northern South America	3	Sandy Point (TOB-1)	bulk shell (*Cittarium pica, Strombus gigas*)	marine shell	Pit 3, L. 10, 45-50	GrN-14962	1840	35	—	Boomert 2000
Trinidad	Trinidad and Tobago	northern South America	2	Atagual (VIC-30)	charcoal	charcoal/ charred material	Area A6, exposed base of midden	Beta-4903	1680	115	-25.85	Boomert 2000

Trinidad	Trinidad and Tobago	northern South America	2	Atagual (VIC-30)	charcoal	charcoal/ charred material	Area A6, exposed base of midden	Beta-4904	1350	85	-25.55	Boomert 2000
Trinidad	Trinidad and Tobago	northern South America	2	Atagual (VIC-30)	charcoal	charcoal/ charred material	Lower part Stratum 2, 17-34 cm	I-10766	540	75	—	Harris, pers comm. In Boomert 2000
Trinidad	Trinidad and Tobago	northern South America	2	Atagual (VIC-30)	charcoal	charcoal/ charred material	Pit A1, L. 5, 40-50 cm	Beta-4898	1040	260	-25.3	Boomert 2000
Trinidad	Trinidad and Tobago	northern South America	2	Atagual (VIC-30)	charcoal	charcoal/ charred material	Pit A1, L. 6, 50-60	Beta-4899	1755	150	-25.3	Boomert 2000
Trinidad	Trinidad and Tobago	northern South America	2	Atagual (VIC-30)	charcoal	charcoal/ charred material	Pit A1, L.7 60-70	Beta-4900	1145	65	-25.5	Boomert 2000
Trinidad	Trinidad and Tobago	northern South America	2	Atagual (VIC-30)	charcoal	charcoal/ charred material	Pit A2, L. 6, 50-60	Beta-4901	1300	110	-25.52	Boomert 2000
Trinidad	Trinidad and Tobago	northern South America	2	Atagual (VIC-30)	charcoal	charcoal/ charred material	Pit A2, L. 7, 60-70	Beta-4902	1805	90	-24.59	Boomert 2000
Trinidad	Trinidad and Tobago	northern South America	3	Banwari Trace (SPA-28)	bulk carbon	bulk carbon	Pit C, level 1, 25 cmbs	UGa-14932	4770	25	—	Tankersley et al. 2018
Trinidad	Trinidad and Tobago	northern South America	2	Banwari Trace (SPA-28)	charcoal	charcoal/ charred material	Pit C, level 2, 50 cmbs	UGa-14458	6100	25	—	Tankersley et al. 2018
Trinidad	Trinidad and Tobago	northern South America	2	Banwari Trace (SPA-28)	charcoal	charcoal/ charred material	Pit C, level 2, 85 cmbs	UGa-14459	6370	25	—	Tankersley et al. 2018
Trinidad	Trinidad and Tobago	northern South America	2	Banwari Trace (SPA-28)	charcoal	charcoal/ charred material	Pit C, level 3, 115 cmbs	UGa-14460	7030	25	—	Tankersley et al. 2018
Trinidad	Trinidad and Tobago	northern South America	2	Banwari Trace (SPA-28)	cortical artiodactyl bioapatite	faunal material	Pit C, level 1, 40 cmbs	UGa-14457	5300	25	—	Tankersley et al. 2018

Trinidad	Trinidad and Tobago	northern South America	4	Banwari Trace (SPA-28)	charcoal	charcoal/ charred material	Excavation A, 0-25 cmbs	IVIC-784	2550	100	—	Tamers 1973:309-310
Trinidad	Trinidad and Tobago	northern South America	2	Banwari Trace (SPA-28)	charcoal	charcoal/ charred material	Excavation A, 100-125 cmbs	IVIC-891	6190	100	—	Tamers 1973:309-310
Trinidad	Trinidad and Tobago	northern South America	2	Banwari Trace (SPA-28)	charcoal	charcoal/ charred material	Excavation A, 125-150 cmbs	IVIC-889	6780	70	—	Tamers 1973:309-310
Trinidad	Trinidad and Tobago	northern South America	2	Banwari Trace (SPA-28)	charcoal	charcoal/ charred material	Excavation A, 175-200 cmbs	IVIC-888	7180	80	—	Tamers 1973:309-310
Trinidad	Trinidad and Tobago	northern South America	2	Banwari Trace (SPA-28)	charcoal	charcoal/ charred material	Excavation A, 25-50 cmbs	IVIC-783	5650	100	—	Tamers 1973:309-310
Trinidad	Trinidad and Tobago	northern South America	2	Banwari Trace (SPA-28)	charcoal	charcoal/ charred material	Excavation A, 50-75 cmbs	IVIC-887	6170	90	—	Tamers 1973:309-310
Trinidad	Trinidad and Tobago	northern South America	2	Banwari Trace (SPA-28)	charcoal	charcoal/ charred material	Excavation A, 75-100 cmbs	IVIC-890	6100	90	—	Tamers 1973:309-310
Trinidad	Trinidad and Tobago	northern South America	2	Batiment Crase 1 (SPA-26)	charcoal	charcoal/ charred material	Testpit A, L. 2, 3, & 4	Beta-6808	650	50	-26.02	Boomert 2000
Trinidad	Trinidad and Tobago	northern South America	2	Batiment Crase 1 (SPA-26)	*Tivela mactroides*	marine shell	Testpit A, L. 3 & 4, 40-80	Beta-6809	990	50	+4.0	Boomert 1985
Trinidad	Trinidad and Tobago	northern South America	2	Blanchisseuse (SGE-8)	charred material	charcoal/ charred material	Context 1	Beta-189113	1570	40	-26.0	Reid, personal communications
Trinidad	Trinidad and Tobago	northern South America	2	Blanchisseuse (SGE-8)	charred material	charcoal/ charred material	Context 1	Beta-196706	1650	40	-26.3	Reid, personal communications
Trinidad	Trinidad and Tobago	northern South America	2	Blanchisseuse (SGE-8)	charred material	charcoal/ charred material	Context 1	Beta-196707	740	40	-27.5	Reid, personal communications

Trinidad	Trinidad and Tobago	northern South America	2	Blanchisseuse (SGE-8)	charred material	charcoal/ charred material	Context 1	Beta-196708	1920	40	-27.5	Reid, personal communication s
Trinidad	Trinidad and Tobago	northern South America	2	Blanchisseuse (SGE-8)	charred material	charcoal/ charred material	Context 1	Beta-196709	1880	40	-26.9	Reid, personal communication s
Trinidad	Trinidad and Tobago	northern South America	2	Blanchisseuse (SGE-8)	wood charcoal	charcoal/ charred material	test ecavation at 125W/25N, 40 cmbs,	Beta-134571	1720	50	-26.6	Steadman and Stokes 2002
Trinidad	Trinidad and Tobago	northern South America	2	Cedros (SPA-1)	charcoal	charcoal/ charred material	A1, L. 2, 25-50	IVIC-642	2140	70	—	Olsen 1974, Boomert 2000
Trinidad	Trinidad and Tobago	northern South America	2	Cedros (SPA-1)	charcoal	charcoal/ charred material	A1, L. 3, 50-75	IVIC-643	1850	80	—	Olsen 1974, Boomert 2000
Trinidad	Trinidad and Tobago	northern South America	2	Guayaguayare (MAY-16)	charcoal	charcoal/ charred material	Testpit C, L. 1, 0-25	IVIC-785	1260	100	—	Rouse et al. 1978
Trinidad	Trinidad and Tobago	northern South America	2	Guayaguayare (MAY-16)	charcoal	charcoal/ charred material	Testpit C, L. 2, 25-50	IVIC-786	1720	90	—	Rouse et al. 1978
Trinidad	Trinidad and Tobago	northern South America	4	Cedros swamp	organic sediment	sediment	CE07-1, 128 cm	AA-82470	2490	40	-28.3	Farrell et al. 2018
Trinidad	Trinidad and Tobago	northern South America	4	Cedros swamp	organic sediment	sediment	CE07-1, 315 cm	AA-82469	4280	40	-28.1	Farrell et al. 2018
Trinidad	Trinidad and Tobago	northern South America	4	Cedros swamp	organic sediment	sediment	CE07-1, 433-436 cm	AA-77444	4730	40	-27.9	Siegel et al. 2015
Trinidad	Trinidad and Tobago	northern South America	2	Clairboy (SGE-44)	seed or nutshell	charcoal/ charred material	Flot Sample Fea. 1	ISGS-A2628	1210	15	-27.4	Lopinot and Ray 2018
Trinidad	Trinidad and Tobago	northern South America	2	Clairboy (SGE-44)	charcoal	charcoal/ charred material	Feature 3 from base of Ap horizon	ISGS-A2629	410	20	-25.2	Lopinot and Ray 2018

Trinidad	Trinidad and Tobago	northern South America	4	Hernandez Site (SGE-43)	charcoal	charcoal/ charred material	Unit 2, level 2	IGS-A2360	—	—	—	Lopinot 2013
Trinidad	Trinidad and Tobago	northern South America	3	Guayaguayare (MAY-16)	bulk shell(*Donax* sp., *Melongena melongena*)	marine shell	Testpit D, L. 2, 5-10 cm	Beta-6823	550	50	+2.77	Boomert 1985a:table 6
Trinidad	Trinidad and Tobago	northern South America	3	Guayaguayare (MAY-16)	bulk shell (*Donax* sp., *Tivela mactroides*)	marine shell	Testpit D, L. 3 & 4, 10-20	Beta-6824	780	60	+3.37	Boomert 1985a:table 6
Trinidad	Trinidad and Tobago	northern South America	3	Guayaguayare (MAY-16)	bulk shell (*Donax sp.*, *Tivela mactroides*)	marine shell	Testpit D, L.7 & 8, 30-40	Beta-6825	1200	60	+2.6	Boomert 1985a:table 6
Trinidad	Trinidad and Tobago	northern South America	2	Icacos (SPA-7)	charcoal	charcoal/ charred material	Testpit A, Lev. 3 & 4, 50-100	Beta-6807	1130	50	-27.8	Boomert 1985, table 6
Trinidad	Trinidad and Tobago	northern South America	2	La Reconnaissance (SGE-34B)	charcoal	charcoal/ charred material	Unit 17; PP#2	Beta-296726	1210	30	-26.8	Lopinot and Ray 2018
Trinidad	Trinidad and Tobago	northern South America	2	La Reconnaissance (SGE-34B)	charcoal	charcoal/ charred material	Unit 17; Stata IIb, 82 cmbs	Beta-296724	1490	30	-26.6	Lopinot and Ray 2018
Trinidad	Trinidad and Tobago	northern South America	2	La Reconnaissance (SGE-34B)	charcoal	charcoal/ charred material	Unit 17; Stata I, 48 cmbs	Beta-296723	1400	30	-25.3	Lopinot and Ray 2018
Trinidad	Trinidad and Tobago	northern South America	2	Hernandez (SGE-43)	charcoal	charcoal/ charred material	Unit 2, level 2	ISGS-A2630	385	20	-26.8	Lopinot and Ray 2018
Trinidad	Trinidad and Tobago	northern South America	4	Manzanilla	charcoal	charcoal/ charred material	Feature 1-B-7	GrA-13866	39000	500	—	Nieweg and Dorst 2001, Delsol and Grouard 2016

Trinidad	Trinidad and Tobago	northern South America	2	Manzanilla	charcoal	charcoal/ charred material	Feature 1-A-14	GrA-13865	1590	40	—	Nieweg and Dorst 2001; Delsol and Grouard 2016
Trinidad	Trinidad and Tobago	northern South America	2	Manzanilla	charcoal	charcoal/ charred material	Feature 1-B-4	GrA-13867	1220	40	—	Nieweg and Dorst 2001, Delsol and Grouard 2016
Trinidad	Trinidad and Tobago	northern South America	2	Manzanilla	human bone	human bone/teeth	Ft. 16	Beta-193442	630	40	—	Healy et al. 2013
Trinidad	Trinidad and Tobago	northern South America	2	Manzanilla	human bone	human bone/teeth	Ft. 18	Beta-193443	620	40	—	Healy et al. 2013
Trinidad	Trinidad and Tobago	northern South America	4	Maracas Swamp	organic sediment	sediment	M 210-225 cm	BGS-2396	2930	80	—	Ramcharan 2004
Trinidad	Trinidad and Tobago	northern South America	4	Maracas Swamp	organic sediment	sediment	M 350-385 cm	Beta-124614	3960	60	—	Ramcharan 2004
Trinidad	Trinidad and Tobago	northern South America	4	Maracas Swamp	organic sediment	sediment	M 805-840 cm	Beta-124615	5880	60	—	Ramcharan 2004
Trinidad	Trinidad and Tobago	northern South America	4	Nariva Swamp	preserved plant matter	plant material	NV08-1, 100-105 cm	Beta-379162	1750	30	-26.5	Siegel et al. 2015
Trinidad	Trinidad and Tobago	northern South America	4	Nariva Swamp	organic sediment	sediment	NV08-1, 100-105 cm	Beta-378825	3220	30	-27.4	Siegel et al. 2015
Trinidad	Trinidad and Tobago	northern South America	4	Nariva Swamp	organic sediment	sediment	NV08-1, 100-105 cm	Beta-382069	3260	30	-27.2	Siegel et al. 2015
Trinidad	Trinidad and Tobago	northern South America	4	Nariva Swamp	preserved wood	wood	NV08-1, 208-210 cm	Beta-343380	5900	30	-25.0	Siegel et al. 2015

Trinidad	Trinidad and Tobago	northern South America	4	Nariva Swamp	preserved wood	wood	NV08-1, 250-251 cm	AA-82681	6160	70	-30.4	Siegel et al. 2015
Trinidad	Trinidad and Tobago	northern South America	4	Nariva Swamp	preserved wood	wood	NV08-2, 374 cm	AA-82679	3260	50	-26.5	Farrell et al. 2018
Trinidad	Trinidad and Tobago	northern South America	4	Nariva Swamp	preserved wood	wood	NV08-3, 196-204 cm	Beta-343381	2480	30	-27.0	Farrell et al. 2018
Trinidad	Trinidad and Tobago	northern South America	4	Nariva Swamp	preserved wood	wood	NV08-3, 445-447 cm	AA-84719	3990	35	-29.2	Farrell et al. 2018
Trinidad	Trinidad and Tobago	northern South America	4	Nariva Swamp	preserved wood	wood	NV08-4, 280-281 cm	AA-85865	3280	45	-29.3	Farrell et al. 2018
Trinidad	Trinidad and Tobago	northern South America	4	Nariva Swamp	preserved wood	wood	NV08-4, 685-686 cm	AA-82680	5910	50	-28.6	Siegel et al. 2015
Trinidad	Trinidad and Tobago	northern South America	4	Nariva Swamp	preserved wood	wood	NV08-4, 235 cm	AA-85864	3575	45	-25.7	Siegel et al. 2015
Trinidad	Trinidad and Tobago	northern South America	4	Nariva Swamp Raphael	organic sediment	sediment	N(R) 125-145 cm	GrN-9097	1360	50	—	Ramcharan 2004
Trinidad	Trinidad and Tobago	northern South America	4	Nariva Swamp Sand Hill West	organic sediment	sediment	N(SHW) 220-225 cm	GrN-9094	2720	55	—	Ramcharan 2004
Trinidad	Trinidad and Tobago	northern South America	4	Nariva Swamp Sand Hill West	organic sediment	sediment	N(SHW) 475-525 cm	GrN-9326	4790	70	—	Ramcharan 2004
Trinidad	Trinidad and Tobago	northern South America	4	Nariva Swamp Sand Hill West	organic sediment	sediment	N(SHW) 638-693 cm	GrN-9095	5260	70	—	Ramcharan 2004
Trinidad	Trinidad and Tobago	northern South America	4	Nariva Swamp Trough	organic sediment	sediment	N(T) 160-180 cm	GrN-9327	555	45	—	Ramcharan 2004

Trinidad	Trinidad and Tobago	northern South America	4	Nariva Swamp Trough	organic sediment	sediment	N(T) 525-590 cm	GrN-9096	4250	70	—	Ramcharan 2004
Trinidad	Trinidad and Tobago	northern South America	2	Ortoire	charcoal	charcoal/ charred material	Trench A, two combined sections, 80-100 cm, Zones I and II	Y-260-1	2750	130	—	Rouse 1960:10-11; Bullen and Sleight 1963:42; Rouse et al. 1978:457
Trinidad	Trinidad and Tobago	northern South America	3	Ortoire	bulk carbon	bulk carbon	Trench A, two combined sections, 100-140 cm, Zone 1	Y-260-2	2760	130	—	Boomert 2000
Trinidad	Trinidad and Tobago	northern South America	4	Oropuche Lagoon, St. John	organic sediment	sediment	SJ07-2, 165-170 cm	Beta-378826	820	30	-26.4	Farrell et al. 2018
Trinidad	Trinidad and Tobago	northern South America	4	Oropuche Lagoon, St. John	organic sediment	sediment	SJ07-2, 464 cm	AA-77388	4790	40	-28.4	Farrell et al. 2018
Trinidad	Trinidad and Tobago	northern South America	2	Palo Seco (SPA-30)	charcoal	charcoal/ charred material	Midden 1, Section D4, L. 2, 25-50	IVIC-638	2130	80	—	Rouse et al. 1978:table 13.4
Trinidad	Trinidad and Tobago	northern South America	2	Palo Seco (SPA-30)	charcoal	charcoal/ charred material	Midden 1, Section D4, L. 3, 50-75	IVIC-639	1480	70	—	Rouse et al. 1978:table 13.4
Trinidad	Trinidad and Tobago	northern South America	2	Palo Seco (SPA-30)	charcoal	charcoal/ charred material	Midden 1, Section D4, L. 5, 100-125	IVIC-641	2060	70	—	Rouse et al. 1978:table 13.4

Trinidad	Trinidad and Tobago	northern South America	2	Palo Seco (SPA-30)	charcoal	charcoal/ charred material	Midden 1, Section D4, L. 75-100	IVIC-640	1990	70	—	Rouse et al. 1978:table 13.4
Trinidad	Trinidad and Tobago	northern South America	2	Pitch Lake	*Andira* sp.	plant material	museum	OxA-19174	1538	29	-25.1	Ostapkowicz et al. 2011
Trinidad	Trinidad and Tobago	northern South America	4	Point Radix 1 (MAY-1)	bulk shell (*Donax* sp., *Tivela mactroides*, *Astraea tuber*)	marine shell	Testpit A, L. 4, 15-20	Beta-6826	moder n	—	-1.51	Boomert 1985:table 6
Trinidad	Trinidad and Tobago	northern South America	3	Point Radix 1 (MAY-1)	bulk shell (*Donax sp.*, *Tivela mactroides*, *Astraea tuber*)	marine shell	Testpit A, L. 5, 20-25	Beta-6827	960	50	-0.57	Boomert 1985:table 6
Trinidad	Trinidad and Tobago	northern South America	2	Poonah Road	charcoal	charcoal/ charred material	Excavation B, level 2, 25-35 cm	I-6444	2120	135	—	Boomert 2000
Trinidad	Trinidad and Tobago	northern South America	2	St. John (SPA-11)	charcoal	charcoal/ charred material	Unit 1, 40-50 cm	UGa-12303	6890	30	-26.7	Pagán-Jiménez et al. 2015
Trinidad	Trinidad and Tobago	northern South America	3	St. John (SPA-11)	bulk shell	bulk sample	Excavation B, no depth	ARC-1153	6866	50	—	Boomert 2000
Trinidad	Trinidad and Tobago	northern South America	3	St. John (SPA-11)	shell	marine shell	Unit 1	Beta-264892	5490	50	-8.8	Reid, personal communication s
Trinidad	Trinidad and Tobago	northern South America	3	St. John (SPA-11)	shell	marine shell	Unit 1, 40-50 cm	UGa-12304	6870	25	-8.1	Pagán-Jiménez et al. 2015
Trinidad	Trinidad and Tobago	northern South America	3	St. John (SPA-11)	shell	marine shell	Unit 1, 50-60 cm	UGa-12305	6980	30	-8.6	Pagán-Jiménez et al. 2015

Trinidad	Trinidad and Tobago	northern South America	3	St. John (SPA-11)	shell	marine shell	Unit 2	Beta-264893	6560	50	-6.7	Reid, personal communications
Trinidad	Trinidad and Tobago	northern South America	3	St. John (SPA-11)	shell	marine shell	Unit 2, 50-60 cm	UGa-12306	6710	25	-9.3	Pagán-Jiménez et al. 2015
Trinidad	Trinidad and Tobago	northern South America	3	St. John (SPA-11)	shell	marine shell	Unit 3, 10-20 cm	UGa-12307	6190	25	-10.9	Pagán-Jiménez et al. 2015
Trinidad	Trinidad and Tobago	northern South America	3	St. John (SPA-11)	shell	marine shell	Unit 3, 20-30 cm	UGa-12308	6050	25	-9.2	Pagán-Jiménez et al. 2015
Trinidad	Trinidad and Tobago	northern South America	3	St. John (SPA-11)	shell	marine shell	Unit 3, 30-40	UGa-13634	5080	30	-10.9	Pagán-Jiménez et al. 2015
Union Island	St. Vincent and the Grenadines	Lesser Antilles	3	Chatham Bay	*Strombus gigas*	marine shell	—	RL-70	1470	110	—	Bullen and Bullen 1972:25, 77; Rouse 1989:397; Haviser 1997:60
Vieques	Puerto Rico	Greater Antilles	3	Cerro Martineau	shell	marine shell	deposit 1, Unit S-1	Beta-152062	1210	60	—	Narganes Storde 2005:280-281
Vieques	Puerto Rico	Greater Antilles	3	Cerro Martineau	shell	marine shell	deposit 1, Unit S-1	Beta-152063	500	70	—	Narganes Storde 2005:280-281
Vieques	Puerto Rico	Greater Antilles	2	La Hueca	charcoal	charcoal/ charred material	Block Z (newest sample)	Beta-129948	1810	60	—	Rodríguez-Ramos et al. 2010; Narganes Storde 1991
Vieques	Puerto Rico	Greater Antilles	2	La Hueca	charcoal	charcoal/ charred material	Block Z: Z-11 (190-200 cmbs)	I-10980	1735	85	—	Rodríguez-Ramos et al. 2010

Vieques	Puerto Rico	Greater Antilles	2	La Hueca	charcoal	charcoal/ charred material	Block Z: Z-15 (200-220 cmbs)	I-11140	1730	80	—	Rodríguez-Ramos et al. 2010
Vieques	Puerto Rico	Greater Antilles	2	La Hueca	charcoal	charcoal/ charred material	Block Z: Z-15 (240-260 cmbs)	I-11139	1800	80	—	Rodríguez-Ramos et al. 2010
Vieques	Puerto Rico	Greater Antilles	2	La Hueca	charcoal	charcoal/ charred material	Block Z: Z-16 (160-180 cmbs)	I-11141	1705	80	—	Rodríguez-Ramos et al. 2010
Vieques	Puerto Rico	Greater Antilles	2	La Hueca	charcoal	charcoal/ charred material	Block Z: Z-8 (200-210 cmbs)	I-10979	1820	85	—	Rodríguez-Ramos et al. 2010
Vieques	Puerto Rico	Greater Antilles	2	La Hueca	charcoal	charcoal/ charred material	Block Z: Z-V (160-170cmbs)	I-11321	1845	80	—	Rodríguez-Ramos et al. 2010
Vieques	Puerto Rico	Greater Antilles	2	La Hueca	charcoal	charcoal/ charred material	Block Z: Z-W (160-170 cmbs)	I-11320	1770	80	—	Rodríguez-Ramos et al. 2010
Vieques	Puerto Rico	Greater Antilles	2	La Hueca	charcoal	charcoal/ charred material	Block Z: Z-X (170-180 cmbs)	I-11322	1945	80	—	Rodríguez-Ramos et al. 2010
Vieques	Puerto Rico	Greater Antilles	2	La Hueca	charcoal	charcoal/ charred material	Block Z-T-2: K-7 (20-40cmbs)	I-12742	900	80	—	Rodríguez-Ramos et al. 2010; Narganes Storde 1991
Vieques	Puerto Rico	Greater Antilles	2	La Hueca	charcoal	charcoal/ charred material	Block Z-T-2: K-9 (20-40 cmbs)	I-12744	1640	80	—	Rodríguez-Ramos et al. 2010; Narganes Storde 1991
Vieques	Puerto Rico	Greater Antilles	2	La Hueca	charcoal	charcoal/ charred material	Block Z-T-2: L-8 (20-40 cmbs)	I-12743	950	80	—	Rodríguez-Ramos et al. 2010; Narganes Storde 1991

Vieques	Puerto Rico	Greater Antilles	2	La Hueca	charcoal	charcoal/ charred material	Block Z-T-2: L-9 (20-40 cmbs)	I-12745	1560	80	—	Rodríguez-Ramos et al. 2010; Narganes Storde 1991
Vieques	Puerto Rico	Greater Antilles	2	La Hueca	charcoal	charcoal/ charred material	Block Z-T-2: LL-9 (20-40 cmbs)	I-12746	1600	80	—	Rodríguez-Ramos et al. 2010; Narganes Storde 1991
Vieques	Puerto Rico	Greater Antilles	2	La Hueca	charcoal	charcoal/ charred material	Block Z-T-B: B-3 (100 cmbs)	I-12858	1820	80	—	Rodríguez-Ramos et al. 2010
Vieques	Puerto Rico	Greater Antilles	2	La Hueca	charcoal	charcoal/ charred material	Block Z-T-B: C-1 (120 cmbs)	I-12860	1780	80	—	Rodríguez-Ramos et al. 2010
Vieques	Puerto Rico	Greater Antilles	2	La Hueca	charcoal	charcoal/ charred material	Block Z-T-B: C-4 (100 cmbs)	I-12859	1880	80	—	Rodríguez-Ramos et al. 2010
Vieques	Puerto Rico	Greater Antilles	2	La Hueca	charcoal	charcoal/ charred material	Block Z-T-B: C-8 (80 cmbs)	I-12856	1810	80	—	Rodríguez-Ramos et al. 2010
Vieques	Puerto Rico	Greater Antilles	2	La Hueca	charcoal	charcoal/ charred material	New Extension, Block Z: A-9 (150 cmbs)	I-15188	700	70	—	Rodríguez-Ramos et al. 2010
Vieques	Puerto Rico	Greater Antilles	2	La Hueca	charcoal	charcoal/ charred material	New Extension, Block Z: B-10 (190 cmbs)	I-15238	570	80	—	Rodríguez-Ramos et al. 2010; Narganes Storde 1991
Vieques	Puerto Rico	Greater Antilles	2	La Hueca	charcoal	charcoal/ charred material	New Extension, Block Z: B-10 (200 cmbs)	I-15239	660	80	—	Rodríguez-Ramos et al. 2010; Narganes Storde 1991

Vieques	Puerto Rico	Greater Antilles	2	La Hueca	charcoal	charcoal/ charred material	New Extension, Block Z: B-10 (210 cmbs)	I-15240	630	80	—	Rodríguez-Ramos et al. 2010; Narganes Storde 1991
Vieques	Puerto Rico	Greater Antilles	2	La Hueca	charcoal	charcoal/ charred material	New Extension, Block Z: B-9 (100 cmbs)	I-15187	690	80	—	Rodríguez-Ramos et al. 2010; Narganes Storde 1991
Vieques	Puerto Rico	Greater Antilles	2	La Hueca	charcoal	charcoal/ charred material	New Extension, Block Z: B-9 (160 cmbs)	I-11189	790	85	—	Rodríguez-Ramos et al. 2010
Vieques	Puerto Rico	Greater Antilles	2	La Hueca	charcoal	charcoal/ charred material	New Extension, Block Z: C-10 (80 cmbs)	I-15186	520	80	—	Rodríguez-Ramos et al. 2010; Narganes Storde 1991
Vieques	Puerto Rico	Greater Antilles	2	La Hueca	charcoal	charcoal/ charred material	New Extension, Block Z: C-12 (60cmbs)	I-15185	540	80	—	Rodríguez-Ramos et al. 2010
Vieques	Puerto Rico	Greater Antilles	2	La Hueca	wood	wood	Block Z: Z-20 (20-40 cmbs)	I-11142	405	75	—	Rodríguez-Ramos et al. 2010
Vieques	Puerto Rico	Greater Antilles	3	La Hueca	charcoal	charcoal/ charred material	pit z 11	—	244	85	—	Chanlatte-Baik and Narganes 1980
Vieques	Puerto Rico	Greater Antilles	3	La Hueca	charcoal	charcoal/ charred material	pit z 8	—	159	85	—	Chanlatte-Baik and Narganes 1980

Vieques	Puerto Rico	Greater Antilles	3	La Hueca	marine shell	marine shell	Block Z (newest sample)	I-18448	1710	80	—	Rodríguez-Ramos et al. 2010; Narganes Storde 2005
Vieques	Puerto Rico	Greater Antilles	3	La Hueca	marine shell	marine shell	Block Z (newest sample)	I-18449	1740	80	—	Rodríguez-Ramos et al. 2010; Narganes Storde 2005
Vieques	Puerto Rico	Greater Antilles	3	La Hueca	marine shell	marine shell	Block Z (newest sample)	I-18450	1640	80	—	Rodríguez-Ramos et al. 2010; Narganes Storde 2005:280-281
Vieques	Puerto Rico	Greater Antilles	3	La Hueca	marine shell	marine shell	Block Z (newest sample)	I-18660	1650	80	—	Rodríguez-Ramos et al. 2010; Narganes Storde 2005:280-281
Vieques	Puerto Rico	Greater Antilles	3	La Hueca	marine shell	marine shell	Block Z (newest sample)	I-18661	1670	80	—	Rodríguez-Ramos et al. 2010; Narganes Storde 2005
Vieques	Puerto Rico	Greater Antilles	3	La Hueca	marine shell	marine shell	Block Z (newest sample)	I-18662	1480	80	—	Rodríguez-Ramos et al. 2010; Narganes Storde 2005:280-281

Vieques	Puerto Rico	Greater Antilles	3	La Hueca	marine shell	marine shell	Block Z (newest sample)	I-18723	1500	80	—	Rodríguez-Ramos et al. 2010; Narganes Storde 2005:280-281
Vieques	Puerto Rico	Greater Antilles	3	La Hueca	marine shell	marine shell	Block Z (newest sample)	I-18724	1350	80	—	Rodríguez-Ramos et al. 2010; Narganes Storde 2005:280-281
Vieques	Puerto Rico	Greater Antilles	3	La Hueca	marine shell	marine shell	Block Z (newest sample), Area P	I-15241	1880	80	—	Rodríguez-Ramos et al. 2010; Narganes Storde 1991, 2005:280-281
Vieques	Puerto Rico	Greater Antilles	3	La Hueca	marine shell	marine shell	Block Z: Z-9 (150-160 cmbs)	I-10553	1565	80	—	Rodríguez-Ramos et al. 2010
Vieques	Puerto Rico	Greater Antilles	3	La Hueca	marine shell	marine shell	Block Z-T-2: K-7 (20 cmbs)	I-13426	1810	80	—	Rodríguez-Ramos et al. 2010; Narganes Storde 1991
Vieques	Puerto Rico	Greater Antilles	3	La Hueca	marine shell	marine shell	Block Z-T-3: H-4 (20 cmbs)	I-13427	1840	80	—	Rodríguez-Ramos et al. 2010; Narganes Storde 1991
Vieques	Puerto Rico	Greater Antilles	3	La Hueca	marine shell	marine shell	Block Z-T-4: E-5 (20-40 cmbs)	I-13428	1930	80	—	Rodríguez-Ramos et al. 2010

Vieques	Puerto Rico	Greater Antilles	3	La Hueca	marine shell	marine shell	Block Z-T-5: H-10 (40 cmbs)	I-15242	1230	80	—	Rodríguez-Ramos et al. 2010; Narganes Storde 1991
Vieques	Puerto Rico	Greater Antilles	3	La Hueca	marine shell	marine shell	Block Z-T-6: G-5 (20-40 cmbs)	I-13429	1640	80	—	Rodríguez-Ramos et al. 2010; Narganes Storde 1991
Vieques	Puerto Rico	Greater Antilles	2	La Hueca	*Cittarium pica*	marine shell	Block Z: Z-9 (60-70 cmbs)	I-10549	1525	85	—	Rodríguez-Ramos et al. 2010; Narganes Storde 1991
Vieques	Puerto Rico	Greater Antilles	3	La Siembra	shell	marine shell	deposit 1, Unit S-1	Beta-175762	1260	60	—	Narganes Storde 2005:280-281
Vieques	Puerto Rico	Greater Antilles	2	Puerto Ferro	*Cittarium pica*	marine shell	deposit 1	I-16899	3780	100	—	Narganes Storde 2005:280-281
Vieques	Puerto Rico	Greater Antilles	2	Puerto Ferro	*Cittarium pica*	marine shell	Unit I-11	I-16898	2770	90	—	Narganes Storde 2005:280-281
Vieques	Puerto Rico	Greater Antilles	2	Puerto Ferro	*Cittarium pica*	marine shell	Unit I-12	I-16896	2650	90	—	Narganes Storde 2005:280-281
Vieques	Puerto Rico	Greater Antilles	2	Puerto Ferro	*Cittarium pica*	marine shell	Unit I-12	I-16897	3470	100	—	Narganes Storde 2005:280-281

Vieques	Puerto Rico	Greater Antilles	2	Puerto Ferro	*Strombus gigas*	marine shell	Unit J-15	I-18971	4095	80	—	Narganes Storde 2005:280-281
Vieques	Puerto Rico	Greater Antilles	2	Puerto Ferro	*Cittarium pica*	marine shell	Unit I-11	I-16406	3850	100	—	Narganes Storde 2015
Vieques	Puerto Rico	Greater Antilles	2	Puerto Ferro	*Cittarium pica*	marine shell	Unit I-12	I-16397	3530	100	—	Narganes Storde 2015
Vieques	Puerto Rico	Greater Antilles	2	Puerto Ferro	*Cittarium pica*	marine shell	Unit I-12	I-16396	3510	100	—	Narganes Storde 2015
Vieques	Puerto Rico	Greater Antilles	2	Puerto Ferro	*Cittarium pica*	marine shell	Unit I-12	I-16395	2790	100	—	Narganes Storde 2015
Vieques	Puerto Rico	Greater Antilles	2	Puerto Ferro	*Cittarium pica*	marine shell	Unit K-12	I-16407	2740	100	—	Narganes Storde 2015
Vieques	Puerto Rico	Greater Antilles	2	Sorcé	charcoal	charcoal/ charred material	Block Area P (new)	I-16151	1700	80	—	Rodríguez-Ramos et al. 2010; Narganes Storde 2005:280-281
Vieques	Puerto Rico	Greater Antilles	2	Sorcé	charcoal	charcoal/ charred material	Block Area P (new)	I-16152	1650	80	—	Rodríguez-Ramos et al. 2010; Narganes Storde 2005:280-281
Vieques	Puerto Rico	Greater Antilles	2	Sorcé	charcoal	charcoal/ charred material	Block Area P (new)	I-16153	2590	90	—	Rodríguez-Ramos et al. 2010; Narganes Storde 2005:280-281

Vieques	Puerto Rico	Greater Antilles	2	Sorcé	charcoal	charcoal/ charred material	Block Area P (new)	I-16154	1620	80	—	Rodríguez-Ramos et al. 2010; Narganes Storde 2005:280-281
Vieques	Puerto Rico	Greater Antilles	2	Sorcé	charcoal	charcoal/ charred material	Block Area P (new)	I-16173	1590	80	—	Rodríguez-Ramos et al. 2010; Narganes Storde 2005:280-281
Vieques	Puerto Rico	Greater Antilles	2	Sorcé	charcoal	charcoal/ charred material	Block Area P (new)	I-16174	1600	80	—	Rodríguez-Ramos et al. 2010; Narganes Storde 2005:280-281
Vieques	Puerto Rico	Greater Antilles	2	Sorcé	charcoal	charcoal/ charred material	Block Area P (new)	I-16175	1450	80	—	Rodríguez-Ramos et al. 2010; Narganes Storde 2005:280-281
Vieques	Puerto Rico	Greater Antilles	2	Sorcé	charcoal	charcoal/ charred material	Block Area X	I-10548	1440	85	—	Rodríguez-Ramos et al. 2010; Narganes Storde 1991
Vieques	Puerto Rico	Greater Antilles	2	Sorcé	charcoal	charcoal/ charred material	Block Area X	I-10550	1505	85	—	Rodríguez-Ramos et al. 2010; Narganes Storde 1991

Vieques	Puerto Rico	Greater Antilles	2	Sorcé	charcoal	charcoal/ charred material	Block Area X-T-3	I-14813	1180	80	—	Rodríguez-Ramos et al. 2010; Narganes Storde 1991
Vieques	Puerto Rico	Greater Antilles	2	Sorcé	charcoal	charcoal/ charred material	Block Area YTA-1	I-11318	1490	75	—	Rodríguez-Ramos et al. 2010; Narganes Storde 1991
Vieques	Puerto Rico	Greater Antilles	2	Sorcé	charcoal	charcoal/ charred material	Block Area YTA-1	I-11319	1915	80	—	Rodríguez-Ramos et al. 2010
Vieques	Puerto Rico	Greater Antilles	2	Sorcé	charcoal	charcoal/ charred material	Block Area YTA-2	I-11686	1575	80	—	Rodríguez-Ramos et al. 2010
Vieques	Puerto Rico	Greater Antilles	2	Sorcé	charcoal	charcoal/ charred material	Block Area YTA-2	I-11925	1665	80	—	Rodríguez-Ramos et al. 2010
Vieques	Puerto Rico	Greater Antilles	2	Sorcé	charcoal	charcoal/ charred material	Block Area YTA-2	I-11926	1720	80	—	Rodríguez-Ramos et al. 2010
Vieques	Puerto Rico	Greater Antilles	2	Sorcé	charcoal	charcoal/ charred material	Block Area YTA-2	I-11927	1565	80	—	Rodríguez-Ramos et al. 2010
Vieques	Puerto Rico	Greater Antilles	2	Sorcé	charcoal	charcoal/ charred material	Block Area YTA-3	I-10547	1575	85	—	Rodríguez-Ramos et al. 2010; Narganes Storde 1991
Vieques	Puerto Rico	Greater Antilles	2	Sorcé	charcoal	charcoal/ charred material	Block Area Z-T-A	I-13425	2110	80	—	Rodríguez-Ramos et al. 2010
Vieques	Puerto Rico	Greater Antilles	2	Sorcé	charcoal	charcoal/ charred material	Block Area Z-T-B	I-12857	1580	80	—	Rodríguez-Ramos et al. 2010

Vieques	Puerto Rico	Greater Antilles	2	Sorcé	charcoal	charcoal/ charred material	Block Area Z-T-B P (new)	I-16176	1270	90	—	Rodríguez-Ramos et al. 2010; Narganes Storde 2005:280-281
Vieques	Puerto Rico	Greater Antilles	2	Sorcé	charcoal	charcoal/ charred material	Block X (new)	I-15657	410	80	—	Rodríguez-Ramos et al. 2010; Narganes Storde 2005:280-281
Vieques	Puerto Rico	Greater Antilles	2	Sorcé	charcoal	charcoal/ charred material	Block X (new)	I-15658	470	80	—	Rodríguez-Ramos et al. 2010; Narganes Storde 2005:280-281
Vieques	Puerto Rico	Greater Antilles	2	Sorcé	charcoal	charcoal/ charred material	Block YTA-1: G-5	I-11316	1555	75	—	Rodríguez-Ramos et al. 2010
Vieques	Puerto Rico	Greater Antilles	2	Sorcé	charcoal	charcoal/ charred material	Block YTA-1: L-36	I-11685	1740	75	—	Rodríguez-Ramos et al. 2010
Vieques	Puerto Rico	Greater Antilles	2	Sorcé	charcoal	charcoal/ charred material	Block YTA-1: L-5	I-11317	1615	75	—	Rodríguez-Ramos et al. 2010
Vieques	Puerto Rico	Greater Antilles	2	Sorcé	charcoal	charcoal/ charred material	Block YTA-2: I-22	I-11687	1565	75	—	Rodríguez-Ramos et al. 2010
Vieques	Puerto Rico	Greater Antilles	2	Sorcé	charcoal	charcoal/ charred material	midden Z, unit B-9	I- 15188	700	80	—	Narganes Storde 1991
Vieques	Puerto Rico	Greater Antilles	2	Sorcé	charcoal	charcoal/ charred material	midden Z, unit B-9	I-15189	790	80	—	Narganes Storde 1991

Vieques	Puerto Rico	Greater Antilles	3	Sorcé	marine shell	marine shell	Block Area X-T-3	I-14845	1080	80	—	Rodríguez-Ramos et al. 2010; Narganes Storde 1991
Vieques	Puerto Rico	Greater Antilles	3	Sorcé	marine shell	marine shell	Block Area X-T-3	I-14846	1150	80	—	Rodríguez-Ramos et al. 2010; Narganes Storde 1991
Vieques	Puerto Rico	Greater Antilles	3	Sorcé	marine shell	marine shell	Block Area X-T-3	I-14847	1220	80	—	Rodríguez-Ramos et al. 2010; Narganes Storde 1991
Vieques	Puerto Rico	Greater Antilles	3	Sorcé	marine shell	marine shell	Block Area X-T-3	I-14848	1190	80	—	Rodríguez-Ramos et al. 2010; Narganes Storde 1991
Vieques	Puerto Rico	Greater Antilles	3	Sorcé	marine shell	marine shell	Block Area X-T-3	I-14850	1340	80	—	Rodríguez-Ramos et al. 2010; Narganes Storde 1991
Vieques	Puerto Rico	Greater Antilles	3	Sorcé	marine shell	marine shell	Block Area X-T-3(new)	I-18725	780	80	—	Rodríguez-Ramos et al. 2010; Narganes Storde 2005:280-281

Vieques	Puerto Rico	Greater Antilles	3	Sorcé	marine shell	marine shell	Block Area X-T-3(new)	I-18972	1715	70	—	Rodríguez-Ramos et al. 2010; Narganes Storde 2005:280-281
Vieques	Puerto Rico	Greater Antilles	3	Sorcé	marine shell	marine shell	Block Area X-T-3(new)	I-18973	1960	110	—	Rodríguez-Ramos et al. 2010; Narganes Storde 2005:280-281
Vieques	Puerto Rico	Greater Antilles	3	Sorcé	marine shell	marine shell	Block Area X-T-3, Unit I-16	I-18726	1810	80	—	Rodríguez-Ramos et al. 2010
Vieques	Puerto Rico	Greater Antilles	3	Sorcé	marine shell	marine shell	Block Area YTA-3	I-10551	1210	85	—	Rodríguez-Ramos et al. 2010; Narganes Storde 1991
Vieques	Puerto Rico	Greater Antilles	3	Sorcé	marine shell	marine shell	Block Area YTA-3	I-10552	1230	80	—	Rodríguez-Ramos et al. 2010; Narganes Storde 1991
Vieques	Puerto Rico	Greater Antilles	3	Sorcé	marine shell	marine shell	Block Area Z-T	I-14815	1380	80	—	Rodríguez-Ramos et al. 2010; Narganes Storde 1991

Vieques	Puerto Rico	Greater Antilles	3	Sorcé	marine shell	marine shell	Block Area Z-T	I-14816	1350	80	—	Rodríguez-Ramos et al. 2010; Narganes Storde 1991
Vieques	Puerto Rico	Greater Antilles	3	Sorcé	marine shell	marine shell	Block Area Z-T (new)	Beta-129949	1920	60	—	Rodríguez-Ramos et al. 2010; Narganes Storde 2005:280-281
Vieques	Puerto Rico	Greater Antilles	3	Sorcé	marine shell	marine shell	Block Area Z-T-A	I-14814	1240	80	—	Rodríguez-Ramos et al. 2010; Narganes Storde 1991
Vieques	Puerto Rico	Greater Antilles	3	Sorcé	marine shell	marine shell	Block Area Z-T-A (new)	I-18970	1765	70	—	Rodríguez-Ramos et al. 2010; Narganes Storde 2005:280-281
Vieques	Puerto Rico	Greater Antilles	3	Sorcé	marine shell	marine shell	Block X (new)	I-15718	1270	80	—	Rodríguez-Ramos et al. 2010; Narganes Storde 2005:280-281
Vieques	Puerto Rico	Greater Antilles	3	Sorcé	marine shell	marine shell	Block X (new)	I-15719	1320	80	—	Rodríguez-Ramos et al. 2010; Narganes Storde 2005:280-281

Vieques	Puerto Rico	Greater Antilles	3	Sorcé	marine shell	marine shell	Block X (new)	I-15727	1350	80	—	Rodríguez-Ramos et al. 2010; Narganes Storde 2005:280-281
Vieques	Puerto Rico	Greater Antilles	3	Sorcé	marine shell	marine shell	Block X (new)	I-15728	1340	80	—	Rodríguez-Ramos et al. 2010; Narganes Storde 2005:280-281
Vieques	Puerto Rico	Greater Antilles	3	Sorcé	marine shell	marine shell	Block YTA-2(new)	Beta-129950	1680	60	—	Rodríguez-Ramos et al. 2010; Narganes Storde 2005:280-281
Vieques	Puerto Rico	Greater Antilles	3	Sorcé	shell	marine shell	midden Z, unit B-9	I- 10553	1565	85	—	Narganes Storde 1991
Vieques	Puerto Rico	Greater Antilles	3	Sorcé	shell	marine shell	X-T-3	I-18762	1810	80	—	Narganes Storde 2005:280-281
Vieques	Puerto Rico	Greater Antilles	3	Sorcé	charcoal	charcoal/ charred material	Block X (new)	I-15656	300	80	—	Rodríguez-Ramos et al. 2010; Narganes Storde 2005:280-281
Vieques	Puerto Rico	Greater Antilles	3	Sorcé	charcoal	charcoal/ charred material	Midden X, Unit K-10	I-15655	290	80	—	Narganes Storde 2005:280-281

Vieques	Puerto Rico	Greater Antilles	2	Sorcé	*Cittarium pica*	marine shell	Midden P, Unit F-24	Beta-259410	1840	50	—	Narganes Storde 2015
Vieques	Puerto Rico	Greater Antilles	3	Sorcé	marine shell	marine shell	Midden P, Unit F-25	Beta-259409	1570	50	—	Narganes Storde 2015
Vieques	Puerto Rico	Greater Antilles	3	Sorcé	marine shell	marine shell	Midden YTA-2, Unit M-21	Beta-259407	1960	50	—	Narganes Storde 2015
Vieques	Puerto Rico	Greater Antilles	3	Sorcé	marine shell	marine shell	Midden YTA-2, Unit S-2	Beta-129950	1680	40	—	Narganes Storde 2015
Vieques	Puerto Rico	Greater Antilles	3	Sorcé	marine shell	marine shell	Midden XT-3, Unit I-16	Beta-276589	2130	40	—	Narganes Storde 2015
Vieques	Puerto Rico	Greater Antilles	3	Sorcé	marine shell	marine shell	Midden XT-3, Unit I-16	Beta-276590	1780	40	—	Narganes Storde 2015
Vieques	Puerto Rico	Greater Antilles	3	Sorcé	marine shell	marine shell	Midden XT-3, Unit H-14	Beta-276591	1750	40	—	Narganes Storde 2015
Vieques	Puerto Rico	Greater Antilles	3	Sorcé	marine shell	marine shell	Midden XT-3, Unit H-9	Beta-301604	1700	50	—	Narganes Storde 2015
Vieques	Puerto Rico	Greater Antilles	3	Sorcé	marine shell	marine shell	Midden XT-3, Unit H-9	Beta-301605	1620	50	—	Narganes Storde 2015
Vieques	Puerto Rico	Greater Antilles	2	Sorcé	*Cittarium pica*	marine shell	Midden z, Unit Z-58	Beta-276588	2240	40	—	Narganes Storde 2015
Water Island	U.S. Virgin Islands	Lesser Antilles	2	12VAm3-56	*Strombus gigas*	marine shell	50 cm below surface	Beta-58095	800	60	-25.0 (est.)	Anderson 1998
Water Island	U.S. Virgin Islands	Lesser Antilles	2	12VAm3-56	*Strombus gigas*	marine shell	base of midden	Beta-58094	1420	60	-25.0 (est.)	Anderson 1998
Water Island	U.S. Virgin Islands	Lesser Antilles	2	12VAm3-56	*Strombus gigas*	marine shell	surface of midden	Beta-58096	740	60	-25.0 (est.)	Anderson 1998

Water Island	U.S. Virgin Islands	Lesser Antilles	2	Banana Bay South (12VAM210)	*Strombus gigas*	marine shell	EU 5, Level 8	Beta-144769	790	50	+1.0	Anderson et al. 2003
Water Island	U.S. Virgin Islands	Lesser Antilles	2	Banana Bay South (12VAM210)	*Strombus gigas*	marine shell	EU1, Level 6	Beta-144767	940	70	+2.1	Anderson et al. 2003
Water Island	U.S. Virgin Islands	Lesser Antilles	2	Banana Bay South (12VAM210)	*Strombus gigas*	marine shell	EU2, Level 7	Beta-144768	940	50	+2.5	Anderson et al. 2003
Water Island	U.S. Virgin Islands	Lesser Antilles	2	Banana Bay South (12VAM210)	*Strombus costatus*	marine shell	EU5, Level 8	Beta-144770	620	40	+3.2	Anderson et al. 2003
West Caicos	Turks and Caicos	Bahamian Archipelago	3	WC-2	shell	marine shell	—	Beta-70800	820	60	—	Carlson 1999

S4. SQL code for 100 yr outlier models, 1,000 yr outlier models, and single-phase models.

100 yr Outlier Model SQL Code

Anguilla

```
Plot()
 {
  Outlier_Model("Charcoal",Exp(1,-10,0),U(0,2),"t");
  Sequence()
  {
   Boundary("Anguilla Start");
   Phase()
   {
    Curve("IntCal13","IntCal13.14c");
    R_Date("Beta-19957", 1550, 70)
    {
     Outlier("Charcoal", 1);
    };
    R_Date("Beta-15824", 1530, 140)
    {
     Outlier("Charcoal", 1);
    };
```

```
R_Date("Beta-18740", 1430, 70)
{
 Outlier("Charcoal", 1);
};
R_Date("Beta-21858", 1410, 60)
{
 Outlier("Charcoal", 1);
};
R_Date("Beta-110397", 1310, 80)
{
 Outlier("Charcoal", 1);
};
R_Date("Beta-19956", 1290, 60)
{
 Outlier("Charcoal", 1);
};
R_Date("Beta-110396", 1290, 60)
{
 Outlier("Charcoal", 1);
};
R_Date("Beta-106439", 1270, 60)
{
 Outlier("Charcoal", 1);
```

```
};
R_Date("Beta-110394", 1230, 70)
{
 Outlier("Charcoal", 1);
};
Curve("Marine13","Marine13.14c");
R_Date("Beta-15485", 1220, 70);
R_Date("Beta-106444", 1180, 60);
R_Date("Beta-106443", 1180, 60);
Curve("IntCal13","IntCal13.14c");
R_Date("PITT-0546", 1180, 45)
{
 Outlier("Charcoal", 1);
};
R_Date("Beta-110395", 1170, 80)
{
 Outlier("Charcoal", 1);
};
R_Date("Beta-19955", 1150, 60)
{
 Outlier("Charcoal", 1);
};
R_Date("Beta-110393", 1140, 60)
```

```
{
 Outlier("Charcoal", 1);
};
R_Date("PITT-0545", 1135, 40)
{
 Outlier("Charcoal", 1);
};
Curve("Marine13","Marine13.14c");
R_Date("Beta-15486", 1130, 80);
Curve("IntCal13","IntCal13.14c");
R_Date("Beta-106442", 1120, 70)
{
 Outlier("Charcoal", 1);
};
R_Date("Beta-18738", 1120, 70)
{
 Outlier("Charcoal", 1);
};
R_Date("PITT-0547", 1085, 55)
{
 Outlier("Charcoal", 1);
};
R_Date("Beta-21861", 1080, 90)
```

```
{
 Outlier("Charcoal", 1);
};
R_Date("Beta-18739", 1000, 110)
{
 Outlier("Charcoal", 1);
};
R_Date("Beta-120152", 950, 70)
{
 Outlier("Charcoal", 1);
};
R_Date("Beta-21863", 940, 80)
{
 Outlier("Charcoal", 1);
};
Curve("Marine13","Marine13.14c");
R_Date("Beta-257181", 910, 40);
R_Date("Beta-257182", 890, 40);
Curve("IntCal13","IntCal13.14c");
R_Date("Beta-21862", 880, 90)
{
 Outlier("Charcoal", 1);
};
```

```
R_Date("Beta-120157", 880, 80)
{
 Outlier("Charcoal", 1);
};
Curve("Marine13","Marine13.14c");
R_Date("Beta-257184", 860, 40);
Curve("IntCal13","IntCal13.14c");
R_Date("Beta-120154", 850, 60)
{
 Outlier("Charcoal", 1);
};
R_Date("Beta-106441", 840, 80)
{
 Outlier("Charcoal", 1);
};
Curve("Marine13","Marine13.14c");
R_Date("Beta-257185", 780, 40);
Curve("IntCal13","IntCal13.14c");
R_Date("Beta-110398", 780, 80)
{
 Outlier("Charcoal", 1);
};
Curve("Marine13","Marine13.14c");
```

```
R_Date("Beta-141202", 740, 60);
Curve("IntCal13","IntCal13.14c");
R_Date("Beta-120153", 740, 60)
{
 Outlier("Charcoal", 1);
};
R_Date("Beta-120156", 710, 80)
{
 Outlier("Charcoal", 1);
};
Curve("Marine13","Marine13.14c");
R_Date("Beta-257183", 680, 40);
Curve("IntCal13","IntCal13.14c");
R_Date("Beta-106440", 510, 80)
{
 Outlier("Charcoal", 1);
};
R_Date("Beta-120155", 440, 70)
{
 Outlier("Charcoal", 1);
};
Curve("Marine13","Marine13.14c");
R_Date("Beta-60776", 400, 60);
```

```
   };
   Boundary("Anguilla End");
  };
 };
```

Antigua

```
Plot()
 {
  Outlier_Model("Charcoal",Exp(1,-10,0),U(0,2),"t");
  Sequence("Antigua")
  {
   Boundary("Antigua Start");
   Phase()
   {
    Curve("IntCal13","IntCal13.14c");
    R_Date("I-7830", 2785, 80)
    {
     Outlier("Charcoal", 1);
    };
    R_Date("I-7842", 2785, 80)
    {
     Outlier("Charcoal", 1);
    };
```

```
R_Date("I-7980", 1915, 80)
{
 Outlier("Charcoal", 1);
};
R_Date("I-7981", 1855, 80)
{
 Outlier("Charcoal", 1);
};
R_Date("I-7979", 1790, 85)
{
 Outlier("Charcoal", 1);
};
R_Date("I-7855", 1765, 80)
{
 Outlier("Charcoal", 1);
};
R_Date("I-7838", 1750, 80)
{
 Outlier("Charcoal", 1);
};
R_Date("I-7837", 1715, 80)
{
 Outlier("Charcoal", 1);
```

```
};
R_Date("I-7854", 1670, 80)
{
 Outlier("Charcoal", 1);
};
R_Date("Beta- 124127", 1610, 80)
{
 Outlier("Charcoal", 1);
};
R_Date("Beta-124126", 1600, 50)
{
 Outlier("Charcoal", 1);
};
R_Date("I-7355", 1505, 85)
{
 Outlier("Charcoal", 1);
};
R_Date("I-7356", 1505, 85)
{
 Outlier("Charcoal", 1);
};
R_Date("I-7352", 1440, 85)
{
```

```
    Outlier("Charcoal", 1);
   };
   R_Date("Beta-101500", 1430, 50)
   {
    Outlier("Charcoal", 1);
   };
   R_Date("I-7353", 1230, 85)
   {
    Outlier("Charcoal", 1);
   };
   Curve("IntCal13","IntCal13.14c")
   Curve("Marine13","Marine13.14c");
   Mix_Curve("Mixed","IntCal13","Marine13",50,12);
   R_Date("SUERC-34163", 950, 30);
   Curve("IntCal13","IntCal13.14c");
   R_Date("Beta-101499", 720, 50)
   {
    Outlier("Charcoal", 1);
   };
  };
  Boundary("Antigua End");
 };
};
```

Aruba

```
Plot()
 {
  Outlier_Model("Charcoal",Exp(1,-10,0),U(0,2),"t");
  Sequence("Aruba")
  {
   Boundary("Aruba Start");
   Phase()
   {
    Curve("IntCal13","IntCal13.14c");
    R_Date("GrN-7341", 3300, 35)
    {
     Outlier("Charcoal", 1);
    };
    Curve("IntCal13","IntCal13.14c");
    Curve("Marine13","Marine13.14c");
    Mix_Curve("Mixed","IntCal13","Marine13",50,12);
    R_Date("Ua-1501", 2210, 95);
    R_Date("Ua-1341", 1740, 110);
    R_Date("Ua-1342", 1520, 100);
    R_Date("Ua-1340", 1520, 110);
    R_Date("Ua-1514", 1420, 150);
```

```
Curve("IntCal13","IntCal13.14c");
R_Date("GrN-2788", 1080, 50)
{
 Outlier("Charcoal", 1);
};
R_Date("GrN-7339", 1040, 45)
{
 Outlier("Charcoal", 1);
};
R_Date("GrN-21665", 1030, 40)
{
 Outlier("Charcoal", 1);
};
R_Date("GrN-21666", 1030, 30)
{
 Outlier("Charcoal", 1);
};
R_Date("GrN-7340", 1000, 30)
{
 Outlier("Charcoal", 1);
};
R_Date("GrN-7342", 990, 30)
{
```

```
 Outlier("Charcoal", 1);
};
R_Date("GrA-2789", 990, 50)
{
 Outlier("Charcoal", 1);
};
R_Date("GrN-7338", 940, 25)
{
 Outlier("Charcoal", 1);
};
R_Date("GrN-21656", 910, 30)
{
 Outlier("Charcoal", 1);
};
Curve("IntCal13","IntCal13.14c");
Curve("Marine13","Marine13.14c");
Mix_Curve("Mixed","IntCal13","Marine13",50,12);
R_Date("GrN-17460", 910, 170);
R_Date("GrN-17459", 870, 80);
Curve("IntCal13","IntCal13.14c");
R_Date("GrN-21664", 860, 40)
{
 Outlier("Charcoal", 1);
```

```
};
R_Date("GrA-2785", 860, 50)
{
 Outlier("Charcoal", 1);
};
R_Date("GrA-2778", 830, 50)
{
 Outlier("Charcoal", 1);
};
R_Date("GrN-16915", 825, 30)
{
 Outlier("Charcoal", 1);
};
R_Date("I-4025", 765, 110)
{
 Outlier("Charcoal", 1);
};
R_Date("GrA-2784", 750, 50)
{
 Outlier("Charcoal", 1);
};
R_Date("I-4026", 740, 105)
{
```

```
    Outlier("Charcoal", 1);
   };
   R_Date("GrA-2790", 340, 50)
   {
    Outlier("Charcoal", 1);
   };
  };
  Boundary("Aruba End");
 };
};
```

Barbados

```
Plot()
 {
  Outlier_Model("Charcoal",Exp(1,-10,0),U(0,2),"t");
  Sequence("Barbados")
  {
   Boundary("Barbados Start");
   Phase()
   {
    Curve("Marine13","Marine13.14c");
    R_Date("D-AMS 001792", 4366, 32);
    R_Date("Beta-297522", 4360, 40);
```

```
   R_Date("D-AMS 001793", 4278, 29);
   R_Date("Beta-297521", 4230, 50);
   R_Date("D-AMS 001794", 4091, 27);
   R_Date("I-16840", 3980, 100);
   Curve("IntCal13","IntCal13.14c");
   R_Date("Beta-20723", 1950, 150)
   {
    Outlier("Charcoal", 1);
   };
   R_Date("I-2486", 1570, 95)
   {
    Outlier("Charcoal", 1);
   };
   Curve("Marine13","Marine13.14c");
   R_Date("1-16189", 1120, 80);
  };
  Boundary("Barbados End");
 };
};
```

Barbuda

```
Plot()
 {
```

```
Outlier_Model("Charcoal",Exp(1,-10,0),U(0,2),"t");
Sequence("Barbuda")
{
 Boundary("Barbuda Start");
 Phase()
 {
  Curve("Marine13","Marine13.14c");
  R_Date("UCI-107938", 3430, 15);
  R_Date("SUERC-33604 (GU-23530)", 3280, 35);
  R_Date("SUERC 33605 (GU-23531)", 2790, 35);
  R_Date("UCI-107937", 2565, 20);
  R_Date("Beta-103891", 2030, 60);
  Curve("IntCal13","IntCal13.14c");
  R_Date("SUERC 18562", 2025, 35)
  {
   Outlier("Charcoal", 1);
  };
  R_Date("SUERC 18560", 2005, 35)
  {
   Outlier("Charcoal", 1);
  };
  R_Date("SUERC 18561", 1920, 35)
  {
```

```
 Outlier("Charcoal", 1);
};
R_Date("SUERC 18558", 1785, 35)
{
 Outlier("Charcoal", 1);
};
R_Date("SUERC 18557", 1755, 35)
{
 Outlier("Charcoal", 1);
};
R_Date("SUERC 34971", 1565, 35)
{
 Outlier("Charcoal", 1);
};
Curve("Marine13","Marine13.14c");
R_Date("Beta-103894", 1400, 60);
R_Date("PITT-1234", 1365, 45);
R_Date("Beta-103892", 1360, 60);
R_Date("Beta-103893", 1350, 60);
R_Date("Beta-103890", 1210, 60);
R_Date("PITT-1233", 1135, 50);
R_Date("PITT-1231", 1050, 30);
Curve("IntCal13","IntCal13.14c");
```

```
  R_Date("SUERC 18556", 820, 35)
  {
   Outlier("Charcoal", 1);
  };
 };
 Boundary("Barbuda End");
};
};
```

Bonaire

```
Plot()
 {
  Outlier_Model("Charcoal",Exp(1,-10,0),U(0,2),"t");
  Sequence("Bonaire")
  {
   Boundary("Bonaire Start");
   Phase()
   {
    Curve("Marine13","Marine13.14c");
    R_Date("GrN-32756", 3610, 25);
    R_Date("GrN-32758", 3410, 20);
    R_Date("GrN-32751", 3245, 25);
    R_Date("GrN-32750", 3095, 20);
```

```
R_Date("GrN-32749", 2785, 20);
R_Date("GrN-32755", 2735, 25);
R_Date("GrN-32752", 2705, 30);
R_Date("GrN-32757", 2680, 25);
R_Date("GrN-32754", 2665, 20);
R_Date("GrN-32753", 2575, 20);
R_Date("GrN-32748", 2412, 15);
Curve("IntCal13","IntCal13.14c");
R_Date("PITT-0267", 1480, 25)
{
 Outlier("Charcoal", 1);
};
R_Date("PITT-0268", 885, 45)
{
 Outlier("Charcoal", 1);
};
R_Date("PITT-0265", 710, 65)
{
 Outlier("Charcoal", 1);
};
R_Date("PITT-0264", 560, 40)
{
 Outlier("Charcoal", 1);
```

```
    };
    R_Date("PITT-0266", 505, 35)
    {
     Outlier("Charcoal", 1);
    };
   };
   Boundary("Bonaire End");
  };
 };
```

Carriacou

```
Plot()
 {
  Outlier_Model("Charcoal",Exp(1,-10,0),U(0,2),"t");
  Sequence("Carriacou")
  {
   Boundary("Carriacou Start");
   Phase()
   {
    Curve("Marine13","Marine13.14c");
    R_Date("AA-62278", 1917, 37);
    R_Date("Beta-206685", 1870, 70);
    R_Date("AA-62280b", 1822, 41);
```

```
R_Date("AA-62280a", 1789, 38);
Curve("IntCal13","IntCal13.14c");
R_Date("AA-67535", 1588, 36)
{
 Outlier("Charcoal", 1);
};
R_Date("AA-67536", 1584, 36)
{
 Outlier("Charcoal", 1);
};
Curve("Marine13","Marine13.14c");
R_Date("GX-30424", 1570, 60);
Curve("IntCal13","IntCal13.14c");
Curve("Marine13","Marine13.14c");
Mix_Curve("Mixed","IntCal13","Marine13",50,12);
R_Date("UCIAMS-111935", 1565, 15);
Curve("Marine13","Marine13.14c");
R_Date("GX-30425", 1460, 60);
R_Date("GX-30423", 1400, 60);
Curve("IntCal13","IntCal13.14c");
R_Date("AA-62281", 1339, 36)
{
 Outlier("Charcoal", 1);
```

```
};
R_Date("AA-67534", 1333, 57)
{
 Outlier("Charcoal", 1);
};
R_Date("D-AMS 016647", 1328, 20)
{
 Outlier("Charcoal", 1);
};
R_Date("D-AMS 16649", 1321, 20)
{
 Outlier("Charcoal", 1);
};
R_Date("D-AMS 016648", 1315, 20)
{
 Outlier("Charcoal", 1);
};
Curve("Marine13","Marine13.14c");
R_Date("Beta-233647", 1310, 40);
R_Date("UCIAMS-94046", 1265, 20);
Curve("IntCal13","IntCal13.14c");
R_Date("AA-62279", 1243, 36)
{
```

```
 Outlier("Charcoal", 1);
};
R_Date("AA-62282", 1227, 36)
{
 Outlier("Charcoal", 1);
};
R_Date("OS-71467", 1220, 20)
{
 Outlier("Charcoal", 1);
};
R_Date("AA-67533", 1172, 36)
{
 Outlier("Charcoal", 1);
};
R_Date("AA-81055", 1158, 45)
{
 Outlier("Charcoal", 1);
};
R_Date("OS-71463", 1140, 15)
{
 Outlier("Charcoal", 1);
};
R_Date("AA-67531", 1133, 38)
```

```
{
 Outlier("Charcoal", 1);
};
R_Date("OS-71464", 1100, 20)
{
 Outlier("Charcoal", 1);
};
R_Date("OS-71465", 1080, 15)
{
 Outlier("Charcoal", 1);
};
R_Date("AA-67532", 1073, 38)
{
 Outlier("Charcoal", 1);
};
Curve("IntCal13","IntCal13.14c");
Curve("Marine13","Marine13.14c");
Mix_Curve("Mixed","IntCal13","Marine13",50,12);
R_Date("AA-62283", 1062, 44);
Curve("IntCal13","IntCal13.14c");
R_Date("AA-67530", 1039, 35)
{
 Outlier("Charcoal", 1);
```

```
};
R_Date("OS-41358", 1030, 30)
{
 Outlier("Charcoal", 1);
};
R_Date("UCIAMS-94045", 1020, 20)
{
 Outlier("Charcoal", 1);
};
Curve("IntCal13","IntCal13.14c");
Curve("Marine13","Marine13.14c");
Mix_Curve("Mixed","IntCal13","Marine13",50,12);
R_Date("UCIAMS-120951", 1015, 15);
Curve("IntCal13","IntCal13.14c");
R_Date("AA-81056", 994, 45)
{
 Outlier("Charcoal", 1);
};
R_Date("UCIAMS-94044", 990, 20)
{
 Outlier("Charcoal", 1);
};
R_Date("AA-67529", 988, 42)
```

```
{
 Outlier("Charcoal", 1);
};
R_Date("OS-71462", 975, 20)
{
 Outlier("Charcoal", 1);
};
R_Date("OS-71408", 970, 15)
{
 Outlier("Charcoal", 1);
};
R_Date("OS-71407", 960, 15)
{
 Outlier("Charcoal", 1);
};
R_Date("RL-29", 940, 100)
{
 Outlier("Charcoal", 1);
};
R_Date("OS-71409", 925, 15)
{
 Outlier("Charcoal", 1);
};
```

```
  Curve("IntCal13","IntCal13.14c");
  Curve("Marine13","Marine13.14c");
  Mix_Curve("Mixed","IntCal13","Marine13",50,12);
  R_Date("Beta-257793", 870, 40);
  Curve("IntCal13","IntCal13.14c");
  R_Date("OS-71466", 680, 15)
  {
   Outlier("Charcoal", 1);
  };
  R_Date("AA-81054", 657, 44)
  {
   Outlier("Charcoal", 1);
  };
  Curve("IntCal13","IntCal13.14c");
  Curve("Marine13","Marine13.14c");
  Mix_Curve("Mixed","IntCal13","Marine13",50,12);
  R_Date("UCIAMS-111933", 715, 15);
  R_Date("UCIAMS-111934", 690, 15);
 };
 Boundary("Carriacou End");
};
};
```

Cuba

```
Plot()
 {
  Outlier_Model("Charcoal",Exp(1,-10,0),U(0,2),"t");
  Sequence("Cuba")
  {
   Boundary("Cuba Start");
   Phase()
   {
    Curve("IntCal13","IntCal13.14c");
    R_Date("LE-4283", 5270, 120)
    {
     Outlier("Charcoal", 1);
    };
    R_Date("GD-250", 5140, 170)
    {
     Outlier("Charcoal", 1);
    };
    R_Date("MC-860", 4420, 100)
    {
     Outlier("Charcoal", 1);
    };
    Curve("Marine13","Marine13.14c");
```

```
R_Date("OxA-15267", 4408, 37);
Curve("IntCal13","IntCal13.14c");
R_Date("MC-859", 4240, 100)
{
 Outlier("Charcoal", 1);
};
R_Date("UBAR-170", 4200, 79)
{
 Outlier("Charcoal", 1);
};
R_Date("Beta-140079", 4180, 80)
{
 Outlier("Charcoal", 1);
};
R_Date("LE-1783", 4110, 50)
{
 Outlier("Charcoal", 1);
};
R_Date("SI-429", 4000, 150)
{
 Outlier("Charcoal", 1);
};
R_Date("LE-1784", 3870, 40)
```

```
{
 Outlier("Charcoal", 1);
};
Curve("Marine13","Marine13.14c");
R_Date("OxA-15180", 3861, 28);
Curve("IntCal13","IntCal13.14c");
R_Date("LE-1782", 3760, 40)
{
 Outlier("Charcoal", 1);
};
R_Date("Beta-133951", 3720, 70)
{
 Outlier("Charcoal", 1);
};
R_Date("UNAM-0716", 3460, 60)
{
 Outlier("Charcoal", 1);
};
R_Date("GD-204", 3460, 160)
{
 Outlier("Charcoal", 1);
};
Curve("Marine13","Marine13.14c");
```

```
R_Date("OxA-15264", 3273, 33);
R_Date("OxA-15263", 3271, 29);
Curve("IntCal13","IntCal13.14c");
R_Date("Y-1764", 3250, 100)
{
 Outlier("Charcoal", 1);
};
R_Date("LE-4270", 3110, 180)
{
 Outlier("Charcoal", 1);
};
R_Date("SI-428", 3110, 200)
{
 Outlier("Charcoal", 1);
};
R_Date("UBAR-169", 3060, 180)
{
 Outlier("Charcoal", 1);
};
R_Date("AA-101053", 3057, 39)
{
 Outlier("Charcoal", 1);
};
```

```
R_Date("LE-4288", 3030, 180)
{
 Outlier("Charcoal", 1);
};
R_Date("LE-4287", 3030, 180)
{
 Outlier("Charcoal", 1);
};
Curve("IntCal13","IntCal13.14c");
Curve("Marine13","Marine13.14c");
Mix_Curve("Mixed","IntCal13","Marine13",50,12);
R_Date("AA-101054", 2999, 61);
R_Date("AA-101057", 2996, 53);
Curve("Marine13","Marine13.14c");
R_Date("Beta-184894", 2980, 70);
Curve("IntCal13","IntCal13.14c");
Curve("Marine13","Marine13.14c");
Mix_Curve("Mixed","IntCal13","Marine13",50,12);
R_Date("AA-89061", 2960, 33);
R_Date("AA-101052", 2946, 57);
Curve("IntCal13","IntCal13.14c");
R_Date("LE-4282", 2930, 300)
{
```

```
 Outlier("Charcoal", 1);
};
R_Date("GD-591", 2930, 80)
{
 Outlier("Charcoal", 1);
};
Curve("IntCal13","IntCal13.14c");
Curve("Marine13","Marine13.14c");
Mix_Curve("Mixed","IntCal13","Marine13",50,12);
R_Date("AA-89063", 2922, 34);
Curve("IntCal13","IntCal13.14c");
R_Date("GD-613", 2880, 70)
{
 Outlier("Charcoal", 1);
};
R_Date("A-14316", 2845, 90)
{
 Outlier("Charcoal", 1);
};
R_Date("GD-1046", 2840, 60)
{
 Outlier("Charcoal", 1);
};
```

```
R_Date("GD-601", 2805, 60)
{
 Outlier("Charcoal", 1);
};
Curve("IntCal13","IntCal13.14c");
Curve("Marine13","Marine13.14c");
Mix_Curve("Mixed","IntCal13","Marine13",50,12);
R_Date("AA-101059", 2791, 51);
Curve("IntCal13","IntCal13.14c");
R_Date("Beta-133950", 2780, 40)
{
 Outlier("Charcoal", 1);
};
R_Date("LE-4272", 2750, 160)
{
 Outlier("Charcoal", 1);
};
R_Date("GD-614", 2720, 65)
{
 Outlier("Charcoal", 1);
};
R_Date("LE-2720", 2680, 40)
{
```

```
 Outlier("Charcoal", 1);
};
Curve("Marine13","Marine13.14c");
R_Date("Beta-184896", 2680, 60);
Curve("IntCal13","IntCal13.14c");
R_Date("LE-4290", 2610, 120)
{
 Outlier("Charcoal", 1);
};
R_Date("LE-4281", 2610, 120)
{
 Outlier("Charcoal", 1);
};
R_Date("LE-2718", 2610, 40)
{
 Outlier("Charcoal", 1);
};
R_Date("LE-4275", 2580, 90)
{
 Outlier("Charcoal", 1);
};
Curve("Marine13","Marine13.14c");
R_Date("Beta-318171", 2570, 30);
```

```
Curve("IntCal13","IntCal13.14c");
R_Date("UNAM-0717", 2520, 60)
{
 Outlier("Charcoal", 1);
};
R_Date("A-14315", 2515, 75)
{
 Outlier("Charcoal", 1);
};
R_Date("SI-427", 2510, 200)
{
 Outlier("Charcoal", 1);
};
R_Date("LE-4273", 2420, 100)
{
 Outlier("Charcoal", 1);
};
R_Date("LE-4279", 2390, 170)
{
 Outlier("Charcoal", 1);
};
R_Date("LE-4271", 2380, 80)
{
```

```
 Outlier("Charcoal", 1);
};
Curve("Marine13","Marine13.14c");
R_Date("Beta-422938", 2350, 30);
Curve("IntCal13","IntCal13.14c");
R_Date("LE-4276", 2250, 150)
{
 Outlier("Charcoal", 1);
};
R_Date("LE-4267", 2220, 160)
{
 Outlier("Charcoal", 1);
};
R_Date("GD-1039", 2160, 55)
{
 Outlier("Charcoal", 1);
};
R_Date("LE-2719", 2160, 40)
{
 Outlier("Charcoal", 1);
};
R_Date("SI-426", 2070, 150)
{
```

```
 Outlier("Charcoal", 1);
};
R_Date("LC-H 1034", 2070, 110)
{
 Outlier("Charcoal", 1);
};
R_Date("LE-4274", 2030, 160)
{
 Outlier("Charcoal", 1);
};
Curve("Marine13","Marine13.14c");
R_Date("Beta-214957", 2020, 50);
Curve("IntCal13","IntCal13.14c");
R_Date("Lv-2063", 2020, 80)
{
 Outlier("Charcoal", 1);
};
R_Date("LE-2717", 2010, 40)
{
 Outlier("Charcoal", 1);
};
Curve("Marine13","Marine13.14c");
R_Date("OxA-15262", 2005, 27);
```

```
Curve("IntCal13","IntCal13.14c");
R_Date("GD-1051", 1990, 80)
{
 Outlier("Charcoal", 1);
};
Curve("Marine13","Marine13.14c");
R_Date("OxA-15266", 1978, 33);
R_Date("Beta-214958", 1910, 50);
Curve("IntCal13","IntCal13.14c");
R_Date("Beta-93862", 1890, 60)
{
 Outlier("Charcoal", 1);
};
Curve("Marine13","Marine13.14c");
R_Date("OxA-15183", 1873, 26);
Curve("IntCal13","IntCal13.14c");
R_Date("Beta-93866", 1850, 50)
{
 Outlier("Charcoal", 1);
};
Curve("Marine13","Marine13.14c");
R_Date("Beta-318170", 1750, 30);
Curve("IntCal13","IntCal13.14c");
```

```
R_Date("UM-1953", 1745, 175)
{
 Outlier("Charcoal", 1);
};
Curve("Marine13","Marine13.14c");
R_Date("OxA-15184", 1686, 26);
Curve("IntCal13","IntCal13.14c");
Curve("Marine13","Marine13.14c");
Mix_Curve("Mixed","IntCal13","Marine13",50,12);
R_Date("Beta-72801", 1670, 70);
R_Date("AA-101055", 1661, 52);
Curve("IntCal13","IntCal13.14c");
R_Date("Beta-133948", 1640, 130)
{
 Outlier("Charcoal", 1);
};
R_Date("SI-424", 1620, 150)
{
 Outlier("Charcoal", 1);
};
R_Date("AA-89064", 1617, 46)
{
 Outlier("Charcoal", 1);
```

```
};
Curve("IntCal13","IntCal13.14c");
Curve("Marine13","Marine13.14c");
Mix_Curve("Mixed","IntCal13","Marine13",50,12);
R_Date("OxA-15260", 1617, 29);
R_Date("Beta-72802", 1590, 60);
Curve("Marine13","Marine13.14c");
R_Date("OxA-15181", 1561, 24);
R_Date("OxA-15146", 1557, 25);
Curve("IntCal13","IntCal13.14c");
Curve("Marine13","Marine13.14c");
Mix_Curve("Mixed","IntCal13","Marine13",50,12);
R_Date("AA-89062", 1536, 51);
Curve("IntCal13","IntCal13.14c");
R_Date("GD-617", 1495, 60)
{
 Outlier("Charcoal", 1);
};
R_Date("LE-4269", 1470, 110)
{
 Outlier("Charcoal", 1);
};
R_Date("LC-H 1035", 1450, 70)
```

```
{
 Outlier("Charcoal", 1);
};
Curve("IntCal13","IntCal13.14c");
Curve("Marine13","Marine13.14c");
Mix_Curve("Mixed","IntCal13","Marine13",50,12);
R_Date("AA-89060", 1420, 59);
Curve("IntCal13","IntCal13.14c");
R_Date("TO-7621", 1404, 60)
{
 Outlier("Charcoal", 1);
};
R_Date("GD-616", 1350, 70)
{
 Outlier("Charcoal", 1);
};
R_Date("Beta-93863", 1350, 50)
{
 Outlier("Charcoal", 1);
};
R_Date("TO-7624", 1320, 60)
{
 Outlier("Charcoal", 1);
```

```
};
Curve("IntCal13","IntCal13.14c");
Curve("Marine13","Marine13.14c");
Mix_Curve("Mixed","IntCal13","Marine13",50,12);
R_Date("AA-101056", 1289, 46);
Curve("IntCal13","IntCal13.14c");
R_Date("Beta-140078", 1280, 60)
{
 Outlier("Charcoal", 1);
};
R_Date("Beta-133947", 1210, 60)
{
 Outlier("Charcoal", 1);
};
R_Date("GD-619", 1170, 90)
{
 Outlier("Charcoal", 1);
};
R_Date("Y-1994", 1120, 160)
{
 Outlier("Charcoal", 1);
};
Curve("Marine13","Marine13.14c");
```

```
R_Date("OxA-15179", 1112, 26);
Curve("IntCal13","IntCal13.14c");
R_Date("LC-H-1106", 1100, 130)
{
 Outlier("Charcoal", 1);
};
R_Date("SI-347", 1020, 100)
{
 Outlier("Charcoal", 1);
};
R_Date("GD-203", 1010, 110)
{
 Outlier("Charcoal", 1);
};
R_Date("Mo-399", 1000, 105)
{
 Outlier("Charcoal", 1);
};
R_Date("Y-1556", 970, 80)
{
 Outlier("Charcoal", 1);
};
R_Date("SI-352", 970, 100)
```

```
{
 Outlier("Charcoal", 1);
};
R_Date("Y-465", 960, 60)
{
 Outlier("Charcoal", 1);
};
R_Date("LC-H 565", 960, 50)
{
 Outlier("Charcoal", 1);
};
Curve("Marine13","Marine13.14c");
R_Date("OxA-15151", 950, 24);
R_Date("OxA-15152", 939, 24);
Curve("IntCal13","IntCal13.14c");
R_Date("GD-618", 910, 85)
{
 Outlier("Charcoal", 1);
};
Curve("Marine13","Marine13.14c");
R_Date("OxA-15148", 891, 23);
Curve("IntCal13","IntCal13.14c");
R_Date("FS AC 2418", 880, 40)
```

```
{
 Outlier("Charcoal", 1);
};
R_Date("Beta-148961", 880, 80)
{
 Outlier("Charcoal", 1);
};
Curve("Marine13","Marine13.14c");
R_Date("OxA-15145", 879, 26);
R_Date("OxA-15149", 874, 25);
Curve("IntCal13","IntCal13.14c");
Curve("Marine13","Marine13.14c");
Mix_Curve("Mixed","IntCal13","Marine13",50,12);
R_Date("Beta-148956", 870, 70);
Curve("Marine13","Marine13.14c");
R_Date("OxA-15182", 857, 24);
R_Date("OxA-15259", 827, 36);
R_Date("OxA-15154", 820, 24);
Curve("IntCal13","IntCal13.14c");
R_Date("Y-206", 810, 80)
{
 Outlier("Charcoal", 1);
};
```

```
Curve("Marine13","Marine13.14c");
R_Date("OxA-15261", 782, 26);
Curve("IntCal13","IntCal13.14c");
R_Date("Lv-2062", 780, 100)
{
 Outlier("Charcoal", 1);
};
R_Date("FS AC 2414", 770, 35)
{
 Outlier("Charcoal", 1);
};
Curve("Marine13","Marine13.14c");
R_Date("OxA-15265", 763, 25);
Curve("IntCal13","IntCal13.14c");
R_Date("Y-1555", 760, 60)
{
 Outlier("Charcoal", 1);
};
R_Date("Beta-148957", 730, 60)
{
 Outlier("Charcoal", 1);
};
Curve("Marine13","Marine13.14c");
```

```
R_Date("OxA-15153", 714, 25);
Curve("IntCal13","IntCal13.14c");
R_Date("OxA-15123", 710, 27)
{
 Outlier("Charcoal", 1);
};
Curve("Marine13","Marine13.14c");
R_Date("OxA-15178", 709, 26);
Curve("IntCal13","IntCal13.14c");
R_Date("GD-621", 705, 65)
{
 Outlier("Charcoal", 1);
};
R_Date("FS AC 2419", 690, 50)
{
 Outlier("Charcoal", 1);
};
R_Date("Beta-148949", 690, 60)
{
 Outlier("Charcoal", 1);
};
R_Date("FS AC 2415", 690, 50)
{
```

```
 Outlier("Charcoal", 1);
};
R_Date("Beta-148958", 670, 70)
{
 Outlier("Charcoal", 1);
};
R_Date("GD-1053", 665, 50)
{
 Outlier("Charcoal", 1);
};
R_Date("FS AC 2416", 660, 35)
{
 Outlier("Charcoal", 1);
};
R_Date("OxA-15144", 651, 24)
{
 Outlier("Charcoal", 1);
};
R_Date("SI-425", 650, 200)
{
 Outlier("Charcoal", 1);
};
R_Date("SI-348", 640, 120)
```

```
{
 Outlier("Charcoal", 1);
};
R_Date("FS AC 2417", 620, 30)
{
 Outlier("Charcoal", 1);
};
R_Date("Beta-148962", 620, 60)
{
 Outlier("Charcoal", 1);
};
R_Date("GD-1056", 600, 55)
{
 Outlier("Charcoal", 1);
};
R_Date("SI-353", 590, 90)
{
 Outlier("Charcoal", 1);
};
R_Date("SI-351", 590, 100)
{
 Outlier("Charcoal", 1);
};
```

```
R_Date("GD-1055", 575, 60)
{
 Outlier("Charcoal", 1);
};
R_Date("TO-7628", 560, 50)
{
 Outlier("Charcoal", 1);
};
R_Date("SI-349", 550, 150)
{
 Outlier("Charcoal", 1);
};
R_Date("TO-7626", 540, 50)
{
 Outlier("Charcoal", 1);
};
R_Date("OxA-15150", 531, 23)
{
 Outlier("Charcoal", 1);
};
R_Date("TO-7618", 510, 50)
{
 Outlier("Charcoal", 1);
```

```
};
R_Date("GD-624", 505, 40)
{
 Outlier("Charcoal", 1);
};
R_Date("Beta-148960", 500, 50)
{
 Outlier("Charcoal", 1);
};
R_Date("SI-350", 500, 100)
{
 Outlier("Charcoal", 1);
};
R_Date("GD-1057", 490, 45)
{
 Outlier("Charcoal", 1);
};
R_Date("GD-1054", 485, 50)
{
 Outlier("Charcoal", 1);
};
R_Date("TO-8068", 480, 60)
{
```

```
 Outlier("Charcoal", 1);
};
R_Date("FS AC 2424", 475, 35)
{
 Outlier("Charcoal", 1);
};
R_Date("TO-7627", 460, 50)
{
 Outlier("Charcoal", 1);
};
R_Date("FS AC 2420", 450, 35)
{
 Outlier("Charcoal", 1);
};
R_Date("TO-8072", 430, 60)
{
 Outlier("Charcoal", 1);
};
R_Date("TO-7620", 430, 50)
{
 Outlier("Charcoal", 1);
};
R_Date("FS AC 2422", 420, 45)
```

```
{
 Outlier("Charcoal", 1);
};
Curve("IntCal13","IntCal13.14c");
Curve("Marine13","Marine13.14c");
Mix_Curve("Mixed","IntCal13","Marine13",50,12);
R_Date("ICA 17B/0756", 420, 40);
Curve("IntCal13","IntCal13.14c");
R_Date("TO-7623", 390, 50)
{
 Outlier("Charcoal", 1);
};
R_Date("FS AC 2421", 375, 25)
{
 Outlier("Charcoal", 1);
};
Curve("IntCal13","IntCal13.14c");
Curve("Marine13","Marine13.14c");
Mix_Curve("Mixed","IntCal13","Marine13",50,12);
R_Date("Beta-148955", 360, 80);
Curve("IntCal13","IntCal13.14c");
R_Date("TO-7625", 340, 50)
{
```

```
    Outlier("Charcoal", 1);
   };
   R_Date("TO-7617", 330, 50)
   {
    Outlier("Charcoal", 1);
   };
   R_Date("TO-7622", 320, 40)
   {
    Outlier("Charcoal", 1);
   };
   R_Date("FS AC 2423", 315, 45)
   {
    Outlier("Charcoal", 1);
   };
  };
  Boundary("Cuba End");
 };
};
```

Curaçao

```
Plot()
 {
  Outlier_Model("Charcoal",Exp(1,-10,0),U(0,2),"t");
```

```
Sequence("Curacao")
{
 Boundary("Curacao Start");
 Phase()
 {
  Curve("IntCal13","IntCal13.14c");
  R_Date("IVIC-247", 4490, 60)
  {
   Outlier("Charcoal", 1);
  };
  R_Date("IVIC-246", 4160, 80)
  {
   Outlier("Charcoal", 1);
  };
  R_Date("IVIC-234", 4110, 65)
  {
   Outlier("Charcoal", 1);
  };
  R_Date("IVIC-242", 4070, 65)
  {
   Outlier("Charcoal", 1);
  };
  R_Date("IVIC-240", 3990, 50)
```

```
{
 Outlier("Charcoal", 1);
};
Curve("Marine13","Marine13.14c");
R_Date("PITT-1200", 1965, 35);
Curve("IntCal13","IntCal13.14c");
R_Date("PITT-1183", 1875, 430)
{
 Outlier("Charcoal", 1);
};
Curve("IntCal13","IntCal13.14c");
Curve("Marine13","Marine13.14c");
Mix_Curve("Mixed","IntCal13","Marine13",50,12);
R_Date("GrN-12914", 1500, 200);
Curve("IntCal13","IntCal13.14c");
R_Date("IVIC-237", 1440, 60)
{
 Outlier("Charcoal", 1);
};
R_Date("IVIC-250", 1230, 60)
{
 Outlier("Charcoal", 1);
};
```

```
R_Date("IVIC-233", 910, 50)
{
 Outlier("Charcoal", 1);
};
R_Date("PITT-1198", 875, 35)
{
 Outlier("Charcoal", 1);
};
R_Date("IVIC-244", 830, 60)
{
 Outlier("Charcoal", 1);
};
R_Date("PITT-1196", 775, 60)
{
 Outlier("Charcoal", 1);
};
Curve("IntCal13","IntCal13.14c");
Curve("Marine13","Marine13.14c");
Mix_Curve("Mixed","IntCal13","Marine13",50,12);
R_Date("DIC-3138", 660, 20);
Curve("IntCal13","IntCal13.14c");
R_Date("IVIC-248", 630, 50)
{
```

```
 Outlier("Charcoal", 1);
};
R_Date("IVIC-249", 630, 60)
{
 Outlier("Charcoal", 1);
};
R_Date("GrN-31926", 605, 15)
{
 Outlier("Charcoal", 1);
};
R_Date("PITT-1195", 590, 50)
{
 Outlier("Charcoal", 1);
};
R_Date("PITT-1188", 475, 50)
{
 Outlier("Charcoal", 1);
};
R_Date("GrN-32016", 450, 30)
{
 Outlier("Charcoal", 1);
};
R_Date("GrN-9997", 420, 15)
```

```
   {
    Outlier("Charcoal", 1);
   };
   R_Date("PITT-1197", 395, 115)
   {
    Outlier("Charcoal", 1);
   };
   R_Date("GrN-32017", 370, 25)
   {
    Outlier("Charcoal", 1);
   };
   R_Date("IVIC-241", 340, 50)
   {
    Outlier("Charcoal", 1);
   };
   R_Date("GrN-9998", 325, 35)
   {
    Outlier("Charcoal", 1);
   };
  };
  Boundary("Curacao End");
 };
};
```

Grand Turk

```
Plot()
 {
  Outlier_Model("Charcoal",Exp(1,-10,0),U(0,2),"t");
  Sequence("Grand Turk")
  {
   Boundary("Grand Turk Start");
   Phase()
   {
    Curve("IntCal13","IntCal13.14c");
    R_Date("Beta-80911", 1280, 60)
    R_Date("Beta-98698", 1230, 60)
    {
     Outlier("Charcoal", 1);
    };
    Curve("Marine13","Marine13.14c");
    R_Date("Beta-93912", 1170, 60);
    Curve("IntCal13","IntCal13.14c");
    R_Date("Beta-80910", 1160, 60)
    R_Date("Beta-114924", 1120, 50)
    {
     Outlier("Charcoal", 1);
```

```
};
R_Date("Beta-66151", 1120, 120)
{
 Outlier("Charcoal", 1);
};
R_Date("Beta-98697", 1010, 50)
{
 Outlier("Charcoal", 1);
};
R_Date("Beta-96700", 940, 60)
Curve("Marine13","Marine13.14c");
R_Date("Beta-93913", 930, 60);
Curve("IntCal13","IntCal13.14c");
R_Date("Beta-242672", 910, 40)
{
 Outlier("Charcoal", 1);
};
R_Date("Beta-98699", 900, 50)
{
 Outlier("Charcoal", 1);
};
Curve("Marine13","Marine13.14c");
R_Date("Beta-242675", 850, 50);
```

```
   R_Date("Beta-242673", 790, 50);
   Curve("IntCal13","IntCal13.14c");
   R_Date("Beta-253527", 780, 40)
   {
    Outlier("Charcoal", 1);
   };
   R_Date("Beta 242670", 690, 40)
   {
    Outlier("Charcoal", 1);
   };
   R_Date("Beta-242671", 610, 40)
   {
    Outlier("Charcoal", 1);
   };
   Curve("Marine13","Marine13.14c");
   R_Date("Beta-242674", 460, 40);
  };
  Boundary("Grand Turk End");
 };
};
```

Grenada

```
Plot()
```

```
{
 Outlier_Model("Charcoal",Exp(1,-10,0),U(0,2),"t");
 Sequence("Grenada")
 {
  Boundary("Grenada Start");
  Phase()
  {
   Curve("Marine13","Marine13.14c");
   R_Date("PSUAMS-3017", 2820, 20);
   R_Date("PSUAMS-3022", 2145, 20);
   Curve("IntCal13","IntCal13.14c");
   R_Date("PSUAMS-1317", 1685, 20)
   {
    Outlier("Charcoal", 1);
   };
   Curve("Marine13","Marine13.14c");
   R_Date("PSUAMS-3020", 1510, 20);
   Curve("IntCal13","IntCal13.14c");
   R_Date("PSUAMS-1287", 1500, 25)
   {
    Outlier("Charcoal", 1);
   };
   Curve("Marine13","Marine13.14c");
```

```
R_Date("UCIAMS-179806", 1380, 20);
Curve("IntCal13","IntCal13.14c");
R_Date("Beta-85941", 1270, 50)
{
 Outlier("Charcoal", 1);
};
R_Date("PSUAMS-1565", 1215, 20)
{
 Outlier("Charcoal", 1);
};
R_Date("PSUAMS-3946", 1215, 20)
{
 Outlier("Charcoal", 1);
};
R_Date("PSUAMS-1320", 1180, 25)
{
 Outlier("Charcoal", 1);
};
R_Date("Beta-85935", 1110, 40)
{
 Outlier("Charcoal", 1);
};
R_Date("Beta-98365", 1080, 50)
```

```
{
 Outlier("Charcoal", 1);
};
R_Date("Beta-86831", 1050, 90)
{
 Outlier("Charcoal", 1);
};
R_Date("Beta-98368", 980, 60)
{
 Outlier("Charcoal", 1);
};
R_Date("Beta-86827", 900, 60)
{
 Outlier("Charcoal", 1);
};
R_Date("Beta-85938", 850, 40)
{
 Outlier("Charcoal", 1);
};
R_Date("PSUAMS-1322", 835, 25)
{
 Outlier("Charcoal", 1);
};
```

```
R_Date("Beta-86833", 810, 50)
{
 Outlier("Charcoal", 1);
};
R_Date("Beta-86832", 790, 60)
{
 Outlier("Charcoal", 1);
};
R_Date("Beta-85939", 770, 60)
{
 Outlier("Charcoal", 1);
};
R_Date("Beta-86830", 770, 50)
{
 Outlier("Charcoal", 1);
};
R_Date("Beta-86828", 650, 40)
{
 Outlier("Charcoal", 1);
};
R_Date("Beta-86829", 550, 60)
{
 Outlier("Charcoal", 1);
```

```
    };
    R_Date("Beta-98367", 510, 60)
    {
     Outlier("Charcoal", 1);
    };
    R_Date("PSUAMS-3945", 380, 25)
    {
     Outlier("Charcoal", 1);
    };
    R_Date("Beta-98366", 340, 50)
    {
     Outlier("Charcoal", 1);
    };
   };
   Boundary("Grenada End");
  };
 };
```

Guadeloupe

```
Plot()
 {
  Outlier_Model("Charcoal",Exp(1,-10,0),U(0,2),"t");
  Sequence("Guadeloupe")
```

```
{
 Boundary("Guadeloupe Start");
 Phase()
 {
  Curve("IntCal13","IntCal13.14c");
  R_Date("Erl-10156", 3052, 41)
  {
   Outlier("Charcoal", 1);
  };
  R_Date("Ly-9162", 1815, 30)
  {
   Outlier("Charcoal", 1);
  };
  R_Date("Ly-9161", 1580, 30)
  {
   Outlier("Charcoal", 1);
  };
  R_Date("KIA-36672", 1340, 25)
  {
   Outlier("Charcoal", 1);
  };
  R_Date("KIA-36677", 1245, 30)
  {
```

```
 Outlier("Charcoal", 1);
};
R_Date("KIA-36671", 1230, 30)
{
 Outlier("Charcoal", 1);
};
R_Date("KIA-31187", 1210, 20)
{
 Outlier("Charcoal", 1);
};
R_Date("Y-1246", 1100, 80)
{
 Outlier("Charcoal", 1);
};
R_Date("KIA-36678", 1065, 30)
{
 Outlier("Charcoal", 1);
};
R_Date("Erl-10159", 1056, 36)
{
 Outlier("Charcoal", 1);
};
R_Date("KIA-36684", 1000, 30)
```

```
{
 Outlier("Charcoal", 1);
};
R_Date("KIA-36673", 945, 35)
{
 Outlier("Charcoal", 1);
};
R_Date("KIA-36674", 945, 30)
{
 Outlier("Charcoal", 1);
};
Curve("IntCal13","IntCal13.14c");
Curve("Marine13","Marine13.14c");
Mix_Curve("Mixed","IntCal13","Marine13",50,12);
R_Date("KIA-36675", 915, 50);
Curve("IntCal13","IntCal13.14c");
R_Date("Ly-8466", 770, 30)
{
 Outlier("Charcoal", 1);
};
R_Date("KIA-36680", 690, 30)
{
 Outlier("Charcoal", 1);
```

```
};
Curve("IntCal13","IntCal13.14c");
Curve("Marine13","Marine13.14c");
Mix_Curve("Mixed","IntCal13","Marine13",50,12);
R_Date("KIA-36682", 650, 140);
Curve("IntCal13","IntCal13.14c");
R_Date("KIA-36679", 625, 30)
{
 Outlier("Charcoal", 1);
};
Curve("IntCal13","IntCal13.14c");
Curve("Marine13","Marine13.14c");
Mix_Curve("Mixed","IntCal13","Marine13",50,12);
R_Date("KIA-36681", 625, 25);
R_Date("KIA-36681", 620, 25);
R_Date("KIA-36676", 565, 25);
R_Date("KIA-36676", 431, 22);
R_Date("KIA-36676", 348, 39);
Curve("IntCal13","IntCal13.14c");
R_Date("KIA-36683", 330, 25)
{
 Outlier("Charcoal", 1);
};
```

```
  };
  Boundary("Guadeloupe End");
 };
};
```

Hispaniola

```
Plot()
 {
  Outlier_Model("Charcoal",Exp(1,-10,0),U(0,2),"t");
  Sequence("Hispaniola")
  {
   Boundary("Hispaniola Start");
   Phase()
   {
    Curve("IntCal13","IntCal13.14c");
    R_Date("I-6756", 3890, 95)
    {
     Outlier("Charcoal", 1);
    };
    R_Date("I-5940", 3840, 130)
    {
     Outlier("Charcoal", 1);
    };
```

```
Curve("Marine13","Marine13.14c");
R_Date("I-9541", 3575, 90);
Curve("IntCal13","IntCal13.14c");
R_Date("I-9539", 3205, 90)
{
 Outlier("Charcoal", 1);
};
R_Date("I-6781", 2585, 90)
{
 Outlier("Charcoal", 1);
};
R_Date("I-5818", 2095, 135)
{
 Outlier("Charcoal", 1);
};
R_Date("SI-991", 1805, 70)
{
 Outlier("Charcoal", 1);
};
Curve("Marine13","Marine13.14c");
R_Date("GrN-29933", 1750, 30);
R_Date("GrN-31416", 1745, 20);
R_Date("GrN-31413", 1705, 20);
```

```
R_Date("GrN-30532", 1525, 25);
R_Date("GrN-31415", 1520, 20);
R_Date("GrN-29932", 1495, 30);
R_Date("GrN-31414", 1435, 20);
R_Date("Beta-293244", 1340, 40);
Curve("IntCal13","IntCal13.14c");
R_Date("GrN-31412", 1230, 40)
{
 Outlier("Charcoal", 1);
};
Curve("Marine13","Marine13.14c");
R_Date("GrN-30531", 1170, 25);
R_Date("Beta-293242", 1120, 40);
Curve("IntCal13","IntCal13.14c");
R_Date("GrN-29934", 1110, 25);
Curve("Marine13","Marine13.14c");
R_Date("GrN-30533", 1040, 25);
R_Date("Beta-293243", 1030, 40);
Curve("IntCal13","IntCal13.14c");
R_Date("Beta-108313", 990, 70)
{
 Outlier("Charcoal", 1);
};
```

```
R_Date("Beta-107023", 940, 30);
R_Date("GrN-31418", 925, 30)
{
 Outlier("Charcoal", 1);
};
R_Date("GrN-31417", 915, 20)
{
 Outlier("Charcoal", 1);
};
R_Date("Beta-112400", 910, 40)
{
 Outlier("Charcoal", 1);
};
R_Date("Beta-96782", 870, 60)
{
 Outlier("Charcoal", 1);
};
R_Date("GrN-29931", 815, 35)
{
 Outlier("Charcoal", 1);
};
R_Date("Beta-47758", 810, 70)
{
```

```
 Outlier("Charcoal", 1);
};
R_Date("Beta-46760", 800, 60)
{
 Outlier("Charcoal", 1);
};
R_Date("Beta-46759", 720, 50)
{
 Outlier("Charcoal", 1);
};
R_Date("Beta-18173", 680, 80)
{
 Outlier("Charcoal", 1);
};
R_Date("Beta-96781", 680, 60)
{
 Outlier("Charcoal", 1);
};
R_Date("Beta-01527", 640, 260)
{
 Outlier("Charcoal", 1);
};
R_Date("Beta-108314", 620, 70)
```

```
{
 Outlier("Charcoal", 1);
};
R_Date("Beta-18172", 600, 70)
{
 Outlier("Charcoal", 1);
};
R_Date("GrN-30534", 600, 25)
{
 Outlier("Charcoal", 1);
};
R_Date("GrN-30535", 580, 30)
{
 Outlier("Charcoal", 1);
};
R_Date("Beta-108315", 540, 50)
{
 Outlier("Charcoal", 1);
};
R_Date("GrN-29035", 535, 25)
{
 Outlier("Charcoal", 1);
};
```

```
   R_Date("Beta-018469", 440, 60)
   {
    Outlier("Charcoal", 1);
   };
   R_Date("Beta-10526", 430, 80)
   {
    Outlier("Charcoal", 1);
   };
   R_Date("Beta-010528", 340, 70)
   {
    Outlier("Charcoal", 1);
   };
   R_Date("Beta-046761", 320, 70)
   {
    Outlier("Charcoal", 1);
   };
  };
  Boundary("Hispaniola End");
 };
};
```

Jamaica

```
Plot()
```

```
{
 Outlier_Model("Charcoal",Exp(1,-10,0),U(0,2),"t");
 Sequence("Jamaica")
 {
  Boundary("Jamaica Start");
  Phase()
  {
   Curve("IntCal13","IntCal13.14c");
   R_Date("Beta-153378", 970, 40)
   {
    Outlier("Charcoal", 1);
   };
   R_Date("WK 43115", 938, 20)
   {
    Outlier("Charcoal", 1);
   };
   R_Date("Beta-167740", 680, 60)
   {
    Outlier("Charcoal", 1);
   };
   R_Date("A-6140", 630, 40)
   {
    Outlier("Charcoal", 1);
```

```
};
R_Date("WK 43114", 627, 20)
{
 Outlier("Charcoal", 1);
};
R_Date("OxA-21058", 615, 24)
{
 Outlier("Charcoal", 1);
};
R_Date("A-6058", 570, 45)
{
 Outlier("Charcoal", 1);
};
R_Date("A-6061", 525, 45)
{
 Outlier("Charcoal", 1);
};
R_Date("OxA-21057", 396, 24)
{
 Outlier("Charcoal", 1);
};
R_Date("OxA- 21056", 384, 24)
{
```

```
    Outlier("Charcoal", 1);
   };
  };
  Boundary("Jamaica End");
 };
};
```

Montserrat

```
Plot()
 {
  Outlier_Model("Charcoal",Exp(1,-10,0),U(0,2),"t");
  Sequence("Montserrat")
  {
   Boundary("Montserrat Start");
   Phase()
   {
    Curve("IntCal13","IntCal13.14c");
    R_Date("Beta-83043", 2770, 60)
    {
     Outlier("Charcaol", 1);
    };
    R_Date("Beta-83050", 2140, 110)
    {
```

```
 Outlier("Charcaol", 1);
};
R_Date("Beta-83046", 2050, 80)
{
 Outlier("Charcaol", 1);
};
R_Date("Beta-83045", 1950, 90)
{
 Outlier("Charcaol", 1);
};
R_Date("Beta-83048", 1860, 100)
{
 Outlier("Charcaol", 1);
};
R_Date("Beta-83049", 1730, 100)
{
 Outlier("Charcaol", 1);
};
R_Date("Beta-83044", 1650, 130)
{
 Outlier("Charcaol", 1);
};
R_Date("Beta-83051", 1540, 120)
```

```
{
 Outlier("Charcaol", 1);
};
R_Date("Beta-83047", 1270, 130)
{
 Outlier("Charcaol", 1);
};
R_Date("Beta-282302", 1120, 40)
{
 Outlier("Charcaol", 1);
};
R_Date("Beta-282300", 1070, 40)
{
 Outlier("Charcaol", 1);
};
R_Date("Beta-277241", 1010, 40)
{
 Outlier("Charcaol", 1);
};
R_Date("Beta-282301", 980, 40)
{
 Outlier("Charcaol", 1);
};
```

```
    R_Date("Beta-282299", 980, 40)
    {
     Outlier("Charcaol", 1);
    };
    R_Date("Beta-277242", 880, 40)
    {
     Outlier("Charcaol", 1);
    };
   };
   Boundary("Montserrat End");
  };
 };
```

Nevis

```
Plot()
 {
  Outlier_Model("Charcoal",Exp(1,-10,0),U(0,2),"t");
  Sequence("Nevis")
  {
   Boundary("Nevis Start");
   Phase()
   {
    Curve("Marine13","Marine13.14c");
```

```
R_Date("D-AMS 007668", 1541, 33);
R_Date("D-AMS 07667", 1464, 24);
R_Date("Beta-290341", 1420, 40);
R_Date("Beta-290340", 1350, 40);
Curve("IntCal13","IntCal13.14c");
R_Date("Beta-47807", 1070, 70)
{
 Outlier("Charcoal", 1);
};
R_Date("Beta-46940", 1060, 50)
{
 Outlier("Charcoal", 1);
};
R_Date("Beta-46944a", 940, 60)
{
 Outlier("Charcoal", 1);
};
R_Date("Beta-46942", 880, 60)
{
 Outlier("Charcoal", 1);
};
Curve("Marine13","Marine13.14c");
R_Date("Beta-324952", 720, 30);
```

```
   R_Date("Beta-324951", 570, 30);
  };
  Boundary("Nevis End");
 };
};
```

Puerto Rico

```
Plot()
 {
  Outlier_Model("Charcoal",Exp(1,-10,0),U(0,2),"t");
  Sequence("Puerto Rico")
  {
   Boundary("Puerto Rico Start");
   Phase()
   {
    Curve("IntCal13","IntCal13.14c");
    R_Date("Beta-77165", 4060, 60)
    {
     Outlier("Charcoal", 1);
    };
    R_Date("Beta-178680", 4110, 40)
    {
     Outlier("Charcoal", 1);
```

```
};
R_Date("GX-28807", 3920, 40)
{
 Outlier("Charcoal", 1);
};
Curve("Marine13","Marine13.14c");
R_Date("UGM-17566", 4250, 25);
Curve("IntCal13","IntCal13.14c");
R_Date("Beta-116372", 3820, 70)
{
 Outlier("Charcoal", 1);
};
R_Date("UGM-17565", 3810, 25)
{
 Outlier("Charcoal", 1);
};
R_Date("GX-28814", 3740, 100)
{
 Outlier("Charcoal", 1);
};
R_Date("UGM-5106", 3740, 30)
{
 Outlier("Charcoal", 1);
```

```
};
Curve("Marine13","Marine13.14c");
R_Date("UGM-5108", 3740, 30);
Curve("IntCal13","IntCal13.14c");
R_Date("GX-28805", 3700, 30)
{
 Outlier("Charcoal", 1);
};
R_Date("Beta-294434", 3680, 40)
{
 Outlier("Charcoal", 1);
};
R_Date("GX-28808", 3670, 40)
{
 Outlier("Charcoal", 1);
};
Curve("Marine13","Marine13.14c");
R_Date("UGM-17561", 3640, 25);
Curve("IntCal13","IntCal13.14c");
R_Date("Beta-130451", 3640, 70)
{
 Outlier("Charcoal", 1);
};
```

```
Curve("Marine13","Marine13.14c");
R_Date("UGM-17562", 3630, 25);
Curve("IntCal13","IntCal13.14c");
R_Date("GX-28806", 3570, 40)
{
 Outlier("Charcoal", 1);
};
Curve("Marine13","Marine13.14c");
R_Date("UGM-5107", 3520, 30);
Curve("IntCal13","IntCal13.14c");
R_Date("GX-28809", 3470, 40)
{
 Outlier("Charcoal", 1);
};
R_Date("I-14745", 3340, 90)
{
 Outlier("Charcoal", 1);
};
Curve("Marine13","Marine13.14c");
R_Date("UGM-5105", 3170, 30);
Curve("IntCal13","IntCal13.14c");
R_Date("UGM-30042", 3140, 40)
{
```

```
 Outlier("Charcoal", 1);
};
Curve("Marine13","Marine13.14c");
R_Date("UGM-17564", 3120, 20);
Curve("IntCal13","IntCal13.14c");
R_Date("UGM-30031", 2910, 50)
{
 Outlier("Charcoal", 1);
};
R_Date("Beta-130450", 2730, 70)
{
 Outlier("Charcoal", 1);
};
R_Date("Beta-178678", 2520, 40)
{
 Outlier("Charcoal", 1);
};
R_Date("UGM-30033", 2390, 35)
{
 Outlier("Charcoal", 1);
};
R_Date("Beta-178677", 2330, 110)
{
```

```
 Outlier("Charcoal", 1);
};
R_Date("I-14744", 2270, 80)
{
 Outlier("Charcoal", 1);
};
R_Date("Beta-294435", 2120, 30)
{
 Outlier("Charcoal", 1);
};
Curve("Marine13","Marine13.14c");
R_Date("I-14979", 2120, 80);
Curve("IntCal13","IntCal13.14c");
R_Date("I-11296", 2100, 80)
{
 Outlier("Charcoal", 1);
};
R_Date("Beta-9970", 2060, 70)
{
 Outlier("Charcoal", 1);
};
R_Date("Beta-14380", 2060, 60)
{
```

```
 Outlier("Charcoal", 1);
};
R_Date("I-14978", 2020, 80)
{
 Outlier("Charcoal", 1);
};
R_Date("I-13855", 2020, 80)
{
 Outlier("Charcoal", 1);
};
R_Date("I-11297", 1995, 80)
{
 Outlier("Charcoal", 1);
};
R_Date("Beta-14381", 1960, 90)
{
 Outlier("Charcoal", 1);
};
R_Date("I-13930", 1950, 80)
{
 Outlier("Charcoal", 1);
};
R_Date("Y-1235", 1920, 120)
```

```
{
 Outlier("Charcoal", 1);
};
R_Date("Beta-87611", 1920, 80)
{
 Outlier("Charcoal", 1);
};
R_Date("Beta-347456", 1910, 30);
R_Date("Y-1234", 1910, 100)
{
 Outlier("Charcoal", 1);
};
R_Date("I-11266", 1865, 80)
{
 Outlier("Charcoal", 1);
};
R_Date("Beta-9972", 1840, 50);
R_Date("Y-1233", 1830, 80)
{
 Outlier("Charcoal", 1);
};
R_Date("Beta-14993", 1810, 60)
{
```

```
 Outlier("Charcoal", 1);
};
R_Date("Beta-14997", 1810, 70)
{
 Outlier("Charcoal", 1);
};
R_Date("I-10914", 1780, 85)
{
 Outlier("Charcoal", 1);
};
R_Date("I-13922", 1780, 85)
{
 Outlier("Charcoal", 1);
};
R_Date("I-9680", 1775, 80)
{
 Outlier("Charcoal", 1);
};
R_Date("I-10916", 1720, 80)
{
 Outlier("Charcoal", 1);
};
R_Date("I-10921", 1705, 85)
```

```
{
 Outlier("Charcoal", 1);
};
R_Date("Beta-14992", 1660, 100)
{
 Outlier("Charcoal", 1);
};
R_Date("I-14361", 1650, 80)
{
 Outlier("Charcoal", 1);
};
R_Date("I-14431", 1650, 80)
{
 Outlier("Charcoal", 1);
};
Curve("IntCal13","IntCal13.14c");
Curve("Marine13","Marine13.14c");
Mix_Curve("Mixed","IntCal13","Marine13",50,12);
R_Date("Beta-222869", 1630, 40);
Curve("IntCal13","IntCal13.14c");
R_Date("I-14430", 1610, 80)
{
 Outlier("Charcoal", 1);
```

```
};
R_Date("I-14427", 1610, 80)
{
 Outlier("Charcoal", 1);
};
Curve("IntCal13","IntCal13.14c");
Curve("Marine13","Marine13.14c");
Mix_Curve("Mixed","IntCal13","Marine13",50,12);
R_Date("AA-6809", 1600, 55);
Curve("IntCal13","IntCal13.14c");
R_Date("I-14428", 1600, 150)
{
 Outlier("Charcoal", 1);
};
R_Date("I-14383", 1600, 80);
Curve("IntCal13","IntCal13.14c");
Curve("Marine13","Marine13.14c");
Mix_Curve("Mixed","IntCal13","Marine13",50,12);
R_Date("AA-75810", 1582, 46);
Curve("IntCal13","IntCal13.14c");
R_Date("Y-1232", 1580, 80)
{
 Outlier("Charcoal", 1);
```

```
};
R_Date("Beta-17637", 1580, 120)
{
 Outlier("Charcoal", 1);
};
R_Date("Beta-178670", 1580, 90)
{
 Outlier("Charcoal", 1);
};
Curve("IntCal13","IntCal13.14c");
Curve("Marine13","Marine13.14c");
Mix_Curve("Mixed","IntCal13","Marine13",50,12);
R_Date("AA-79415", 1566, 46);
Curve("IntCal13","IntCal13.14c");
R_Date("I-14362", 1560, 80)
{
 Outlier("Charcoal", 1);
};
Curve("IntCal13","IntCal13.14c");
Curve("Marine13","Marine13.14c");
Mix_Curve("Mixed","IntCal13","Marine13",50,12);
R_Date("AA-78513", 1557, 44);
Curve("IntCal13","IntCal13.14c");
```

```
R_Date("Beta-87610", 1550, 60)
{
 Outlier("Charcoal", 1);
};
R_Date("Beta-272032", 1550, 40)
{
 Outlier("Charcoal", 1);
};
R_Date("I-14429", 1550, 80)
{
 Outlier("Charcoal", 1);
};
R_Date("I-6595", 1545, 90)
{
 Outlier("Charcoal", 1);
};
Curve("IntCal13","IntCal13.14c");
Curve("Marine13","Marine13.14c");
Mix_Curve("Mixed","IntCal13","Marine13",50,12);
R_Date("AA-75128", 1539, 43);
Curve("IntCal13","IntCal13.14c");
R_Date("Beta-17631", 1530, 90)
{
```

```
 Outlier("Charcoal", 1);
};
R_Date("I-14382", 1530, 80)
{
 Outlier("Charcoal", 1);
};
Curve("IntCal13","IntCal13.14c");
Curve("Marine13","Marine13.14c");
Mix_Curve("Mixed","IntCal13","Marine13",50,12);
R_Date("AA-6805", 1525, 55);
Curve("IntCal13","IntCal13.14c");
R_Date("Beta-14994", 1520, 50)
{
 Outlier("Charcoal", 1);
};
R_Date("Beta-178681", 1520, 40)
{
 Outlier("Charcoal", 1);
};
Curve("IntCal13","IntCal13.14c");
Curve("Marine13","Marine13.14c");
Mix_Curve("Mixed","IntCal13","Marine13",50,12);
R_Date("AA-4100", 1515, 50);
```

```
Curve("IntCal13","IntCal13.14c");
R_Date("I-9677", 1515, 80)
{
 Outlier("Charcoal", 1);
};
Curve("IntCal13","IntCal13.14c");
Curve("Marine13","Marine13.14c");
Mix_Curve("Mixed","IntCal13","Marine13",50,12);
R_Date("AA-78495", 1505, 44);
Curve("IntCal13","IntCal13.14c");
R_Date("I-13932", 1500, 80)
{
 Outlier("Charcoal", 1);
};
Curve("IntCal13","IntCal13.14c");
Curve("Marine13","Marine13.14c");
Mix_Curve("Mixed","IntCal13","Marine13",50,12);
R_Date("AA-74638", 1493, 45);
Curve("IntCal13","IntCal13.14c");
R_Date("I-13923", 1490, 80)
{
 Outlier("Charcoal", 1);
};
```

```
R_Date("I-9108", 1480, 95)
{
 Outlier("Charcoal", 1);
};
R_Date("I-13924", 1480, 80)
{
 Outlier("Charcoal", 1);
};
R_Date("Beta-178674", 1470, 40)
{
 Outlier("Charcoal", 1);
};
Curve("IntCal13","IntCal13.14c");
Curve("Marine13","Marine13.14c");
Mix_Curve("Mixed","IntCal13","Marine13",50,12);
R_Date("AA-82397", 1469, 47);
Curve("IntCal13","IntCal13.14c");
R_Date("Beta-223566", 1460, 60)
{
 Outlier("Charcoal", 1);
};
R_Date("I-14360", 1460, 80)
{
```

```
 Outlier("Charcoal", 1);
};
R_Date("I-9873", 1460, 80)
{
 Outlier("Charcoal", 1);
};
Curve("IntCal13","IntCal13.14c");
Curve("Marine13","Marine13.14c");
Mix_Curve("Mixed","IntCal13","Marine13",50,12);
R_Date("AA-79371", 1456, 45);
R_Date("AA-75816", 1455, 46);
Curve("IntCal13","IntCal13.14c");
R_Date("Beta-178666", 1450, 40)
{
 Outlier("Charcoal", 1);
};
Curve("IntCal13","IntCal13.14c");
Curve("Marine13","Marine13.14c");
Mix_Curve("Mixed","IntCal13","Marine13",50,12);
R_Date("AA-72872", 1443, 50);
Curve("IntCal13","IntCal13.14c");
R_Date("UGM-30035", 1440, 30)
{
```

```
   Outlier("Charcoal", 1);
  };
  R_Date("Beta-17641", 1440, 70)
  {
   Outlier("Charcoal", 1);
  };
  R_Date("Beta-87601", 1440, 60)
  {
   Outlier("Charcoal", 1);
  };
  Curve("IntCal13","IntCal13.14c");
  Curve("Marine13","Marine13.14c");
  Mix_Curve("Mixed","IntCal13","Marine13",50,12);
  R_Date("AA-74637", 1434, 45);
  R_Date("AA-78492", 1434, 44);
 };
 Boundary("Puerto Rico End");
};
};
```

San Salvador

```
Plot()
 {
```

```
Outlier_Model("Charcoal",Exp(1,-10,0),U(0,2),"t");
Sequence("San Salvador")
{
 Boundary("San Salvador Start");
 Phase()
 {
  Curve("Marine13","Marine13.14c");
  R_Date("UM-2275", 1384, 65);
  Curve("IntCal13","IntCal13.14c");
  R_Date("YSU #3", 1130, 40)
  {
   Outlier("Charcoal", 1);
  };
  Curve("Marine13","Marine13.14c");
  R_Date("UGa-00836", 1054, 37);
  R_Date("AA-51432", 1028, 34);
  Curve("IntCal13","IntCal13.14c");
  R_Date("YSU #1", 840, 40)
  {
   Outlier("Charcoal", 1);
  };
  R_Date("UM-2244", 660, 100)
  {
```

```
 Outlier("Charcoal", 1);
};
R_Date("UM-2274", 620, 70)
{
 Outlier("Charcoal", 1);
};
R_Date("UM-2273", 580, 90)
{
 Outlier("Charcoal", 1);
};
R_Date("Beta-16732", 530, 65)
{
 Outlier("Charcoal", 1);
};
R_Date("YSU #4", 470, 60)
{
 Outlier("Charcoal", 1);
};
R_Date("Beta-105988", 450, 50)
{
 Outlier("Charcoal", 1);
};
R_Date("YSU #2", 350, 70)
```

```
    {
     Outlier("Charcoal", 1);
    };
    R_Date("UM-2271", 305, 75)
    {
     Outlier("Charcoal", 1);
    };
    Curve("Marine13","Marine13.14c");
    R_Date("UM-2245", 425, 75);
   };
   Boundary("San Salvador End");
  };
 };
```

St. Eustatius

```
Plot()
 {
  Outlier_Model("Charcoal",Exp(1,-10,0),U(0,2),"t");
  Sequence("St Eustatius")
  {
   Boundary("St Eustatius Start");
   Phase()
   {
```

```
Curve("IntCal13","IntCal13.14c");
Curve("Marine13","Marine13.14c");
Mix_Curve("Mixed","IntCal13","Marine13",50,12);
R_Date("Ua-1488", 1735, 220);
Curve("IntCal13","IntCal13.14c");
R_Date("GrN-11512", 1755, 20)
{
 Outlier("Charcoal", 1);
};
R_Date("GrN-11513", 1635, 20)
{
 Outlier("Charcoal", 1);
};
R_Date("GrN-11510", 1545, 35)
{
 Outlier("Charcoal", 1);
};
R_Date("GrN-11509", 1415, 30)
{
 Outlier("Charcoal", 1);
};
R_Date("GrN-11514", 1350, 60)
{
```

```
 Outlier("Charcoal", 1);
};
R_Date("GrN-11516", 1340, 20)
{
 Outlier("Charcoal", 1);
};
R_Date("GrN-17074", 1325, 30)
{
 Outlier("Charcoal", 1);
};
R_Date("GrN-17075", 1260, 30)
{
 Outlier("Charcoal", 1);
};
R_Date("GrN-11517", 1210, 20)
{
 Outlier("Charcoal", 1);
};
R_Date("GrN-11515", 1205, 30)
{
 Outlier("Charcoal", 1);
};
};
```

```
  Boundary("St Eustatius End");
 };
};
```

St. John

```
Plot()
 {
  Outlier_Model("Charcoal",Exp(1,-10,0),U(0,2),"t");
  Sequence("St. John")
  {
   Boundary("St. John Start");
   Phase()
   {
    Curve("IntCal13","IntCal13.14c");
    R_Date("Beta-17080", 1630, 100)
    {
     Outlier("Charcoal", 1);
    };
    R_Date("Beta-32239", 1460, 80)
    {
     Outlier("Charcoal", 1);
    };
    R_Date("Beta-16647", 1210, 80)
```

```
{
 Outlier("Charcoal", 1);
};
Curve("IntCal13","IntCal13.14c");
Curve("Marine13","Marine13.14c");
Mix_Curve("Mixed","IntCal13","Marine13",50,12);
R_Date("Beta-27793", 1170, 80);
Curve("IntCal13","IntCal13.14c");
R_Date("Beta-192223", 1160, 40)
{
 Outlier("Charcoal", 1);
};
R_Date("Beta-192224", 1140, 40)
{
 Outlier("Charcoal", 1);
};
R_Date("Beta-25891", 1130, 70)
{
 Outlier("Charcoal", 1);
};
R_Date("Beta-59781", 1120, 100)
{
 Outlier("Charcoal", 1);
```

```
};
R_Date("Beta-20605", 1050, 60)
{
 Outlier("Charcoal", 1);
};
R_Date("Beta-59780", 970, 80)
{
 Outlier("Charcoal", 1);
};
R_Date("Beta-18513", 970, 70)
{
 Outlier("Charcoal", 1);
};
R_Date("Beta-26964", 900, 100)
{
 Outlier("Charcoal", 1);
};
Curve("IntCal13","IntCal13.14c");
Curve("Marine13","Marine13.14c");
Mix_Curve("Mixed","IntCal13","Marine13",50,12);
R_Date("Beta-191882", 840, 40);
Curve("IntCal13","IntCal13.14c");
R_Date("Beta-19863", 660, 60)
```

```
    {
     Outlier("Charcoal", 1);
    };
   };
   Boundary("St. John End");
  };
 };
```

St. Lucia

```
Plot()
 {
  Outlier_Model("Charcoal",Exp(1,-10,0),U(0,2),"t");
  Sequence("St. Lucia")
  {
   Boundary("St. Lucia Start");
   Phase()
   {
    Curve("IntCal13","IntCal13.14c");
    R_Date("Y-1115", 1460, 80)
    {
     Outlier("Charcoal", 1);
    };
    R_Date("Y-650", 1220, 100)
```

```
{
 Outlier("Charcoal", 1);
};
Curve("Marine13","Marine13.14c");
R_Date("RL-30", 1240, 100);
R_Date("RL-31", 1120, 100);
Curve("IntCal13","IntCal13.14c");
Curve("Marine13","Marine13.14c");
Mix_Curve("Mixed","IntCal13","Marine13",50,12);
R_Date("GrN-46607", 1000, 40);
R_Date("GrN-32330", 960, 35);
R_Date("GrN-32324", 920, 25);
R_Date("GrN-32326", 865, 35);
R_Date("GrN-32328", 820, 35);
R_Date("GrN-32325", 790, 35);
R_Date("GrN-32319", 770, 35);
R_Date("GrN-31944", 750, 30);
R_Date("GrN-32327", 745, 30);
R_Date("GrN-32314", 740, 30);
R_Date("GrN-32317", 725, 35);
R_Date("GrN-32315", 720, 35);
Curve("IntCal13","IntCal13.14c");
R_Date("GrN-46604", 645, 35)
```

```
    {
     Outlier("Charcoal", 1);
    };
    Curve("IntCal13","IntCal13.14c");
    Curve("Marine13","Marine13.14c");
    Mix_Curve("Mixed","IntCal13","Marine13",50,12);
    R_Date("GrN-32329", 620, 40);
   };
   Boundary("St. Lucia End");
  };
 };
```

St. Martin

```
Plot()
 {
  Outlier_Model("Charcoal",Exp(1,-10,0),U(0,2),"t");
  Sequence("St. Martin")
  {
   Boundary("St. Martin Start");
   Phase()
   {
    Curve("Marine13","Marine13.14c");
    R_Date("KIA-28815", 4830, 40);
```

```
R_Date("KIA-28108", 4770, 40);
R_Date("KIA-28116", 4505, 35);
R_Date("KIA-28115", 4275, 30);
R_Date("Erl-9066", 4200, 50);
Curve("IntCal13","IntCal13.14c");
R_Date("KIA-28121", 3828, 27)
{
 Outlier("Charcoal", 1);
};
Curve("Marine13","Marine13.14c");
R_Date("KIA-28114", 3800, 30);
R_Date("KIA-28112", 3775, 30);
R_Date("Erl-9071", 3750, 50);
Curve("IntCal13","IntCal13.14c");
R_Date("KIA-28123", 3684, 27)
{
 Outlier("Charcoal", 1);
};
R_Date("KIA-28119", 3655, 25)
{
 Outlier("Charcoal", 1);
};
Curve("Marine13","Marine13.14c");
```

```
R_Date("Erl-9072", 3610, 50);
Curve("IntCal13","IntCal13.14c");
R_Date("KIA-28124", 3598, 29)
{
 Outlier("Charcoal", 1);
};
Curve("Marine13","Marine13.14c");
R_Date("Beta-41782", 3580, 90);
Curve("IntCal13","IntCal13.14c");
R_Date("Erl-9074", 3515, 45)
{
 Outlier("Charcoal", 1);
};
Curve("Marine13","Marine13.14c");
R_Date("Erl-9073", 3510, 50);
Curve("IntCal13","IntCal13.14c");
R_Date("Beta-190805", 3490, 40)
{
 Outlier("Charcoal", 1);
};
Curve("Marine13","Marine13.14c");
R_Date("Erl-9064", 3460, 50);
R_Date("Beta-187936", 3450, 40);
```

```
Curve("IntCal13","IntCal13.14c");
R_Date("KIA-28126", 3447, 26)
{
 Outlier("Charcoal", 1);
};
R_Date("KIA-28127", 3429, 35)
{
 Outlier("Charcoal", 1);
};
Curve("Marine13","Marine13.14c");
R_Date("KIA-28111", 3380, 40);
Curve("IntCal13","IntCal13.14c");
R_Date("KIA-28120", 3366, 27)
{
 Outlier("Charcoal", 1);
};
Curve("Marine13","Marine13.14c");
R_Date("Erl-9065", 3340, 50);
R_Date("KIA-28113", 3320, 30);
R_Date("Beta-224793", 3240, 60);
Curve("IntCal13","IntCal13.14c");
R_Date("KIA-28125", 3235, 26)
{
```

```
 Outlier("Charcoal", 1);
};
Curve("Marine13","Marine13.14c");
R_Date("KIA-28110", 3185, 30);
Curve("IntCal13","IntCal13.14c");
R_Date("Beta-187937", 3140, 40)
{
 Outlier("Charcoal", 1);
};
Curve("Marine13","Marine13.14c");
R_Date("KIA-28109", 3105, 30);
Curve("IntCal13","IntCal13.14c");
R_Date("KIA-28117", 3095, 23)
{
 Outlier("Charcoal", 1);
};
R_Date("KIA-28118", 2951, 52)
{
 Outlier("Charcoal", 1);
};
Curve("Marine13","Marine13.14c");
R_Date("Beta-146427", 2850, 60);
Curve("IntCal13","IntCal13.14c");
```

```
R_Date("Beta-224792", 2610, 40)
{
 Outlier("Charcoal", 1);
};
R_Date("PITT-0450", 2510, 40)
{
 Outlier("Charcoal", 1);
};
R_Date("Beta-145372", 2420, 40)
{
 Outlier("Charcoal", 1);
};
R_Date("PITT-0449", 2300, 55)
{
 Outlier("Charcoal", 1);
};
R_Date("PITT-0219", 2275, 60)
{
 Outlier("Charcoal", 1);
};
R_Date("Beta-146425", 2270, 40)
{
 Outlier("Charcoal", 1);
```

```
};
R_Date("PITT-0220", 2250, 45)
{
 Outlier("Charcoal", 1);
};
R_Date("PITT-0446", 2250, 45)
{
 Outlier("Charcoal", 1);
};
Curve("IntCal13","IntCal13.14c");
Curve("Marine13","Marine13.14c");
Mix_Curve("Mixed","IntCal13","Marine13",50,12);
R_Date("Erl-8235", 2070, 50);
Curve("IntCal13","IntCal13.14c");
R_Date("PITT-0448", 2050, 45)
{
 Outlier("Charcoal", 1);
};
R_Date("Beta-146424", 2020, 40)
{
 Outlier("Charcoal", 1);
};
R_Date("Beta-106230", 1960, 60)
```

```
{
 Outlier("Charcoal", 1);
};
R_Date("Beta-82159", 1910, 50)
{
 Outlier("Charcoal", 1);
};
Curve("Marine13","Marine13.14c");
R_Date("KIA-32785", 1900, 25);
Curve("IntCal13","IntCal13.14c");
R_Date("Beta-82156", 1870, 60)
{
 Outlier("Charcoal", 1);
};
Curve("Marine13","Marine13.14c");
R_Date("Beta-187941", 1810, 40);
Curve("IntCal13","IntCal13.14c");
R_Date("Beta-82158", 1800, 50)
{
 Outlier("Charcoal", 1);
};
R_Date("Beta-82157", 1800, 60)
{
```

```
 Outlier("Charcoal", 1);
};
R_Date("Beta-106228", 1770, 50)
{
 Outlier("Charcoal", 1);
};
R_Date("LGQ-1099", 1760, 160)
{
 Outlier("Charcoal", 1);
};
R_Date("Beta-82160", 1760, 50)
{
 Outlier("Charcoal", 1);
};
R_Date("Beta-82154", 1710, 60)
{
 Outlier("Charcoal", 1);
};
R_Date("Beta-106233", 1710, 70)
{
 Outlier("Charcoal", 1);
};
R_Date("Beta-106229", 1670, 50)
```

```
{
 Outlier("Charcoal", 1);
};
R_Date("PITT-0452", 1660, 55)
{
 Outlier("Charcoal", 1);
};
R_Date("Beta-106232", 1650, 70)
{
 Outlier("Charcoal", 1);
};
R_Date("LGQ-1098", 1610, 150)
{
 Outlier("Charcoal", 1);
};
R_Date("Beta-82153", 1590, 70)
{
 Outlier("Charcoal", 1);
};
Curve("Marine13","Marine13.14c");
R_Date("KIA-28963", 1585, 25);
Curve("IntCal13","IntCal13.14c");
R_Date("Beta-187940", 1560, 40)
```

```
{
 Outlier("Charcoal", 1);
};
R_Date("Beta-106231", 1560, 60)
{
 Outlier("Charcoal", 1);
};
R_Date("Beta-82155", 1540, 50)
{
 Outlier("Charcoal", 1);
};
Curve("Marine13","Marine13.14c");
R_Date("Beta-187938", 1540, 40);
Curve("IntCal13","IntCal13.14c");
R_Date("GrN-20170", 1535, 30);
R_Date("GrN-20168", 1530, 30);
R_Date("GrN-20169", 1520, 35);
R_Date("KIA-28122", 1494, 26)
{
 Outlier("Charcoal", 1);
};
R_Date("PITT-0445", 1490, 35)
{
```

```
 Outlier("Charcoal", 1);
};
Curve("Marine13","Marine13.14c");
R_Date("Beta-200098", 1330, 60);
Curve("IntCal13","IntCal13.14c");
R_Date("Ly-9163", 1230, 30)
{
 Outlier("Charcoal", 1);
};
R_Date("GrN-20161", 1225, 30);
R_Date("GrN-20160", 1180, 30);
R_Date("GrN-20162", 1170, 30);
Curve("Marine13","Marine13.14c");
R_Date("GrN- 20164", 1170, 30);
Curve("IntCal13","IntCal13.14c");
R_Date("Beta-82165", 1000, 50);
Curve("IntCal13","IntCal13.14c");
Curve("Marine13","Marine13.14c");
Mix_Curve("Mixed","IntCal13","Marine13",50,12);
R_Date("Ly-2019(OxA)", 895, 30);
Curve("IntCal13","IntCal13.14c");
R_Date("Ly-11437", 890, 30)
{
```

```
    Outlier("Charcoal", 1);
   };
   R_Date("Ly-11435", 890, 30)
   {
    Outlier("Charcoal", 1);
   };
  };
  Boundary("St. Martin End");
 };
};
```

St. Thomas

```
Plot()
 {
  Outlier_Model("Charcoal",Exp(1,-10,0),U(0,2),"t");
  Sequence("St. Thomas")
  {
   Boundary("St. Thomas End");
   Phase()
   {
    Curve("Marine13","Marine13.14c");
    R_Date("I-8640", 2830, 85);
    R_Date("Beta-7022", 2860, 70);
```

```
Curve("IntCal13","IntCal13.14c");
R_Date("Beta-111459", 2710, 120)
{
 Outlier("Charcoal", 1);
};
R_Date("I-8641", 2775, 85)
{
 Outlier("Charcoal", 1);
};
Curve("Marine13","Marine13.14c");
R_Date("SI-5851", 2700, 65);
R_Date("L-1380B", 2410, 60);
R_Date("I-621", 2400, 175);
R_Date("I-620", 2175, 160);
R_Date("SI-5850", 2130, 60);
Curve("IntCal13","IntCal13.14c");
R_Date("Beta-108917", 2090, 50)
{
 Outlier("Charcoal", 1);
};
R_Date("Beta-111462", 1980, 50)
{
 Outlier("Charcoal", 1);
```

```
};
Curve("Marine13","Marine13.14c");
R_Date("L-1380A", 1900, 70);
R_Date("SI-5848", 1805, 75);
Curve("IntCal13","IntCal13.14c");
R_Date("Beta-65474", 1800, 80)
{
 Outlier("Charcoal", 1);
};
R_Date("GX-12845", 1770, 235)
{
 Outlier("Charcoal", 1);
};
R_Date("Beta-108888", 1720, 140)
{
 Outlier("Charcoal", 1);
};
R_Date("Beta-50066", 1610, 70)
{
 Outlier("Charcoal", 1);
};
Curve("Marine13","Marine13.14c");
R_Date("SI-5849", 1595, 75);
```

```
Curve("IntCal13","IntCal13.14c");
R_Date("Beta-65472", 1580, 50)
{
 Outlier("Charcoal", 1);
};
R_Date("Beta-65473", 1570, 60)
{
 Outlier("Charcoal", 1);
};
R_Date("Beta-54646", 1560, 90)
{
 Outlier("Charcoal", 1);
};
R_Date("CAMS-10696", 1550, 50)
{
 Outlier("Charcoal", 1);
};
R_Date("Beta-108889", 1500, 50)
{
 Outlier("Charcoal", 1);
};
R_Date("Beta-62568", 1430, 90)
{
```

```
 Outlier("Charcoal", 1);
};
R_Date("Beta-62569", 1400, 120)
{
 Outlier("Charcoal", 1);
};
Curve("IntCal13","IntCal13.14c");
Curve("Marine13","Marine13.14c");
Mix_Curve("Mixed","IntCal13","Marine13",50,12);
R_Date("Beta-88345", 1390, 40);
R_Date("Beta-83011", 1390, 40);
R_Date("Beta-83003", 1390, 30);
Curve("IntCal13","IntCal13.14c");
R_Date("Beta-62570", 1380, 90)
{
 Outlier("Charcoal", 1);
};
Curve("IntCal13","IntCal13.14c");
Curve("Marine13","Marine13.14c");
Mix_Curve("Mixed","IntCal13","Marine13",50,12);
R_Date("Beta-83000", 1330, 30);
R_Date("Beta-83001", 1330, 30);
Curve("IntCal13","IntCal13.14c");
```

```
R_Date("Beta-65469", 1310, 60)
{
 Outlier("Charcoal", 1);
};
Curve("IntCal13","IntCal13.14c");
Curve("Marine13","Marine13.14c");
Mix_Curve("Mixed","IntCal13","Marine13",50,12);
R_Date("Beta-83009", 1300, 30);
R_Date("Beta-83006", 1280, 40);
R_Date("Beta-73392", 1190, 60);
R_Date("Beta-83010", 1090, 30);
Curve("IntCal13","IntCal13.14c");
R_Date("Beta-49751", 1040, 150)
{
 Outlier("Charcoal", 1);
};
R_Date("Beta-48742", 810, 140)
{
 Outlier("Charcoal", 1);
};
R_Date("Beta-43437", 810, 70)
{
 Outlier("Charcoal", 1);
```

```
};
R_Date("Beta-42277", 730, 80)
{
 Outlier("Charcoal", 1);
};
R_Date("Beta-51355", 720, 120)
{
 Outlier("Charcoal", 1);
};
R_Date("Beta-111461", 650, 50)
{
 Outlier("Charcoal", 1);
};
Curve("IntCal13","IntCal13.14c");
Curve("Marine13","Marine13.14c");
Mix_Curve("Mixed","IntCal13","Marine13",50,12);
R_Date("Beta-73390", 640, 60);
R_Date("Beta-73394", 630, 60);
R_Date("Beta-73393", 600, 60);
R_Date("Beta-83005", 600, 30);
R_Date("Beta-73395", 590, 90);
R_Date("Beta-73391", 580, 60);
Curve("IntCal13","IntCal13.14c");
```

```
R_Date("Beta-51354", 560, 120)
{
 Outlier("Charcoal", 1);
};
Curve("IntCal13","IntCal13.14c");
Curve("Marine13","Marine13.14c");
Mix_Curve("Mixed","IntCal13","Marine13",50,12);
R_Date("Beta-88347", 560, 40);
Curve("IntCal13","IntCal13.14c");
R_Date("Beta-111452", 560, 80)
{
 Outlier("Charcoal", 1);
};
Curve("IntCal13","IntCal13.14c");
Curve("Marine13","Marine13.14c");
Mix_Curve("Mixed","IntCal13","Marine13",50,12);
R_Date("Beta-83008", 540, 30);
R_Date("Beta-83004", 500, 30);
R_Date("Beta-109071", 480, 50);
R_Date("Beta-88348", 470, 40);
R_Date("Beta-88349", 460, 40);
R_Date("Beta-109070", 450, 50);
R_Date("Beta-88346", 390, 40);
```

```
    R_Date("Beta-109072", 380, 50);
    R_Date("Beta-83007", 340, 30);
    R_Date("Beta-88344", 300, 40);
   };
   Boundary("St. Thomas End");
  };
 };
```

Tobago

```
Plot()
 {
  Outlier_Model("Charcoal",Exp(1,-10,0),U(0,2),"t");
  Sequence("Tobago")
  {
   Boundary("Tobago Start");
   Phase()
   {
    Curve("IntCal13","IntCal13.14c");
    R_Date("Beta-15351", 2700, 40)
    R_Date("Beta-15936", 1750, 40)
    R_Date("Beta-172211", 1700, 40)
    R_Date("Y-1336", 1300, 120)
    {
```

```
 Outlier("Charcaol", 1);
};
R_Date("Beta-172209", 1180, 40)
{
 Outlier("Charcaol", 1);
};
R_Date("Beta-153150", 1170, 40)
{
 Outlier("Charcaol", 1);
};
R_Date("Beta-172210", 1110, 40)
{
 Outlier("Charcaol", 1);
};
R_Date("Beta-153149", 900, 40)
{
 Outlier("Charcaol", 1);
};
Curve("IntCal13","IntCal13.14c");
Curve("Marine13","Marine13.14c");
Mix_Curve("Mixed","IntCal13","Marine13",50,12);
R_Date("Beta-221321", 850, 40);
R_Date("Beta-221319", 810, 40);
```

```
   R_Date("Beta-221320", 810, 40);
   Curve("IntCal13","IntCal13.14c");
   R_Date("Beta-4905", 760, 105)
   {
    Outlier("Charcaol", 1);
   };
   R_Date("Beta-129265", 600, 50)
   {
    Outlier("Charcaol", 1);
   };
   R_Date("Beta-129262", 590, 40)
   {
    Outlier("Charcaol", 1);
   };
   R_Date("Beta-129264", 550, 40)
   {
    Outlier("Charcaol", 1);
   };
  };
  Boundary("Tobago End");
 };
};
```

Trinidad

```
Plot()
 {
  Outlier_Model("Charcoal",Exp(1,-10,0),U(0,2),"t");
  Sequence("Trinidad Start")
  {
   Boundary("Trinidad End");
   Phase()
   {
    R_Date("IVIC-888", 7180, 80)
    {
     Outlier("charcoal", 1);
    };
    R_Date("UGa-14460", 7030, 25)
    {
     Outlier("charcoal", 1);
    };
    R_Date("UGa-12303", 6890, 30)
    {
     Outlier("charcoal", 1);
    };
    R_Date("IVIC-889", 6780, 70)
    {
```

```
 Outlier("charcoal", 1);
};
R_Date("UGa-14459", 6370, 25)
{
 Outlier("charcoal", 1);
};
R_Date("IVIC-891", 6190, 100)
{
 Outlier("charcoal", 1);
};
R_Date("IVIC-887", 6170, 90)
{
 Outlier("charcoal", 1);
};
R_Date("UGa-14458", 6100, 25)
{
 Outlier("charcoal", 1);
};
R_Date("IVIC-890", 6100, 90)
{
 Outlier("charcoal", 1);
};
R_Date("IVIC-783", 5650, 100)
```

```
{
 Outlier("charcoal", 1);
};
R_Date("UGa-14457", 5300, 25);
R_Date("Y-260-1", 2750, 130)
{
 Outlier("charcoal", 1);
};
R_Date("IVIC-642", 2140, 70)
{
 Outlier("charcoal", 1);
};
R_Date("IVIC-638", 2130, 80)
{
 Outlier("charcoal", 1);
};
R_Date("I-6444", 2120, 135)
{
 Outlier("charcoal", 1);
};
R_Date("IVIC-641", 2060, 70)
{
 Outlier("charcoal", 1);
```

```
};
R_Date("IVIC-640", 1990, 70)
{
 Outlier("charcoal", 1);
};
R_Date("Beta-196708", 1920, 40)
{
 Outlier("charcoal", 1);
};
R_Date("Beta-196709", 1880, 40)
{
 Outlier("charcoal", 1);
};
R_Date("IVIC-643", 1850, 80)
{
 Outlier("charcoal", 1);
};
R_Date("Beta-4902", 1805, 90)
{
 Outlier("charcoal", 1);
};
R_Date("Beta-4899", 1755, 150)
{
```

```
 Outlier("charcoal", 1);
};
R_Date("Beta-134571", 1720, 50)
{
 Outlier("charcoal", 1);
};
R_Date("IVIC-786", 1720, 90)
{
 Outlier("charcoal", 1);
};
R_Date("Beta-4903", 1680, 115)
{
 Outlier("charcoal", 1);
};
R_Date("Beta-196706", 1650, 40)
{
 Outlier("charcoal", 1);
};
R_Date("GrA-13865", 1590, 40)
{
 Outlier("charcoal", 1);
};
R_Date("Beta-189113", 1570, 40)
```

```
{
 Outlier("charcoal", 1);
};
R_Date("OxA-19174", 1538, 29)
{
 Outlier("charcoal", 1);
};
R_Date("Beta-296724", 1490, 30)
{
 Outlier("charcoal", 1);
};
R_Date("IVIC-639", 1480, 70)
{
 Outlier("charcoal", 1);
};
R_Date("Beta-296723", 1400, 30)
{
 Outlier("charcoal", 1);
};
R_Date("Beta-4904", 1350, 85)
{
 Outlier("charcoal", 1);
};
```

```
R_Date("Beta-4901", 1300, 110)
{
 Outlier("charcoal", 1);
};
R_Date("IVIC-785", 1260, 100)
{
 Outlier("charcoal", 1);
};
R_Date("GrA-13867", 1220, 40)
{
 Outlier("charcoal", 1);
};
R_Date("Beta-296726", 1210, 30)
{
 Outlier("charcoal", 1);
};
R_Date("ISGS-A2628", 1210, 15)
{
 Outlier("charcoal", 1);
};
R_Date("Beta-4900", 1145, 65)
{
 Outlier("charcoal", 1);
```

```
};
R_Date("Beta-6807", 1130, 50)
{
 Outlier("charcoal", 1);
};
R_Date("Beta-4898", 1040, 260)
{
 Outlier("charcoal", 1);
};
Curve("Marine13","Marine13.14c");
R_Date("Beta-6809", 990, 50);
Curve("IntCal13","IntCal13.14c");
R_Date("Beta-196707", 740, 40)
{
 Outlier("charcoal", 1);
};
R_Date("Beta-6808", 650, 50)
{
 Outlier("charcoal", 1);
};
Curve("IntCal13","IntCal13.14c");
Curve("Marine13","Marine13.14c");
Mix_Curve("Mixed","IntCal13","Marine13",50,12);
```

```
   R_Date("Beta-193442", 630, 40);
   Curve("IntCal13","IntCal13.14c");
   Curve("Marine13","Marine13.14c");
   Mix_Curve("Mixed","IntCal13","Marine13",50,12);
   R_Date("Beta-193443", 620, 40);
   Curve("IntCal13","IntCal13.14c");
   R_Date("I-10766", 540, 75)
   {
    Outlier("charcoal", 1);
   };
   R_Date("ISGS-A2629", 410, 20)
   {
    Outlier("charcoal", 1);
   };
   R_Date("ISGS-A2630", 385, 20)
   {
    Outlier("charcoal", 1);
   };
  };
  Boundary("Trinidad");
 };
};
```

Vieques

```
Plot()
 {
  Outlier_Model("Charcoal",Exp(1,-10,0),U(0,2),"t");
  Sequence("Vieques")
  {
   Boundary("Vieques Start");
   Phase()
   {
    Curve("Marine13","Marine13.14c");
    R_Date("I-18971", 4095, 80);
    R_Date("I-16406", 3850, 100);
    R_Date("I-16899", 3780, 100);
    R_Date("I-16397", 3530, 100);
    R_Date("I-16396", 3510, 100);
    R_Date("I-16897", 3470, 100);
    R_Date("I-16395", 2790, 100);
    R_Date("I-16898", 2770, 90);
    R_Date("I-16407", 2740, 100);
    R_Date("I-16896", 2650, 90);
    Curve("IntCal13","IntCal13.14c");
    R_Date("I-16153", 2590, 90)
    {
```

```
 Outlier("Charcoal", 1);
};
Curve("Marine13","Marine13.14c");
R_Date("Beta-276588", 2240, 40);
Curve("IntCal13","IntCal13.14c");
R_Date("I-13425", 2110, 80)
{
 Outlier("Charcoal", 1);
};
R_Date("I-11322", 1945, 80)
{
 Outlier("Charcoal", 1);
};
R_Date("I-11319", 1915, 80)
{
 Outlier("Charcoal", 1);
};
R_Date("I-12859", 1880, 80)
{
 Outlier("Charcoal", 1);
};
R_Date("I-11321", 1845, 80)
{
```

```
 Outlier("Charcoal", 1);
};
Curve("Marine13","Marine13.14c");
R_Date("Beta-259410", 1840, 50);
Curve("IntCal13","IntCal13.14c");
R_Date("I-10979", 1820, 85)
{
 Outlier("Charcoal", 1);
};
R_Date("I-12858", 1820, 80)
{
 Outlier("Charcoal", 1);
};
R_Date("I-12856", 1810, 80)
{
 Outlier("Charcoal", 1);
};
R_Date("Beta-129948", 1810, 60)
{
 Outlier("Charcoal", 1);
};
R_Date("I-11139", 1800, 80)
{
```

```
 Outlier("Charcoal", 1);
};
R_Date("I-12860", 1780, 80)
{
 Outlier("Charcoal", 1);
};
R_Date("I-11320", 1770, 80)
{
 Outlier("Charcoal", 1);
};
R_Date("I-11685", 1740, 75)
{
 Outlier("Charcoal", 1);
};
R_Date("I-10980", 1735, 85)
{
 Outlier("Charcoal", 1);
};
R_Date("I-11140", 1730, 80)
{
 Outlier("Charcoal", 1);
};
R_Date("I-11926", 1720, 80)
```

```
{
 Outlier("Charcoal", 1);
};
R_Date("I-11141", 1705, 80)
{
 Outlier("Charcoal", 1);
};
R_Date("I-16151", 1700, 80)
{
 Outlier("Charcoal", 1);
};
R_Date("I-11925", 1665, 80)
{
 Outlier("Charcoal", 1);
};
R_Date("I-16152", 1650, 80)
{
 Outlier("Charcoal", 1);
};
R_Date("I-12744", 1640, 80)
{
 Outlier("Charcoal", 1);
};
```

```
R_Date("I-16154", 1620, 80)
{
 Outlier("Charcoal", 1);
};
R_Date("I-11317", 1615, 75)
{
 Outlier("Charcoal", 1);
};
R_Date("I-12746", 1600, 80)
{
 Outlier("Charcoal", 1);
};
R_Date("I-16174", 1600, 80)
{
 Outlier("Charcoal", 1);
};
R_Date("I-16173", 1590, 80)
{
 Outlier("Charcoal", 1);
};
R_Date("I-12857", 1580, 80)
{
 Outlier("Charcoal", 1);
```

```
};
R_Date("I-11686", 1575, 80)
{
 Outlier("Charcoal", 1);
};
R_Date("I-10547", 1575, 85)
{
 Outlier("Charcoal", 1);
};
R_Date("I-11687", 1565, 75)
{
 Outlier("Charcoal", 1);
};
R_Date("I-11927", 1565, 80)
{
 Outlier("Charcoal", 1);
};
R_Date("I-12745", 1560, 80)
{
 Outlier("Charcoal", 1);
};
R_Date("I-11316", 1555, 75)
{
```

```
 Outlier("Charcoal", 1);
};
Curve("Marine13","Marine13.14c");
R_Date("I-10549", 1525, 85);
Curve("IntCal13","IntCal13.14c");
R_Date("I-10550", 1505, 85)
{
 Outlier("Charcoal", 1);
};
R_Date("I-11318", 1490, 75)
{
 Outlier("Charcoal", 1);
};
R_Date("I-16175", 1450, 80)
{
 Outlier("Charcoal", 1);
};
R_Date("I-10548", 1440, 85)
{
 Outlier("Charcoal", 1);
};
R_Date("I-16176", 1270, 90)
{
```

```
 Outlier("Charcoal", 1);
};
R_Date("I-14813", 1180, 80)
{
 Outlier("Charcoal", 1);
};
R_Date("I-12743", 950, 80)
{
 Outlier("Charcoal", 1);
};
R_Date("I-12742", 900, 80);
R_Date("I-11189", 790, 85)
{
 Outlier("Charcoal", 1);
};
R_Date("I-15189", 790, 80)
{
 Outlier("Charcoal", 1);
};
R_Date("I- 15188", 700, 80)
{
 Outlier("Charcoal", 1);
};
```

```
R_Date("I-15188", 700, 70)
{
 Outlier("Charcoal", 1);
};
R_Date("I-15187", 690, 80)
{
 Outlier("Charcoal", 1);
};
R_Date("I-15239", 660, 80)
{
 Outlier("Charcoal", 1);
};
R_Date("I-15240", 630, 80)
{
 Outlier("Charcoal", 1);
};
R_Date("I-15238", 570, 80)
{
 Outlier("Charcoal", 1);
};
R_Date("I-15185", 540, 80)
{
 Outlier("Charcoal", 1);
```

```
   };
   R_Date("I-15186", 520, 80)
   {
    Outlier("Charcoal", 1);
   };
   R_Date("I-15658", 470, 80)
   {
    Outlier("Charcoal", 1);
   };
   R_Date("I-15657", 410, 80)
   {
    Outlier("Charcoal", 1);
   };
   R_Date("I-11142", 405, 75)
   {
    Outlier("Charcoal", 1);
   };
  };
  Boundary("Vieques End");
 };
};
```

1,000 yr Outlier Model SQL Code

Anguilla

```
Plot()
 {
  Outlier_Model("Charcoal",Exp(1,-10,0),U(0,3),"t");
  Sequence()
  {
   Boundary("Anguilla Start");
   Phase()
   {
    Curve("IntCal13","IntCal13.14c");
    R_Date("Beta-19957", 1550, 70)
    {
     Outlier("Charcoal", 1);
    };
    R_Date("Beta-15824", 1530, 140)
    {
     Outlier("Charcoal", 1);
    };
    R_Date("Beta-18740", 1430, 70)
    {
     Outlier("Charcoal", 1);
    };
```

```
R_Date("Beta-21858", 1410, 60)
{
 Outlier("Charcoal", 1);
};
R_Date("Beta-110397", 1310, 80)
{
 Outlier("Charcoal", 1);
};
R_Date("Beta-19956", 1290, 60)
{
 Outlier("Charcoal", 1);
};
R_Date("Beta-110396", 1290, 60)
{
 Outlier("Charcoal", 1);
};
R_Date("Beta-106439", 1270, 60)
{
 Outlier("Charcoal", 1);
};
R_Date("Beta-110394", 1230, 70)
{
 Outlier("Charcoal", 1);
```

```
};
Curve("Marine13","Marine13.14c");
R_Date("Beta-15485", 1220, 70);
R_Date("Beta-106444", 1180, 60);
R_Date("Beta-106443", 1180, 60);
Curve("IntCal13","IntCal13.14c");
R_Date("PITT-0546", 1180, 45)
{
 Outlier("Charcoal", 1);
};
R_Date("Beta-110395", 1170, 80)
{
 Outlier("Charcoal", 1);
};
R_Date("Beta-19955", 1150, 60)
{
 Outlier("Charcoal", 1);
};
R_Date("Beta-110393", 1140, 60)
{
 Outlier("Charcoal", 1);
};
R_Date("PITT-0545", 1135, 40)
```

```
{
 Outlier("Charcoal", 1);
};
Curve("Marine13","Marine13.14c");
R_Date("Beta-15486", 1130, 80);
Curve("IntCal13","IntCal13.14c");
R_Date("Beta-106442", 1120, 70)
{
 Outlier("Charcoal", 1);
};
R_Date("Beta-18738", 1120, 70)
{
 Outlier("Charcoal", 1);
};
R_Date("PITT-0547", 1085, 55)
{
 Outlier("Charcoal", 1);
};
R_Date("Beta-21861", 1080, 90)
{
 Outlier("Charcoal", 1);
};
R_Date("Beta-18739", 1000, 110)
```

```
{
 Outlier("Charcoal", 1);
};
R_Date("Beta-120152", 950, 70)
{
 Outlier("Charcoal", 1);
};
R_Date("Beta-21863", 940, 80)
{
 Outlier("Charcoal", 1);
};
Curve("Marine13","Marine13.14c");
R_Date("Beta-257181", 910, 40);
R_Date("Beta-257182", 890, 40);
Curve("IntCal13","IntCal13.14c");
R_Date("Beta-21862", 880, 90)
{
 Outlier("Charcoal", 1);
};
R_Date("Beta-120157", 880, 80)
{
 Outlier("Charcoal", 1);
};
```

```
Curve("Marine13","Marine13.14c");
R_Date("Beta-257184", 860, 40);
Curve("IntCal13","IntCal13.14c");
R_Date("Beta-120154", 850, 60)
{
 Outlier("Charcoal", 1);
};
R_Date("Beta-106441", 840, 80)
{
 Outlier("Charcoal", 1);
};
Curve("Marine13","Marine13.14c");
R_Date("Beta-257185", 780, 40);
Curve("IntCal13","IntCal13.14c");
R_Date("Beta-110398", 780, 80)
{
 Outlier("Charcoal", 1);
};
Curve("Marine13","Marine13.14c");
R_Date("Beta-141202", 740, 60);
Curve("IntCal13","IntCal13.14c");
R_Date("Beta-120153", 740, 60)
{
```

```
   Outlier("Charcoal", 1);
  };
  R_Date("Beta-120156", 710, 80)
  {
   Outlier("Charcoal", 1);
  };
  Curve("Marine13","Marine13.14c");
  R_Date("Beta-257183", 680, 40);
  Curve("IntCal13","IntCal13.14c");
  R_Date("Beta-106440", 510, 80)
  {
   Outlier("Charcoal", 1);
  };
  R_Date("Beta-120155", 440, 70)
  {
   Outlier("Charcoal", 1);
  };
  Curve("Marine13","Marine13.14c");
  R_Date("Beta-60776", 400, 60);
 };
 Boundary("Anguilla End");
};
};
```

Antigua

```
Plot()
 {
  Outlier_Model("Charcoal",Exp(1,-10,0),U(0,3),"t");
  Sequence("Antigua")
  {
   Boundary("Antigua Start");
   Phase()
   {
    Curve("IntCal13","IntCal13.14c");
    R_Date("I-7830", 2785, 80)
    {
     Outlier("Charcoal", 1);
    };
    R_Date("I-7842", 2785, 80)
    {
     Outlier("Charcoal", 1);
    };
    R_Date("I-7980", 1915, 80)
    {
     Outlier("Charcoal", 1);
    };
```

```
R_Date("I-7981", 1855, 80)
{
 Outlier("Charcoal", 1);
};
R_Date("I-7979", 1790, 85)
{
 Outlier("Charcoal", 1);
};
R_Date("I-7855", 1765, 80)
{
 Outlier("Charcoal", 1);
};
R_Date("I-7838", 1750, 80)
{
 Outlier("Charcoal", 1);
};
R_Date("I-7837", 1715, 80)
{
 Outlier("Charcoal", 1);
};
R_Date("I-7854", 1670, 80)
{
 Outlier("Charcoal", 1);
```

```
};
R_Date("Beta- 124127", 1610, 80)
{
 Outlier("Charcoal", 1);
};
R_Date("Beta-124126", 1600, 50)
{
 Outlier("Charcoal", 1);
};
R_Date("I-7355", 1505, 85)
{
 Outlier("Charcoal", 1);
};
R_Date("I-7356", 1505, 85)
{
 Outlier("Charcoal", 1);
};
R_Date("I-7352", 1440, 85)
{
 Outlier("Charcoal", 1);
};
R_Date("Beta-101500", 1430, 50)
{
```

```
     Outlier("Charcoal", 1);
    };
    R_Date("I-7353", 1230, 85)
    {
     Outlier("Charcoal", 1);
    };
    Curve("IntCal13","IntCal13.14c")
    Curve("Marine13","Marine13.14c");
    Mix_Curve("Mixed","IntCal13","Marine13",50,12);
    R_Date("SUERC-34163", 950, 30);
    Curve("IntCal13","IntCal13.14c");
    R_Date("Beta-101499", 720, 50)
    {
     Outlier("Charcoal", 1);
    };
   };
   Boundary("Antigua End");
  };
 };
```

Aruba

```
Plot()
 {
```

```
Outlier_Model("Charcoal",Exp(1,-10,0),U(0,3),"t");
Sequence("Aruba")
{
 Boundary("Aruba Start");
 Phase()
 {
  Curve("IntCal13","IntCal13.14c");
  R_Date("GrN-7341", 3300, 35)
  {
   Outlier("Charcoal", 1);
  };
  Curve("IntCal13","IntCal13.14c");
  Curve("Marine13","Marine13.14c");
  Mix_Curve("Mixed","IntCal13","Marine13",50,12);
  R_Date("Ua-1501", 2210, 95);
  R_Date("Ua-1341", 1740, 110);
  R_Date("Ua-1342", 1520, 100);
  R_Date("Ua-1340", 1520, 110);
  R_Date("Ua-1514", 1420, 150);
  Curve("IntCal13","IntCal13.14c");
  R_Date("GrN-2788", 1080, 50)
  {
   Outlier("Charcoal", 1);
```

```
};
R_Date("GrN-7339", 1040, 45)
{
 Outlier("Charcoal", 1);
};
R_Date("GrN-21665", 1030, 40)
{
 Outlier("Charcoal", 1);
};
R_Date("GrN-21666", 1030, 30)
{
 Outlier("Charcoal", 1);
};
R_Date("GrN-7340", 1000, 30)
{
 Outlier("Charcoal", 1);
};
R_Date("GrN-7342", 990, 30)
{
 Outlier("Charcoal", 1);
};
R_Date("GrA-2789", 990, 50)
{
```

```
 Outlier("Charcoal", 1);
};
R_Date("GrN-7338", 940, 25)
{
 Outlier("Charcoal", 1);
};
R_Date("GrN-21656", 910, 30)
{
 Outlier("Charcoal", 1);
};
Curve("IntCal13","IntCal13.14c");
Curve("Marine13","Marine13.14c");
Mix_Curve("Mixed","IntCal13","Marine13",50,12);
R_Date("GrN-17460", 910, 170);
R_Date("GrN-17459", 870, 80);
Curve("IntCal13","IntCal13.14c");
R_Date("GrN-21664", 860, 40)
{
 Outlier("Charcoal", 1);
};
R_Date("GrA-2785", 860, 50)
{
 Outlier("Charcoal", 1);
```

```
};
R_Date("GrA-2778", 830, 50)
{
 Outlier("Charcoal", 1);
};
R_Date("GrN-16915", 825, 30)
{
 Outlier("Charcoal", 1);
};
R_Date("I-4025", 765, 110)
{
 Outlier("Charcoal", 1);
};
R_Date("GrA-2784", 750, 50)
{
 Outlier("Charcoal", 1);
};
R_Date("I-4026", 740, 105)
{
 Outlier("Charcoal", 1);
};
R_Date("GrA-2790", 340, 50)
{
```

```
    Outlier("Charcoal", 1);
   };
  };
  Boundary("Aruba End");
 };
};
```

Barbados

```
Plot()
 {
  Outlier_Model("Charcoal",Exp(1,-10,0),U(0,3),"t");
  Sequence("Barbados")
  {
   Boundary("Barbados Start");
   Phase()
   {
    Curve("Marine13","Marine13.14c");
    R_Date("D-AMS 001792", 4366, 32);
    R_Date("Beta-297522", 4360, 40);
    R_Date("D-AMS 001793", 4278, 29);
    R_Date("Beta-297521", 4230, 50);
    R_Date("D-AMS 001794", 4091, 27);
    R_Date("I-16840", 3980, 100);
```

```
    Curve("IntCal13","IntCal13.14c");
    R_Date("Beta-20723", 1950, 150)
    {
     Outlier("Charcoal", 1);
    };
    R_Date("I-2486", 1570, 95)
    {
     Outlier("Charcoal", 1);
    };
    Curve("Marine13","Marine13.14c");
    R_Date("1-16189", 1120, 80);
   };
   Boundary("Barbados End");
  };
 };
```

Barbuda

```
Plot()
 {
  Outlier_Model("Charcoal",Exp(1,-10,0),U(0,3),"t");
  Sequence("Barbuda")
  {
   Boundary("Barbuda Start");
```

```
Phase()
{
 Curve("Marine13","Marine13.14c");
 R_Date("UCI-107938", 3430, 15);
 R_Date("SUERC-33604 (GU-23530)", 3280, 35);
 R_Date("SUERC 33605 (GU-23531)", 2790, 35);
 R_Date("UCI-107937", 2565, 20);
 R_Date("Beta-103891", 2030, 60);
 Curve("IntCal13","IntCal13.14c");
 R_Date("SUERC 18562", 2025, 35)
 {
  Outlier("Charcoal", 1);
 };
 R_Date("SUERC 18560", 2005, 35)
 {
  Outlier("Charcoal", 1);
 };
 R_Date("SUERC 18561", 1920, 35)
 {
  Outlier("Charcoal", 1);
 };
 R_Date("SUERC 18558", 1785, 35)
 {
```

```
 Outlier("Charcoal", 1);
};
R_Date("SUERC 18557", 1755, 35)
{
 Outlier("Charcoal", 1);
};
R_Date("SUERC 34971", 1565, 35)
{
 Outlier("Charcoal", 1);
};
Curve("Marine13","Marine13.14c");
R_Date("Beta-103894", 1400, 60);
R_Date("PITT-1234", 1365, 45);
R_Date("Beta-103892", 1360, 60);
R_Date("Beta-103893", 1350, 60);
R_Date("Beta-103890", 1210, 60);
R_Date("PITT-1233", 1135, 50);
R_Date("PITT-1231", 1050, 30);
Curve("IntCal13","IntCal13.14c");
R_Date("SUERC 18556", 820, 35)
{
 Outlier("Charcoal", 1);
};
```

```
  };
  Boundary("Barbuda End");
 };
};
```

Bonaire

```
Plot()
 {
  Outlier_Model("Charcoal",Exp(1,-10,0),U(0,3),"t");
  Sequence("Bonaire")
  {
   Boundary("Bonaire Start");
   Phase()
   {
    Curve("Marine13","Marine13.14c");
    R_Date("GrN-32756", 3610, 25);
    R_Date("GrN-32758", 3410, 20);
    R_Date("GrN-32751", 3245, 25);
    R_Date("GrN-32750", 3095, 20);
    R_Date("GrN-32749", 2785, 20);
    R_Date("GrN-32755", 2735, 25);
```

```
R_Date("GrN-32752", 2705, 30);
R_Date("GrN-32757", 2680, 25);
R_Date("GrN-32754", 2665, 20);
R_Date("GrN-32753", 2575, 20);
R_Date("GrN-32748", 2412, 15);
Curve("IntCal13","IntCal13.14c");
R_Date("PITT-0267", 1480, 25)
{
 Outlier("Charcoal", 1);
};
R_Date("PITT-0268", 885, 45)
{
 Outlier("Charcoal", 1);
};
R_Date("PITT-0265", 710, 65)
{
 Outlier("Charcoal", 1);
};
R_Date("PITT-0264", 560, 40)
{
 Outlier("Charcoal", 1);
};
R_Date("PITT-0266", 505, 35)
```

```
    {
     Outlier("Charcoal", 1);
    };
   };
   Boundary("Bonaire End");
  };
 };
```

Carriacou

```
Plot()
 {
  Outlier_Model("Charcoal",Exp(1,-10,0),U(0,3),"t");
  Sequence("Carriacou")
  {
   Boundary("Carriacou Start");
   Phase()
   {
    Curve("Marine13","Marine13.14c");
    R_Date("AA-62278", 1917, 37);
    R_Date("Beta-206685", 1870, 70);
    R_Date("AA-62280b", 1822, 41);
    R_Date("AA-62280a", 1789, 38);
    Curve("IntCal13","IntCal13.14c");
```

```
R_Date("AA-67535", 1588, 36)
{
 Outlier("Charcoal", 1);
};
R_Date("AA-67536", 1584, 36)
{
 Outlier("Charcoal", 1);
};
Curve("Marine13","Marine13.14c");
R_Date("GX-30424", 1570, 60);
Curve("IntCal13","IntCal13.14c");
Curve("Marine13","Marine13.14c");
Mix_Curve("Mixed","IntCal13","Marine13",50,12);
R_Date("UCIAMS-111935", 1565, 15);
Curve("Marine13","Marine13.14c");
R_Date("GX-30425", 1460, 60);
R_Date("GX-30423", 1400, 60);
Curve("IntCal13","IntCal13.14c");
R_Date("AA-62281", 1339, 36)
{
 Outlier("Charcoal", 1);
};
R_Date("AA-67534", 1333, 57)
```

```
{
 Outlier("Charcoal", 1);
};
R_Date("D-AMS 016647", 1328, 20)
{
 Outlier("Charcoal", 1);
};
R_Date("D-AMS 16649", 1321, 20)
{
 Outlier("Charcoal", 1);
};
R_Date("D-AMS 016648", 1315, 20)
{
 Outlier("Charcoal", 1);
};
Curve("Marine13","Marine13.14c");
R_Date("Beta-233647", 1310, 40);
R_Date("UCIAMS-94046", 1265, 20);
Curve("IntCal13","IntCal13.14c");
R_Date("AA-62279", 1243, 36)
{
 Outlier("Charcoal", 1);
};
```

```
R_Date("AA-62282", 1227, 36)
{
 Outlier("Charcoal", 1);
};
R_Date("OS-71467", 1220, 20)
{
 Outlier("Charcoal", 1);
};
R_Date("AA-67533", 1172, 36)
{
 Outlier("Charcoal", 1);
};
R_Date("AA-81055", 1158, 45)
{
 Outlier("Charcoal", 1);
};
R_Date("OS-71463", 1140, 15)
{
 Outlier("Charcoal", 1);
};
R_Date("AA-67531", 1133, 38)
{
 Outlier("Charcoal", 1);
```

```
};
R_Date("OS-71464", 1100, 20)
{
 Outlier("Charcoal", 1);
};
R_Date("OS-71465", 1080, 15)
{
 Outlier("Charcoal", 1);
};
R_Date("AA-67532", 1073, 38)
{
 Outlier("Charcoal", 1);
};
Curve("IntCal13","IntCal13.14c");
Curve("Marine13","Marine13.14c");
Mix_Curve("Mixed","IntCal13","Marine13",50,12);
R_Date("AA-62283", 1062, 44);
Curve("IntCal13","IntCal13.14c");
R_Date("AA-67530", 1039, 35)
{
 Outlier("Charcoal", 1);
};
R_Date("OS-41358", 1030, 30)
```

```
{
 Outlier("Charcoal", 1);
};
R_Date("UCIAMS-94045", 1020, 20)
{
 Outlier("Charcoal", 1);
};
Curve("IntCal13","IntCal13.14c");
Curve("Marine13","Marine13.14c");
Mix_Curve("Mixed","IntCal13","Marine13",50,12);
R_Date("UCIAMS-120951", 1015, 15);
Curve("IntCal13","IntCal13.14c");
R_Date("AA-81056", 994, 45)
{
 Outlier("Charcoal", 1);
};
R_Date("UCIAMS-94044", 990, 20)
{
 Outlier("Charcoal", 1);
};
R_Date("AA-67529", 988, 42)
{
 Outlier("Charcoal", 1);
```

```
};
R_Date("OS-71462", 975, 20)
{
 Outlier("Charcoal", 1);
};
R_Date("OS-71408", 970, 15)
{
 Outlier("Charcoal", 1);
};
R_Date("OS-71407", 960, 15)
{
 Outlier("Charcoal", 1);
};
R_Date("RL-29", 940, 100)
{
 Outlier("Charcoal", 1);
};
R_Date("OS-71409", 925, 15)
{
 Outlier("Charcoal", 1);
};
Curve("IntCal13","IntCal13.14c");
Curve("Marine13","Marine13.14c");
```

```
   Mix_Curve("Mixed","IntCal13","Marine13",50,12);
   R_Date("Beta-257793", 870, 40);
   Curve("IntCal13","IntCal13.14c");
   R_Date("OS-71466", 680, 15)
   {
    Outlier("Charcoal", 1);
   };
   R_Date("AA-81054", 657, 44)
   {
    Outlier("Charcoal", 1);
   };
   Curve("IntCal13","IntCal13.14c");
   Curve("Marine13","Marine13.14c");
   Mix_Curve("Mixed","IntCal13","Marine13",50,12);
   R_Date("UCIAMS-111933", 715, 15);
   R_Date("UCIAMS-111934", 690, 15);
  };
  Boundary("Carriacou End");
 };
};
```

Cuba

```
Plot()
```

```
{
 Outlier_Model("Charcoal",Exp(1,-10,0),U(0,3),"t");
 Sequence("Cuba")
 {
  Boundary("Cuba Start");
  Phase()
  {
   Curve("IntCal13","IntCal13.14c");
   R_Date("LE-4283", 5270, 120)
   {
    Outlier("Charcoal", 1);
   };
   R_Date("GD-250", 5140, 170)
   {
    Outlier("Charcoal", 1);
   };
   R_Date("MC-860", 4420, 100)
   {
    Outlier("Charcoal", 1);
   };
   Curve("Marine13","Marine13.14c");
   R_Date("OxA-15267", 4408, 37);
   Curve("IntCal13","IntCal13.14c");
```

```
R_Date("MC-859", 4240, 100)
{
 Outlier("Charcoal", 1);
};
R_Date("UBAR-170", 4200, 79)
{
 Outlier("Charcoal", 1);
};
R_Date("Beta-140079", 4180, 80)
{
 Outlier("Charcoal", 1);
};
R_Date("LE-1783", 4110, 50)
{
 Outlier("Charcoal", 1);
};
R_Date("SI-429", 4000, 150)
{
 Outlier("Charcoal", 1);
};
R_Date("LE-1784", 3870, 40)
{
 Outlier("Charcoal", 1);
```

```
};
Curve("Marine13","Marine13.14c");
R_Date("OxA-15180", 3861, 28);
Curve("IntCal13","IntCal13.14c");
R_Date("LE-1782", 3760, 40)
{
 Outlier("Charcoal", 1);
};
R_Date("Beta-133951", 3720, 70)
{
 Outlier("Charcoal", 1);
};
R_Date("UNAM-0716", 3460, 60)
{
 Outlier("Charcoal", 1);
};
R_Date("GD-204", 3460, 160)
{
 Outlier("Charcoal", 1);
};
Curve("Marine13","Marine13.14c");
R_Date("OxA-15264", 3273, 33);
R_Date("OxA-15263", 3271, 29);
```

```
Curve("IntCal13","IntCal13.14c");
R_Date("Y-1764", 3250, 100)
{
 Outlier("Charcoal", 1);
};
R_Date("LE-4270", 3110, 180)
{
 Outlier("Charcoal", 1);
};
R_Date("SI-428", 3110, 200)
{
 Outlier("Charcoal", 1);
};
R_Date("UBAR-169", 3060, 180)
{
 Outlier("Charcoal", 1);
};
R_Date("AA-101053", 3057, 39)
{
 Outlier("Charcoal", 1);
};
R_Date("LE-4288", 3030, 180)
{
```

```
 Outlier("Charcoal", 1);
};
R_Date("LE-4287", 3030, 180)
{
 Outlier("Charcoal", 1);
};
Curve("IntCal13","IntCal13.14c");
Curve("Marine13","Marine13.14c");
Mix_Curve("Mixed","IntCal13","Marine13",50,12);
R_Date("AA-101054", 2999, 61);
R_Date("AA-101057", 2996, 53);
Curve("Marine13","Marine13.14c");
R_Date("Beta-184894", 2980, 70);
Curve("IntCal13","IntCal13.14c");
Curve("Marine13","Marine13.14c");
Mix_Curve("Mixed","IntCal13","Marine13",50,12);
R_Date("AA-89061", 2960, 33);
R_Date("AA-101052", 2946, 57);
Curve("IntCal13","IntCal13.14c");
R_Date("LE-4282", 2930, 300)
{
 Outlier("Charcoal", 1);
};
```

```
R_Date("GD-591", 2930, 80)
{
 Outlier("Charcoal", 1);
};
Curve("IntCal13","IntCal13.14c");
Curve("Marine13","Marine13.14c");
Mix_Curve("Mixed","IntCal13","Marine13",50,12);
R_Date("AA-89063", 2922, 34);
Curve("IntCal13","IntCal13.14c");
R_Date("GD-613", 2880, 70)
{
 Outlier("Charcoal", 1);
};
R_Date("A-14316", 2845, 90)
{
 Outlier("Charcoal", 1);
};
R_Date("GD-1046", 2840, 60)
{
 Outlier("Charcoal", 1);
};
R_Date("GD-601", 2805, 60)
{
```

```
 Outlier("Charcoal", 1);
};
Curve("IntCal13","IntCal13.14c");
Curve("Marine13","Marine13.14c");
Mix_Curve("Mixed","IntCal13","Marine13",50,12);
R_Date("AA-101059", 2791, 51);
Curve("IntCal13","IntCal13.14c");
R_Date("Beta-133950", 2780, 40)
{
 Outlier("Charcoal", 1);
};
R_Date("LE-4272", 2750, 160)
{
 Outlier("Charcoal", 1);
};
R_Date("GD-614", 2720, 65)
{
 Outlier("Charcoal", 1);
};
R_Date("LE-2720", 2680, 40)
{
 Outlier("Charcoal", 1);
};
```

```
Curve("Marine13","Marine13.14c");
R_Date("Beta-184896", 2680, 60);
Curve("IntCal13","IntCal13.14c");
R_Date("LE-4290", 2610, 120)
{
 Outlier("Charcoal", 1);
};
R_Date("LE-4281", 2610, 120)
{
 Outlier("Charcoal", 1);
};
R_Date("LE-2718", 2610, 40)
{
 Outlier("Charcoal", 1);
};
R_Date("LE-4275", 2580, 90)
{
 Outlier("Charcoal", 1);
};
Curve("Marine13","Marine13.14c");
R_Date("Beta-318171", 2570, 30);
Curve("IntCal13","IntCal13.14c");
R_Date("UNAM-0717", 2520, 60)
```

```
{
 Outlier("Charcoal", 1);
};
R_Date("A-14315", 2515, 75)
{
 Outlier("Charcoal", 1);
};
R_Date("SI-427", 2510, 200)
{
 Outlier("Charcoal", 1);
};
R_Date("LE-4273", 2420, 100)
{
 Outlier("Charcoal", 1);
};
R_Date("LE-4279", 2390, 170)
{
 Outlier("Charcoal", 1);
};
R_Date("LE-4271", 2380, 80)
{
 Outlier("Charcoal", 1);
};
```

```
Curve("Marine13","Marine13.14c");
R_Date("Beta-422938", 2350, 30);
Curve("IntCal13","IntCal13.14c");
R_Date("LE-4276", 2250, 150)
{
 Outlier("Charcoal", 1);
};
R_Date("LE-4267", 2220, 160)
{
 Outlier("Charcoal", 1);
};
R_Date("GD-1039", 2160, 55)
{
 Outlier("Charcoal", 1);
};
R_Date("LE-2719", 2160, 40)
{
 Outlier("Charcoal", 1);
};
R_Date("SI-426", 2070, 150)
{
 Outlier("Charcoal", 1);
};
```

```
R_Date("LC-H 1034", 2070, 110)
{
 Outlier("Charcoal", 1);
};
R_Date("LE-4274", 2030, 160)
{
 Outlier("Charcoal", 1);
};
Curve("Marine13","Marine13.14c");
R_Date("Beta-214957", 2020, 50);
Curve("IntCal13","IntCal13.14c");
R_Date("Lv-2063", 2020, 80)
{
 Outlier("Charcoal", 1);
};
R_Date("LE-2717", 2010, 40)
{
 Outlier("Charcoal", 1);
};
Curve("Marine13","Marine13.14c");
R_Date("OxA-15262", 2005, 27);
Curve("IntCal13","IntCal13.14c");
R_Date("GD-1051", 1990, 80)
```

```
{
 Outlier("Charcoal", 1);
};
Curve("Marine13","Marine13.14c");
R_Date("OxA-15266", 1978, 33);
R_Date("Beta-214958", 1910, 50);
Curve("IntCal13","IntCal13.14c");
R_Date("Beta-93862", 1890, 60)
{
 Outlier("Charcoal", 1);
};
Curve("Marine13","Marine13.14c");
R_Date("OxA-15183", 1873, 26);
Curve("IntCal13","IntCal13.14c");
R_Date("Beta-93866", 1850, 50)
{
 Outlier("Charcoal", 1);
};
Curve("Marine13","Marine13.14c");
R_Date("Beta-318170", 1750, 30);
Curve("IntCal13","IntCal13.14c");
R_Date("UM-1953", 1745, 175)
{
```

```
 Outlier("Charcoal", 1);
};
Curve("Marine13","Marine13.14c");
R_Date("OxA-15184", 1686, 26);
Curve("IntCal13","IntCal13.14c");
Curve("Marine13","Marine13.14c");
Mix_Curve("Mixed","IntCal13","Marine13",50,12);
R_Date("Beta-72801", 1670, 70);
R_Date("AA-101055", 1661, 52);
Curve("IntCal13","IntCal13.14c");
R_Date("Beta-133948", 1640, 130)
{
 Outlier("Charcoal", 1);
};
R_Date("SI-424", 1620, 150)
{
 Outlier("Charcoal", 1);
};
R_Date("AA-89064", 1617, 46)
{
 Outlier("Charcoal", 1);
};
Curve("IntCal13","IntCal13.14c");
```

```
Curve("Marine13","Marine13.14c");
Mix_Curve("Mixed","IntCal13","Marine13",50,12);
R_Date("OxA-15260", 1617, 29);
R_Date("Beta-72802", 1590, 60);
Curve("Marine13","Marine13.14c");
R_Date("OxA-15181", 1561, 24);
R_Date("OxA-15146", 1557, 25);
Curve("IntCal13","IntCal13.14c");
Curve("Marine13","Marine13.14c");
Mix_Curve("Mixed","IntCal13","Marine13",50,12);
R_Date("AA-89062", 1536, 51);
Curve("IntCal13","IntCal13.14c");
R_Date("GD-617", 1495, 60)
{
 Outlier("Charcoal", 1);
};
R_Date("LE-4269", 1470, 110)
{
 Outlier("Charcoal", 1);
};
R_Date("LC-H 1035", 1450, 70)
{
 Outlier("Charcoal", 1);
```

```
};
Curve("IntCal13","IntCal13.14c");
Curve("Marine13","Marine13.14c");
Mix_Curve("Mixed","IntCal13","Marine13",50,12);
R_Date("AA-89060", 1420, 59);
Curve("IntCal13","IntCal13.14c");
R_Date("TO-7621", 1404, 60)
{
 Outlier("Charcoal", 1);
};
R_Date("GD-616", 1350, 70)
{
 Outlier("Charcoal", 1);
};
R_Date("Beta-93863", 1350, 50)
{
 Outlier("Charcoal", 1);
};
R_Date("TO-7624", 1320, 60)
{
 Outlier("Charcoal", 1);
};
Curve("IntCal13","IntCal13.14c");
```

```
Curve("Marine13","Marine13.14c");
Mix_Curve("Mixed","IntCal13","Marine13",50,12);
R_Date("AA-101056", 1289, 46);
Curve("IntCal13","IntCal13.14c");
R_Date("Beta-140078", 1280, 60)
{
 Outlier("Charcoal", 1);
};
R_Date("Beta-133947", 1210, 60)
{
 Outlier("Charcoal", 1);
};
R_Date("GD-619", 1170, 90)
{
 Outlier("Charcoal", 1);
};
R_Date("Y-1994", 1120, 160)
{
 Outlier("Charcoal", 1);
};
Curve("Marine13","Marine13.14c");
R_Date("OxA-15179", 1112, 26);
Curve("IntCal13","IntCal13.14c");
```

```
    R_Date("LC-H-1106", 1100, 130)
    {
     Outlier("Charcoal", 1);
    };
    R_Date("SI-347", 1020, 100)
    {
     Outlier("Charcoal", 1);
    };
    Boundary("Cuba End");
   };
  };
 };
```

Curaçao

```
Plot()
 {
  Outlier_Model("Charcoal",Exp(1,-10,0),U(0,3),"t");
  Sequence("Curacao")
  {
   Boundary("Curacao Start");
   Phase()
   {
    Curve("IntCal13","IntCal13.14c");
```

```
R_Date("IVIC-247", 4490, 60)
{
 Outlier("Charcoal", 1);
};
R_Date("IVIC-246", 4160, 80)
{
 Outlier("Charcoal", 1);
};
R_Date("IVIC-234", 4110, 65)
{
 Outlier("Charcoal", 1);
};
R_Date("IVIC-242", 4070, 65)
{
 Outlier("Charcoal", 1);
};
R_Date("IVIC-240", 3990, 50)
{
 Outlier("Charcoal", 1);
};
Curve("Marine13","Marine13.14c");
R_Date("PITT-1200", 1965, 35);
Curve("IntCal13","IntCal13.14c");
```

```
R_Date("PITT-1183", 1875, 430)
{
 Outlier("Charcoal", 1);
};
Curve("IntCal13","IntCal13.14c");
Curve("Marine13","Marine13.14c");
Mix_Curve("Mixed","IntCal13","Marine13",50,12);
R_Date("GrN-12914", 1500, 200);
Curve("IntCal13","IntCal13.14c");
R_Date("IVIC-237", 1440, 60)
{
 Outlier("Charcoal", 1);
};
R_Date("IVIC-250", 1230, 60)
{
 Outlier("Charcoal", 1);
};
R_Date("IVIC-233", 910, 50)
{
 Outlier("Charcoal", 1);
};
R_Date("PITT-1198", 875, 35)
{
```

```
 Outlier("Charcoal", 1);
};
R_Date("IVIC-244", 830, 60)
{
 Outlier("Charcoal", 1);
};
R_Date("PITT-1196", 775, 60)
{
 Outlier("Charcoal", 1);
};
Curve("IntCal13","IntCal13.14c");
Curve("Marine13","Marine13.14c");
Mix_Curve("Mixed","IntCal13","Marine13",50,12);
R_Date("DIC-3138", 660, 20);
Curve("IntCal13","IntCal13.14c");
R_Date("IVIC-248", 630, 50)
{
 Outlier("Charcoal", 1);
};
R_Date("IVIC-249", 630, 60)
{
 Outlier("Charcoal", 1);
};
```

```
R_Date("GrN-31926", 605, 15)
{
 Outlier("Charcoal", 1);
};
R_Date("PITT-1195", 590, 50)
{
 Outlier("Charcoal", 1);
};
R_Date("PITT-1188", 475, 50)
{
 Outlier("Charcoal", 1);
};
R_Date("GrN-32016", 450, 30)
{
 Outlier("Charcoal", 1);
};
R_Date("GrN-9997", 420, 15)
{
 Outlier("Charcoal", 1);
};
R_Date("PITT-1197", 395, 115)
{
 Outlier("Charcoal", 1);
```

```
    };
    R_Date("GrN-32017", 370, 25)
    {
     Outlier("Charcoal", 1);
    };
    R_Date("IVIC-241", 340, 50)
    {
     Outlier("Charcoal", 1);
    };
    R_Date("GrN-9998", 325, 35)
    {
     Outlier("Charcoal", 1);
    };
   };
   Boundary("Curacao End");
  };
 };
```

Grand Turk

```
Plot()
 {
  Outlier_Model("Charcoal",Exp(1,-10,0),U(0,3),"t");
  Sequence("Grand Turk")
```

```
{
 Boundary("Grand Turk Start");
 Phase()
 {
  Curve("IntCal13","IntCal13.14c");
  R_Date("Beta-80911", 1280, 60)
  R_Date("Beta-98698", 1230, 60)
  {
   Outlier("Charcoal", 1);
  };
  Curve("Marine13","Marine13.14c");
  R_Date("Beta-93912", 1170, 60);
  Curve("IntCal13","IntCal13.14c");
  R_Date("Beta-80910", 1160, 60)
  R_Date("Beta-114924", 1120, 50)
  {
   Outlier("Charcoal", 1);
  };
  R_Date("Beta-66151", 1120, 120)
  {
   Outlier("Charcoal", 1);
  };
  R_Date("Beta-98697", 1010, 50)
```

```
{
 Outlier("Charcoal", 1);
};
R_Date("Beta-96700", 940, 60)
Curve("Marine13","Marine13.14c");
R_Date("Beta-93913", 930, 60);
Curve("IntCal13","IntCal13.14c");
R_Date("Beta-242672", 910, 40)
{
 Outlier("Charcoal", 1);
};
R_Date("Beta-98699", 900, 50)
{
 Outlier("Charcoal", 1);
};
Curve("Marine13","Marine13.14c");
R_Date("Beta-242675", 850, 50);
R_Date("Beta-242673", 790, 50);
Curve("IntCal13","IntCal13.14c");
R_Date("Beta-253527", 780, 40)
{
 Outlier("Charcoal", 1);
};
```

```
   R_Date("Beta 242670", 690, 40)
   {
    Outlier("Charcoal", 1);
   };
   R_Date("Beta-242671", 610, 40)
   {
    Outlier("Charcoal", 1);
   };
   Curve("Marine13","Marine13.14c");
   R_Date("Beta-242674", 460, 40);
  };
  Boundary("Grand Turk End");
 };
};
```

Grenada

```
Plot()
 {
  Outlier_Model("Charcoal",Exp(1,-10,0),U(0,3),"t");
  Sequence("Grenada")
  {
   Boundary("Grenada Start");
   Phase()
```

```
{
 Curve("Marine13","Marine13.14c");
 R_Date("PSUAMS-3017", 2820, 20);
 R_Date("PSUAMS-3022", 2145, 20);
 Curve("IntCal13","IntCal13.14c");
 R_Date("PSUAMS-1317", 1685, 20)
 {
  Outlier("Charcoal", 1);
 };
 Curve("Marine13","Marine13.14c");
 R_Date("PSUAMS-3020", 1510, 20);
 Curve("IntCal13","IntCal13.14c");
 R_Date("PSUAMS-1287", 1500, 25)
 {
  Outlier("Charcoal", 1);
 };
 Curve("Marine13","Marine13.14c");
 R_Date("UCIAMS-179806", 1380, 20);
 Curve("IntCal13","IntCal13.14c");
 R_Date("Beta-85941", 1270, 50)
 {
  Outlier("Charcoal", 1);
 };
```

```
R_Date("PSUAMS-1565", 1215, 20)
{
 Outlier("Charcoal", 1);
};
R_Date("PSUAMS-3946", 1215, 20)
{
 Outlier("Charcoal", 1);
};
R_Date("PSUAMS-1320", 1180, 25)
{
 Outlier("Charcoal", 1);
};
R_Date("Beta-85935", 1110, 40)
{
 Outlier("Charcoal", 1);
};
R_Date("Beta-98365", 1080, 50)
{
 Outlier("Charcoal", 1);
};
R_Date("Beta-86831", 1050, 90)
{
 Outlier("Charcoal", 1);
```

```
};
R_Date("Beta-98368", 980, 60)
{
 Outlier("Charcoal", 1);
};
R_Date("Beta-86827", 900, 60)
{
 Outlier("Charcoal", 1);
};
R_Date("Beta-85938", 850, 40)
{
 Outlier("Charcoal", 1);
};
R_Date("PSUAMS-1322", 835, 25)
{
 Outlier("Charcoal", 1);
};
R_Date("Beta-86833", 810, 50)
{
 Outlier("Charcoal", 1);
};
R_Date("Beta-86832", 790, 60)
{
```

```
 Outlier("Charcoal", 1);
};
R_Date("Beta-85939", 770, 60)
{
 Outlier("Charcoal", 1);
};
R_Date("Beta-86830", 770, 50)
{
 Outlier("Charcoal", 1);
};
R_Date("Beta-86828", 650, 40)
{
 Outlier("Charcoal", 1);
};
R_Date("Beta-86829", 550, 60)
{
 Outlier("Charcoal", 1);
};
R_Date("Beta-98367", 510, 60)
{
 Outlier("Charcoal", 1);
};
R_Date("PSUAMS-3945", 380, 25)
```

```
   {
    Outlier("Charcoal", 1);
   };
   R_Date("Beta-98366", 340, 50)
   {
    Outlier("Charcoal", 1);
   };
  };
  Boundary("Grenada End");
 };
};
```

Guadeloupe

```
Plot()
 {
  Outlier_Model("Charcoal",Exp(1,-10,0),U(0,3),"t");
  Sequence("Guadeloupe")
  {
   Boundary("Guadeloupe Start");
   Phase()
   {
    Curve("IntCal13","IntCal13.14c");
    R_Date("Erl-10156", 3052, 41)
```

```
{
 Outlier("Charcoal", 1);
};
R_Date("Ly-9162", 1815, 30)
{
 Outlier("Charcoal", 1);
};
R_Date("Ly-9161", 1580, 30)
{
 Outlier("Charcoal", 1);
};
R_Date("KIA-36672", 1340, 25)
{
 Outlier("Charcoal", 1);
};
R_Date("KIA-36677", 1245, 30)
{
 Outlier("Charcoal", 1);
};
R_Date("KIA-36671", 1230, 30)
{
 Outlier("Charcoal", 1);
};
```

```
R_Date("KIA-31187", 1210, 20)
{
 Outlier("Charcoal", 1);
};
R_Date("Y-1246", 1100, 80)
{
 Outlier("Charcoal", 1);
};
R_Date("KIA-36678", 1065, 30)
{
 Outlier("Charcoal", 1);
};
R_Date("Erl-10159", 1056, 36)
{
 Outlier("Charcoal", 1);
};
R_Date("KIA-36684", 1000, 30)
{
 Outlier("Charcoal", 1);
};
R_Date("KIA-36673", 945, 35)
{
 Outlier("Charcoal", 1);
```

```
};
R_Date("KIA-36674", 945, 30)
{
 Outlier("Charcoal", 1);
};
Curve("IntCal13","IntCal13.14c");
Curve("Marine13","Marine13.14c");
Mix_Curve("Mixed","IntCal13","Marine13",50,12);
R_Date("KIA-36675", 915, 50);
Curve("IntCal13","IntCal13.14c");
R_Date("Ly-8466", 770, 30)
{
 Outlier("Charcoal", 1);
};
R_Date("KIA-36680", 690, 30)
{
 Outlier("Charcoal", 1);
};
Curve("IntCal13","IntCal13.14c");
Curve("Marine13","Marine13.14c");
Mix_Curve("Mixed","IntCal13","Marine13",50,12);
R_Date("KIA-36682", 650, 140);
Curve("IntCal13","IntCal13.14c");
```

```
  R_Date("KIA-36679", 625, 30)
  {
   Outlier("Charcoal", 1);
  };
  Curve("IntCal13","IntCal13.14c");
  Curve("Marine13","Marine13.14c");
  Mix_Curve("Mixed","IntCal13","Marine13",50,12);
  R_Date("KIA-36681", 625, 25);
  R_Date("KIA-36681", 620, 25);
  R_Date("KIA-36676", 565, 25);
  R_Date("KIA-36676", 431, 22);
  R_Date("KIA-36676", 348, 39);
  Curve("IntCal13","IntCal13.14c");
  R_Date("KIA-36683", 330, 25)
  {
   Outlier("Charcoal", 1);
  };
 };
 Boundary("Guadeloupe End");
};
};
```

Hispaniola

```
Plot()
 {
  Outlier_Model("Charcoal",Exp(1,-10,0),U(0,3),"t");
  Sequence("Hispaniola")
  {
   Boundary("Hispaniola Start");
   Phase()
   {
    Curve("IntCal13","IntCal13.14c");
    R_Date("I-6756", 3890, 95)
    {
     Outlier("Charcoal", 1);
    };
    R_Date("I-5940", 3840, 130)
    {
     Outlier("Charcoal", 1);
    };
    Curve("Marine13","Marine13.14c");
    R_Date("I-9541", 3575, 90);
    Curve("IntCal13","IntCal13.14c");
    R_Date("I-9539", 3205, 90)
    {
     Outlier("Charcoal", 1);
```

```
};
R_Date("I-6781", 2585, 90)
{
 Outlier("Charcoal", 1);
};
R_Date("I-5818", 2095, 135)
{
 Outlier("Charcoal", 1);
};
R_Date("SI-991", 1805, 70)
{
 Outlier("Charcoal", 1);
};
Curve("Marine13","Marine13.14c");
R_Date("GrN-29933", 1750, 30);
R_Date("GrN-31416", 1745, 20);
R_Date("GrN-31413", 1705, 20);
R_Date("GrN-30532", 1525, 25);
R_Date("GrN-31415", 1520, 20);
R_Date("GrN-29932", 1495, 30);
R_Date("GrN-31414", 1435, 20);
R_Date("Beta-293244", 1340, 40);
Curve("IntCal13","IntCal13.14c");
```

```
R_Date("GrN-31412", 1230, 40)
{
 Outlier("Charcoal", 1);
};
Curve("Marine13","Marine13.14c");
R_Date("GrN-30531", 1170, 25);
R_Date("Beta-293242", 1120, 40);
Curve("IntCal13","IntCal13.14c");
R_Date("GrN-29934", 1110, 25);
Curve("Marine13","Marine13.14c");
R_Date("GrN-30533", 1040, 25);
R_Date("Beta-293243", 1030, 40);
Curve("IntCal13","IntCal13.14c");
R_Date("Beta-108313", 990, 70)
{
 Outlier("Charcoal", 1);
};
R_Date("Beta-107023", 940, 30);
R_Date("GrN-31418", 925, 30)
{
 Outlier("Charcoal", 1);
};
R_Date("GrN-31417", 915, 20)
```

```
{
 Outlier("Charcoal", 1);
};
R_Date("Beta-112400", 910, 40)
{
 Outlier("Charcoal", 1);
};
R_Date("Beta-96782", 870, 60)
{
 Outlier("Charcoal", 1);
};
R_Date("GrN-29931", 815, 35)
{
 Outlier("Charcoal", 1);
};
R_Date("Beta-47758", 810, 70)
{
 Outlier("Charcoal", 1);
};
R_Date("Beta-46760", 800, 60)
{
 Outlier("Charcoal", 1);
};
```

```
R_Date("Beta-46759", 720, 50)
{
 Outlier("Charcoal", 1);
};
R_Date("Beta-18173", 680, 80)
{
 Outlier("Charcoal", 1);
};
R_Date("Beta-96781", 680, 60)
{
 Outlier("Charcoal", 1);
};
R_Date("Beta-01527", 640, 260)
{
 Outlier("Charcoal", 1);
};
R_Date("Beta-108314", 620, 70)
{
 Outlier("Charcoal", 1);
};
R_Date("Beta-18172", 600, 70)
{
 Outlier("Charcoal", 1);
```

```
};
R_Date("GrN-30534", 600, 25)
{
 Outlier("Charcoal", 1);
};
R_Date("GrN-30535", 580, 30)
{
 Outlier("Charcoal", 1);
};
R_Date("Beta-108315", 540, 50)
{
 Outlier("Charcoal", 1);
};
R_Date("GrN-29035", 535, 25)
{
 Outlier("Charcoal", 1);
};
R_Date("Beta-018469", 440, 60)
{
 Outlier("Charcoal", 1);
};
R_Date("Beta-10526", 430, 80)
{
```

```
    Outlier("Charcoal", 1);
   };
 R_Date("Beta-010528", 340, 70)
   {
    Outlier("Charcoal", 1);
   };
 R_Date("Beta-046761", 320, 70)
   {
    Outlier("Charcoal", 1);
   };
  };
  Boundary("Hispaniola End");
 };
};
```

Jamaica

```
Plot()
 {
  Outlier_Model("Charcoal",Exp(1,-10,0),U(0,3),"t");
  Sequence("Jamaica")
  {
   Boundary("Jamaica Start");
   Phase()
```

```
{
 Curve("IntCal13","IntCal13.14c");
 R_Date("Beta-153378", 970, 40)
 {
  Outlier("Charcoal", 1);
 };
 R_Date("WK 43115", 938, 20)
 {
  Outlier("Charcoal", 1);
 };
 R_Date("Beta-167740", 680, 60)
 {
  Outlier("Charcoal", 1);
 };
 R_Date("A-6140", 630, 40)
 {
  Outlier("Charcoal", 1);
 };
 R_Date("WK 43114", 627, 20)
 {
  Outlier("Charcoal", 1);
 };
 R_Date("OxA-21058", 615, 24)
```

```
{
 Outlier("Charcoal", 1);
};
R_Date("A-6058", 570, 45)
{
 Outlier("Charcoal", 1);
};
R_Date("A-6061", 525, 45)
{
 Outlier("Charcoal", 1);
};
R_Date("OxA-21057", 396, 24)
{
 Outlier("Charcoal", 1);
};
R_Date("OxA- 21056", 384, 24)
{
 Outlier("Charcoal", 1);
};
};
Boundary("Jamaica End");
};
};
```

Montserrat

```
Plot()
 {
  Outlier_Model("Charcoal",Exp(1,-10,0),U(0,3),"t");
  Sequence("Montserrat")
  {
   Boundary("Montserrat Start");
   Phase()
   {
    Curve("IntCal13","IntCal13.14c");
    R_Date("Beta-83043", 2770, 60)
    {
     Outlier("Charcaol", 1);
    };
    R_Date("Beta-83050", 2140, 110)
    {
     Outlier("Charcaol", 1);
    };
    R_Date("Beta-83046", 2050, 80)
    {
     Outlier("Charcaol", 1);
    };
```

```
R_Date("Beta-83045", 1950, 90)
{
 Outlier("Charcaol", 1);
};
R_Date("Beta-83048", 1860, 100)
{
 Outlier("Charcaol", 1);
};
R_Date("Beta-83049", 1730, 100)
{
 Outlier("Charcaol", 1);
};
R_Date("Beta-83044", 1650, 130)
{
 Outlier("Charcaol", 1);
};
R_Date("Beta-83051", 1540, 120)
{
 Outlier("Charcaol", 1);
};
R_Date("Beta-83047", 1270, 130)
{
 Outlier("Charcaol", 1);
```

```
};
R_Date("Beta-282302", 1120, 40)
{
 Outlier("Charcaol", 1);
};
R_Date("Beta-282300", 1070, 40)
{
 Outlier("Charcaol", 1);
};
R_Date("Beta-277241", 1010, 40)
{
 Outlier("Charcaol", 1);
};
R_Date("Beta-282301", 980, 40)
{
 Outlier("Charcaol", 1);
};
R_Date("Beta-282299", 980, 40)
{
 Outlier("Charcaol", 1);
};
R_Date("Beta-277242", 880, 40)
{
```

```
    Outlier("Charcaol", 1);
   };
  };
  Boundary("Montserrat End");
 };
};
```

Nevis

```
Plot()
 {
  Outlier_Model("Charcoal",Exp(1,-10,0),U(0,3),"t");
  Sequence("Nevis")
  {
   Boundary("Nevis Start");
   Phase()
   {
    Curve("Marine13","Marine13.14c");
    R_Date("D-AMS 007668", 1541, 33);
    R_Date("D-AMS 07667", 1464, 24);
    R_Date("Beta-290341", 1420, 40);
    R_Date("Beta-290340", 1350, 40);
    Curve("IntCal13","IntCal13.14c");
    R_Date("Beta-47807", 1070, 70)
```

```
    {
     Outlier("Charcoal", 1);
    };
    R_Date("Beta-46940", 1060, 50)
    {
     Outlier("Charcoal", 1);
    };
    R_Date("Beta-46944a", 940, 60)
    {
     Outlier("Charcoal", 1);
    };
    R_Date("Beta-46942", 880, 60)
    {
     Outlier("Charcoal", 1);
    };
    Curve("Marine13","Marine13.14c");
    R_Date("Beta-324952", 720, 30);
    R_Date("Beta-324951", 570, 30);
   };
  Boundary("Nevis End");
 };
};
```

Puerto Rico

```
Plot()
 {
  Outlier_Model("Charcoal",Exp(1,-10,0),U(0,3),"t");
  Sequence("Puerto Rico")
  {
   Boundary("Puerto Rico Start");
   Phase()
   {
    Curve("IntCal13","IntCal13.14c");
    R_Date("Beta-77165", 4060, 60)
    {
     Outlier("Charcoal", 1);
    };
    R_Date("Beta-178680", 4110, 40)
    {
     Outlier("Charcoal", 1);
    };
    R_Date("GX-28807", 3920, 40)
    {
     Outlier("Charcoal", 1);
    };
    Curve("Marine13","Marine13.14c");
```

```
R_Date("UGM-17566", 4250, 25);
Curve("IntCal13","IntCal13.14c");
R_Date("Beta-116372", 3820, 70)
{
 Outlier("Charcoal", 1);
};
R_Date("UGM-17565", 3810, 25)
{
 Outlier("Charcoal", 1);
};
R_Date("GX-28814", 3740, 100)
{
 Outlier("Charcoal", 1);
};
R_Date("UGM-5106", 3740, 30)
{
 Outlier("Charcoal", 1);
};
Curve("Marine13","Marine13.14c");
R_Date("UGM-5108", 3740, 30);
Curve("IntCal13","IntCal13.14c");
R_Date("GX-28805", 3700, 30)
{
```

```
 Outlier("Charcoal", 1);
};
R_Date("Beta-294434", 3680, 40)
{
 Outlier("Charcoal", 1);
};
R_Date("GX-28808", 3670, 40)
{
 Outlier("Charcoal", 1);
};
Curve("Marine13","Marine13.14c");
R_Date("UGM-17561", 3640, 25);
Curve("IntCal13","IntCal13.14c");
R_Date("Beta-130451", 3640, 70)
{
 Outlier("Charcoal", 1);
};
Curve("Marine13","Marine13.14c");
R_Date("UGM-17562", 3630, 25);
Curve("IntCal13","IntCal13.14c");
R_Date("GX-28806", 3570, 40)
{
 Outlier("Charcoal", 1);
```

```
};
Curve("Marine13","Marine13.14c");
R_Date("UGM-5107", 3520, 30);
Curve("IntCal13","IntCal13.14c");
R_Date("GX-28809", 3470, 40)
{
 Outlier("Charcoal", 1);
};
R_Date("I-14745", 3340, 90)
{
 Outlier("Charcoal", 1);
};
Curve("Marine13","Marine13.14c");
R_Date("UGM-5105", 3170, 30);
Curve("IntCal13","IntCal13.14c");
R_Date("UGM-30042", 3140, 40)
{
 Outlier("Charcoal", 1);
};
Curve("Marine13","Marine13.14c");
R_Date("UGM-17564", 3120, 20);
Curve("IntCal13","IntCal13.14c");
R_Date("UGM-30031", 2910, 50)
```

```
{
 Outlier("Charcoal", 1);
};
R_Date("Beta-130450", 2730, 70)
{
 Outlier("Charcoal", 1);
};
R_Date("Beta-178678", 2520, 40)
{
 Outlier("Charcoal", 1);
};
R_Date("UGM-30033", 2390, 35)
{
 Outlier("Charcoal", 1);
};
R_Date("Beta-178677", 2330, 110)
{
 Outlier("Charcoal", 1);
};
R_Date("I-14744", 2270, 80)
{
 Outlier("Charcoal", 1);
};
```

```
R_Date("Beta-294435", 2120, 30)
{
 Outlier("Charcoal", 1);
};
Curve("Marine13","Marine13.14c");
R_Date("I-14979", 2120, 80);
Curve("IntCal13","IntCal13.14c");
R_Date("I-11296", 2100, 80)
{
 Outlier("Charcoal", 1);
};
R_Date("Beta-9970", 2060, 70)
{
 Outlier("Charcoal", 1);
};
R_Date("Beta-14380", 2060, 60)
{
 Outlier("Charcoal", 1);
};
R_Date("I-14978", 2020, 80)
{
 Outlier("Charcoal", 1);
};
```

```
R_Date("I-13855", 2020, 80)
{
 Outlier("Charcoal", 1);
};
R_Date("I-11297", 1995, 80)
{
 Outlier("Charcoal", 1);
};
R_Date("Beta-14381", 1960, 90)
{
 Outlier("Charcoal", 1);
};
R_Date("I-13930", 1950, 80)
{
 Outlier("Charcoal", 1);
};
R_Date("Y-1235", 1920, 120)
{
 Outlier("Charcoal", 1);
};
R_Date("Beta-87611", 1920, 80)
{
 Outlier("Charcoal", 1);
```

```
};
R_Date("Beta-347456", 1910, 30);
R_Date("Y-1234", 1910, 100)
{
 Outlier("Charcoal", 1);
};
R_Date("I-11266", 1865, 80)
{
 Outlier("Charcoal", 1);
};
R_Date("Beta-9972", 1840, 50);
R_Date("Y-1233", 1830, 80)
{
 Outlier("Charcoal", 1);
};
R_Date("Beta-14993", 1810, 60)
{
 Outlier("Charcoal", 1);
};
R_Date("Beta-14997", 1810, 70)
{
 Outlier("Charcoal", 1);
};
```

```
R_Date("I-10914", 1780, 85)
{
 Outlier("Charcoal", 1);
};
R_Date("I-13922", 1780, 85)
{
 Outlier("Charcoal", 1);
};
R_Date("I-9680", 1775, 80)
{
 Outlier("Charcoal", 1);
};
R_Date("I-10916", 1720, 80)
{
 Outlier("Charcoal", 1);
};
R_Date("I-10921", 1705, 85)
{
 Outlier("Charcoal", 1);
};
R_Date("Beta-14992", 1660, 100)
{
 Outlier("Charcoal", 1);
```

```
};
R_Date("I-14361", 1650, 80)
{
 Outlier("Charcoal", 1);
};
R_Date("I-14431", 1650, 80)
{
 Outlier("Charcoal", 1);
};
Curve("IntCal13","IntCal13.14c");
Curve("Marine13","Marine13.14c");
Mix_Curve("Mixed","IntCal13","Marine13",50,12);
R_Date("Beta-222869", 1630, 40);
Curve("IntCal13","IntCal13.14c");
R_Date("I-14430", 1610, 80)
{
 Outlier("Charcoal", 1);
};
R_Date("I-14427", 1610, 80)
{
 Outlier("Charcoal", 1);
};
Curve("IntCal13","IntCal13.14c");
```

```
Curve("Marine13","Marine13.14c");
Mix_Curve("Mixed","IntCal13","Marine13",50,12);
R_Date("AA-6809", 1600, 55);
Curve("IntCal13","IntCal13.14c");
R_Date("I-14428", 1600, 150)
{
 Outlier("Charcoal", 1);
};
R_Date("I-14383", 1600, 80);
Curve("IntCal13","IntCal13.14c");
Curve("Marine13","Marine13.14c");
Mix_Curve("Mixed","IntCal13","Marine13",50,12);
R_Date("AA-75810", 1582, 46);
Curve("IntCal13","IntCal13.14c");
R_Date("Y-1232", 1580, 80)
{
 Outlier("Charcoal", 1);
};
R_Date("Beta-17637", 1580, 120)
{
 Outlier("Charcoal", 1);
};
R_Date("Beta-178670", 1580, 90)
```

```
{
 Outlier("Charcoal", 1);
};
Curve("IntCal13","IntCal13.14c");
Curve("Marine13","Marine13.14c");
Mix_Curve("Mixed","IntCal13","Marine13",50,12);
R_Date("AA-79415", 1566, 46);
Curve("IntCal13","IntCal13.14c");
R_Date("I-14362", 1560, 80)
{
 Outlier("Charcoal", 1);
};
Curve("IntCal13","IntCal13.14c");
Curve("Marine13","Marine13.14c");
Mix_Curve("Mixed","IntCal13","Marine13",50,12);
R_Date("AA-78513", 1557, 44);
Curve("IntCal13","IntCal13.14c");
R_Date("Beta-87610", 1550, 60)
{
 Outlier("Charcoal", 1);
};
R_Date("Beta-272032", 1550, 40)
{
```

```
 Outlier("Charcoal", 1);
};
R_Date("I-14429", 1550, 80)
{
 Outlier("Charcoal", 1);
};
R_Date("I-6595", 1545, 90)
{
 Outlier("Charcoal", 1);
};
Curve("IntCal13","IntCal13.14c");
Curve("Marine13","Marine13.14c");
Mix_Curve("Mixed","IntCal13","Marine13",50,12);
R_Date("AA-75128", 1539, 43);
Curve("IntCal13","IntCal13.14c");
R_Date("Beta-17631", 1530, 90)
{
 Outlier("Charcoal", 1);
};
R_Date("I-14382", 1530, 80)
{
 Outlier("Charcoal", 1);
};
```

```
Curve("IntCal13","IntCal13.14c");
Curve("Marine13","Marine13.14c");
Mix_Curve("Mixed","IntCal13","Marine13",50,12);
R_Date("AA-6805", 1525, 55);
Curve("IntCal13","IntCal13.14c");
R_Date("Beta-14994", 1520, 50)
{
 Outlier("Charcoal", 1);
};
R_Date("Beta-178681", 1520, 40)
{
 Outlier("Charcoal", 1);
};
Curve("IntCal13","IntCal13.14c");
Curve("Marine13","Marine13.14c");
Mix_Curve("Mixed","IntCal13","Marine13",50,12);
R_Date("AA-4100", 1515, 50);
Curve("IntCal13","IntCal13.14c");
R_Date("I-9677", 1515, 80)
{
 Outlier("Charcoal", 1);
};
Curve("IntCal13","IntCal13.14c");
```

```
Curve("Marine13","Marine13.14c");

Mix_Curve("Mixed","IntCal13","Marine13",50,12);

R_Date("AA-78495", 1505, 44);

Curve("IntCal13","IntCal13.14c");

R_Date("I-13932", 1500, 80)

{

 Outlier("Charcoal", 1);

};

Curve("IntCal13","IntCal13.14c");

Curve("Marine13","Marine13.14c");

Mix_Curve("Mixed","IntCal13","Marine13",50,12);

R_Date("AA-74638", 1493, 45);

Curve("IntCal13","IntCal13.14c");

R_Date("I-13923", 1490, 80)

{

 Outlier("Charcoal", 1);

};

R_Date("I-9108", 1480, 95)

{

 Outlier("Charcoal", 1);

};

R_Date("I-13924", 1480, 80)

{
```

```
 Outlier("Charcoal", 1);
};
R_Date("Beta-178674", 1470, 40)
{
 Outlier("Charcoal", 1);
};
Curve("IntCal13","IntCal13.14c");
Curve("Marine13","Marine13.14c");
Mix_Curve("Mixed","IntCal13","Marine13",50,12);
R_Date("AA-82397", 1469, 47);
Curve("IntCal13","IntCal13.14c");
R_Date("Beta-223566", 1460, 60)
{
 Outlier("Charcoal", 1);
};
R_Date("I-14360", 1460, 80)
{
 Outlier("Charcoal", 1);
};
R_Date("I-9873", 1460, 80)
{
 Outlier("Charcoal", 1);
};
```

```
Curve("IntCal13","IntCal13.14c");
Curve("Marine13","Marine13.14c");
Mix_Curve("Mixed","IntCal13","Marine13",50,12);
R_Date("AA-79371", 1456, 45);
R_Date("AA-75816", 1455, 46);
Curve("IntCal13","IntCal13.14c");
R_Date("Beta-178666", 1450, 40)
{
 Outlier("Charcoal", 1);
};
Curve("IntCal13","IntCal13.14c");
Curve("Marine13","Marine13.14c");
Mix_Curve("Mixed","IntCal13","Marine13",50,12);
R_Date("AA-72872", 1443, 50);
Curve("IntCal13","IntCal13.14c");
R_Date("UGM-30035", 1440, 30)
{
 Outlier("Charcoal", 1);
};
R_Date("Beta-17641", 1440, 70)
{
 Outlier("Charcoal", 1);
};
```

```
    R_Date("Beta-87601", 1440, 60)
    {
     Outlier("Charcoal", 1);
    };
    Curve("IntCal13","IntCal13.14c");
    Curve("Marine13","Marine13.14c");
    Mix_Curve("Mixed","IntCal13","Marine13",50,12);
    R_Date("AA-74637", 1434, 45);
    R_Date("AA-78492", 1434, 44);
   };
   Boundary("Puerto Rico End");
  };
 };
```

San Salvador

```
Plot()
 {
  Outlier_Model("Charcoal",Exp(1,-10,0),U(0,3),"t");
  Sequence("San Salvador")
  {
   Boundary("San Salvador Start");
   Phase()
   {
```

```
Curve("Marine13","Marine13.14c");
R_Date("UM-2275", 1384, 65);
Curve("IntCal13","IntCal13.14c");
R_Date("YSU #3", 1130, 40)
{
 Outlier("Charcoal", 1);
};
Curve("Marine13","Marine13.14c");
R_Date("UGa-00836", 1054, 37);
R_Date("AA-51432", 1028, 34);
Curve("IntCal13","IntCal13.14c");
R_Date("YSU #1", 840, 40)
{
 Outlier("Charcoal", 1);
};
R_Date("UM-2244", 660, 100)
{
 Outlier("Charcoal", 1);
};
R_Date("UM-2274", 620, 70)
{
 Outlier("Charcoal", 1);
};
```

```
R_Date("UM-2273", 580, 90)
{
 Outlier("Charcoal", 1);
};
R_Date("Beta-16732", 530, 65)
{
 Outlier("Charcoal", 1);
};
R_Date("YSU #4", 470, 60)
{
 Outlier("Charcoal", 1);
};
R_Date("Beta-105988", 450, 50)
{
 Outlier("Charcoal", 1);
};
R_Date("YSU #2", 350, 70)
{
 Outlier("Charcoal", 1);
};
R_Date("UM-2271", 305, 75)
{
 Outlier("Charcoal", 1);
```

```
    };
    Curve("Marine13","Marine13.14c");
    R_Date("UM-2245", 425, 75);
   };
   Boundary("San Salvador End");
  };
 };
```

St. John

```
Plot()
 {
  Outlier_Model("Charcoal",Exp(1,-10,0),U(0,3),"t");
  Sequence("St. John")
  {
   Boundary("St. John Start");
   Phase()
   {
    Curve("IntCal13","IntCal13.14c");
    R_Date("Beta-17080", 1630, 100)
    {
     Outlier("Charcoal", 1);
    };
    R_Date("Beta-32239", 1460, 80)
```

```
{
 Outlier("Charcoal", 1);
};
R_Date("Beta-16647", 1210, 80)
{
 Outlier("Charcoal", 1);
};
Curve("IntCal13","IntCal13.14c");
Curve("Marine13","Marine13.14c");
Mix_Curve("Mixed","IntCal13","Marine13",50,12);
R_Date("Beta-27793", 1170, 80);
Curve("IntCal13","IntCal13.14c");
R_Date("Beta-192223", 1160, 40)
{
 Outlier("Charcoal", 1);
};
R_Date("Beta-192224", 1140, 40)
{
 Outlier("Charcoal", 1);
};
R_Date("Beta-25891", 1130, 70)
{
 Outlier("Charcoal", 1);
```

```
};
R_Date("Beta-59781", 1120, 100)
{
 Outlier("Charcoal", 1);
};
R_Date("Beta-20605", 1050, 60)
{
 Outlier("Charcoal", 1);
};
R_Date("Beta-59780", 970, 80)
{
 Outlier("Charcoal", 1);
};
R_Date("Beta-18513", 970, 70)
{
 Outlier("Charcoal", 1);
};
R_Date("Beta-26964", 900, 100)
{
 Outlier("Charcoal", 1);
};
Curve("IntCal13","IntCal13.14c");
Curve("Marine13","Marine13.14c");
```

```
    Mix_Curve("Mixed","IntCal13","Marine13",50,12);
    R_Date("Beta-191882", 840, 40);
    Curve("IntCal13","IntCal13.14c");
    R_Date("Beta-19863", 660, 60)
    {
     Outlier("Charcoal", 1);
    };
   };
   Boundary("St. John End");
  };
 };
```

St. Lucia

```
Plot()
 {
  Outlier_Model("Charcoal",Exp(1,-10,0),U(0,3),"t");
  Sequence("St. Lucia")
  {
   Boundary("St. Lucia Start");
   Phase()
   {
```

```
Curve("IntCal13","IntCal13.14c");
R_Date("Y-1115", 1460, 80)
{
 Outlier("Charcoal", 1);
};
R_Date("Y-650", 1220, 100)
{
 Outlier("Charcoal", 1);
};
Curve("Marine13","Marine13.14c");
R_Date("RL-30", 1240, 100);
R_Date("RL-31", 1120, 100);
Curve("IntCal13","IntCal13.14c");
Curve("Marine13","Marine13.14c");
Mix_Curve("Mixed","IntCal13","Marine13",50,12);
R_Date("GrN-46607", 1000, 40);
R_Date("GrN-32330", 960, 35);
R_Date("GrN-32324", 920, 25);
R_Date("GrN-32326", 865, 35);
R_Date("GrN-32328", 820, 35);
R_Date("GrN-32325", 790, 35);
R_Date("GrN-32319", 770, 35);
R_Date("GrN-31944", 750, 30);
```

```
   R_Date("GrN-32327", 745, 30);
   R_Date("GrN-32314", 740, 30);
   R_Date("GrN-32317", 725, 35);
   R_Date("GrN-32315", 720, 35);
   Curve("IntCal13","IntCal13.14c");
   R_Date("GrN-46604", 645, 35)
   {
    Outlier("Charcoal", 1);
   };
   Curve("IntCal13","IntCal13.14c");
   Curve("Marine13","Marine13.14c");
   Mix_Curve("Mixed","IntCal13","Marine13",50,12);
   R_Date("GrN-32329", 620, 40);
  };
  Boundary("St. Lucia End");
 };
};
```

St. Martin

```
Plot()
 {
  Outlier_Model("Charcoal",Exp(1,-10,0),U(0,3),"t");
  Sequence("St. Martin")
```

```
{
 Boundary("St. Martin Start");
 Phase()
 {
  Curve("Marine13","Marine13.14c");
  R_Date("KIA-28815", 4830, 40);
  R_Date("KIA-28108", 4770, 40);
  R_Date("KIA-28116", 4505, 35);
  R_Date("KIA-28115", 4275, 30);
  R_Date("Erl-9066", 4200, 50);
  Curve("IntCal13","IntCal13.14c");
  R_Date("KIA-28121", 3828, 27)
  {
   Outlier("Charcoal", 1);
  };
  Curve("Marine13","Marine13.14c");
  R_Date("KIA-28114", 3800, 30);
  R_Date("KIA-28112", 3775, 30);
  R_Date("Erl-9071", 3750, 50);
  Curve("IntCal13","IntCal13.14c");
  R_Date("KIA-28123", 3684, 27)
  {
   Outlier("Charcoal", 1);
```

```
};
R_Date("KIA-28119", 3655, 25)
{
 Outlier("Charcoal", 1);
};
Curve("Marine13","Marine13.14c");
R_Date("Erl-9072", 3610, 50);
Curve("IntCal13","IntCal13.14c");
R_Date("KIA-28124", 3598, 29)
{
 Outlier("Charcoal", 1);
};
Curve("Marine13","Marine13.14c");
R_Date("Beta-41782", 3580, 90);
Curve("IntCal13","IntCal13.14c");
R_Date("Erl-9074", 3515, 45)
{
 Outlier("Charcoal", 1);
};
Curve("Marine13","Marine13.14c");
R_Date("Erl-9073", 3510, 50);
Curve("IntCal13","IntCal13.14c");
R_Date("Beta-190805", 3490, 40)
```

```
{
 Outlier("Charcoal", 1);
};
Curve("Marine13","Marine13.14c");
R_Date("Erl-9064", 3460, 50);
R_Date("Beta-187936", 3450, 40);
Curve("IntCal13","IntCal13.14c");
R_Date("KIA-28126", 3447, 26)
{
 Outlier("Charcoal", 1);
};
R_Date("KIA-28127", 3429, 35)
{
 Outlier("Charcoal", 1);
};
Curve("Marine13","Marine13.14c");
R_Date("KIA-28111", 3380, 40);
Curve("IntCal13","IntCal13.14c");
R_Date("KIA-28120", 3366, 27)
{
 Outlier("Charcoal", 1);
};
Curve("Marine13","Marine13.14c");
```

```
R_Date("Erl-9065", 3340, 50);
R_Date("KIA-28113", 3320, 30);
R_Date("Beta-224793", 3240, 60);
Curve("IntCal13","IntCal13.14c");
R_Date("KIA-28125", 3235, 26)
{
 Outlier("Charcoal", 1);
};
Curve("Marine13","Marine13.14c");
R_Date("KIA-28110", 3185, 30);
Curve("IntCal13","IntCal13.14c");
R_Date("Beta-187937", 3140, 40)
{
 Outlier("Charcoal", 1);
};
Curve("Marine13","Marine13.14c");
R_Date("KIA-28109", 3105, 30);
Curve("IntCal13","IntCal13.14c");
R_Date("KIA-28117", 3095, 23)
{
 Outlier("Charcoal", 1);
};
R_Date("KIA-28118", 2951, 52)
```

```
{
 Outlier("Charcoal", 1);
};
Curve("Marine13","Marine13.14c");
R_Date("Beta-146427", 2850, 60);
Curve("IntCal13","IntCal13.14c");
R_Date("Beta-224792", 2610, 40)
{
 Outlier("Charcoal", 1);
};
R_Date("PITT-0450", 2510, 40)
{
 Outlier("Charcoal", 1);
};
R_Date("Beta-145372", 2420, 40)
{
 Outlier("Charcoal", 1);
};
R_Date("PITT-0449", 2300, 55)
{
 Outlier("Charcoal", 1);
};
R_Date("PITT-0219", 2275, 60)
```

```
{
 Outlier("Charcoal", 1);
};
R_Date("Beta-146425", 2270, 40)
{
 Outlier("Charcoal", 1);
};
R_Date("PITT-0220", 2250, 45)
{
 Outlier("Charcoal", 1);
};
R_Date("PITT-0446", 2250, 45)
{
 Outlier("Charcoal", 1);
};
Curve("IntCal13","IntCal13.14c");
Curve("Marine13","Marine13.14c");
Mix_Curve("Mixed","IntCal13","Marine13",50,12);
R_Date("Erl-8235", 2070, 50);
Curve("IntCal13","IntCal13.14c");
R_Date("PITT-0448", 2050, 45)
{
 Outlier("Charcoal", 1);
```

```
};
R_Date("Beta-146424", 2020, 40)
{
 Outlier("Charcoal", 1);
};
R_Date("Beta-106230", 1960, 60)
{
 Outlier("Charcoal", 1);
};
R_Date("Beta-82159", 1910, 50)
{
 Outlier("Charcoal", 1);
};
Curve("Marine13","Marine13.14c");
R_Date("KIA-32785", 1900, 25);
Curve("IntCal13","IntCal13.14c");
R_Date("Beta-82156", 1870, 60)
{
 Outlier("Charcoal", 1);
};
Curve("Marine13","Marine13.14c");
R_Date("Beta-187941", 1810, 40);
Curve("IntCal13","IntCal13.14c");
```

```
R_Date("Beta-82158", 1800, 50)
{
 Outlier("Charcoal", 1);
};
R_Date("Beta-82157", 1800, 60)
{
 Outlier("Charcoal", 1);
};
R_Date("Beta-106228", 1770, 50)
{
 Outlier("Charcoal", 1);
};
R_Date("LGQ-1099", 1760, 160)
{
 Outlier("Charcoal", 1);
};
R_Date("Beta-82160", 1760, 50)
{
 Outlier("Charcoal", 1);
};
R_Date("Beta-82154", 1710, 60)
{
 Outlier("Charcoal", 1);
```

```
};
R_Date("Beta-106233", 1710, 70)
{
 Outlier("Charcoal", 1);
};
R_Date("Beta-106229", 1670, 50)
{
 Outlier("Charcoal", 1);
};
R_Date("PITT-0452", 1660, 55)
{
 Outlier("Charcoal", 1);
};
R_Date("Beta-106232", 1650, 70)
{
 Outlier("Charcoal", 1);
};
R_Date("LGQ-1098", 1610, 150)
{
 Outlier("Charcoal", 1);
};
R_Date("Beta-82153", 1590, 70)
{
```

```
 Outlier("Charcoal", 1);
};
Curve("Marine13","Marine13.14c");
R_Date("KIA-28963", 1585, 25);
Curve("IntCal13","IntCal13.14c");
R_Date("Beta-187940", 1560, 40)
{
 Outlier("Charcoal", 1);
};
R_Date("Beta-106231", 1560, 60)
{
 Outlier("Charcoal", 1);
};
R_Date("Beta-82155", 1540, 50)
{
 Outlier("Charcoal", 1);
};
Curve("Marine13","Marine13.14c");
R_Date("Beta-187938", 1540, 40);
Curve("IntCal13","IntCal13.14c");
R_Date("GrN-20170", 1535, 30);
R_Date("GrN-20168", 1530, 30);
R_Date("GrN-20169", 1520, 35);
```

```
R_Date("KIA-28122", 1494, 26)
{
 Outlier("Charcoal", 1);
};
R_Date("PITT-0445", 1490, 35)
{
 Outlier("Charcoal", 1);
};
Curve("Marine13","Marine13.14c");
R_Date("Beta-200098", 1330, 60);
Curve("IntCal13","IntCal13.14c");
R_Date("Ly-9163", 1230, 30)
{
 Outlier("Charcoal", 1);
};
R_Date("GrN-20161", 1225, 30);
R_Date("GrN-20160", 1180, 30);
R_Date("GrN-20162", 1170, 30);
Curve("Marine13","Marine13.14c");
R_Date("GrN- 20164", 1170, 30);
Curve("IntCal13","IntCal13.14c");
R_Date("Beta-82165", 1000, 50);
Curve("IntCal13","IntCal13.14c");
```

```
    Curve("Marine13","Marine13.14c");
    Mix_Curve("Mixed","IntCal13","Marine13",50,12);
    R_Date("Ly-2019(OxA)", 895, 30);
    Curve("IntCal13","IntCal13.14c");
    R_Date("Ly-11437", 890, 30)
    {
     Outlier("Charcoal", 1);
    };
    R_Date("Ly-11435", 890, 30)
    {
     Outlier("Charcoal", 1);
    };
   };
   Boundary("St. Martin End");
  };
 };
```

St. Thomas

```
Plot()
 {
  Outlier_Model("Charcoal",Exp(1,-10,0),U(0,3),"t");
  Sequence("St. Thomas")
  {
```

```
Boundary("St. Thomas End");
Phase()
{
 Curve("Marine13","Marine13.14c");
 R_Date("I-8640", 2830, 85);
 R_Date("Beta-7022", 2860, 70);
 Curve("IntCal13","IntCal13.14c");
 R_Date("Beta-111459", 2710, 120)
 {
  Outlier("Charcoal", 1);
 };
 R_Date("I-8641", 2775, 85)
 {
  Outlier("Charcoal", 1);
 };
 Curve("Marine13","Marine13.14c");
 R_Date("SI-5851", 2700, 65);
 R_Date("L-1380B", 2410, 60);
 R_Date("I-621", 2400, 175);
 R_Date("I-620", 2175, 160);
 R_Date("SI-5850", 2130, 60);
 Curve("IntCal13","IntCal13.14c");
 R_Date("Beta-108917", 2090, 50)
```

```
{
 Outlier("Charcoal", 1);
};
R_Date("Beta-111462", 1980, 50)
{
 Outlier("Charcoal", 1);
};
Curve("Marine13","Marine13.14c");
R_Date("L-1380A", 1900, 70);
R_Date("SI-5848", 1805, 75);
Curve("IntCal13","IntCal13.14c");
R_Date("Beta-65474", 1800, 80)
{
 Outlier("Charcoal", 1);
};
R_Date("GX-12845", 1770, 235)
{
 Outlier("Charcoal", 1);
};
R_Date("Beta-108888", 1720, 140)
{
 Outlier("Charcoal", 1);
};
```

```
R_Date("Beta-50066", 1610, 70)
{
 Outlier("Charcoal", 1);
};
Curve("Marine13","Marine13.14c");
R_Date("SI-5849", 1595, 75);
Curve("IntCal13","IntCal13.14c");
R_Date("Beta-65472", 1580, 50)
{
 Outlier("Charcoal", 1);
};
R_Date("Beta-65473", 1570, 60)
{
 Outlier("Charcoal", 1);
};
R_Date("Beta-54646", 1560, 90)
{
 Outlier("Charcoal", 1);
};
R_Date("CAMS-10696", 1550, 50)
{
 Outlier("Charcoal", 1);
};
```

```
R_Date("Beta-108889", 1500, 50)
{
 Outlier("Charcoal", 1);
};
R_Date("Beta-62568", 1430, 90)
{
 Outlier("Charcoal", 1);
};
R_Date("Beta-62569", 1400, 120)
{
 Outlier("Charcoal", 1);
};
Curve("IntCal13","IntCal13.14c");
Curve("Marine13","Marine13.14c");
Mix_Curve("Mixed","IntCal13","Marine13",50,12);
R_Date("Beta-88345", 1390, 40);
R_Date("Beta-83011", 1390, 40);
R_Date("Beta-83003", 1390, 30);
Curve("IntCal13","IntCal13.14c");
R_Date("Beta-62570", 1380, 90)
{
 Outlier("Charcoal", 1);
};
```

```
Curve("IntCal13","IntCal13.14c");
Curve("Marine13","Marine13.14c");
Mix_Curve("Mixed","IntCal13","Marine13",50,12);
R_Date("Beta-83000", 1330, 30);
R_Date("Beta-83001", 1330, 30);
Curve("IntCal13","IntCal13.14c");
R_Date("Beta-65469", 1310, 60)
{
 Outlier("Charcoal", 1);
};
Curve("IntCal13","IntCal13.14c");
Curve("Marine13","Marine13.14c");
Mix_Curve("Mixed","IntCal13","Marine13",50,12);
R_Date("Beta-83009", 1300, 30);
R_Date("Beta-83006", 1280, 40);
R_Date("Beta-73392", 1190, 60);
R_Date("Beta-83010", 1090, 30);
Curve("IntCal13","IntCal13.14c");
R_Date("Beta-49751", 1040, 150)
{
 Outlier("Charcoal", 1);
};
R_Date("Beta-48742", 810, 140)
```

```
{
 Outlier("Charcoal", 1);
};
R_Date("Beta-43437", 810, 70)
{
 Outlier("Charcoal", 1);
};
R_Date("Beta-42277", 730, 80)
{
 Outlier("Charcoal", 1);
};
R_Date("Beta-51355", 720, 120)
{
 Outlier("Charcoal", 1);
};
R_Date("Beta-111461", 650, 50)
{
 Outlier("Charcoal", 1);
};
Curve("IntCal13","IntCal13.14c");
Curve("Marine13","Marine13.14c");
Mix_Curve("Mixed","IntCal13","Marine13",50,12);
R_Date("Beta-73390", 640, 60);
```

```
R_Date("Beta-73394", 630, 60);

R_Date("Beta-73393", 600, 60);

R_Date("Beta-83005", 600, 30);

R_Date("Beta-73395", 590, 90);

R_Date("Beta-73391", 580, 60);

Curve("IntCal13","IntCal13.14c");

R_Date("Beta-51354", 560, 120)

{

 Outlier("Charcoal", 1);

};

Curve("IntCal13","IntCal13.14c");

Curve("Marine13","Marine13.14c");

Mix_Curve("Mixed","IntCal13","Marine13",50,12);

R_Date("Beta-88347", 560, 40);

Curve("IntCal13","IntCal13.14c");

R_Date("Beta-111452", 560, 80)

{

 Outlier("Charcoal", 1);

};

Curve("IntCal13","IntCal13.14c");

Curve("Marine13","Marine13.14c");

Mix_Curve("Mixed","IntCal13","Marine13",50,12);

R_Date("Beta-83008", 540, 30);
```

```
   R_Date("Beta-83004", 500, 30);
   R_Date("Beta-109071", 480, 50);
   R_Date("Beta-88348", 470, 40);
   R_Date("Beta-88349", 460, 40);
   R_Date("Beta-109070", 450, 50);
   R_Date("Beta-88346", 390, 40);
   R_Date("Beta-109072", 380, 50);
   R_Date("Beta-83007", 340, 30);
   R_Date("Beta-88344", 300, 40);
  };
  Boundary("St. Thomas End");
 };
};
```

Tobago

```
Plot()
 {
  Outlier_Model("Charcoal",Exp(1,-10,0),U(0,3),"t");
  Sequence("Tobago")
  {
   Boundary("Tobago Start");
   Phase()
   {
```

```
Curve("IntCal13","IntCal13.14c");
R_Date("Beta-15351", 2700, 40)
R_Date("Beta-15936", 1750, 40)
R_Date("Beta-172211", 1700, 40)
R_Date("Y-1336", 1300, 120)
{
 Outlier("Charcaol", 1);
};
R_Date("Beta-172209", 1180, 40)
{
 Outlier("Charcaol", 1);
};
R_Date("Beta-153150", 1170, 40)
{
 Outlier("Charcaol", 1);
};
R_Date("Beta-172210", 1110, 40)
{
 Outlier("Charcaol", 1);
};
R_Date("Beta-153149", 900, 40)
{
 Outlier("Charcaol", 1);
```

```
};
Curve("IntCal13","IntCal13.14c");
Curve("Marine13","Marine13.14c");
Mix_Curve("Mixed","IntCal13","Marine13",50,12);
R_Date("Beta-221321", 850, 40);
R_Date("Beta-221319", 810, 40);
R_Date("Beta-221320", 810, 40);
Curve("IntCal13","IntCal13.14c");
R_Date("Beta-4905", 760, 105)
{
 Outlier("Charcaol", 1);
};
R_Date("Beta-129265", 600, 50)
{
 Outlier("Charcaol", 1);
};
R_Date("Beta-129262", 590, 40)
{
 Outlier("Charcaol", 1);
};
R_Date("Beta-129264", 550, 40)
{
 Outlier("Charcaol", 1);
```

```
    };
   };
   Boundary("Tobago End");
  };
 };
```

Trinidad

```
Plot()
 {
  Outlier_Model("Charcoal",Exp(1,-10,0),U(0,3),"t");
  Sequence("Trinidad")
  {
   Boundary("Trinidad Start");
   Phase()
   {
    Curve("IntCal13","IntCal13.14c");
    R_Date("IVIC-888", 7180, 80)
    {
     Outlier("charcoal", 1);
    };
    R_Date("UGa-14460", 7030, 25)
    {
     Outlier("charcoal", 1);
```

```
};
R_Date("UGa-12303", 6890, 30)
{
 Outlier("charcoal", 1);
};
R_Date("IVIC-889", 6780, 70)
{
 Outlier("charcoal", 1);
};
R_Date("UGa-14459", 6370, 25)
{
 Outlier("charcoal", 1);
};
R_Date("IVIC-891", 6190, 100)
{
 Outlier("charcoal", 1);
};
R_Date("IVIC-887", 6170, 90)
{
 Outlier("charcoal", 1);
};
R_Date("UGa-14458", 6100, 25)
{
```

```
 Outlier("charcoal", 1);
};
R_Date("IVIC-890", 6100, 90)
{
 Outlier("charcoal", 1);
};
R_Date("IVIC-783", 5650, 100)
{
 Outlier("charcoal", 1);
};
R_Date("UGa-14457", 5300, 25);
R_Date("Y-260-1", 2750, 130)
{
 Outlier("charcoal", 1);
};
R_Date("IVIC-642", 2140, 70)
{
 Outlier("charcoal", 1);
};
R_Date("IVIC-638", 2130, 80)
{
 Outlier("charcoal", 1);
};
```

```
R_Date("I-6444", 2120, 135)
{
 Outlier("charcoal", 1);
};
R_Date("IVIC-641", 2060, 70)
{
 Outlier("charcoal", 1);
};
R_Date("IVIC-640", 1990, 70)
{
 Outlier("charcoal", 1);
};
R_Date("Beta-196708", 1920, 40)
{
 Outlier("charcoal", 1);
};
R_Date("Beta-196709", 1880, 40)
{
 Outlier("charcoal", 1);
};
R_Date("IVIC-643", 1850, 80)
{
 Outlier("charcoal", 1);
```

```
};
R_Date("Beta-4902", 1805, 90)
{
 Outlier("charcoal", 1);
};
R_Date("Beta-4899", 1755, 150)
{
 Outlier("charcoal", 1);
};
R_Date("Beta-134571", 1720, 50)
{
 Outlier("charcoal", 1);
};
R_Date("IVIC-786", 1720, 90)
{
 Outlier("charcoal", 1);
};
R_Date("Beta-4903", 1680, 115)
{
 Outlier("charcoal", 1);
};
R_Date("Beta-196706", 1650, 40)
{
```

```
 Outlier("charcoal", 1);
};
R_Date("GrA-13865", 1590, 40)
{
 Outlier("charcoal", 1);
};
R_Date("Beta-189113", 1570, 40)
{
 Outlier("charcoal", 1);
};
R_Date("OxA-19174", 1538, 29)
{
 Outlier("charcoal", 1);
};
R_Date("Beta-296724", 1490, 30)
{
 Outlier("charcoal", 1);
};
R_Date("IVIC-639", 1480, 70)
{
 Outlier("charcoal", 1);
};
R_Date("Beta-296723", 1400, 30)
```

```
{
 Outlier("charcoal", 1);
};
R_Date("Beta-4904", 1350, 85)
{
 Outlier("charcoal", 1);
};
R_Date("Beta-4901", 1300, 110)
{
 Outlier("charcoal", 1);
};
R_Date("IVIC-785", 1260, 100)
{
 Outlier("charcoal", 1);
};
R_Date("GrA-13867", 1220, 40)
{
 Outlier("charcoal", 1);
};
R_Date("Beta-296726", 1210, 30)
{
 Outlier("charcoal", 1);
};
```

```
R_Date("ISGS-A2628", 1210, 15)
{
 Outlier("charcoal", 1);
};
R_Date("Beta-4900", 1145, 65)
{
 Outlier("charcoal", 1);
};
R_Date("Beta-6807", 1130, 50)
{
 Outlier("charcoal", 1);
};
R_Date("Beta-4898", 1040, 260)
{
 Outlier("charcoal", 1);
};
Curve("Marine13","Marine13.14c");
R_Date("Beta-6809", 990, 50);
Curve("IntCal13","IntCal13.14c");
R_Date("Beta-196707", 740, 40)
{
 Outlier("charcoal", 1);
};
```

```
    R_Date("Beta-6808", 650, 50)
    {
     Outlier("charcoal", 1);
    };
    Curve("IntCal13","IntCal13.14c");
    Curve("Marine13","Marine13.14c");
    Mix_Curve("Mixed","IntCal13","Marine13",50,12);
    R_Date("Beta-193442", 630, 40);
    R_Date("Beta-193443", 620, 40);
   };
   Boundary("Trinidad End");
  };
 };
```

Vieques

```
Plot()
 {
  Outlier_Model("Charcoal",Exp(1,-10,0),U(0,2),"t");
  Sequence("Vieques")
  {
   Boundary("Vieques Start");
   Phase()
   {
```

```
Curve("Marine13","Marine13.14c");
R_Date("I-18971", 4095, 80);
R_Date("I-16406", 3850, 100);
R_Date("I-16899", 3780, 100);
R_Date("I-16397", 3530, 100);
R_Date("I-16396", 3510, 100);
R_Date("I-16897", 3470, 100);
R_Date("I-16395", 2790, 100);
R_Date("I-16898", 2770, 90);
R_Date("I-16407", 2740, 100);
R_Date("I-16896", 2650, 90);
Curve("IntCal13","IntCal13.14c");
R_Date("I-16153", 2590, 90)
{
 Outlier("Charcoal", 1);
};
Curve("Marine13","Marine13.14c");
R_Date("Beta-276588", 2240, 40);
Curve("IntCal13","IntCal13.14c");
R_Date("I-13425", 2110, 80)
{
 Outlier("Charcoal", 1);
};
```

```
R_Date("I-11322", 1945, 80)
{
 Outlier("Charcoal", 1);
};
R_Date("I-11319", 1915, 80)
{
 Outlier("Charcoal", 1);
};
R_Date("I-12859", 1880, 80)
{
 Outlier("Charcoal", 1);
};
R_Date("I-11321", 1845, 80)
{
 Outlier("Charcoal", 1);
};
Curve("Marine13","Marine13.14c");
R_Date("Beta-259410", 1840, 50);
Curve("IntCal13","IntCal13.14c");
R_Date("I-10979", 1820, 85)
{
 Outlier("Charcoal", 1);
};
```

```
R_Date("I-12858", 1820, 80)
{
 Outlier("Charcoal", 1);
};
R_Date("I-12856", 1810, 80)
{
 Outlier("Charcoal", 1);
};
R_Date("Beta-129948", 1810, 60)
{
 Outlier("Charcoal", 1);
};
R_Date("I-11139", 1800, 80)
{
 Outlier("Charcoal", 1);
};
R_Date("I-12860", 1780, 80)
{
 Outlier("Charcoal", 1);
};
R_Date("I-11320", 1770, 80)
{
 Outlier("Charcoal", 1);
```

```
};
R_Date("I-11685", 1740, 75)
{
 Outlier("Charcoal", 1);
};
R_Date("I-10980", 1735, 85)
{
 Outlier("Charcoal", 1);
};
R_Date("I-11140", 1730, 80)
{
 Outlier("Charcoal", 1);
};
R_Date("I-11926", 1720, 80)
{
 Outlier("Charcoal", 1);
};
R_Date("I-11141", 1705, 80)
{
 Outlier("Charcoal", 1);
};
R_Date("I-16151", 1700, 80)
{
```

```
 Outlier("Charcoal", 1);
};
R_Date("I-11925", 1665, 80)
{
 Outlier("Charcoal", 1);
};
R_Date("I-16152", 1650, 80)
{
 Outlier("Charcoal", 1);
};
R_Date("I-12744", 1640, 80)
{
 Outlier("Charcoal", 1);
};
R_Date("I-16154", 1620, 80)
{
 Outlier("Charcoal", 1);
};
R_Date("I-11317", 1615, 75)
{
 Outlier("Charcoal", 1);
};
R_Date("I-12746", 1600, 80)
```

```
{
 Outlier("Charcoal", 1);
};
R_Date("I-16174", 1600, 80)
{
 Outlier("Charcoal", 1);
};
R_Date("I-16173", 1590, 80)
{
 Outlier("Charcoal", 1);
};
R_Date("I-12857", 1580, 80)
{
 Outlier("Charcoal", 1);
};
R_Date("I-11686", 1575, 80)
{
 Outlier("Charcoal", 1);
};
R_Date("I-10547", 1575, 85)
{
 Outlier("Charcoal", 1);
};
```

```
R_Date("I-11687", 1565, 75)
{
 Outlier("Charcoal", 1);
};
R_Date("I-11927", 1565, 80)
{
 Outlier("Charcoal", 1);
};
R_Date("I-12745", 1560, 80)
{
 Outlier("Charcoal", 1);
};
R_Date("I-11316", 1555, 75)
{
 Outlier("Charcoal", 1);
};
Curve("Marine13","Marine13.14c");
R_Date("I-10549", 1525, 85);
Curve("IntCal13","IntCal13.14c");
R_Date("I-10550", 1505, 85)
{
 Outlier("Charcoal", 1);
};
```

```
R_Date("I-11318", 1490, 75)
{
 Outlier("Charcoal", 1);
};
R_Date("I-16175", 1450, 80)
{
 Outlier("Charcoal", 1);
};
R_Date("I-10548", 1440, 85)
{
 Outlier("Charcoal", 1);
};
R_Date("I-16176", 1270, 90)
{
 Outlier("Charcoal", 1);
};
R_Date("I-14813", 1180, 80)
{
 Outlier("Charcoal", 1);
};
R_Date("I-12743", 950, 80)
{
 Outlier("Charcoal", 1);
```

```
};
R_Date("I-12742", 900, 80);
R_Date("I-11189", 790, 85)
{
 Outlier("Charcoal", 1);
};
R_Date("I-15189", 790, 80)
{
 Outlier("Charcoal", 1);
};
R_Date("I- 15188", 700, 80)
{
 Outlier("Charcoal", 1);
};
R_Date("I-15188", 700, 70)
{
 Outlier("Charcoal", 1);
};
R_Date("I-15187", 690, 80)
{
 Outlier("Charcoal", 1);
};
R_Date("I-15239", 660, 80)
```

```
{
 Outlier("Charcoal", 1);
};
R_Date("I-15240", 630, 80)
{
 Outlier("Charcoal", 1);
};
R_Date("I-15238", 570, 80)
{
 Outlier("Charcoal", 1);
};
R_Date("I-15185", 540, 80)
{
 Outlier("Charcoal", 1);
};
R_Date("I-15186", 520, 80)
{
 Outlier("Charcoal", 1);
};
R_Date("I-15658", 470, 80)
{
 Outlier("Charcoal", 1);
};
```

```
   R_Date("I-15657", 410, 80)
   {
    Outlier("Charcoal", 1);
   };
   R_Date("I-11142", 405, 75)
   {
    Outlier("Charcoal", 1);
   };
  };
  Boundary("Vieques End");
 };
};
```

Single Phase Model SQL Code

Anguilla

```
Plot()
 {
  Sequence("Anguilla")
  {
   Boundary("Anguilla Start");
   Phase()
   {
```

```
Curve("IntCal13","IntCal13.14c");
R_Date("Beta-19957", 1550, 70);
R_Date("Beta-15824", 1530, 140);
R_Date("Beta-18740", 1430, 70);
R_Date("Beta-21858", 1410, 60);
R_Date("Beta-110397", 1310, 80);
R_Date("Beta-19956", 1290, 60);
R_Date("Beta-110396", 1290, 60);
R_Date("Beta-106439", 1270, 60);
R_Date("Beta-110394", 1230, 70);
Curve("Marine13","Marine13.14c");
R_Date("Beta-15485", 1220, 70);
R_Date("Beta-106444", 1180, 60);
R_Date("Beta-106443", 1180, 60);
Curve("IntCal13","IntCal13.14c");
R_Date("PITT-0546", 1180, 45);
R_Date("Beta-110395", 1170, 80);
R_Date("Beta-19955", 1150, 60);
R_Date("Beta-110393", 1140, 60);
R_Date("PITT-0545", 1135, 40);
Curve("Marine13","Marine13.14c");
R_Date("Beta-15486", 1130, 80);
Curve("IntCal13","IntCal13.14c");
```

```
R_Date("Beta-106442", 1120, 70);
R_Date("Beta-18738", 1120, 70);
R_Date("PITT-0547", 1085, 55);
R_Date("Beta-21861", 1080, 90);
R_Date("Beta-18739", 1000, 110);
R_Date("Beta-120152", 950, 70);
R_Date("Beta-21863", 940, 80);
Curve("Marine13","Marine13.14c");
R_Date("Beta-257181", 910, 40);
R_Date("Beta-257182", 890, 40);
Curve("IntCal13","IntCal13.14c");
R_Date("Beta-21862", 880, 90);
R_Date("Beta-120157", 880, 80);
Curve("Marine13","Marine13.14c");
R_Date("Beta-257184", 860, 40);
Curve("IntCal13","IntCal13.14c");
R_Date("Beta-120154", 850, 60);
R_Date("Beta-106441", 840, 80);
Curve("Marine13","Marine13.14c");
R_Date("Beta-257185", 780, 40);
Curve("IntCal13","IntCal13.14c");
R_Date("Beta-110398", 780, 80);
Curve("Marine13","Marine13.14c");
```

```
  R_Date("Beta-141202", 740, 60);
  Curve("IntCal13","IntCal13.14c");
  R_Date("Beta-120153", 740, 60);
  R_Date("Beta-120156", 710, 80);
  Curve("Marine13","Marine13.14c");
  R_Date("Beta-257183", 680, 40);
  Curve("IntCal13","IntCal13.14c");
  R_Date("Beta-106440", 510, 80);
  R_Date("Beta-120155", 440, 70);
  Curve("Marine13","Marine13.14c");
  R_Date("Beta-60776", 400, 60);
 };
 Boundary("Anguilla End");
};
};
```

Antigua

```
Plot()
 {
  Sequence("Antigua")
  {
   Boundary("Antigua Start");
   Phase()
```

```
{
 Curve("IntCal13","IntCal13.14c");
 R_Date("I-7830", 2785, 80);
 R_Date("I-7842", 2785, 80);
 R_Date("I-7980", 1915, 80);
 R_Date("I-7981", 1855, 80);
 R_Date("I-7979", 1790, 85);
 R_Date("I-7855", 1765, 80);
 R_Date("I-7838", 1750, 80);
 R_Date("I-7837", 1715, 80);
 R_Date("I-7854", 1670, 80);
 R_Date("Beta- 124127", 1610, 80);
 R_Date("Beta-124126", 1600, 50);
 R_Date("I-7355", 1505, 85);
 R_Date("I-7356", 1505, 85);
 R_Date("I-7352", 1440, 85);
 R_Date("Beta-101500", 1430, 50);
 R_Date("I-7353", 1230, 85);
 R_Date("SUERC-34163", 950, 30);
 R_Date("Beta-101499", 720, 50);
};
Boundary("Antigua End");
};
```

```
};
```

Aruba

```
Plot()
{
 Sequence("Aruba")
 {
  Boundary("Aruba Start");
  Phase()
  {
   Curve("IntCal13","IntCal13.14c");
   R_Date("GrN-7341", 3300, 35);
   Curve("IntCal13","IntCal13.14c");
   Curve("Marine13","Marine13.14c");
   Mix_Curve("Mixed","IntCal13","Marine13",50,12);
   R_Date("Ua-1501", 2210, 95);
   R_Date("Ua-1341", 1740, 110);
   R_Date("Ua-1342", 1520, 100);
   R_Date("Ua-1340", 1520, 110);
   R_Date("Ua-1514", 1420, 150);
   Curve("IntCal13","IntCal13.14c");
   R_Date("GrN-2788", 1080, 50);
   R_Date("GrN-7339", 1040, 45);
```

```
 R_Date("GrN-21665", 1030, 40);
 R_Date("GrN-21666", 1030, 30);
 R_Date("GrN-7340", 1000, 30);
 R_Date("GrN-7342", 990, 30);
 R_Date("GrA-2789", 990, 50);
 R_Date("GrN-7338", 940, 25);
 R_Date("GrN-21656", 910, 30);
 Curve("IntCal13","IntCal13.14c");
 Curve("Marine13","Marine13.14c");
 Mix_Curve("Mixed","IntCal13","Marine13",50,12);
 R_Date("GrN-17460", 910, 170);
 R_Date("GrN-17459", 870, 80);
 Curve("IntCal13","IntCal13.14c");
 R_Date("GrN-21664", 860, 40);
 R_Date("GrA-2785", 860, 50);
 R_Date("GrA-2778", 830, 50);
 R_Date("GrN-16915", 825, 30);
 R_Date("I-4025", 765, 110);
 R_Date("GrA-2784", 750, 50);
 R_Date("I-4026", 740, 105);
 R_Date("GrA-2790", 340, 50);
};
Boundary("Aruba End");
```

```
 };
};
```

Barbados

```
Plot()
 {
  Sequence("Barbados")
  {
   Boundary("Barbados Start");
   Phase()
   {
    Curve("Marine13","Marine13.14c");
    R_Date("D-AMS 001792", 4366, 32);
    R_Date("Beta-297522", 4360, 40);
    R_Date("D-AMS 001793", 4278, 29);
    R_Date("Beta-297521", 4230, 50);
    R_Date("D-AMS 001794", 4091, 27);
    R_Date("I-16840", 3980, 100);
    Curve("IntCal13","IntCal13.14c");
    R_Date("Beta-20723", 1950, 150);
    R_Date("I-2486", 1570, 95);
    Curve("Marine13","Marine13.14c");
    R_Date("1-16189", 1120, 80);
```

```
  };
  Boundary("Barbados End");
 };
};
```

Barbuda

```
Plot()
 {
  Sequence("Barbuda")
  {
   Boundary("Barbuda Start");
   Phase()
   {
    Curve("Marine13","Marine13.14c");
    R_Date("UCI-107938", 3430, 15);
    R_Date("SUERC-33604 (GU-23530)", 3280, 35);
    R_Date("SUERC 33605 (GU-23531)", 2790, 35);
    R_Date("UCI-107937", 2565, 20);
    R_Date("Beta-103891", 2030, 60);
    Curve("IntCal13","IntCal13.14c");
    R_Date("SUERC 18562", 2025, 35);
    R_Date("SUERC 18560", 2005, 35);
    R_Date("SUERC 18561", 1920, 35);
```

```
  R_Date("SUERC 18558", 1785, 35);
  R_Date("SUERC 18557", 1755, 35);
  R_Date("SUERC 34971", 1565, 35);
  Curve("Marine13","Marine13.14c");
  R_Date("Beta-103894", 1400, 60);
  R_Date("PITT-1234", 1365, 45);
  R_Date("Beta-103892", 1360, 60);
  R_Date("Beta-103893", 1350, 60);
  R_Date("Beta-103890", 1210, 60);
  R_Date("PITT-1233", 1135, 50);
  R_Date("PITT-1231", 1050, 30);
  Curve("IntCal13","IntCal13.14c");
  R_Date("SUERC 18556", 820, 35);
 };
 Boundary("Barbuda End");
};
};
```

Bonaire

```
Plot()
{
 Sequence("Bonaire")
 {
```

```
Boundary("Bonaire Start");
Phase()
{
 Curve("Marine13","Marine13.14c");
 R_Date("GrN-32756", 3610, 25);
 R_Date("GrN-32758", 3410, 20);
 R_Date("GrN-32751", 3245, 25);
 R_Date("GrN-32750", 3095, 20);
 R_Date("GrN-32749", 2785, 20);
 R_Date("GrN-32755", 2735, 25);
 R_Date("GrN-32752", 2705, 30);
 R_Date("GrN-32757", 2680, 25);
 R_Date("GrN-32754", 2665, 20);
 R_Date("GrN-32753", 2575, 20);
 R_Date("GrN-32748", 2412, 15);
 Curve("IntCal13","IntCal13.14c");
 R_Date("PITT-0267", 1480, 25);
 R_Date("PITT-0268", 885, 45);
 R_Date("PITT-0265", 710, 65);
 R_Date("PITT-0264", 560, 40);
 R_Date("PITT-0266", 505, 35);
};
Boundary("Bonaire End");
```

```
  };
 };
```

Carriacou

```
Plot()
 {
  Sequence("Carriacou")
  {
   Boundary("Carriacou Start");
   Phase()
   {
    Curve("Marine13","Marine13.14c");
    R_Date("AA-62278", 1917, 37);
    R_Date("Beta-206685", 1870, 70);
    R_Date("AA-62280b", 1822, 41);
    R_Date("AA-62280a", 1789, 38);
    Curve("IntCal13","IntCal13.14c");
    R_Date("AA-67535", 1588, 36);
    R_Date("AA-67536", 1584, 36);
    Curve("Marine13","Marine13.14c");
    R_Date("GX-30424", 1570, 60);
    Curve("IntCal13","IntCal13.14c");
    Curve("Marine13","Marine13.14c");
```

```
Mix_Curve("Mixed","IntCal13","Marine13",50,12);

R_Date("UCIAMS-111935", 1565, 15);

Curve("Marine13","Marine13.14c");

R_Date("GX-30425", 1460, 60);

R_Date("GX-30423", 1400, 60);

Curve("IntCal13","IntCal13.14c");

R_Date("AA-62281", 1339, 36);

R_Date("AA-67534", 1333, 57);

R_Date("D-AMS 016647", 1328, 20);

R_Date("D-AMS 16649", 1321, 20);

R_Date("D-AMS 016648", 1315, 20);

Curve("Marine13","Marine13.14c");

R_Date("Beta-233647", 1310, 40);

R_Date("UCIAMS-94046", 1265, 20);

Curve("IntCal13","IntCal13.14c");

R_Date("AA-62279", 1243, 36);

R_Date("AA-62282", 1227, 36);

R_Date("OS-71467", 1220, 20);

R_Date("AA-67533", 1172, 36);

R_Date("AA-81055", 1158, 45);

R_Date("OS-71463", 1140, 15);

R_Date("AA-67531", 1133, 38);

R_Date("OS-71464", 1100, 20);
```

```
R_Date("OS-71465", 1080, 15);
R_Date("AA-67532", 1073, 38);
Curve("IntCal13","IntCal13.14c");
Curve("Marine13","Marine13.14c");
Mix_Curve("Mixed","IntCal13","Marine13",50,12);
R_Date("AA-62283", 1062, 44);
Curve("IntCal13","IntCal13.14c");
R_Date("AA-67530", 1039, 35);
R_Date("OS-41358", 1030, 30);
R_Date("UCIAMS-94045", 1020, 20);
Curve("IntCal13","IntCal13.14c");
Curve("Marine13","Marine13.14c");
Mix_Curve("Mixed","IntCal13","Marine13",50,12);
R_Date("UCIAMS-120951", 1015, 15);
Curve("IntCal13","IntCal13.14c");
R_Date("AA-81056", 994, 45);
R_Date("UCIAMS-94044", 990, 20);
R_Date("AA-67529", 988, 42);
R_Date("OS-71462", 975, 20);
R_Date("OS-71408", 970, 15);
R_Date("OS-71407", 960, 15);
R_Date("RL-29", 940, 100);
R_Date("OS-71409", 925, 15);
```

```
   Curve("IntCal13","IntCal13.14c");
   Curve("Marine13","Marine13.14c");
   Mix_Curve("Mixed","IntCal13","Marine13",50,12);
   R_Date("Beta-257793", 870, 40);
   Curve("IntCal13","IntCal13.14c");
   R_Date("OS-71466", 680, 15);
   R_Date("AA-81054", 657, 44);
   Curve("IntCal13","IntCal13.14c");
   Curve("Marine13","Marine13.14c");
   Mix_Curve("Mixed","IntCal13","Marine13",50,12);
   R_Date("UCIAMS-111933", 715, 15);
   R_Date("UCIAMS-111934", 690, 15);
  };
  Boundary("Carriacou End");
 };
};
```

Cuba

```
Plot()
 {
 Sequence("Cuba")
  {
  Boundary("Cuba Start");
```

```
Phase()
{
 Curve("IntCal13","IntCal13.14c");
 R_Date("LE-4283", 5270, 120);
 R_Date("GD-250", 5140, 170);
 R_Date("MC-860", 4420, 100);
 Curve("Marine13","Marine13.14c");
 R_Date("OxA-15267", 4408, 37);
 Curve("IntCal13","IntCal13.14c");
 R_Date("MC-859", 4240, 100);
 R_Date("UBAR-170", 4200, 79);
 R_Date("Beta-140079", 4180, 80);
 R_Date("LE-1783", 4110, 50);
 R_Date("SI-429", 4000, 150);
 R_Date("LE-1784", 3870, 40);
 Curve("Marine13","Marine13.14c");
 R_Date("OxA-15180", 3861, 28);
 Curve("IntCal13","IntCal13.14c");
 R_Date("LE-1782", 3760, 40);
 R_Date("Beta-133951", 3720, 70);
 R_Date("UNAM-0716", 3460, 60);
 R_Date("GD-204", 3460, 160);
 Curve("Marine13","Marine13.14c");
```

```
R_Date("OxA-15264", 3273, 33);
R_Date("OxA-15263", 3271, 29);
Curve("IntCal13","IntCal13.14c");
R_Date("Y-1764", 3250, 100);
R_Date("LE-4270", 3110, 180);
R_Date("SI-428", 3110, 200);
R_Date("UBAR-169", 3060, 180);
R_Date("AA-101053", 3057, 39);
R_Date("LE-4288", 3030, 180);
R_Date("LE-4287", 3030, 180);
Curve("IntCal13","IntCal13.14c");
Curve("Marine13","Marine13.14c");
Mix_Curve("Mixed","IntCal13","Marine13",50,12);
R_Date("AA-101054", 2999, 61);
R_Date("AA-101057", 2996, 53);
Curve("Marine13","Marine13.14c");
R_Date("Beta-184894", 2980, 70);
Curve("IntCal13","IntCal13.14c");
Curve("Marine13","Marine13.14c");
Mix_Curve("Mixed","IntCal13","Marine13",50,12);
R_Date("AA-89061", 2960, 33);
R_Date("AA-101052", 2946, 57);
Curve("IntCal13","IntCal13.14c");
```

```
R_Date("LE-4282", 2930, 300);
R_Date("GD-591", 2930, 80);
Curve("IntCal13","IntCal13.14c");
Curve("Marine13","Marine13.14c");
Mix_Curve("Mixed","IntCal13","Marine13",50,12);
R_Date("AA-89063", 2922, 34);
Curve("IntCal13","IntCal13.14c");
R_Date("GD-613", 2880, 70);
R_Date("A-14316", 2845, 90);
R_Date("GD-1046", 2840, 60);
R_Date("GD-601", 2805, 60);
Curve("IntCal13","IntCal13.14c");
Curve("Marine13","Marine13.14c");
Mix_Curve("Mixed","IntCal13","Marine13",50,12);
R_Date("AA-101059", 2791, 51);
Curve("IntCal13","IntCal13.14c");
R_Date("Beta-133950", 2780, 40);
R_Date("LE-4272", 2750, 160);
R_Date("GD-614", 2720, 65);
R_Date("LE-2720", 2680, 40);
Curve("Marine13","Marine13.14c");
R_Date("Beta-184896", 2680, 60);
Curve("IntCal13","IntCal13.14c");
```

```
R_Date("LE-4290", 2610, 120);
R_Date("LE-4281", 2610, 120);
R_Date("LE-2718", 2610, 40);
R_Date("LE-4275", 2580, 90);
Curve("Marine13","Marine13.14c");
R_Date("Beta-318171", 2570, 30);
Curve("IntCal13","IntCal13.14c");
R_Date("UNAM-0717", 2520, 60);
R_Date("A-14315", 2515, 75);
R_Date("SI-427", 2510, 200);
R_Date("LE-4273", 2420, 100);
R_Date("LE-4279", 2390, 170);
R_Date("LE-4271", 2380, 80);
Curve("Marine13","Marine13.14c");
R_Date("Beta-422938", 2350, 30);
Curve("IntCal13","IntCal13.14c");
R_Date("LE-4276", 2250, 150);
R_Date("LE-4267", 2220, 160);
R_Date("GD-1039", 2160, 55);
R_Date("LE-2719", 2160, 40);
R_Date("SI-426", 2070, 150);
R_Date("LC-H 1034", 2070, 110);
R_Date("LE-4274", 2030, 160);
```

```
Curve("Marine13","Marine13.14c");
R_Date("Beta-214957", 2020, 50);
Curve("IntCal13","IntCal13.14c");
R_Date("Lv-2063", 2020, 80);
R_Date("LE-2717", 2010, 40);
Curve("Marine13","Marine13.14c");
R_Date("OxA-15262", 2005, 27);
Curve("IntCal13","IntCal13.14c");
R_Date("GD-1051", 1990, 80);
Curve("Marine13","Marine13.14c");
R_Date("OxA-15266", 1978, 33);
R_Date("Beta-214958", 1910, 50);
Curve("IntCal13","IntCal13.14c");
R_Date("Beta-93862", 1890, 60);
Curve("Marine13","Marine13.14c");
R_Date("OxA-15183", 1873, 26);
Curve("IntCal13","IntCal13.14c");
R_Date("Beta-93866", 1850, 50);
Curve("Marine13","Marine13.14c");
R_Date("Beta-318170", 1750, 30);
Curve("IntCal13","IntCal13.14c");
R_Date("UM-1953", 1745, 175);
Curve("Marine13","Marine13.14c");
```

```
R_Date("OxA-15184", 1686, 26);
Curve("IntCal13","IntCal13.14c");
Curve("Marine13","Marine13.14c");
Mix_Curve("Mixed","IntCal13","Marine13",50,12);
R_Date("Beta-72801", 1670, 70);
R_Date("AA-101055", 1661, 52);
Curve("IntCal13","IntCal13.14c");
R_Date("Beta-133948", 1640, 130);
R_Date("SI-424", 1620, 150);
R_Date("AA-89064", 1617, 46);
Curve("IntCal13","IntCal13.14c");
Curve("Marine13","Marine13.14c");
Mix_Curve("Mixed","IntCal13","Marine13",50,12);
R_Date("OxA-15260", 1617, 29);
R_Date("Beta-72802", 1590, 60);
Curve("Marine13","Marine13.14c");
R_Date("OxA-15181", 1561, 24);
R_Date("OxA-15146", 1557, 25);
Curve("IntCal13","IntCal13.14c");
Curve("Marine13","Marine13.14c");
Mix_Curve("Mixed","IntCal13","Marine13",50,12);
R_Date("AA-89062", 1536, 51);
Curve("IntCal13","IntCal13.14c");
```

```
R_Date("GD-617", 1495, 60);
R_Date("LE-4269", 1470, 110);
R_Date("LC-H 1035", 1450, 70);
Curve("IntCal13","IntCal13.14c");
Curve("Marine13","Marine13.14c");
Mix_Curve("Mixed","IntCal13","Marine13",50,12);
R_Date("AA-89060", 1420, 59);
Curve("IntCal13","IntCal13.14c");
R_Date("TO-7621", 1404, 60);
R_Date("GD-616", 1350, 70);
R_Date("Beta-93863", 1350, 50);
R_Date("TO-7624", 1320, 60);
Curve("IntCal13","IntCal13.14c");
Curve("Marine13","Marine13.14c");
Mix_Curve("Mixed","IntCal13","Marine13",50,12);
R_Date("AA-101056", 1289, 46);
Curve("IntCal13","IntCal13.14c");
R_Date("Beta-140078", 1280, 60);
R_Date("Beta-133947", 1210, 60);
R_Date("GD-619", 1170, 90);
R_Date("Y-1994", 1120, 160);
Curve("Marine13","Marine13.14c");
R_Date("OxA-15179", 1112, 26);
```

```
Curve("IntCal13","IntCal13.14c");
R_Date("LC-H-1106", 1100, 130);
R_Date("SI-347", 1020, 100);
R_Date("GD-203", 1010, 110);
R_Date("Mo-399", 1000, 105);
R_Date("Y-1556", 970, 80);
R_Date("SI-352", 970, 100);
R_Date("Y-465", 960, 60);
R_Date("LC-H 565", 960, 50);
Curve("Marine13","Marine13.14c");
R_Date("OxA-15151", 950, 24);
R_Date("OxA-15152", 939, 24);
Curve("IntCal13","IntCal13.14c");
R_Date("GD-618", 910, 85);
Curve("Marine13","Marine13.14c");
R_Date("OxA-15148", 891, 23);
Curve("IntCal13","IntCal13.14c");
R_Date("FS AC 2418", 880, 40);
R_Date("Beta-148961", 880, 80);
Curve("Marine13","Marine13.14c");
R_Date("OxA-15145", 879, 26);
R_Date("OxA-15149", 874, 25);
Curve("IntCal13","IntCal13.14c");
```

```
Curve("Marine13","Marine13.14c");
Mix_Curve("Mixed","IntCal13","Marine13",50,12);
R_Date("Beta-148956", 870, 70);
Curve("Marine13","Marine13.14c");
R_Date("OxA-15182", 857, 24);
R_Date("OxA-15259", 827, 36);
R_Date("OxA-15154", 820, 24);
Curve("IntCal13","IntCal13.14c");
R_Date("Y-206", 810, 80);
Curve("Marine13","Marine13.14c");
R_Date("OxA-15261", 782, 26);
Curve("IntCal13","IntCal13.14c");
R_Date("Lv-2062", 780, 100);
R_Date("FS AC 2414", 770, 35);
Curve("Marine13","Marine13.14c");
R_Date("OxA-15265", 763, 25);
Curve("IntCal13","IntCal13.14c");
R_Date("Y-1555", 760, 60);
R_Date("Beta-148957", 730, 60);
Curve("Marine13","Marine13.14c");
R_Date("OxA-15153", 714, 25);
Curve("IntCal13","IntCal13.14c");
R_Date("OxA-15123", 710, 27);
```

```
Curve("Marine13","Marine13.14c");
R_Date("OxA-15178", 709, 26);
Curve("IntCal13","IntCal13.14c");
R_Date("GD-621", 705, 65);
R_Date("FS AC 2419", 690, 50);
R_Date("Beta-148949", 690, 60);
R_Date("FS AC 2415", 690, 50);
R_Date("Beta-148958", 670, 70);
R_Date("GD-1053", 665, 50);
R_Date("FS AC 2416", 660, 35);
R_Date("OxA-15144", 651, 24);
R_Date("SI-425", 650, 200);
R_Date("SI-348", 640, 120);
R_Date("FS AC 2417", 620, 30);
R_Date("Beta-148962", 620, 60);
R_Date("GD-1056", 600, 55);
R_Date("SI-353", 590, 90);
R_Date("SI-351", 590, 100);
R_Date("GD-1055", 575, 60);
R_Date("TO-7628", 560, 50);
R_Date("SI-349", 550, 150);
R_Date("TO-7626", 540, 50);
R_Date("OxA-15150", 531, 23);
```

```
R_Date("TO-7618", 510, 50);
R_Date("GD-624", 505, 40);
R_Date("Beta-148960", 500, 50);
R_Date("SI-350", 500, 100);
R_Date("GD-1057", 490, 45);
R_Date("GD-1054", 485, 50);
R_Date("TO-8068", 480, 60);
R_Date("FS AC 2424", 475, 35);
R_Date("TO-7627", 460, 50);
R_Date("FS AC 2420", 450, 35);
R_Date("TO-8072", 430, 60);
R_Date("TO-7620", 430, 50);
R_Date("FS AC 2422", 420, 45);
Curve("IntCal13","IntCal13.14c");
Curve("Marine13","Marine13.14c");
Mix_Curve("Mixed","IntCal13","Marine13",50,12);
R_Date("ICA 17B/0756", 420, 40);
Curve("IntCal13","IntCal13.14c");
R_Date("TO-7623", 390, 50);
R_Date("FS AC 2421", 375, 25);
Curve("IntCal13","IntCal13.14c");
Curve("Marine13","Marine13.14c");
Mix_Curve("Mixed","IntCal13","Marine13",50,12);
```

```
   R_Date("Beta-148955", 360, 80);
   Curve("IntCal13","IntCal13.14c");
   R_Date("TO-7625", 340, 50);
   R_Date("TO-7617", 330, 50);
   R_Date("TO-7622", 320, 40);
   R_Date("FS AC 2423", 315, 45);
  };
  Boundary("Cuba End");
 };
};
```

Curaçao

```
Plot()
 {
  Sequence("Curacao")
  {
   Boundary("Curacao Start");
   Phase()
   {
    Curve("IntCal13","IntCal13.14c");
    R_Date("IVIC-247", 4490, 60);
    R_Date("IVIC-246", 4160, 80);
    R_Date("IVIC-234", 4110, 65);
```

```
R_Date("IVIC-242", 4070, 65);
R_Date("IVIC-240", 3990, 50);
Curve("Marine13","Marine13.14c");
R_Date("PITT-1200", 1965, 35);
Curve("IntCal13","IntCal13.14c");
R_Date("PITT-1183", 1875, 430);
Curve("IntCal13","IntCal13.14c");
Curve("Marine13","Marine13.14c");
Mix_Curve("Mixed","IntCal13","Marine13",50,12);
R_Date("GrN-12914", 1500, 200);
Curve("IntCal13","IntCal13.14c");
R_Date("IVIC-237", 1440, 60);
R_Date("IVIC-250", 1230, 60);
R_Date("IVIC-233", 910, 50);
R_Date("PITT-1198", 875, 35);
R_Date("IVIC-244", 830, 60);
R_Date("PITT-1196", 775, 60);
Curve("IntCal13","IntCal13.14c");
Curve("Marine13","Marine13.14c");
Mix_Curve("Mixed","IntCal13","Marine13",50,12);
R_Date("DIC-3138", 660, 20);
Curve("IntCal13","IntCal13.14c");
R_Date("IVIC-248", 630, 50);
```

```
   R_Date("IVIC-249", 630, 60);
   R_Date("GrN-31926", 605, 15);
   R_Date("PITT-1195", 590, 50);
   R_Date("PITT-1188", 475, 50);
   R_Date("GrN-32016", 450, 30);
   R_Date("GrN-9997", 420, 15);
   R_Date("PITT-1197", 395, 115);
   R_Date("GrN-32017", 370, 25);
   R_Date("IVIC-241", 340, 50);
   R_Date("GrN-9998", 325, 35);
  };
  Boundary("Curacao End");
 };
};
```

Grand Turk

```
Plot()
 {
  Sequence("Grand Turk")
  {
   Boundary("Grand Turk Start");
   Phase()
   {
```

```
Curve("IntCal13","IntCal13.14c");
R_Date("Beta-80911", 1280, 60);
R_Date("Beta-98698", 1230, 60);
Curve("Marine13","Marine13.14c");
R_Date("Beta-93912", 1170, 60);
Curve("IntCal13","IntCal13.14c");
R_Date("Beta-80910", 1160, 60);
R_Date("Beta-114924", 1120, 50);
R_Date("Beta-66151", 1120, 120);
R_Date("Beta-98697", 1010, 50);
R_Date("Beta-96700", 940, 60);
Curve("Marine13","Marine13.14c");
R_Date("Beta-93913", 930, 60);
Curve("IntCal13","IntCal13.14c");
R_Date("Beta-242672", 910, 40);
R_Date("Beta-98699", 900, 50);
Curve("Marine13","Marine13.14c");
R_Date("Beta-242675", 850, 50);
R_Date("Beta-242673", 790, 50);
Curve("IntCal13","IntCal13.14c");
R_Date("Beta-253527", 780, 40);
R_Date("Beta 242670", 690, 40);
R_Date("Beta-242671", 610, 40);
```

```
   Curve("Marine13","Marine13.14c");
   R_Date("Beta-242674", 460, 40);
  };
  Boundary("Grand Turk End");
 };
};
```

Grenada

```
Plot()
 {
  Sequence("Grenada")
  {
   Boundary("Grenada Start");
   Phase()
   {
    Curve("Marine13","Marine13.14c");
    R_Date("PSUAMS-3017", 2820, 20);
    R_Date("PSUAMS-3022", 2145, 20);
    Curve("IntCal13","IntCal13.14c");
    R_Date("PSUAMS-1317", 1685, 20);
    Curve("Marine13","Marine13.14c");
    R_Date("PSUAMS-3020", 1510, 20);
    Curve("IntCal13","IntCal13.14c");
```

```
R_Date("PSUAMS-1287", 1500, 25);
Curve("Marine13","Marine13.14c");
R_Date("UCIAMS-179806", 1380, 20);
Curve("IntCal13","IntCal13.14c");
R_Date("Beta-85941", 1270, 50);
R_Date("PSUAMS-1565", 1215, 20);
R_Date("PSUAMS-3946", 1215, 20);
R_Date("PSUAMS-1320", 1180, 25);
R_Date("Beta-85935", 1110, 40);
R_Date("Beta-98365", 1080, 50);
R_Date("Beta-86831", 1050, 90);
R_Date("Beta-98368", 980, 60);
R_Date("Beta-86827", 900, 60);
R_Date("Beta-85938", 850, 40);
R_Date("PSUAMS-1322", 835, 25);
R_Date("Beta-86833", 810, 50);
R_Date("Beta-86832", 790, 60);
R_Date("Beta-85939", 770, 60);
R_Date("Beta-86830", 770, 50);
R_Date("Beta-86828", 650, 40);
R_Date("Beta-86829", 550, 60);
R_Date("Beta-98367", 510, 60);
R_Date("PSUAMS-3945", 380, 25);
```

```
    R_Date("Beta-98366", 340, 50);
   };
   Boundary("Grenada End");
  };
 };
```

Guadeloupe

```
Plot()
 {
  Sequence("Guadeloupe")
  {
   Boundary("Guadeloupe Start");
   Phase()
   {
    Curve("IntCal13","IntCal13.14c");
    R_Date("Erl-10156", 3052, 41);
    R_Date("Ly-9162", 1815, 30);
    R_Date("Ly-9161", 1580, 30);
    R_Date("KIA-36672", 1340, 25);
    R_Date("KIA-36677", 1245, 30);
    R_Date("KIA-36671", 1230, 30);
    R_Date("KIA-31187", 1210, 20);
    R_Date("Y-1246", 1100, 80);
```

```
R_Date("KIA-36678", 1065, 30);

R_Date("Erl-10159", 1056, 36);

R_Date("KIA-36684", 1000, 30);

R_Date("KIA-36673", 945, 35);

R_Date("KIA-36674", 945, 30);

Curve("IntCal13","IntCal13.14c");

Curve("Marine13","Marine13.14c");

Mix_Curve("Mixed","IntCal13","Marine13",50,12);

R_Date("KIA-36675", 915, 50);

Curve("IntCal13","IntCal13.14c");

R_Date("Ly-8466", 770, 30);

R_Date("KIA-36680", 690, 30);

Curve("IntCal13","IntCal13.14c");

Curve("Marine13","Marine13.14c");

Mix_Curve("Mixed","IntCal13","Marine13",50,12);

R_Date("KIA-36682", 650, 140);

Curve("IntCal13","IntCal13.14c");

R_Date("KIA-36679", 625, 30);

Curve("IntCal13","IntCal13.14c");

Curve("Marine13","Marine13.14c");

Mix_Curve("Mixed","IntCal13","Marine13",50,12);

R_Date("KIA-36681", 625, 25);

R_Date("KIA-36681", 620, 25);
```

```
   R_Date("KIA-36676", 565, 25);
   R_Date("KIA-36676", 431, 22);
   R_Date("KIA-36676", 348, 39);
   Curve("IntCal13","IntCal13.14c");
   R_Date("KIA-36683", 330, 25);
  };
  Boundary("Guadeloupe End");
 };
};
```

Hispaniola

```
Plot()
 {
  Sequence("Hispaniola")
  {
  Boundary("Hispaniola Start");
  Phase()
  {
   Curve("IntCal13","IntCal13.14c");
   R_Date("I-6756", 3890, 95);
   R_Date("I-5940", 3840, 130);
   Curve("Marine13","Marine13.14c");
```

```
R_Date("I-9541", 3575, 90);
Curve("IntCal13","IntCal13.14c");
R_Date("I-9539", 3205, 90);
R_Date("I-6781", 2585, 90);
R_Date("I-5818", 2095, 135);
R_Date("SI-991", 1805, 70);
Curve("Marine13","Marine13.14c");
R_Date("GrN-29933", 1750, 30);
R_Date("GrN-31416", 1745, 20);
R_Date("GrN-31413", 1705, 20);
R_Date("GrN-30532", 1525, 25);
R_Date("GrN-31415", 1520, 20);
R_Date("GrN-29932", 1495, 30);
R_Date("GrN-31414", 1435, 20);
R_Date("Beta-293244", 1340, 40);
Curve("IntCal13","IntCal13.14c");
R_Date("GrN-31412", 1230, 40);
Curve("Marine13","Marine13.14c");
R_Date("GrN-30531", 1170, 25);
R_Date("Beta-293242", 1120, 40);
Curve("IntCal13","IntCal13.14c");
R_Date("GrN-29934", 1110, 25);
Curve("Marine13","Marine13.14c");
```

```
R_Date("GrN-30533", 1040, 25);
R_Date("Beta-293243", 1030, 40);
Curve("IntCal13","IntCal13.14c");
R_Date("Beta-108313", 990, 70);
R_Date("Beta-107023", 940, 30);
R_Date("GrN-31418", 925, 30);
R_Date("GrN-31417", 915, 20);
R_Date("Beta-112400", 910, 40);
R_Date("Beta-96782", 870, 60);
R_Date("GrN-29931", 815, 35);
R_Date("Beta-47758", 810, 70);
R_Date("Beta-46760", 800, 60);
R_Date("Beta-46759", 720, 50);
R_Date("Beta-18173", 680, 80);
R_Date("Beta-96781", 680, 60);
R_Date("Beta-01527", 640, 260);
R_Date("Beta-108314", 620, 70);
R_Date("Beta-18172", 600, 70);
R_Date("GrN-30534", 600, 25);
R_Date("GrN-30535", 580, 30);
R_Date("Beta-108315", 540, 50);
R_Date("GrN-29035", 535, 25);
R_Date("Beta-018469", 440, 60);
```

```
    R_Date("Beta-10526", 430, 80);
    R_Date("Beta-010528", 340, 70);
    R_Date("Beta-046761", 320, 70);
   };
   Boundary("Hispaniola End");
  };
 };
```

Jamaica

```
Plot()
 {
  Sequence("Jamaica")
  {
   Boundary("Jamaica Start");
   Phase()
   {
    Curve("IntCal13","IntCal13.14c");
    R_Date("Beta-153378", 970, 40);
    R_Date("WK 43115", 938, 20);
    R_Date("Beta-167740", 680, 60);
    R_Date("A-6140", 630, 40);
    R_Date("WK 43114", 627, 20);
    R_Date("OxA-21058", 615, 24);
```

```
  R_Date("A-6058", 570, 45);
  R_Date("A-6061", 525, 45);
  R_Date("OxA-21057", 396, 24);
  R_Date("OxA- 21056", 384, 24);
 };
 Boundary("Jamaica End");
};
};
```

Montserrat

```
Plot()
{
 Sequence("Montserrat")
 {
  Boundary("Montserrat Start");
  Phase()
  {
   Curve("IntCal13","IntCal13.14c");
   R_Date("Beta-83043", 2770, 60);
   R_Date("Beta-83050", 2140, 110);
   R_Date("Beta-83046", 2050, 80);
   R_Date("Beta-83045", 1950, 90);
   R_Date("Beta-83048", 1860, 100);
```

```
   R_Date("Beta-83049", 1730, 100);
   R_Date("Beta-83044", 1650, 130);
   R_Date("Beta-83051", 1540, 120);
   R_Date("Beta-83047", 1270, 130);
   R_Date("Beta-282302", 1120, 40);
   R_Date("Beta-282300", 1070, 40);
   R_Date("Beta-277241", 1010, 40);
   R_Date("Beta-282301", 980, 40);
   R_Date("Beta-282299", 980, 40);
   R_Date("Beta-277242", 880, 40);
  };
  Boundary("Montserrat End");
 };
};
```

Nevis

```
Plot()
 {
  Sequence("Nevis")
  {
   Boundary("Nevis Start");
   Phase()
   {
```

```
   Curve("Marine13","Marine13.14c");
   R_Date("D-AMS 007668", 1541, 33);
   R_Date("D-AMS 07667", 1464, 24);
   R_Date("Beta-290341", 1420, 40);
   R_Date("Beta-290340", 1350, 40);
   Curve("IntCal13","IntCal13.14c");
   R_Date("Beta-47807", 1070, 70);
   R_Date("Beta-46940", 1060, 50);
   R_Date("Beta-46944a", 940, 60);
   R_Date("Beta-46942", 880, 60);
   Curve("Marine13","Marine13.14c");
   R_Date("Beta-324952", 720, 30);
   R_Date("Beta-324951", 570, 30);
  };
  Boundary("Nevis End");
 };
};
```

Puerto Rico

```
Plot()
 {
  Sequence("Puerto Rico")
  {
```

```
Boundary("Puerto Rico Start");
Phase()
{
 Curve("IntCal13","IntCal13.14c");
 R_Date("Beta-77165", 4060, 60);
 R_Date("Beta-178680", 4110, 40);
 R_Date("GX-28807", 3920, 40);
 Curve("Marine13","Marine13.14c");
 R_Date("UGM-17566", 4250, 25);
 Curve("IntCal13","IntCal13.14c");
 R_Date("Beta-116372", 3820, 70);
 R_Date("UGM-17565", 3810, 25);
 R_Date("GX-28814", 3740, 100);
 R_Date("UGM-5106", 3740, 30);
 Curve("Marine13","Marine13.14c");
 R_Date("UGM-5108", 3740, 30);
 Curve("IntCal13","IntCal13.14c");
 R_Date("GX-28805", 3700, 30);
 R_Date("Beta-294434", 3680, 40);
 R_Date("GX-28808", 3670, 40);
 Curve("Marine13","Marine13.14c");
 R_Date("UGM-17561", 3640, 25);
 Curve("IntCal13","IntCal13.14c");
```

```
R_Date("Beta-130451", 3640, 70);
Curve("Marine13","Marine13.14c");
R_Date("UGM-17562", 3630, 25);
Curve("IntCal13","IntCal13.14c");
R_Date("GX-28806", 3570, 40);
Curve("Marine13","Marine13.14c");
R_Date("UGM-5107", 3520, 30);
Curve("IntCal13","IntCal13.14c");
R_Date("GX-28809", 3470, 40);
R_Date("I-14745", 3340, 90);
Curve("Marine13","Marine13.14c");
R_Date("UGM-5105", 3170, 30);
Curve("IntCal13","IntCal13.14c");
R_Date("UGM-30042", 3140, 40);
Curve("Marine13","Marine13.14c");
R_Date("UGM-17564", 3120, 20);
Curve("IntCal13","IntCal13.14c");
R_Date("UGM-30031", 2910, 50);
R_Date("Beta-130450", 2730, 70);
R_Date("Beta-178678", 2520, 40);
R_Date("UGM-30033", 2390, 35);
R_Date("Beta-178677", 2330, 110);
R_Date("I-14744", 2270, 80);
```

```
R_Date("Beta-294435", 2120, 30);

Curve("Marine13","Marine13.14c");

R_Date("I-14979", 2120, 80);

Curve("IntCal13","IntCal13.14c");

R_Date("I-11296", 2100, 80);

R_Date("Beta-9970", 2060, 70);

R_Date("Beta-14380", 2060, 60);

R_Date("I-14978", 2020, 80);

R_Date("I-13855", 2020, 80);

R_Date("I-11297", 1995, 80);

R_Date("Beta-14381", 1960, 90);

R_Date("I-13930", 1950, 80);

R_Date("Y-1235", 1920, 120);

R_Date("Beta-87611", 1920, 80);

R_Date("Beta-347456", 1910, 30);

R_Date("Y-1234", 1910, 100);

R_Date("I-11266", 1865, 80);

R_Date("Beta-9972", 1840, 50);

R_Date("Y-1233", 1830, 80);

R_Date("Beta-14993", 1810, 60);

R_Date("Beta-14997", 1810, 70);

R_Date("I-10914", 1780, 85);

R_Date("I-13922", 1780, 85);
```

```
R_Date("I-9680", 1775, 80);
R_Date("I-10916", 1720, 80);
R_Date("I-10921", 1705, 85);
R_Date("Beta-14992", 1660, 100);
R_Date("I-14361", 1650, 80);
R_Date("I-14431", 1650, 80);
Curve("IntCal13","IntCal13.14c");
Curve("Marine13","Marine13.14c");
Mix_Curve("Mixed","IntCal13","Marine13",50,12);
R_Date("Beta-222869", 1630, 40);
Curve("IntCal13","IntCal13.14c");
R_Date("I-14430", 1610, 80);
R_Date("I-14427", 1610, 80);
Curve("IntCal13","IntCal13.14c");
Curve("Marine13","Marine13.14c");
Mix_Curve("Mixed","IntCal13","Marine13",50,12);
R_Date("AA-6809", 1600, 55);
Curve("IntCal13","IntCal13.14c");
R_Date("I-14428", 1600, 150);
R_Date("I-14383", 1600, 80);
Curve("IntCal13","IntCal13.14c");
Curve("Marine13","Marine13.14c");
Mix_Curve("Mixed","IntCal13","Marine13",50,12);
```

```
R_Date("AA-75810", 1582, 46);

Curve("IntCal13","IntCal13.14c");

R_Date("Y-1232", 1580, 80);

R_Date("Beta-17637", 1580, 120);

R_Date("Beta-178670", 1580, 90);

Curve("IntCal13","IntCal13.14c");

Curve("Marine13","Marine13.14c");

Mix_Curve("Mixed","IntCal13","Marine13",50,12);

R_Date("AA-79415", 1566, 46);

Curve("IntCal13","IntCal13.14c");

R_Date("I-14362", 1560, 80);

Curve("IntCal13","IntCal13.14c");

Curve("Marine13","Marine13.14c");

Mix_Curve("Mixed","IntCal13","Marine13",50,12);

R_Date("AA-78513", 1557, 44);

Curve("IntCal13","IntCal13.14c");

R_Date("Beta-87610", 1550, 60);

R_Date("Beta-272032", 1550, 40);

R_Date("I-14429", 1550, 80);

R_Date("I-6595", 1545, 90);

Curve("IntCal13","IntCal13.14c");

Curve("Marine13","Marine13.14c");

Mix_Curve("Mixed","IntCal13","Marine13",50,12);
```

```
R_Date("AA-75128", 1539, 43);
Curve("IntCal13","IntCal13.14c");
R_Date("Beta-17631", 1530, 90);
R_Date("I-14382", 1530, 80);
Curve("IntCal13","IntCal13.14c");
Curve("Marine13","Marine13.14c");
Mix_Curve("Mixed","IntCal13","Marine13",50,12);
R_Date("AA-6805", 1525, 55);
Curve("IntCal13","IntCal13.14c");
R_Date("Beta-14994", 1520, 50);
R_Date("Beta-178681", 1520, 40);
Curve("IntCal13","IntCal13.14c");
Curve("Marine13","Marine13.14c");
Mix_Curve("Mixed","IntCal13","Marine13",50,12);
R_Date("AA-4100", 1515, 50);
Curve("IntCal13","IntCal13.14c");
R_Date("I-9677", 1515, 80);
Curve("IntCal13","IntCal13.14c");
Curve("Marine13","Marine13.14c");
Mix_Curve("Mixed","IntCal13","Marine13",50,12);
R_Date("AA-78495", 1505, 44);
Curve("IntCal13","IntCal13.14c");
R_Date("I-13932", 1500, 80);
```

```
Curve("IntCal13","IntCal13.14c");

Curve("Marine13","Marine13.14c");

Mix_Curve("Mixed","IntCal13","Marine13",50,12);

R_Date("AA-74638", 1493, 45);

Curve("IntCal13","IntCal13.14c");

R_Date("I-13923", 1490, 80);

R_Date("I-9108", 1480, 95);

R_Date("I-13924", 1480, 80);

R_Date("Beta-178674", 1470, 40);

Curve("IntCal13","IntCal13.14c");

Curve("Marine13","Marine13.14c");

Mix_Curve("Mixed","IntCal13","Marine13",50,12);

R_Date("AA-82397", 1469, 47);

Curve("IntCal13","IntCal13.14c");

R_Date("Beta-223566", 1460, 60);

R_Date("I-14360", 1460, 80);

R_Date("I-9873", 1460, 80);

Curve("IntCal13","IntCal13.14c");

Curve("Marine13","Marine13.14c");

Mix_Curve("Mixed","IntCal13","Marine13",50,12);

R_Date("AA-79371", 1456, 45);

R_Date("AA-75816", 1455, 46);

Curve("IntCal13","IntCal13.14c");
```

```
R_Date("Beta-178666", 1450, 40);
Curve("IntCal13","IntCal13.14c");
Curve("Marine13","Marine13.14c");
Mix_Curve("Mixed","IntCal13","Marine13",50,12);
R_Date("AA-72872", 1443, 50);
Curve("IntCal13","IntCal13.14c");
R_Date("UGM-30035", 1440, 30);
R_Date("Beta-17641", 1440, 70);
R_Date("Beta-87601", 1440, 60);
Curve("IntCal13","IntCal13.14c");
Curve("Marine13","Marine13.14c");
Mix_Curve("Mixed","IntCal13","Marine13",50,12);
R_Date("AA-74637", 1434, 45);
R_Date("AA-78492", 1434, 44);
Curve("IntCal13","IntCal13.14c");
R_Date("Beta-223977", 1430, 70);
Curve("IntCal13","IntCal13.14c");
Curve("Marine13","Marine13.14c");
Mix_Curve("Mixed","IntCal13","Marine13",50,12);
R_Date("AA-78512", 1430, 43);
R_Date("AA-72896", 1428, 42);
R_Date("AA-78483", 1427, 44);
R_Date("AA-78493", 1424, 44);
```

```
R_Date("AA-79362", 1422, 46);
R_Date("AA-79409", 1421, 48);
R_Date("AA-83951", 1413, 64);
R_Date("AA-79364", 1411, 45);
Curve("IntCal13","IntCal13.14c");
R_Date("I-10920", 1410, 85);
Curve("IntCal13","IntCal13.14c");
Curve("Marine13","Marine13.14c");
Mix_Curve("Mixed","IntCal13","Marine13",50,12);
R_Date("AA-79384", 1408, 46);
R_Date("AA-4110", 1405, 50);
R_Date("AA-74656", 1403, 44);
R_Date("AA-75804", 1401, 45);
Curve("IntCal13","IntCal13.14c");
R_Date("I-13854", 1400, 150);
Curve("IntCal13","IntCal13.14c");
Curve("Marine13","Marine13.14c");
Mix_Curve("Mixed","IntCal13","Marine13",50,12);
R_Date("AA-79363", 1397, 50);
R_Date("AA-78490", 1392, 43);
R_Date("AA-72895", 1392, 42);
Curve("IntCal13","IntCal13.14c");
R_Date("I-10915", 1390, 85);
```

```
Curve("IntCal13","IntCal13.14c");
Curve("Marine13","Marine13.14c");
Mix_Curve("Mixed","IntCal13","Marine13",50,12);
R_Date("AA-79383", 1389, 45);
R_Date("AA-79410", 1387, 45);
R_Date("AA-83942", 1381, 43);
R_Date("AA-75130", 1374, 43);
R_Date("AA-75137", 1372, 44);
Curve("IntCal13","IntCal13.14c");
R_Date("Beta-223565", 1370, 40);
R_Date("Beta-15003", 1370, 60);
R_Date("I-13853", 1370, 80);
Curve("IntCal13","IntCal13.14c");
Curve("Marine13","Marine13.14c");
Mix_Curve("Mixed","IntCal13","Marine13",50,12);
R_Date("AA-75805", 1369, 45);
R_Date("AA-79374", 1369, 45);
R_Date("AA-79367", 1367, 45);
R_Date("AA-72894", 1366, 44);
R_Date("AA-74636", 1365, 45);
R_Date("AA-79366", 1364, 45);
Curve("IntCal13","IntCal13.14c");
R_Date("Beta-17635", 1360, 70);
```

```
Curve("IntCal13","IntCal13.14c");
Curve("Marine13","Marine13.14c");
Mix_Curve("Mixed","IntCal13","Marine13",50,12);
R_Date("AA-4107", 1360, 50);
Curve("IntCal13","IntCal13.14c");
R_Date("I-13931", 1360, 80);
Curve("IntCal13","IntCal13.14c");
Curve("Marine13","Marine13.14c");
Mix_Curve("Mixed","IntCal13","Marine13",50,12);
R_Date("AA-79369", 1359, 50);
R_Date("AA-79365", 1358, 48);
R_Date("AA-74663", 1355, 54);
R_Date("AA-82391", 1355, 46);
R_Date("AA-83940", 1353, 43);
R_Date("AA-72871", 1352, 43);
R_Date("AA-75799", 1351, 44);
R_Date("AA-72897", 1351, 44);
Curve("IntCal13","IntCal13.14c");
R_Date("Beta-77164", 1350, 70);
Curve("IntCal13","IntCal13.14c");
Curve("Marine13","Marine13.14c");
Mix_Curve("Mixed","IntCal13","Marine13",50,12);
R_Date("AA-75809", 1350, 46);
```

```
Curve("IntCal13","IntCal13.14c");

R_Date("I-13933", 1350, 110);

Curve("IntCal13","IntCal13.14c");

Curve("Marine13","Marine13.14c");

Mix_Curve("Mixed","IntCal13","Marine13",50,12);

R_Date("AA-82378", 1347, 45);

R_Date("AA-74643", 1347, 45);

R_Date("AA-79370", 1344, 62);

Curve("IntCal13","IntCal13.14c");

R_Date("Beta-221018", 1340, 40);

Curve("IntCal13","IntCal13.14c");

Curve("Marine13","Marine13.14c");

Mix_Curve("Mixed","IntCal13","Marine13",50,12);

R_Date("AA-75812", 1339, 45);

R_Date("AA-78496", 1338, 43);

R_Date("AA-78489", 1336, 43);

R_Date("AA-4103", 1335, 45);

R_Date("AA-4109", 1335, 45);

R_Date("AA-75803", 1331, 68);

R_Date("AA-4097", 1330, 45);

R_Date("AA-83938", 1326, 44);

R_Date("AA-72887", 1322, 42);

R_Date("AA-74662", 1322, 44);
```

```
R_Date("AA-82383", 1321, 46);

Curve("IntCal13","IntCal13.14c");

R_Date("Beta-9971", 1320, 70);

Curve("IntCal13","IntCal13.14c");

Curve("Marine13","Marine13.14c");

Mix_Curve("Mixed","IntCal13","Marine13",50,12);

R_Date("AA-74639", 1319, 42);

Curve("IntCal13","IntCal13.14c");

R_Date("AA-4114", 1315, 45);

R_Date("I-10913", 1315, 85);

R_Date("Beta-17633", 1310, 60);

R_Date("Beta-272023", 1310, 40);

R_Date("I-15408", 1310, 80);

Curve("IntCal13","IntCal13.14c");

Curve("Marine13","Marine13.14c");

Mix_Curve("Mixed","IntCal13","Marine13",50,12);

R_Date("AA-74657", 1305, 44);

R_Date("AA-82416", 1302, 45);

R_Date("AA-72869", 1302, 42);

R_Date("AA-74665", 1301, 43);

Curve("IntCal13","IntCal13.14c");

R_Date("Beta-17640", 1300, 70);

R_Date("Beta-272028", 1300, 40);
```

```
R_Date("UM-398", 1300, 90);
R_Date("AA-4115", 1295, 45);
Curve("IntCal13","IntCal13.14c");
Curve("Marine13","Marine13.14c");
Mix_Curve("Mixed","IntCal13","Marine13",50,12);
R_Date("AA-6810", 1295, 60);
Curve("IntCal13","IntCal13.14c");
R_Date("I-10912", 1295, 85);
Curve("IntCal13","IntCal13.14c");
Curve("Marine13","Marine13.14c");
Mix_Curve("Mixed","IntCal13","Marine13",50,12);
R_Date("AA-82407", 1289, 46);
R_Date("AA-78511", 1287, 43);
Curve("IntCal13","IntCal13.14c");
R_Date("I-9107", 1285, 95);
Curve("IntCal13","IntCal13.14c");
Curve("Marine13","Marine13.14c");
Mix_Curve("Mixed","IntCal13","Marine13",50,12);
R_Date("AA-74664", 1285, 43);
Curve("IntCal13","IntCal13.14c");
R_Date("UGM-30037", 1280, 30);
Curve("IntCal13","IntCal13.14c");
Curve("Marine13","Marine13.14c");
```

```
Mix_Curve("Mixed","IntCal13","Marine13",50,12);

R_Date("AA-79411", 1271, 45);

Curve("IntCal13","IntCal13.14c");

R_Date("Beta-386615", 1270, 30);

R_Date("Beta-178673", 1270, 70);

R_Date("Beta-109680", 1270, 40);

R_Date("Beta-386071", 1260, 30);

R_Date("Beta-386068", 1260, 30);

R_Date("Beta-17638", 1260, 60);

R_Date("I-15410", 1260, 80);

Curve("IntCal13","IntCal13.14c");

Curve("Marine13","Marine13.14c");

Mix_Curve("Mixed","IntCal13","Marine13",50,12);

R_Date("AA-75129", 1260, 42);

R_Date("AA-82377", 1260, 46);

R_Date("AA-79412", 1257, 47);

R_Date("AA-79414", 1255, 45);

R_Date("AA-79368", 1253, 52);

R_Date("AA-72881", 1251, 42);

Curve("IntCal13","IntCal13.14c");

R_Date("Beta-272025", 1250, 40);

Curve("IntCal13","IntCal13.14c");

Curve("Marine13","Marine13.14c");
```

```
Mix_Curve("Mixed","IntCal13","Marine13",50,12);

R_Date("AA-78491", 1249, 43);

Curve("IntCal13","IntCal13.14c");

R_Date("Beta-127523", 1240, 40);

R_Date("I-14748", 1240, 80);

R_Date("Beta-272030", 1240, 40);

Curve("IntCal13","IntCal13.14c");

Curve("Marine13","Marine13.14c");

Mix_Curve("Mixed","IntCal13","Marine13",50,12);

R_Date("AA-79382", 1235, 45);

R_Date("AA-75807", 1231, 77);

Curve("IntCal13","IntCal13.14c");

R_Date("Beta-386073", 1230, 30);

R_Date("Beta-386074", 1230, 30);

R_Date("UGM-30026", 1230, 65);

R_Date("Beta-178667", 1230, 60);

R_Date("I-15679", 1230, 80);

Curve("IntCal13","IntCal13.14c");

Curve("Marine13","Marine13.14c");

Mix_Curve("Mixed","IntCal13","Marine13",50,12);

R_Date("AA-75808", 1228, 47);

Curve("IntCal13","IntCal13.14c");

R_Date("Beta-225064", 1220, 40);
```

```
R_Date("Beta-272027", 1220, 40);
Curve("Marine13","Marine13.14c");
R_Date("I-15431", 1220, 80);
Curve("IntCal13","IntCal13.14c");
R_Date("I-9679", 1220, 80);
R_Date("OxA-15142", 1219, 26);
Curve("IntCal13","IntCal13.14c");
Curve("Marine13","Marine13.14c");
Mix_Curve("Mixed","IntCal13","Marine13",50,12);
R_Date("AA-75815", 1218, 46);
R_Date("AA-75813", 1214, 46);
R_Date("AA-79408", 1208, 45);
Curve("IntCal13","IntCal13.14c");
R_Date("GrN-30059", 1200, 40);
Curve("IntCal13","IntCal13.14c");
Curve("Marine13","Marine13.14c");
Mix_Curve("Mixed","IntCal13","Marine13",50,12);
R_Date("AA-75824", 1200, 44);
R_Date("AA-4104", 1195, 45);
R_Date("AA-82402", 1191, 48);
Curve("IntCal13","IntCal13.14c");
R_Date("Beta-283565", 1190, 40);
R_Date("Beta-272026", 1190, 40);
```

```
Curve("IntCal13","IntCal13.14c");
Curve("Marine13","Marine13.14c");
Mix_Curve("Mixed","IntCal13","Marine13",50,12);
R_Date("AA-78510", 1189, 45);
R_Date("AA-6807", 1188, 55);
R_Date("AA-75806", 1186, 45);
Curve("IntCal13","IntCal13.14c");
R_Date("GrN-24767", 1180, 40);
R_Date("I-14746", 1180, 80);
Curve("IntCal13","IntCal13.14c");
Curve("Marine13","Marine13.14c");
Mix_Curve("Mixed","IntCal13","Marine13",50,12);
R_Date("AA-6811", 1180, 85);
Curve("IntCal13","IntCal13.14c");
R_Date("Beta-81848", 1180, 70);
Curve("IntCal13","IntCal13.14c");
Curve("Marine13","Marine13.14c");
Mix_Curve("Mixed","IntCal13","Marine13",50,12);
R_Date("AA-78509", 1179, 43);
R_Date("AA-75814", 1175, 45);
R_Date("AA-82380", 1174, 45);
R_Date("AA-75133", 1173, 42);
Curve("IntCal13","IntCal13.14c");
```

```
R_Date("I-15678", 1170, 80);
Curve("IntCal13","IntCal13.14c");
Curve("Marine13","Marine13.14c");
Mix_Curve("Mixed","IntCal13","Marine13",50,12);
R_Date("AA-75801", 1168, 43);
R_Date("AA-72893", 1168, 42);
R_Date("AA-72888", 1164, 41);
R_Date("AA-82404", 1162, 60);
R_Date("AA-79381", 1162, 45);
Curve("IntCal13","IntCal13.14c");
R_Date("Beta-17636", 1160, 70);
R_Date("I-14749", 1160, 80);
Curve("IntCal13","IntCal13.14c");
Curve("Marine13","Marine13.14c");
Mix_Curve("Mixed","IntCal13","Marine13",50,12);
R_Date("AA-75127", 1160, 42);
R_Date("AA-82399", 1156, 46);
R_Date("AA-79413", 1154, 44);
Curve("IntCal13","IntCal13.14c");
R_Date("Beta-17639", 1150, 70);
Curve("IntCal13","IntCal13.14c");
Curve("Marine13","Marine13.14c");
Mix_Curve("Mixed","IntCal13","Marine13",50,12);
```

```
R_Date("AA-82409", 1150, 45);
R_Date("AA-82401", 1147, 87);
R_Date("AA-6806", 1145, 55);
R_Date("AA-79402", 1141, 45);
Curve("IntCal13","IntCal13.14c");
R_Date("GrN-24769", 1140, 40);
R_Date("Beta-17634", 1140, 60);
Curve("IntCal13","IntCal13.14c");
Curve("Marine13","Marine13.14c");
Mix_Curve("Mixed","IntCal13","Marine13",50,12);
R_Date("AA-4096", 1140, 45);
R_Date("AA-82406", 1140, 47);
R_Date("AA-78494", 1138, 43);
R_Date("AA-75817", 1135, 45);
Curve("IntCal13","IntCal13.14c");
R_Date("Beta-15006", 1130, 60);
Curve("IntCal13","IntCal13.14c");
Curve("Marine13","Marine13.14c");
Mix_Curve("Mixed","IntCal13","Marine13",50,12);
R_Date("AA-78479", 1128, 49);
R_Date("AA-75818", 1127, 45);
R_Date("AA-79404", 1125, 45);
R_Date("AA-79351", 1121, 44);
```

```
Curve("IntCal13","IntCal13.14c");
R_Date("Beta-386698", 1120, 30);
Curve("IntCal13","IntCal13.14c");
Curve("Marine13","Marine13.14c");
Mix_Curve("Mixed","IntCal13","Marine13",50,12);
R_Date("AA-72884", 1118, 44);
R_Date("AA-4111", 1110, 50);
Curve("IntCal13","IntCal13.14c");
R_Date("Beta-272029", 1100, 40);
Curve("IntCal13","IntCal13.14c");
Curve("Marine13","Marine13.14c");
Mix_Curve("Mixed","IntCal13","Marine13",50,12);
R_Date("AA-79355", 1099, 44);
R_Date("AA-79345", 1099, 45);
R_Date("AA-82410", 1098, 45);
R_Date("AA-79354", 1098, 44);
R_Date("AA-75134", 1098, 43);
R_Date("AA-75141", 1094, 44);
R_Date("AA-83935", 1092, 42);
R_Date("AA-79347", 1090, 45);
Curve("IntCal13","IntCal13.14c");
R_Date("UM-399", 1090, 100);
Curve("IntCal13","IntCal13.14c");
```

```
Curve("Marine13","Marine13.14c");
Mix_Curve("Mixed","IntCal13","Marine13",50,12);
R_Date("AA-83929", 1086, 46);
R_Date("AA-78488", 1085, 43);
R_Date("AA-78480", 1084, 46);
R_Date("AA-75135", 1082, 42);
Curve("IntCal13","IntCal13.14c");
R_Date("I-14747", 1080, 80);
Curve("IntCal13","IntCal13.14c");
Curve("Marine13","Marine13.14c");
Mix_Curve("Mixed","IntCal13","Marine13",50,12);
R_Date("AA-6812", 1080, 55);
Curve("IntCal13","IntCal13.14c");
R_Date("Beta-81846", 1080, 60);
R_Date("Beta-136326", 1080, 60);
Curve("IntCal13","IntCal13.14c");
Curve("Marine13","Marine13.14c");
Mix_Curve("Mixed","IntCal13","Marine13",50,12);
R_Date("AA-78487", 1078, 46);
R_Date("AA-79356", 1075, 44);
R_Date("AA-83927", 1073, 45);
R_Date("AA-75798", 1071, 43);
Curve("IntCal13","IntCal13.14c");
```

```
R_Date("Beta-17632", 1070, 70);
Curve("IntCal13","IntCal13.14c");
Curve("Marine13","Marine13.14c");
Mix_Curve("Mixed","IntCal13","Marine13",50,12);
R_Date("AA-79344", 1070, 45);
R_Date("AA-82381", 1070, 45);
R_Date("AA-4113", 1065, 50);
R_Date("AA-83930", 1065, 45);
R_Date("AA-75822", 1062, 43);
R_Date("AA-75136", 1061, 42);
Curve("IntCal13","IntCal13.14c");
R_Date("GrN-24764", 1060, 40);
R_Date("Beta-178663", 1060, 40);
R_Date("Beta-81843", 1060, 60);
Curve("IntCal13","IntCal13.14c");
Curve("Marine13","Marine13.14c");
Mix_Curve("Mixed","IntCal13","Marine13",50,12);
R_Date("AA-75122", 1055, 41);
Curve("IntCal13","IntCal13.14c");
R_Date("I-9678", 1055, 80);
Curve("IntCal13","IntCal13.14c");
Curve("Marine13","Marine13.14c");
Mix_Curve("Mixed","IntCal13","Marine13",50,12);
```

```
R_Date("AA-82415", 1054, 44);
R_Date("AA-72874", 1053, 42);
R_Date("AA-78482", 1053, 42);
Curve("IntCal13","IntCal13.14c");
R_Date("UGM-30034", 1050, 30);
R_Date("UGM-30036", 1050, 80);
R_Date("Beta-81850", 1050, 50);
Curve("IntCal13","IntCal13.14c");
Curve("Marine13","Marine13.14c");
Mix_Curve("Mixed","IntCal13","Marine13",50,12);
R_Date("AA-4106", 1045, 45);
R_Date("AA-4099", 1045, 45);
R_Date("AA-79407", 1041, 44);
Curve("IntCal13","IntCal13.14c");
R_Date("Beta-15007", 1040, 50);
Curve("IntCal13","IntCal13.14c");
Curve("Marine13","Marine13.14c");
Mix_Curve("Mixed","IntCal13","Marine13",50,12);
R_Date("AA-4112", 1040, 45);
R_Date("AA-79406", 1040, 44);
Curve("IntCal13","IntCal13.14c");
R_Date("Beta-136325", 1040, 50);
Curve("IntCal13","IntCal13.14c");
```

```
Curve("Marine13","Marine13.14c");
Mix_Curve("Mixed","IntCal13","Marine13",50,12);
R_Date("AA-79348", 1039, 45);
R_Date("AA-79372", 1038, 47);
R_Date("AA-72876", 1036, 42);
Curve("IntCal13","IntCal13.14c");
R_Date("UGM-30023", 1030, 20);
R_Date("Beta-178660", 1030, 50);
Curve("IntCal13","IntCal13.14c");
Curve("Marine13","Marine13.14c");
Mix_Curve("Mixed","IntCal13","Marine13",50,12);
R_Date("AA-82411", 1027, 44);
R_Date("AA-82414", 1026, 44);
R_Date("AA-79353", 1026, 44);
R_Date("AA-4108", 1025, 55);
R_Date("AA-75140", 1016, 45);
R_Date("AA-78478", 1014, 43);
R_Date("AA-75139", 1011, 42);
R_Date("Beta-220582", 1010, 40);
Curve("IntCal13","IntCal13.14c");
R_Date("Beta-178676", 1010, 40);
Curve("IntCal13","IntCal13.14c");
Curve("Marine13","Marine13.14c");
```

```
Mix_Curve("Mixed","IntCal13","Marine13",50,12);

R_Date("AA-75124", 1010, 42);

Curve("IntCal13","IntCal13.14c");

R_Date("Beta-136327", 1010, 40);

Curve("IntCal13","IntCal13.14c");

Curve("Marine13","Marine13.14c");

Mix_Curve("Mixed","IntCal13","Marine13",50,12);

R_Date("AA-82400", 1008, 46);

R_Date("AA-82382", 1007, 47);

R_Date("AA-72886", 1006, 41);

R_Date("AA-75142", 1004, 44);

R_Date("AA-78484", 1004, 45);

R_Date("AA-83936", 1002, 43);

Curve("IntCal13","IntCal13.14c");

R_Date("I-15432", 1000, 110);

Curve("IntCal13","IntCal13.14c");

Curve("Marine13","Marine13.14c");

Mix_Curve("Mixed","IntCal13","Marine13",50,12);

R_Date("AA-75826", 997, 44);

R_Date("AA-83933", 991, 43);

Curve("IntCal13","IntCal13.14c");

R_Date("GrN-24768", 990, 40);

R_Date("Beta-81841", 990, 50);
```

```
R_Date("Beta-198877", 990, 40);
R_Date("OxA-15141", 990, 24);
Curve("IntCal13","IntCal13.14c");
Curve("Marine13","Marine13.14c");
Mix_Curve("Mixed","IntCal13","Marine13",50,12);
R_Date("AA-79400", 983, 44);
Curve("IntCal13","IntCal13.14c");
R_Date("Beta-77168", 980, 50);
Curve("IntCal13","IntCal13.14c");
Curve("Marine13","Marine13.14c");
Mix_Curve("Mixed","IntCal13","Marine13",50,12);
R_Date("AA-72875", 980, 41);
R_Date("AA-75123", 973, 41);
Curve("IntCal13","IntCal13.14c");
R_Date("GrN-24759", 970, 30);
R_Date("Beta-81845", 970, 50);
R_Date("Beta-178668", 970, 40);
Curve("IntCal13","IntCal13.14c");
Curve("Marine13","Marine13.14c");
Mix_Curve("Mixed","IntCal13","Marine13",50,12);
R_Date("AA-75126", 966, 42);
R_Date("AA-72892", 966, 41);
R_Date("AA-75820", 964, 44);
```

```
R_Date("AA-82405", 963, 46);

Curve("IntCal13","IntCal13.14c");

R_Date("Beta-81844", 960, 50);

R_Date("Beta-178669", 960, 130);

R_Date("Beta-178672", 960, 40);

Curve("IntCal13","IntCal13.14c");

Curve("Marine13","Marine13.14c");

Mix_Curve("Mixed","IntCal13","Marine13",50,12);

R_Date("AA-82408", 953, 46);

R_Date("AA-75121", 952, 41);

R_Date("AA-83934", 951, 42);

R_Date("AA-75823", 951, 42);

Curve("IntCal13","IntCal13.14c");

R_Date("Beta-178665", 950, 60);

R_Date("Beta-87603", 950, 60);

R_Date("Beta-136324", 950, 40);

Curve("IntCal13","IntCal13.14c");

Curve("Marine13","Marine13.14c");

Mix_Curve("Mixed","IntCal13","Marine13",50,12);

R_Date("AA-75144", 941, 44);

Curve("IntCal13","IntCal13.14c");

R_Date("Beta-247738", 940, 40);

R_Date("Beta-247739", 940, 40);
```

```
R_Date("Beta-77174", 940, 60);
R_Date("Beta-178661", 940, 60);
Curve("IntCal13","IntCal13.14c");
Curve("Marine13","Marine13.14c");
Mix_Curve("Mixed","IntCal13","Marine13",50,12);
R_Date("AA-83928", 935, 44);
R_Date("AA-75143", 932, 44);
Curve("IntCal13","IntCal13.14c");
R_Date("Beta-178679", 930, 40);
R_Date("Beta-136328", 930, 40);
Curve("IntCal13","IntCal13.14c");
Curve("Marine13","Marine13.14c");
Mix_Curve("Mixed","IntCal13","Marine13",50,12);
R_Date("AA-83931", 927, 45);
Curve("IntCal13","IntCal13.14c");
R_Date("Beta-178662", 910, 40);
R_Date("Beta-87600", 910, 60);
Curve("IntCal13","IntCal13.14c");
Curve("Marine13","Marine13.14c");
Mix_Curve("Mixed","IntCal13","Marine13",50,12);
R_Date("AA-75800", 907, 45);
R_Date("AA-82412", 904, 44);
Curve("IntCal13","IntCal13.14c");
```

```
R_Date("GrN-24761", 900, 60);
Curve("IntCal13","IntCal13.14c");
Curve("Marine13","Marine13.14c");
Mix_Curve("Mixed","IntCal13","Marine13",50,12);
R_Date("AA-82413", 900, 44);
Curve("IntCal13","IntCal13.14c");
R_Date("Beta-110631", 900, 60);
Curve("IntCal13","IntCal13.14c");
Curve("Marine13","Marine13.14c");
Mix_Curve("Mixed","IntCal13","Marine13",50,12);
R_Date("AA-72889", 893, 41);
Curve("IntCal13","IntCal13.14c");
R_Date("GrN-24766", 890, 30);
R_Date("Beta-109679", 890, 40);
R_Date("AA-79346", 885, 44);
R_Date("GrN24762", 880, 40);
R_Date("Beta-103329", 880, 50);
Curve("IntCal13","IntCal13.14c");
Curve("Marine13","Marine13.14c");
Mix_Curve("Mixed","IntCal13","Marine13",50,12);
R_Date("AA-83932", 873, 42);
Curve("IntCal13","IntCal13.14c");
R_Date("UGM-30028", 870, 40);
```

```
R_Date("Beta-87604", 870, 80);
Curve("IntCal13","IntCal13.14c");
Curve("Marine13","Marine13.14c");
Mix_Curve("Mixed","IntCal13","Marine13",50,12);
R_Date("AA-79401", 870, 44);
Curve("IntCal13","IntCal13.14c");
R_Date("GrN-24763", 860, 40);
R_Date("Beta-272022", 860, 40);
Curve("Marine13","Marine13.14c");
R_Date("I-15429", 860, 80);
R_Date("I-15430", 850, 80);
Curve("IntCal13","IntCal13.14c");
R_Date("Beta-81849", 840, 60);
R_Date("Beta-77175", 830, 80);
Curve("IntCal13","IntCal13.14c");
Curve("Marine13","Marine13.14c");
Mix_Curve("Mixed","IntCal13","Marine13",50,12);
R_Date("AA-83926", 829, 45);
R_Date("AA-75825", 804, 43);
R_Date("AA-78481", 798, 45);
R_Date("Beta-220581", 790, 40);
Curve("IntCal13","IntCal13.14c");
R_Date("GrN-16414", 790, 50);
```

```
R_Date("GrN-24757", 760, 70);
R_Date("Beta-198876", 750, 40);
Curve("IntCal13","IntCal13.14c");
Curve("Marine13","Marine13.14c");
Mix_Curve("Mixed","IntCal13","Marine13",50,12);
R_Date("AA-83925", 735, 44);
Curve("IntCal13","IntCal13.14c");
R_Date("UGM-30045", 730, 35);
R_Date("Beta-178675", 730, 40);
Curve("IntCal13","IntCal13.14c");
Curve("Marine13","Marine13.14c");
Mix_Curve("Mixed","IntCal13","Marine13",50,12);
R_Date("AA-79403", 725, 43);
Curve("IntCal13","IntCal13.14c");
R_Date("Beta-386072", 720, 30);
R_Date("GrN-30058", 710, 40);
Curve("IntCal13","IntCal13.14c");
Curve("Marine13","Marine13.14c");
Mix_Curve("Mixed","IntCal13","Marine13",50,12);
R_Date("AA-75802", 710, 43);
Curve("IntCal13","IntCal13.14c");
R_Date("Beta-272031", 710, 40);
Curve("IntCal13","IntCal13.14c");
```

```
  Curve("Marine13","Marine13.14c");
  Mix_Curve("Mixed","IntCal13","Marine13",50,12);
  R_Date("AA-72877", 699, 52);
  Curve("IntCal13","IntCal13.14c");
  R_Date("I-15407", 690, 80);
  R_Date("GrN-24758", 680, 50);
  R_Date("GrN-24765", 680, 40);
  R_Date("GrN-26412", 650, 25);
  R_Date("UGM-30019", 640, 45);
  R_Date("Beta-77177", 640, 60);
  R_Date("GrN-30052", 640, 30);
  R_Date("GrN-30053", 630, 40);
  R_Date("UGM-30039", 630, 20);
  R_Date("UGM-30043", 630, 50);
  R_Date("Beta-178664", 630, 40);
  R_Date("Beta-77183", 630, 50);
  R_Date("GrN-30051", 625, 25);
 };
 Boundary("Puerto Rico End");
};
};
```

San Salvador

```
Plot()
 {
  Sequence("San Salvador")
  {
   Boundary("San Salvador Start");
   Phase()
   {
    Curve("Marine13","Marine13.14c");
    R_Date("UM-2275", 1384, 65);
    Curve("IntCal13","IntCal13.14c");
    R_Date("YSU #3", 1130, 40);
    Curve("Marine13","Marine13.14c");
    R_Date("UGa-00836", 1054, 37);
    R_Date("AA-51432", 1028, 34);
    Curve("IntCal13","IntCal13.14c");
    R_Date("YSU #1", 840, 40);
    R_Date("UM-2244", 660, 100);
    R_Date("UM-2274", 620, 70);
    R_Date("UM-2273", 580, 90);
    R_Date("Beta-16732", 530, 65);
    R_Date("YSU #4", 470, 60);
    R_Date("Beta-105988", 450, 50);
    R_Date("YSU #2", 350, 70);
```

```
  R_Date("UM-2271", 305, 75);
  Curve("Marine13","Marine13.14c");
  R_Date("UM-2245", 425, 75);
 };
 Boundary("San Salvador End");
};
};
```

St. Eustatius

```
Plot()
{
 Sequence("St. Eustatius")
 {
  Boundary("St. Eustatius Start");
  Phase()
  {
   Curve("IntCal13","IntCal13.14c");
   Curve("Marine13","Marine13.14c");
   Mix_Curve("Mixed","IntCal13","Marine13",50,12);
   R_Date("Ua-1488", 1735, 220);
   Curve("IntCal13","IntCal13.14c");
   R_Date("GrN-11512", 1755, 20);
   R_Date("GrN-11513", 1635, 20);
```

```
    R_Date("GrN-11510", 1545, 35);
    R_Date("GrN-11509", 1415, 30);
    R_Date("GrN-11514", 1350, 60);
    R_Date("GrN-11516", 1340, 20);
    R_Date("GrN-17074", 1325, 30);
    R_Date("GrN-17075", 1260, 30);
    R_Date("GrN-11517", 1210, 20);
    R_Date("GrN-11515", 1205, 30);
   };
   Boundary("St. Eustatius End");
  };
 };
```

St. John

```
Plot()
 {
  Sequence("St. John")
  {
   Boundary("St. John Start");
   Phase()
   {
    Curve("IntCal13","IntCal13.14c");
    R_Date("Beta-17080", 1630, 100);
```

```
 R_Date("Beta-32239", 1460, 80);
 R_Date("Beta-16647", 1210, 80);
 Curve("IntCal13","IntCal13.14c");
 Curve("Marine13","Marine13.14c");
 Mix_Curve("Mixed","IntCal13","Marine13",50,12);
 R_Date("Beta-27793", 1170, 80);
 Curve("IntCal13","IntCal13.14c");
 R_Date("Beta-192223", 1160, 40);
 R_Date("Beta-192224", 1140, 40);
 R_Date("Beta-25891", 1130, 70);
 R_Date("Beta-59781", 1120, 100);
 R_Date("Beta-20605", 1050, 60);
 R_Date("Beta-59780", 970, 80);
 R_Date("Beta-18513", 970, 70);
 R_Date("Beta-26964", 900, 100);
 Curve("IntCal13","IntCal13.14c");
 Curve("Marine13","Marine13.14c");
 Mix_Curve("Mixed","IntCal13","Marine13",50,12);
 R_Date("Beta-191882", 840, 40);
 Curve("IntCal13","IntCal13.14c");
 R_Date("Beta-19863", 660, 60);
};
Boundary("St. John End");
```

```
 };
};
```

St. Lucia

```
Plot()
 {
  Sequence("St. Lucia")
  {
   Boundary("St. Lucia Start");
   Phase()
   {
    Curve("IntCal13","IntCal13.14c");
    R_Date("Y-1115", 1460, 80);
    R_Date("Y-650", 1220, 100);
    Curve("Marine13","Marine13.14c");
    R_Date("RL-30", 1240, 100);
    R_Date("RL-31", 1120, 100);
    Curve("IntCal13","IntCal13.14c");
    Curve("Marine13","Marine13.14c");
    Mix_Curve("Mixed","IntCal13","Marine13",50,12);
    R_Date("GrN-46607", 1000, 40);
    R_Date("GrN-32330", 960, 35);
    R_Date("GrN-32324", 920, 25);
```

```
  R_Date("GrN-32326", 865, 35);
  R_Date("GrN-32328", 820, 35);
  R_Date("GrN-32325", 790, 35);
  R_Date("GrN-32319", 770, 35);
  R_Date("GrN-31944", 750, 30);
  R_Date("GrN-32327", 745, 30);
  R_Date("GrN-32314", 740, 30);
  R_Date("GrN-32317", 725, 35);
  R_Date("GrN-32315", 720, 35);
  Curve("IntCal13","IntCal13.14c");
  R_Date("GrN-46604", 645, 35);
  Curve("IntCal13","IntCal13.14c");
  Curve("Marine13","Marine13.14c");
  Mix_Curve("Mixed","IntCal13","Marine13",50,12);
  R_Date("GrN-32329", 620, 40);
 };
 Boundary("St. Lucia End");
};
};
```

St. Martin

```
Plot()
{
```

```
Sequence("St. Martin")
{
 Boundary("St. Martin Start");
 Phase()
 {
  Curve("Marine13","Marine13.14c");
  R_Date("KIA-28815", 4830, 40);
  R_Date("KIA-28108", 4770, 40);
  R_Date("KIA-28116", 4505, 35);
  R_Date("KIA-28115", 4275, 30);
  R_Date("Erl-9066", 4200, 50);
  Curve("IntCal13","IntCal13.14c");
  R_Date("KIA-28121", 3828, 27);
  Curve("Marine13","Marine13.14c");
  R_Date("KIA-28114", 3800, 30);
  R_Date("KIA-28112", 3775, 30);
  R_Date("Erl-9071", 3750, 50);
  Curve("IntCal13","IntCal13.14c");
  R_Date("KIA-28123", 3684, 27);
  R_Date("KIA-28119", 3655, 25);
  Curve("Marine13","Marine13.14c");
  R_Date("Erl-9072", 3610, 50);
  Curve("IntCal13","IntCal13.14c");
```

```
R_Date("KIA-28124", 3598, 29);
Curve("Marine13","Marine13.14c");
R_Date("Beta-41782", 3580, 90);
Curve("IntCal13","IntCal13.14c");
R_Date("Erl-9074", 3515, 45);
Curve("Marine13","Marine13.14c");
R_Date("Erl-9073", 3510, 50);
Curve("IntCal13","IntCal13.14c");
R_Date("Beta-190805", 3490, 40);
Curve("Marine13","Marine13.14c");
R_Date("Erl-9064", 3460, 50);
R_Date("Beta-187936", 3450, 40);
Curve("IntCal13","IntCal13.14c");
R_Date("KIA-28126", 3447, 26);
R_Date("KIA-28127", 3429, 35);
Curve("Marine13","Marine13.14c");
R_Date("KIA-28111", 3380, 40);
Curve("IntCal13","IntCal13.14c");
R_Date("KIA-28120", 3366, 27);
Curve("Marine13","Marine13.14c");
R_Date("Erl-9065", 3340, 50);
R_Date("KIA-28113", 3320, 30);
R_Date("Beta-224793", 3240, 60);
```

```
Curve("IntCal13","IntCal13.14c");
R_Date("KIA-28125", 3235, 26);
Curve("Marine13","Marine13.14c");
R_Date("KIA-28110", 3185, 30);
Curve("IntCal13","IntCal13.14c");
R_Date("Beta-187937", 3140, 40);
Curve("Marine13","Marine13.14c");
R_Date("KIA-28109", 3105, 30);
Curve("IntCal13","IntCal13.14c");
R_Date("KIA-28117", 3095, 23);
R_Date("KIA-28118", 2951, 52);
Curve("Marine13","Marine13.14c");
R_Date("Beta-146427", 2850, 60);
Curve("IntCal13","IntCal13.14c");
R_Date("Beta-224792", 2610, 40);
R_Date("PITT-0450", 2510, 40);
R_Date("Beta-145372", 2420, 40);
R_Date("PITT-0449", 2300, 55);
R_Date("PITT-0219", 2275, 60);
R_Date("Beta-146425", 2270, 40);
R_Date("PITT-0220", 2250, 45);
R_Date("PITT-0446", 2250, 45);
Curve("IntCal13","IntCal13.14c");
```

```
Curve("Marine13","Marine13.14c");
Mix_Curve("Mixed","IntCal13","Marine13",50,12);
R_Date("Erl-8235", 2070, 50);
Curve("IntCal13","IntCal13.14c");
R_Date("PITT-0448", 2050, 45);
R_Date("Beta-146424", 2020, 40);
R_Date("Beta-106230", 1960, 60);
R_Date("Beta-82159", 1910, 50);
Curve("Marine13","Marine13.14c");
R_Date("KIA-32785", 1900, 25);
Curve("IntCal13","IntCal13.14c");
R_Date("Beta-82156", 1870, 60);
Curve("Marine13","Marine13.14c");
R_Date("Beta-187941", 1810, 40);
Curve("IntCal13","IntCal13.14c");
R_Date("Beta-82158", 1800, 50);
R_Date("Beta-82157", 1800, 60);
R_Date("Beta-106228", 1770, 50);
R_Date("LGQ-1099", 1760, 160);
R_Date("Beta-82160", 1760, 50);
R_Date("Beta-82154", 1710, 60);
R_Date("Beta-106233", 1710, 70);
R_Date("Beta-106229", 1670, 50);
```

```
R_Date("PITT-0452", 1660, 55);
R_Date("Beta-106232", 1650, 70);
R_Date("LGQ-1098", 1610, 150);
R_Date("Beta-82153", 1590, 70);
Curve("Marine13","Marine13.14c");
R_Date("KIA-28963", 1585, 25);
Curve("IntCal13","IntCal13.14c");
R_Date("Beta-187940", 1560, 40);
R_Date("Beta-106231", 1560, 60);
R_Date("Beta-82155", 1540, 50);
Curve("Marine13","Marine13.14c");
R_Date("Beta-187938", 1540, 40);
Curve("IntCal13","IntCal13.14c");
R_Date("GrN-20170", 1535, 30);
R_Date("GrN-20168", 1530, 30);
R_Date("GrN-20169", 1520, 35);
R_Date("KIA-28122", 1494, 26);
R_Date("PITT-0445", 1490, 35);
Curve("Marine13","Marine13.14c");
R_Date("Beta-200098", 1330, 60);
Curve("IntCal13","IntCal13.14c");
R_Date("Ly-9163", 1230, 30);
R_Date("GrN-20161", 1225, 30);
```

```
  R_Date("GrN-20160", 1180, 30);
  R_Date("GrN-20162", 1170, 30);
  Curve("Marine13","Marine13.14c");
  R_Date("GrN- 20164", 1170, 30);
  Curve("IntCal13","IntCal13.14c");
  R_Date("Beta-82165", 1000, 50);
  Curve("IntCal13","IntCal13.14c");
  Curve("Marine13","Marine13.14c");
  Mix_Curve("Mixed","IntCal13","Marine13",50,12);
  R_Date("Ly-2019(OxA)", 895, 30);
  Curve("IntCal13","IntCal13.14c");
  R_Date("Ly-11437", 890, 30);
  R_Date("Ly-11435", 890, 30);
 };
 Boundary("St. Martin End");
};
};
```

St. Thomas

```
Plot()
 {
  Sequence("St. Thomas")
  {
```

```
Boundary("St. Thomas Start");
Phase()
{
 Curve("Marine13","Marine13.14c");
 R_Date("I-8640", 2830, 85);
 R_Date("Beta-7022", 2860, 70);
 Curve("IntCal13","IntCal13.14c");
 R_Date("Beta-111459", 2710, 120);
 R_Date("I-8641", 2775, 85);
 Curve("Marine13","Marine13.14c");
 R_Date("SI-5851", 2700, 65);
 R_Date("L-1380B", 2410, 60);
 R_Date("I-621", 2400, 175);
 R_Date("I-620", 2175, 160);
 R_Date("SI-5850", 2130, 60);
 Curve("IntCal13","IntCal13.14c");
 R_Date("Beta-108917", 2090, 50);
 R_Date("Beta-111462", 1980, 50);
 Curve("Marine13","Marine13.14c");
 R_Date("L-1380A", 1900, 70);
 R_Date("SI-5848", 1805, 75);
 Curve("IntCal13","IntCal13.14c");
 R_Date("Beta-65474", 1800, 80);
```

```
R_Date("GX-12845", 1770, 235);
R_Date("Beta-108888", 1720, 140);
R_Date("Beta-50066", 1610, 70);
Curve("Marine13","Marine13.14c");
R_Date("SI-5849", 1595, 75);
Curve("IntCal13","IntCal13.14c");
R_Date("Beta-65472", 1580, 50);
R_Date("Beta-65473", 1570, 60);
R_Date("Beta-54646", 1560, 90);
R_Date("CAMS-10696", 1550, 50);
R_Date("Beta-108889", 1500, 50);
R_Date("Beta-62568", 1430, 90);
R_Date("Beta-62569", 1400, 120);
Curve("IntCal13","IntCal13.14c");
Curve("Marine13","Marine13.14c");
Mix_Curve("Mixed","IntCal13","Marine13",50,12);
R_Date("Beta-88345", 1390, 40);
R_Date("Beta-83011", 1390, 40);
R_Date("Beta-83003", 1390, 30);
Curve("IntCal13","IntCal13.14c");
R_Date("Beta-62570", 1380, 90);
Curve("IntCal13","IntCal13.14c");
Curve("Marine13","Marine13.14c");
```

```
Mix_Curve("Mixed","IntCal13","Marine13",50,12);
R_Date("Beta-83000", 1330, 30);
R_Date("Beta-83001", 1330, 30);
Curve("IntCal13","IntCal13.14c");
R_Date("Beta-65469", 1310, 60);
Curve("IntCal13","IntCal13.14c");
Curve("Marine13","Marine13.14c");
Mix_Curve("Mixed","IntCal13","Marine13",50,12);
R_Date("Beta-83009", 1300, 30);
R_Date("Beta-83006", 1280, 40);
R_Date("Beta-73392", 1190, 60);
R_Date("Beta-83010", 1090, 30);
Curve("IntCal13","IntCal13.14c");
R_Date("Beta-49751", 1040, 150);
R_Date("Beta-48742", 810, 140);
R_Date("Beta-43437", 810, 70);
R_Date("Beta-42277", 730, 80);
R_Date("Beta-51355", 720, 120);
R_Date("Beta-111461", 650, 50);
Curve("IntCal13","IntCal13.14c");
Curve("Marine13","Marine13.14c");
Mix_Curve("Mixed","IntCal13","Marine13",50,12);
R_Date("Beta-73390", 640, 60);
```

```
R_Date("Beta-73394", 630, 60);
R_Date("Beta-73393", 600, 60);
R_Date("Beta-83005", 600, 30);
R_Date("Beta-73395", 590, 90);
R_Date("Beta-73391", 580, 60);
Curve("IntCal13","IntCal13.14c");
R_Date("Beta-51354", 560, 120);
Curve("IntCal13","IntCal13.14c");
Curve("Marine13","Marine13.14c");
Mix_Curve("Mixed","IntCal13","Marine13",50,12);
R_Date("Beta-88347", 560, 40);
Curve("IntCal13","IntCal13.14c");
R_Date("Beta-111452", 560, 80);
Curve("IntCal13","IntCal13.14c");
Curve("Marine13","Marine13.14c");
Mix_Curve("Mixed","IntCal13","Marine13",50,12);
R_Date("Beta-83008", 540, 30);
R_Date("Beta-83004", 500, 30);
R_Date("Beta-109071", 480, 50);
R_Date("Beta-88348", 470, 40);
R_Date("Beta-88349", 460, 40);
R_Date("Beta-109070", 450, 50);
R_Date("Beta-88346", 390, 40);
```

```
    R_Date("Beta-109072", 380, 50);
    R_Date("Beta-83007", 340, 30);
    R_Date("Beta-88344", 300, 40);
   };
   Boundary("St. Thomas End");
  };
 };
```

Tobago

```
Plot()
 {
  Sequence("Tobago")
  {
   Boundary("Tobago Start");
   Phase()
   {
    Curve("IntCal13","IntCal13.14c");
    R_Date("Beta-15351", 2700, 40);
    R_Date("Beta-15936", 1750, 40);
    R_Date("Beta-172211", 1700, 40);
    R_Date("Y-1336", 1300, 120);
    R_Date("Beta-172209", 1180, 40);
    R_Date("Beta-153150", 1170, 40);
```

```
   R_Date("Beta-172210", 1110, 40);
   R_Date("Beta-153149", 900, 40);
   Curve("IntCal13","IntCal13.14c");
   Curve("Marine13","Marine13.14c");
   Mix_Curve("Mixed","IntCal13","Marine13",50,12);
   R_Date("Beta-221321", 850, 40);
   R_Date("Beta-221319", 810, 40);
   R_Date("Beta-221320", 810, 40);
   Curve("IntCal13","IntCal13.14c");
   R_Date("Beta-4905", 760, 105);
   R_Date("Beta-129265", 600, 50);
   R_Date("Beta-129262", 590, 40);
   R_Date("Beta-129264", 550, 40);
  };
  Boundary("Tobago End");
 };
};
```

Trinidad

```
Plot()
 {
  Sequence("Trinidad")
  {
```

```
Boundary("Trinidad Start");
Phase()
{
 Curve("IntCal13","IntCal13.14c");
 R_Date("IVIC-888", 7180, 80);
 R_Date("UGa-14460", 7030, 25);
 R_Date("UGa-12303", 6890, 30);
 R_Date("IVIC-889", 6780, 70);
 R_Date("UGa-14459", 6370, 25);
 R_Date("IVIC-891", 6190, 100);
 R_Date("IVIC-887", 6170, 90);
 R_Date("UGa-14458", 6100, 25);
 R_Date("IVIC-890", 6100, 90);
 R_Date("IVIC-783", 5650, 100);
 R_Date("UGa-14457", 5300, 25);
 R_Date("Y-260-1", 2750, 130);
 R_Date("IVIC-642", 2140, 70);
 R_Date("IVIC-638", 2130, 80);
 R_Date("I-6444", 2120, 135);
 R_Date("IVIC-641", 2060, 70);
 R_Date("IVIC-640", 1990, 70);
 R_Date("Beta-196708", 1920, 40);
 R_Date("Beta-196709", 1880, 40);
```

```
R_Date("IVIC-643", 1850, 80);
R_Date("Beta-4902", 1805, 90);
R_Date("Beta-4899", 1755, 150);
R_Date("Beta-134571", 1720, 50);
R_Date("IVIC-786", 1720, 90);
R_Date("Beta-4903", 1680, 115);
R_Date("Beta-196706", 1650, 40);
R_Date("GrA-13865", 1590, 40);
R_Date("Beta-189113", 1570, 40);
R_Date("OxA-19174", 1538, 29);
R_Date("Beta-296724", 1490, 30);
R_Date("IVIC-639", 1480, 70);
R_Date("Beta-296723", 1400, 30);
R_Date("Beta-4904", 1350, 85);
R_Date("Beta-4901", 1300, 110);
R_Date("IVIC-785", 1260, 100);
R_Date("GrA-13867", 1220, 40);
R_Date("Beta-296726", 1210, 30);
R_Date("ISGS-A2628", 1210, 15);
R_Date("Beta-4900", 1145, 65);
R_Date("Beta-6807", 1130, 50);
R_Date("Beta-4898", 1040, 260);
Curve("Marine13","Marine13.14c");
```

```
    R_Date("Beta-6809", 990, 50);
    Curve("IntCal13","IntCal13.14c");
    R_Date("Beta-196707", 740, 40);
    R_Date("Beta-6808", 650, 50);
    Curve("IntCal13","IntCal13.14c");
    Curve("Marine13","Marine13.14c");
    Mix_Curve("Mixed","IntCal13","Marine13",50,12);
    R_Date("Beta-193442", 630, 40);
    Curve("IntCal13","IntCal13.14c");
    Curve("Marine13","Marine13.14c");
    Mix_Curve("Mixed","IntCal13","Marine13",50,12);
    R_Date("Beta-193443", 620, 40);
    Curve("IntCal13","IntCal13.14c");
    R_Date("I-10766", 540, 75);
    R_Date("ISGS-A2629", 410, 20);
    R_Date("ISGS-A2630", 385, 20);
   };
   Boundary("Trinidad End");
  };
 };
```

Vieques

```
Plot()
```

```
{
 Sequence("Vieques")
 {
  Boundary("Vieques Start");
  Phase()
  {
   Curve("Marine13","Marine13.14c");
   R_Date("I-18971", 4095, 80);
   R_Date("I-6406", 3850, 100);
   R_Date("I-16899", 3780, 100);
   R_Date("I-6397", 3530, 100);
   R_Date("I-6396", 3510, 100);
   R_Date("I-16897", 3470, 100);
   R_Date("I-6395", 2790, 100);
   R_Date("I-16898", 2770, 90);
   R_Date("I-6407", 2740, 100);
   R_Date("I-16896", 2650, 90);
   Curve("IntCal13","IntCal13.14c");
   R_Date("I-16153", 2590, 90);
   Curve("Marine13","Marine13.14c");
   R_Date("Beta-276588", 2240, 40);
   Curve("IntCal13","IntCal13.14c");
   R_Date("I-13425", 2110, 80);
```

```
R_Date("I-11322", 1945, 80);
R_Date("I-11319", 1915, 80);
R_Date("I-12859", 1880, 80);
Curve("Marine13","Marine13.14c");
R_Date("Beta-259140", 1840, 50);
Curve("IntCal13","IntCal13.14c");
R_Date("I-11321", 1845, 80);
R_Date("I-10979", 1820, 85);
R_Date("I-12858", 1820, 80);
R_Date("I-12856", 1810, 80);
R_Date("Beta-129948", 1810, 60);
R_Date("I-11139", 1800, 80);
R_Date("I-12860", 1780, 80);
R_Date("I-11320", 1770, 80);
R_Date("I-11685", 1740, 75);
R_Date("I-10980", 1735, 85);
R_Date("I-11140", 1730, 80);
R_Date("I-11926", 1720, 80);
R_Date("I-11141", 1705, 80);
R_Date("I-16151", 1700, 80);
R_Date("I-11925", 1665, 80);
R_Date("I-16152", 1650, 80);
R_Date("I-12744", 1640, 80);
```

```
R_Date("I-16154", 1620, 80);
R_Date("I-11317", 1615, 75);
R_Date("I-12746", 1600, 80);
R_Date("I-16174", 1600, 80);
R_Date("I-16173", 1590, 80);
R_Date("I-12857", 1580, 80);
R_Date("I-11686", 1575, 80);
R_Date("I-10547", 1575, 85);
R_Date("I-11687", 1565, 75);
R_Date("I-11927", 1565, 80);
R_Date("I-12745", 1560, 80);
R_Date("I-11316", 1555, 75);
Curve("Marine13","Marine13.14c");
R_Date("I-10549", 1525, 85);
Curve("IntCal13","IntCal13.14c");
R_Date("I-10550", 1505, 85);
R_Date("I-11318", 1490, 75);
R_Date("I-16175", 1450, 80);
R_Date("I-10548", 1440, 85);
R_Date("I-16176", 1270, 90);
R_Date("I-14813", 1180, 80);
R_Date("I-12743", 950, 80);
R_Date("I-12742", 900, 80);
```

```
  R_Date("I-11189", 790, 85);
  R_Date("I-15189", 790, 80);
  R_Date("I- 15188", 700, 80);
  R_Date("I-15188", 700, 70);
  R_Date("I-15187", 690, 80);
  R_Date("I-15239", 660, 80);
  R_Date("I-15240", 630, 80);
  R_Date("I-15238", 570, 80);
  R_Date("I-15185", 540, 80);
  R_Date("I-15186", 520, 80);
  R_Date("I-15658", 470, 80);
  R_Date("I-15657", 410, 80);
  R_Date("I-11142", 405, 75);
 };
 Boundary("Vieques End");
};
};
```

Table 2. Originally reported sample materials with current taxonomic identification.

Original reported sample type	Current taxonomic identification
Strombus gigas	*Lobatus gigas*
Eustrombus gigas	*Lobatus gigas*
Oliva recticularis/reticularis	*Americoliva reticularis*
Xancus angulatus	*Turbinella* sp.
Lucina pectinatus/pectinata	*Phacoides pectinatus* or *Ctena Mexicana*
Livonia pica	*Cittarium pica* or *Livona* sp.
Lima scabra	*Ctenoides scaber*
agouti	*Dasyprocta* sp.
iguana	*Iguana* sp.
peccary	*Tayassu/pecari* sp.
Astraea tuber	*Astraea* sp.

Table 3. Radiocarbon laboratory abbreviation, name, and country of operation. Asterisk denotes laboratories no longer in operation.

Prefix	Laboratory Name	Country
A-	University of Arizona	USA
AA-	University of Arizona; National Science Foundation	USA
AAINA	Lab is IVIC, but reported as AAINA	Venezuela
Alpha-	Alpha Analytic	USA
ARC-	A.E. Lalonde AMS Laboratories, University of Ottawa	Canada
Beta-	Beta Analytic	USA
CAMS-	Center for Accelerated Mass Spectrometry	USA
CSIS	Instituto Rocasola, Instituto Superior de Investigaciones Científicas	Spain
DIC-*	Dicar Corp and Dicarb Radioisotope Company	USA
Erl-*	Erlangen AMS Facility	Germany
Esso-*	Esso Research and Engineering Company	USA
FS AC*	Igneis(?)	Argentina(?)
GD-*	Gdansk	Poland
GrA-	Groningen Accelerator	The Netherlands
GrN-*	Groningen	The Netherlands
GX-	Geochron Laboratories	USA
I-*	Teledyne Isotopes	USA
ICA	International Chemical Analysis, Inc.	USA
IGS-*	Institute of Geological Science	Sweden
IVIC-*	Caracas	Venezuela
KIA-	Kiel AMS	Germany
Kreuger Ent.	Geochron Laboratories Kreuger Enterprises Isotopic	USA
L-*	Lamont-Doherty	USA

LC-H-	University of Bern, Laboratory of Radiochemistry and Environmental Chemistry, Paul Scherrer Institute	USA
LE-	Leningrad	Russia
LGQ-	Laboratoire de Géologie du Quaternaire, CNRS, Marseilles	France
Lv-*	Louvain-la-Neuve	Belgium
Ly-	University of Lyon	France
MC-*	Centre Scientifique de Monaco	Monaco
Mo-*	Verdanski Inst. of Geochemistry, Moscow	Russia
N-	Rikagaku Laboratories	Japan
Ny-*	Nancy, Centre de Recherches Radiogéologiques	France
O-*	Humble Oil & Refining	USA
ORAU-	Oxford Radiocarbon Accelerator Unit	England
OS-	NOSAMS Woods Hole	USA
OxA-	Oxford Radiocarbon Accelerator Unit	England
PITT-*	University of Pittsburgh	USA
Poz-	Poznán	Poland
PSUAMS-	Penn State University Radiocarbon ^{14}C Laboratory	USA
RL-*	Radiocarbon, Ltd.	USA
S-*	Saskatchewan	Canada
SI-*	Smithsonian Institution	USA
SUERC-	Scottish Universities Environmental Research Centre	Scotland
TO-	IsoTrace Laboratory	Canada
Tx-*	Texas	USA
Ua-	Uppsala Accelerator	Sweden
UBAR-*	University of Barcelona	Spain
UCI-	University of California, Irvine	USA
UCLA-*	University of California, Los Angeles	USA
Uga-	Center for Applies Isotope Studies, the University of Georgia	USA
UGAMS	Center for Applies Isotope Studies, the University of Georgia	USA
UM-*	University of Miami	USA
WK-	University of Waikato	New Zealand
X-*	Whitworth College	USA
Y-*	Yale University	USA
YSU-*	Youngstown State University	USA

Table 4. Bibliographic information for radiocarbon dates.

Author(s)	Publication Year	Title	Book/Volume Title/Journal; Publisher
Allsworth-Jones, Philip	2008	*Pre-Columbian Jamaica*	Tuscaloosa: University of Alabama Press
Anderson, David G., David W. Knight, and Emily M. Yates	2003	The Archaeology and History of Water Island, U.S. Virgin Islands	Report prepared for Office of Insular Affairs, U.S. Department of Interior, Washington D.C.
Angelbello, Sylivia T.	2002	Fincas azucareras enclavadas en la zona del Central Trinidad. Cronología y Patrimonio Cultural	IV Evento Nacional de Patrimonio Histórico Azucarero. Matanzas, Cuba.
Antczak, M. Magdalena, Andrezej Antczak, and J.B. Haviser	1991	Arqueologia Prehistorica Del Archipielago de Los Roques, Venezuela: Informe Preliminar	In *Proceedings of the 13th Congress of the the International Association for Caribbean Archaeology*, edited by E.N. Ayubi, 494–508. Curaçao: Reports of the Archaeological-Anthropological Institute of the Netherlands Antilles.
Atiles, Gabriel, and Adolfo López	2006	El Sitio Arqueologico La Punta de Bayahibe: Primeros Agricultores Tempranos de Las Antillas Asentados En La Costa Sureste de La Isla de Santo Domingo	Dominican Republic: Editora de Revistas, 537–51.
Ayubi, E.W.	1990	The Study of the Aesthetic Aspects of the Precolumbian Pottery of Aruba, Curacao & Bonaire	In *Proceedings of the 11th Congress of the International Association of Caribbean Archaeology*, Puerto Rico 1985, pp. 128-140.
Bain, Allison, Anne-Marie Faucher, Lisa M. Kennedy, Allison R. LeBlanc, Michael J. Burn, Rebecca Boger, and Sophia Perdikaris	2017	Landscape Transformation During Ceramic Age and Colonial Occupations of Barbuda, West Indies	*Environmental Archaeology* doi: 10.1080/1461403.2017.1345115
Banks, T.J.	1988	Archaeological Excavation at the Grand Anse Beach Site, Grenada, W.I., Foundation for Field Research.	Report on file at the Grenada National Museum, St. George's, Grenada.
Bates, Brian David	2001	Ceramic Period Settlement in the Virgin Island Group, United States and British Virgin Islands	PhD Dissertation, London, United Kingdom: University of London.
Berard, Benoit	2007	The 'South-Dominica' archaeological Mission: The Soufrière Site	In *Proceedings of the 22nd Congress of the International Association of Caribbean Archaeology*. Kingston, Jamaica: Jamaica National Heritage Trust.
Berman, Mary Jane, and Perry L. Gnivecki	1991	The Colonization of the Bahamas Archipelago: A View from the Three Dog Site, San Salvador Island	In *Proceedings of the 14th Congress of the International Association for Caribbean Archaeology*, 170–86. Barbados: The Barbados Museum and Historical Society.
Berman, Mary Jane, and Perry L Gnivecki	1995	The Colonization of the Bahama Archipelago: A Reappraisal	*World Archaeology* 26 (3): 421–41.
Blick, Jeffrey, B. Rathcke, and W. Hayes	2007	A New Projectile Point Type from Barker's Point Shell Midden (SS-37), San Salvador, Bahamas	In *Proceedings of the Eleventh Symposium on the Natural History of the Bahamas*, 158–169. San Salvador: Gerace Research Center.
Bonnissent, Dominique	1998	Les Caractéristiques de La Céramique Du Site de Hope Estate, Île de Saint-Martin	In *Proceedings of the 16th International Congress for the Archaeology of the Caribbean*, 333–45. Guadeloupe: Conseil Régional de la Guadeloupe, Mission Archéologique et du Patrimoine.
Bonnissent, Dominique	2008	Archéologie Précolombienne de L'île de Saint-Martin, Petites, Antilles (3300 BC–1600 AD)	PhD Dissertation, Marseille, France: Université de Provence, Aix-Marseille I.

Bonnissent, D., P. Bertran, A. Chancerel, S. Grouard, T. Romon, N. Serrand, C. Stouvenot, and C. Tardy	2002	Les sites de la Baie Orientale. Occupations précéramiques et post-Saladoïde, Saint-Martin, Guadeloupe, Petites Antilles	Document Final de Synthèse auprès du Service Régional d'Archéologie de Guadeloupe.
Bonnissent, D., P. Bertran, A. Chancerel, T. Romon, N. Serrand, and C. Tardy	2001	Saint-Martin, Baie Orientale	*Bilan Scientifique* 2000: 43–51.
Bonnissent, D., and C. Stouvenot	2005	Un site d'habitat postsaladoïde dans les Terres Basses (Plum Bay): Baie aux Prunes (Saint-Martin, Petites Antilles)	In *Proceedings of the 20th Congress of the International Association for Caribbean Archaeology*, edited by Clenis Tavárez María and Manuel A. García Arévalo, 31–39. Santo Domingo: Museo del Hombre Domincano and Fundación García Arévalo.
Bonnissent, D., N. Serrand, L. Bruxelles, P. Fouéré, S. Grouard, N. Sellier-Ségard, and C. Stouvenot	2016	Archéoécologie des Sociétés Insulaires des Petites Antilles au Mésoindien. L'enjeu des Ressources à Saint-Martin.	*Séances de la Société Préhistorique Française de Rennes* 6:213-60.
Boomert, A	1985	The Guayabitoid and Mayoid Series: Amerindian Culture History in Trinidad during Late Prehistoric and Protohistoric Times	In *Proceedings of the 10th Congress of the International Association for Caribbean Archaeology*, 93-148. Montréal: Centre de Recherches Caraïbes.
Boomert, Arie	2000	*Trinidad, Tobago and the Lower Orinoco Interaction Sphere: An Archaeological/Ethnohistorical Study*	Leiden: Leiden University.
Boomert, Arie, Angus A.A. Mol, Corinne L. Hofman, Menno L.P. Hoogland, Jason E. Laffoon, and Jimmy L.J.A. Mans	2017	Archaeological rescue investigations at the multi-component indigenous site of Brighton Beach: New insights into the cultural history of St. Vincent and The Grenadines	In *Proceedings of the 26th Congress of the International Association of Caribbean Archaeology*, edited by C.B. Velasquez and J.B. Haviser. SIMARC Heritage Series No. 15, Sint Maarten.
Bright, Alistair J	2011	*Blood Is Thicker than Water: Amerindian Intra- and Inter-Insular Relationships and Social Organization in the Pre-Colonial Windward Islands*	Leiden: Sidestone Press.
Brock, Fiona, Joanna Ostapkowicz, Christopher Bronk Ramsey, Alex Wiedenhoeft, and Caroline Cartwright	2012	Paired Dating of Pith and Outer Edge (Terminus) Samples from Pre-Hispanic Caribbean Wooden Sculptures	*Radiocarbon* 54 (3–4): 677–88.
Bullen, Adelaide K., and Ripley P. Bullen	1970	The Lavoutte Site, St. Lucia: A Carib Ceremonial Centre	In *Proceedings of the 3rd International Congress for the Study of Pre-Columbian Cultures of the Lesser Antilles*, 61–86. Grenada: Grenada National Museum.
Bullen, Ripley P., and Adelaide K. Bullen	1972	Archaeological Investigations of St. Vincent and the Grenadines, West Indies	Orlando, Florida: Wm. L. Bryant Foundation, American Studies.
Bullen, Ripley P. and Adelaide K. Bullen	1968	Barbados Archaeology: 1966	In *Proceedings of the Second International Congress for the Study of the Pre-Columbian Cultures of the Lesser Antilles*, edited by Ripley P. Bullen, 134–44. Barbados: Barbados Musem.
Bullen, Ripley P., and Frederick W. Sleight	1963	The Krum Bay Site: A Preceramic Site on St. Thomas, US Virgin Islands	William L. Bryant Foundation for American Studies Report 5. William L. Bryant Foundation for American Studies Report.

Caesar, M., Caesar, P., and Lungberg, E	1991	The Calabash Boom Site, St. John, USVI: Preliminary Report	In *Proceedings of the Twelfth Congress of the International Association for Caribbean Archaeology*, edited by Robinson, L.S., 203–16. Martinique: International Association for Caribbean Archaeology.
Carlson, Lisabeth Anne	1999	Aftermath of a Feast: Human Colonization of the Southern Bahamian Archipelago and Its Effects on the Indigenous Fauna	PhD Dissertation, University of Florida: Gainesville.
Carlson, Lisabeth A., and David W. Steadman	2009	Examining Temporal Differences in Faunal Exploitation at Two Ceramic Age Sites in Puerto Rico	*The Journal of Island and Coastal Archaeology* 4 (2): 207–22.
Carlson, Lisabeth A., Christopher F. Altes, Darell S. Gundrum	2017	Manatee exploitation at the Early Ostinoid site of CE-34, Eastern Puerto Rico	In *Proceedings of the 26th Congress of the International Association of Caribbean Archaeology*, edited by C.B. Velasquez and J.B. Haviser. SIMARC Heritage Series No. 15, Sint Maarten.
Casto, Kara I.	2015	Spatial Analysis of Archaeological Assemblages from the Late Ceramic Age (AD 400-1400) site of Grand Bay, Carriacou, West Indies.	M.A. Thesis, University of South Florida: Tampa.
Chanlatte-Baik, Luis A., Narganes, Yvonne M	1980	La Hueca Vieques: Nuevo Complejo Cultural Agroalfarero En La Arqueologia Antillana	In *Proceedings of the Eighth International Congress for the Study of the Pre-Columbian Cultures of the Lesser Antilles*, edited by Lewenstein, Suzanne M., 501–23. Tempe: Arizona State University.
Cinquino, Michael A., Michele H. Hayward, and Inez Reed Hoffman	1999	1994 Excavations at the Aklis Site, Sandy Point National Wildlife Refuge, St. Croix, U.S.V.I.	In *Proceedings of the 16th Congress of the International Association for Caribbean Archaeology*, edited by G. Richard, 67–82. Guadeloupe.
Clark, Jeffrey J., Walker, Jeff, and Rodrigues-Ramos, Reniel	2003	Depositional History and Evolution of the Paso Del Indio Site, Vega Baja, Puerto Rico	*Geoarchaeology* 18 (6): 625–48.
Clerc, Edgar	1968	Sites précolombiens de la côte nord-est de la Grande-Terre de Guadeloupe	In *Proceedings of the Second International Congress for the Study of Pre-Columbian Cultures in the Lesser Antilles*, 47–60. Barbados: Barbados Museum.
Cody, A.K.	1991	From the Site of Pearls, Grenada: Exotic Lithics & Radiocarbon Dates	In *Proceedings of the XIII Congress of the International Association for Caribbean Archaeology*, edited by Haviser Ayubi, E.N. J.B. Curacao: Archaeological-Anthropological Institute of the Netherlands Antilles.
Cody Holdren, A.K.	1998	Raiders and Traders: Caraïbe social and political networks at the time of European contact and colonization in the Eastern Caribbean	PhD dissertation, University of California Los Angeles.
Colten, Roger H., Elizabeth Terese Newman and Brian Worthington	2009	Preceramic Faunal Exploitation at the Las Obas Site, Cuba	Bulletin of the Peabody Museum of Natural History 50(1): 75-84.
Colten, Roger H., and Brian Worthington	2014	Faunal Remains from the Archaic and Archaic with Ceramic Site of Vega Del Palmar, Cuba	*Journal of Caribbean Archaeology* 14: 23–49.
Colten, Roger H., and Brian Worthington	2019	Museum collections and Archaic era vertebrate faunal remains from Cuba	Environmental Archaeology 24 (2):211-227.
Conolley, Ivor C.		Montego Bay Pottery and Cultura in Western Jamaica: Significance and Implications for Jamaican Taino Pre-History	PhD Dissertation, The University of the West Indies: Mona.
Conrad, Geoffrey W., John W. Foster, and Charles D. Beeker	2001	Organic Artifacts from the Manantial de La Aleta, Dominican Republic: Preliminary Observations and Interpretations	*Journal of Caribbean Archaeology* 2: 1–20.

Cooper, Jago, and Kenneth D. Thomas	2012	Constructing Caribbean Chronologies: Comparative Radiocarbon Dating of Shell and Wood Artefacts from pre-Columbian Sites in Cuba	*Archaeometry* 54 (2): 401–25.
Crock, John Gordon	2001	*Interisland Interaction and the Development of Chiefdoms in the Eastern Caribbean*	Pittsburgh, Pennsylvania: University of Pittsburgh.
Crock, John Gordon, James B. Petersen, and Nik Douglas	1995	Preceramic Anguilla: A View from the Whitehead's Bluff Site	In *Proceedings of the Fifteenth Annual Congress for Caribbean Archaeology*, edited by R.E. Alegria and M. Rodriguez, 15:283–92. San Juan, Puerto Rico: Centro de Estudios Avanzados de Puerto Rico y el Caribe.
Crock, John G., Petersen, J.B.	2001	Stratified Sites and Storm Events: The Formation and Destruction of Beach Sites in Anguilla, West Indies	In *Proceedings of the Nineteenth Congress of the International Congress of the International Association of Caribbean Archaeology*, edited by Dijkhoff Alofs, L. R.A.C.F., 204–13. Aruba: Publications of the Archaeological Museum Aruba.
Cruxent, Jose	1965	IVIC-241	*American Journal of Science*, Radiocarbon 9: 243.
Curet, L.A.	2010	The Archaeological Project of the Ceremonial Center of Tibes	*Tibes: People, Power, and Ritual at the Center of the Cosmos*, edited by Stringer Curet, L.A. L.M., 38–59. Tuscaloosa: University of Alabama Press.
Curet, L. Antonio, Lee A. Newsom, and Susan D. deFrance	2006	Prehispanic Social and Cultural Changes at Tibes, Puerto Rico	*Journal of Field Archaeology*, no. 31: 1.
Dacal Moure, Ramón and Manuel Rivero de la Calle	1997	*Art and Archaeology of Pre-Columbian Cuba*	Pittsburgh: University of Pittsburgh Press.
Dávila Dávila, Ovidio	2003	Arqueología de la isla de Mona	San Juan: Instituto de Cultura Puertorriqueña.
Davis, Dave D	1982	Archaic Settlement and Resource Exploitation in the Lesser Antilles: Preliminary Information from Antigua	*Caribbean Journal of Science* 17 (1–4): 107–22.
Davis, Dave D	1988	Calibration of the Ceramic Period Chronology for Antigua, West Indies	*Southeastern Archaeology* 7 (1): 52–60.
Davis, Dave D	2000	Jolly Beach and the Preceramic Occupation of Antigua, West Indies	Yale University Publications in Anthropology 84. New Haven, Connecticut: The Yale Peabody Museum.
Davis, Dave, and Kevin Oldfield	2003	Archaeological Reconnaissance of Anegada, British Virgin Islands	*Journal of Caribbean Archaeology* 4: 1–27.
Davis, Deborah Diane	2011	Out of the Shadows: A Review of the Archaeological Evidence for the Isolation, Interaction, and Abandonment of the British Virgin Islands in the Pre-Columbian Caribbean	Master's Thesis, Leicester: University of Leicester.
Deagan, Kathleen	2004	Reconsidering Taíno Social Dynamics after Spanish Contact: Gender and Class in Culture Contact Studies	American Antiquity 69 (4): 597–626.
Deevey, Edward, LJ Gralenski, and Vaino Hoffren	1959	Yale Natural Radiocarbon Measurements, [Part] 4	*Radiocarbon* 1 (1): 144–72.
Delsol, Nicolas, and Sandrine Grouard	2016	Comments on Amerindian Hunting Practices in Trinidad (West Indies): Tetrapods From the Manzanilla Site (Late Ceramic Age 300–900 AD)	*The Journal of Island and Coastal Archaeology* 11(3): 385-410.
Doran, Glen H.	1990	Osteological Analysis of the Human Skeletal Remains from the Aklis Site, St. Croix, Virgin Islands	Report to the National Park Service NADB 550819. Atlanta, Georgia: Interagency Archeological Service.

Douglas, Nik	1991	Recent Amerindian Finds on Anguilla	In *Proceedings of the 13th Congress of the International Association for Caribbean Archaeology*, edited by Edwin N. Ayubi and Jay B. Haviser, 576–88. Willemstad: Archaeological-Anthropological Institute of the Netherlands Antilles.
Drewett, Peter L.	1989	Early Ceramic Population Lifeways and Adaptive Strategies in Barbados	*Early Ceramic Population Lifeways and Adaptive Strategies in the Caribbean*, edited by Peter E. Siegel, 79–118. B.A.R.
Drewett, Peter	1991	*Prehistoric Barbados*	London, UK: Institute of Archaeology, University of London.
Drewett, Peter L.	2000	Prehistoric Settlements in the Caribbean: Fieldwork in Barbados, Tórtola and the Cayman Islands	Bridgetown, Barbados: Barbados Museum and Historical Society.
Drewett, Peter L.	2006	Dating the Prehistoric Settlement of Barbados	*The Journal of the Barbados Museum and Historical Society* 52: 202–14.
Drewett, Peter L.	1993	Excavations at Heywoods, Barbados, and the Economic Basis of the Suazoid Period in the Lesser Antilles	Proceedings of the Prehistoric Society 59: 113–37.
Dunning, Nicholas P., John G. Jones, Neil A. Duncan, Deborah M. Pearsall, and Peter E. Siegel	2018a	Curaçao	In *Island Historical Ecology: Socionatural landscapes of the eastern and southern Caribbean*, edited by Peter E. Siegel, 155-181. New York, Berghan.
Dunning, Nicholas P., John G. Jones, Deborah M. Pearsall, and Peter E. Siegel	2018b	Barbados	In *Island Historical Ecology: Socionatural landscapes of the eastern and southern Caribbean*, edited by Peter E. Siegel, 182-202. New York, Berghan.
Eldridge, K. L.; J. J. Stipp, and J. Hattner	1976	University of Miami Radiocarbon Dates V	*Radiocarbon* 18(1): 116-124
Espenshade, Christopher	2014	The Cultural Landscape of Jácana: Archaeological Investigations of Site PO-29, Municipio de Pone, Puerto Rico	US Army Corps of Engineers, Jackonsville District.
Faucher, Anne-Marie, Elise-Audrée Guay, and Allison Bain	2011	Archaeobotanical Studies on Barbuda, Preliminary Results from 2011	New York: Barbuda Archaeological Research Center.
Figueredo, Alfredo E.	1976	Caño Hondo, Un Residuario Precerámico En La Isla de Vieques	In *Proceedings of the 6th International Congress for the Study of Pre-Columbian Cultures of the Lesser Antilles*, edited by Ripley P. Bullen, 247–52. Gainesville: Florida State Museum, University of Florida.
Fitzpatrick, Scott	2006	A Critical Approach to Dating in the Caribbean: Using Chronometric Hygiene to Evaluate Chronological Control and Prehistoric Settlement	*Latin American Antiquity* 17 (4): 389–418.
Fitzpatrick, Scott M.	2011	Verification of an Archaic Age Occupation on Barbados, Southern Lesser Antilles	*Radiocarbon* 53: 595–604.
Fitzpatrick, Scott M., and Christina M. Giovas	2011	New Radiocarbon Dates for the Grenadine Islands (West Indies)	*Radiocarbon* 53 (3): 451–60.
Fitzpatrick, Scott M., Quetta Kaye, and Michiel Kappers	2004	A Radiocarbon Sequence for the Sabazan Site, Carriacou, West Indies	*Journal of Caribbean Archaeology* 5: 1–11.
Frank, E.F.	1998	A Radiocarbon Date of 380+/-60 for a Taino Site Negra, Isla de Mona, Puerto Rico	*Journal of Cave and Karst Studies* 60: 101–2.

Friðriksson, A., G. Gudmundsson, F. Feeley, V. Rousseau, O. Vésteinsson, J. Vobornick, and T. MicGovern	2011	Investigations at the RIVER Site (BAA 004) Field Report	Unpublished Field Report. New York: City University of New York
Fouéré, P., Sa. Sailon, D. Bonnissent, A. Chancerel, P. Courtaud, M.-F. Deguilloux, S. Grouard, A. Lenoble, P. Mora, J. Monney, K. Pinçon, A. Queffelec, and C. Stouvenout	2015	La Grotte de Morne Rita, Capesterre de Marie-Galante (Guadeloupe): Nouvelles Données.	Paper presented at the 26th Congress of the International Association for Caibbean Archaeology, 20-24 July, Sint Maarten.
Richard, Gerard	1994	Premier Indice D'une Occupation Preceramique En Guadeloupe Continentale	*Journal de La Societe Des Americanistes* 80 (1): 241–42
Giovas, Christina M., Meagan Clark, Scott M. Fitzpatrick, and Jessica Stone	2013	Intensifying Collection and Size Increase of the Tessellated Nerite Snail (Nerita Tessellata) at the Coconut Walk Site, Nevis, Northern Lesser Antilles, AD 890–1440	*Journal of Archaeological Science* 40 (11): 4024–38.
Giovas, Christina M., Michelle J. LeFebvre, and Scott M. Fitzpatrick	2012	New records for prehistoric introduction of Neotropical mammals ot the West Indies: evidence from Carriacou, Lesser Antilles.	*Journal of Biogeography* 39(3): 476-87.
Godo Torres, P.P.	1994	Industrias de La Concha Y de La Piedra No Lascada Del Sitio Arqueologico Mesolitico Victoria I, Provincia de Camaguey	*Estudios Arqueologicos*, edited by Dominguez Febles, J. L., 140–65. La Habana: Editorial Academia.
Godo, P.P.	2001	Contextos Arqueológicos del Protoagrícola en el Centro Occidente de Cuba	*El Caribe Arqueológico* 5:62-75
Goodwin, Christopher R.	1978	The Lesser Antillean Archaic: New Data from St. Kitts	*Journal of the Virgin Islands Archaeological Society* 5: 6–16.
Gould, Stephen J.	1971	The Paleontology and Evolution of Cerion II: Age and Fauna of Indian Shell Middens on Curaçao and Aruba	*Breviora* 372: 1–26.
Gross, Jeffrey M.	1976	The Archaic Period of the Virgin Islands: New Investigations	In *Proceedings of the 6th Congress of the International Association for Caribbean Archaeology*, 232–38. Gainesville: Florida State Museum, University of Florida.
Grouard, Sandrine, Bonnissent, Dominique, Fouere Courtard, Patrice Pierrick, Richard Lenoble, Arnaud Gerard, Serrand Romon, Thomas Nathalie, and Stouvenot, Christian	2014	Frequentation Amerindienne Des Cavites Des Petites Antilles	*Archeologie Caraibe*, edited by Losier Berard, Benoit Catherine, 277–95. Leiden: Sidestone Press.
Hackenberger, Steven	1988	An Abstract of Archaeological Investigations by the Barbados Museum, 1986	*Journal of the Barbados Museum and Historical Society* 38 (2): 155–162.
Hanna, Jonathan A.	2019	Camáhogne's chronology: The radiocarbon settlement sequence on Grenada, West Indies	Journal of Anthropological Archaeology 55:101075.
Hansen, Tiffany	2015	Bioarchaeology, Barbados, Eastern Caribbean: Isotopic analyses of teeth and bone from human remains	Thesis, Science Honors Research Program, Central Washington University.
Harris, Peter O.B.	1973	Preliminary Report on Banwari Trace, a Preceramic Site in Trinidad	In *Proceedings of the 4th International Congress for the Study of Pre-Columbian Cultures of the Lesser Antilles*, 115–25. Castries, St. Lucia: St. Lucia Archaeological and Historical Society.

Harvey, Virginia L., Victoria M. Egerton, Andrew T. Chamberlain, Phillip L. Manning, and Michael Buckley	2016	Collagen Fingerprinting: A New Screening Technique for Radiocarbon Dating Ancient Bone	*PLoS ONE* 11(3): e0150650.
Hastings, Alexander K., John Krigbaum, David W. Steadman, and Nancy A. Albury	2014	Domination by Reptiles in a Terrestrial Food Web of the Bahamas Prior to Human Occupation	*Journal of Herpetology* 48(3): 380-388.
Haviser, Jay B.	1985	Prehistoric Human Remains on Curacao	In *Proceedings from the XI International Congress for Caribbean Archaeology*, edited by Iraida Vargas Arenas Agamemnon Gus Pantel Tekakis and Mario Sanoja, 11–21. Puerto Rico: La Fundación Arqueológica, Antropológica e Histórica de Puerto Rico.
Haviser, Jay B.	1987	Amerindian Cultural Geography of Curaçao	PhD Dissertation, Leiden, Netherlands: Leiden University.
Haviser, Jay B.	1988	An Archaeological Survey of St. Martin-St. Maarten	Institute of Archaeology and Anthropology of the Netherlands Antilles (AAINA).
Haviser, Jay B.	1991	Preliminary Results from Test Excavations at the Hope Estate Site (SM-026), St. Martin	In *Proceedings from the Thirteenth International Congress of Caribbean Archaeology*, edited by Haviser Ayubi, E.N. J.B., 647–66. Curacao: Archaeological-Anthropological Institute of the Netherlands Antilles.
Haviser, Jay B.	1997	Settlement Strategies in the Early Ceramic Age.	In *The Indigenous Peoples of the Caribbean*, edited by Samuel Wilson, pp. 59-69. University Press of Florida, Gainesville.
Haviser, Jay B.	2001	New Data for the Archaic Age on Curaçao	In *Proceedings of the 19th Congress of the International Association for Caribbean Archaeology*, 9:110–23. edited by Dijkhoff Alofs, L. R.A.C.F.Aruba: Publications of the Archaeological Museum Aruba.
Haviser, Jay B.	2010	The 'Old Netherlands Style' and Seventeenth-Century Dutch Fortifications of The Caribbean	In *First Forts*, Edited by Eric Kingelhofer, pp. 167-188, Brill: Leiden.
Haviser, Jay B., and	1995	Excavations at the Zuurzac site: A possible 17th century Dutch slave camp on Curaçao, Netherlands Antilles	In *Proceedings of the 15th International Congress for Caribbean Archaeology*, pp. 71-82. Centro de Estudios Avanzados de Puerto Rico y el Caribe, San Juan, Puerto Rico.
Hayward, Michele H., and Michael A. Cinquino	2002	Archaeological Investigations at the Aklis Site. Sandy Point National Wildlife Refuge, St. Croix, U.S. Virgin Islands	SEAC Technical Reports 10. Tallahassee, Florida: Southeast Archaeological Center.
Healy, Paul F., and A Reg. Murphy	1995	Excavations at the Muddy Bay Site (PH-14), Antigua: Preliminary Report on the 1994 Investigations	In *Proceedings of the 16th Congress of the International Association for Caribbean Archaeology*, 287–99. Basseterre, Guadeloupe: Archaeological Mission for Patrimony.
Healy, Paul F., A. Reg Murphy, and David M. Cruz	2001	Excavations at the Royall's Site (Jo-11), Antigua: An Inland Saladoid Settlement	In *Proceedings of the 18th Congress of the International Association for Caribbean Archaeology*, 216–32. St. George, Grenada: l'Association Internationale des Archéologues de la Caraïbe Région, Guadeloupe.
Healy, Paul F., Keenleyside, A., and Dorst, M.C.	2013	Isotope Analysis and Radiocarbon Dating of Prehistoric Human Bone from the Manzanilla (SAN 1) Site, Trinidad	*Caribbean Connections* 3 1: 30–45.

Healy, Paul F., Thornton, Erin, and Fuess, Martin T.	2003	The Post Saladoid Faunal Assemblage from The Coconut Hall Site, Antigua, West Indies	In *Proceedings of the Twentieth International Congress for Caribbean Archaeology*, edited by Garcia Arevale Tavarez, C. M.A., 20–22. Santo Domingo: Museo del Hombre Dominicano and Fundacion Garcia Arevalo.
Heidecker, L., and M.I. Siegel	1969	Preliminary Report on the Excavation Henrıquez-I Site, Tanki Flip, Aruba, Netherland Antilles	*The Florida Anthropologist* 22: 12–26.
Hénocq, Christophe	1995a	Saint-Martin. Anse Des Peres. Bilan Scientifique de La Region Guadeloupe. 1992-1994	Service Regional de l'Archeologie. Ministere de la Culture et de la Francophonie. Direction du Patrimoine.
Hénocq, Christophe	1995b	Saint-Martin. Baie Orientale. Bilan Scientifique de La Region Guadeloupe. 1992-1994	Service Regional de l'Archeologie. Ministere de la Culture et de la Francophonie. Direction du Patrimoine.
Hénocq, Christophe, and François Petit	1998	Présentation de six sites archéologiques de Saint-Martin et de leur environnement	In *Proceedings of the 16th Congress of the International Association for Caribbean Archaeology*, edited by G. Richard, 300–315. Basseterre, Guadeloupe: Editions du Ponant.
Hénocq, Christophe	1998	Baie Rouge, Gisement Archéologique Tardif de Saint-Martin	In *Proceedings of the 16th Congress of the International Association for Caribbean Archaeology*, edited by G. Richard, 316–32. Basseterre, Guadeloupe: Editions du Ponant.
Higham, Thomas FG, Christopher Bronk Ramsey, Fiona Brock, D Baker, and P Ditchfield	2007	Radiocarbon Dates from the Oxford AMS System: Archaeometry Datelist 32	*Archaeometry* 49 (s1): S1–60.
Hofman, Corinne L.	1993	In Search of the Native Population of Precolumbian Saba (400-1450 A.D.) Part One. Pottery Styles and Their Implications	PhD Dissertation, Leiden, The Netherlands: Leiden University.
Hofman, Corinne L.	1995	Grande Anse, Terre-de-Bas, Guadeloupe	Rapport de fouille programmée, DRAC Guadeloupe 18. Leiden, Netherlands: University of Leiden.
Hofman, Corinne L., and Menno L.P. Hoogland	2003	Evidence for Archaic Seasonal Occupation on Saba, Northern Lesser Antilles around 3300 BP	*Journal of Caribbean Archaeology* 4: 12–27.
Hofman, Corinne L., Menno L.P. Hoogland, Hayley L. Mickleburgh, Jason E. Laffoon, Darlene A. Weston, and Mike H. Field	2012	Life and Death at Precolumbian Lavoutte, Saint Lucia, Lesser Antilles	*Journal of Field Archaeology* 37 (3): 209–25.
Hofman, Corinne L., Lewis Borck, Emma Slayton, and Menno L.P. Hoogland	2019	Archaic Age voyaging, networks and resource mobility around the Caribbean Sea	In *Early Settlers of the Insular Caribbean: Dearchaizing the Archaic*, edited by Corinne L. Hofman and Andrzej T. Antczak, 245-62. Leiden, Sidestone Press.
Hooghiemstra, Henry, Thomas Olijhoek, Menno Hoogland, Maarten Prins, Bas van Geel, Timme Donders, William Gosling, and Corinne Hofman	2018	Columbus' environmental impact in the New World: Land use change in the Yaque River Valley, Dominican Republic	The Holocene 28 (11): 1818-35.
Hoogland, Menno L.P.	1995	Sainte-Anne. Pointe Helleux. Bilan scientifique de la Région Guadeloupe. 1992-1992.	Direction Régional de L'Archéologie. Ministère de la Culture et de la Francophonie. Direction du Patriomonie. Sous-direction de l'Archéologie.

Hoogland, Menno L.P.	1999	Methods and Strategy, Part Three, Hope Estate	Archaelogical Investigations on St. Martin (Lesser Antilles). The Sites of Norman Estate, Anse Des Pères and Hope Estate with a Contribution to the" La Hueca Problem, 127–47. Leiden, Netherlands: Archaeological Studies, Leiden University Faculty of Archaeology.
Hoogland, Menno LP, and Corinne L. Hofman	2011	Archaeological Investigations at Spanish Water, Curaçao	In *Proceedings of the 23rd International Association for Caribbean Archaeology*, edited by R. Murphy, 631–639. Antigua.
Hoogland, M., Hofman, C.	1993	Kelbey's Ridge 2, A 14th Century Taino Settlement on Saba, Netherlands Antilles	*Analecta Praehistorica Leidensia* 26 26: 163–81.
Horn, Sally P., Kenneth H. Orvis, Lisa M. Kennedy, and G. Michael Clark	2000	Prehistoric Fires in the Highlands of the Dominican Republic: Evidence from Charcoal in Soils and Sediments	*Caribbean Journal of Science* 36 (1–2): 10–18.
Jew, Nicholas P., Scott M. Fitzpatrick, and Kelsey J. Sullivan	2016	δ^{18}O analysis of Donax denticulatus: Evaluating a proxy for sea surface temperature and nearshore paleoenvironmental reconstructions for the northern Caribbean	*Journal of Archaeological Science*: Reports 8: 216-223.
Jones, John G., Nicholas P. Dunning, Neil A. Duncan	2018a	Antigua	In *Island Historical Ecology: Socionatural landscapes of the eastern and southern Caribbean*, edited by Peter E. Siegel, 239–69. New York, Berghan.
Jones, John G., Nicholas P. Dunning, Neil A. Duncan, Deborah M. Pearsall, and Peter Siegel	2018b	Barbuda	In *Island Historical Ecology: Socionatural landscapes of the eastern and southern Caribbean*, edited by Peter E. Siegel, 270–84. New York, Berghan.
Keegan, William F.	1993	Inagua Archaeology	51. Miscellaneous Project Report. Florida Museum of Natural History, Department of Anthropology.
Keegan, William F.	2001	Archaeological investigations on Ile A Rat, Haiti: Avoid the oid	In Proceedings of the XVIII International Congress for Caribbean Archaeology 2: 233-239.
Keegan, William F., Roger W. Portell, and John Slapcinsky	2003	Changes in Invertebrate Taxa at Two Pre-Columbian Sites in Southwestern Jamaica, AD 800–1500	*Journal of Archaeological Science* 30 (12): 1607–17.
Kelly, Harold, and Corinne L. Hofman	2019	The Archaic Age of Aruba: New evidence on the first migrations to the island	In *Early Settlers of the Insular Caribbean: Dearchaizing the Archaic*, edited by Corinne L. Hofman and Andrzej T. Antczak, 147-62. Leiden, Sidestone Press.
Kendall, Aaron, Manigault, Norie, Schreiner Guðmundsson, Garðar Amanda, Williams Khalsa, Santmukh Lucretia, Riggle Witter, Lauren Rebecca, Olavarria Plummer, Jeanette Grissel, and Adkins, Rachel	2011	Preliminary Report of the 2011 Excavation at Seaview, Barbuda, Antigua/Barbuda	BARC Report 2011-4. New York: Barbuda Archaeological Research Center.
Kepecs, Susan L. Antonio Curet and Gabino La Rosa Corzo	2010	*Beyond the Blockade: New Currents in Cuban Archaeology*	2nd ed. Tuscaloosa, Alabama, USA: University of Alabama Press.
Kjellmark, Eric W., and Jeffrey P. Blick	2016	Analysis of a sediment core from Triangle Pond, San Salvador Island, Bahamas: Pollen, paleoclimate, human impacts, and insights into Lucayan Lifeways	in Glumac, Bosiljka and Michael Savarese (eds.) *The 16th Symposium on the Geology of the Bahamas and other Carbonate Regions*, Gerace Research Centre, San Salvador, Bahamas.

Knippenberg, S.	2001	Flint Collecting Strategies on Long Island	In *Proceedings of the 19th Congress of the International Association for Caribbean Archaeology*, edited by L. Alofs and R.A.C.F. Dijkhoff, 88–98. Oranjestad, Aruba: Archaeological Museum Aruba.
Kraan, Claudia, Amy Victorina, Scott M. Fitzpatrick, Taylor Dodrill, Maggie Gebhardt, Paul Gerard, Haden Kingrey, Natasha Minugh, Martin Nelson-Harrington and Mark Rempel	2017	New Archaeological Research on Curaçao	*The Journal of Island and Coastal Archaeology* 12(1): 138-144.
Lalueza-Fox, Carles, M. Thomas P. Gilbert, Antonio J. Martínez Fuentes, Francesc Calafell, and Jaume Bertranpetit	2003	Mitochondrial DNA from pre-Columbian Ciboneys from Cuba and the Prehistoric Colonization of the Caribbean	*American Journal of Physical Anthropology* 121 (2): 97–108.
Lane, Chad S., Sally P. Horn, and Kenneth H. Orvis	2008	The Earliest Evidence of Ostionoid Maize Agriculture from the Interior of Hispaniola	*Caribbean Journal of Science* 44 (1): 43–52.
Lazell, James	2005	*Island: Fact and Theory in Nature*	Berkeley, California: University of California Press.
Lenoble, Arnaud, Alain Bertrand, Laurant Charles, Jean-Bapstise Mallye, and Nathalie Serrand	2018	Quaternary occurrence of the rare land snail *Amphibulima patula* (Bruguière, 1789) in Guadeloupe (mollusca; amphibulimidae): ecological and paleoenvironmental implications	*Quaternaire* 29 (2):121-130.
Lopinot, Neal H.	2013	Summary of Archaeological Research by the Center for Archaeological Research, Missouri State University- March 21-April 3, 2013	The University of the West Indies.
Lopinot, Neal H. and Jack H. Ray	2018	Investigating Amerindian Occupations in the Northern Range of Trinidad	*Journal of Caribbean Archaeology* 18:34-69
Lundberg, Emily R.	1985	Interpreting the Cultural Associations of Aceramic Deposits in the Virgin Islands	*Journal of Field Archaeology* 12 (2): 201–12.
Lundberg, Emily R.	1989	*Preceramic Procurement Patterns at Krum Bay, Virgin Islands*	Ph.D. thesis, University of Illinois at Urbana-Champaign. University Microfilms International, Ann Arbor, MI.
Lundberg, Emily R.	2001	A Vessel-Analysis Approach to Early Ostionoid Pottery from Peter Bay, Virgin Islands	In *Proceedings of the 18th Congress of the International Association for Caribbean Archaeology*, 214–224. St. George, Guadeloupe: L'Association Internationale des Archéologues de la Caraïbe.
Lundberg, Emily R.	2002	Tutu Pottery and Ceramic Chronology	In *The Tutu Archaeological Village Site: A Multidisciplinary Case Study in Human Adaptation*, edited by Elizabeth Righter, 166–98. New York: Routledge.
Lundberg, Emily R.	2005	The Calabash Boom Site (VAm2-25), St. John, USVI: Phase II and III Cultural Resource Investigation of Parcel 3B-11 in Johnson Bay Estates	Report prepared for Robert L. Lechner and Mercedes K. C. Dullum, submitted to the Virgin Islands State Historic Preservation Office, St. Thomas, USVI.
Lundberg, Emily R., Elizabeth C. Righter, and Margaret D. Casesar	1992	The Late Ceramic Age in the Northern Virgin Islands	Paper presented at the 57th Annual Meeting of the Society for American Archaeology, April 11, 1992, Pittsburgh.
Veloz Maggiolo, Marcio	1975	*Cayo Cofresí, Un Sitio Precerámico de Puerto Rico*	Santo Domingo: Ediciones de Taller.
Martias, R.	2005	Saint-Martin, Étang Rouge 3. Lot 411 (97150 Guadeloupe), Les Terres Basses	Unpublished. Rapport de Diagnostic INRAP. DRAC Guadeloupe.

Martínez Fuentes, A., Lalueza Fox, C., Lazo Valdivia Gilbert, T. P. A., and Bertranpetit Callafell, F. J.	2003	El Poblamiento Antiguo Del Caribe. Analisis Del ADN Mitocondrial En Preagroalfareros de La Region Occidental de Cuba	*Catauro: Revista Cubana de Antropologia* 5 (8): 62–74.
Mielke, James E., and Austin Long	1969	Smithsonian Institution Radiocarbon Measurements V	*Radiocarbon* 11 (1): 163–82.
de Mille, Christy	2011	New Evidence and Understanding of the Antiguan Preceramic	In *Proceedings of the 23rd Congress of the International Association of Caribbean Archaeology*, 428–46. Antigua: Dockyard Museum.
de Mille, Christy, A. Reg Murphy, and Paul F. Healy	1999	Preliminary Archaeological Investigations at Winthorpe's Bay, Antigua	In *Proceedings of the 17th Congress of the International Association for Caribbean Archaeology*, edited by J.H. Winter, 105–21. Rockville Centre, New York: Molloy College.
Moore, Clark	1991	Cabaret: Lithic Workshop Sites in Haiti	9. Reports of the Archaeological-Anthropological Institute of the Netherlands Antilles.
Moore, C.R., and N. Tremmel	1997	Settlement Patterns in pre-Columbian Haiti: An Inventory of Archaeological Sites.	Manuscript in archive, Bureau National d'Etnologie, Port au Prince.
Morbán Laucer, F.	1979	Cronología de Radiocarbono (C-14) para la Isla de Santo Domingo	Boletín del Museo del Hombre Dominicano 12:147-159.
Morse, Birgit Faber, and Irving Rouse	1995	The Indian Creek Period: A Late Saladoid Manifestation on the Island of Antigua	In *Proceedings of the 16th Congress of the International Association of Caribbean Archaeology*, edited by G. Richard, 312–21. Basseterre, Guadeloupe.
Murphy, Arthur Reginald	1999	The Prehistory of Antigua, Ceramic Age: Subsistence, Settlement, Culture and Adaptation within an Insular Environment	PhD Dissertation, Calgary: University of Calgary.
Narganes Storde, Y.M.	1991	Los Restos Faunísticos Del Sitio de Puerto Ferro, Vieques, Puerto Rico	In *Proceedings of the 14th Congress of the International Association for Caribbean Archaeology*, 94–114. Barbados: Barbados Museum and Historical Society.
Narganes Storde, Yvonne M.	2005	Nueva Cronologia de Varios Sitios de Puerto Rico Y Vieques	In *Proceedings of the 21st Congress of the International Association for Caribbean Archaeology*, 275–94. St. Augustine, Trinidad: University of the West Indies.
Narganes Storde, Yvonne M.	2015	Sorcé, historia de una aldea Saladoide de pescadores	PhD Dissertation, Puerto Rico: Centro Estudios Avanzados de Puerto Rico y el Caribe.
Navarrete, Ramon	1990	Caimanes III: Arqueologia	Havana: Editorial de Ciencias Sociales.
Nicholson, Desmond V.	1975	Precolumbian Seafaring Capabilities in the Lesser Antilles	In *Proceedings of the 6th Congress of the International Association for Caribbean Archaeology*, edited by Ripley P. Bullen, 98–105. Gainesville, Florida: Florida State Museum, University of Florida.
Nieweg, D.C., and M.C. Dorst	2001	The Manzanilla 1 (SAN-1) Site, Trinidad	In *Proceedings of the 19th Congress of the International Association for Caribbean Archaeology*, 9:173–85. Oranjestand, Aruba: Archaeological Museum Aruba.
Nodine, Bruce K.	1990	Aceramic Interactions in the Lesser Antilles: Evidence from Antigua, West Indies	Las Vegas, Nevada.
Nold, Katherine D.	2018	Geological examination of archaeological middens in the Dominican Republic	PhD Dissertation, Bloomington, Indiana: Indiana University.

O'Day, Sharyn Jones, and William F. Keegan	2001	Expedient Shell Tools from the Northern West Indies	*Latin American Antiquity* 12 (3): 274–90.
Oliver, José R., Narganes Storde, Y.	2003	The Zooarcheaological Remains from Juan Miguel Cave and Finca de Doña Rosa, Barrio Caguana, Puerto Rico	In *Proceedings of the XV International Congress of Caribbean Archaeology*, edited by Arévalo Clenis, Tavárez María Manuel Antonio García, 227–42. Santo Domingo: Museo del Hombre Dominicano.
Oliver, José R., and Isabel Rivera Collazo	2015	A Reassessment of María de La Cruz Cave Site, Puerto Rico: The 2012 Excavations	In *Proceedings of the 25th International Congress of Caribbean Archaeology*, pp. 94-125. Instituto de Cultura Puertorriqueña, el Centro de Estudios Avanzados de Puerto Rico y el Caribe y la Universidad de Puerto Rico, Recinto de Río Piedras: San Juan.
Oliver, José R., and Juan Rivera Fontán	2007	Bateyes de Viví (U-1), Utuado, Puerto Rico: Archaeological Documentaion for its Inclusion in the NRHP	US Department of the Interior, National Park Service Cultural Resources
Olsen, Fred	1961	Arawak Campsites on Antigua	In *Proceedings of the First International Conference for the Study of Pre-Columbian Civilization in the Caribbean*, pp. 95-102. Société d'Histoire de la Martinique: Fort-de-France.
Olsen, Fred	1974	*Indian Creek; Arawak Site on Antigua, West Indies: 1973 Excavation by Yale University and the Antigua Archeological Society*	Norman, Oklahoma: University of Oklahoma Press.
Ortega, Elpidio, Gabriel Atiles, and Jorge Ulloa Hung	2003	Investigaciones Arqueológicas En El Yacimiento La Iglesia. Provincia La Altagracia, República Dominicana	In *Proceedings of the 20th Congress of the International Association of Caribbean Archaeology*, 407–16. Santo Domingo: Museo del Hombre Dominicano and Fundación García Arévalo.
Ostapkowicz, Joanna	2015	Either a piece of domestic furniture of the Indiands of one of their Gods: The study of Lucayan duhos	*Journal of Caribbean Archaeology* 15:62-101.
Ostapkowicz, Joanna, Christopher Bronk Ramsey, Alex C. Widenhoeft, Fiona Brock, Tom Highan, and Samuel M. Wilson	2011	This Relic of Antiquity': Fifth to fifteenth century wood carvings from the southern Lesser Antilles.	In *Communities in Contact: Essays in archaeology, ethnohistory and ethnography of the Amerindian circum-Caribbean.* Edited by Corinne L. Hofman and Anne van Dujvenbode, pp. 137-170. Sidestone Press: Leiden.
Ostapkowicz, Joanna, Christopher Bronk Ramsey, Fiona Brock, Caroline Cartwright, Rebecca Stacey, and Mike Richards	2013	Birdmen, Cemís and Duhos: Material Studies and AMS 14 C Dating of Pre-Hispanic Caribbean Wood Sculptures in the British Museum	*Journal of Archaeological Science* 40(12):4675-4687.
Ostapkowicz, Joanna, Christopher Bronk Ramsey, Fiona Brock, Thomas Higham, Alex C. Widenhoeft, Erika Ribechini, Jeanette J. Lucejko, and Samuel Wilson	2012	Chronologies in Wood and Resin: AMS 14 C Dating of Pre-Hispanic Caribbean Wood Sculpture	*Journal of Archaeological Science* 39 (7): 2238–51.
Pagán-Jiménez, Jaime R., Reniel Rodríguez-Ramos, Basil A. Reid, Martijn van den Bel, and Corinne L. Hofman	2015	Early Dispersals of Maize and Other Food Plants into the Southern Caribbean and Northeastern South America	*Quaternary Science Reviews* 123: 231–46.

Pantel, A.G.	1994	Evaluación de Recursos Culturales de Fase II. Yacimiento Precolombino Maruca, Barrio Canas. Municipio de Ponce, Puerto Rico	Submitted to the Cansejo para la Protección del Patrimonion Arqueológico Terrestre de Puerto Rico.
Payne, T.M.	1995	Research Progress Report, Robin Bay Site (12V Aml-27) St. Croix, U.S.V.I.: A Site in the Ceramic Age	In *Proceedings of the XV Congress of the International Association for Caribbean Archaeology*, edited by Miguel Rodriguez Ricardo E. Alegria, 15–40. San Juan: Asociacion Internacional de Arqueología del Caribe Centro de Estudios Avanzados de Puerto Rico y el Caribe
Pazdur, Anna, Romuald Awsiuk, Andrzej Bluszcz, M.F. Pazdur, Adam Walanus, and Andrzej Zastawny	1982	Gliwice Radiocarbon Dates VII	*Radiocarbon* 24 (2): 171–81
Pendergast, David M., Elizabeth Graham, R. Jorge Calvera, and M. Juan Jardines	2002	The Houses in Which They Dwelt: The Excavation and Dating of Taino Wooden Structures at Los Buchillones, Cuba	*Journal of Wetland Archaeology* 2 (1): 61–75.
Pestle, William J.	2010	Diet and Society in Prehistoric Puerto Rico: An Isotopic Approach	PhD Dissertation, Chicago, Illinois: University of Illinois at Chicago.
Pestle, William J.	2013	Fishing Down a Prehistoric Caribbean Marine Food Web: Isotopic Evidence From Punta Candelero, Puerto Rico	*The Journal of Island and Coastal Archaeology* 8: 228–54.
Petersen, James B., Robert N. Bartone, and David R. Watters	1999	Pyroclastic, Storm Surge, and Saladoid Villager Deposits: The Archaeological and Geological Stratigraphy of the Trants Site, Montserrat	In *Proceedings of the 16th Congress of the International Association for Caribbean Archaeology*, 40–51. Basseterre, Guadeloupe: Editions du Ponant.
Petersen, James B., and John G. Crock	2001	Late Saladoid to Late Prehistoric Occupation in Anguilla: Site Setting, Chronology and Settlement Hierarchy	In *Proceedings of the 18th Congress of the International Association for Caribbean Archaeology*, edited by Richard, G., 124–35. St. George, Grenada: L'Association Internationale des Archéologues de la Caraïbe Région Guadeloupe.
Petitjean-Roget, J.	1970	L'Archéologie Martiniquaise	*Parallèles* 36/37: 4-67.
Pino, M.	1995	*Actualizacion de Fechados Radiocarbónicos de Sitios Arqueológicos de Cuba Hasta Diciembre de 1993*	La Habana: Editorial Academia.
Ramcharan, Eugene K.	2004	Mid-to-late Holocene sea level inflluence on coastal wetland development in Trinidad	*Quaternary International* 120 (1): 145-151.
Ramcharan, Eugene K.	2005	Late Holocene ecological development of the Graeme Hall Swamp, Barbados, West Indies	*Caribbean Journal of Science* 41: 147-150.
Rankin, S.	1994	Estudio Del Sitio Arqueologico de 'Cabagan', Circuito Sur, Provincia de Santi Spiritus	*Estudio Arqueologicos*, edited by J. Febles, L. Dominguez, F. Ortega, F. La Rosa, A. Martinez, and A. Rives. Havana: Editorial Academia.
Reid, Basil	1992	Arawak Archaeology in Jamaica: New Approaches, New Perspectives	*Caribbean Quarterly* 38 (2–3): 15–20.
Richard, Gérard	1994	Premier Indice D'une Occupation Précéramique En Guadeloupe Continentale	*Journal de La Société Des Américanistes* 80: 241–42
Richard, Gérard	2003	The Archaeological Site Of Roseau's Seaside At Capesterre Belle Eau. Revealer Of Insular Carib's Occupation In Guadeloupe	In *Proceedings of the 20th Congress of the International Association for Caribbean Archaeology*, edited by Clenis Tavárez María and Manuel A. García Arévalo, 15–22. Santo Domingo: Museo del Hombre Dominicano and Fundación García Arévalo.

Righter, Elizabeth	2002	Post hole patterns: Structures, chronology and spatial distribution at the Tute site	In *The Tutu Archaeological Village Site: A Multidisciplinary Case Study in Human Adaptation*, edited by Elizabeth Righter, 284-341. New York: Routledge.
Rímoli, R., and J. Nadal	1983	*El Horizonte Ceramista Temprano en Santo Domingo y Otras Antillas*	Editorial de la Universidad Autónoma de Santo Domingo, Santo Domingo.
Rivera-Collazo, Isabel, Amos Winter, Denis Scholz, Augusto Magini, Thomas Miller, Yochanan Kushnir, and David Black	2015	Human Adaptation Strategies to Abrupt Climate Change in Puerto Rico Ca. 3.5 Ka.	*Holocene* 25 (4): 627–40.
Rodríguez, Miguel	1989	The Zoned Incised Crosshatch (ZIC) Ware of Early Precolumbian Ceramic Age Sites in Puerto Rico and Vieques Island	Early Ceramic Populatbn Lifways and Adaptive Strategies in the Caribbean, edited by Peter E. Siegel, 249–66. B.A.R.
Rodríguez, Miguel	1991	Arqueologica de Punta Candelero, Puerto Rico	In *Proceedings of the 13th International Congress of the International Association for Caribbean Archaeology*, 9:605–27. Willemstad, Curaçao: Archaeological-Anthropological Institute of the Netherlands Antilles
Rodríguez López, M.	2004	*Excavaciones en el Yacimiento Arcaico de Maruca, Ponce, Puerto Rico: Informe Final*	Consejo para la Protección del Patrimonio Arqueológico Terrestre de Puerto Rico, San Juan.
Rodríguez López, M., and Virginia Rivera	1991	Puerto Rico and the Caribbean Pre-Saladoïd 'Crosshatch Connection	In *Proceedings of the 12th Congress of the International Association for Caribbean Archaeology*, edited by Linda S. Robinson, 217–26. Fort-de-France, French Guiana: L'Association Internationale des Archéologues de la Caraïbe.
Rodríguez Ramos, Reniel	2017	La temporalidad absoluta del arte rupestre pictográfico en Puerto Rico	Report to Oficina Estatl de Conservacíon Histórica Proyecto subvencionado con un Historic Preservation Fund Grant (#2017-1550)
Rodríguez Ramos, Reniel	2014	La Ocupación Temprana del Interior Montañoso de Puerto Rico: Los Casos de Cueva Ventana y Salto Arriba	Report to Oficina Estatl de Conservacíon Histórica Proyecto subvencionado con un Historic Preservation Fund Grant (#2014-155062)
Rodriguez-Ramos, R., Torres, J., and Oliver, J.	2010	Rethinking Time in Caribbean Archaeology: The Puerto Rico Case Study	In *Island Shores, Distant Pasts: Archaeological and Biological Approaches to the Pre-Columbian Settlement of the Caribbean*, edited by Fitzpatrick, S.M., and A.H. Ross, 21–53. Gainesville: University Press of Florida.
Roksandic, Mirjana, William M. Buhay, Yadira Chinique des Armas, Roberto Rodríguez Suárez, Matthew C. Peros, Ivan Roksandic, Stephanie Mowat, et al.	2015	Radiocarbon and Stratigraphic Chronology of Canímar Abajo, Matanzas, Cuba	*Radiocarbon* 57 (5): 1–9.
Roobol, M.J., A.L. Smith, and S.M. Lewenstein	1980	Archaeological Implications of Some Radiocarbon Dating on Saba and St. Kitts	In *Proceedings of the 8th International Congress for the Study of the Pre-Colombian Cultures of the Lesser Antilles*, 22:168–176. Anthropological Research Papers. Tempe, Arizona: Arizona State University.
Rose, Richard	1982	The Pigeon Creek Site, San Salvador, Bahamas	*The Florida Anthropologist* 35(4): 129-145.

Rose, Richard	1987	Lucayan Lifeways at the Time of Columbus	In *Proceedings of the First San Salvador Conference Columbus and His World*, edited by D.T. Gerace, 321–39. Fort Lauderdale, Florida: CCFL Bahamian Field Station.
Rouse, Irving	1961	Archaeology in Lowland South America and the Caribbean, 1935-60	*American Antiquity* 27 (1): 56–62.
Rouse, Irving	1989	Peoples and Cultures of the Saladoid Frontier in the Greater Antilles	In *Early Ceramic Population Lifeways and Adaptive Strategies*, edited by P. E. Siegel, pp. 383–403. BAR International Series 506. British Archaeological Reports, Oxford.
Rouse, Irving	1963	Final Technical Report NSF-G24069: Dating of Caribbean Cultures	NSF-G2069. New Haven.
Rouse, Irving	1960	The Entry of Man into the West Indies	Vol. 61. Yale University Publications in Anthropology. New Haven: Yale University Press.
Rouse, Irving, and Ricardo E. Alegria	1990	Excavations at Maria de La Cruz Cave and Hacienda Grande Village Site, Loiza, Puerto Rico	New Haven, Connecticut: Yale University Publications in Anthropology.
Rouse, Irving, Louis Allaire, and C Meighan	1978	Caribbean	In *Chronologies in the New World*, edited by R Taylor, 432–78. New York, New York: Academic Press.
Rouse, Irving, and Brigit Faber Morse	1999	Excavations at the Indian Creek Site, Antigua, West Indies	New Haven, Connecticut: Yale University, Department of Anthropology and Peabody Museum of Natural History.
Rousseau, V.	2011	Preliminary Analyses from the River Site, Barbuda	BARC Report 2011-3. Universite du Laval.
Rousseau, V.	2012	Investigations at the Burton's Field (BuF12), and Cattle Field (CaF12) Sites, Barbuda Survey and Field Report, January 2012	New York: Barbuda Archaeological Research Center.
Samson, Alice Victoria Maud	2010	*Renewing the House: Trajectories of Social Life in the Yucayeque (Community) of El Cabo, Higüey, Dominican Republic, AD 800 to 1504*	Leiden: Sidestone Press.
Samson, Alice V.M., Lucy J. Wrapson, Caroline R. Cartwright, Diana Sahy, Rebecca J. Stacey, Jago Cooper	2017	*Artists before Columbus: A multi-method characterization of the material and practices of Caribbean cave art*	*Journal of Archaeological Science* 88: 24-36
Santos, Ana Luísa, Michael T. Gardner, and Philip Allsworth-Jones	2013	Treponematosis in Pre-Columbian Jamaica: A Biocultural Approach to the Human Cranium Found in Bull Savannah	*Journal of Archaeological Science* 40: 490–96.
Sara, Timothy R., Bruce J. Larson, William F. Keegan, Juan Jose Ortize Aguilú, Betsy Carlson, Lee Newsom and Rich Macphail	2007	An Archaeological Survey of U.S. Naval Station Guantanamo Bay, Cuba	In *Proceedings of the 21st Congress of the International Association for Caribbean Archaeology*, 177-190. St. Augustine, Trinidad: University of the West Indies.
Schaffer, William C., Robert S. Carr, J.S. Day, and M.P. Pateman	2012	Lucayan–Taíno Burials from Preacher's Cave, Eleuthera, Bahamas	*International Journal of Osteoarchaeology* 22 (1): 45–69.

Schroeder, Hannes, Martin Sikora, Shyam Gopalakrishnan, Lara M. Cassidy, Pierpaolo Maisano Delser, Marcela Sandoval Velasco, Joshua G. Schraiber, Simon Rasmussen, Julian R. Homburger, María C. Ávila-Arcos, Morten E. Allentoft, J. Víctor Moreno-Mayar, Gabriel Renaud, Alberto Gómez-Carballa, Jason E. Laffoon, Rachel J. A. Hopkins, Thomas F. G. Higham, Robert S. Carr, William C. Schaffer, Jane S. Day, Menno Hoogland, Antonio Salas, Carlos D. Bustamante, Rasmus Nielsen, Daniel G. Bradley, Corinne L. Hofman, and Eske Willerslev	2018	Origins and genetic legacies of the Caribbean Taino	*Proceedings of the National Academy of Sciences* 115 (10): 2341-6.
Scudder, Sylvia, and Irvy Quitmyer	1998	Evaluation of evidence of pre-Columbian human occupation at Great Cave, Cayman Brac, Cayman Islands	*Caribbean Journal of Science* 34:41-49.
Sellier-Ségard, N.	2016	COM Saint-Martin, Marigot, Rue Maurasse	Inrap. Rapport de diagnostic archéologique.
Sellier-Ségard, Nathalie, and Clara Samuelian	2017	Un village de bord de mer du Néoindian récent à grand-case (Saint Martin, Petites Antilles)	In *Proceedings of the 26th Congress of the International Association of Caribbean Archaeology*, edited by C.B. Velasquez and J.B. Haviser. SIMARC Heritage Series No. 15, Sint Maarten.
Serrand, N.	2009	Baie Nettlé, Pierre à Chaux, Saint-Martin, Petites Antilles, avec les Contributions de D. Todisco, P. Texier, F. Casagrande, O. Armand	Rapport d'opération de diagnostic archéologique, Inrap GSO DOM-TOM, Bègles, Service régional de l'archéologie de Guadeloupe.
Siegel, Peter E.	1996	Ideology and Culture Change in Prehistoric Puerto Rico: A View from the Community	*Journal of Field Archaeology* 23 (3): 313–33.
Serrand, N.	1999	Occurrence of Exogenous Freshwater Bivalves (Unionida) in the Lesser Antilles during the 1st Millennium AD: Example from the Hope Estate Saladoïde Site (St. Martin, French Lesser Antilles)	In *Proceedings of the 18th Congress of the International Association for Caribbean Archaeology*, 136–52. St. George, Grenada: L'Association Internationale des Archéologues de la Caraïbe Région Guadeloupe.
Shaklee, R., G. Fry, and T. Delvaux	2007	An Archaeological Report on the Storr's Lake Site, San Salvador	*Bahamas Naturalist and Journal of Science* 2(1): 31-39.
Shearn, Isaac	2014	Pre-Columbian Regional Community Integration in Dominica, West Indies	PhD Dissertation, University of Florida: Gainesville.
Siegel, Peter E.	1989	Site Structure, Demography, and Social Complexity in the Early Ceramic Age of the Caribbean.	*Early Ceramic Population Lifeways and Adaptive Strategies in the Caribbean*, 194–245. B.A.R.
Siegel, Peter E., John G. Jones, Deborah M. Pearsall, Nicholas P. Dunning, Pat Farrell, Neil A. Duncan, Jason H. Curtis, and Sushant K. Singh	2015	Paleoenvironmental Evidence for First Human Colonization of the Eastern Caribbean	*Quaternary Science Reviews* 129: 275-295.

Siegel, Peter E., John G. Jones, Deborah M. Pearsall, and Daniel P. Wagner	2005	Environmental and Cultural Correlates in the West Indies: A View from Puerto Rico	In *Ancient Borinquen: Archaeology and Ethnohistory of Native Puerto Rico*, 88–121. Tuscaloosa: University of Alabama Press.
Sinelli, Peter T.	2001	Archaeological Investigations of Two Prehistoric Sites Representing a Hispaniolan Colonization of Middle Caicos, Turks and Caicos Islands	Master's Thesis, Gainesville, Florida: University of Florida.
Sinelli, Peter T.	2010	All Islands Great and Small: The Role of Small Cay Environments in Indigenous Settlement Strategies in the Turks & Caicos Islands	PhD Dissertation, Gainesville, Florida: University of Florida.
Steadman, David W., Nancy A. Albury, Jim I Mead, J. Angel Soto-Centeno, and Janet Franklin	2017	Holocene vertebrates from a dry cave on Eleuthera Island, Commonwealth of The Bahamas	*The Holocene* 28(5): 806-813.
Steadman, David W., Richard Franz, Gary S. Morgan, Nancy A. Albury, Brian Kakuk, Kenneth Broad, Shelley E. Franz, et al.	2007	Exceptionally Well Preserved Late Quaternary Plant and Vertebrate Fossils from a Blue Hole on Abaco, The Bahamas	*Proceedings of the National Academy of Sciences* 104(50): 19897-19902.
Steadman, David W., and Sharyn Jones	2006	Long-Term Trends in Prehistoric Fishing and Hunting on Tobago, West Indies	*Latin American Antiquity* 17(3): 316-334.
Steadman, David W., and Anne V. Stokes	2002	Changing Exploitation of Terrestrial Vertebrates during the Past 3000 Years on Tobago, West Indies	*Human Ecology* 30(3): 339-367.
Steadman, David W., Nancy A. Albury, Perry Maillis, Jim I Mead, John Slapcinsky, Kenneth L. Krysko, Hayley M. Singleton, and Janet Franklin	2014	Late-Holocene faunal landscape change in the Bahamas	*The Holocene* 24(2): 220-230
Steadman, David W., Hayley M. Singleton, Kelly M. Delancy, Nancy A. Albury, J. Angel Soto-Centeno, Harlan Gough, Neil Duncan, Janet Franklin, and William F. Keegan	2017	Late Holocene Historical Ecology: The Timing of Vertebrate Extirpation on Crooked Island, Commonwealth of The Bahamas	*Journal of Island and Coastal Archaeology* 12(4): 572-584.
Stouvenot, Christian, Jacques Beauchêne, Dominique Bonnissent, and Christine Oberlin	2013	Datations radiocarbone et le «problème vieux bois» dans l'arc antillais: état de la question	In *Proceedings of the 25th Congress of the International Association for Caribbean Archaeology*, 459–94. Puerto Rico.
Stouvenot, Christian, Sandrine Grouard, Salvador Bailon, Dominique Bonnissent, Arnaud Lenoble, Nathalie Serrand, and Victor Sierpe	2014	L'abri Sous Roche Cadet 3 (Marie-Galante): Un Gisement À Accumulations de Faune et À Vestiges Archéologiques	In *Proceedings of the 24th Congress of the International Association for Caribbean Archaeology*. Fort-de-France, Martinique. pp.126-140.
Stuckenrath, Robert, and James E. Mielke	1973	Smithsonian Institution Radiocarbon Measurements VIII	*Radiocarbon* 15(2): 388-424.
Stuiver, Minze	1969	Yale Natural Radiocarbon Measurements IX	*Radiocarbon* 11(2): 545-658.
Tacoma, Jouke	1980	Studies on the Physical Anthropology of the Netherlands Antilles: IV: A Prae-Columbian Skeleton from Bonaire	Nieuwe West-Indische Gids/New West Indian Guide, 54(3/4): 229-258.

Tacoma, Jouke	1990	Skeletal Remains from de Savaan Region, Curacao	In *Proceedings of the Eleventh Congress of the International Association for Caribbean Archaeology*, 217–23. San Juan: La Fundación Arqueológica, Antropológica e Histórica de Puerto Rico.
Tamers, M.A.	1973	Instituto Venezolano de Investigaciones Cientificas Natural Radiocarbon Measurements VI	*Radiocarbon* 13(1): 32-44.
Tankersley, Kenneth Barnett, Nicholas P. Dunning, Lewis A. Owen, and Janine Sparks	2018	Geochronology and paleoenvironmental framework for the oldest archaeological site (7800-7900 cal BP) in the West Indies, Banwari Trace, Trinidad	*Latin American Antiquity* 29 (4): 681-695.
Tilden, Bruce E.	1976	The Arboretum Complex: A Pre-Ceramic Culture of the Virgin Islands	In *Proceedings of the 6th International Congress for the Study of Pre-Columbian Cultures of the Lesser Antilles*, 239–46. Gainesville, Florida: Florida State Museum, University of Florida.
Toftgaard, Casper Jacobsen	2019	The Krum Bay sites revisited: The excavations in the Krum Bay area on St. Thomas, U.S. Virgin Islands	In *Early Settlers of the Insular Caribbean: Dearchaizing the Archaic*, edited by Corinne L. Hofman and Andrzej T. Antczak, 215-228. Leiden, Sidestone Press.
Turvey, Samuel T., J.R. Oliver, Y. M. Narganes Storde, and P. Rye	2007	Late Holocene Extinction of Puerto Rican Native Land Mammals	*Biology Letters* 3(2): 193-196.
Ulloa Hung, J.	2008	Una Nota al Margen. Crónica de una Datación Olvidad.	*El Caribe Arqueológico* 11:106-10.
Ulloa Hung, J. and R. Valcárel Rojas	2002	Cerámica Temprana En El Centro Del Oriente de Cuba	Santo Domingo: Videograph.
Valcárcel Rojas, Roberto, and César Rodríguez Arce	2003	Chorro De Maíta. Muerte Y Desigualdad Social	In *Proceedings of the 20th Congress of the International Association for Caribbean Archaeology*, 507–14. Santo Domingo: Museo del Hombre Dominican and Fundación García Arévalo.
Valcarecel Rojas, Roberto	2002	Banes Precolombino: La Ocupacion Agricultora	Coleccion Premio de La Ciudad. Holguin: Ediciones Holguin.
Van den Bel, Martijn	2017	Mysterious LCA pits in the hinterland of Grande-Terre, Guadeloupe	In *Proceedings of the 26th Congress of the International Association of Caribbean Archaeology*, edited by C.B. Velasquez and J.B. Haviser. SIMARC Heritage Series No. 15, Sint Maarten.
Van den Bel, Martijn, and Thomas Romon	2010	A Troumassoid site at Trois-Riviéres, Guadeloupe FWI Funerary practices and house patters at La Pointe de Grande Anse.	*Journal of Caribbean Archaeology* 9:1-17.
van Klinken, G.J.	1991	Dating and Dietary Reconstruction by Isotopic Analysis of Amino Acids in Fossil Bone Collagen-with Special Reference to the Caribbean	Publications of the Foundation for Scientific Research in the Carribbean Region 128. Amsterdam: University of Groningen.
Veloz Maggiolo, M. and E. Ortega	1973	El Precerámico de Santo Domingo, Nuevos Lugares y su Posible Relación con otros Puntos del Área Antillana	Museo del Hombre Dominicano, Papeles Ocasionales 1.
Veloz Maggiolo, M. and E. Ortega	1976	The Preceramic of the Dominican Republic: Some New Finds and Their Possible Relationships	In Proceedings of the First Puerto Rican Symposium on Archaeology, edited by L. Robinson, 147-201. Fundación Arqueológica, Anthropológica e Histórica de Puerto Rico, San Juan.
Veloz Maggiolo, M., E. Ortega, J. Nadal, F. Luna Calderón, and R. Rímoli	1977	*Arqueología de Cueva de Berna*	Ediciones de la Universidad Central del Este, San Pedro de Macorís.

Versteeg, Aad H.	1991	A Preceramic Burial Site at Malmok (Aruba)	In *Proceedings from the Thirteenth International Congress of Caribbean Archaeology*, 105–126. Reports of the Archaeological-Anthropological Institute of the Netherlands Antilles 9. Curacao: Archaeological-Anthropological Institute of the Netherlands Antilles.
Versteeg, Aad H., and Kees Schinkel	1992	The Archaeology of St.Eustatius: The Golden Rock Site Vol. 2	Amsterdam: St. Eustatius Historical Foundation.
Versteeg, Aad H., Kees Schinkel, and Samuel L. Wilson.	1993	Large-Scale Excavations versus Surveys: Examples from Nevis, St. Eustatius and St. Kitts in the Northern Caribbean	Analecta Praehistorica Leidensia 26: 24.
Versteeg, Aad H., Jouke Tacoma, and Pieter Van de Velde	1990	Archaeological Investigations on Aruba: The Malmok Cemetery. Vol. 2.	Publication of the Archaeological Museum Aruba. Oranjestad: Archaeological Museum Aruba.
Versteeg, Aad H.	1997	The Archaeology of Aruba: The Tanki Flip Site	Publication of the Archaeological Museum Aruba 8. Publications of the Foundation for Scientific Research in the Caribbean Region 141.
Vésteinsson, Orri	2011	Reconnaissance of a Prehistoric Shell-ridge in Barbuda, West Indies	Fornleifastofnun Íslands, FS462-11032, Reykjavík.
Vidal, Nathalie	1999	Le Site Precolumbien de la Plage Dizac au Diamant, Martinique	In *Proceedings of the 16th Congress of the International Association of Caribbean Archaeology*, pp. 7-16. Basseterre, Guadeloupe: Editions du Ponant.
Vinogradov, A.P., A.L. Devirts, E.I. Dobkina, and N. Markova	1968	Radiocarbon Dating in the Vernadsky Institute I-IV	*Radiocarbon* 8: 292-323.
Walker, Jeffery B.	2005	The Paso Del Indio Site, Vega Baja, Puerto Rico: A Progress Report	In *Ancient Borinquen: Archaeology and Ethnohistory of Native Puerto Rico*, 55–87. Tuscaloosa: University of Alabama Press.
Waters, Michael R., John R. Giardino, Derek W. Ryter, James M. Parrent	1993	Geoarchaeological Investigation of St. Ann's Bay, Jamaica: The Search for Columbus Caravels and an Assessment of 1000 Years of Human Land Use	Geoarchaeology 8(4): 259-279.
Watters, David, and Jack Donahue	1990	Geoarchaeological Research on Barbuda, Antigua, and Montserrat	In *Proceedings of the 10th Congress of the International Association for Caribbean Archaeology*, 375–79. Montréal: Centre de recherches caraïbes, Université de Montréal.
Watters, David R.	1997	Maritime trade in the prehistoric eastern Caribbean.	In *Indigenous People of the Caribbean*, Edited by: Wilson, S.M. 88-99. Gainesville: University Press Florida.
Watters, David R.	1999	Composition of the Molluscan Fauna at the Gravenor Bay Shell Ridge, Barbuda	In *Proceedings of the 17th Congress of the International Association for Caribbean Archaeology*, 181–96. Rockville Centre, New York: Molloy College.
Watters, David R., Jack Donahue, and Robert Stuckenrath	1992	Paleoshorelines and the Prehistory of Barbuda, West Indies	In *Paleoshorelines and Prehistory: An Investigation of Metho*d, 15–52. Boca Raton, Florida: CRC Press.
Watters, David R. and James B. Petersen	1991	Preliminary Report on the Archaeology of the Rendezvous Bay Site, Anguilla	In *Proceedings of the 14th Congress of the International Association for Caribbean Archaeology*, 25–33. St. Michael, Barbados: Barbados Museum and Historical Society.
Watters, David R.	1991	Archaeology of Fountain Cavern, Anguilla, West Indies	*Annals of Carnegie Museum* 60: 255-320.
Wild, Kenneth S.	2013	A Timeline of Taíno Development in the Virgin Islands	Paper presented at the 25th Congress for the International Association for Caribbean Archaeology, Puerto Rico.
Wilson, Samuel M.	1989	The Prehistoric Settlement Pattern of Nevis, West Indies	*Journal of Field Archaeology* 16(4): 427-450.

Wilson, Samuel M.	2006	*The Prehistory of Nevis, a Small Island in the Lesser Antilles*	New Haven: Yale University Press.
Wing, Elizabeth S., S.D. deFrance, and L. Kozuch	2002	Faunal Remains from the Tutu Site	In *The Tutu Archaeological Village Site: A Multidisciplinary Case Study in Human Adaptation*, 141–65. New York: Routledge.
Winter, John H.	1978a	The Clifton Pier Rockshelter, New Providence, Bahamas	*Journal of the Virgin Islands Archaeological Society* 6: 45-48.
Winter, John H.	1978b	Preliminary Work from the McKay Site on Crooked Island	In *Proceedings of the 7th International Congress for the Study of the Pre-Columbian Cultures of the Lesser Antilles*, 237–42. Montréal: Centre de recherches caraïbes, Université de Montréal.
Winter, John H.	1987	San Salvador in 1492: Its Geography and Ecology	In *Proceedings of the First San Salvador Conference*, 313–20. Fort Lauderdale, Florida: CCFL Bahamian Field Station.
Winter, John H., and Jerry Stipp	1983	Preliminary Investigations of the Minnis/Ward Site, San Salvador, Bahamas	In *Proceedings of the 9th International Congress for Caribbean Archaeology*, 155–62. Montréal: Centre de recherches caraïbes, Université de Montréal.
Winter, John H., Elizabeth S. Wing, and Lee A. Newsom	1999	A Lucayan Funeral Offering	In *Proceedings of the 17th Congress of the International Association for Caribbean Archaeology*, 197–210. New York: Molloy College.

APPENDIX B

SUPPLEMENTARY MATERIAL FOR CHAPTER III

Table 1. ΔR data for R markdown file.

Lab_Code	Region	FKRT_zone	Terrestrial_Influence	deltaR	deltar_error	Reference
L-576B	Bahamas	?	?	-175	42	Broecker and Olsen 1961
L-576G	Bahamas	?	?	-104	59	Broecker and Olsen 1961
SI-?	Bahamas	?	?	-12	66	Lighty et al. 1982
D-AMS 004869	Bahamas	?	?	-452	43	DiNapoli_etal_2020
D-AMS 004870	Bahamas	?	?	-232	33	DiNapoli_etal_2020
D-AMS 004871	Bahamas	?	?	-237	30	DiNapoli_etal_2020
D-AMS 004872	Bahamas	?	?	-213	37	DiNapoli_etal_2020
D-AMS 004876	Cuba	?	?	-363	37	DiNapoli_etal_2020
D-AMS 004877	Cuba	?	?	-66	24	DiNapoli_etal_2020
D-AMS 004878	Cuba	?	?	-154	32	DiNapoli_etal_2020
D-AMS 004879	Cuba	?	?	-119	26	DiNapoli_etal_2020
LAC-150280	Cuba	?	?	-131	39	Diaz,_et_al,_2017
LAC-150269	Cuba	?	?	-106	41	Diaz,_et_al,_2017
LAC-150281	Cuba	?	?	-33	53	Diaz,_et_al,_2017
LAC-150276	Cuba	?	?	-129	84	Diaz,_et_al,_2017
LAC-150271	Cuba	?	?	-153	38	Diaz,_et_al,_2017
LAC-150272	Cuba	?	?	-136	38	Diaz,_et_al,_2017
LAC-150270	Cuba	?	?	-53	40	Diaz,_et_al,_2017
LAC-150277	Cuba	?	?	-39	41	Diaz,_et_al,_2017
LAC-150278	Cuba	?	?	88	38	Diaz,_et_al,_2017
LAC-150279	Cuba	?	?	-69	41	Diaz,_et_al,_2017
LAC-150284	Cuba	?	?	-93	40	Diaz,_et_al,_2017
LAC-150286	Cuba	?	?	-103	42	Diaz,_et_al,_2017
LAC-150283	Cuba	?	?	49	41	Diaz,_et_al,_2017
LAC-150285	Cuba	?	?	-128	38	Diaz,_et_al,_2017
LAC-150282	Cuba	?	?	-185	38	Diaz,_et_al,_2017
LAC-150273	Cuba	?	?	-95	40	Diaz,_et_al,_2017
LAC-150287	Cuba	?	?	-170	39	Diaz,_et_al,_2017
LAC-150274	Cuba	?	?	-96	41	Diaz,_et_al,_2017
UGAMS-14896A	Apalachicola_Bay	?	?	-198	23	Hadden,_Cherkinsky_2015

UGAMS-14894	Apalachicola_Bay	?	?	-154	23	Hadden,_Cherkinsky_2015
UGAMS-14897A	Apalachicola_Bay	?	?	427	23	Hadden,_Cherkinsky_2015
UGAMS-14897B	Apalachicola_Bay	?	?	517	23	Hadden,_Cherkinsky_2015
UGAMS-14895	Apalachicola_Bay	?	?	-73	23	Hadden,_Cherkinsky_2015
UGAMS-14891	Apalachicola_Bay	?	?	-153	23	Hadden,_Cherkinsky_2015
UGAMS-14893	Apalachicola_Bay	?	?	-154	23	Hadden,_Cherkinsky_2015
UGAMS-14890	Apalachicola_Bay	?	?	-93	23	Hadden,_Cherkinsky_2015
UGAMS-23653.01	Apalachicola_Bay	?	?	-79	32	Hadden,_Cherkinsky_2017
UGAMS-23653.02	Apalachicola_Bay	?	?	-43	33	Hadden,_Cherkinsky_2017
UGAMS-23653.03	Apalachicola_Bay	?	?	-58	34	Hadden,_Cherkinsky_2017
GX-28109	Biscayne_National_Park	Biscayne_National_Park	Nearshore	-170	61	Toth_et_al._2017
CAMS-167728	Biscayne_National_Park	Biscayne_National_Park	Nearshore	-155	31	Toth_et_al._2017
CAMS-142674	Biscayne_National_Park	Biscayne_National_Park	Nearshore	-242	27	Toth_et_al._2017
CAMS-142681	Biscayne_National_Park	Biscayne_National_Park	Nearshore	-227	36	Toth_et_al._2017
CAMS-167734	Biscayne_National_Park	Biscayne_National_Park	Nearshore	-282	34	Toth_et_al._2017
CAMS-167736	Biscayne_National_Park	Biscayne_National_Park	Nearshore	-166	29	Toth_et_al._2017
UGAMS-23652B.02	Apalachicola_Bay	?	?	-28	33	Hadden,_Cherkinsky_2017
UGAMS-23652B.03	Apalachicola_Bay	?	?	67	33	Hadden,_Cherkinsky_2017
UGAMS-23652A.01	Apalachicola_Bay	?	?	-3	33	Hadden,_Cherkinsky_2017
UGAMS-23652A.02	Apalachicola_Bay	?	?	-44	33	Hadden,_Cherkinsky_2017
UGAMS-23652A.03	Apalachicola_Bay	?	?	-10	33	Hadden,_Cherkinsky_2017
UGAMS-23652A.04	Apalachicola_Bay	?	?	-18	33	Hadden,_Cherkinsky_2017
CAMS-126062	Dry_Tortugas_National_Park	Dry_Tortugas_National_Park	OpenOcean	-244	31	Toth_et_al._2017

CAMS-126063	Dry_Tortugas_National_Park	Dry_Tortugas_National_Park	OpenOcean	-207	36	Toth_et_al._2017
CAMS-126064	Dry_Tortugas_National_Park	Dry_Tortugas_National_Park	OpenOcean	-211	36	Toth_et_al._2017
CAMS-126056	Dry_Tortugas_National_Park	Dry_Tortugas_National_Park	OpenOcean	-239	36	Toth_et_al._2017
CAMS-123403	Dry_Tortugas_National_Park	Dry_Tortugas_National_Park	OpenOcean	-99	31	Toth_et_al._2017
CAMS-131776	Dry_Tortugas_National_Park	Dry_Tortugas_National_Park	OpenOcean	-125	26	Toth_et_al._2017
CAMS-151246	Dry_Tortugas_National_Park	Dry_Tortugas_National_Park	OpenOcean	-151	31	Toth_et_al._2017
CAMS-168084	Dry_Tortugas_National_Park	Dry_Tortugas_National_Park	OpenOcean	-255	26	Toth_et_al._2017
CAMS-151239	Dry_Tortugas_National_Park	Dry_Tortugas_National_Park	OpenOcean	-252	33	Toth_et_al._2017
CAMS-168089	Dry_Tortugas_National_Park	Dry_Tortugas_National_Park	OpenOcean	-194	26	Toth_et_al._2017
CAMS-126050	Dry_Tortugas_National_Park	Dry_Tortugas_National_Park	OpenOcean	-318	31	Toth_et_al._2017
CAMS-123404	Dry_Tortugas_National_Park	Dry_Tortugas_National_Park	OpenOcean	-287	37	Toth_et_al._2017
CAMS-126046	Dry_Tortugas_National_Park	Dry_Tortugas_National_Park	OpenOcean	-310	36	Toth_et_al._2017
CAMS-126053	Dry_Tortugas_National_Park	Dry_Tortugas_National_Park	OpenOcean	-352	38	Toth_et_al._2017
CAMS-126054	Dry_Tortugas_National_Park	Dry_Tortugas_National_Park	OpenOcean	-286	42	Toth_et_al._2017
CAMS-126060	Dry_Tortugas_National_Park	Dry_Tortugas_National_Park	OpenOcean	-326	36	Toth_et_al._2017
SI-?	Dry_Tortugas_National_Park	Dry_Tortugas_National_Park	OpenOcean	-45	51	Lighty,_R.G.:1982
UGAMS-28225.1	Southwestern_Florida	?	?	247	61	Hadden,_Schwadron_2019
UGAMS-28225.2	Southwestern_Florida	?	?	457	61	Hadden,_Schwadron_2019
UGAMS-28225.3	Southwestern_Florida	?	?	247	61	Hadden,_Schwadron_2019
UGAMS-28224A.1	Southwestern_Florida	?	?	-24	62	Hadden,_Schwadron_2019

UGAMS-28224A.2	Southwestern_Florida	?	?	-64	62	Hadden,_Schwadron_2019
UGAMS-28224A.3	Southwestern_Florida	?	?	-94	62	Hadden,_Schwadron_2019
UGAMS-28224B.1	Southwestern_Florida	?	?	-124	62	Hadden,_Schwadron_2019
UGAMS-28224B.2	Southwestern_Florida	?	?	-124	62	Hadden,_Schwadron_2019
UGAMS-28224B.3	Southwestern_Florida	?	?	-14	62	Hadden,_Schwadron_2019
CAMS-172788	Lower_Keys	Lower_Keys	Nearshore	-285	27	Toth_et_al._2017
CAMS-172458	Lower_Keys	Lower_Keys	Nearshore	-132	26	Toth_et_al._2017
CAMS-168543	Lower_Keys	Lower_Keys	Nearshore	-147	31	Toth_et_al._2017
CAMS-168541	Lower_Keys	Lower_Keys	Nearshore	-221	27	Toth_et_al._2017
CAMS-168542	Lower_Keys	Lower_Keys	Nearshore	-160	27	Toth_et_al._2017
CAMS-168540	Lower_Keys	Lower_Keys	Nearshore	-205	26	Toth_et_al._2017
CAMS-168548	Marquesas	Marquesas	OpenOcean	-132	28	Toth_et_al._2017
CAMS-168552	Marquesas	Marquesas	OpenOcean	-133	26	Toth_et_al._2017
CAMS-168554	Marquesas	Marquesas	OpenOcean	-247	28	Toth_et_al._2017
CAMS-168551	Marquesas	Marquesas	OpenOcean	-249	25	Toth_et_al._2017
CAMS-171499	Middle_Keys	Middle_Keys	Nearshore	-214	26	Toth_et_al._2017
CAMS-167744	Middle_Keys	Middle_Keys	Nearshore	205	26	Toth_et_al._2017
CAMS-171494	Middle_Keys	Middle_Keys	Nearshore	-196	27	Toth_et_al._2017
CAMS-172468	Middle_Keys	Middle_Keys	Nearshore	-110	36	Toth_et_al._2017
CAMS-167745	Middle_Keys	Middle_Keys	Nearshore	-156	31	Toth_et_al._2017
CAMS-171496	Middle_Keys	Middle_Keys	Nearshore	-181	37	Toth_et_al._2017
UGAMS-14892A	Apalachicola_Bay	?	?	56	23	Hadden,_Cherkinsky_2015
UGAMS-28226.1	Southwestern_Florida	?	?	57	60	Hadden,_Schwadron_2019
UGAMS-28226.2	Southwestern_Florida	?	?	-53	60	Hadden,_Schwadron_2019
ucid941	Pickles_Reef	Upper_Keys	Nearshore	-145	26	Druffel,_E.R.M._1997
ucid940	Pickles_Reef	Upper_Keys	Nearshore	-147	25	Druffel,_E.R.M._1997
WH1454	Pickles_Reef	Upper_Keys	Nearshore	-234	18	Druffel,_E.R.M._1997
WH1479	Pickles_Reef	Upper_Keys	Nearshore	-188	18	Druffel,_E.R.M._1997
WH1492	Pickles_Reef	Upper_Keys	Nearshore	-191	19	Druffel,_E.R.M._1997
ucid1051	Pickles_Reef	Upper_Keys	Nearshore	-203	30	Druffel,_E.R.M._1997
ucid1375	Pickles_Reef	Upper_Keys	Nearshore	-204	24	Druffel,_E.R.M._1997
ucid1368	Pickles_Reef	Upper_Keys	Nearshore	-405	23	Druffel,_E.R.M._1997

WH1476	Pickles_Reef	Upper_Keys	Nearshore	-207	19	Druffel,_E.R.M._1997
WH1460	Pickles_Reef	Upper_Keys	Nearshore	-199	19	Druffel,_E.R.M._1997
WH1466	Pickles_Reef	Upper_Keys	Nearshore	-277	23	Druffel,_E.R.M._1997
WH1458	Pickles_Reef	Upper_Keys	Nearshore	-211	21	Druffel,_E.R.M._1997
WH1470	Pickles_Reef	Upper_Keys	Nearshore	-272	23	Druffel,_E.R.M._1997
WH1457	Pickles_Reef	Upper_Keys	Nearshore	-160	19	Druffel,_E.R.M._1997
WH1472	Pickles_Reef	Upper_Keys	Nearshore	-170	20	Druffel,_E.R.M._1997
WH1463	Pickles_Reef	Upper_Keys	Nearshore	-104	20	Druffel,_E.R.M._1997
WH1478	Pickles_Reef	Upper_Keys	Nearshore	-190	20	Druffel,_E.R.M._1997
WH1464	Pickles_Reef	Upper_Keys	Nearshore	-217	22	Druffel,_E.R.M._1997
ucid1050	Pickles_Reef	Upper_Keys	Nearshore	-191	28	Druffel,_E.R.M._1997
WH1475	Pickles_Reef	Upper_Keys	Nearshore	-190	31	Druffel,_E.R.M._1997
WH1461	Pickles_Reef	Upper_Keys	Nearshore	-153	24	Druffel,_E.R.M._1997
ucid939	Pickles_Reef	Upper_Keys	Nearshore	-187	25	Druffel,_E.R.M._1997
ucid1049	Pickles_Reef	Upper_Keys	Nearshore	-171	44	Druffel,_E.R.M._1997
WH1477	Pickles_Reef	Upper_Keys	Nearshore	-129	20	Druffel,_E.R.M._1997
WH1467	Pickles_Reef	Upper_Keys	Nearshore	-201	18	Druffel,_E.R.M._1997
WH1468	Pickles_Reef	Upper_Keys	Nearshore	-151	17	Druffel,_E.R.M._1997
WH1459	Pickles_Reef	Upper_Keys	Nearshore	-199	18	Druffel,_E.R.M._1997
WH1462	Pickles_Reef	Upper_Keys	Nearshore	-97	20	Druffel,_E.R.M._1997
WH1474	Pickles_Reef	Upper_Keys	Nearshore	-158	20	Druffel,_E.R.M._1997
WH1493	Pickles_Reef	Upper_Keys	Nearshore	-161	18	Druffel,_E.R.M._1997
WH1469	Pickles_Reef	Upper_Keys	Nearshore	-178	19	Druffel,_E.R.M._1997
WH1456	Pickles_Reef	Upper_Keys	Nearshore	-190	18	Druffel,_E.R.M._1997
LJ4122	The_Rocks	Upper_Keys	Nearshore	-166	59	Druffel_&_Linick_1978
LJ4121	The_Rocks	Upper_Keys	Nearshore	-122	60	Druffel_&_Linick_1978
LJ4051	The_Rocks	Upper_Keys	Nearshore	-95	86	Druffel_&_Linick_1978
LJ4262	The_Rocks	Upper_Keys	Nearshore	-154	68	Druffel_&_Linick_1978
LJ4123	The_Rocks	Upper_Keys	Nearshore	-102	60	Druffel_&_Linick_1978
LJ4127	The_Rocks	Upper_Keys	Nearshore	-195	59	Druffel_&_Linick_1978
LJ4125	The_Rocks	Upper_Keys	Nearshore	-160	68	Druffel_&_Linick_1978
LJ4126	The_Rocks	Upper_Keys	Nearshore	-167	68	Druffel_&_Linick_1978
LJ3815	The_Rocks	Upper_Keys	Nearshore	-123	51	Druffel_&_Linick_1978
LJ3816	The_Rocks	Upper_Keys	Nearshore	-190	51	Druffel_&_Linick_1978
LJ3817	The_Rocks	Upper_Keys	Nearshore	-172	51	Druffel_&_Linick_1978
LJ3818	The_Rocks	Upper_Keys	Nearshore	-196	42	Druffel_&_Linick_1978
LJ3819	The_Rocks	Upper_Keys	Nearshore	-178	51	Druffel_&_Linick_1978
LJ4288	The_Rocks	Upper_Keys	Nearshore	-143	68	Druffel_&_Linick_1978

LJ4261	The_Rocks	Upper_Keys	Nearshore	-179	59	Druffel_&_Linick_1978
LJ4403	The_Rocks	Upper_Keys	Nearshore	-143	34	Druffel_&_Linick_1978
LJ4234	The_Rocks	Upper_Keys	Nearshore	-150	51	Druffel_&_Linick_1978
LJ4280	The_Rocks	Upper_Keys	Nearshore	-189	34	Druffel_&_Linick_1978
LJ4193	The_Rocks	Upper_Keys	Nearshore	-162	34	Druffel_&_Linick_1978
LJ4281	The_Rocks	Upper_Keys	Nearshore	-136	51	Druffel_&_Linick_1978
LJ4196	The_Rocks	Upper_Keys	Nearshore	-144	34	Druffel_&_Linick_1978
LJ4179	The_Rocks	Upper_Keys	Nearshore	-153	34	Druffel_&_Linick_1978
LJ4184	The_Rocks	Upper_Keys	Nearshore	-153	51	Druffel_&_Linick_1978
LJ4344	The_Rocks	Upper_Keys	Nearshore	-203	25	Druffel_&_Linick_1978
LJ4206	The_Rocks	Upper_Keys	Nearshore	-152	25	Druffel_&_Linick_1978
LJ4207	The_Rocks	Upper_Keys	Nearshore	-150	68	Druffel_&_Linick_1978
LJ4283	The_Rocks	Upper_Keys	Nearshore	-166	34	Druffel_&_Linick_1978
LJ4186	The_Rocks	Upper_Keys	Nearshore	-62	43	Druffel_&_Linick_1978
LJ4277	The_Rocks	Upper_Keys	Nearshore	-120	34	Druffel_&_Linick_1978
LJ4232	The_Rocks	Upper_Keys	Nearshore	-136	34	Druffel_&_Linick_1978
LJ4342	The_Rocks	Upper_Keys	Nearshore	-126	34	Druffel_&_Linick_1978
LJ4165	The_Rocks	Upper_Keys	Nearshore	-89	43	Druffel_&_Linick_1978
LJ4278	The_Rocks	Upper_Keys	Nearshore	-95	34	Druffel_&_Linick_1978
LJ4236	The_Rocks	Upper_Keys	Nearshore	-161	51	Druffel_&_Linick_1978
LJ4340	The_Rocks	Upper_Keys	Nearshore	-101	34	Druffel_&_Linick_1978
LJ4185	The_Rocks	Upper_Keys	Nearshore	-153	59	Druffel_&_Linick_1978
LJ4343	The_Rocks	Upper_Keys	Nearshore	-139	59	Druffel_&_Linick_1978
LJ4233	The_Rocks	Upper_Keys	Nearshore	-133	34	Druffel_&_Linick_1978
LJ4284	The_Rocks	Upper_Keys	Nearshore	-137	34	Druffel_&_Linick_1978
LJ4194	The_Rocks	Upper_Keys	Nearshore	-165	51	Druffel_&_Linick_1978
LJ4926	The_Rocks	Upper_Keys	Nearshore	-142	25	Druffel,_E.R.M._1982
LJ4924	The_Rocks	Upper_Keys	Nearshore	-181	25	Druffel,_E.R.M._1982
LJ4927	The_Rocks	Upper_Keys	Nearshore	-141	42	Druffel,_E.R.M._1982
LJ4925	The_Rocks	Upper_Keys	Nearshore	-164	34	Druffel,_E.R.M._1982
LJ4930	The_Rocks	Upper_Keys	Nearshore	-172	34	Druffel,_E.R.M._1982
LJ4928	The_Rocks	Upper_Keys	Nearshore	-195	42	Druffel,_E.R.M._1982
LJ4929	The_Rocks	Upper_Keys	Nearshore	-152	42	Druffel,_E.R.M._1982
LJ4740	The_Rocks	Upper_Keys	Nearshore	-177	34	Druffel,_E.R.M._1982
LJ4889	The_Rocks	Upper_Keys	Nearshore	-187	34	Druffel,_E.R.M._1982
LJ4893	The_Rocks	Upper_Keys	Nearshore	-172	34	Druffel,_E.R.M._1982
LJ4742	The_Rocks	Upper_Keys	Nearshore	-149	42	Druffel,_E.R.M._1982
LJ4786	The_Rocks	Upper_Keys	Nearshore	-124	25	Druffel,_E.R.M._1982

LJ4738	The_Rocks	Upper_Keys	Nearshore	-158	42	Druffel,_E.R.M._1982
LJ4913	The_Rocks	Upper_Keys	Nearshore	-121	34	Druffel,_E.R.M._1982
LJ4197	The_Rocks	Upper_Keys	Nearshore	-177	51	Druffel,_E.R.M._1982
LJ4912	The_Rocks	Upper_Keys	Nearshore	-117	25	Druffel,_E.R.M._1982
LJ4737	The_Rocks	Upper_Keys	Nearshore	-183	25	Druffel,_E.R.M._1982
LJ4741	The_Rocks	Upper_Keys	Nearshore	-163	34	Druffel,_E.R.M._1982
LJ4265	The_Rocks	Upper_Keys	Nearshore	-196	25	Druffel,_E.R.M._1982
LJ4782	The_Rocks	Upper_Keys	Nearshore	-102	25	Druffel,_E.R.M._1982
LJ4775	The_Rocks	Upper_Keys	Nearshore	-117	34	Druffel,_E.R.M._1982
LJ4739	The_Rocks	Upper_Keys	Nearshore	-132	25	Druffel,_E.R.M._1982
LJ4408	The_Rocks	Upper_Keys	Nearshore	-174	50	Druffel,_E.R.M._1982
LJ4408	The_Rocks	Upper_Keys	Nearshore	-173	50	Druffel,_E.R.M._1982
LJ4770	The_Rocks	Upper_Keys	Nearshore	-105	34	Druffel,_E.R.M._1982
LJ4784	The_Rocks	Upper_Keys	Nearshore	-136	25	Druffel,_E.R.M._1982
LJ4235	The_Rocks	Upper_Keys	Nearshore	-135	34	Druffel,_E.R.M._1982
LJ4777	The_Rocks	Upper_Keys	Nearshore	-100	34	Druffel,_E.R.M._1982
LJ4231	The_Rocks	Upper_Keys	Nearshore	-184	59	Druffel,_E.R.M._1982
LJ4794	The_Rocks	Upper_Keys	Nearshore	-141	25	Druffel,_E.R.M._1982
LJ4286	The_Rocks	Upper_Keys	Nearshore	-140	59	Druffel,_E.R.M._1982
LJ4752	The_Rocks	Upper_Keys	Nearshore	-190	34	Druffel,_E.R.M._1982
LJ4833	The_Rocks	Upper_Keys	Nearshore	-188	67	Druffel,_E.R.M._1982
LJ4192	The_Rocks	Upper_Keys	Nearshore	-111	59	Druffel,_E.R.M._1982
LJ4783	The_Rocks	Upper_Keys	Nearshore	-93	25	Druffel,_E.R.M._1982
LJ4773	The_Rocks	Upper_Keys	Nearshore	-117	34	Druffel,_E.R.M._1982
LJ4282	The_Rocks	Upper_Keys	Nearshore	-158	42	Druffel,_E.R.M._1982
LJ4792	The_Rocks	Upper_Keys	Nearshore	-198	25	Druffel,_E.R.M._1982
LJ4237	The_Rocks	Upper_Keys	Nearshore	-145	59	Druffel,_E.R.M._1982
LJ4750	The_Rocks	Upper_Keys	Nearshore	-212	25	Druffel,_E.R.M._1982
LJ4287	The_Rocks	Upper_Keys	Nearshore	-147	25	Druffel,_E.R.M._1982
LJ4751	The_Rocks	Upper_Keys	Nearshore	-121	34	Druffel,_E.R.M._1982
LJ4778	The_Rocks	Upper_Keys	Nearshore	-161	34	Druffel,_E.R.M._1982
LJ4238	The_Rocks	Upper_Keys	Nearshore	-153	25	Druffel,_E.R.M._1982
LJ4890	The_Rocks	Upper_Keys	Nearshore	-153	42	Druffel,_E.R.M._1982
LJ4284	The_Rocks	Upper_Keys	Nearshore	-255	41	Druffel,_E.R.M._1982
LJ4785	The_Rocks	Upper_Keys	Nearshore	-104	25	Druffel,_E.R.M._1982
LJ4892	The_Rocks	Upper_Keys	Nearshore	-180	42	Druffel,_E.R.M._1982
LJ4793	The_Rocks	Upper_Keys	Nearshore	-140	34	Druffel,_E.R.M._1982
LJ4780	The_Rocks	Upper_Keys	Nearshore	-55	34	Druffel,_E.R.M._1982

LJ4772	The_Rocks	Upper_Keys	Nearshore	-83	25	Druffel,_E.R.M._1982
LJ4429	The_Rocks	Upper_Keys	Nearshore	-142	34	Druffel,_E.R.M._1982
LJ4832	The_Rocks	Upper_Keys	Nearshore	-185	34	Druffel,_E.R.M._1982
LJ4894	The_Rocks	Upper_Keys	Nearshore	-119	42	Druffel,_E.R.M._1982
LJ4831	The_Rocks	Upper_Keys	Nearshore	-120	34	Druffel,_E.R.M._1982
LJ4428	The_Rocks	Upper_Keys	Nearshore	-146	25	Druffel,_E.R.M._1982
LJ4891	The_Rocks	Upper_Keys	Nearshore	-88	34	Druffel,_E.R.M._1982
LJ4430	The_Rocks	Upper_Keys	Nearshore	-136	25	Druffel,_E.R.M._1982
LJ4406	The_Rocks	Upper_Keys	Nearshore	-131	34	Druffel,_E.R.M._1982
LJ4431	The_Rocks	Upper_Keys	Nearshore	-160	25	Druffel,_E.R.M._1982
LJ4404	The_Rocks	Upper_Keys	Nearshore	-197	25	Druffel,_E.R.M._1982
LJ4409	The_Rocks	Upper_Keys	Nearshore	-176	25	Druffel,_E.R.M._1982
LJ4432	The_Rocks	Upper_Keys	Nearshore	-146	25	Druffel,_E.R.M._1982
UGAMS-27881.1	Southwestern_Florida	?	?	7	61	Hadden,_Schwadron_2019
UGAMS-27881.2	Southwestern_Florida	?	?	-13	61	Hadden,_Schwadron_2019
UGAMS-27881.3	Southwestern_Florida	?	?	-63	61	Hadden,_Schwadron_2019
CAMS-151940	Upper_Keys	Upper_Keys	Nearshore	-229	36	Toth_et_al._2017
CAMS-151942	Upper_Keys	Upper_Keys	Nearshore	-277	31	Toth_et_al._2017
CAMS-168534	Upper_Keys	Upper_Keys	Nearshore	-205	27	Toth_et_al._2017
CAMS-172457	Upper_Keys	Upper_Keys	Nearshore	-177	26	Toth_et_al._2017
CAMS-171489	Upper_Keys	Upper_Keys	Nearshore	-194	26	Toth_et_al._2017
CAMS-168532	Upper_Keys	Upper_Keys	Nearshore	-262	26	Toth_et_al._2017
CAMS-168533	Upper_Keys	Upper_Keys	Nearshore	-78	26	Toth_et_al._2017
CAMS-168538	Upper_Keys	Upper_Keys	Nearshore	-149	27	Toth_et_al._2017
CAMS-151943	Upper_Keys	Upper_Keys	Nearshore	-163	31	Toth_et_al._2017
CAMS-168528	Upper_Keys	Upper_Keys	Nearshore	-213	27	Toth_et_al._2017
CAMS-151938	Upper_Keys	Upper_Keys	Nearshore	-126	32	Toth_et_al._2017
CAMS-169545	Upper_Keys	Upper_Keys	Nearshore	-174	32	Toth_et_al._2017
CAMS-171037	Upper_Keys	Upper_Keys	Nearshore	-295	28	Toth_et_al._2017
Beta-173037	Upper_Keys	Upper_Keys	Nearshore	-116	71	Toth_et_al._2017
UGAMS-40210	Loggerhead_Key_Light	Dry_Tortugas_National_Park	OpenOcean	-137	18	this_publication
D-AMS-015389	Loggerhead_Key_Light	Dry_Tortugas_National_Park	OpenOcean	-91	21	this_publication
D-AMS-015390	Looe_Key_Reef	Lower_Keys	Nearshore	-117	21	this_publication
D-AMS-015391	Key_West,_Sand_Key	Lower_Keys	Nearshore	-192	20	this_publication

D-AMS-015392	Loggerhead_Key_Light	Dry_Tortugas_National_Park	OpenOcean	-138	21	this_publication
D-AMS-015393	Loggerhead_Key_Light	Dry_Tortugas_National_Park	OpenOcean	-160	22	this_publication
UGAMS-40207	Plantation_Key,_Conch_Reef	Upper_Keys	Nearshore	-192	18	this_publication
D-AMS-015396	Plantation_Key,_Conch_Reef	Upper_Keys	Nearshore	-257	21	this_publication
UGAMS-40206	Lower_Matecumbe_Key	Upper_Keys	Nearshore	-176	19	this_publication
D-AMS-015397	Lower_Matecumbe_Key	Upper_Keys	Nearshore	-121	22	this_publication
UGAMS-40211	Plantation_Key,_Conch_Reef	Upper_Keys	Nearshore	-88	18	this_publication
D-AMS-015398	Plantation_Key,_Conch_Reef	Upper_Keys	Nearshore	-34	22	this_publication

R markdown for ΔR calculations

Supplementary analyses for Napolitano et al. ‘New MarineReservoir Corrections for the Florida Keys’

Introduction

This supplementary document contains the code used to calculate the error-weighted pooled means and uncertainties presented in the main text, as well as code necessary to reproduce Figures.

Load Packages

```
library(here) library(ggplot2)
library(gridExtra)
```

Set Working Directory

```
setwd(here())
```

Pooled Mean and Chi-Square Function

The function below calculates the error-weighted pooled means and uncertainty as described in DiNapoli et al. 2020. Also executes chi-square tests and pooled means withexternal variance added.

```
w_mean_fun <- function (df, delta_r, delta_r_error){
  pooled_mean <- sum(delta_r/(delta_r_error^2))/sum(1/(delta_r_error^2))
#error weighted pooled mean
  weighted_uncertainty <- sqrt(1/sum(1/(delta_r_error^2)))#pooled sd t_chi_sq <-
  sum(((delta_r-pooled_mean)^2)/(delta_r_error^2)) #t valuedegree_freedom <- nrow(df)-1
  t_crit  <-  qchisq(p=0.05,  df=degree_freedom,  lower.tail=F) normalized_chi_sq  <-
  t_chi_sq/(nrow(df)-1)
  est_se <- weighted_uncertainty*sqrt(nrow(df)) #estimated standard error ext_var <-
  sqrt((sd(delta_r)^2)-(est_se^2)) #external variance T_uncertainty <-
  sqrt((weighted_uncertainty^2)+(ext_var^2)) #delta r with
external variance
  if(normalized_chi_sq  >  1){ outliers  <-
    "outlier(s)"
  } else {
    outliers <- "no outliers"
  }

    return(data.frame(deparse(substitute(df)), pooled_mean,
 weighted_uncertainty,
                    t_chi_sq, degree_freedom, t_crit, normalized_chi_sq,outliers, T_uncertainty))
 }
```

Load Delta R's

Load Delta R values.

```
all_delta_rs <- read.csv("Supplemental_DeltaR_Table.csv")
```

Calculate pooled means for nearshore and open-ocean locations inthe Keys

```
TI <- subset(all_delta_rs, Terrestrial_Influence !="?") #terrestrialinfluence for Keys
TI_s <- split(TI, TI$Terrestrial_Influence) #split based on terrestrialinfluence
attach(TI_s)
NS <- w_mean_fun(Nearshore, Nearshore$deltaR, Nearshore$deltar_error) #pooledmean for nearshore locations
NS

## deparse.substitute.df.. pooled_mean weighted_uncertainty t_chi_sq## 1
Nearshore -166.4076 2.148214 786.2193
## degree_freedom t_crit normalized_chi_sq outliers T_uncertainty ## 1
174 205.7786 4.518502 outlier(s) 48.20992

OO <- w_mean_fun(OpenOcean, OpenOcean$deltaR, OpenOcean$deltar_error) #pooled mean for open-ocean locations
OO

## deparse.substitute.df.. pooled_mean weighted_uncertainty t_chi_sq## 1
OpenOcean -190.1344 5.673323 170.186
## degree_freedom t_crit normalized_chi_sq outliers T_uncertainty## 1 24
36.41503 7.091082 outlier(s) 78.17629

#boxplot of variability by terrestrial influence
p1 <- ggplot(TI, aes(x=Terrestrial_Influence, y=deltaR))+
  geom_boxplot() + labs(x="", y="Delta R")
p1
```

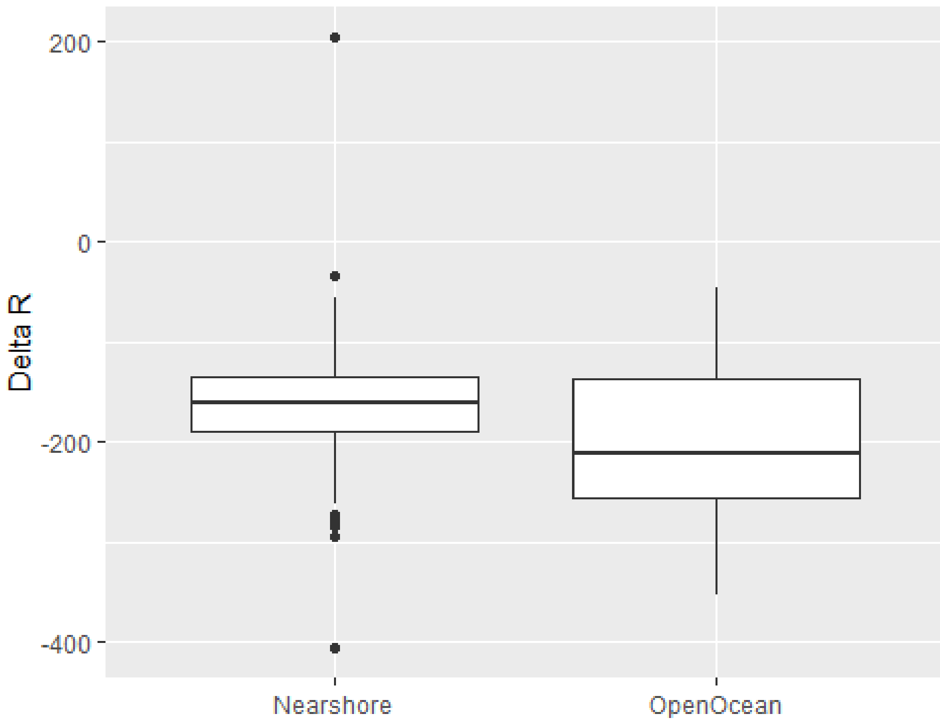


```
# #Terrestrial Influence figure
# tiff("Terrestrial_Influence.tiff", width=5, height=4, compression="lzw",units="in", res=2400)
# p1
# dev.off()

detach(TI_s)
```

Calculate pooled means for different geographic locations in theregion

```
FKRT_g <- subset(all_delta_rs, FKRT_zone!="?")
FRKT_g_s <- split(FKRT_g, FKRT_g$FKRT_zone)
attach(FRKT_g_s)

u_keys <- w_mean_fun(Upper_Keys, Upper_Keys$deltaR, Upper_Keys$deltar_error)
#pooled mean for upper keys
u_keys


##      deparse.substitute.df.. pooled_mean weighted_uncertainty t_chi_sq
## 1                Upper_Keys   -166.8064             2.285565 517.5299
##      degree_freedom      t_crit normalized_chi_sq      outliers T_uncertainty
## 1               154 183.9586          3.360584 outlier(s)      38.53406
```

```
m_keys <- w_mean_fun(Middle_Keys, Middle_Keys$deltaR,
Middle_Keys$deltar_error) #pooled mean for middle keysm_keys

##     deparse.substitute.df.. pooled_mean weighted_uncertainty t_chi_sq## 1
        Middle_Keys     -96.26054            12.06223 177.5146
##     degree_freedom   t_crit normalized_chi_sq      outliers       T_uncertainty       ##
1                         5 11.0705                   35.50293 outlier(s)                     155.5287

l_keys <- w_mean_fun(Lower_Keys, Lower_Keys$deltaR, Lower_Keys$deltar_error)
#pooled mean for lower keys
l_keys

##     deparse.substitute.df.. pooled_mean weighted_uncertainty t_chi_sq## 1
        Lower_Keys       -179.3494            8.810671 32.79863
##     degree_freedom     t_crit normalized_chi_sq      outliers     T_uncertainty     ##     1
                          7 14.06714                   4.685519 outlier(s)           49.8399

d_tort <- w_mean_fun(Dry_Tortugas_National_Park, Dry_Tortugas_National_Park$deltaR,
Dry_Tortugas_National_Park$deltar_error)#pooled mean for dry tortugas
d_tort

##          deparse.substitute.df..     pooled_mean     weighted_uncertainty     t_chi_sq    ##     1
Dry_Tortugas_National_Park     -189.818                 6.269805             151.3749           ##
        degree_freedom   t_crit normalized_chi_sq    outliers T_uncertainty ## 1
            20 31.41043             7.568746 outlier(s) 82.0759

b_nat <- w_mean_fun(Biscayne_National_Park, Biscayne_National_Park$deltaR,
Biscayne_National_Park$deltar_error) #pooled mean for biscayne bay
b_nat

##    deparse.substitute.df..     pooled_mean     weighted_uncertainty     t_chi_sq     ##     1
Biscayne_National_Park     -209.8177                                          13.47568
11.99168##    degree_freedom    t_crit normalized_chi_sq    outliers T_uncertainty## 1    5
11.0705    2.398336 outlier(s)    41.14401

marq <- w_mean_fun(Marquesas, Marquesas$deltaR, Marquesas$deltar_error)
#pooled mean for marquesas
marq

##     deparse.substitute.df.. pooled_mean weighted_uncertainty t_chi_sq## 1
        Marquesas           -191.5639          13.32704 18.79699
##     degree_freedom     t_crit normalized_chi_sq      outliers     T_uncertainty     ##     1
                          3 7.814728                   6.265664 outlier(s)          62.56799

#boxplot of variability by geographic location
p2 <- ggplot(FKRT_g, aes(x=FKRT_zone,
    y=deltaR))+geom_boxplot() + labs(x='', y='Delta
    R')
p2
```

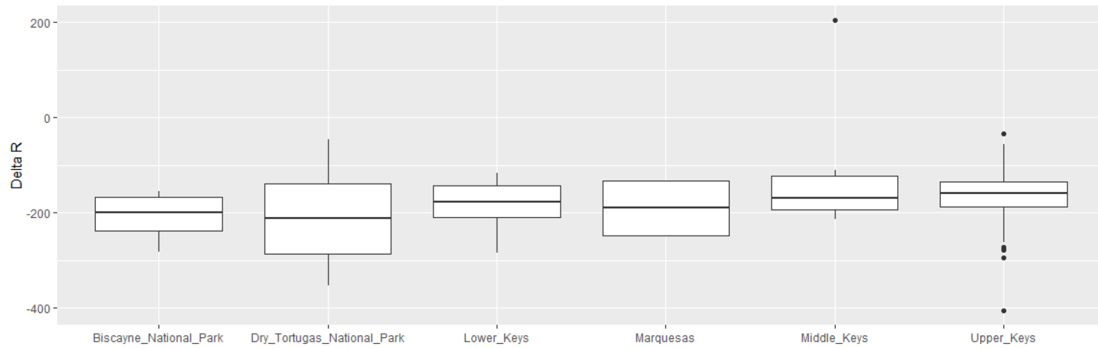


```
# #FKRT zone figure
# tiff("FKRT_zone.tiff", width=12, height=4, compression="lzw", units="in",res=2400)
# p2
# dev.off()

detach(FRKT_g_s)
```

Pooled means for Southwestern Florida and Apalachicola Bay

```
SW_FL <- subset(all_delta_rs, Region=="Southwestern_Florida")
SW_FL_m <- w_mean_fun(SW_FL, SW_FL$deltaR, SW_FL$deltar_error)SW_FL_m


##      deparse.substitute.df.. pooled_mean weighted_uncertainty t_chi_sq
## 1                       SW_F    32.88892             16.37607 99.25841
##      degree_freedom    t_crit normalized_chi_sq       outliers T_uncertainty
## 1                13 22.36203          7.635262 outlier(s)         158.4278

ACB <- subset(all_delta_rs, Region=="Apalachicola_Bay")
ACB_m <- w_mean_fun(ACB, ACB$deltaR, ACB$deltar_error)ACB_m


##      deparse.substitute.df.. pooled_mean weighted_uncertainty t_chi_sq
## 1                         AC    5.179331             6.289089 1107.358
##      degree_freedom    t_crit normalized_chi_sq       outliers T_uncertainty
## 1                17 27.58711          65.13868 outlier(s)         185.4008
```

Pooled means for different islands within the Florida Keys

```
#calculate pooled mean for Loggerhead Key
LK <- subset(all_delta_rs, Region=="Loggerhead_Key_Light")LK_m <-
w_mean_fun(LK, LK$deltaR, LK$deltar_error)
LK_m

##      deparse.substitute.df.. pooled_mean weighted_uncertainty t_chi_sq
## 1                          L   -131.3722             10.15991 5.586601
##      degree_freedom     t_crit normalized_chi_sq      outliers T_uncertainty
## 1                 3 7.814728            1.8622 outlier(s)      23.06502
```

```
#calculate pooled mean for Plantation Key
PK <- subset(all_delta_rs, Region=="Plantation_Key,_Conch_Reef")PK_m <-
w_mean_fun(PK, PK$deltaR, PK$deltar_error)
PK_m

##      deparse.substitute.df.. pooled_mean weighted_uncertainty t_chi_sq
## 1                          P   -144.4066             9.755968 70.74304
##      degree_freedom     t_crit normalized_chi_sq      outliers T_uncertainty
## 1                 3 7.814728          23.58101 outlier(s)       99.0726

#calculate pooled mean for Lower Matecumbe Key
LMK <- subset(all_delta_rs, Region=="Lower_Matecumbe_Key")
LMK_m <- w_mean_fun(LMK, LMK$deltaR, LMK$deltar_error)
LMK_m

##      deparse.substitute.df.. pooled_mean weighted_uncertainty t_chi_sq
## 1                         LM    -152.503             14.37964 3.579882
##      degree_freedom     t_crit normalized_chi_sq      outliers T_uncertainty
## 1                 1 3.841459          3.579882 outlier(s)      36.13483
```

Pooled mean for the Clupper site combining measurements fromPlantation Key and Lower Matecumbe Key

```
clupper <- subset(all_delta_rs, Region %in%
c("Plantation_Key,_Conch_Reef","Lower_Matecumbe_Key"))
clupper_m <- w_mean_fun(clupper, clupper$deltaR, clupper$deltar_error)clupper_m

##      deparse.substitute.df.. pooled_mean weighted_uncertainty t_chi_sq
## 1                    clupper   -146.9586             8.073256 74.54001
##      degree_freedom     t_crit normalized_chi_sq      outliers T_uncertainty
## 1                 5 11.0705            14.908 outlier(s)       77.7559
```

SQL Code for all OxCal models from the Clupper Site, Upper Matecumbe Key, Florida

Associated dates from Test Pit 4 with Plantation Key/Lower Matecumbe Key ΔR

```
Options()
 {
  kIterations=1000;
 };
 // Delta_R values updated for Marine20
 Plot()
 {
  Sequence()
  {
   Boundary("End");
   Phase("TP4 Layer 1 and 2 2")
   {
    Curve("IntCal20","intcal20.14c");
    R_Date("UGAMS 52040", 1270, 20);
    R_Date("UGAMS 52038", 1270, 20);
    R_Date("UGAMS 52039", 1180, 20);
    Curve("Marine20","marine20.14c");
    Delta_R("LocalMarine",-147,78);
    R_Date("UGAMS-52370", 1280, 20);
    R_Date("UGAMS 52369", 1260, 20);
```

```
   R_Date("UGAMS-52368", 1340, 20);
  };
  Boundary("Start");
 };
};
```

Associated dates from Test Pit 4 with Florida Keys ΔR

```
Options()
 {
  kIterations=1000;
 };
 // Delta_R values updated for Marine20
 Plot()
 {
  Sequence()
  {
   Boundary("End");
   Phase("TP4 Layer 1 and 2 2")
   {
    Curve("IntCal20","intcal20.14c");
    R_Date("UGAMS 52040", 1270, 20);
    R_Date("UGAMS 52038", 1270, 20);
    R_Date("UGAMS 52039", 1180, 20);
```

```
   Curve("Marine20","marine20.14c");
   Delta_R("LocalMarine",-169,55);
   R_Date("UGAMS-52370", 1280, 20);
   R_Date("UGAMS 52369", 1260, 20);
   R_Date("UGAMS-52368", 1340, 20);
  };
  Boundary("Start");
 };
};
```

Associated dates from Test Pit 4 with Upper Keys ΔR

```
Options()
 {
  kIterations=1000;
 };
 // Delta_R values updated for Marine20
 Plot()
 {
  Sequence()
  {
   Boundary("End");
   Phase("TP4 Layer 1 and 2 2")
   {
```

```
   Curve("IntCal20","intcal20.14c");
   R_Date("UGAMS 52040", 1270, 20);
   R_Date("UGAMS 52038", 1270, 20);
   R_Date("UGAMS 52039", 1180, 20);
   Curve("Marine20","marine20.14c");
   Delta_R("LocalMarine",-167,39);
   R_Date("UGAMS-52370", 1280, 20);
   R_Date("UGAMS 52369", 1260, 20);
   R_Date("UGAMS-52368", 1340, 20);
  };
  Boundary("Start");
 };
};
```

All radiocarbon dates with Plantation Key/Lower Matecumbe Key ΔR

```
// Delta_R values updated for Marine20
 Options()
 {
  kIterations=1000;
 };
 // Delta_R values updated for Marine20
 Plot()
 {
```

```
 Sequence()
 {
  Boundary("End");
  Phase("TP4 Layer 1 and 2 2")
  {
   Curve("IntCal20","intcal20.14c");
   R_Date("UGAMS 52040", 1270, 20);
   R_Date("UGAMS 52038", 1270, 20);
   R_Date("UGAMS 52039", 1180, 20);
   Curve("Marine20","marine20.14c");
   Delta_R("LocalMarine",-147,78);
   R_Date("UGAMS-52370", 1280, 20);
   R_Date("UGAMS 52369", 1260, 20);
   R_Date("UGAMS-52368", 1340, 20);
  };
  Boundary("Start");
 };
};
Plot()
{
 Curve("Marine20","marine20.14c");
 Delta_R("LocalMarine",-147,78);
 R_Date("D-AMS 013325", 1323, 21);
```

```
R_Date("Beta-410911", 1280, 30);

R_Date("D-AMS 013326", 1278, 27);

R_Date("D-AMS 013327", 1463, 22);

};
```

Table 2. Results of single-phase Bayesian model of stratigraphically associated dates in Test Pit 4, Clupper site, Upper Matecumbe Key.

Name	**Unmodelled (BP)**			**Modelled (BP)**		
	from	to	%	from	to	%
Sequence						
Boundary End				1600	1150	95.449973
Phase TP4 Layer 1 and 2 2						
Curve IntCal20						
R_Date UGAMS 52040	1280	1150	95.449973	1280	1130	95.449974
R_Date UGAMS 52038	1280	1150	95.449973	1280	1130	95.449974
R_Date UGAMS 52039	1180	1005	95.449974	1180	1005	95.449974
Curve Marine20						
Delta_R LocalMarine	-304	10	95.449974	-425.5	-75	95.449974
R_Date UGAMS-52370	1020	625	95.449974	1175	710	95.449974
R_Date UGAMS 52369	1000	610	95.449974	1170	700	95.449974
R_Date UGAMS-52368	1075	665	95.449974	1220	760	95.449974
Boundary Start				1170	450	95.449974

Table 3. Model specification for single-phase Bayesian model of stratigraphically associated dates in Test Pit 4, Clupper site, Upper Matecumbe Key

Parameter	**Name**	**Type**	**z**	**mu**	**sigma**	**llim**	**ulim**
0	intcal20	NoOp				-53054.5	1960.5
1		NoOp				NaN	NaN
2	End	Boundary		630.204	127.451	-549.5	900.5
3		NoOp				NaN	NaN
4	IntCal20	Curve				-53054.5	1960.5
5	UGAMS 52040	R_Date		735.459	34.752	640.5	900.5
6	UGAMS 52038	R_Date		735.4	34.6897	640.5	900.5
7	UGAMS 52039	R_Date		843.787	41.4494	665.5	1005.5
8	Marine20	Curve				-53054.5	1965.5
9	LocalMarine	Delta_R		-249.518	93.8454	-575	290
10	UGAMS-52370	R_Date		1008.5	122.508	620.5	1650.5

11	UGAMS 52369	R_Date		1020.86	123.908	635.5	1670.5
12	UGAMS-52368	R_Date		963.358	118.854	560.5	1575.5
13	Start	Boundary		1138.78	198.635	665.5	2780.5

Table 4. Results of single-phase Bayesian model with the error weighted average ΔR from the Upper Keys.

Name	Unmodelled (BC/AD)			Modelled (BC/AD)		
	from	to	%	from	to	%
Sequence						
Boundary End				295	770	95.449973
Phase TP4 Layer 1 and 2 2						
Curve IntCal20						
R_Date UGAMS 52040	670	800	95.449973	670	820	95.449973
R_Date UGAMS 52038	670	800	95.449973	670	820	95.449974
R_Date UGAMS 52039	770	945	95.449974	770	945	95.449973
Curve Marine20						
Delta_R LocalMarine	-245.5	-88.5	95.449974	-266	-102.5	95.449974
R_Date UGAMS-52370	980	1275	95.449974	925	1235	95.449974
R_Date UGAMS 52369	1000	1285	95.449974	950	1255	95.449974
R_Date UGAMS-52368	900	1220	95.449974	880	1200	95.449974
Boundary Start				970	1590	95.449974

Table 5. Model specification for single-phase Bayesian model with error weighted average ΔR from the Upper Keys.

Parameter	Name	Type	z	mu	sigma	llim	ulim
0	intcal20	NoOp				-53054.5	1960.5
1		NoOp				NaN	NaN
2	End	Boundary		607.554	135.02	-229.5	900.5
3		NoOp				NaN	NaN
4	IntCal20	Curve				-53054.5	1960.5
5	UGAMS 52040	R_Date		732.419	33.9469	640.5	900.5
6	UGAMS 52038	R_Date		732.432	33.9192	640.5	900.5
7	UGAMS 52039	R_Date		846.428	41.7501	665.5	1005.5
8	Marine20	Curve				-53054.5	1965.5
9	LocalMarine	Delta_R		-183.832	40.35	-391	64
10	UGAMS-52370	R_Date		1085.6	74.2892	685.5	1495.5
11	UGAMS 52369	R_Date		1099.13	73.2906	700.5	1510.5
12	UGAMS-52368	R_Date		1036.19	78.7004	650.5	1455.5

13	Start	Boundary		1236.62	166.975	700.5	2380.5

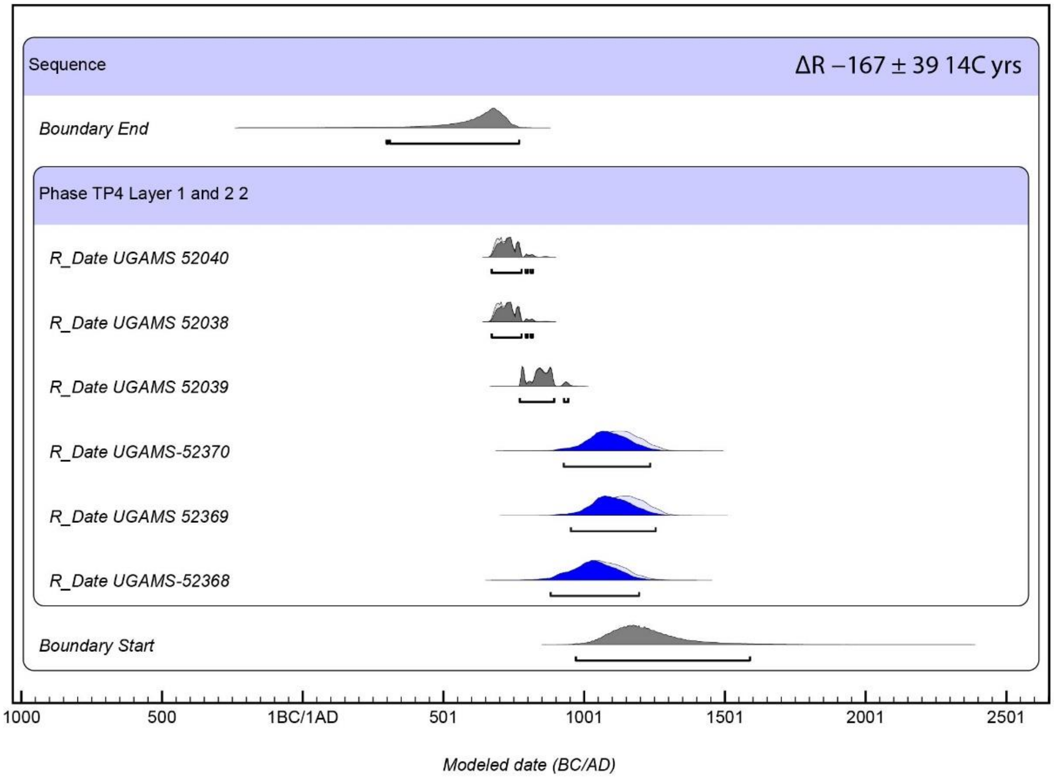

Figure 1. Plot of single-phase Bayesian model with error weighted average ΔR from the Upper Keys

Table 6. Results of single-phase Bayesian model with error weighted average ΔR from the Florida Keys

Name	**Unmodelled (BC/AD)**			**Modelled (BC/AD)**		
	from	to	%	from	to	%
Sequence						
Boundary End				320	775	95.449974
Phase TP4 Layer 1 and 2 2						
Curve IntCal20						
R_Date UGAMS 52040	670	800	95.449973	670	820	95.449974
R_Date UGAMS 52038	670	800	95.449973	670	820	95.449974
R_Date UGAMS 52039	770	945	95.449974	770	945	95.449974
Curve Marine20						
Delta_R LocalMarine	-279	-59	95.449974	-335	-92.5	95.449974
R_Date UGAMS-52370	955	1290	95.449974	865	1240	95.449974
R_Date UGAMS 52369	975	1300	95.449974	885	1255	95.449974
R_Date UGAMS-52368	880	1240	95.449974	810	1190	95.449974

Boundary Start				895	1565	95.449974

Table 7. Model specification for single-phase Bayesian model with error weighted average ΔR from the Florida Keys

Parameter	Name	Type	z	mu	sigma	llim	ulim
0	intcal20	NoOp				-53054.5	1960.5
1		NoOp				NaN	NaN
2	End	Boundary		614.364	133.315	-304.5	900.5
3		NoOp				NaN	NaN
4	IntCal20	Curve				-53054.5	1960.5
5	UGAMS 52040	R_Date		733.165	34.163	640.5	900.5
6	UGAMS 52038	R_Date		733.213	34.0525	640.5	900.5
7	UGAMS 52039	R_Date		846.079	41.5895	665.5	1005.5
8	Marine20	Curve				-53054.5	1965.5
9	LocalMarine	Delta_R		-209.709	61.5387	-474	146
10	UGAMS-52370	R_Date		1056	92.2311	655.5	1530.5
11	UGAMS 52369	R_Date		1069.72	92.1109	665.5	1545.5
12	UGAMS-52368	R_Date		1007.09	93.5504	620.5	1480.5
13	Start	Boundary		1201.32	177.959	665.5	2470.5

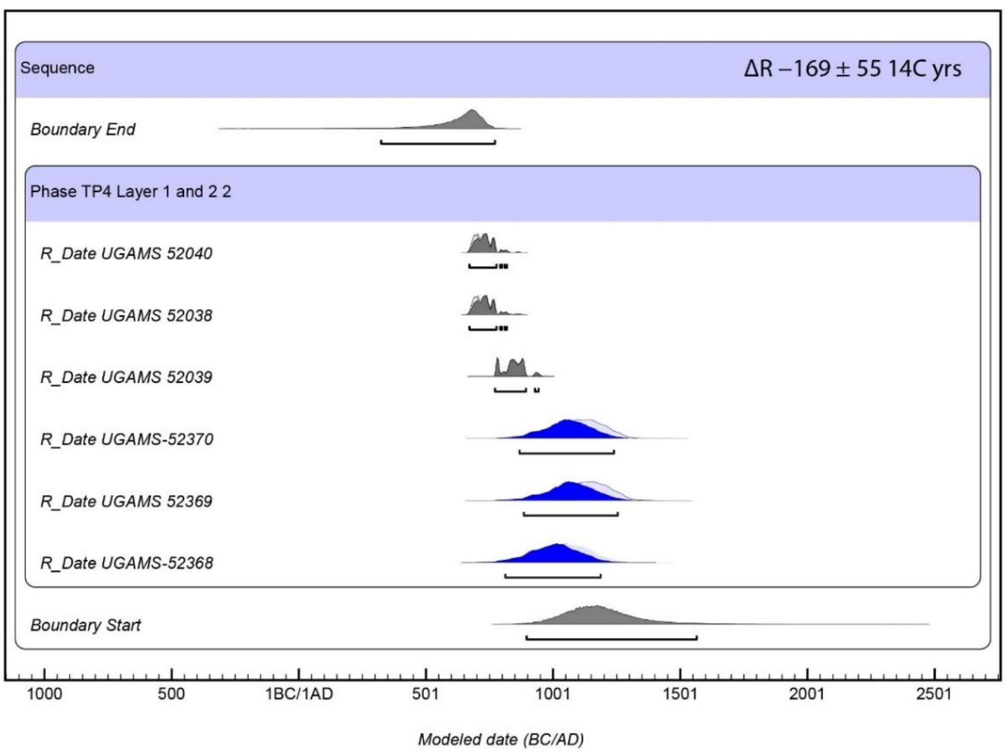

Figure 1. Plot of single-phase Bayesian model with error weighted average ΔR from the Florida Keys

APPENDIX C

SUPPLEMENTAL MATERIAL FOR CHAPTER IV

Table 1. Results of Bayesian modeled stratgraphically associated radiocarbon dates

Name	**Unmodelled (BP)**					**Modelled (BP)**					**Indices** **Amodel 121.6** **Aoverall 115**				
	from	to	%	mu	sigma	from	to	%	mu	sigma	Acomb	A	L	P	C
Curve Marine20															
Delta_R LocalMarine1	-300	300	95.449974	0	171.464	-234.6	268.2	95.449974	-0.751962	128.043		100			99.1
Sequence															
Boundary Yap Start						2655	1755	95.449974	2130	290					97.6
Phase Layer 5															
Curve =LocalMarine1															
R_Date YP-1	2430	1525	95.449974	1985	225	2285	1635	95.449974	1945	160		113.6			99.6
Curve IntCal20															
R_Date YP-8	1940	1745	95.449974	1860	45	1940	1745	95.449974	1860	45		99.9			99.9
Boundary Transition 5/4						1920	1340	95.449974	1670	155					99.6
Phase Layer 4															
Curve =LocalMarine1															
R_Date D-AMS 019908	2030	1170	95.449974	1590	215	1830	1260	95.449974	1555	145		114.8			99.7
R_Date D-AMS 019907	1790	955	95.449974	1380	205	1805	1210	95.449974	1505	150		99.1			99.6
Boundary Transition 4/3						1775	1165	95.449974	1465	155					99.6
Phase Layer 3															
Curve =LocalMarine1															
R_Date D-AMS 019906	1920	1090	95.449974	1500	205	1730	1125	95.449974	1430	150		109.1			99.6
Boundary Yap End						1770	720	95.449974	1290	295					97.4

Table 2. Model specification for Bayesian modeled stratgraphically associated radiocarbon dates

Parameter	Name	Type	z	mu	sigma	llim	ulim
0	intcal20	NoOp				-53054.5	1960.5
1	Charcoal	Outlier_Model		-158.195	181.909	-1010	20
2		Sum		-1.87337	2.1722	-10.1	0.2
3		U		1.92532	0.0598321	0	2
4	Marine20	Curve				-53054.5	1965.5
5	LocalMarine1	Delta_R		-130.823	70.5603	-300	300
6		NoOp				NaN	NaN
7	Yap Start	Boundary		-384.13	165.318	-3029.5	320.5
8		NoOp				NaN	NaN
10	D-AMS 019909	R_Date		-248.92	122.962	-1339.5	1045.5
11	YP-1	R_Date		-183.542	114.219	-1179.5	1090.5
12	IntCal20	Curve				-53054.5	1960.5
13	YP-9	R_Date		-209.666	110.137	-3029.5	1440.5
14	YP-8	R_Date		77.1667	42.8895	-159.5	320.5
15	YP-10	R_Date		-65.3257	94.9222	-3029.5	1440.5
16	Transition 5/4	Boundary		170.09	64.2624	-159.5	1440.5
17		NoOp				NaN	NaN
19	D-AMS 019908	R_Date		253.142	74.4024	-159.5	1440.5
20	IntCal20	Curve				-53054.5	1960.5
21	YP-6	R_Date		237.213	61.9576	-159.5	1480.5
22	YP-7	R_Date		254.394	59.3968	-159.5	1480.5
24	D-AMS 019907	R_Date		297.855	86.4836	-159.5	1480.5
25	Transition 4/3	Boundary		337.553	92.1077	-159.5	1480.5
26		NoOp				NaN	NaN
28	D-AMS 019906	R_Date		389.204	93.1476	-159.5	1480.5
29	Transition 3/2	Boundary		550.559	146.909	-159.5	1965.5

30		NoOp				NaN	NaN
32	D-AMS 019905	R_Date		910.147	105.194	15.5	1965.5
33	IntCal20	Curve				-53054.5	1960.5
34	YP-3	R_Date		1364.44	58.9143	-159.5	1965.5
35	YP-4	R_Date		750.142	116.092	-159.5	1965.5
37	D-AMS 019904	R_Date		1475.41	61.7578	1015.5	1965.5
38	Transition 2/1	Boundary		1489.57	62.8186	1015.5	1965.5
39		NoOp				NaN	NaN
41	D-AMS 019903	R_Date		1500.45	64.6954	1015.5	1965.5
42	D-AMS 019902	R_Date		1520.25	72.1426	1015.5	1965.5
43	IntCal20	Curve				-53054.5	1960.5
44	YP-2	R_Date		1513.68	71.7963	1015.5	2760.5
45	Yap End	Boundary		1553.25	102.147	1015.5	2760.5

Supplemental text

Bayesian modeled ΔR SQL Code

```
// Delta_R values updated for Marine20
 Options()
 {
  kIterations=1000;
 };
 Plot()
 {
  Curve("Marine20","marine20.14c");
  Delta_R("LocalMarine1",U(-300,300));
  Sequence()
  {
   Boundary("Yap Start");
   Phase("Layer 5")
   {
    Curve("=LocalMarine1");
    R_Date("YP-1", 2500, 30);
    Curve("IntCal20","intcal20.14c");
    R_Date("YP-8", 1939, 29);
   };
   Boundary("Transition 5/4");
```

```
  Phase("Layer 4")
  {
   Curve("=LocalMarine1");
   R_Date("D-AMS 019908", 2161, 57);
   R_Date("D-AMS 019907", 1969, 57);
  };
  Boundary("Transition 4/3");
  Phase("Layer 3")
  {
   Curve("=LocalMarine1");
   R_Date("D-AMS 019906", 2078, 37);
  };
  Boundary("Yap End");
 };
};
```

SQL Code for Bayesian modeled colonization estimate with Saipan ΔR

```
// Delta_R values updated for Marine20
 Plot()
 {
  Outlier_Model("Charcoal",Exp(1,-10,0),U(0,2),"t");
  Sequence()
  {
```

```
Boundary("Yap Start");
Phase()
{
 Curve("Marine20","marine20.14c");
 Delta_R("LocalMarine",218,57);
 R_Date("D-AMS 019909", 2592, 58);
 R_Date("YP-1", 2500, 30);
 R_Date("D-AMS 026548", 2344, 28);
 Curve("IntCal20","intcal20.14c");
 R_Date("YP-9", 2298, 30)
 {
  Outlier("Charcoal", 1);
 };
 R_Date("S-ANU-57912", 2239, 22)
 {
  Outlier("Charcoal", 1);
 };
 Curve("Marine20","marine20.14c");
 Delta_R("LocalMarine",218,57);
 R_Date("D-AMS 019908", 2161, 57);
 R_Date("D-AMS 038879", 2123, 23);
 Curve("IntCal20","intcal20.14c");
 R_Date("YP-10", 2122, 35)
```

```
{
 Outlier("Charcoal", 1);
};
Curve("Marine20","marine20.14c");
Delta_R("LocalMarine",218,57);
R_Date("D-AMS 026457", 2114, 26);
R_Date("D-AMS 019906", 2078, 37);
R_Date("D-AMS 038880", 2059, 24);
R_Date("D-AMS 038877", 2055, 22);
R_Date("D-AMS 038878", 1995, 25);
R_Date("D-AMS 019907", 1969, 57);
Curve("IntCal20","intcal20.14c");
R_Date("S-ANU-57911", 1946, 22)
{
 Outlier("Charcoal", 1);
};
R_Date("YP-8", 1939, 29)
{
 Outlier("Charcoal", 1);
};
R_Date("S-ANU-57910", 1923, 22)
{
 Outlier("Charcoal", 1);
```

```
};
R_Date("NZ 6668", 1905, 65)
{
 Outlier("Charcoal", 1);
};
R_Date("YP-6", 1901, 30)
{
 Outlier("Charcoal", 1);
};
R_Date("YP-7", 1844, 29)
{
 Outlier("Charcoal", 1);
};
Curve("Marine20","marine20.14c");
Delta_R("LocalMarine",218,57);
R_Date("D-AMS 038871", 1716, 22);
R_Date("D-AMS 038874", 1541, 22);
R_Date("D-AMS 019905", 1520, 43);
R_Date("D-AMS 038873", 1519, 22);
Curve("IntCal20","intcal20.14c");
R_Date("YP-4", 1467, 29)
{
 Outlier("Charcoal", 1);
```

```
};
R_Date("AA-21211", 1456, 40)
{
 Outlier("Charcoal", 1);
};
Curve("Marine20","marine20.14c");
Delta_R("LocalMarine",218,57);
R_Date("D-AMS 019903", 1175, 35);
Curve("IntCal20","intcal20.14c");
R_Date("YP-2", 1107, 35)
{
 Outlier("Charcoal", 1);
};
R_Date("AA-21208", 1037, 39)
{
 Outlier("Charcoal", 1);
};
Curve("Marine20","marine20.14c");
Delta_R("LocalMarine",218,57);
R_Date("D-AMS 019902", 797, 40);
Curve("IntCal20","intcal20.14c");
R_Date("YP-3", 704, 29)
{
```

```
 Outlier("Charcoal", 1);
};
Curve("Marine20","marine20.14c");
Delta_R("LocalMarine",218,57);
R_Date("D-AMS 019904", 621, 30);
R_Date("D-AMS 038872", 592, 22);
Curve("IntCal20","intcal20.14c");
R_Date("NZ 6625", 507, 133)
{
 Outlier("Charcoal", 1);
};
R_Date("AA-21209", 504, 38)
{
 Outlier("Charcoal", 1);
};
R_Date("NZ 6651", 469, 66)
{
 Outlier("Charcoal", 1);
};
Curve("Marine20","marine20.14c");
Delta_R("LocalMarine",218,57);
R_Date("D-AMS 038875", 441, 21);
R_Date("D-AMS 038876", 430, 19);
```

```
    Curve("IntCal20","intcal20.14c");
    R_Date("NZ 6680", 364, 54)
    {
     Outlier("Charcoal", 1);
    };
    R_Date("Crane M-631", 320, 200)
    {
     Outlier("Charcoal", 1);
    };
    R_Date("AA-21210", 317, 38)
    {
     Outlier("Charcoal", 1);
    };
   };
   Boundary("Yap End");
  };
 };
```

SQL Code for Bayesian modeled colonization estimate

```
// Delta_R values updated for Marine20
 Plot()
 {
  Outlier_Model("Charcoal",Exp(1,-10,0),U(0,2),"t");
```

```
Sequence()
{
 Boundary("Yap Start");
 Phase()
 {
  Curve("Marine20","marine20.14c");
  Delta_R("LocalMarine",-1,128);
  R_Date("D-AMS 019909", 2592, 58);
  R_Date("YP-1", 2500, 30);
  R_Date("D-AMS 026548", 2344, 28);
  Curve("IntCal20","intcal20.14c");
  R_Date("YP-9", 2298, 30)
  {
   Outlier("Charcoal", 1);
  };
  R_Date("S-ANU-57912", 2239, 22);
  Curve("Marine20","marine20.14c");
  Delta_R("LocalMarine",-1,128);
  R_Date("D-AMS 019908", 2161, 57);
  R_Date("D-AMS 038879", 2123, 23);
  Curve("IntCal20","intcal20.14c");
  R_Date("YP-10", 2122, 35)
  {
```

```
 Outlier("Charcoal", 1);
};
Curve("Marine20","marine20.14c");
Delta_R("LocalMarine",-1,128);
R_Date("D-AMS 026457", 2114, 26);
R_Date("D-AMS 019906", 2078, 37);
R_Date("D-AMS 038880", 2059, 24);
R_Date("D-AMS 038877", 2055, 22);
R_Date("D-AMS 038878", 1995, 25);
R_Date("D-AMS 019907", 1969, 57);
Curve("IntCal20","intcal20.14c");
R_Date("S-ANU-57911", 1946, 22)
{
 Outlier("Charcoal", 1);
};
R_Date("YP-8", 1939, 29);
R_Date("S-ANU-57910", 1923, 22)
{
 Outlier("Charcoal", 1);
};
R_Date("NZ 6668", 1905, 65)
{
 Outlier("Charcoal", 1);
```

```
};
R_Date("YP-6", 1901, 30)
{
 Outlier("Charcoal", 1);
};
R_Date("YP-7", 1844, 29)
{
 Outlier("Charcoal", 1);
};
Delta_R("LocalMarine",-1,128);
R_Date("D-AMS 038871", 1716, 22);
R_Date("D-AMS 038874", 1541, 22);
R_Date("D-AMS 019905", 1520, 43);
R_Date("D-AMS 038873", 1519, 22);
Curve("IntCal20","intcal20.14c");
R_Date("YP-4", 1467, 29)
{
 Outlier("Charcoal", 1);
};
R_Date("AA-21211", 1456, 40)
{
 Outlier("Charcoal", 1);
};
```

```
Curve("Marine20","marine20.14c");
Delta_R("LocalMarine",-1,128);
R_Date("D-AMS 019903", 1175, 35);
Curve("IntCal20","intcal20.14c");
R_Date("YP-2", 1107, 35);
R_Date("AA-21208", 1037, 39)
{
 Outlier("Charcoal", 1);
};
Curve("Marine20","marine20.14c");
Delta_R("LocalMarine",-1,128);
R_Date("D-AMS 019902", 797, 40);
Curve("IntCal20","intcal20.14c");
R_Date("YP-3", 704, 29);
Curve("Marine20","marine20.14c");
Delta_R("LocalMarine",-1,128);
R_Date("D-AMS 019904", 621, 30);
R_Date("D-AMS 038872", 592, 22);
Curve("IntCal20","intcal20.14c");
R_Date("NZ 6625", 507, 133)
{
 Outlier("Charcoal", 1);
};
```

```
 R_Date("AA-21209", 504, 38)
 {
  Outlier("Charcoal", 1);
 };
 R_Date("NZ 6651", 469, 66)
 {
  Outlier("Charcoal", 1);
 };
 Curve("Marine20","marine20.14c");
 Delta_R("LocalMarine",-1,128);
 R_Date("D-AMS 038875", 441, 21);
 R_Date("D-AMS 038876", 430, 19);
 Curve("IntCal20","intcal20.14c");
 R_Date("NZ 6680", 364, 54)
 {
  Outlier("Charcoal", 1);
 };
 R_Date("AA-21210", 317, 38)
 {
  Outlier("Charcoal", 1);
 };
};
Boundary("Yap End");
```

```
 };

  Before("Fais pottery")

  {

   R_Date("NUTA2167", 1794, 152);

  };

};
```

Table 3. Model specification for single-phase Bayesian modeled with Class 1 and 2 dates.

Parameter	Name	Type	z	mu	sigma	llim	ulim
0	intcal20	NoOp				-53054.5	1960.5
1	Charcoal	Outlier_Model		-27.4302	45.8888	-1010	20
2		Sum		-1.05573	1.00038	-10.1	0.2
3		U		1.10299	0.584846	0	2
4		NoOp				NaN	NaN
5	Yap Start	Boundary		-344.7	78.7131	-4184.5	-89.5
6		NoOp				NaN	NaN
7	Marine20	Curve				-53054.5	1965.5
8	LocalMarine	Delta_R		28.266	107.365	-689	701
9	D-AMS 019909	R_Date		-97.1031	150.795	-1109.5	795.5
10	YP-1	R_Date		4.4796	153.405	-919.5	855.5
11	D-AMS 026548	R_Date		194.285	149.661	-774.5	1030.5
12	IntCal20	Curve				-53054.5	1960.5
13	YP-9	R_Date		-262.587	75.2589	-4184.5	5040.5
14	S-ANU-57912	R_Date		-260.168	43.7491	-414.5	-89.5
15	Marine20	Curve				-53054.5	1965.5
16	LocalMarine	Delta_R		-14.6352	122.589	-689	701
17	D-AMS 019908	R_Date		356.3	167.961	-589.5	1260.5
18	D-AMS 038879	R_Date		401.804	155.173	-434.5	1250.5
19	IntCal20	Curve				-53054.5	1960.5
20	YP-10	R_Date		-113.176	80.6138	-4184.5	5040.5
21	Marine20	Curve				-53054.5	1965.5
22	LocalMarine	Delta_R		-52.7101	121.547	-689	701
23	D-AMS 026457	R_Date		368.885	155.824	-424.5	1265.5
24	D-AMS 019906	R_Date		409.095	156.284	-409.5	1300.5

25	D-AMS 038880	R_Date		431.112	151.918	-389.5	1305.5
26	D-AMS 038877	R_Date		435.694	151.146	-389.5	1305.5
27	D-AMS 038878	R_Date		500.792	147.239	-349.5	1350.5
28	D-AMS 019907	R_Date		525.83	155.693	-364.5	1420.5
29	IntCal20	Curve				-53054.5	1960.5
30	S-ANU-57911	R_Date		106.85	58.2315	-4184.5	5040.5
31	YP-8	R_Date		90.0244	46.4997	-159.5	320.5
32	S-ANU-57910	R_Date		140.71	63.6908	-4184.5	5040.5
33	NZ 6668	R_Date		154.423	92.6704	-4184.5	5040.5
34	YP-6	R_Date		171.422	63.7071	-4184.5	5040.5
35	YP-7	R_Date		223.543	62.6481	-4184.5	5040.5
36	LocalMarine	Delta_R		-70.3799	114.594	-689	701
37	D-AMS 038871	R_Date		269.286	130.972	-419.5	1040.5
38	D-AMS 038874	R_Date		456.345	119.697	-359.5	1235.5
39	D-AMS 019905	R_Date		471.838	123.514	-364.5	1280.5
40	D-AMS 038873	R_Date		473.571	118.734	-354.5	1265.5
41	IntCal20	Curve				-53054.5	1960.5
42	YP-4	R_Date		632.35	51.0823	-4184.5	5040.5
43	AA-21211	R_Date		633.503	50.2169	-4184.5	5040.5
44	Marine20	Curve				-53054.5	1965.5
45	LocalMarine	Delta_R		-7.47356	133.886	-689	701
46	D-AMS 019903	R_Date		1355.31	129.827	640.5	1965.5
47	IntCal20	Curve				-53054.5	1960.5
48	YP-2	R_Date		938.904	42.8599	665.5	1170.5
49	AA-21208	R_Date		1034.07	69.8782	-4184.5	5040.5
50	Marine20	Curve				-53054.5	1965.5
51	LocalMarine	Delta_R		-18.5533	111.216	-689	701
52	D-AMS 019902	R_Date		1667.17	121.393	1010.5	1965.5
53	IntCal20	Curve				-53054.5	1960.5
54	YP-3	R_Date		1304	35.5564	1170.5	1420.5
55	Marine20	Curve				-53054.5	1965.5
56	LocalMarine	Delta_R		-120.23	86.694	-689	701
57	D-AMS 019904	R_Date		1734.33	104.66	1210.5	1965.5
58	D-AMS 038872	R_Date		1755.68	100.251	1245.5	1965.5
59	IntCal20	Curve				-53054.5	1960.5
60	NZ 6625	R_Date		1469.52	122.507	-4184.5	5040.5
61	AA-21209	R_Date		1443.81	52.7494	-4184.5	5040.5
62	NZ 6651	R_Date		1483.52	83.7363	-4184.5	5040.5
63	Marine20	Curve				-53054.5	1965.5

64	LocalMarine	Delta_R		-241.111	75.4783	-689	701
65	D-AMS 038875	R_Date		1778.06	91.43	1325.5	1965.5
66	D-AMS 038876	R_Date		1784.52	89.9471	1335.5	1965.5
67	IntCal20	Curve				-53054.5	1960.5
68	NZ 6680	R_Date		1569.78	72.443	-4184.5	5040.5
69	AA-21210	R_Date		1590.45	64.3481	-4184.5	5040.5
70	Yap End	Boundary		1889	92.4888	1335.5	5040.5
71		NoOp				NaN	NaN
72	NUTA2167	R_Date		237.782	178.003	-814.5	1035.5

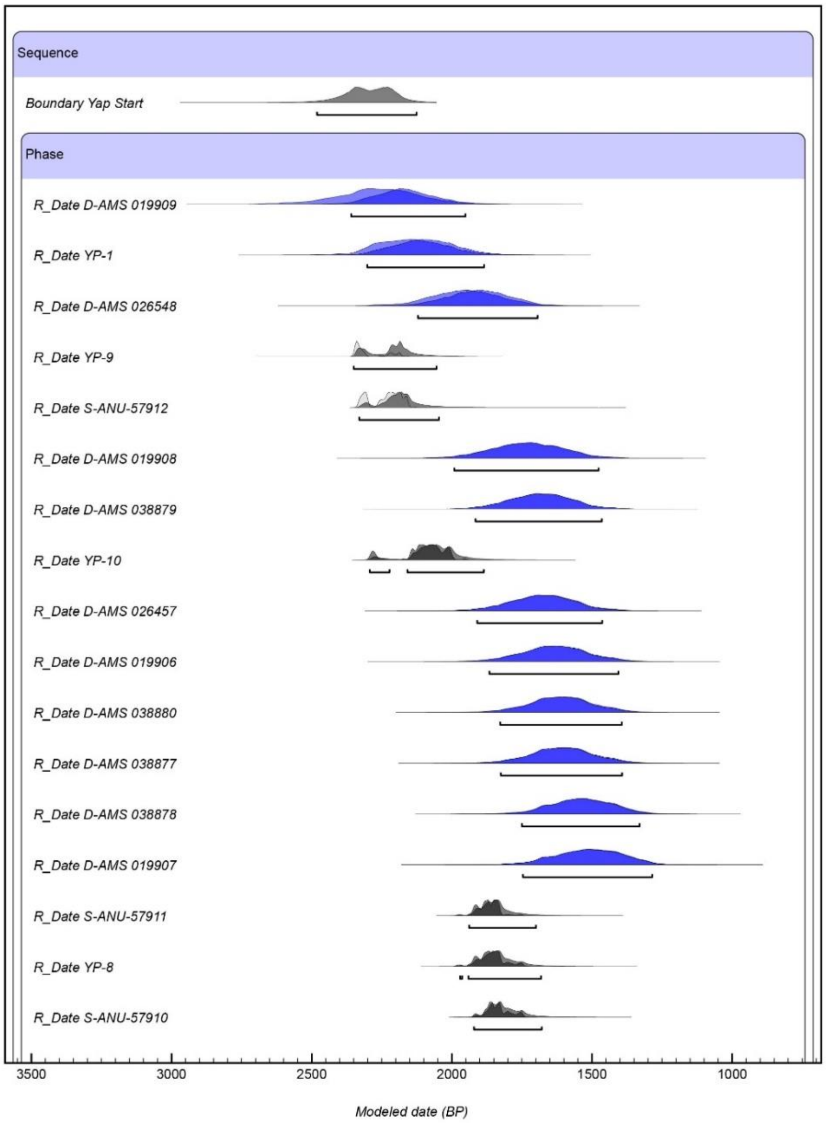

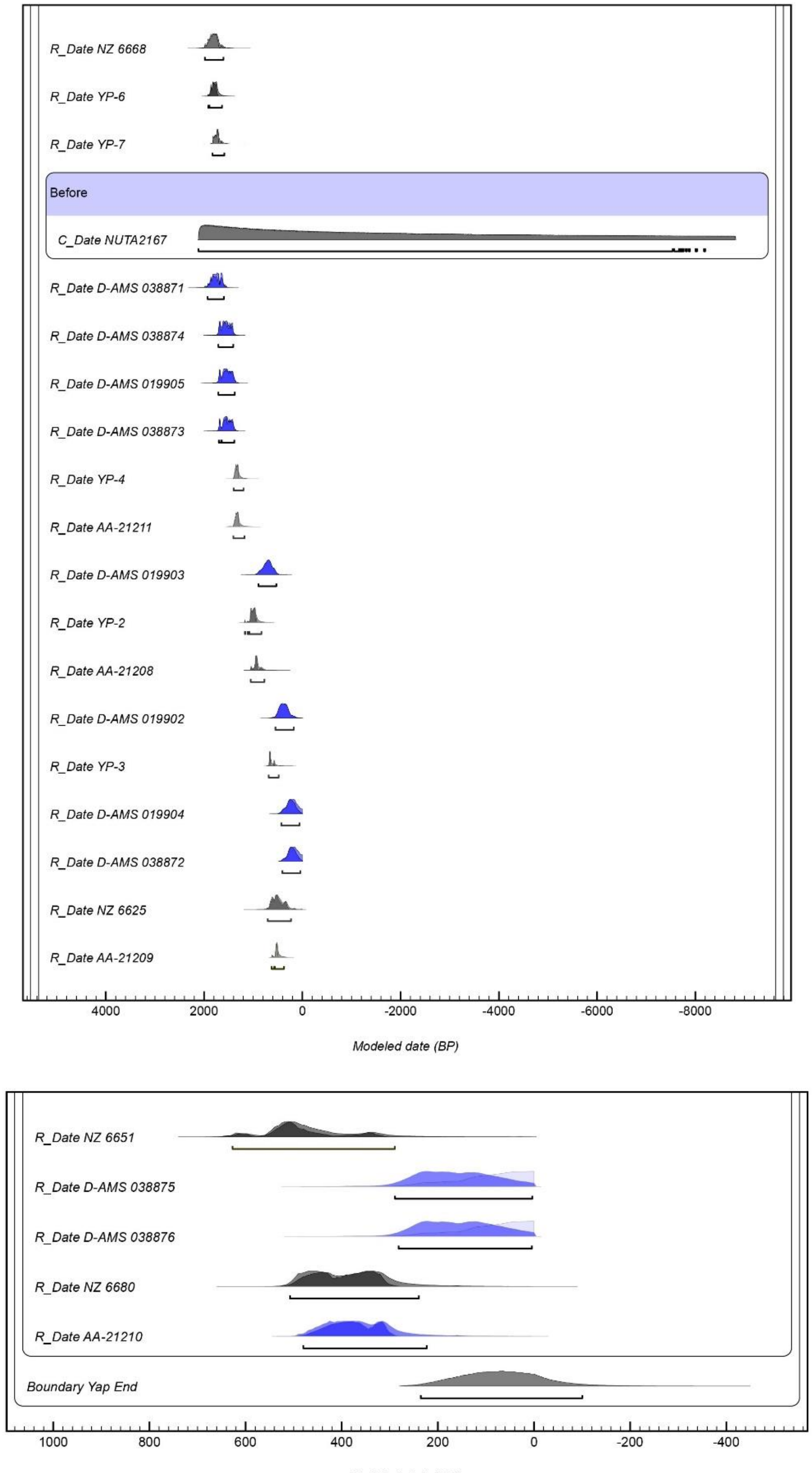

Figures 1. Plots of single phase Bayesian modeled Class 1 and 2 dates .

APPENDIX D

SUPPLEMENTAL MATERIAL FOR CHAPTER V

Table 1. Complete elemental analysis for glass beads from Chelechol ra Orrak.

Catalog No.	SiO2	Na2O	MgO	Al2O3	P2O5	Cl	K2O	CaO	MnO	Fe2O3	CuO	SnO2	PbO	Li	Be	B
4	75.57	0.78	0.18	0.46	0.35	0.03	15.63	6.63	0.08	0.16	0.02	0.00	0.05	7	0	47
5	40.56	0.11	0.08	0.46	0.11	0.02	3.07	0.37	0.03	0.16	0.06	0.01	54.91	6	1	61
6	74.11	0.61	0.15	0.49	0.27	0.03	13.19	7.25	0.15	0.27	3.00	0.03	0.39	5	0	66
7	40.49	1.25	0.12	1.07	0.07	0.09	9.68	0.77	0.37	0.56	0.29	0.28	44.87	28	1	2513
8	64.35	2.37	0.21	4.91	0.05	0.14	19.75	7.95	0.01	0.24	0.01	0.00	0.00	5	1	9
9	74.62	0.69	0.15	0.47	0.23	0.03	12.77	7.21	0.12	0.26	3.03	0.03	0.33	5	0	68
10	42.75	0.45	0.10	0.98	0.05	0.04	7.87	1.03	0.03	0.42	0.84	1.01	44.31	15	1	865
11	74.41	0.60	0.15	0.46	0.27	0.02	12.92	7.13	0.15	0.27	3.11	0.03	0.43	5	0	69
17	65.92	2.03	4.32	1.06	0.01	0.11	12.39	12.49	0.04	0.38	0.65	0.03	0.07	8	0	14
19	48.15	0.75	0.11	0.86	0.01	0.05	7.84	2.28	0.04	0.25	0.23	0.29	39.05	12	1	1353
111STNsp	46.96	1.43	0.22	1.49	0.12	0.07	13.30	4.33	0.02	0.23	0.80	0.04	30.81	9	2	1724
19STNsp	35.51	0.14	0.20	0.67	0.21	0.03	5.96	1.16	0.05	0.28	0.12	0.03	55.49	6	0	16
26STNsp	35.61	0.14	0.20	0.76	0.22	0.03	5.65	1.31	0.05	0.29	0.12	0.04	55.43	6	0	16
27MIXSP-A (refit w/ 51STNsp1)	33.67	0.12	0.24	0.99	0.18	0.11	5.28	1.40	0.04	0.34	0.11	0.02	57.35	9	0	18
27MIXSP-B	9.95	2.02	1.41	0.99	12.59	2.31	1.11	19.45	0.00	0.41	0.02	0.13	49.56	6	0	249
27MIXSP-C	65.25	0.63	0.62	1.30	0.18	0.12	16.64	11.06	0.12	0.50	3.34	0.05	0.10	9	0	137
37 (exterior)	60.82	11.76	2.03	2.44	1.08	0.23	3.07	8.58	0.74	2.45	2.04	0.02	3.28	14	0	162
37 (interior)	62.19	12.20	1.88	1.93	0.62	0.17	3.09	8.50	0.68	1.79	1.56	0.01	3.84	16	0	155
40STNsp	38.94	0.12	0.17	0.64	0.16	0.10	3.69	1.10	0.03	0.28	0.07	0.02	54.60	5	0	14
46STNsp-A	33.45	0.11	0.24	0.92	0.18	0.10	5.17	1.30	0.04	0.32	0.11	0.02	57.90	9	0	18
46STNsp-B	33.57	0.11	0.25	0.90	0.18	0.11	5.33	1.35	0.04	0.32	0.11	0.02	57.55	9	0	18
46STNsp-C	34.20	0.12	0.22	0.80	0.19	0.11	5.42	1.34	0.04	0.34	0.11	0.02	56.93	9	0	18
46STNsp-D	33.38	0.12	0.24	0.96	0.18	0.11	5.32	1.29	0.04	0.32	0.11	0.02	57.77	9	0	18
46STNsp-E	33.34	0.12	0.24	0.95	0.19	0.11	5.29	1.29	0.04	0.31	0.11	0.02	57.86	9	0	18
50STNsp-A	35.39	0.13	0.21	0.68	0.21	0.03	5.92	1.14	0.05	0.27	0.12	0.03	55.67	6	0	15
50STNsp-B	36.17	0.14	0.20	0.82	0.19	0.03	5.65	1.13	0.05	0.26	0.11	0.03	55.07	6	0	16
51STNsp1 (refit w/ 27MIXsp-A)	39.28	0.12	0.18	0.63	0.16	0.10	3.67	1.08	0.03	0.27	0.07	0.02	54.30	5	0	14
64STNsp	35.05	0.14	0.21	0.82	0.20	0.03	5.93	1.06	0.05	0.26	0.11	0.03	55.96	6	0	15
69STNsp	38.05	0.15	0.20	0.90	0.19	0.03	5.55	1.04	0.04	0.25	0.11	0.03	53.29	5	0	14
6STNSP-A	51.56	2.05	0.22	1.66	0.03	0.28	11.17	5.38	0.02	0.24	0.70	0.08	26.37	14	1	2831
6STNSP-B	36.39	0.14	0.18	0.69	0.15	0.11	3.66	0.97	0.04	0.26	0.10	0.01	57.29	9	1	70
6STNSP-C	38.31	0.12	0.21	0.64	0.20	0.12	4.45	1.08	0.04	0.27	0.11	0.03	54.28	9	0	22
6STNSP-D	38.17	0.12	0.21	0.68	0.21	0.13	4.38	1.20	0.04	0.28	0.11	0.03	54.30	9	0	23
6STNSP-E	38.44	0.12	0.20	0.68	0.20	0.12	4.53	1.12	0.05	0.27	0.11	0.03	54.01	10	0	24
6STNSP-F	41.80	0.39	0.21	0.61	0.28	0.13	3.60	0.92	0.06	0.16	0.03	0.00	51.71	9	0	3100
6STNSP-G	50.98	9.61	0.25	0.83	0.07	1.04	4.59	5.27	0.11	0.17	0.01	0.03	26.87	16	1	33
72STNSP-A	39.68	0.11	0.18	0.63	0.16	0.10	3.58	1.04	0.03	0.27	0.07	0.02	54.03	5	0	14
72STNSP-B	39.36	0.11	0.16	0.63	0.16	0.10	3.68	1.07	0.03	0.27	0.07	0.02	54.25	5	0	14

72STNSP-C	39.95	0.12	0.17	0.64	0.25	0.13	3.66	1.11	0.03	0.27	0.07	0.02	53.49	5	0	16
85STNsp2	39.97	0.18	0.10	0.61	0.03	0.13	7.32	0.77	0.02	0.33	0.54	0.84	49.05	9	2	98

Catalog No.	**Sc**	**Ti**	**V**	**Cr**	**Ni**	**Co**	**Zn**	**As**	**Rb**	**Sr**	**Zr**	**Nb**	**Ag**	**In**	**Sb**	**Cs**	**Ba**	**La**	**Ce**	**Pr**
4	5	213	5	5	627	460	55	3016	80	84	52	1	1	0	8	1	48	4	7	1
5	2	101	2	2	3	2	19	88	26	12	7	1	94	0	188	0	14	1	3	0
6	5	259	5	18	50	7	319	1045	135	92	60	1	7	1	80	1	85	4	8	1
7	3	285	8	4	53	344	207	3199	88	26	13	1	26	10	170	1	111	3	46	1
8	5	790	10	5	3	1	26	4	27	260	103	4	0	0	1	0	207	8	16	2
9	5	257	5	17	51	6	353	887	117	88	60	1	6	1	83	1	70	4	8	1
10	3	227	5	4	17	12	528	337	29	36	17	1	57	35	275	1	39	3	7	1
11	5	245	5	18	51	7	338	1093	131	89	57	1	8	1	84	1	82	4	8	1
17	4	287	5	2	34	13	3628	27	7	135	51	2	2	1	24	0	664	8	20	2
19	3	204	3	2	21	215	219	4993	18	60	42	1	31	10	121	1	80	3	9	1
111STNsp	5	284	5	2	11	24	766	3965	14	114	41	2	40	1	258	1	86	4	9	1
19STNsp	4	165	4	3	11	3	152	2952	26	19	12	1	62	1	548	0	19	2	3	0
26STNsp	4	177	4	3	13	4	117	3476	24	24	12	1	62	1	535	0	21	2	4	0
27MIXSP-A (refit w/ 51STNsp1)	5	159	5	3	9	3	216	4955	30	25	13	1	59	1	691	0	17	2	4	0
27MIXSP-B	2	104	34	115	2	1	217	83766	6	1467	6	1	3	5	187	0	39	1	3	0
27MIXSP-C	9	312	13	7	173	25	448	4451	161	169	75	2	8	2	113	1	108	5	9	1
37 (exterior)	5	668	13	51	44	30	90	325	12	644	44	3	4	1	8479	0	166	6	11	1
37 (interior)	5	538	12	15	42	32	71	276	10	591	36	2	3	1	8899	0	180	5	9	1
40STNsp	4	158	3	3	10	3	143	2363	26	25	12	1	65	1	475	1	23	3	5	1
46STNsp-A	6	147	4	3	8	3	212	4339	28	23	12	1	60	1	692	0	16	2	4	0
46STNsp-B	6	151	4	3	8	3	209	4345	30	23	12	1	59	1	685	0	16	2	4	0
46STNsp-C	6	159	5	4	9	3	210	3983	29	24	12	1	58	1	682	0	16	2	4	0
46STNsp-D	6	148	4	3	8	3	200	4898	30	22	12	1	59	1	686	0	15	2	4	0
46STNsp-E	6	149	4	3	8	3	196	5050	28	22	12	1	60	1	685	0	15	2	4	0
50STNsp-A	4	164	4	3	11	3	151	3329	23	18	11	1	63	1	562	0	18	2	3	0
50STNsp-B	4	159	4	2	10	3	141	3320	25	18	11	1	61	1	538	0	19	2	3	0
51STNsp1 (refit w/ 27MIXsp-A)	4	155	3	3	10	3	142	2376	25	25	12	1	66	1	502	0	22	3	5	1
64STNsp	4	155	4	3	10	3	142	3433	22	17	10	1	62	1	562	0	18	2	3	0
69STNsp	4	149	3	2	10	3	138	3439	21	17	10	1	60	1	547	0	17	2	3	0

6STNSP-A	10	332	6	3	19	60	2411	7216	19	163	59	2	22	3	155	0	115	5	11	1
6STNSP-B	8	148	4	3	8	2	52	1076	41	27	12	1	46	0	140	1	27	2	4	0
6STNSP-C	8	164	5	3	10	3	246	4071	31	26	13	1	71	1	806	0	17	2	4	0
6STNSP-D	8	173	5	3	11	3	269	4269	31	28	14	1	71	1	812	0	18	2	4	0
6STNSP-E	8	166	5	4	10	4	250	4053	44	26	13	1	69	1	785	1	17	2	4	0
6STNSP-F	8	144	4	3	1	0	42	43	59	21	10	1	49	0	603	0	24	1	3	0
6STNSP-G	9	216	7	4	8	2	214	31249	26	128	41	2	4	1	642	0	314	2	4	0
72STNSP-A	4	151	3	2	10	3	144	2377	24	24	11	1	67	1	519	0	22	3	5	1
72STNSP-B	4	154	3	2	10	3	144	2381	26	25	12	1	66	1	463	1	22	3	5	1
72STNSP-C	4	154	4	3	10	3	140	2678	26	31	12	1	65	1	529	0	22	2	5	1
85STNsp2	4	128	3	2	12	17	594	1148	20	24	11	1	50	53	359	1	23	2	5	1

Catalog No.	**Ta**	**Au**	**Y**	**Bi**	**U**	**W**	**Mo**	**Nd**	**Sm**	**Eu**	**Gd**	**Tb**	**Dy**	**Ho**	**Er**	**Tm**	**Yb**	**Lu**	**Hf**	**Th**
4	0	0	5	236	44	1	6	3	1	0	1	0	1	0	1	0	0	0	2	2
5	0	19	1	26	0	1	0	1	0	0	0	0	0	0	0	0	0	0	0	1
6	0	0	4	5	1	1	2	4	1	0	1	0	1	0	0	0	0	0	2	2
7	0	1	3	45	1	1	1	2	1	0	1	0	1	0	0	0	0	0	0	1
8	0	0	6	0	1	0	0	7	1	0	1	0	1	0	1	0	1	0	3	4
9	0	0	4	5	1	1	2	3	1	0	1	0	1	0	0	0	0	0	2	2
10	0	1	2	70	0	1	1	2	0	0	0	0	0	0	0	0	0	0	0	1
11	0	0	3	5	1	1	2	3	1	0	1	0	1	0	0	0	0	0	2	2
17	0	0	4	2	1	0	0	6	1	0	1	0	1	0	0	0	0	0	2	3
19	0	0	2	19	1	1	0	2	0	0	0	0	0	0	0	0	0	0	1	1
111STNsp	0	1	3	65	1	1	0	4	1	0	1	0	1	0	0	0	0	0	1	2
19STNsp	0	23	2	336	0	0	0	1	0	0	0	0	0	0	0	0	0	0	0	1
26STNsp	0	27	2	335	0	0	0	1	0	0	0	0	0	0	0	0	0	0	0	1
27MIXSP-A (refit w/ 51STNsp1)	0	23	2	346	0	0	0	1	0	0	0	0	0	0	0	0	0	0	0	1
27MIXSP-B	0	30	1	8	3	0	1	1	0	0	0	0	0	0	0	0	0	0	0	0
27MIXSP-C	0	0	5	8	1	1	2	3	1	0	1	0	1	0	0	0	0	0	2	1
37 (exterior)	0	0	5	43	2	0	1	5	1	0	1	0	1	0	0	0	0	0	1	2
37 (interior)	0	0	4	29	2	0	1	4	1	0	1	0	1	0	0	0	0	0	1	1
40STNsp	0	27	2	386	0	0	0	2	0	0	0	0	0	0	0	0	0	0	0	2
46STNsp-A	0	24	2	356	0	0	0	1	0	0	0	0	0	0	0	0	0	0	0	1
46STNsp-B	0	24	2	357	0	0	0	1	0	0	0	0	0	0	0	0	0	0	0	1
46STNsp-C	0	23	2	342	0	0	0	1	0	0	0	0	0	0	0	0	0	0	0	1
46STNsp-D	0	23	2	345	0	0	0	1	0	0	0	0	0	0	0	0	0	0	0	1
46STNsp-E	0	23	2	343	0	0	0	1	0	0	0	0	0	0	0	0	0	0	0	1

50STNsp-A	0	24	2	342	0	0	0	1	0	0	0	0	0	0	0	0	0	0	0	1
50STNsp-B	0	23	2	331	0	0	0	1	0	0	0	0	0	0	0	0	0	0	0	1
51STNsp1 (refit w/ 27MIXsp-A)	0	27	2	383	0	0	0	2	0	0	0	0	0	0	0	0	0	0	0	1
64STNsp	0	24	1	341	0	0	0	1	0	0	0	0	0	0	0	0	0	0	0	1
69STNsp	0	23	1	325	0	0	0	1	0	0	0	0	0	0	0	0	0	0	0	1
6STNSP-A	0	0	4	8	1	1	0	3	1	0	1	0	1	0	0	0	0	0	1	2
6STNSP-B	0	25	2	8	0	0	0	1	0	0	0	0	0	0	0	0	0	0	0	1
6STNSP-C	0	27	2	397	0	0	0	1	0	0	0	0	0	0	0	0	0	0	0	1
6STNSP-D	0	27	2	403	0	0	0	1	0	0	0	0	0	0	0	0	0	0	0	1
6STNSP-E	0	26	2	378	0	0	0	1	0	0	0	0	0	0	0	0	0	0	0	1
6STNSP-F	0	36	1	37	0	3	1	1	0	0	0	0	0	0	0	0	0	0	0	0
6STNSP-G	0	0	2	31	1	1	1	1	0	0	0	0	0	0	0	0	0	0	1	1
72STNSP-A	0	28	2	393	0	0	0	2	0	0	0	0	0	0	0	0	0	0	0	2
72STNSP-B	0	27	2	387	0	0	0	2	0	0	0	0	0	0	0	0	0	0	0	2
72STNSP-C	0	27	2	377	0	0	0	1	0	0	0	0	0	0	0	0	0	0	0	1
85STNsp2	0	1	2	133	1	1	0	1	0	0	0	0	0	0	0	0	0	0	0	1

REFERENCES CITED

Adams WH. 1997. Yap archaeology: Archaeological survey of Gachlaw village, Gilmon municipality, Yap, Federated States of Micronesia. US National Park Service.

Adelaar K, Himmelmann N. 2013. Austronesian Languages of Asia and Madagascar. Hoboken: Taylor and Francis.

Adhyatman S, Arifin R, 1993. Manik-Manik di Indonesia: Beads in Indonesia. Jakarta: Penerbit Djambatan.

Allen JD. 2010. The Heirloom Beads of Island South East Asia. In: Munan H, Martin F, editors. Journal: Borneo International Beads Conference 2010, Sarawak: Crafthub. p. 67-83.

Allen MS. 1998. Holocene Sea-Level Change on Aitutaki, Cook Islands: Landscape Change and Human Response. Journal of Coastal Research 14(1):10–22.

Allen MS, Wallace R. 2007. New evidence from the East Polynesian gateway: Substantive and methodological results from Aitutaki, southern Cook Islands. Radiocarbon 49(3):1163–1180.

Allen MS. 2014. Marquesan Colonisation Chronologies and Post- Colonisation Interaction: Implications for Hawaiian Origins and the ‘Marquesan Homeland’ Hypothesis. Journal of Pacific Archaeology 5(2):1-17.

Allen MS, Huebert JM. 2014. Short-lived plant materials, long-lived trees, and Polynesian ^{14}C dating: Considerations for ^{14}C sample selection and documentation. Radiocarbon 56(1):257-276.

Allen MS, Morrison AE. 2013. Modelling Site Formation Dynamics: Geoarchaeological, Chronometric and Statistical Approaches to a Stratified Rockshelter Sequence, Polynesia. Journal of Archaeological Science 40(12):4560–475.

Allen MS, Morrison AE, Lorrey AM, Zhao J-X, Jacobsen GE. 2017. Timing, magnitude and effects of Late Holocene sea level drawdown on island habitability Aitutaki, Cook Islands. Archaeology in Oceania 51(2):108-121.

Alves EQ, Macario K, Ascough P, Bronk Ramsey C. 2018. The worldwide marine radiocarbon reservoir effect: Definitions, mechanisms, and Prospects. Reviews of Geophysics 56:278–305.

Ambrose WR. 1994. Obsidian hydration dating of a Pleistocene age site from the Manus Islands, Papua New Guinea. Quaternary Science Reviews 13(2):137-142.

Arneborg J, Heinemeier J, Lynnerup N, Nielsen HL, Rud N, Sveinbjörnsdóttir AE. 1999. Change of diet of the Greenland Vikings determined from stable carbon isotope analysis and 14C dating of their bones. Radiocarbon 41(2):157-168.

Anerson A. 1991. The chronology of colonization in New Zealand. Antiquity 65:767–795.

Anderson A. 1995. Current approaches in East Polynesian colonization research. Journal of the Polynesian Society 104:110-132.

Anderson A. 1996. Was 'Rattus Exulans' in New Zealand 2000 Years Ago? AMS Radiocarbon Ages from Shag River Mouth. Archaeology in Oceania 31(3):178–184.

Anderson A. 2000. Differntial Reliability of ^{14}C AMS Ages of Rattus Exulans Bone Gelatin in South Pacific Prehistory. Journal of the Royal Society of New Zealand 30(3):243–261.

Anderson A. 2008. Traditionalism, interaction, and long-distance seafaring in Polynesia. The Journal of Island and Coastal Archaeology 3:240-250.

Anderson A. 2018. Ecological contingency accounts for earliest seagoing in the western Pacific Ocean. The Journal of Island and Coastal Archaeology 13(2):224-234.

Anovitz LM, Elam JM, Riciputi LR. 1999. The failure of obsidian hydration dating: Sources, implications, and new directions. Journal of Archaeological Science 26:735-752

Aoyagi M. 1982. Islanders and their outside world: A report of the cultural and anthropological research in the Caroline Islands of Micronesia in 1980-1981. Committee for Micronesian Research. Tokyo: St. Paul's (Rikkyo) University.

Ardren T, Lowry JP, Memory M, Flanagan K, Busot A. 2016. Prehistoric human impact on tree island life cycles in the Florida Everglades. The Holocene 26(5):772-780.

Ardren T, Thompson VD, Fitzpatrick SM, Stevenson J, Sierra RL. 2018. When foragers are managers: Social complexity and persistent foraging in the Florida Keys. In: Reid BA, editor. The Archaeology of Caribbean and Circum-Caribbean Farmers (6000 BC – AD 1500). New York: Routledge. p. 311-326.

Ardren T, Thompson VD, Fitzpatrick SM, LeFebvre M, Napolitano, MF. 2018. Archaeological Investigations at the Clupper Site (8MO17) 2014 and 2015 Field Seasons Monroe County, Florida. Bureau of Natural and Cultural Resources, Division of Recreation and Parks, Department of Environmental Protection, Tallahassee, Florida.

Ardren T, Fitzpatrick SM, Thompson VD. 2019. Island chain coastlines: A history of human adaptation in the Florida Keys. In: Reeder-Meyers L, Turk JA, Rick TC, editors.

The Archaeology of Human Environment Dynamics on the North American Atlantic Coast. Gainesville: University Press of Florida. p. 232-259.

Argiriadis E, Battistel D, McWethy DB, Vecchiato M, Kirchgeorg T, Kehrwald NM, Whitlock C, Wilmshurst JM, Barbante C. 2018. Lake sediment fecal and biomass burning biomarkers provide direct evidence for prehistoric human-lit fires in New Zealand. Scientific Reports 8(1):1-9.

Ascough P, Cook C, Dugmore, A. 2005. Methodological approaches to determining the marine radiocarbon reservoir effect. Progress in Physical Geography 29(4)532-547.

Ashmore PJ. 1999. Radiocarbon dating: avoiding errors by avoiding mixed samples. Antiquity 73(279):124.

Athens JS, Ward JV. 2001. Paleoenvironmental evidence for early human settlement in Palau: The Ngerchau core. In: Stevenson CM, Lee G, Morin FJ, eidtors. Pacific 2000: Proceedings of the Fifth International Conference on Easter Island and the Pacific. Easter Island Foundation: Los Angeles. p. 164-177.

Athens JS, Rieth TM, Dye TS. 2014. A paleoenvironmental and archaeological model-based age estimate for the colonization of Hawai'i. American Antiquity 79, 144-155.

Ballendorf DA. 1991. The Obscure Johann Stanislaus Kubary and His Estimable Discourses on Palauan Money. Journal of the Pacific Society 14:19-25.

Ballendorf DA. 1993. Udoud: The Origins of Palaun Traditional Money. Asian Culture Quarterly 21(3):29-33.

Barlett LJ, Williams DR, Prescott GW, Balmford A, Green RE, Eriksson A, Valdes PJ, Singarayer JS, Manica A. 2016. Robustness despite uncertainty: Regional climate data reveal the dominant role of humans in explaining global extinctions of Late Quaternary megafauna. Ecography 39(2): 152-161.

Barnett HG. 1949. Palauan Society: A Study of Contemporary Native Life in the Palau Islands, Eugene: University of Oregon Publications.

Barnett J, Campbell J. 2010. Climate change and small island states: power, knowledge and the South Pacific. London: Earthscan.

Baron J, Clavier J. 1992. Effects of environmental factors on the distribution of the edible bivalves Atactodea striata, Gafrarium tumidum and Anadara scapha on the coast of New Caledonia (SW Pacific). Aquatic Living Resources 5:107–114.

Batt CM, Schmid MME, Vésteinsson O. 2015. Constructing chronologies in Viking Age Iceland: Increasing dating resolution using Bayesian approaches. Journal of Archaeological Science 62:161-174.

Bayliss A. 2009. Rolling out revolution: using radiocarbon dating in archaeology. Radiocarbon 51(1):123-147.

Bayliss A. 2015. Quality in Bayesian chronological models in archaeology. World Archaeology 47(4):677-700.

de Beauclair I. 1963. Some Ancient Beads of Yap and Palau. Journal of the Polynesian Society 72(1): 1-10.

Beck HC. 1928. Classification and Nomenclature of Beads and Pendants. Archaeologia 77:1-76.

Bedford S, Spriggs M, editors. 2019. Debating Lapita: Distribution, chronology, society and subsistence. Terra Australis 52. Canberra: ANU Press.

Bedford S, Spriggs M, Regenvanu R. 2006. The Teouma Lapita site and the early human settlement of the Pacific Islands. Antiquity 80(310):812-828.

Bednarik RG. 2003. Seafaring in the Pleistocene. Cambridge Archaeological Journal 13(1):41-66.

Bell AV, Currie TE, Irwin G, Bradbury C. 2015. Driving factors in the colonization of Oceania: Developing island-level statistical models to test competing hypotheses. American Antiquity 80(2):397-407.

Berg ML. 1992. Yapese Politics, Yapese money, and the sawei tribute network before World War I. Journal of Pacific History 27(2):150-164.

Berger R, Taylor RE, Libby WF. 1966. Radiocarbon content of marine shells from the California and Mexican West Coast. Science 153:864-866.

van den Bergh GD, Kaifu Y, Kurniawan I, Kono RT, Brumm A, Setiyabudi E, Aziz F, Wormwood MJ. 2016. *Homo florensis*-like fossils form the early Middle Pleistocene of Flores. Nature 534: 245-248.

Beesley PL, Ross GJB, Wells A, editors. 1998. Mollusca: The southern synthesis. Fauna of Australia. Volume 5. Melbourne: CSIRO Publishing.

Best E. 1923. Polynesian Voyagers. Monograph 5. Wellington: Dominion Museum.

Bieler R, Mikkelsen PM. 2004. Marine bivalves of the Florida Keys: A qualitative faunal analysis based on original collections, museum holdings and literature data. Malacologia 46(2):503-544.

Billeck WT. 2008. Red-on-white drawn or cornelian beads: A 19th-century temporal marker for the Plains. Beads: Journal of the Society for Bead Research 20:49-61.

Bird MI, Ayliffe LK, Fifield LK, Turney CSM, Cresswell RG, Barrows TT, David B. 1999. Radiocarbon dating of "old" charcoal using a wet oxidation, stepped-combustion procedure. Radiocarbon 41(2): 127-140.

Bird, MI, Levchenko V, Ascough PL, Meredith W, Wurster CM, Williams A, Tilston EL, Snape CE, Apperley DC. 2014. The efficiency of charcoal decontamination for radiocarbon dating by three pre-treatments–ABOX, ABA and hypy. Quaternary Geochronology 22: 25-32.

Blaauw M, Christen JA, Bennett KD, Reimer, PJ. 2018. Double the dates and go for Bayes—Impacts of model choice, dating density and quality on chronologies. Quaternary Science Reviews 188: 58-66.

Blair EH. 2018. Glass Beads. In: Lightfoot KG, Gonzalez S., editors. The archaeology of Metini Village: A historic 19th century Kashaya Pomo village at Fort Ross State Historic Park. Berkeley: University of California. p. 72-78; 176-177.

Blaiyok V. 1993. Archaeology survey of Airai State, Republic of Palau. Report on file with the Bureau of Cultural and Historical Preservation, Republic of Palau.

Blake NJ, Shumway SE. 2006. Bay scallop and calico scallop fisheries, culture and enhancement in eastern North America. In: Shumway SE and Parsons GJ, editors. Scallops: biology, ecology and aquaculture. Elsevier. p. 945–964.

Blakeslee, DJ. 1994. Reassessment of some radiocarbon dates from the Central Plains. Plains Anthropologist, 39(148):103-210.

Blumenstock DI. 1960. Weather and climate. In: Johnson CG, Alvin RJ, Hetzler RL, editors. Military Geology of Yap Islands, Caroline Islands, Honolulu: Intelligence Division, Office of the Engineer HQ, US Army Pacific. p 27-45.

Blust R. 2013. The Austronesian languages. Canberra: Australian National University.

Boivin, NL, Zeder MA, Fuller DQ, Crowther A, Larson G, Erlandson JM, Denham T, Petraglia MD. Ecological consequences of human niche construction: Examining long-term anthropogenic shaping of global species distributions. Proceedings of the National Academy of Sciences 113(23):6388-6396.

Bonsall C, Cook GT, Hedges RE, Higham TF, Pickard C, Radovanović I. 2004. Radiocarbon and stable isotope evidence of dietary change from the Mesolithic to the Middle Ages in the Iron Gates: new results from Lepenski Vir. Radiocarbon 46(1):293-300.

Braje TJ, Leppard TP, Fitzpatrick SM, Erlandson JM. 2017. Archaeology, historical ecology and anthropogenic island ecosystems. Environmental Conservation 44(3): 286-297.

Brill RH. 1964. Application of fission-track dating to historic and prehistoric glasses. Archaeometry 7:51-57.

Brill RH. 1999. Chemical analysis of early glasses, volume 2: The tables. Corning: The Corning Museum of Glass.

Brill RH, Tong SSC, Dohrenwend D. 1991. Chemical analyses of some early Chinese glasses. In: Brill RH, Martin JH, editors. Scientific research in early Chinese glass: Proceedings of the archaeometry of glass sessions of the 1984 International Symposium on Glass, Beijin, September 7, 1984, with supplementary papers. New York: Hudson Hills Press. pp. 31-64.

Brock F, Higham T, Ditchfield P, Bronk Ramsey C. 2010. Current pretreatment methods for AMS radiocarbon dating at the Oxford Radiocarbon Accelerator Unit (ORAU). Radiocarbon 52(1):103-112.

Broecker WS, Olson EA. 1961. Lamont radiocarbon measurements VIII. Radiocarbon 3:176-204.

Broom MJ. 1985. The biology and culture of marine bivalve molluscs of the genus *Anadara*. In: ICLARM Studies and Reviews. International Center for Living Aquatic Resources Management, Manila, Volume 12.

Bronk Ramsey C. 2009a. Bayesian analysis of radiocarbon dates. Radiocarbon 51:337-360.

Bronk Ramsey C. 2009b. Dealing with outliers and offsets in radiocarbon dating. Radiocarbon 51: 1023-1045.

Bronk Ramsey C. 2015. Bayesian approaches to the building of archaeological chronologies. In: Barceló JA, Bogdonovic I, editors. Mathematics and archaeology. Boca Raton: CRC Press. p. 272-292.

Bronk Ramsey C, Higham T, Bowles A, Hedges R. 2004. Improvements to the pretreatment of bone at Oxford. Radiocarbon 46(1):155-163.

Brumm AG. Jensen M, van den Bergh GD, Wormwood MJ, Kurniawan I, Aziz F, Storey M. 2010. Hominin on Flores, Indonesia, by one million years ago. Nature 464:748-752.

Brumm AG, van den Bergh GD, Storey M, Kurniawan I, Alloway BV, Setiawan R, Setiyabudi E, Grün R, Moore MW, Yurnaldi D, Puspaningrum MR, Wibowo UP, Insani H, Sutisna I, Westgate JA, Pearce NJG, Duval M, Meijer HJM, Aziz F, Sutikna T, van der Kaars S, Flude S, Morwood MJ. 2016. Age and context of the oldest known hominin fossibls from Flores. Nature 534: 249-253.

Buck CE, Higham TF, Lowe DJ. 2003. Bayesian tools for tephrochronology. The Holocene 13(5):639-647.

Bulbeck D. 2007. Where river meets sea: A parsimonious model for *Homo sapiens* colonization of the Indian Ocean rim and Sahul. Current Anthropology 48:315-321.

Burgess LE, Dussubieux L. 2007. Chemical composition of late 18th- and 19th-century glass beads from western North America: Clues to sourcing beads. Beads: Journal of the Society of Bead Research 19:58-73.

Burley D, Weisler MI, Zhao J-X. 2012. High precision U/Th dating of first Polynesian settlement. PloS One 7(11):e48769.

Burley D, Edinborough K, Weisler M, Zhao J-X. 2015. Bayesian modeling and chronological precision for Polynesian settlement of Tonga. PloS One 10: e0120795.

Caffrey MA, Horn SP. 2015. Long-term fire trends in Hispaniola and Puerto Rico from sedimentary charcoal: A comparison of three records. The Professional Geographer 67:229-241.

Callaghan RT. 2001. Ceramic age seafaring and the interaction potential in the Antilles. Current Anthropology 42:308-313.

Callaghan RT. 2008. On the question of the absence of Archaic Age sites on Jamaica. The Journal of Island and Coastal Archaeology 3:54-71.

Callaghan RT. 2010. Crossing the Guadeloupe passage in the Archaic Age. In: Fitzpatrick SM, Ross AH, editors. Island shores and distant pasts: Archaeological and biological approaches to Pre-Columbian settlement of the Caribbean. Gainesville: University of Florida Press. p. 127-147.

Callaghan R, Fitzpatrick SM. 2007. On the relative isolation of a Micronesian archipelago during the historic period: The Palau case study. International Journal of Nautical Archaeology 36(2):353-364.

Carlson LA. 1999. First contact: The Coralie site, Grand Turk, Turks and Caicos Islands. Ph.D. dissertation, Gainesville: University of Florida.

Carlson LA, Keegan WF. 2004. Resource depletion in the prehistoric northern West Indies. In: Fitzpatrick SM, editor. Voyages of discovery: The archaeology of islands. Westport: Praeger. p. 85-107.

Carlson LA, Steadman DW. 2009. Examining temporal differences in faunal exploitation at two Ceramic Age sites in Puerto Rico. The Journal of Island and Coastal Archaeology 4:207-222.

Carpenter KE, Niem VH. 1998. The living marine resources of the western central Pacific. Vol. 1. Seaweeds, corals, bivalves and gastropods. Rome: Food and Agriculture Organization of the United Nations.

Carson MT, Peterson JA. 2012. Radiocarbon dating of algal bioclasts in beach sites of Guam. The Journal of Island and Coastal Archaeology 7(1):64–75.

Carter AK. 2016. The production and exchange of glass and stone beads in Southeast Asia from 500 BCE to the early second millennium CE: An assessment of the work of Peter Francis in light of recent research. Archaeological Research in Asia 6:16-29.

Carter AK, Abraham SA, Kelly GO. 2016a. Updating Asia's maritime bead trade: An introduction. Archaeological Research in Asia 6:1-3.

Carter AK, Dussubieux L, Beavan N. 2016b. Glass beads from 15th–17th century CE jar burial sites in Cambodia's Cardamom Mountains. Archaeometry 58:401-412.

Cherkinsky A, Culp RA, Dvoracek DK, Noakes JE. 2010. Status of AMS facility at the University of Georgia. Nuclear Instruments and Methods in Physics Research B. 268: 867-870.

Cherkinsky A, Pluckhahn TJ, Thompson VD. 2014. Variation in Radiocarbon Age Determinations from the Crystal River Archaeological Site, Florida. Radiocarbon 56(2):801-810.

Cherry JF, Leppard TP. 2015. Experimental archaeology and the earliest seafaring: The limitations of inference. World Archaeology 47:740-755.

Cherry JF, Leppard TP. 2018. The Balearic paradox: Why were the islands colonized so late? Pyrenae 49(1): 49-70.

Chinique de Armas Y, González Herrera UM, Buhay WM, Yero Masdeu JM, Viera Sanfiel LM, Burchell M, Crann C, Grau González-Quevedo ER, Roksandic M. Chronology of the archaeological site of Playa Del Mango, Rio Cauto, Granma, Cuba. 2020. Radiocarbon 62(5):1221-1236.

Chisholm, BS, Nelson, DE, Schwarcz, HP. 1982. Stable-carbon isotope ratios as a measure of marine versus terrestrial protein in ancient diets. Science 216(4550):1131-1132.

Church MJ, Arge SV, Edwards KJ, Ascough PL, Bond JM, Cook GT, Dockrill SJ, Dugmore AJ, McGovern TH, Nesbitt C, Simpson IA. 2013. The Vikings were not the first colonizers of the Faroe Islands. Quaternary Science Reviews 77(1): 228-232.

Cílová Z, Woitsch J. 2011. Potash-A key raw material of glass batch for Bohemian glasses from 14th-17th centuries? Journal Archaeological Science 39:371-380.

Clark GR. 2005. A 3000-year culture sequence from Palau, Western Micronesia. Asian Perspectives 44(2):349–80.

Clark G. 2007. Culture contact in the Palau Islands, 1783. Journal Pacific History 42:89-97.

Clark G, Anderson A, Wright, D. 2006. Human colonization of the Palau islands, Western Micronesia. The Journal of Island and Coastal Archaeology 1:215-232.

Clark G, Petchey F, Hawkins S, Reepmeyer C, Smith I, Masse WB. 2013. Distribution and extirpation of pigs in Pacific Islands: A case study from Palau. Archaeology in Oceania 48(3): 141-153.

Clarkson C, Jacobs Z, Marwick B, Fullagar R, Wallis L, Smith M, Roberts RG, Hayes E, Lowe K, Carah X. 2017. Human occupation of northern Australia by 65,000 years ago. Nature 547: 306.

Cochrane EE, Rieth TM. 2016. Sāmoan artefact provenance reveals limited artefact transfer within and beyond the archipelago. Archaeology in Oceania 51(2):150-157.

Connor SE, van Leeuwen JFN, Rittenour TM, van der Knaap WO, Ammann B, Björck S. 2012. The ecological impact of oceanic island colonization – a palaeoecological perspective from the Azores. Journal of Biogeography 39(6):1007-1023.

Conrad GW, Foster JW, Beeker CD. 2001. Organic artifacts from the Manantial de La Aleta, Dominican Republic: Preliminary observations and interpretations. Journal of Caribbean Archaeology 2:1-20.

Cook GT, Bonsall C, Hedges RE, McSweeney K, Boronean, V, Pettitt PB. 2001. A freshwater diet-derived 14C reservoir effect at the Stone Age sites in the Iron Gates Gorge. Radiocarbon 43(2A):453-460.

Cook GT, Bonsall C, Hedges RE, McSweene, K, Boroneant V, Bartosiewicz L, Pettitt PB. 2002. Problems of dating human bones from the Iron Gates. Antiquity 76(291):77-85.

Cook GT, Ascough PL, Bonsall C, Hamilton WD, Russell N, Sayle KL, Marian Scott E, Bownes JM. 2015. Best practice methodology for ^{14}C calibration of marine and mixed terrestrial/marine samples. Quaternary Geochronology 27:164-171.

Corbett DR, Chanton J, Burnett W, Dillon K, Rutowski C. 1999. Patterns of groundwater discharge into Florida Bay. Limnology and Oceanography 44(4):1045-1055.

Cordy R. 1986. Archaeological settlement patterns on Yap. No. 16. Micronesian Archaeological Survey, Office of Historic Preservation, Office of the High Commissioner, Trust Territory of the Pacific Islands.

Cormie AB, Schwarcz HP. 1994. Stable isotopes of nitrogen and carbon of North American white-tailed deer and implications for paleodietary and other food web studies. Palaeogeography, Palaeoclimatology, Palaeoecology 107:27-241.

Couthard RD, Furze MFA, Pieńkowski AJ, Chantel Nixon F, England JH. 2010. New marine ΔR values for Arctic Canada. Quaternary Geochronology 5(4):419-434.

Craib J, Price S. 1978. An archaeological reconnaissance of selected areas on Yap, Western Caroline Islands. Report submitted to the Trust Territory of the Pacific Islands Historic Preservation Office, Saipan.

Crock JG. 2000. Interisland interaction and the development of chiefdoms in the Eastern Caribbean. Ph.D. dissertation. Pittsburgh: University of Pittsburgh.

Crock JG. 2004. Archaeological evidence of eastern Taínos: Late Ceramic Age interaction between the Greater Antilles and the northern Lesser Antilles. In: Tavárez MC, García Arévalo MA, editors. Proceedings of the International Congress for Caribbean Archaeology 20. Santo Domingo: Departamento de Difusion y Relaciones Públicas del Museo del Hombre Dominicano. p. 835-842.

Crock JG, Petersen J. 2004. Inter-island exchange, settlement hierarchy, and a Taíno-related chiefdom on the Anguilla Bank, Northern Lesser Antilles. In: Delpuech A, Hofman CL, editors. Late Ceramic Age Societies in the Eastern Caribbean. Oxford: British Archaeological Reports. p. 139-158.

Culleton BJ, Kennett DJ, Ingram BL, Erlandson JM, Southon JR. 2006. Intrashell radiocarbon variability in marine mollusks. Radiocarbon 48(3):387–400.

Cushing Falanruw MJ, Ruegorong F. 2007. Indigenous fallow management on Yap Island. In: Cairns M, editor. Voices from the Forest: Integrating Indigenous Knowledge into Sustainable Upland Farming. New York: Routledge.

Davenport J, Wong TM. 1986. Responses of the blood cockle *Anadara granos*a (L.) (Bivalvia: Arcidae) to salinity, hypoxia and aerial exposure. Aquaculture 56(2):151-162.

Davis DD. 2000. Jolly Beach and the Preceramic Occupation of Antigua, West Indies. New Haven: Yale University Press.

Dee M, Bronk Ramsey C. 2014. High-precision Bayesian modeling of samples susceptible to inbuilt age. Radiocarbon 56:83-94.

Descantes, C., 2005. Integrating archaeology and ethnohistory: The development of exchange betweeen Yap and Ulithi, Western Caroline Islands. BAR International Series 1344. Oxford: Bar Publishing.

Descantes C, Intoh M, Neff H, Glascock MD. 2004. Chemical characterization of Yapese clays and ceramics by instrumental neutron activation analysis. Journal of Radioanalytical and Nuclear Chemistry 262(1):83-91.

Dewar G, Pfeiffer S. 2010. Approaches to estimating marine protein in human collagen for radiocarbon date calibration. Radiocarbon 52(4):1611-1625.

Diaz M, Macario KD, Gomes PRS, Álvarez-Lajonchere L, Aguilera O, Alves EQ, Radiocarbon marine reservoir effect on the northwestern coast of Cuba. Radiocarbon 59: 333-341.

Dickinson WR. 1982. Temper sands from prehistoric sherds excavated at Pemrang site on Yap and from nearby Ngulu Atoll. Journal of the Indo-Pacific Prehistory Association 3:115-117.

Dickinson WR. 1999. Holocene sea-level record on Funafuti and potential impact of global warming on central Pacific atolls. Quaternary Research 51(2):124-132.

Dickinson WR. 2003. Impact of mid-Holocene hydro-isostatic highstand in regional sea level on habitability of islands in Pacific Oceania. Journal of Coastal Research 19(3):489-502.

Dickinson WR. 2014. Beach ridges as favored locales for human settlement on Pacific Islands. Geoarchaeology 29:249-267.

Dickinson WR, Athens JS. 2007. Holocene paleoshoreline and paleoenvironmental history of Palau: Implications for human settlement. The Journal of Island and Coastal Archaeology 2(2):175-196.

Dickinson WR, Shutler R. 2000. Implications of petrographic temper analysis for Oceanian prehistory. Journal of World Prehistory 14(3):203-266.

DiNapoli RJ, Rieth TM, Lipo CP, Hunt TL. 2020. A model-based approach to the tempo of “collapse”: The case of Rapa Nui (Easter Island). Journal of Archaeological Science 116:105094.

DiNapoli RJ, Fitzpatrick SM, Napolitano MF, Rick TC, Stone JH, Jew N. 2021. Marine Reservoir Correction (ΔR) for the Caribbean Illustrate High Intra- and Inter-Island Variability. Quaternary Geochronology. doi.org/10.1016/j.quageo.2020.101126.

Dodrill TN, Jew NP, Fitzpatrick SM. 2018. $\delta^{18}O$ Analyses of the humpbacked conch (*Gibberulus gibberulus*): Evaluating a proxy for reconstructing sea-surface temperature at Chelechol ra Orrak, Palau. Environmental Archaeology 23:403-415.

Dodson JR, Intoh M. 1999. Prehistory and palaeoecology of Yap, Federated States of Micronesia. Quaternary International 59:17–26.

Donohue M, Denham T. 2010. Farming and language in Island Southeast Asia: Reframing Austronesian history. Current Anthropology 51(2): 223-256.

Douglass K, Zinke J. 2015. Forging ahead by land and by sea: Archaeology and paleoclimate reconstruction in Madagascar. African Archaeological Research 32: 267-299.

Douglass K, Walz J, Morales EQ, Marcus R, Myers G, Pollini J. 2019. Historical perspectives on contemporary human–environment dynamics in southeast Africa. Conservation Biology 33(2):260-274.

Druffel ERM. 1982. Banded corals: Changes in oceanic carbon-14 during the Little Ice Age.
Science 218(4567):13-19.

Druffel ERM. 1997. Pulses of rapid ventilation in the North Atlantic surface ocean during the past century. Science 275:1454-1457.

Druffel ERM, Benavides LM. 1986. Input of excess CO2 to the surface ocean based on 13C/12C ratios in a banded Jamaican sclerosponge. Nature 321:58-61.

Druffel ERM, Linick TW. 1978. Radiocarbon in annual coral rings of Florida. Geophysical Research Letters 5(11):913-916.

Druffel ERM, Robinson LF, Griffin S, Halley RB, Southon JR, Adkins JF. 2008. Low reservoir ages for the surface ocean from mid-Holocene Florida corals. Paleoceanography and Paleoclimatology 23(2):PA2209.

Dupont C. 2018a. Gifts of the gods: Objects of foreign origin in traditional exchange systems in Palau. In: Brandherm D, Heymans E, Hofmann D, editors. Gifts, goods, and money: Comparing currency and circulation systems in past societies. Archaeopress, Oxford. p. 195-223.

Dupont C. 2018b. Wertobjekte und gabentausch auf Palau (Ozeanien): Eine ethnologische studie zu transformationen von geld und prestige. Reimer: Dietrich.

Dye TS. 1994. Apparent ages of marine shells: implications for the archaeology of Hawai’i. Radiocarbon 36(1):51-57.

Dye TS. 2000. “Effects of 14C Sample Selection in Archaeology: An Example from Hawai’i.” Radiocarbon 42 (2):203–217.

Dye TS. 2015. Dating human dispersal in Remote Oceania: A Bayesian view from Hawai’i. World Archaeology 47:661-676.

Dye TS. 2016. Long-term rhythms in the development of Hawaiian social stratification. Journal of Archaeological Science 71:1-9.

Dye TS, Buck CE. 2015. Archaeological sequence diagrams and Bayesian chronological models. Journal of Archaeological Science 63: 84-93.

Elliot MB, Striewski B, Flenley JR, Sutton D. 1995. Palynological and sedimentological evidence for a radiocarbon chronology of environmental change and Polynesian deforestation from Lake Taumatawhana, Northland, New Zealand
1. Radiocarbon 37(3):899-916.

Emiliani C, Hudson JH, Shinn EA, George RY. 1966. Oxygen and carbon isotopic growth record in a reef coral from the Florida Keys and a deep-sea coral from Blake Plateau. Science 202(4):627-629.

Enos P, Perkins RD. 1979. Evolution of Florida Bay from island stratigraphy. Bulletin of the Geological Society of America 90(1):59–83.

Epstein S, Mayeda T. 1953. Variation of ^{18}O content of waters from natural sources. Geochim Cosmochim Acta 4:213-224 450.

Epstein S, Buchsbaum R, Lowenstam HA, Urey HC. 1953. Revised carbonate-water isotopic temperature scale. Geological Society of America Bulletin 64:1315-1326.

Erlandson JM. 2008. Racing a rising tide: Global warming, rising seas, and the erosion of human history. The Journal of Island and Coastal Archaeology 3(2):167-169.

Erlandson JM. 2010. Neptune’s children: The evolution of human seafaring. In: Anderson AA, Barrett JH, Boyle KV, editors. The Global Origins and Development of Seafaring. McDonald Institute Monographs. Cambridge: University of Cambridge. p. 19-28.

Erlandson JM. 2012. As the world warms: Rising seas, coastal archaeology, and the erosion of maritime history. Journal of Coastal Conservation 16(2):137-142.

Erlandson JM, Moss ML. 1999. The Systematic Use of Radiocarbon Dating in Archaeological Surveys in Coastal and Other Erosional Environments. American Antiquity 64(3):431–43.

Erlandson, JM, Rick TC. 2010. Archaeology meets marine ecology: the antiquity of maritime cultures and human impacts on marine fisheries and ecosystems. Annual Review of Marine Science 2:231-251.

Etpison M, Dupont C, 2017. Palau in Europe. Etpison Museum, Palau.

Gifford EW, Gifford DS. 1959. Archaeological excavations in Yap. Anthropological Records 18(2). Berkeley: University of California.

Gladwin T. 2009. East is a big bird: Navigation and logic on Puluwat Atoll. Cambridge: Harvard University Press.

Falanruw, MVC. 2015. Trees of Yap: A field guide. General Technical Report PSW-GTR-249, United States Department of Agriculture.

Feinman GM, Neitzel JE. 2020. Excising culture history from contemporary archaeology. Journal of Anthropological Archaeology 60:101230.

Ferentinos, G., M. Gkioni, M. Geraga, and G. Papatheodorou. 2012. Early seafaring activity in the southern Ionian Islands, Mediterranean Sea. Journal of Archaeological Science 39(7): 2167-2176.

Field J, Fillios M, Wroe S. 2008. Chronological overlap between humans and megafauna in Sahul (Pleistocene Australia-New Guinea): A review of the evidence. Earth Science Reviews 89(3-4): 97-115.

Field J, Wroe S, Trueman CN, Garvey J, Wyatt-Spratt S. 2013. Looking for the archaeological signature in Australian megafaunal extinctions. Quaternary International 285(8):76-88.

Finney B. 1996. Colonizing an island world. Transactions of the American Philosophical Society 86(5):71-116.

Finney JC. 1998. The Yapese language: Whence and how. Papers from the fifth annual meeting of the Southeastern Asian Linguistics Society, 1995:97-114.

Fitzpatrick SM. 2001. Archaeological investigations of Omis Cave: A Yapese stone money quarry in Palau. Archaeology in Oceania 36:153-162.

Fitzpatrick SM. 2002. A Radiocarbon chronology of Yapese stone money quarries in Palau. Micronesica 34(2):227-242.

Fitzpatrick SM. 2003a. Stones of the butterfly: An archaeological investigation of Yapese stone money quarries in Palau, Western Micronesia. PhD dissertation. Eugene: University of Oregon.

Fitzpatrick SM. 2003b. Early human burials in the Western Pacific: Evidence for a c.3000 year old occupation on Palau. Antiquity 77(298):719-731.

Fitzpatrick SM. 2003c. An archaeological study on the extraction of flowstone from caves and rockshelters for producing stone money in Western Micronesia. Cave Karst Science 30(2):75-82.

Fitzpatrick SM. 2006. A critical approach to 14C dating in the Caribbean: Using chronometric hygiene to evaluate chronological control and prehistoric settlement. Latin American Antiquity 17:281-290.

Fitzpatrick SM. 2008. Maritime interregional interaction in Micronesia: Deciphering multi-group contacts and exchange systems through time. Journal of Anthropological Archaeology 27:131-147.

Fitzpatrick SM. 2013. Seafaring capabilities in the Pre-Columbian Caribbean. Journal of Maritime Archaeology 8:101-138.

Fitzpatrick SM. 2015. The Pre-Columbian Caribbean: Colonization, population dispersal, and island adaptations. PaleoAmerica 1:305-331.

Fitzpatrick SM. 2016. Yap’s famous stone money. In: Haselgrove C. Krmnicek S, editors. The archaeology of money. Leicester Archaeology Monographs 24. Leicester: University of Leicester. p. 43-65.

Fitzpatrick SM, Callaghan RT. 2008. Seafaring simulations and the origins of prehistoric settlers to Madagascar. In: O’Connor S, Clark G, Leach F, editors. Islands of inquiry: Colonisation and the archaeology of maritime landscapes. Terra Australis 29. Canberra: ANU E Press. p. 47-58.

Fitzpatrick SM, Jew NP. 2018. Radiocarbon dating and Bayesian modelling of one of Remote Oceania's oldest cemeteries at Chelechol ra Orrak, Palau. Antiquity 92(361):149-164.

Fitzpatrick SM, McKeon S. 2020. Banking on stone money: Ancient antecedents to bitcoin. Economic Anthropology 7(1):7-21.

Fitzpatrick SM, Caruso AC, Peterson JE. 2006. Metal tools and the transformation of an oceanic exchange systems. Journal of Historical Archaeology 40:9-27.

Fitzpatrick SM, Kappers M, Giovas CM. 2010. The southward route hypothesis: examining Carriacou’s chronological position in Antillean prehistory. In: Fitzpatrick SM, Ross AH, editors. Island shores and distant pasts: Archaeological and biological approaches to the Pre-Columbian settlement of the Caribbean. Gainesville: University Press of Florida. p. 163-176.

Fitzpatrick SM, Thompson VD, Poteate AS, Napolitano MF, Erlandson JM. 2016. Marginalization of the margins: The importance of smaller islands in prehistory. The Journal of Islands and Coastal Archaeology 11(2):155-170.

Fitzpatrick SM, Napolitano MF, Stone JH. 2021. What is the most parsimonious explanation for where pre-Columbian Caribbean peoples originated? In: Napolitano MF, Stone JH, DiNapoli RJ, editors. The archaeology of island colonization: Global approaches to initial human settlement. Gainesville: University Press of Florida. p. 231-264.

Florin SA, Fairbairn AS, Nango M, Djandjomerr D, Marwick B, Fullagar R, Smith M, Wallis LA, Clarkson C. 2020. The first Australian plant foods at Madjedbebe, 65,000–53,000 years ago" Nature Communications 11(1):1-8.

Force RW. 1959. Palauan Money: Some Preliminary Comments on Material and Origins. Journal of the Polynesian Society 68:40-44.

Francis P, Jr. 1979. The Czech bead story. Lake Placid: Lapis Route Books.

Francis P, Jr. 1988. The glass trade beads of Europe: Their manufacture, their history, and their identification. Lapis Route Books: Lake Placid.

Francis P, Jr. 1991. Beads in Indonesia. Asian Perspectives 30:217-241.

Francis P, Jr. 1994. Beads at the crossroads of continents. In: Fitzhugh WW, Chaussonnet V, editors. Anthropology of the North Pacific Rim, Washington D.C.: Smithsonian Institution Press. p. 281-305.

Francis P, Jr. 1997. Palau heirloom beads. The Margaretologist 10:14.

Francis P, Jr. 2002. Asia's maritime bead trade: 300 B.C. to the present. Honolulu: University of Hawai'i Press.

Francis P, Jr, 2009a. Glass beads from other manufacturing centers. In: Blair EH, Pendleton LSA, Francis P, Jr., editors. The beads of St. Catherines Island. Anthropological Papers of the American Museum of Natural History. New York: American Museum of Natural History. p. 97-100.

Francis P, Jr, 2009b. The glass beads of the paternostri of Venice. In: Blair EH, Pendleton, LSA, Francis P, Jr, editors. The beads of St. Catherines Island. Anthropological Papers of the American Museum of Natural History. New York: American Museum of Natural History. p. 65-71.

Friedman I, Smith RL. 1960. A new dating method using obsidian: Part 1, the development of the method. American Antiquity 25(4):476-522.

Furness WH. 1910. The island of stone money: Uap of the Carolines. Philadelphia: Lippincott.

Giovas CM. 2018. Pre-Columbian Amerindian lifeways at the Sabazan Site, Carriacou, West Indies. The Journal of Island and Coastal Archaeology 13:161-190.

Giovas CM, Fitzpatrick SM. 2014. Prehistoric migration in the Caribbean: Past perspectives, new models and the Ideal Free Distribution of West Indian colonization. World Archaeology 46:569-589.

Glassow MA. 2015. Chronology of red abalone middens on Santa Cruz Island, California, and evidence for subsistence and settlement change. American Antiquity 80(4):745-759.

Goodwin ID, Browning SA, Anderson AJ. 2014. Climate windows for Polynesian voyaging to New Zealand and Easter Island. Proceedings of the National Academy of Sciences 111(41):14716–14721.

Gratuze B. 1999. Obsidian characterization by laser ablation ICP-MS and its application to prehistoric trade in the Mediterranean and the Near East: Sources and distribution of obsidian within the Aegean and Anatolia. Journal of Archaeological Science 26:869-81.

Gratuze B, Soulier I, Blet M, Vallauri L. 1996. De L' Origine du cobalt: Du verre à la céramique. Revue d'Archéométrie 20, 77-94.

Green RC, Jones M, Sheppard P. 2008. The reconstructed environment and absolute dating of SE-SZ-8 Lapita site on Nendö, Santa Cruz, Solomon Islands. Archaeology in Oceania 43(2):49-61.

Griffin JW. 1988. The archaeology of Everglades National Park: A synthesis. Tallahassee: Southeast Archaeological Center, National Park Service.

Griffin JW. 2002. Archaeology of the Everglades. Gainesville: University Press of Florida.

Guiry E. 2019. Complexities of stable carbon and nitrogen isotope biochemistry in ancient freshwater ecosystems: Implications for the study of past subsistence and environmental change. Frontiers in Ecology and Evolution 313.

Hadden CS, Cherkinsky A. 2015. ^{14}C variations in pre-bomb nearshore habitats of the Florida panhandle, USA. Radiocarbon 57(3):469-479.

Hadden CS, Cherkinsky A. 2017. Carbon reservoir effects in eastern oyster from Apalachicola Bay, USA. Radiocarbon 59(5):1497-1506.

Hadden CS, Schwadron M. 2019. Marine reservoir effects in eastern oyster (*Crassostrea virginia*) from Southwestern Florida, USA. Radiocarbon 61(5):1501-1510.

Halley RB, Vacher HL, Shinn EA. 1997. Geology and Hydrogeology of the Florida Keys. In: Vacher HL, Quinn T, editors. Geology and hydrogeology of carbonate islands. San Diego: Elsevier. p. 217–248.

Hamilton WD, Krus AM. 2018. The myths and realities of Bayesian chronological modeling revealed. American Antiquity 83:187-203.

Hamm G, Mitchell P, Arnold LJ, Prideaux GJ, Questiaux D, Spooner NA, Levchenko VA, Foley EC, Worthy TH, et al. 2016. Cultural innovation and megafauna interaction in the early settlement of arid Australia. Nature 539: 280-283.

Hann JH. 1991. Missions to the Calusa. Gainesville: University of Florida Press.

Hanna JA. 2019. Camáhogne's chronology: The radiocarbon settlement sequence on Grenada, West Indies. Journal of Anthropological Archaeology 55:101075.

Harris E. 1989. Introduction to faceted beads. In: Picard J, Picard R, editors. Russian blues, faceted and fancy beads from the West African trade. Carmel: Picard African Imports. p. 3-6.

Harris M, Weisler M. 2017. Intertidal foraging on atolls. Prehistoric forager decision-making at Ebon Atoll, Marshall Islands. The Journal of Island and Coastal Archaeology 12(2):200-223.

Hassan FA, Robinson SW. 1987. High-precision radiocarbon chronometry of ancient Egypt, and comparisons with Nubia, Palestine and Mesopotamia. Antiquity 61:119-135.

Heaton T, Köhler P, Butzin M, Bard E, Reimer R, Austin W, Bronk Ramsey C, Grootes P, Hughen K, Kromer B, Reimer P, Adkins J, Burke A, Cook M, Olsen J, Skinner L. 2020. Marine20 – the marine radiocarbon age calibration curve (0-55,000 cal BP). 2020. Radiocarbon 62(4):779-820.

Hess HH. 1948. Major structural features of the Western North Pacific, an interpretation of H.O. 5485 bathymetric chart, Korea to New Guinea. Geological Society of American Bulletin 59(5):417-446.

Hezel FX. 1972. Early European contact with the Western Carolines. Journal of Pacific History 7:26–44.

Hezel FX. 1979. Foreign ships in Micronesia: A compendium of ship contacts with the Caroline and Marshall Islands, 1521–1885. Saipan.

Hezel FX. 1983. The first taint of civilization: A history of the Caroline and Marshall Islands in pre-colonial days, 1521–1885. Honolulu.

Hijikata H. 1993. Collective works of Hijikata Hisakatsu: Society and life in Palau. Tokyo: Sasakawa Peace Foundation.

Hīroa TR. 1938. Vikings of the sunrise. New York: Lippincott.

Hofman CL, Antczak AT, editors. Early settlers of the insular Caribbean: Dearchaizing the Archaic. Leiden: Sidestone Press.

Hofman CL, Bright AJ, Hoogland MLP, Keegan WF. 2008. Attractive ideas, desirable goods: Examining the Late Ceramic Age relationships between Greater and Lesser Antillean Societies. Journal of Island and Coastal Archaeology 3:17-34.

Hofman CL, Hoogland MLP, Michleburgh HL, Laffoon JE, Weston DA, Field MH. 2012. Life and death at Pre-Columbian Lavoutte, Saint Lucia, Lesser Antilles. Journal of Field Archaeology 37:209-225.

Hoffmeister JE, Multer HG. 1968. Geology and origin of the Florida Keys. Geological Society of America Bulletin 79:1487–1502.

Hoogland MCPL, Hofman C. 1993. Kelby's Ridge 2, A 14th century Taino settlement on Saba, Netherlands Antilles. Analecta Praehistorica Leidensia 26:163-181.

Hoogland MLP, Hofman CL. 2013. From corpse taphonomy to mortuary behavior in the Caribbean. The Oxford handbook of Caribbean archaeology 52:452.

Houk P, Benavente D, Fread V. 2012. Characterization and evaluation of coral reefs around Yap Proper, Federated States of Micronesia. Biodiversity Conservation 21:2045-2059.

Horrocks M, Ogden J. 1998. The effects of the Taupo Tephra eruption of c. 1718 BP on the vegetation of Mt Hauhungatahi, central North Island, New Zealand. Journal of Biogeography 25(4):649-660.

Hua Q, Barbetti M. 2004. Review of tropospheric bomb ^{14}C data for carbon cycle modeling and age calibration purposes. Radiocarbon 46(3):1273-1298.

Hunt LB. 1976. The true story of purple of cassius. Gold Bulletin 9:134-139.

Hunt TL, Lipo, CP. 2006. Late colonization of Easter island. Science. 311(5767):1603-1606.

Hunter-Anderson RL. 1981. Yapese stone fish traps. Asian Perspectives 24(1):81-90.

Hunter-Anderson RL. 1983. Yapese settlement patterns: An ethnoarchaeological approach. Agana: Pacific Studies Institute.

Hunter-Anderson RL. 1984. Recent observations on traditional Yapese settlement patterns. New Zealand Journal of Archaeology 6:95-105.

Hunter-Anderson RL. 1991. A review of traditional Micronesian high island horticulture in Belau, Yap, Chuuk, Pohnpei, and Kosrae. Micronesica 24(1):1-56.

Hunter-Anderson RL, Zan Y. 1996. Demystifying the Sawei, a traditional interisland exchange system. ISLA: Journal of Micronesian Studies 4(1):1-45.

Hutchinson I. 2020. Spatiotemporal variation in ΔR on the West Coast of North America in the Late Holocene: Implications for dating the shells of marine mollusks. American Antiquity 85(4):676-693.

Hutchinson DL, Norr, L. 2006. Nutrition and health at contact in late prehistoric central Gulf Coast Florida. American Journal of Physical Anthropology 129:375-386.

Ihm P. 2005. A contribution to the history of seriation in archaeology. In: Weihs C, Gaul W, editors. Classification – the ubiquitous challenge. Studies in classification, data analysis, and knowledge organization. Berlin: Springer.

Ingram BL, Southon JR. 1996. Reservoir ages in eastern Pacific coastal and estuarine waters. Radiocarbon 38(3):573-582.

Intoh M. 1989. Changing prehistoric Yapese pottery technology: A case study of adaptive transformation. PhD dissertation. University of Otago.

Intoh M. 2017. Colonisation and/or cultural contacts: A discussion of the Western Micronesia Case. In: Piper PJ, Hirofumi M, Bulbeck D, editors, New perspectives in Southeast Asian and Pacific prehistory. Terra Australis 45. Canberra: ANU Press. p. 233-241.

Intoh M, Leach F. 1985. Archaeological investigations in the Yap Islands, Micronesia: First millennium B.C. to present day. BAR International Series 277. Oxford: BAR Publishing.

Intoh M, Shigehara N. 2004. Prehistoric pig and dog remains from Fais Island, Micronesia. Anthropological Science 112:257-267.

Irwin G. 1989. Against, across and down the wind: A case for the systematic exploration of the remote Pacific Islands. The Journal of the Polynesian Society 98(2):167-206.

Irwin G. 1992. The Prehistoric exploration and colonisation of the Pacific. Cambridge: Cambridge University Press.

Irwin G. 2008. Pacific seascapes, canoe performance, and a review of Lapita voyaging with regard to theories of migration. Asian Perspectives 47(1):12-27.

Jacomb C, Holdaway RN, Allentoft ME, Bunce M, Oskam CL, Walter R., Brooks E. 2014. High-precision dating and ancient DNA profiling of moa (Aves: Dinornithiformes) eggshell documents a complex feature at Wairau Bar and refines the chronology of New Zealand settlement by Polynesians. Journal of Archaeological Science 50:24–30.

Jeffery B. 2013. Reviving community spirit: Furthering the sustainable, historical and economic role of fish weirs and traps. Journal of Maritime Archaeology 8:29-57.

Jew NP, Fitzpatrick SM. 2015. $\delta^{18}O$ analysis of *Atactodea striata*: evaluating a proxy for sea-surface temperature and shellfish foraging from a prehistoric rockshelter in Palau, Micronesia. Journal of Archaeological Science: Reports 4: 477-486.

Johnson CG, Alvis RJ, Hetzler RL, Blumenstock DI. 1960. Military geology of Yap main islands, Caroline Islands. Headquarters U.S. Army Pacific, Office of the Engineer.

Kalish JM. 1993. Pre- and post-bomb radiocarbon in fish otoliths. Earth and Planetary Science Letters 114:549-554.

Kane HH, Fletcher CH, Cochrane EE, Mitrovica JX, Habel S, Barbee M. 2017. Coastal plain stratigraphy records tectonic, environmental, and human habitability changes related to sea-level drawdown,‘Upolu, Sāmoa. Quaternary Research 87(2):246-257.

Karklins K. 1982. Guide to the description and classification of glass beads. Ottowa: National Historic Parks and Sites Branch, Parks Canada, Environment Canada.

Karklins K. 2012. Guide to the description and classification of glass beads found in the Americas. Beads: Journal of the Society of Bead Research 24:62-90.

Kaspers F. 2014. Beads from Jablonec: A History in Beads. Marblings Publishing.

Kayanne H, Yasukochi T, Yamaguchi T, Yamano H, Yoneda M. 2011. Rapid settlement of Majuro Atoll, central Pacific, following its emergence at 2000 years cal BP. Geophysical Research Letters 38(20):doi.org/10.1029/2011GL049163.

Keate G. 1789. An account of the Pelew Islands. Basil: J.J. Tourneisen.

Keegan WF. 1989. Creating the Guanahatabey (Ciboney): The modern genesis of an extinct culture. Antiquity 69:373-379.

Keegan WF. 1994. West Indian archaeology. 1. Overview and foragers. Journal of Archaeological Research 2:255-284.

Keegan WF. 2000. West Indian archaeology. 3. Ceramic Age. Journal of Archaeological Reports 8:135-167.

Keegan WF, Diamond JM. 1987. Colonization of islands by humans: A biogeographical perspective. In: Schiffer MB, editors. Advances in archaeological method and theory, vol. 10. San Diego: Academic Press. p. 49-92.

Keegan WF, DeNiro MJ. 1988. Stable carbon- and nitrogen-isotope ratios of bone collagen used to study coral-reef and terrestrial components of prehistoric Bahamian diet. American Antiquity 53:320-336.

Keegan WF, Hofman CL. 2017. The Caribbean before Columbus. New York: Oxford University Press.

Keith ML, Anderson GM, Eichler R. 1964. Carbon and oxygen isotopic composition of mollusk shells from marine and freshwater environments. Geochim Cosmochim Acta 28:1757–1786.

Kelman I. 2010. Hearing local voices from small island developing states for climate change. Local Environment 15(7): 605-619.

Kelman I, West JJ. 2009. Climate change and small island developing states: a critical review. Ecological and Environmental Anthropology 5(1):1-16.

Kennett D, Ingram BL, Erlandson JM, Walker P. 1997. Evidence for temporal fluctuations in marine radiocarbon reservoir ages in the Santa Barbara Channel, southern California. Journal of Archaeological Science 24(11):1051-1059.

Kenyon I, Kenyon S, Hancock RGV, Aufreiter S. 1995. Neutron activation analysis of some 19th-century facetted glass trade beads from Ontario, Canada, that have chemical compositions resembling Bohemian glass. The Bead Forum 27:4-9.

Kidd KE, Kidd MA. 1970. A classification system for glass beads for the use of field archaeologists. Canadian historic sites, Occasional Papers in Archaeology and History 1:45-89.

Kirch PV. 1984. The evolution of the Polynesian chiefdoms. Cambridge: Cambridge University Press.

Kirch PV. 1986. Rethinking East Polynesian Prehistory. The Journal of the Polynesian Society 95(1): 9-40.

Kirch PV. 1997. The Lapita peoples: Ancestors of the Oceanic world. The Peoples of South-East Asia and the Pacific. Cambridge: Blackwell.

Kirch PV. 2017. On the roads of the winds: An archaeological history of the Pacific Islands before European Contact. Berkeley: University of California Press.

Kirch PV, Sharp WD. 2005. Coral ^{230}Th dating of the imposition of a ritual control hierarchy in precontact Hawaii. Science 307(5706):102-104.

Kirch PV, Flenley JR, Steadman DW, Lamont, F, Dawson S. 1992. Ancient environmental degradation. Research and Exploration 8(2):166-179.

Kitalong AH. 2008. Forests of Palau: a long-term perspective. Micronesica 40(1/2):9-31.

Klimstra WD, Dooley AL. 1990. Food of the Key deer. Florida Scientist 53(4):264-273.

Klumpp DW, Bayne BL, Hawkins AJS. 1992. Nutrition of the giant clam *Tridacna gigas* (L.) I. Contribution of filter feeding and photosynthates to respiration and growth. Journal of Experimental marine Biology and Ecology 155:105-122.

Krämer A. 1926. Palau Volume 3. Hamburg: L. Friederichsen & Co. Translated by M.E. Locker.

Krigbaum J, Fitzpatrick SM, Bankaitis J. 2013. Human paleodiet at Grand Bay, Carriacou, Lesser Antilles. The Journal of Island and Coastal Archaeology 8: 210-227.

Krus AM, Cook R, Hamilton WD. 2015. Bayesian chronological modeling of SunWatch, a Fort Ancient village in Dayton, Ohio. Radiocarbon 57(5):965-977.

Kubary JS. 1873. Die Palau-Inseln in der Südsee. Journal des Museum Godeffroy 1:177-238. HRAF unofficial translation.

Kubary JS. 1895. Ethnographische beiträge zur kenntnis des Karolinen archipels. Leiden: Verlag Von P.W.M. Trap. HRAF unofficial translation.

Kuzmin, YV, Burr GS, Gorbunov SV, Rakov VA, and Razjigaeva NG. 2007. A Tale of two seas: Reservoir age correction values, (R, ΔR) for the Sakhalin Island (Sea of Japan and Okhotsk Sea). Nuclear Instruments and Methods in Physics Research Section B: Beam Interactions with Materials and Atoms 259(1):460-462.

Laffoon JE, Hoogland MLP, Davies GR, Hofman CL. Human dietary assessment in the pre-colonial Lesser Antilles: New stable isotope evidence from Lavoutte, Saint Lucia. Journal Archaeological. Science: Reports 5:168-180.

Lamb K, Swart PK. 2008. The carbon and nitrogen isotopic values of particulate organic material from the Florida Keys: A temporal and spatial study. Coral Reefs 27:351-362.

Land LS, Lundelius EL, Valastro Jr S. 1980. Isotopic ecology of deer bones. Palaeogeography, Palaeoclimatology, Palaeoecology 32:143-151.

Langhamer A. 2003. The legend of Bohemian glass: A thousand years of glassmaking in the heart of Europe. Czech Republich: Tigris.

Lanting JN, van der Plicht J. 1998. Reservoir effects and apparent 14C-ages. The Journal of Irish Archaeology 9:151-165.

Lartaud F, Emmanuel L, de Rafelis M, Pouvreau S, Renard M. 2010. Influence of food supply on the $\delta^{13}C$ signature of mollusc shells: Implications for palaeoenvironmental reconstitutions. Geo-Marine Letters 30(1):23-34.

Lawson IT, Edwards KJ, Church MJ, Newton AJ, Cook GT, Gathorne-Hardy FJ, Dugmore AJ. 2008. Human impact on an island ecosystem: pollen data from Sandoy, Faroe Islands. Journal of Biogeography 35(6):1130-1152.

Lee TN, Johns WE, Zantopp J, Fillenbaum E. 1996. Moored observations of volume transport and variability in western boundary currents of the subtropical North Atlantic at 26.5° N. Journal of Physical Oceanography 26:446-466.

Lee TN, Williams E. 1999. Mean distribution and seasonal variability of coastal currents and temperature in the Florida Keys with implications for larval recruitment. Bulletin of Marine Science 64(1):35-56.

LeGrande AN, Schmidt GA. 2006. Global gridded data set of the oxygen isotopic composition in seawater. Geophysical Research Letters 33(12):L12604.

LeGrande AN, Schmidt GA. 2009. Sources of Holocene variability of oxygen isotopes in paleoclimate archives. Climate in the Past 5:441-455.

Leppard TP, Runnels C. 2017. Maritime hominin dispersals in the Pleistocene: advancing the debate. Antiquity 91(356): 510–519.

Leppard TP, Smith AJ, Cherry JF. 2021. The initial colonization and settlement of the Mediterranean Islands. In: Napolitano MF, Stone JH, DiNapoli RJ, editors. The Archaeology of Island Colonization: Global Approaches to Initial Human Settlement. Gainesville: University Press of Florida. p. 265-292.

Lepofsky D, Lyons N, Moss ML. 2003. The use of driftwood on the North Pacific Coast: an example from Southeast Alaska. Journal of Ethnobiology 23(1):125-142.

Libby W. 1955. Radiocarbon dating. Chicago: University of Chicago Press.

Lidz BH, Shinn EA. 1991. Paleoshorelines, reefs, and a rising sea: South Florida, U.S.A. Journal of Coastal Research 7(1):203-229.

Lighty RG, MacIntyre IG, Stuckernath R. 1982. Acropora palmata reef framework: A reliable indicator of sea level in the Western Atlantic for the past 10,000 years. Coral Reefs 1(2):125-130.

Lin G, Sternberg LSL. 1992. Differences in morphology, carbon isotope ratios, and photosynthesis between scrub and fringe mangroves in Florida, USA. Aquatic Botany 42:303-313.

Liritzis I, Laskaris N. 2011. Fifty years of obsidian hydration dating in archaeology. Journal of Non-Crystalline Solids 357(10):2011-2023.

Lipo CP, Hunt TL, DiNapoli RJ. 2021.Temporal systematics: The colonization of Rapa Nui (Easter Island) and the conceptualization of time. In: Napolitano MF, Stone JH, DiNapoli RJ, editors. The Archaeology of Island Colonization: Global Approaches to Initial Human Settlement. Gainesville: University Press of Florida. p. 61-86.

Liston J. 2005. An assessment of radiocarbon dates from Palau, western Micronesia. Radiocarbon 47(2):295-354.

Liston J. 2007a. Palau Compact Road archaeological investigations, Babeldaob Island, Republic of Palau, phase II: Archaeological data recovery, volume VIII: Appendices. Honolulu: International Archaeological Research Institute, Inc.

Liston J. 2007b. Palau Compact Road archaeological investigations, Babeldaob Island, Republic of Palau, phase II: Historic preservation investigations, volume VII: Laboratory analyses, synthesis, and recommendations. Honolulu: International Archaeological Research Institute, Inc.

Liston J. 2010. Archaeological data recovery at Ngerumelong, Ngermid (OR-1:1), Koror State, Republic of Palau, Prepared for: Minister Sandra S. Pierantozzi, Koror.

Liston J. 2011a. Palau Compact Road archaeological investigations, Babeldaob Island, Republic of Palau, phase IV: Archaeological monitoring, volume XI: Fieldwork reports. Honolulu: International Archaeological Research Institute, Inc.

Liston J. 2011b. Palau Compact Road archaeological investigations, Babeldaob Island, Republic of Palau, phase IV: Archaeological monitoring, volume XII: Laboratory analyses and synthesis. Honolulu: International Archaeological Research Institute, Inc.

Liston J. 2011c. Palau Compact Road archaeological investigations, Babeldaob Island, Republic of Palau, phase IV: Archaeological monitoring, Volume XIII: Appendices. Honolulu: International Archaeological Research Institute, Inc.

Louys J, Braje TJ, Chang C-H, Cosgrove R, Fitzpatrick SM, Fujity M, Hawkins S, Ingicco T, Kawamura A, MacPhee RDE, McDowell MC, et al. 2021. No evidence for widespread island extinctions after Pleistocene hominin arrival. Proceedings of the National Academy of Sciences 118(20):e2023005118.

Lövgren L. 2011. Glass bead money: Traditional glass bead money in Palau, Western Micronesia, and a case study of a sample of small beads. Unpublished BA thesis. Visby: Gotland University.

Lowe DJ, Newnham RM, McFadgen BG, Higham TFG. 2000. Tephras and New Zealand Archaeology. Journal of Archaeological Science 27:859-870.

Loy TH, Spriggs M, Wickler S. 1992. Direct evidence for human use of plants 28,000 years ago: Starch residues on stone artefacts from the northern Solomon Islands. Antiquity 66(253):898-912.

Lum JK, Cann RL. 2000. mtDNA lineage analyses: Origins and migrations of Micronesians and Polynesians. American Journal of Physical Anthropology 113(2):151-168.

Lynch J, Ross M, Crowley T. 2013. The Oceanic languages. Language family series. Hoboken: Taylor and Francis.

MacArthur RH, Wilson EO. 1967. The theory of island biogeography. Princeton: Princeton University Press.

Machida H, Blong RJ, Specht J, Moriwaki H, Torrence R, Hayakawa Y, Talai B, Lolok D, Pain CF. 1996. Holocene explosive eruptions of Witori and Dakataua caldera volcanoes in west New Britain, Papua New Guinea. Quaternary International 34: 65-78.

Mangerud J, Bondevik S, Gulliksen S, Karin Hufthammer A, Høisæter T. 2006. Marine ^{14}C reservoir ages for 19th century whales and molluscs from the North Atlantic. Quaternary Science Reviews 25(23):3228-3245.

Marquardt WH, Krus A, Thompson VD. 2020. Rethinking the Estero Island Site: A possible satellite village of Mound Key. Journal of Anthropological Archaeology. https://doi.org/10.1016/j.jaa.2020.101145.

Martinsson-Wallin H, Wallin P, Anderson A, Solsvik R. 2013. Chronogeographic variation in initial East Polynesian construction of monumental ceremonial sites. The Journal of Island and Coastal Archaeology. 8(3):405-421.

Masse WB, Snyder D. 1982. The final report of the 1981 field season of the Southern Illinois University Palau Archaeological Project, Center for Archaeological Investigations. Carbondale: Southern Illinois University.

Maul GA, Martin DM. 1993. Sea level rise at Key West, Florida, 1846-1992: America's longest instrument record? Geophysical Research Letters 20(18):1955-1958.

McCoy MD**,** Alderson HA**,** Thompson A. 2015. A new archaeological field survey of the site of Nan Madol, Pohnpei. Rapa Nui Journal 29(1):5–22

McCoy MD, Alderson HA, Hemi R, Cheng H, Edwards RL. 2016. Earliest direct evidence of monument building at the archaeological site of Nan Madol (Pohnpei, Micronesia) identified using 230Th/U coral dating and geochemical sourcing of megalithic architectural stone. Quaternary research 86(3):295-303.

McKinnon H. 1999. Investigation of a hard water effect at Aotea Harbour, North Island, New Zealand. Masters of Science dissertation. New Zealand: University of Waikato.

McWethy DB, Wilmshurst JM, Whitlock C, Wood JR, McGlone MS. 2014. A high-resolution chronology of rapid forest transitions following Polynesian arrival in New Zealand. PLoS One 9(11): e111328.

McWethy, DB, Whitlock C, Wilmshurst JM, McGlone MS, Fromont M, Li X, Dieffenbacher-Krall A, Hobbs WO, Fritz SC, Cook ER. 2010. Rapid landscape transformation in South Island, New Zealand, following initial Polynesian settlement. Proceedings of the National Academy of Sciences 107(50):21343-21348.

Micó R. 2006. Radiocarbon dating and Balearic prehistory: reviewing the periodization of the prehistoric sequence. Radiocarbon 48(3):421-434.

Mickleburgh HL, Pagán-Jiménez JR. New insights into the consumption of maize and other food plants in the pre-Columbian Caribbean from starch grains trapped in human dental calculus. Journal of Archaeological Science 39(7): 2468-2478.

Morgan A. 1996. Mystery in the eye of the beholder: Cross-cultural encounters on 19th century Yap. Journal of Pacific History 31(1):27-41.

Mulrooney MA, Bickler SH, Allen MS, Ladefoged TN. 2011. High-precision dating of colonization and settlement in East Polynesia. Proceedings of the National Academy of Sciences 108(23): E192-E194.

Napolitano MF, Fitzpatrick SM, Clark G, Stone JH. 2019a. New Investigations of Early Prehistoric Settlement on Yap, Western Caroline Islands. The Journal of Island and Coastal Archaeology 14(1):101-107.

Napolitano MF, DiNapoli RJ, Stone JH, Levin MJ, Jew NP, O'Connor JT, Lane BG, Fitzpatrick SM. 2019b. Reevaluating human colonization of the Caribbean using chronometric hygiene and Bayesian modeling. Science Advances 5(12):eaar7806.

Napolitano MF, DiNapoli RJ, Stone JH. 2021. Introduction: The archaeology of island colonization. In: Napolitano MF, Stone JH, DiNapoli RJ, editors. The Archaeology of Island Colonization: Global Approaches to Initial Human Settlement. Society and Ecology in Island and Coastal Archaeology. Gainesville: University Press of Florida. p. 1-34.

Nelson GC, Fitzpatrick SM. 2005. Preliminary Investigations of the Chelechol ra Orrak Cemetery, Republic of Palau: I, Skeletal Biology and Paleopathology. Journal of Anthropological Science 113(3):1-12.

Nero KL. 1996. State Histories: Representations of Koror. Paper presented at the 11th PHA Conference, Hilo, Hawaii.

Neuwirth W. 1994. Beads From Gablonz: Historicism, art nouveau. Vienna: Privately Printed.

Neuwirth W. 2011. Beads from Gablonz, Beads: Journal of the Society of Bead Research 23:3-111.

Newnham RM, Lowe DJ, McGlone MS, Wilmshurst JM, Higham TFG. 1998. The Kaharoa Tephra as a critical datum for earliest human impact in northern New Zealand. Journal of Archaeological Science 25(6):533-544.

Newsom LA, Wing ES. 2004. On land and sea: Native American uses of biological resources in the West Indies. Tuscaloosa: University of Alabama Press.

Nunn PD, Petchey F. 2013. Bayesian Re-Evaluation of Lapita Settlement in Fiji: Radiocarbon Analysis of the Lapita Occupation at Bourewa and Nearby Sites on the Rove Peninsula, Viti Levu Island. Journal of Pacific Archaeology 4(2):21–34.

Nunn PD, Runman J, Falanruw M, Kumar R. 2017. Culturally grounded responses to coastal change on islands in the Federates States of Micronesia, northwest Pacific Ocean. Regional Environmental Change 17:959-971.

Nuttle WK, Fourqurean JW, Cosby BJ, Zieman JC, Robblee MB. 2000. Influence of net freshwater supply on salinity in Florida Bay. Water Resources Research 36(7):1805-1822.

O’Connell JF, Allen J, Williams MAJ, Williams AN, Turney CSM, Spooner NA, Kamming J, Brown G, Cooper A. 2018. When did *Homo sapiens* first reach Southeast Asia and Sahul? Proceedings of the National Academy of Sciences 115(34):8482-8490.

O’Connor S, Ulm S, Fallon SJ, Barham A, Loch I. 2010. Pre-bomb marine reservoir variability in the Kimberly Region, western Australia. Radiocarbon 52(2-3):1158-1165.

O'Sullivan PB, Morwood M, Hobbs D, Suminto FA, Situmorang M, Raza A, Maas R. 2001. Archaeological implications of the geology and chronology of the Sao basin, Flores, Indonesia. Geology 29(7): 607-610.

Opitz CJ. 2004. Traditional money on Yap and Palau. Ocala: First Impressions Printing, Inc.

Osborne D. 1958. The Palau Islands: Stepping stones into the Pacific. Archaeology 11:162-171.

Osborne D. 1966. The Archaeology of the Palau Islands: An intensive survey. Honolulu: Bishop Museum Press.

Papoulia C. 2017. Seaward dispersals to the NE Mediterranean islands in the Pleistocene: The lithic evidence in retrospect. Quaternary International 431:64-87.
Petchey F. 2009. Dating marine shell in Oceania: issues and prospects. In: Fairbairn A, O'Connor S, Marwick B, editors. New Directions in Archaeological Science. Terra Australis 28. Canberra: ANU E Press. p. 157-172.

Parmentier RJ. 1985. Times of the signs: Modalities of history and levels of social structure in Belau. In: Mertz E, Parmentier RJ, editors. Semiotic mediation: Sociocultural and psychological perspectives. Orlando: Academic Press. p. 131-154.

Parmentier RJ. 2002. Money walks, people talk. L'Homme: Revue Française d'Anthropologie 162:49-79.

Pearce NJG, Perkins WT, Westgate JA, Gorton MT, Jackson SE, Neal CR, Chenery SP. 1997. A compilation of new and published major and trace element data for NIST SRM 610 and SRM 612 glass reference materials. Geostandards Newsletter XXI:114-115.

Perkins RM, Krause SM. 2018. Adapting to climate change impacts in Yap State, Dederated States of Micronesia: The importance of environmental conditions and intangible cultural heritage. Island Studies Journal 13(1):65-78.

Petchey F. 2009. Dating marine shell in Oceania: issues and prospects. In: Fairbairn A, O'Connor S, Marwick B, editors. New Directions in Archaeological Science. Terra Australis 28. Canberra: ANU E Press. p. 157-172.

Petchey F, Green R. 2005. Use of three isotopes to calibrate human bone radiocarbon determinations from Kainapirina (SAC), Watom Island, Papua New Guinea. Radiocarbon, 47(2): 181-192.

Petchey F, Clark G. 2010. A marine reservoir correction value (ΔR) for the Palauan Archipelago: Environmental and oceanographic considerations. The Journal of Island and Coastal Archaeology 5(2):236-252.

Petchey F, Clark G. 2011. Tongatapu hardwater: investigation into the 14C marine reservoir offset in lagoon, reef and open ocean environments of a limestone island. Quaternary Geochronology 6:539-549.

Petchey F, Kirch PV. 2019. The importance of shell: Redating of the To'aga site (Ofu Island, Manu'a) and a revised chronology for the Lapita to Polynesian Plainware transition in Tonga and Samoa. PlosOne 14(9): e0211990.

Petchey F, Clark G. 2021. Clarifying the age of initial settlement horizon in the Mariana Islands and the impact of hard water: A response to Carson (2020). Radiocarbon doi:10.1017/RDC.2021.27.

Petchey F, Schmid MME. 2020. Vital evidence: Change in the marine 14C reservoir around New Zealand (Aotearoa) and implications for the timing of early settlement. Scientific Reports 10(14266).

Petchey F, Anderson A, Zondervan A, Ulm S, Hogg A. 2008a. New marine ΔR values for the South Pacific subtropical gyre region. Radiocarbon 50(3):373-397.

Petchey F, Anderson A, Hogg A, Zondervan A. 2008b. The marine reservoir effect in the Southern Ocean: An evaluation of extant and new ΔR values and their application to archaeological chronologies. Journal of the Royal Society of New Zealand 38(4):243-262.

Petchey F, Allen MS, Addison DJ, Anderson A. 2009. Stability in the South Pacific surface marine ^{14}C reservoir over the last 750 years: Evidence from American Sāmoa, the southern Cook Islands and the Marquesas. Journal of Archaeological Science 36(10):2234-2243.

Petchey F, Spriggs M, Leach F, Seed M, Sand C, Pietrusewsky M, Anderson, K. 2011. Testing the human factor: radiocarbon dating the first peoples of the South Pacific. Journal of Archaeological Science. 38(1):29-44.

Petchey F, Ulm S, David B, McNiven IJ, Asmussen B, Tomkins H, Dolby N, Aplin K, Richards T, Rowe C, and Leavesley M. 2013. High-resolution radiocarbon dating of marine materials in archaeological contexts: Radiocarbon marine reservoir variability between *Anadara, Gafrarium*, Batissa, *Polymesoda* spp., and Echinoidea at Caution Bay, Southern Coastal Papua New Guinea. Archaeological and Anthropological Sciences 5(1):69-80.

Petchey F, Spriggs M, Bedford S, Valentin F, Buckley, H. 2014. Radiocarbon dating of burials from the Teouma Lapita cemetery, Efate, Vanuatu. Journal of Archaeological Science 50:227-242.

Petchey F, Spriggs M, Bedford S, Valentin F. 2015. The chronology of occupation at Teouma, Vanuatu: Use of a modified chronometric hygiene protocol and Bayesian modeling to evaluate midden remains. Journal of Archaeological Science: Reports 4:95-105.

Petchey F, Ulm S, David B, McNiven IJ, Asmussen B, Tomkins H, Richards T, Rowe C, Leavesley M, Mandui H, Stanisic J. 2016. ^{14}C marine reservoir variability in herbivores and deposit-feedings gastropods from an open coastline, Papua New Guinea. Radiocarbon 54(3-4):967-978.

Petchey F, Clark G, Winter O, O'Day P, Litster M. 2017. Colonisation of Remote Oceania: New dates for the Bapot-1 site in the Mariana Islands. Archaeology in Oceania 52:108-126.

Petchey F, Clark G, Lindeman I, O'Day P, Southon J, Dabell K, Winter O. 2018. Forgotten news: Shellfish isotope insight into changing sea-level and associated impact on the first settlers of the Mariana Archipelago. Quaternary Geochronology 48:180-194.

Petrie CA, Torrence R. 2008. Assessing the effects of volcanic disasters on human settlement in the Willaumez Peninsula, Papua New Guinea: a Bayesian approach to radiocarbon calibration. The Holocene 18(5):729-744.

Pitts PA. 1994. An investigation of near-bottom flow patterns along and across Hawk Channel, Florida Keys. Bulletin of Marine Science 54(3):610–20.

Pope KO, Terrell JE. 2008. Environmental setting of human migrations in the circum-Pacific region. Journal of Biogeography 35(1):1-21.

Power EM. 2011. Historic beads. In: Liston J, editor. Palau Compact Road archaeological investigations, Babeldaob Island, Republic of Palau, phase IV: Archaeological monitoring, volume XII: Laboratory analyses and synthesis. Honolulu: International Archaeological Research Institute, Inc. p. 371-385.

Prasad GVR, Culp R, Cherkinsky A. 2019. $\delta^{13}C$ correction to AMS data: Values derived from AMS vs IRMS values. Nuclear Instruments and Methods in Physics Research Section B: Beam Interactions with Materials and Atoms 455:244-249.

Prebble M, Wilmshurst JE. 2009. Detecting the initial impact of humans and introduced species on island environments in Remote Oceania using palaeoecology. Biological Invasions 11:1529-1556.

Randall HA. 1964. A study of the growth and other aspects of the biology of the West Indian topshell, *Cittarium pica* (Linnaeus). Bulletin of Marine Science of the Gulf and Caribbean 14(3):424-443.

Rawlence NJ, Collins CJ, Andersen CNK, Maxwell JJ, Smith IWG, Robertson BC, Knapp M, Horsburgh A, Stanton JL, Scofield RP, et al. 2016. Human-mediated extirpation of the unique Chatham Islands sea lion and implications for the conservation management of remaining New Zealand sea lion populations. Molecular Ecology 25(16):3950-3961.

Reid DG, Dyal P, Lozouet P, Glaubrecht M, Williams ST. 2008. Mudwhelks and mangroves: The evolutionary history of an ecological association (Gastropoda: Potamididae). Molecular Phylogenetics and Evolution 47(2): 680-699.

Reimer RW, Reimer PJ. 2017. An online application for ΔR calculation. Radiocarbon 59(5):1623-1627.

Reimer PJ, Bard E, Bayliss A, Beck JW, Blackwell PG, Bronk Ramsey C, Buck CE, Cheng H, Edwards RL, Friedrich M, et al. 2013. IntCal13 and Marine13 radiocarbon age calibration curves 0-50,000 years cal BP. Radiocarbon 55(3):1869-1887.

Reimer P, Austin W, Bard E, Bayliss A, Blackwell P, Bronk Ramsey C, Butzin M, Cheng H, Edwards R, Friedrich M, et al. 2020. The IntCal 20 Northern Hemisphere radiocarbon age calibration curve (0-55 cal kBP). Radiocarbon 62(4):725-757.

Remengesau FK. 1997. Traditional udoud of Palau: Mysteries, recordings, and Future Use. Journal of the Pacific Society 19:9-18.

Reynolds LK, Berg P, Zieman JC. 2007. Lucinid clam influence on the biochemistry of the seagrass *Thalassia testudinum* sediments. Estuaries and Coasts 30(3):482-490.

Robertson R. 2003. The edible West Indian “Whelk” *Cittarium pica* (Gastropoda: Trochidae): Natural history with new observations. Proceedings of the National Academy of Natural Sciences of Philadelphia 153:27-47.

Richards ZT, Chuan-Chou S, Hobbs J-P A, Wu C-C, Jiang X, Beardsley F. 2015. New precise dates for the ancient and sacred coral pyramidal tombs of Leluh (Kosrae, Micronesia). Science Advances 1(2):e1400060.

Rick TC, Vellanoweth RL, Erlandson, JM. 2005. Radiocarbon dating and the “old shell” problem: Direct dating of artifacts and cultural chronologies in coastal and other aquatic regions. Journal of Archaeological Science 32(11):1641-1648.

Rick TC, Henkes GA, Lowery DL, Colman SM, Culleton BJ. 2012. Marine Radiocarbon Reservoir Corrections (ΔR) for Chesapeake Bay and the Middle Atlantic Coast of North America. Quaternary Research 77(1):205–210.

Rick TC, Kirch PV, Erlandson JM, Fitzpatrick SM. 2013. Archeology, deep history, and the human transformation of island ecosystems. Anthropocene 4: 33-45.

Ridings R. 1996. Where in the world does obsidian hydration dating work? American Antiquity
61(1):136-148.

Rieth TM, Hunt TL. 2008. A radiocarbon chronology for Samoan prehistory. Journal of Archaeological Science 35(7): 1901-1927.

Rieth TM, Athens, JS. 2019. Late Holocene human expansion into Near and Remote Oceania: A Bayesian model of chronologies of the Mariana Islands and Bismarck Archipelago. Journal of Island and Coastal Archaeology 14(1):5-16.

Rieth TM, Hamilton WD. 2021. Improving dating accuracy and precision for Mid-Late Holocene island colonization. In: Napolitano MF, Stone JH, DiNapoli RJ, editors. The Archaeology of Island Colonization: Global Approaches to Initial Human Settlement. Gainesville: University Press of Florida. p. 180-206.

Rieth TM, Morrison AE, Addison DJ. 2008. The temporal and spatial patterning of the initial settlement of Sāmoa. The Journal of Island and Coastal Archaeology 3(2):214-239.

Rieth TM, Hunt TL, Lipo C, Wilmshurst JM. 2011. The 13th century Polynesian colonization of Hawai'i Island. Journal of Archaeological Science 38(10):2740-2749.

Rijsdijk KF, Zinke J, de Louw PG, Hume JP, van der Plicht H, Hooghiemstra H, Meijer HJM, Vonhof HB, Porch N, Florens FBV, et al. 2011. Mid-Holocene (4200 kyr BP) mass mortalities in Mauritius (Mascarenes): insular vertebrates resilient to climatic extremes but vulnerable to human impact. The Holocene 21(8):1179-1194.

Rizal Y, Westaway KE, Zaim Y, van den Bergh GD, Bettis EA, Morwood MJ, Huffman OF, Grün, Joannes-Boyau R, Bailey RM, et al. 2020. Last appearance of *Homo erectus* at Ngandong, Java, 117,000-108,000 years ago. Nature 577:381-385.

Ritzenthaler RE. 1954. Native money of Palau. Milwaukee: Milwaukee Public Museum Publications in Anthropology.

Ross LA. 1997. Glass and ceramic trade beads from the Native Alaskan neighborhood. In: Lightfoot KG, Schiff AM, Wake TA, editors. The archaeology and ethnohistory of Fort Ross, California, volume 2: The Native Alaskan neighborhood: A multiethnic community at Colony Ross. Contributions of the University of California Archaeological Research Facility. Berkeley: University of California. p. 179-212.

Ross LA. 2003. Bohemian faceted-spheroidal mold-pressed glass bead attributes: Hypothesized terminus post quem dates for the 19th century. Beads: Journal for the Society of Bead Researchers 15:41-52.

Ross LA, Pflanz, B. 1989. Bohemian glass bead making: Translation and discussion of a 1913 German technical article. Beads: Journal of the Society of Bead Researchers 1:81-94.

Ross M. 1996. Is Yapese Oceanic? In: Nothofer B, editor. Reconstruction, classification, description: Festschrift in honor of Isidore Dyen. Meyer: Abera-Verl. p. 121-166.

Rouse I. 1986. Migrations in prehistory. New Haven: Yale University Press.

Runnels C. 2014. Early Palaeolithic on the Greek Islands? Journal of Mediterranean Archaeology 27(2):211-230.

Runnels C. 2021. The Paleolithic exploration of the Greek Islands and Middle Pleistocene Hominin dispersals: The case for behavioral variability over behavioral modernity. In: Napolitano MF, Stone JH, DiNapoli RJ, editors. The Archaeology of Island Colonization: Global Approaches to Initial Human Settlement. Gainesville: University Press of Florida. p. 87-103.

Sanchez GM, Rick TC, Culleton BJ, Kennett DJ, Buckley M, Erlandson JM, Losey RL. 2018. Radiocarbon dating legacy collections: A Bayesian analysis of high-precision AMS ^{14}C dates from the Par-Tee site, Oregon. Journal of Archaeological Science: Reports 21:833-848.

Schreyer JA. 1790. Kommerz, Fabriken und Manufakturen des Königreichs Böhmen, Theil, Prag-Leipzig.

Schiffer MB. 1986. Radiocarbon dating and the "old wood" problem: The case of the Hohokam chronology. Journal of Archaeological Science 13(1):13-30.

Schmid MM, Wood R, Newton AJ, Vesteinsson O, Dugmore AJ. 2019. Enhancing radiocarbon chronologies of colonization: chronometric hygiene revisited. Radiocarbon 61:629-647.

Schmid MM, Dugmore AJ, Foresta L, Newton AJ, Vésteinsson O, Wood R. How ^{14}C dates on wood charcoal increase precision when dating colonization: The examples of Iceland and Polynesia. Quaternary Geochronology 48:64-71.

Schmid MME, Dugmore AJ, Newton AJ, Vesteinsson O. 2021. Multidisciplinary chronological data from Iceland indicate a Viking Age settlement flood, rather than a flow or a trickle. In Napolitano MF, Stone JH, DiNapoli RJ, editors. The Archaeology of Island Colonization: Global Approaches to Initial Human Settlement. Gainesville: University Press of Florida. p. 132-179.

Schoeninger MJ, DeNiro MJ. 1984. Nitrogen and carbon isotopic composition of bone collagen from marine and terrestrial animals. Geochimica et Cosmochimica Acta 48:625-639.

Schott FA, Lee TN, Zantopp R. 1988. Variability of structure and transport of the Florida Current in the period range of days to seasonal. Journal of Physical Oceanography 18:1209-1230.

Schulting RJ**,** Richards MP**.** 2002. Finding the coastal Mesolithic in southwest Britain: AMS dates and stable isotope results on human remains from Caldey Island, South Wales. Antiquity 76:1011–1025.

Sear DA, Allen MS, Hassall JD, Maloney AE, Langdon PG, Morrison AE, Henderson ACG, Mackay H, Croudace IW, Clarke C, et al. 2020. Human settlement of East Polynesia earlier, incremental, and coincident with prolonged South Pacific drought. Proceedings of the National Academy of Sciences 117(16): 8813-8819.

Seersholm FV, Cole TL, Grealy A, Rawlence NJ, Greig K, Knapp M, Stat M, Hansen AJ, Easton LJ, Shepherd L, et al. 2018. Subsistence practices, past biodiversity, and anthropogenic impacts revealed by New Zealand-wide ancient DNA survey. Proceedings of the National Academy of Sciences 115(30):7771-7776.

Sepkoski Jr. JJ. 2002. A compendium of fossil marine animal genera. Bulletins of American Paleontology 363:1-560.

Shade PJ, Anthony SS, Takasaki KJ. 1992. Ground-water resources reconnaissance of the Yap main islands, Federated States of Micronesia. Water-Resources Investigations Report 90-4074. U.S. Geological Survey, Honolulu.

Shane P. 2000. Tephrochonology: A New Zealand case study. Earth Science Reviews 49(1-
4):223-259.

Sharp WD, Kahn JG, Polito CM, Kirch PV. 2010. Rapid evolution of ritual architecture in central Polynesia indicated by precise 230Th/U coral dating. Proceedings of the National Academy of Sciences 107(30):13234-13239.

Sheppard P. 2019. Early Lapita colonisation of Remote Oceania: An update on the leapfrog hypothesis. In: Bedford S, Spriggs M, editors. Debating Lapita: Distribution, chronology, society and subsistence. Terra Australis 52. Canberra: ANU Press. p. 135-154.

Shinn A, Hudson H, Halley RB, Lidz B. 1977. Topographic control and accumulation rate of some Holocene coral reefs: South Florida and Dry Tortugas. Proceedings: Third International Coral Reef Symposium. Miami: Coastal and Marine Geology Program.

Siegel PE, editor. 2018. Island historical ecology: Socionatural landscapes of the Eastern and Southern Caribbean. New York: Berghahn Books.

Siegel PE, Jones JG, Pearsall DM, Dunning NP, Farrell P, Duncan NA, Curtis JH, Singh SK. Paleoenvironmental evidence for first human colonization of the eastern Caribbean. Quaternary Science Reviews 129:275-295.

Siegel PE, Jones JG, Pearsall DM, Dunning NP, Farrell P, Duncan NA, Curtis JH. 2019. In: Hofman CL, Antczak, AT, editors. Ecosystem engineering during the human occupations of the Lesser Antilles, in Early Settlers of the Insular Caribbean: Dearchaizing the Archaic. Leiden: Sidestone Press. p. 77-88.

Smith CW. 1983. Soil surveys of Islands of Yap Federated States of Micronesia. U.S. Department of Agriculture Soil Conservation Service.

Smith SP. 1910. Hawaiki the original home of the Maori. Christchurch: Whitcombe and Tombs.

Southon J, Kashgarian M, Fontugne M, Metivier B, Yim WWS. Marine reservoir corrections for the Indian Ocean and Southeast Asia. Radiocarbon 44(1): 167-180.

Spennemann DHR. 1987. Resources of prehistoric Tongatapu, Tonga: Effects of human predation and changing environment. Archaeology in Oceania 22(3):81-96.

Spriggs M. 1989. The dating of the Island Southeast Asian Neolithic: An attempt at chronometric hygiene and linguistic correlation. Antiquity 63(24):587-613.

Spriggs M. 1990. Dating Lapita: Another view. In: Spriggs M, editor. Lapita design, form and composition: Proceedings of the Lapita design workshop. Canberra: Australian National University. p. 1-27.

Spriggs M. 1991. Lapita origins, distribution, contemporaries and successors, revisited. In:
Bellwood P, editor. Indo-Pacific prehistory 1990: Proceedings of the 14th Congress of the Indo-Pacific Prehistory Association. Canberra: Indo-Pacific Prehistory Association. p. 306–312.

Spriggs M. 2011. Archaeology and the Austronesian expansion: where are we now?. Antiquity 85(328).

Spriggs M, Anderson A. 1993. Late colonization of East Polynesia. Antiquity 67: 200–217.

Stevenson C, Sheppard P, Sutton D, Ambrose W. 1996. Advances in the hydration dating of New Zealand obsidian. Journal of Archaeological Science 23(2): 233-242.

Stevenson CM, Abdelrehim IM, Novak SW. 2001. Infra-red photoacoustic and secondary ion mass spectrometry measurements of obsidian hydration rims. Journal of Archaeological Science 28:109-115.

Stokes AV, Keegan WF. 1996. A reconnaissance for prehistoric archaeological sites on Grand Cayman. Caribbean Journal of Science 32:425-430.

Storlazzi CD, Gingerich SB, van Dongeren A, Cheriton OM, Swarzenski PW, Quataert E, Voss CI, Field DW, Annamalai H, Piniak GA, McCall R. 2018. Most atolls will be uninhabitable by the mid-21st century because of sea-level rise exacerbating wave-driven flooding. Science Advances 4(4):eaap9741.

Stuiver M, Pearson GW. 1986. High-Precision Calibration of the Radiocarbon Time Scale, AD 1950-500 BC. Radiocarbon 28(2B):805–838.

Stuiver M, Braziunas TF. 1993. Modeling Atmospheric ^{14}C Influences and ^{14}C Ages of Marine Samples to 10,000 BC. Radiocarbon 31(1):137-189.

Stuiver M, Pearson GW, Braziunas TF. 1986. Radiocarbon Age Calibration of Marine Samples Back to 9000 Cal Yr BP. Radiocarbon 28(2B):980–1021.

Stuiver M, Reimer PJ, Reimer RW. 2020. CALIB 8.2. www.calib.org.

Sullivan RM, van Hengstum PJ, Donnelly JP, Winkler TS, Mark SE, Albury NA. 2020. Absolute and relative dating of human remains in a Bahamian sinkhole (Great Cistern, Abaco). Journal of Archaeological Science: Reports 32:102441.

Summerhayes GR. 2018. Coconuts on the move: Archaeology of Western Pacific. Journal of Pacific History 53(4):375-396.

Sutton DG. 1994. Origins of the first New Zealanders. Auckland: Auckland University Press.

Sutton DG, Flenley JR, Li X, Todd A, Butler K, Summers R, Chester PI. 2008. The timing of the human discovery and colonization of New Zealand. Quaternary International 184(1):109-121.

Swart PK, Wilson AF, Jell JS. 1983. Oxygen isotope variation on a lagoonal platform reef, Heron Island, Great Barrier Reef. Marine and Freshwater Research 34:813–819.

Swart PK, Healy GF, Dodge RE, Kramer P, Hudson JH, Halley RB, Robblee MB. 1996. The stable oxygen and carbon isotopic record from coral growing in Florida Bay: a 160 year record of climatic and anthropogenic influence. Palaeogeography, Palaeoclimatology, Palaeoecology 124(1-4):219-237.

Swisher CC, Rink WJ, Antón SC, Schwarcz HP, Curtis GH, Widiasmoro AS. 1996) Latest *Homo erectus* of Java: potential contemporaneity with Homo sapiens in Southeast Asia. Science 274(5294):1870-1874.

Semper K. 1873. Die Palau-Inseln im Stillen Ocean. Leipzig: F. A. Brockhaus.

Semper K. 1982 [1873]. Die Palau-Inseln im Stillen Ocean. Translated by M.L. Berg. Leipzig: F. A. Brockhaus.

Silliman SW. 2009. Change and continuity, practice and memory: Native American persistence in Colonial New England. American Antiquity 74(2):211-230.

Stone JH. 2020. The Bioarchaeology of Initial Human Settlement in Palau, Western Micronesia. PhD dissertation. University of Oregon, Eugene.

Stone JH, Fitzpatrick SM, Napolitano MF. 2017. Disproving Claims for Small-bodied Humans in the Palauan Archipelago. Antiquity 91(360):1546-1560.

Taché K, Hart JP. 2013. Chronometric hygiene of radiocarbon databases for early durable cooking vessel technologies in northeastern North America. American Antiquity 78(2):359-372.

Tagliabue A, Bopp L. 2008. Towards understanding global variability in ocean carbon-13. Global Biogeochemical Cycles 22:GB1025.

Takayama J. 1982. A brief report on archaeological investigations of the southern part of Yap Island and nearby Ngulu Atoll. In Aoyagi, T, editor Islanders and Their Outside World: A report of the cultural and anthropological research in the Caroline Islands of Micronesia in 1980-1981. Tokyo: Rikkyo University. Committee for Micronesian Research. P. 77-104.

Tankersly TB, Dunning NP, Owen LA, Sparks J. 2018. Geochronology and paleoenvironmental framework for the oldest archaeological site (7800-7900 cal BP) in the West Indies, Banwari Trace, Trinidad. Latin American Antiquity 29:681-695.

Tebano T, Paulay G. 2000. Variable recruitment and changing environments create a fluctuating resource: the biology of *Anadara uropigmelana* (Bivalvia: Arcidae) on Tarawa Atoll. Atoll Research Bulletin 488. Washington D.C.: National Museum of Natural History Smithsonian Institution. p. 1-5.

Terry JP, Chui TFM. 2012. Evaluating the fate of freshwater lenses on atoll islands after eustatic sea-level rise and cyclone-driven inundation: A modelling approach. Global and Planetary Change 88:76-84.

Thijssen-Etpison M. 1997. Palau: Portrait of Paradise, Revised third ed. Koror:NECO Marine Corporation.

Titchenal PB. 1999. Palauan money beads: An analysis of glass beads found with a child's burial at site B:OR-1:8, Feature 2, Burial Pit 2, Hung Kuo, Koror, Republic of Palau. Honolulu: Jeffrey Pantaleo Consultants.

Titchenal PB. 2001. Description and classification of glass beads and bangles recovered from traditional Palauan burial platforms at the village of Ngerielb, Site B:OR-1:8, Ngermid, Koror, Republic of Palau. Honolulu: Pantaleo Consultants LLC.

Titchenal PB. Drolet R, Pantaleo, J. 1998. Ngiwal: Archaeological data recovery and monitoring in a rural village on Babeldaob in the Republic of Palau. Guam: Garcia and Associates.

Thomas DH. 2008. Native American landscapes of St. Catherines Island. II. The data. Anthropological Papers of the American Museum of Natural History 88(2). New York: American Museum of Natural History.

Thomas FR. 2001. Mollusk habitats and fisheries in Kiribati: An assessment from the Gilbert Islands. Pacific Science 55(1)77-97.

Thomas KD. 2015. Molluscs emergent, Part I: Themes and trends in the scientific investigation of mollusc shells as resources for archaeological research. Journal of Archaeological Science 56:133-140.

Thomas DH, Sanger MC, Hayes RH. 2013. Revising the ^{14}C reservoir correction for St. Catherines Island, Georgia. In: Thompson VD, Thomas DH, editors. Life among the tides: Recent archaeology on the Georgia Bight. Anthropological Papers of the American Museum of Natural History 98. New York: American Museum of Natural History. p. 25-46.

Thompson VD, Krus A. 2018. Contemplating the history and future of radiocarbon dating in the American Southeast. Southeastern Archaeology 37(1):1-11.

Thompson, VD, Marquardt WH, Walker KJ, Roberts Thompson A, Newsom LA. 2018. Collective action, state building, and the rise of the Calusa, Southwest Florida. Journal of Anthropological Archaeology 51:28-44.

Tobler R, Rohrlach A, Soubrier J, Bover P, Llamas B, Tuke J, Bean N, Abdullah-Highfold A, Agius S, O'Donoghue A, O'Loughlin I, Sutton P, Zilio F, Walshe K, Williams AN, Turney CSM, Williams M, Richards SM, Mitchell RJ, Kowal E. 2017. Aboriginal mitogenomes reveal 50,000 years of regionalism in Australia. Nature 544(7649):180-184.

Torrence R. 2008. Punctuated landscapes: Creating cultural places in volcanically active environments. Handbook of Landscape Archaeology 333-343.

Torrence R, Swadling P. 2008. Social networks and the spread of Lapita. Antiquity 82(317): 600-616.

Torrence R, Neall V, Doelman T, Rhodes E, McKee C, Davies H, Bonetti R, Guglielmetti A, Manzoni A, Oddone M, et al. 2004. Pleistocene colonisation of the Bismarck Archipelago: new evidence from West New Britain. Archaeology in Oceania 39(3):101-130.

Toth LT, Cheng H, Edwards RL, Ashe E, Richey JN. 2017. Millennial-scale variability in the local radiocarbon reservoir age of south Florida during the Holocene. Quaternary Geochronology 42:130-143.

Tuniz C, Bird JR, Fink D, Herzog GF. 1998. Accelerated mass spectrometry: Ultrasensitive analysis for global science. Boca Raton: CRC Press.

Turgeon DD, Lyons WG, Mikkelsen P, Rosenberg G, Moretzsohn F. 2009. Bivalvia (Mollusca) of the Gulf of Mexico. In: Felder DL, Camp DK, editors. Gulf of Mexico: Origins, waters, and biota. College Station: Texas A&M University Press. p. 711-744.

Turvey ST, Oliver JT, Narganes Storde YM, Rye P. 2007. Late Holocene extinction of Puerto Rican native land mammals. Biological Letters 3:193-196.

Ulm, S. 2006. Australian marine reservoir effects: a guide to ΔR values. Australian Archaeology 65:57-60.

Ushijima I. 1982. The control of reefs and lagoons: Some aspects of the political structure of Ulithi Atoll. In: Aoyagi M (editor). Islanders and their outside world: A report of the cultural anthropological research in the Caroline Islands of Micronesia in 1980-1981. Committee for Micronesian Research. Tokyo: Rikkyo University.

Vecchi GA, Harrison DE. 2000. Tropical Pacific sea surface temperature anomalies, El Niño, and Equatorial westerly wind events. Journal of Climate 13(111):1814-1830.

Walker K. 2013. The Pineland site complex: Environmental contexts. In: Marquardt WH, Walker KJ, editors. The Archaeology of Pineland: A coastal Southwest Florida site complex, A.D. 50-1710. Gainesville: University Press of Florida. p. 23-52.

Waller T. 1991. Evolutionary relationships among commercial scallops (Mollusca: Bivalvia: Pectinidae). In: Shumway SE, editor. Scallops: Biology, ecology and aquaculture. Amsterdam: Elsevier.

Waller T. 1993. The evolution of "Chlamys" (Mollusca: Bivalvia: Pectinidae) in the tropical westerns Atlantic and eastern Pacific. American Malacological Bulletin 10(2):195-249.

Wang F, Li Y, Wang J. 2016. Intraseasonal variability of the surface zonal currents in the western tropical Pacific Ocean: Characteristics and mechanisms. Journal of Physical Oceanography 46(12):3639-3660.

Watanabe J, Inacio M. n.d. Udoud er a Belau. Koror: Palau Ministry of Education.

Weisler MI, Collerson KD, Feng YX, Zhao JX, Yu, KF 2006. Thorium-230 coral chronology of a late prehistoric Hawaiian chiefdom. Journal of Archaeological Science, 33(2):273-282.

Weisler MI, Yamano H, Hua Q. 2012. A multidisciplinary approach for dating human colonization of Pacific atolls. The Journal of Island and Coastal Archaeology 7(1):102-125.

Wilmshurst JM. 1997. The impact of human settlement on vegetation and soil stability in Hawke's Bay, New Zealand. New Zealand Journal of Botany 35(1):97-111.

Wilmshurst JM, Anderson AJ, Higham TFG, Worthy TH. 2008. Dating the Late Prehistoric Dispersal of Polynesians to New Zealand Using the Commensal Pacific Rat. Proceedings of the National Academy of Sciences of the United States of America 105(22):7676–7680.

Wilmshurst J, Hunt TL, Lipo CL, Anderson AJ. 2011. High-precision radiocarbon dating shows recent and rapid initial human colonization of East Polynesia. Proceedings of the National Academy of Sciences 108:1815-1820.

Wilson SM. 2006. The prehistory of Nevis, a Small island in the Lesser Antilles. New Haven: Yale University Press.

Wilson SM, Iceland HB, Hester TR. 1998. Preceramic connections between Yucatan and the Caribbean. Latin American Antiquity 9:342-352.

Wood R. 2015. From revolution to convention: the past, present and future of radiocarbon dating. Journal of Archaeological Science 56:61-72.

Worth JE. 2014. Discovering Florida: First-contact narratives from Spanish expeditions along the Lower Gulf Coast. Gainesville: University of Florida.

van Wynsberge S, Andréfouët, Gaertner-Mazouni N, Wabnitz CCC, Menoud M, Le Moullac G, Levy P, Gilbert A, Remoissenet G. 2017. Growth, survival and reproduction of the giant clam *Tridanca maxima* (Röding 1978, Bivalvia) in two contrasting lagoons in French Polynesia. Plos One 12(1):e0170565.

Yoneda M, Kitagawa H, van der Plicht J, Uchida M, Tanaka A, Uehiro T, Shibata Y, Morita M, Ohno T. 2000. Pre-bomb marine reservoir ages in the Western North Pacific: Preliminary result on Kyoto University collection. Nuclear Instruments and Methods in Physics Research Section B: Beam Interactions with Materials and Atoms 172(1-4):377–381.

Yoneda M, Uno H, Shibata Y, Suzuki R, Kumamoto Y, Yoshida K, Sasaki T, Suzuki A, Kawahata H. 2007. Radiocarbon marine reservoir ages in the Western Pacific estimated by pre-bomb molluscan shells. Nuclear Instruments and Methods in Physics Research, Section B: Beam Interactions with Materials and Atoms 259(1):432–37.

Yu Z, McCreary Jr. JP, Kessler WS, Kelly KA. 2000. Influence of equatorial dynamics on the Pacific North Equatorial Countercurrent. Journal of Physical Oceanography 30(12):3179-3190.

Yuping C. 2012. The emergence of local entrepreneurs in Palau. Pacific Asia Inquiry 3, 87-101.

Zerega, NJC, Ragone D, Motley T. 2004. Complex origins of breadfruit (*Artocarpus altilis*, Moraceae): Implications for human migrations in Oceania. American Journal of Botany 91(5)760-766.